Spring 5-5-2023

EVALUATING SEX DIFFERENCES IN THE NEUROIMMUNE RESPONSE FOLLOWING NEUROINFLAMMATION AND RELIEF DUE TO NANOTHERANOSTIC TREATMENT

Brooke Deal

EVALUATING SEX DIFFERENCES IN THE NEUROIMMUNE RESPONSE FOLLOWING NEUROINFLAMMATION AND RELIEF DUE TO NANOTHERANOSTIC TREATMENT

A Dissertation

Submitted to the Bayer School of Natural and Environmental Sciences

Duquesne University

In partial fulfilment of the requirements for

the degree of Doctor of Philosophy

By

Brooke S. Deal

May 2023

EVALUATING SEX DIFFERENCES IN THE NEUROIMMUNE RESPONSE FOLLOWING NEUROINFLAMMATION AND RELIEF DUE TO NANOTHERANOSTIC TREATMENT

By

Brooke S. Deal

February 23, 2023

John A. Pollock Professor of Biological Sciences (Committee Chair)	Jelena M. Janjic Associate Professor of Pharmaceutical Sciences (Committee Member)
Jan E. Janecka Associate Professor of Biological Sciences (Committee Member)	Lauren O'Donnell Associate Professor of Pharmaceutical Sciences (Committee Member)
Jill Dembowski Assistant Professor of Biological Sciences (Committee Member)	
Ellen Gawalt Interim Dean, Bayer School of Natural and Environmental Sciences	Jana Patton-Vogt Chair, Biological Sciences Professor of Biological Sciences

ABSTRACT

EVALUATING SEX DIFFERENCES IN THE NEUROIMMUNE RESPONSE FOLLOWING NEUROINFLAMMATION AND RELIEF DUE TO NANOTHERANOSTIC TREATMENT

By

Brooke S. Deal

May 2023

Dissertation supervised by Dr. John A. Pollock

Until recently, the majority of preclinical neuroinflammatory studies were performed on males. Because of this, less is known about the female neuroinflammatory response to injury, formation of pain, or response to pain-relieving therapies. The neuroinflammatory response is multifaceted with neuronal, glial, and immune cells all contributing to the induction and resolution of neuroinflammation. During this response, macrophages typically undergo an upregulation of cyclooxygenase-2 (COX-2) leading to the production of prostaglandin E_2 (PGE_2), which is linked to neuronal sensitization and pain. Non-steroidal anti-inflammatory drugs (NSAIDs) attenuate PGE_2 by the inhibition of COX-2. A limitation with NSAIDs is that due to the systemic dosage needed to achieve neuropathic pain relief there are risks of off-target toxicity. In collaboration with the Janjic Lab, a novel COX-2 inhibiting theranostic nanoemulsion has been seen to alleviate mechanical hypersensitivity in male rats who have

undergone chronic constriction injury (CCI); however, how it works to alleviate female neuropathic pain remained unknown. This study evaluated the efficacy of 1X CXB-NE (0.24 mg/kg) in relieving neuropathic hypersensitivity and saw that females experienced less relief. Increasing the concentration to 10X CXB-NE (2.4 mg/kg) resolved this sex difference with equivalent relief being observed. Knowing the therapeutic works differently in females than in males, we furthered our understanding by transcriptionally evaluating the sex differences during neuroinflammation and relief. Here we found that how males and females responded to treatment was unique. Following neuroinflammatory induction, both sexes had an upregulation of a CREB binding protein, *activating transcription factor 3* (*ATF-3*); following 10X CXB-NE treatment, which only females had a significant down regulation of this gene. Interestingly, it has been seen that ATF-3 is a transcriptional regulator to the COX-2 expression. Males on the other hand appear to have an upregulation of neutrophil involvement, specifically with *S1008A* and *S1009A,* which are markers for the release of neutrophil extracellular traps. This body of work shows for the first time that female neuropathic pain can be relieved using a COX-2 inhibiting theranostic nanoemulsion treatment, and that how COX-2 inhibition provides relief is different in males and females.

Adapted from:

B. Deal, L. Reynolds, C. Patterson, J. M. Janjic, J. A. Pollock. (2022). Behavioral and inflammatory sex differences revealed by celecoxib nanotherapeutic treatment of peripheral neuroinflammation. *Scientific Reports*. 12, 8472. https://doi.org/10.1038/s41598-022-12248-8.

M. Saleem, A. Stevens, **B. Deal**, L. Liu, J. M. Janjic, J. A. Pollock (2019). A new best practice for validating tail vein injections in rat with near infrared labeled agents. *JoVE - J. Vis. Exp.*, (146), e59295, doi:10.3791/59295.

ACKNOWLEDGEMENTS

I am incredibly blessed to have such an amazing support system, without whom, I would not have been able to complete this work. Firstly, I would like to thank my amazing fiancé, Jay, for being my rock through the hard times and my cheerleader during the good ones. You are always willing to listen and help me navigate my next steps. I am eager to continue this throughout the rest of our lives together. Thank you for letting me adopt Biggie during the pandemic. He has been such a spectacular addition to our family and has provided me with so much love and companionship through those lonely days at home alone.

I would also like to thank my parents Bill and Shannon for their never-ending support. It means the world to have you at all of my talks and seminars in person or on zoom. Thank you for pushing me as a kid to do the best that I can; I truly believe that those skills have allowed me to succeed in my adult life. I am beyond grateful to my Aunt Jamie and Uncle Steve for helping me adjust to life in Pittsburgh. Living with you during my first year made my adjustment into graduate school much smoother than I could have imagined. I'd also like to acknowledge my Aunt Ellisa and Uncle John. John, thank you for reading through all of my scientific publications and keeping me on my toes with my word choice. Ellisa, thank you for your empowering words and assistance through my job search. To my sisters, Paige and Sara, thank you for always having my back and teaching me to stand up for myself. Lastly, to my grandparents Chuck and Nancy, I look to you as role models. I see how hard work and dedication can lead to an amazing life and I aspire to be as kind and successful as you both are.

To my advisor, Dr. John A. Pollock, your positivity and guidance have been key in my success as a scientist. "The data is the data", has been a crucial and invaluable lesson while I

have grown at Duquesne. It has helped me feel confident enough to critically think about the data which I have generated and to connect the dots. To my committee members, Dr. Lauren O'Donnell, Dr. Jill Dembowski, Dr. Jan Janecka, and Dr. Jelena Janjic, thank you for pushing me to critically think through my science and for supporting me in my choices. Lauren, thank you for your assistance in helping me choose immune cell markers and for always being a kind face to come and speak with. Jan, thank you for assisting me with everything having to do with CLC, and for supporting me though my decision to repeat my RNA-seq experiment. Jill, thank you for being willing to hop onto my committee midway through my time here. Your willingness to speak with me on drop by visits, and your counsel in my professional development has been appreciated. Dr. J, I am grateful for all that you have done to help me grow both as a presenter and as a scientist. I am especially appreciative for you for arranging for me to attend the microsurgery course at Wake Forest and for connecting me to other outstanding scientists.

I'd also like to give my appreciation to my lab members past and current. To Andrea and Muz, thank you for allowing me to jump in on your science and contribute to your work. Learning alongside you was a privilege. To my undergrads, thank you for your companionship. Laura, Charles, Alyssa, and Alysia, I am forever indebted to you for your time and effort that you put in to helping me process tissues, optimize antibodies, and perform necropsies. Katy, I've enjoyed the friendship that we have developed over our long trips to North Carolina and San Diego; I value you reminding me to enjoy the little things. Your presence and support have pushed me to do what I need to do to finish and not feel guilty about having to do so. Maggie, thank you for being a source of positivity in the lab and providing a new fire to continue exploring. To my summer undergrads, Lauren Bhar, Dylan Bertovich, Essence Williams, Aboubacar Traore, and Malajah Johnson, thank you for spicing things up during the summer and

presenting me with new ideas and questions. To my new undergrads Jeremy Jones and Eli Bartholomew, best of luck in all that you do.

Thank you to the animal facility for providing me the opportunity to complete my research studies. A special thanks to Denise Butler-Buccilli, Denise Capozzi, Christine Close, Rachel Barr, and Ashley Yuhouse. Ashley and Rachel, I can't tell you how appreciative I am for you helping me navigate doing my animal studies during COVID restrictions.

Thank you to the biology department and my fellow graduate students. To the office staff, Pamela Ferchak, Terri Widenhofer, Stephanie Kotsch, and Heather Costello, I value all of the work you do behind the scenes to keep us running, and I appreciate you being willing to answer my never-ending questions.

A special thank you to my unbelievable cohort Brianna Ports, William King, Anton Evans, Emine Kahveci, David MaCar, and our adopted cohort members Manisha Chandwani, Chris Swank, and Marisa Guido. To Will and Bri, thank you for sharing tears with me both happy and sad. Both of your kind words of encouragement throughout the years got me through the day. Thank you to Will for giving me your time and being willing to teach me new skills in the last portion of my wet lab experiments. Bri, your willingness to read and proofread every document I've written in my graduate career is commendable. Having my cohort to lean on through this experience has been invaluable and I know that we have made friendships that will last a lifetime.

TABLE OF CONTENTS

Page

Abstract……...iv

Acknowledgements……vii

List of Tables……xvi

List of Figures……xviii

List of Abbreviations……xx

Chapter I. Introduction & Background……..1

1.1 Impact of Neuropathic Pain……...1

1.2 Mechanisms of Neuropathic Pain Development ……...2

1.2.1 The Neuroimmune Network and Wallerian Degeneration……..2

1.2.2 Transcriptomic Studies……6

1.3 Current Treatments of Neuropathic Pain……...8

1.3.1 Nonsteroidal Anti-inflammatory Treatment……..10

1.3.2 COX-2 Inhibiting Theranostic Nanoemulsion……...12

1.4 Sex Disparity in Neuropathic Pain……...16

1.5 Specific Aims……...19

1.5.1 Specific Aim 1……...19

1.5.2 Background for Specific Aim 1…….....19

1.5.3 Methodology for Specific Aim 1……...20

1.5.4 Specific Aim 2……...21

1.5.5 Background for Specific Aim 2…….22

1.5.6 Methodology for Specific Aim 2……...22

1.5.7 Specific Aim 3……...23

1.5.8 Background for Specific Aim 3…….23

1.5.9 Methodology for Specific Aim 3……...24

Chapter II. Materials and Methods……...26

2.1 Animals and Ethics Statement…….26

2.2 Chronic Constriction Injury…….27

2.3 von Frey Behavioral Testing……27

2.4 Intravenous Tail Vein Injections……..28

2.5 Vaginal Swabs…….29

2.6 Tissue Dissection and Preparation for Histology…….29

2.7 Immunohistochemistry and Microscopy……..30

2.8 Tissue Dissection and Preparation for RNAseq……...31

2.9 RNA-seq DRG Sample Preparation…….32

2.10 Library Preparation and Sequencing……..32

2.11 Bioinformatic Analysis of RNAseq Data (Mapping and Differential Expression Analysis - conducted by Brooke Deal)……..33

2.12 Enrichment Analysis……..34

2.13 cDNA Conversion and RT-qPCR Validation……34

Chapter III. Behavioral and inflammatory sex differences revealed by celecoxib nanotherapeutic treatment of peripheral neuroinflammation.……...36

3.1 Introduction.…….38

3.2 Results.…….41

3.2.1 Treatment Effect on Mechanical Allodynia.…….41

3.2.2 Assessment of Cellular Involvement of Neuroinflammation……..43

3.3 Discussion……...51

3.4 Conclusion……..57

3.5 Materials and Methods……58

3.5.1 Ethics Statement……...58

3.5.2 CCI Surgery……..58

3.5.3 Estrus Cycle Tracking……..59

3.5.4 Behavioral Testing……...59

3.5.5 COX-2 Inhibiting Theranostic Nanoemulsion.....……..59

3.5.6 Tail Vein Injection……60

3.5.7 Tissue Processing……61

3.5.8 Immunofluorescence and Image Analysis……61

3.5.9 Statistical Analysis……...63

Chapter IV. RNA-seq reveals sex differences in gene expression during peripheral neuroinflammation and in relief with COX-2 inhibiting nanotheranostic.…….....……...64

4.1 Introduction……66

4.2 Results……68

4.2.1 Celecoxib nanotheranostic nanoemulsion alleviates mechanical hypersensitivity caused by neuroinflammation in both males and females……68

4.2.2 Mechanical hypersensitivity induced by neuroinflammation and relief following 10X CXB-NE treatment causes a shift in gene expression in the DRG.....71

4.2.3 Female neuroinflammation…….....74

4.2.4 Male neuroinflammation……..78

4.2.5 Female neuroinflammatory relief.……....81

4.2.6 Male neuroinflammatory relief.……83

4.2.7 Shared and unique gene expression changes across male and female neuroinflammation and relief. ……..87

4.3 Discussion.……..…….93

4.3.1 Mechanical allodynia relief from NSAID nanoemulsion....……..94

4.3.2 Male transcriptome changes in the DRG following CCI.....95

4.3.3 Female transcriptome changes in the DRG following CCI.....97

4.3.4 Macrophage associated COX-2 inhibitory effect causes transcriptional differences in the associated male DRG.....…….....98

4.3.5 Macrophage associated COX-2 inhibitory effect causes transcriptional differences in the associated female DRG.....…….....100

4.3.6 CREB protein involvement in the sex differences of neuroinflammation and relief.…….101

4.4 Conclusion.……..104

4.5 Materials and Methods.……....105

4.5.1 Animal Use and Ethics.……105

4.5.2 Up-down von Frey behavior.……...106

4.5.3 Chronic Constriction Injury (CCI) ……107

4.5.4 COX-2 Inhibiting Theranostic Nanoemulsion.....……107

4.5.5 Tail Vein Injection.……..107

4.5.6 Estrus Cycle Tracking.……108

4.5.7 Dorsal Root Ganglion (DRG) Collection.……108

4.5.8 Sample preparation.……109

4.5.9 Library preparation and sequencing.……109

4.5.10 Bioinformatics analysis of RNA-seq data (Mapping and Differential Expression Analysis) ……..110

4.5.11 Enrichment Analysis.……110

4.5.12 cDNA conversion and RT-qPCR validation.……111

4.5.13 Data Deposition.……111

4.5.14 Immunofluorescent Staining and Confocal Imaging.……112

Chapter V. Discussion and Conclusions……..113

5.1 The use of chronic constriction injury and von Frey behavioral analysis to measure neuropathic pain-like behavior……113

5.1.1 Similar patterns of hypersensitivity in males and females……..115

5.1.2 Different responses to CXB-NE treatment…….116

5.2 Neuroimmune response…….....119

5.3 Transcriptional Differences……...124

5.4 10X CXB-NE Influence over COX-1, COX-2 and ATF3.....127

5.5 Future Directions……...129

5.5.1 Longitudinal studies in neuroinflammatory relief……..128

5.5.2 Multiple assessments of neuroinflammatory pain relief.……130

5.5.3 One suture CCI technique to lower variability……...131

5.5.4 Flow cytometry to phenotype immune cells at the site of injury and in the DRG…….131

5.5.5. Assessment of early and long-term use of 10X CXB-NE.....133

Appendix……...……..135

A.1 Tail Vein Injection Protocol……..135

A.1.1 Abstract……..135

A.1.2 Introduction……136

A.1.3 Protocol……..137

A.1.3.1 Preparation and anesthesia……..138

A.1.3.2 Pre-injection……138

A.1.3.3 Tail vein injection with NIRF-containing agent…….139

A.1.3.4 Post-injection……..140

A.1.3.5 Image quantification……...141

A.1.4 Representative Results……...141

A.1.5 Discussion……..141

A.2 Chapter III Supplemental Material…….....143

A.3 Chapter IV Supplemental Material…….....150

References...…… ……..355

LIST OF TABLES

Page

Table 4.1. Top 25 significantly up-regulated genes in the female DRG following CCI of the sciatic nerve……...75

Table 4.2. Top 25 significantly down-regulated genes in the female DRG following CCI of the sciatic nerve. …….75

Table 4.3. Top 25 significantly up-regulated genes in the male DRG following CCI of the sciatic nerve..…….78

Table 4.4. Top 25 significantly down-regulated genes in the male DRG following CCI of the sciatic nerve.……..79

Table 4.5. Most significantly up-regulated genes in the female DRG following neuroinflammatory reduction via COX-2 inhibition.……81

Table 4.6. Most significantly down-regulated genes in the female DRG following neuroinflammatory reduction via COX-2 inhibition…….82

Table 4.7. Top 25 most significantly up-regulated genes in the male DRG following neuroinflammatory reduction via COX-2 inhibition…….84

Table 4.8. Top 25 most significantly down-regulated genes in the male DRG following neuroinflammatory reduction via COX-2 inhibition. ……...85

Table 4.9. List of differentially expressed genes which show unique patterns across sex and or treatment……...90

Table A3.1 Select table of primers used for qPCR including *ATF3*, *SEMA6A*, *VGF*, and the housekeeping gene *GAPDH*……..……..150

Table A3.2. Master list of differentially expressed genes between Female CCI vs Naïve samples with a FDR p-value ≤ 0.05 and a fold change greater than ±1. ……..……152

Table A3.3. Master list of differentially expressed genes between Male CCI vs Naïve samples with a FDR p-value ≤ 0.05 and a fold change greater than ±1……177

Table A3.4. Master list of differentially expressed genes between female 10X CXB-NE vs DF-NE samples with a FDR p-value ≤ 0.05 and a fold change greater than ±1……184

Table A3.5. Master list of differentially expressed genes between male 10X CXB-NE vs DF-NE samples with an FDR p-value ≤ 0.05 and a fold change greater than ±1……185

Table A3.6. Master list of differentially expressed genes between Female CCI vs Naïve samples with a p-value ≤ 0.05 and a fold change greater than ±1. ……..…….193

Table A3.7. Master list of differentially expressed genes between Male CCI vs Naïve samples with a p-value ≤ 0.05 and a fold change greater than ±1…….257

Table A3.8. Master list of differentially expressed genes between female 10X CXB-NE vs DF-NE samples with a p-value ≤ 0.05 and a fold change greater than ±1…….280

Table A3.9. Master list of differentially expressed genes between male 10X CXB-NE vs DF-NE samples with a p-value ≤ 0.05 and a fold change greater than ±1……...289

Table A3.10. Master list of differentially expressed genes between female 10X CXB-NE vs male 10X CXB-NE samples with an FDR p-value ≤ 0.05 and a fold change greater than ±1....328

Table A3.11. Master list of differentially expressed genes between female 10X DF-NE vs male 10X DF-NE samples with an FDR p-value ≤ 0.05 and a fold change greater than ±1.....332

Table A3.12 List of 90 genes from male heat map gene tree (Figure 4.2a).....349

Table A3.13. List of 90 genes from female heat map gene tree (Figure 4.2b).....351

LIST OF FIGURES

Page

Figure 1.1. Healthy neuroinflammatory process and Wallerian degeneration……...5

Figure 1.2. Nerve damage influences immune cells to produce production of neuronal sensitizers……...11

Figure 1.3. Experimental schedule for behavioral testing in both males and females to evaluate the efficiency of CXB-NE and visualize the location *in vivo*……20

Figure 3.1. Mechanical hypersensitivity caused by CCI and the difference in pain relief from celecoxib-loaded nanoemulsion (CXB-NE).…….42

Figure 3.2. Day 12 macrophage infiltration after CCI decreases significantly in both male and female injured nerves treated with CXB-NE. ……...45

Figure 3.3. Nanoemulsion is equally phagocytosed by both male and female macrophages…..46

Figure 3.4. T cells localize to the epineurium of the sciatic nerve……...48

Figure 3.5. CD3e+ T cells are present at a low density in the fasciculated nerve; their number unchanged by CCI surgery, DF-NE or CXB-NE drug delivery……49

Figure 3.6. CD8+ cells are recruited to the site of injury after CCI and recruitment is not significantly affected by CXB-NE treatment.....50

Figure 4.1. Mechanical allodynia relieved by single dose of Celecoxib nanotheranostic in both sexes.…….70

Figure 4.2. Heatmaps displaying the top 90 genes with the highest coefficients of variation in male and female DRGs…..……72

Figure 4.3. Display of comparisons made between RNA-seq generated gene sets……..73

Figure 4.4. Neuroinflammation in females causes differential genes expression in the affected DRG…..……77

Figure 4.5. Neuroinflammation in males causes differential gene expression in the affected DRG…..…….80

Figure 4.6. Neuroinflammatory relief via COX-2 inhibition in females causes differential gene expression in the affected DRG…….83

Figure 4.7. Neuroinflammatory relief via COX-2 inhibition in males causes differential gene expression in the affected DRG.……86

Figure 4.8. Venn diagrams of differentially expressed genes in each sex and shared genes in male and female neuroinflammation and relief…….87

Figure 4.9. Venn Diagram of differentially expressed genes using p-value ≤ 0.05……..88

Figure 4.10. ATF3 change in protein expression in the ipsilateral DRG following hypersensitivity (DF-NE) and relief (CXB-NE).……...92

Figure 4.11. COX-2 feedback loop transcriptionally regulated by ATF3……..102

Figure 5.1. PGE_2 production by COX enzymes and PGE synthase 2.……116

Figure A1.1. NIRF based nanoemulsion and images of tail vein……...142

Figure A1.2. Examples of bad injections……143

Figure A2.1. Vaginal smears were used to stage the ~ 4-day estrous cycle of all of the female rats……147

Figure A2.2. Day 18 macrophage infiltration in CXB-NE heightens to a similar level of CCI and DF-NE as they return to hyperalgesia……..148

Figure A3.1 qPCR Results Looking at Expression Change in *ATF3*…….150

Figure A3.2 qPCR Results Looking at Expression Change in *SEMA6A*……151

LIST OF ABBREVIATIONS

CCI	Chronic constriction injury
CFA	Complete Freud's adjuvant
COX-2	Cyclooxygenase-2
CXB	Celecoxib
CXB-NE	Celecoxib nanoemulsion
DF-NE	Drug-Free nanoemulsion
DRG	Dorsal root ganglia
IL	Interleukin
M1	Pro-inflammatory macrophage
M2	Anti-inflammatory macrophage
NE	Nanoemulsion
NIR	Near-infrared
NSAID	Nonsteroidal anti-inflammatory drug
PGE_2	Prostaglandin E2
TLR	Toll-like Receptor
TCA	Tricyclic antidepressants
SSRI	Selective serotonin reuptake inhibitors

CHAPTER I.

INTRODUCTION

1.1 Impact of neuropathic pain

Pain is an unpleasant sensation that arises due to tissue damage. Although unpleasant, it's purpose is useful in keeping the subject from doing the damaging action again, or from overuse of the injured body part until properly healed[1]. It is when pain extends beyond the tissue healing that it becomes problematic or in other words chronic[1,2]. Chronic pain affects 20% of the world's population with 8% of the world's population afflicted by chronic neuropathic pain[3]. Neuropathic pain has been defined as pain arising from a lesion or disease to the somatosensory system; however, not every nerve injury induces chronic neuropathic pain[4]. It is for this reason that the understanding of the development of chronic neuropathic pain is elusive, and pain management is difficult.

Those suffering from neuropathic pain often experience spontaneous burning, itching, tingling, and sometimes reduced sensitivity[3,5]. Evoked sensations can also be felt such as allodynia where a normally non-painful stimulus is now painful, or hyperalgesia where a stimulus that is normally pain inducing is now more painful than before. These evoked sensations can be due to mechanical pressure, thermal sensitivity, or to a chemical stimulus.

Neuropathic pain can stem from multiple causes from either the central nervous system or peripheral nervous system, but for our purposes, we will focus on the peripheral nervous system. Peripheral neuropathic pain can be binned into five different subtypes such as trigeminal neuralgia (oral facial pain), painful radiculopathy (lesion or disease of the nerve root), painful polyneuropathy (caused by diseases such as diabetes, HIV, or leprosy), postherpetic neuralgia (caused by the herpes zoster virus) and peripheral nerve injury (heterogeneous group caused by

nerve lesion such as amputation)[6]. The research presented here specifically focuses on the latter group with those who have undergone direct nerve injury. This is one of the most commonly studied groups because there are a handful of successful rodent models. Some of these include chronic constriction injury (CCI), spared nerve injury, nerve crush injury, and transected nerve and repair[6].

1.2 Mechanism of neuropathic pain development

1.2.1 The Neuroimmune network and Wallerian Degeneration

Peripheral neuroinflammation following injury is initiated when damaged nervous tissue releases bits of cellular content which are not normally present within the unperturbed tissue milieu such as heat shock proteins, mRNA, or extracellular matrix components[7]. These antigens are able to bind to toll-like receptors (TLRs) on myelinating Schwann cells and resident macrophages; thereby activating them into releasing various interleukins, chemokines, and cytokines[7]. One pro-inflammatory cytokine specifically increased after TLR activation of both Schwann cells and macrophages is NF-κB[1]. NF-κB leads to increased vasodilation and works to bring other immune cells to the site of injury[1,2].

During this neuroinflammatory response, the first few immune cells to localize to the site of inflammation from the blood are from the innate immune system including neutrophils and monocytes. Neutrophils migrate to the injured tissue first within 8 hours and are short-lived, peaking around 24 hours post injury[2,7] (Figure 1.1B). Once activated, monocytes mature into macrophages and follow 3-4 days later [2,7] remaining in the tissue for months[7] (Figure 1.1C). These two cell types specialize in phagocytosis, and work to eliminate any pathogens or cellular debris[2,8].

These phagocytic macrophage cells as well as dedifferentiated Schwann cells are involved in a process known as Wallerian degeneration. During Wallerian degeneration, demyelination and degradation of the axon distal to the injury occurs[9]. This is done in order to clear damaged tissue and debris from the area and give room for the rise of regeneration and reinnervation of new healthy axons[9]. Schwann cells, which are typically wrapping the axon to form the myelin sheath (Figure 1.1A), become activated and convert into a phagocytic cell type[9] (Figure 1.1B). These newly transformed cells, as well as the infiltrating macrophages, then add to the cellular milieu by excreting additional pro-inflammatory cytokines such as TNF-α (tumor necrosis factor - α) and interleukin (IL)-15, which are known to sensitize neurons[1]. Additional activation of the macrophage through TLR4 or from IL-1β can activate signaling cascades that lead to the activation of the cyclooxygenase 2 (COX-2) enzyme and the production of its pro-inflammatory prostaglandin, PGE_2 (prostaglandin E2)[1]. PGE_2 is also well known as a neuronal sensitizer inducing neuropathic pain.

Once the innate cells have localized to the site of neuroinflammation, cells of the adaptive immune system such as T cells are able to migrate into the damaged neuronal tissue[7,10,11] and remain peaking around 14-28 days after injury to help direct a healthy inflammatory response[7] (Figure 1.1D). Helper T cells, denotated CD4+, are able to produce chemicals which influence the inflammatory milieu. Helper T cells can be further broken down into Th1, Th2, and Th17 subtypes with pro-inflammatory types being Th1 (INFγ and IL-2 producing) and Th17 (IL-17 producing) and anti-inflammatory being Th2 (IL-4, IL-10, and IL-13 producing)[1,2,7,12]. Blood serum from patients showed those who were not experiencing pain after nerve injury had higher levels of IL-10 and IL-4 than those who were in pain following nerve injury. This indicates that Th2 helper T cells are important in the resolution of neuropathic

pain. In the case of neuroinflammation, helper T cells commonly act as an inflammatory switch for other immune cells such as macrophages switching them from inflammatory (M1) to anti-inflammatory (M2) once the injury has resolved[13]. CD8+ T cells are termed cytotoxic T cells and are known for inducing apoptosis in virus infected or malignant tumor cells. Their role in neuropathic pain is less understood[12]. Being able to control the strength and length of the inflammatory response is important for maintaining a properly functioning immune response[12]. If the response is too strong, or lasts too long, neuronal plasticity can occur, and the pain phenotype may remain.

Plasticity can change through sensitization. Sensitization occurs when the peripheral neuron's activation threshold gets lowered from activity of ion channels by different interleukins, prostaglandins, and (tumor necrosis factor) TNF. By opening ion channels, it becomes easier for neurons to reach an activation threshold and fire more often leading to allodynia and changes in neuronal plasticity[10,14]. If the decreased threshold remains present after the immune response has cleared, this is when chronic neuropathic pain occurs[2]. Changes in plasticity to lower the activation threshold could include permanently inducing higher levels of gene expression for things such as sodium channels[15].

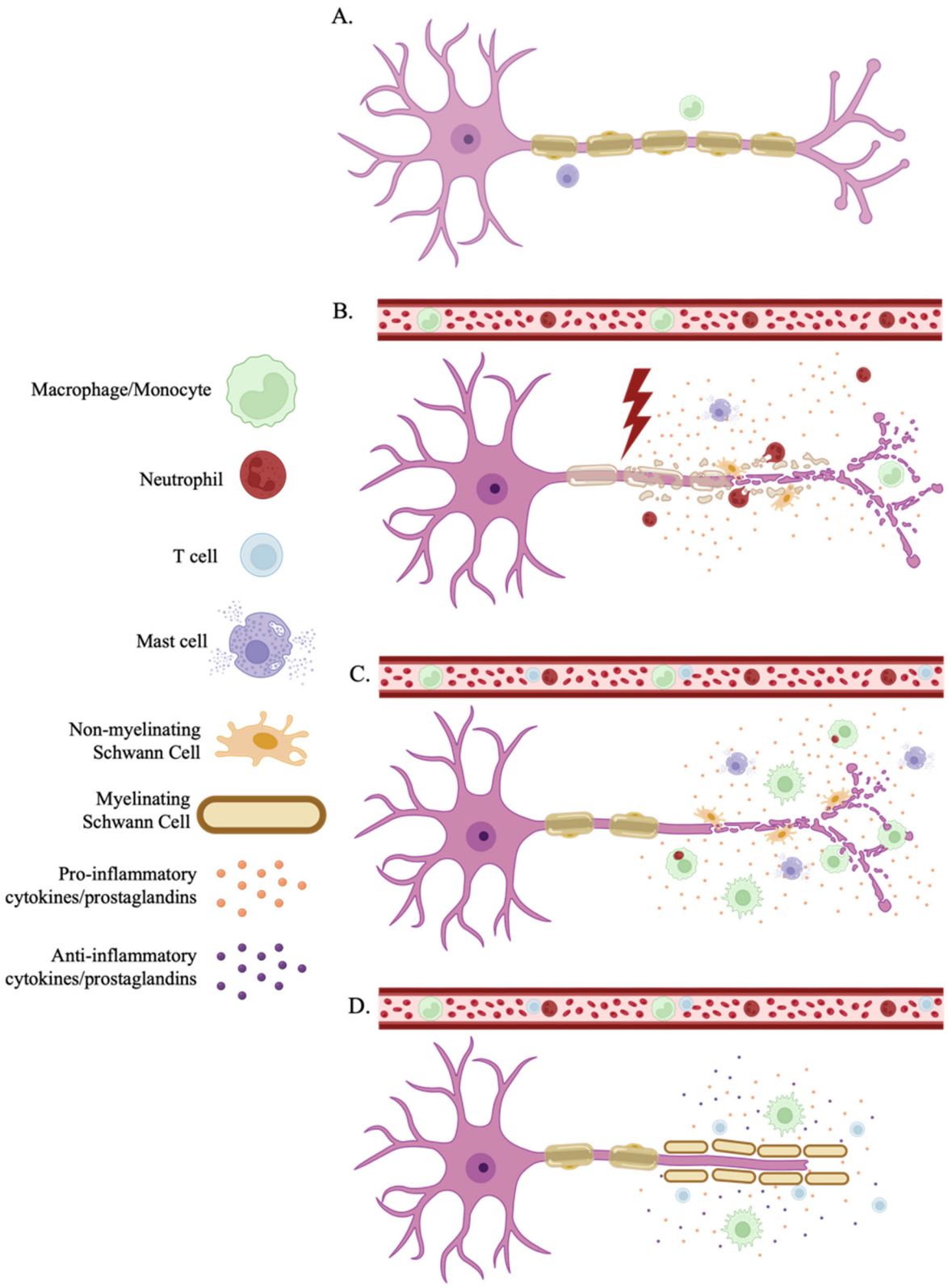

Figure 1.1. Healthy neuroinflammatory process and Wallerian degeneration. A. Healthy peripheral nerve with myelinated axons and resting, resident immune cells such as monocytes

Figure 1.1. (continued) and mast cells. **B.** 24 hours post-peripheral nerve injury, resident immune cells are activated, Schwann cells dedifferentiate, and neutrophils migrate to the site of injury. Pro-inflammatory cytokines, chemokines, and prostaglandins are excreted into the cellular milieu causing neuronal hypersensitivity. **C.** Days following injury, macrophages make up the majority of infiltrating immune cells with additional immune cells such as mast cells being recruited. **D.** Days to weeks following the nerve injury, T helper cells help to secrete anti-inflammatory cytokines influencing the cellular milieu into a neuroregenerative state. Figure created with BioRender.

1.2.2 Transcriptomic studies

Sustained neuroinflammation can cause shifts in the transcriptional fate of neurons and surrounding cells leading to modifications of cellular function. However, the ability to assess these changes didn't exist until the invention of Sanger sequencing in 1977[16, 17] and then the microarray in 1983[18]. Sanger sequencing is time consuming having to manually analyze bands to determine nucleotides, and microarrays had its limits of needing to know your transcript and species of interest to generate probes. With the introduction of next generation sequencing in 2008, sequencing became faster, cheaper, and easier than before. With next generation sequencing platforms such as RNA-seq, the detection of all transcripts no matter the sequence or species could be performed; this gives the scientist the ability to detect the expression of novel unknown transcripts[19]. One study found that from 2008 to 2016 an astonishing 2,808 publications have been released using this technology[19].

The neuroinflammatory field also followed, using next generation sequencing to discover differential expression of key transcriptional changes when neuroinflammation is underway such

as TNFα, IL-1β, substance P, bone derived neurotrophic factor (BDNF), caspase, and COX-2. And further analysis of how these transcriptomic changes differ between sexes began to flourish. For example, baseline differences in gene transcription between males and females[20] revealed that differentially expressed genes in the naïve female DRG had enrichment for inflammation, synaptic transmission, and extracellular matrix processes. Male DRGs had enriched genes for oxidative phosphorylation and metabolism[20].

Other studies compared sex differences in multiple different neuroinflammatory models. Stephens and colleagues used a CCI model of neuroinflammation and found that at baseline only 6% of genes were differentially expressed between males and females; however, in a different study of fourteen days post CCI, 16% of the differentially expressed genes were shared between sexes[21,22]. You will see that in my analysis, 8% of the differentially expressed genes are shared between males and females after CCI. Baseline differences seen in the Stephens et al 2019 study had to do with enriched genes for immune related functions in the females such as NADH dehydrogenase complex assembly and antigen process and presentation of antigen via the major histocompatibility complex II[21]. This is not unexpected, seeing that human females often have higher incidence of autoimmune disorders when compared to age matched males[23]. For example, following CCI, female rats had genes enriched for glucocorticoid and corticosteroid biological processes, and CCI males had enrichment for ion channel activity and substrate specific channel activity[21].

Human studies also compared differences in chronic neuroinflammation between sexes and found that the major differences between male and female neuroinflammation had to do with the immune response. Males had larger changes in differentially expressed genes having to do with macrophages than females[24, 25]. This matches what has been seen in rodent models of pain[26,27].

However, very few studies, if any, have looked at how treatment that relieves pain changes these differences in gene expression when neuroinflammation has been relieved. Doing so, could give insight into how the drug response is affecting the whole neuroinflammatory response and why behavioral differences may exist.

1.3 Current treatments of neuropathic pain

The clinical treatment of inflammatory pain first started with aspirin in 1897[28] as it established itself as the first drug seen to reduce inflammation (which we now know is by the attenuation of prostaglandins). Since then, with the lack of identified physiological processes for the formation of chronic neuroinflammatory pain, treatment has been focused on the symptomatic side[5,29]. Many of the drugs we use today were developed for other reasons, such as anti-depressants or anti-epileptics, and they were later seen to additionally reduce neuroinflammatory pain[29]. Diagnosing neuroinflammatory pain and assigning an effective treatment is a difficult task in itself seeing as there are no symptoms that are specific only to neuropathic pain, but some symptoms are more frequently related[29]. Some of these symptoms include tingling, burning, shooting pain, reduced sensation, or increased sensitivity. However, symptoms are not the only consideration when diagnosing neuropathic pain. According to the International Association for Pain Studies' definition for neuropathic pain, it must stem from a lesion or disease of the somatosensory system; therefore, medical history is also taken into account[4]. Once an official diagnosis is made, a treatment can be selected. Even then, multiple studies have shown that those suffering from neuropathic pain do not feel that they receive adequate treatment for their pain[30-32].

The International Association for Pain Studies recently formed a Neuropathic Pain Special Interest Group which has reevaluated the guidelines in the recommendation for the therapeutic treatment of neuropathic pain[30]. Successful evaluation of the effectiveness of treatments for neuropathic pain has been difficult to assess given that there is a publication bias where reporting of only positive outcome studies take place[30]. Nevertheless, the Neuropathic Pain Special Interest Group's evaluation leads to the recommendation of gabapentinoids, tricyclic antidepressants (TCAs), and selective serotonin reuptake inhibitors (SSRIs) as the first line of drugs for treatment of neuropathic pain. They then suggest that lidocaine, capsaicin, and tramadol be used as second line treatments, and strong opioids and botulinum toxin-A be used as third line treatments[5,30].

These first line drugs are known to work on the central nervous system effecting the body systemically. Gabapentinoids were first developed for anti-epileptic use, and work by binding to calcium channels to decrease calcium influx into the nerve thereby reducing action potentials[5]. They are included in the list of first line drugs and have been seen to cause drowsiness, dizziness, fatigue, edema, blurred vision, and ataxia with extended use[29,33]. Two other drugs suggested for first line use in treating neuropathic pain are TCAs and SSRIs. The primary use of these drugs was first as anti-depressants and work similarly by inhibiting serotonin and noradrenaline reuptake at the synaptic terminals thereby reducing neuronal hyperexcitability[5]. TCAs can have adverse reactions such as weight gain, cardiovascular effects, sedation, orthostatic hypotension, and lethal overdose[29,34]. SSRIs also can cause weight gain, sexual disfunction, constipation, dry mouth, and removal from them too quickly can induce nausea, vertigo, anxiety, trouble sleeping, and odd sensory symptoms[29,34].

The listed second line drugs work on more directly on peripheral nerves, however, lidocaine and capsaicin typically have to be applied as local anesthetics and work for shorter periods of time by blocking sodium (lidocaine)[35] or calcium (capsaicin) channels[36]. Lastly, the assessment of the Neuropathic Pain Special Interest Group's third line of use drugs are the most concerning. Botulinum toxin-A is a neurotoxin and works by inhibiting synaptic exocytosis; this thereby stops neurons from being able to fire[5], and it can cause permanent nerve damage. And strong opioids, although effective at reducing neuropathic pain, are very addictive and lethal overdose is all too common. It is for this reason that the Neuropathic Pain Special Interest Group has recommended them as a last line of defense[30].

None of these treatments come without adverse side effects and long-term use can be detrimental. The need to generate a safer therapeutic aimed at pain producing mechanisms is of great importance.

1.3.1 Nonsteroidal Anti-inflammatory Treatment for inflammatory pain

Injury and inflammation results in experiencing the sensation of pain to varying degrees. The nociceptive sensory system is sensitive to indicators of injury and tissue damage including the production and release of PGE_2 (Figure 1.2), which is produced by the activation of cyclooxygenase (COX) enzymes. Non-steroidal anti-inflammatory drugs are potent inhibitors of COX enzymes and are effective in treatment of certain pain.

NSAIDs are not currently recommended for use to treat chronic neuroinflammatory pain because the systemic dosage needed to achieve sufficient pain relief causes adverse side effects on various off target organs[37]. However, they are quite commonly used to treat inflammatory pain. NSAIDs work by blocking the ability of cyclooxygenase (COX) enzymes from being able

to produce their pro-inflammatory prostaglandin products. There are two types of COX enzymes including COX-1 and COX-2. COX-1 was first discovered in 1976[38] and is known to be constitutively expressed in most tissues acting in housekeeping functions[28]. While COX-2 was unknown until 1991[39, 40], it is known to be inducible during the inflammatory response[28].

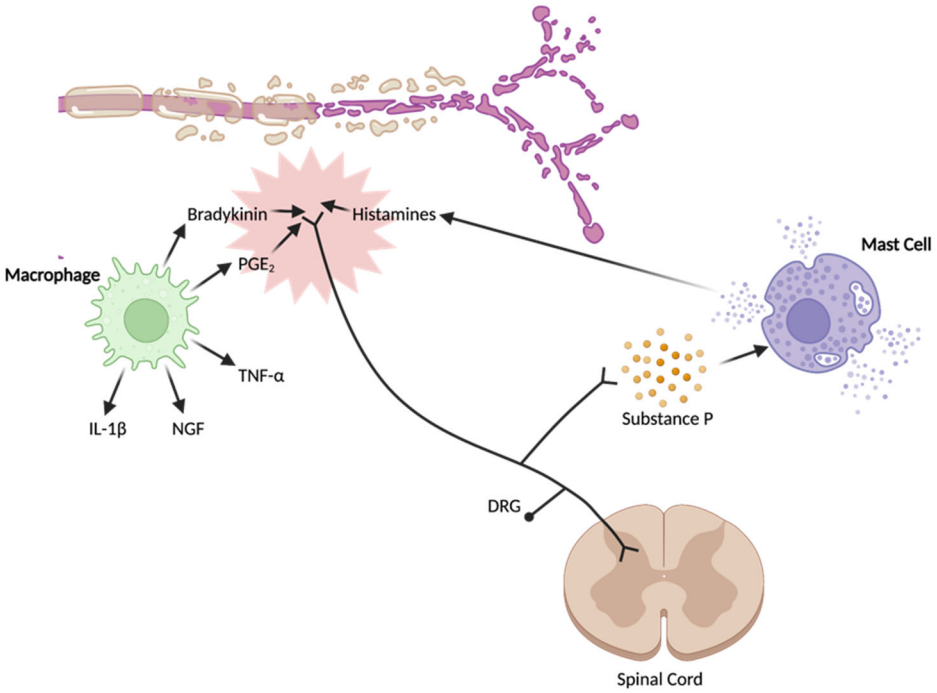

Figure 1.2. Nerve damage influences immune cells to produce production of neuronal sensitizers such as histamines, bradykinin, and PGE_2. Image created in BioRender and adapted from Neuroscience 6th edition, Purves et al (2018) Sinauer, Oxford University Press.

The majority of NSAIDs first to market were non-specific to one type of COX enzymes such as aspirin and ibuprofen[28]. By non-specifically targeting COX enzymes, alterations of housekeeping genes can occur, where long-term use can lead to issues such as abdominal pain, perforations, ulcerations, and bleeding[28]. These effects were later accredited to COX-1 inhibition. Once COX-2 was discovered, the shift towards making more selective drugs began.

Overtime, it was seen that drugs that displayed too strong of a selectivity towards COX-2 such as Limiracoxib or Vioxx had to be withdrawn from market seeing that they began to display increased chance for heart attacks, strokes, and liver failure[28, 41, 42]. Using COX-2 inhibitors with lower selectivity, such as celecoxib, lower rates of gastrointestinal problems occur and decreased rates of cardiovascular issues arise as compared to stronger selective COX-2 inhibitors[43, 44, 28]. The main consumers of celecoxib are women with 85% being prescribed to them[45]. Currently, celecoxib's long-term usage is predominately utilized to treat arthritic pain, but short-term usage to treat acute pain such as post-surgical pain or injury also occurs. Even though celecoxib is a relatively safer pain relieving option, it is still not advised to be used to treat neuropathic pain given that the systemic dosage has to be so high that toxicity and major side effects occur[37].

1.3.2 COX-2 inhibiting theranostic nanoemulsion

Dr. Jelena Janjic and colleagues first began the development of their novel nanoemulsion formulation as a way to both quantitatively and qualitatively track infiltrating inflammatory immune cells such as macrophages[46]. This formulation (PFC-NIR nanoemulsion) is the first to carry both a near-infrared (NIR) dye as well as be constructed with perfluorocarbon (PFC); in doing this, the nanoemulsion could be imaged *in vivo* and *ex vivo* using the NIR dye as well as detailed imaging can be acquired using ^{19}F MRI to detect PFC[46] . In a tumor model Janjic and Balducci were able to assess the ability for the PFC-NIR nanoemulsion to infiltrate the tumor microenvironment and determined that myeloid-derived suppressor cells were the main cell phenotype carrying the PFC-NIR nanoemulsion[46].

To assess whether this dual labeled nanoemulsion could be used to track infiltrating immune cells in additional models, such as neuropathic pain, Dr. Kiran Vasudeva tested this

PFC-NIR nanoemulsion in a CCI sciatic nerve model. Here it was seen that in injured CCI male rats, that the nanoemulsion could be used to visualize increased inflammation at the sciatic nerve using NIR imaging of the live animal, or alternatively ^{19}F MRI. Furthermore, the nanoemulsion could be visualized within the tissue inside CD68 positive macrophages within the sciatic nerve by epi-fluorescent microscopy of the NIR dye[47]. Complementing studies showed that cell culture RAW 264.7 macrophage-like cells would similarly phagocytose the nanoemulsion[48]. Knowing that the nanoemulsion could be incorporated into infiltrating inflammatory macrophages in multiple models, the Janjic Lab then began to test the ability for the nanoemulsion to carry anti-inflammatory therapeutics. The COX-2 inhibiting NSAID celecoxib was selected because it had been FDA approved to be the most clinically safe COX-2 inhibitor[28,44]. This formulation inhibited activity of COX-2 and was able to attenuate the production of PGE_2 in activated RAW 264.7 cell culture[48]. In combining the therapeutic effect of celecoxib and the diagnostic ability of the dual-labeled nanoemulsion, the new nanoemulsion is now a theranostic, and referred to CXB-NE (celecoxib nanoemulsion)[49].

The ability for the theranostic nanoemulsion to shift the inflammatory response was evaluated by Patel *et al*. in the inflammatory complete Freund's adjuvant (CFA) model[49]. In the CFA model heat killed *Mycobacterium tuberculosis* is injected into the palm of the hind paw of a mouse. In doing so, the local inflammatory response is triggered, and inflammatory immune cells infiltrate the paw around the site of injection[50]. In this study, it was seen that both macrophages and neutrophils did infiltrate the inflamed paw, however, only macrophages carried nanoemulsion to the site of injury. Using both live animal imaging as well as immunohistochemical tissue analysis, it was seen that the CXB-NE theranostic nanoemulsion was able to decrease the number of infiltrating macrophages at the site of injury[49].

Knowing that CXB-NE can shift the inflammatory response, further evaluation by Dr. Kiran Vasudeva looked at whether neuroinflammatory pain relief could be achieved through the action of the theranostic nanoemulsion[51]. Here it was found that a single, low dose of CXB-NE was able to relieve neuroinflammatory pain-like behavior for four or more days in male rats. This study also showed that in the sciatic nerve tissue, CXB-NE decreased the number of infiltrating macrophages in the injured tissue when compared to drug free nanoemulsion (DF-NE). The CXB-NE also decreases the presence of its target enzyme, COX-2, and attenuates the production of PGE_2[51]. This finding was unprecedented given that NSAIDs were not thought to be effective in treating neuroinflammatory pain[37]. In fact, other studies that have tried oral delivery of celecoxib to relieve neuroinflammatory pain used 2000-fold or more drug than what was used here to obtain similar relief[52, 53]. The increased efficacy of CXB-NE in relieving neuropathic pain has to do with the fact that it is being phagocytosed and delivered to the injured nerve by the very cells that generate COX-2 during an inflammatory response. This allows for the decreased drug concentration and therefore, decreased chances of toxicity.

In order to further the understanding of how pain relief obtained from the attenuation of PGE_2 can change the neuroimmune response, Dr. Muzamil Saleem set out to examine macrophage and mast cell crosstalk in male rats at the site of the injured sciatic nerve as well as the neuronal cell bodies in the corresponding dorsal root ganglia (DRG) during neuroinflammatory pain, relief, and return to pain[54] when the drug effect of a single dose wears off. In this, the full extent of the drug relief profile was evident, revealing that a single injection provided 6 days of relief from hypersensitivity. Furthermore, similar to what was previously reported, CXB-NE reduced the number of infiltrating macrophages at the site of injury decreasing the percent of COX-2 expressing macrophages and their production of PGE_2. This

resulted in a switch from macrophages being M1, pro-inflammatory, to M2, anti-inflammatory. As a depletion in macrophage pro-inflammatory signaling occurred, the presence of mast cells and mast cell degranulation at the site of injury also decreased. The DRG appeared unaffected by drug treatment while relief was being experienced. However, it was seen when both the DF-NE and CXB-NE reached day 18 (when CXB-NE returned to pain) that there was an increased infiltration of immune cells in the DRG including macrophages and mast cells. This, as well as reduced immune cells at the site of injury at day 18 compared to day 12, suggests that during the initial neuroinflammatory response, the reaction is local to the injury, but the inflammatory response can then spread to the neuronal cell bodies centimeters from the injury where they now appear to influence neuronal inflammatory pain there.

The effect of CXB-NE on the infiltration and function of immune cells is apparent, but how this effects gene transcription and regulation is unclear. Dr. Andrea Stevens saw that in male rats, in the sciatic nerve at the site of injury, genes associated with neuroinflammation such as IL-6, IL-1β, TLR2, and CD4 exhibited changes in transcription following CCI[55]. Interestingly, it was also seen that once treated with CXB-NE, IL-6, IL-1β, CD11b, TRPV1, among other neuro-inflammatory genes all experience reduced levels of mRNA expression. This suggests that the change in neuroinflammatory hypersensitivity towards a pain-relief state could be due to changes in the abundance of different infiltrating cell types as well as the change in gene expression of those genes associated with neuroinflammation. Given that neuronal gene expression occurs at the cell body, and the cell bodies of the sciatic nerve's axons are located within the DRG[56], assessment of transcriptional changes needed to be examined within the DRG itself. Further examination using RNA-seq[57] in male rats showed that hypersensitivity relief by CXB-NE was accompanied by a shift in gene expression changes compared to DF-NE. Some of

these changes included genes identified as influencing axonal outgrowth, synapse formation, neutrophil degranulation, and innate immune system processes.

This body of work created by the Janjic/Pollock collaboration provides insightful information on the development of a non-opioid therapeutic and how the neuroinflammatory response changes due to relief from hypersensitivity in response to CXB-NE treatment. However, this body of work was initially generated using male rodents and cell lines.

Lu Liu evaluated the efficacy of CXB-NE in the relief of pain from an inflammatory model using CFA injection in the paw pad of male and female mice[58]. Liu and co-workers found that CXB-NE did provide relief in both sexes, but that relief in the number of days from inflammatory pain was 21 days less in females as compared to males[58]. Additionally, male and female mice had differential inflammatory patterns 40 days following CFA and CXB-NE treatment once CXB-NE behavior was similar to DF-NE. It was seen that males treated had less inflammation than females at this time point[58]. This was the first report showing sex difference in COX-2 inhibition in a macrophage that correlates to pain behavioral changes between the sexes. Inflammation and neuroinflammation share some characteristics in the development of peripheral pain; however, they do differ in many ways as well such as how they engage the immune system and change gene expression changes in neurons[59]. Seeing this difference in an inflammatory model, made it of upmost importance to additionally evaluate this difference in a neuroinflammatory model.

1.4 Sex disparity in neuropathic pain

With decades of research, the focus until very recently had been almost exclusively on male neuropathic pain. In fact, a systematic review was done to examine this bias in published

articles from 2009 in 10 different fields, and found that male bias was most prominent in the neuroscience field with male studies out numbering female studies 5.5 to 1[60]. This continued sex bias has led to poor translational findings in the clinic; for example, from 1997 to 2000, eight of the ten drugs pulled from market were found to have greater health risks for women than men[61]. Even though the National Institute of Health tried to address this bias in 1993, with requiring females to be included in phase III clinical trials, the foundational problem still existed at the preclinical level. Without both sexes being examined in the early stages, a waste of time and resources occurs by bringing drugs through the process only to reveal sex dependent ineffectiveness due to fundamental biological differences so late in clinical trials[62]. Many scientists wrote opinion articles on this topic[62, 63], and opposing scientists argued that including females would increase variability in the study because of the involvement of the estrus cycle hormones[64]. However, this has been shown to be untrue[65, 66]. Due to push back from scientists, it wasn't until 2016 that the National Institute of Health mandated sex be considered as a biological variable in pre-clinical studies. Since then, researchers in neuroscience, as well as immunology, have been observing the importance of sex differences within their disciplines[67, 26,27, 68].

Some of the primary work that sparked the huge interest in sex differences in neuropathic pain stemmed from Dr. Jeffery Mogil's lab at McGill University[26,27]. Here they found that activating microglia via TLR4 in the spinal cord of both sexes, which function similarly to macrophages in the peripheral nervous system, caused mechanical allodynia in only male mice and not in females[26]. Additionally, castrated males were protected from allodynia induction by TLR4, and allodynia returned when testosterone was administered[26]. Similarly, ovariectomized females when given testosterone also experience allodynia when microglial TLR4 is activated[26]. This appeared to display a unique characteristic for microglia driven neuropathic pain in males,

but not in females. They furthered these studies by examining other cell types that could be mitigating female neuropathic pain[27]. Here the authors examined the importance of both microglia and T cells in inducing male and female neuropathic pain[27]. This time, using a peripheral nerve injury they blocked microglia at the spinal cord and saw again that males had reduced allodynia and females were unaffected[27]. Using mice deficient in T cells, females then experienced relief with a microglial inhibitor, and when T cells were given back, females again were not affected by the microglial inhibitor[27]. This means that in an intact system that female neuropathic pain appears to be driven by the T cell.

These findings are informative to our studies given that TLR4 leads to the activation of COX-2, which is what the celecoxib nanoemulsion is an agonist to. If these sex differences in TLR4 function in inducing neuropathic pain hold true, sex differences in how efficient the therapeutic is at exerting its effect should be apparent with CXB-NE treatment. TLR4 typically functions to recognize pattern recognition receptors such as those stemming from pathogens (PAMPs) or from result of tissue injury (DAMPs). TLR4 binds to antigens such as heat shock proteins, components of the extracellular matrix components, and lipopolysaccharide[69]. Following binding of antigen to TLR-4, MyD88 and other co-factors activates mitogen activated protein (MAP) kinases, which lead to the transcription of the *prostaglandin-endoperoxide synthase 2* (*PTGS2*) gene which leads to the translation of the COX-2 enzyme[69-71]. Additionally, COX-2 transcription can also be activated via IL-R1 binding or the transcription of early genes such as c-jun, c-phos, and c-myc[72].

1.5 Specific Aims

1.5.1 Specific Aim 1

Evaluate the efficiency of a theranostic formulated as COX-2 inhibiting nanoemulsion to alleviate mechanical allodynia and hyperalgesia in both sexes.

1.5.2 Background for Specific Aim 1

As previously mentioned, females have been left out of preclinical studies until recently. Studies examining how chronic pain is triggered in females are on the rise, but how they respond to treatment and how treatment effects the neuroimmune response is still limited. Even though it is being seen that females predominantly use their adaptive immune response to induce neuropathic pain[23], macrophages and microglia still infiltrate the injured area equally to what is seen in their male counterparts[73]. This infiltration of activated macrophages leads to the production of the COX-2 enzyme and ultimately the production the pro-inflammatory and neuronal sensitizing PGE_2 product. The Pollock Lab has previously shown in males that a single dose (0.24 mg/kg) can provide up to 6 days of pain relief. By doing so, a dosage without systemic toxicity and with longer lasting effects is ideal for long-term effective treatment of neuroinflammatory pain. Until now, it has been unknown if this therapy will be effective in treating female neuroinflammatory pain. With the knowledge that females also have macrophage infiltration during a neuroimmune response and knowing that PGE_2 is one of the main triggers of neuropathic pain, **it was hypothesized that CXB-NE could provide pain relief to females like we have seen in males.** However, given that recent studies have been showing sex differences in TLR4 function in the male and female neuroinflammatory response **it was also hypothesized that females given CXB-NE treatment may experience relief differently than the males do.**

1.5.3 Methodology for Specific Aim 1

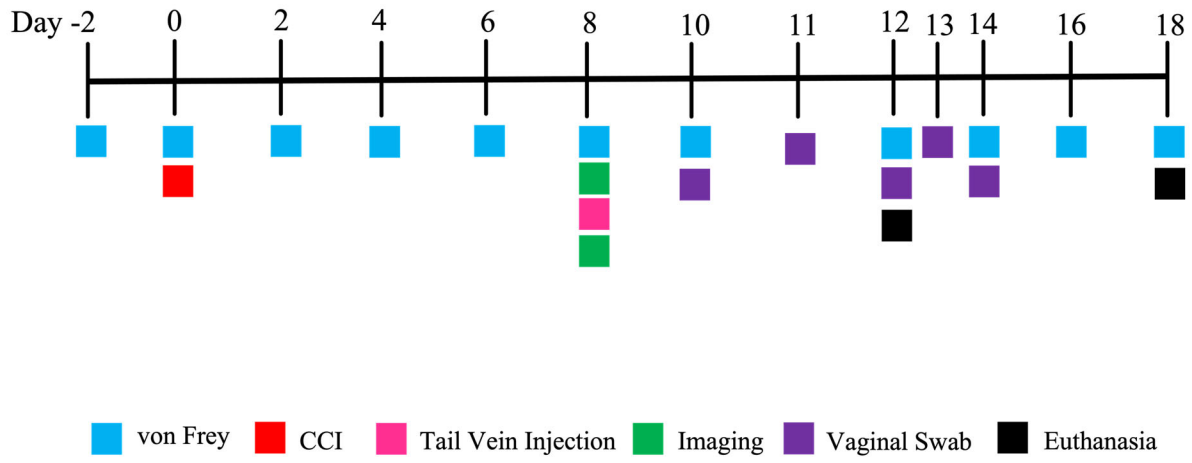

Figure 1.3. Experimental schedule for behavioral testing in both males and females to evaluate the efficiency of CXB-NE and visualize the location *in vivo*. Behavior will be conducted prior to any other procedures scheduled on the same day.

In order to assess the full drug response curve in both sexes, mechanical hypersensitivity was measured over the extent of the time animals experienced mechanical hypersensitivity relief extending to 18 days post-CCI. Figure 1.1 shows that one group of animals was euthanized at the peak of male relief (Day 12) and a second group was chosen to be euthanized once the animals had returned to hypersensitivity (Day 18). If females were still experiencing relief up until this point, the timeline would have been extended.

Male and female Sprague Dawley rats aged 6 - 7 weeks were subjected to CCI surgery and then assessed for pain-like behavior using the von Frey technique to assess mechanical hypersensitivity. This method was also used to assess as the efficacy of CXB-NE to alleviate mechanical allodynia. There were cohorts of male and female rats with the following treatment

groups: naïve, surgical sham, CCI, CCI + DF-NE, and CCI + CXB-NE. Rats were randomly assigned to their groups to avoid any biases and the nanoemulsion injections were blinded by other members of the lab.

Up-down von Frey behavior[74,75] was used in animals prior to CCI or Sham surgery on days -2 and 0 with surgeries occurring on day 0 post behavioral assessment. Either drug free or CXB containing nanoemulsion was given 8 days post-surgery once the animals were in sustained mechanical allodynia as well as once the neuroimmune response was in full blown effect[51,54,55,57,76].

From these first round of studies, using 1X CXB-NE (0.24 mg/kg), I was able to detect a significant sex difference in relief achieved between males and females. Males showed a similar dose response as what we have seen previously[51,54,55,57], obtaining around 5 days of relief, while females only obtained 1 day of relief and at an attenuated response compared to males[68]. This indicates that females were not achieving complete pain relief like males. However, when the celecoxib theranostic nanoemulsion was reformulated by the Janjic lab[77] to contain 10 times the amount of CXB (10X CXB-NE) (2.4 mg/kg), the sex difference in relief resolved with females obtaining nearly identical mechanical allodynia relief as compared to the males.

1.5.4 Specific Aim 2

Evaluate key immunological cell types involved in the neuroimmune response and how their presence is affected by CXB-NE treatment.

1.5.5 *Background for Specific Aim 2*

Given the recent knowledge that females drive neuroinflammatory pain through adaptive immunological aspects and males use more of an innate response, fundamental immunological cell types of both systems were evaluated for their presence and location at the site of injury. Our lab has previously seen that CXB-NE treatment is able to reduce the number of infiltrating $CD68^+$ macrophages at the site of injury when animals are experiencing relief [47,51,54]. We have also seen that when neuroinflammatory pain returns, the difference in number of infiltrating macrophages after treatment no longer stands once the animals have returned to hypersensitivity[54]. Because of this, **it was hypothesized that the presence of CD68+ macrophages in the site of injury is an indicator of behavioral hypersensitivity in both sexes.**

This study also examined adaptive immune cells including CD3+ T cells and subtyping them into helper T cells (CD4+) and cytotoxic T cells (CD8+). It has been seen that CD4+ T cells help contribute to the neuroinflammatory response in both sexes, but their ability to affect neuronal hypersensitivity is primarily a role in females. Therefore, **it was hypothesized that in females, that T cell infiltration will decrease correlating with neuroinflammatory hypersensitivity and they will reflect more of a CD4+ phenotype.**

1.5.6 Methodology for Specific Aim 2

Animals for aims 1 and 3 had their sciatic nerves collected for *ex vivo* analysis of immunological infiltrating cells during relief (day 12) and at return to hypersensitivity (day 18). Tissues were processed, stained, and imaged on the confocal or conventional epifluorescent microscope. It was found that the infiltration of macrophages did correlate with mechanical

hypersensitivity and the density of infiltrating macrophages followed the sex difference in response with 1X CXB-NE, with females having significantly more macrophages present during relief than males. However, T cells were not altered by treatment or exhibit a difference between sexes.

Additionally, we found that *ATF3*, a CREB transcription factor, showed sexual dimorphisms following treatment with 10X CXB-NE and its protein expression was evaluated using immunohistochemistry. Careful examination has shown that ATF3 nuclear condensation does in fact increase in both sexes following CCI, but decreases significantly only in the female DRG following CXB-NE treatment.

1.5.7 Specific Aim 3

Use RNA-seq transcriptional analysis to evaluate the differential gene expression between male and female affected neurons in the dorsal root ganglia (DRG) during neuroinflammation and relief.

1.5.8 Background for Specific Aim 3

Changes in neuronal responsiveness may be the basis of chronic pain. Such changes in neuronal response may originate from differences in transcriptional expression of key genes found in the neuronal cell bodies. Therefore, assessing the transcriptional profile of the DRG is of interest. Although the sciatic nerve is technically innervated by lumbar ganglia L3-L6, more than 98% of the innervation comes from L4 and L5; therefore, for this study purposes only L4 and L5 were collected for transcriptome analysis[56]. There are many different cell types that could be contributing to transcriptional changes. The DRG itself is comprised of both large-bodied

mechanoreceptors and small-bodied nociceptors which serve contrasting functional roles leading to differences within transcription in the DRG itself. The DRG also has resident immune cells, epithelial cells, and satellite glial cells all of which play into the overall transcriptome genotype being expressed in response to a stimulus[78].

Previously, the majority of studies had performed microarray analyses or qPCR to examine a specific set of genes of interest[78-80]. While this is cost effective and usually gives an answer pertaining to what you are looking for, plenty of things can be lost by limiting your scope on a handful of genes. Our study examined total RNA expression in the DRG looking to gain better insight into which part of a signaling cascades are being affected in the pain state and then changing once relief is obtained between males and females. Because of some of the fundamental differences during neuroinflammation that are beginning to be elucidated between males and females as well as preliminary studies finding transcriptional sex differences during neuroinflammation, **it was hypothesized that key differences in biological processes will be revealed in those animals experiencing pain or relief with CXB-NE treatment.**

1.5.9 Methodology for Specific Aim 3

Male and female Sprague Dawley rats were randomly assigned to their respective groups (Naïve, CCI, CCI + 10X CXB-NE, and CCI + DF-NE) and followed the same process from Aim 1 but ending at day 12 where CXB-NE treatment animals are experiencing relief, and DF-NE and CCI are experiencing mechanical hypersensitivity. 10X CXB-NE (2.4 mg/kg) was chosen for more accurate comparison of transcriptional changes considering that with 10X CXB-NE treatment females now experience similar level of relief to males. Therefore, transcriptional

changes aren't due to differences in levels of relief, but changes are due to differences in biological processes.

Once DRGs were collected and sequenced. In order to determine differences due to the neuroinflammatory response, CCI and Naïve groups were compared within sexes given that the only differences between these groups would be the induction of a neuroinflammatory response with CCI. Changes in gene expression due to relief with 10X CXB-NE treatment was assessed by comparing DF-NE and 10X CXB-NE groups within sex, limiting the differences only to the presence/ absence of CXB. Genes normally present in a pain state as well as others were compared between sexes and changes in these genes following treatment were further contrasted.

This analysis showed that of the 977 genes changed with female neuroinflammation, only 89 were significantly shared with males; similarly, 333 genes changed during neuroinflammatory relief in males only 1 gene was shared with females. This alone shows how important it is to include both sexes when evaluating therapeutics given that the male and female responses can differ so greatly.

CHAPTER II.

MATERIALS AND METHODS

2.1 Animals and Ethics Statement

Male (200 - 250 g) and female (150 - 200 g) Sprague-Dawley rats were purchased from Hilltop Lab Animals, Inc. (Springdale, PA). These experiments were carried out following the recommendations in the Guide for Care and Use of Laboratory Animals of the National Institutes of Health and the regulations of the Institutional Animal Care and Use Committee at Duquesne University under approved Protocols #1803-02 and 2009-07 and in compliance with the ARRIVE guidelines (https://arriveguidelines.org). Rats were acclimated and maintained on a 12:12 hour light-dark cycle and housed on paper bedding with access to food and water *ad libitum*. Starting two days prior to surgery, animals were switched onto a special diet (Research Diets, Inc., New Brunswick NJ; Cat # AIN-93G) to avoid autofluorescence during near infrared imaging of the nanoemulsion in live animals. Animals were socially housed during acclimation. They were then individually housed once von Frey began (two days prior to surgery) to establish a baseline behavior. Individual housing was done to avoid rats from opening one another's wounds following surgery. A power analysis was preformed using behavioral data from 1X CXB-NE females compared to DF-NE females as well as 1X CXB-NE males compared to DF-NE males to determine the number of animals needed to detect significance. Using a power of 80% and an alpha value of 0.05, it was determined that a total of 4 animals per condition was needed for these studies. In our behavioral studies, we used between 4-6 animals per condition to achieve statistical significance.

2.2 Chronic Constriction Injury

Male and female rats underwent chronic constriction injury (CCI) of the sciatic nerve as described by Bennett and Xie [75] and in accordance with our prior technique [51,54] to induce neuropathic pain and inflammation. The sciatic nerve was accessed by making an incision with a scalpel a few millimeters beneath the femur bone following the direction of the bone for a 1.5 – 2.0-inch opening. The white connective tissue between the *biceps femoris* and *gluteus superficialis* was bluntly dissected through exposing the sciatic nerve. The nerve was then carefully freed from the loose connective tissue holding it in place. Four sutures (McKesson 4-0 Chromic Gut Sutures, Cat # S635GX) were then loosely tied around the sciatic nerve approximately 1 mm apart in CCI, DF-NE, and CXB-NE treated animals. Sham animals underwent identical surgery to expose the sciatic nerve, but no sutures were tied around the nerve. The separation between *the biceps femoris* and *gluteus superficialis* was then closed using 3 sutures, iodine was applied, and the skin was stapled close with 5-6 autoclips. Animals were monitored until awake and notes of their foot function were acquired.

2.3 von Frey Behavioral Testing

Cohorts of all male or all female rats were tested separately for hypersensitivity with the up down von Frey technique. In each case, behavioral analysis was assessed every other day before and following surgery as outlined in Figure 1.3. Behavioralist was blinded to any treatment received. Rodents were first acclimated for 30 minutes in individual plexiglass containers with mesh floors. Once testing began, the left and right hind paws were probed with calibrated von Frey filaments (Stoelting Co., Catalog # 58011). Filaments (1.202 g, 1.479 g, 2.041 g, 3.630 g, 5.495 g, 8.511 g, 15.136 g) were applied to the hind paw at a 30-degree angle

and for 3 seconds to look for positive (quick lift, flick, vocalization) or negative responses. If no response, the next largest filament would be used. If positive response, the next smallest filament would be used. This pattern continued until 4 responses were collected after the change in response such as used previously[74, 81, 68, 54, 51]. No less than 30 seconds separated probing of the same paw twice. The gram force of the 50% withdrawal threshold was then calculated using Chaplan's 50% withdrawal threshold formula[74].

2.4 Intravenous Tail Vein Injections

Intravenous injections of DF-NE and CXB-NE were performed 8 days after surgery and following von Frey behavior analyses. Injections and near-infrared imaging inspection of injection quality were performed as described by Saleem et al. [76] (See appendix for publication with additional information on technique). Investigators were blinded to the nanoemulsion treatment. Animals were anesthetized with respiratory isoflurane. Tails were warmed in water for 1 minute to dilate the lateral veins. Tails were then dried with gauze and sterilized with an alcohol pad. A 27G needle, bevel up, was placed distally into the lateral tail vein. Upon blood flashback, a syringe containing 300μL of DF-NE or CXB-NE (55.5 ng of celecoxib) was attached and slowly injected into the vein [51,54,76]; this dose was used for all animals. The quality of the tail vein injection was assessed using the near infrared LI-COR fluorescent imager (LI-COR BioSciences, Lincoln, NE). A quality injection should be cleared through the bloodstream, leaving little to no near infrared signal in the tail, except for the possibility of a tiny dot at the injection site. Animals with subcutaneous injections or a ruptured vein leading to an incomplete injection were removed from the study.

2.5 Vaginal Swabs

Female's estrus cycle was tracked for four consecutive days (days 8 – 12 post-surgery) in order to establish where in estrus cycle the individual was when receiving treatment. During this procedure, females were briefly anesthetized with isoflurane, vaginal canals were flushed with saline, and collection was allowed to dry on a slide. Once dry, slides were fixed with 100% methanol and stained with 5% Geisma stain for 20 minutes. Slides were then rinsed briefly with water and allowed to dry before mounting with Permount (FisherScientific, Cat # SP15-100). Using Cora and colleague's description of the estrus cycle[82], each female's cycle was established. Data is included in the appendix.

2.6 Tissue Dissection and Preparation for Histology

Rats were euthanized at the maximum relief from hypersensitivity at 12 days post CCI or 18 days post CCI when the animals returned to pain-like behavior by CO_2 asphyxiation and followed by cervical dislocation. The dorsal root ganglia (DRG), sciatic nerves, testis, ovaries, spleen, kidneys, liver, and heart were immediately collected following euthanasia in this respective order. Ovaries, testis, and a piece of liver were collected for the Selcer Lab and flash frozen in liquid nitrogen. All remaining tissues for IHC were placed in 4% paraformaldehyde in 1X phosphate buffered saline (PBS) solution at 4°C for 24 hours. Tissues were then washed with 1X PBS, transferred into 30% sucrose in 1X PBS solution and kept at 4°C until embedded. Tissues were embedded in optimal cutting temperature compound (Tissue-Tek® OCT) and frozen in a bath of isopentane. Frozen tissue blocks acclimated to the cryostat (-25°C) were then sectioned on the cryostat at 20 μm thickness and collected on gelatin-coated slides

(SouthernBioTech, Birmingham, AL; Cat # 100241-864). Slides were kept at -20°C until immunofluorescence staining was performed.

2.7 Immunohistochemistry and Microscopy

Tissues were stained with standard immunohistochemical protocols and recommendations of the antibody manufacturers as previously described [51,54]. Multistain procedures typically include nuclear staining (DAPI) and two other primary antibodies. Primary antibodies included an anti-CD68 [83] rabbit polyclonal antibody (ab125212) at a 1:400 dilution, an anti-CD3e mouse monoclonal antibody (MA1-90582) at a 1:500 dilution, an anti-CD4 mouse monoclonal antibody (ab33775) at a 1:500 dilution, an anti-CD8 mouse monoclonal antibody (ab33786) at a 1:100 dilution, or anti-ATF3 (HPA001562) at a 1:500 dilution. The secondary antibodies used were ThermoFisher's donkey anti-rabbit IgG Alexa Fluor 488 (A21206), goat anti-mouse IgG1 Alexa Fluor 555 (A21127), or donkey anti-rabbit IgG Alexa Fluor 555 (A31572) all at a 1:200 dilution. After the final washes, the slides were coverslipped with Prolong™ Diamond-DAPI (ThermoFisher).

Images were acquired and analyzed on a Nikon Eclipse Ni-U epifluorescence microscope with a 20X objective using Nikon NIS-Elements BR software (Version 5.02) for DAPI, 488 (FITC), 555 (TRITC), and DIC channels. Investigators were blinded to the treatment conditions while imaging and analyzing. Images were taken between the knots from the CCI surgery where inflammation was at its highest. Infiltrating immune cells were only counted if present within the fasciculated nerve bundle and not within the epineural sheath; this was determined by using the DIC overlay.

Quantification of macrophages and T cells used 7 regions of interest (140 μm x 140 μm) that were placed on the transmitted light image of the fasciculated axons of the sciatic nerve using the DIC view, and then individual CD68 positive or CD3e positive cells were counted. The average number of cells per region was compared across conditions.

When examining the percentage of CD68+ macrophages with the nanoemulsion, images were acquired on a Nikon Ti2 Eclipse inverted A1r confocal microscope. During this analysis, all macrophages in a field of view (212 μm X 212 μm) were counted, and then the number of those containing nanoemulsion were divided by the total number of macrophages in the field of view. Each animal was averaged within their treatment group to determine the percent of nanoemulsion-positive macrophages per sex and treatment.

Counting CD8-positive cells that infiltrated the fasciculated nerve required a different approach. Here, we counted the number of positive cells within the fasciculated nerve and divided this number by the total area counted. The cells per given area were then normalized.

ATF3 images were acquired on a Nikon Ti2 Eclipse inverted A1r confocal microscope using a 40X 1.3 NA oil objective. Images were acquired using 3D Z-stacks through the entire DRG section. Images were then converted to a maximum intensity projection image in order to visualize signal throughout the whole section. All images were taken using the same exposure, gain, and LUTs settings.

2.8 Tissue Dissection and Preparation for RNAseq

Rats that were to be used for RNAseq studies were euthanized on day 12 by CO_2 asphyxiation followed by cervical dislocation. DRGs were immediately excised following euthanasia. To do so, a rectangular incision was made with the scalpel over the spinal column

through the surface muscle. Using bone crushers, this muscle was peeled away. The vertebrae were then further cleared from the surrounding muscle until each vertebra could be clearly seen. The iliac crest of the hip bones was located and exposed. Using bone crushers, 3 – 4 vertebrae up from the iliac crest, the vertebrae were crushed and peeled away exposing the sciatic nerve and DRG. Directly above the iliac crest the 5th right and left lumbar DRGs were located. RL4, LL4, RL5, and LL5 were collected and immediately stored in PCR tubes containing RNA*later* solution (ThermoFisher, Catalog #AM7020). Tissues were stored at room temperature in RNA*later* for 24 hours and then tissues were removed and placed in new, empty tubes and stored at -20°C until sequenced. When shipped, the RL4 and RL5 of the same animal were moved to the same tube and sent on dry ice to Qiagen's Genomic Services in Frederick, Maryland.

2.9 RNA-seq DRG Sample preparation

RNA isolation was performed under contract by Qiagen as follows; RL4 and RL5 DRG were weighed, and 5-7 mg was homogenized for RNA extraction using the RNeasy Plus Universal Mini Kit (Qiagen, Hilden, Germany). In order to include small RNAs, manufacturer instructions for the kit were followed using the Qiagen *Purification of Total RNA Containing miRNA appendix C*.

2.10 Library preparation and sequencing (conducted by Qiagen)

Library preparation and sequencing was performed under contract by Qiagen as follows. Approximately 400 to 500 ng of extracted RNA was first heat fragmented, and then separated from any unwanted ribosomal RNA (rRNA) using the QIAseq FastSelect rRNA and globin depletion kit (Qiagen, Hilden, Germany). Samples were quality controlled by checking the RNA

integrity number (RIN^e) gathered from the Agilent D1000 ScreenTape System (Agilent Technologies, Santa Clara, CA). Using the QIAseq Stranded Total RNA Library Kit (Qiagen, Hilden, Germany), library preparation was done. Briefly, sequencing adapters were added, and cDNA was amplified using PCR. All libraries were pooled in equimolar concentrations. Following the manufacturer's protocol, library pools were clustered on the surface of a flow cell before sequencing on a NextSeq High Output flow cell (Illumina Inc., San Diego, CA) instrument (2x75, 2x8). Libraries were generated with 30 million read depth per animal and average lengths of 75 base pairs.

2.11 Bioinformatics analysis of RNA-seq data (Mapping and Differential Expression Analysis - conducted by Brooke Deal)

RNA-seq fastq data files were received by Brooke Deal from Qiagen and imported into CLC Genomics Workbench 22.0.2 (QIAGEN, Hilden, Germany). CLC was then used for quality assessment, alignment with the *Rattus norvegicus* genome (mRatBN7.2.106), heatmap comparisons, differential expression analyses, volcano plots, and Venn diagram comparisons of the differentially expressed genes.

Mapping was done under the CLC Genomics Workbench default settings in the forward direction. Genes included in most-mapping analyses had an adjusted p-value, false discovery rate (FDR), of ≤ 0.05 and a fold change greater than ± 1. Trimmed mean of M values (TMM) normalization is internally used for DE, heatmaps, and principal component analyses (PCA).

To identify genes that were regulated by neuroinflammation (CCI vs Naïve) or relief (CXB-NE vs DF-NE) in each sex, DE analyses were performed. These gene sets that were differentially

changed by neuroinflammation, or relief were then compared between sexes via Venn diagram to see which genes are shared or distinct for a given sex under these conditions.

2.12 Enrichment Analysis

Metascape (metascape.org) was used for enrichment analyses. Metascape is updated monthly and incorporates Gene Ontology (GO) processes, Kyoto Encyclopedia of Genes and Genomics (KEGG) pathways, Reactome gene sets, Cytoscape and NCBI as well as other publicly available resources all incorporated into one platform[84]. This allows for reduced redundancy among ontology terms.

Up or down regulated gene sets of differentially expressed genes due to neuroinflammation or relief in each sex were then imported into Metascape using the express analysis version with the default settings. Enrichment heatmaps and protein interaction networks were then visualized for interpretation.

2.13 cDNA conversion and RT-qPCR validation

RNA was received from Qiagen and at Duquesne University Brooke Deal converted it to cDNA using the Verso cDNA conversion kit (ThermoFisher Scientific, Waltham, MA; AB-1453/A). RNA (500 ng) conversion was performed at 42°C for 1 hour and then inactivated for 2 minutes at 65°C. cDNA conversion was confirmed to be successful via PCR using GAPDH primers and visualization on an agarose gel.

Real time quantitative PCR (RT-qPCR) was done to verify gene expression changes in a subset of genes (ATF3 and Sema6a) (see Appendix A3. Figures A3.1 and A3.2). Maxima SYBR Green/ROX qPCR Master Mix (2X) (ThermoScientific, Catalog # K0221) was used on the Step

One Plus qRT-PCR Instrument (Applied Biosystems, Waltham, MA). Primers are listed in Supplementary table 1. Briefly, 250 ng of template DNA was used in a 25µL reaction. Following the manufacturer's protocol, 40 cycles were run under the two-step reaction protocol.

CHAPTER III.

BEHAVIORAL AND INFLAMMATORY SEX DIFFERENCES REVEALED BY CELECOXIB NANOTHERAPEUTIC TREATMENT OF PERIPHERAL NEUROINFLAMMATION

Abstract

Neuropathic pain affects millions of people worldwide, yet the molecular mechanisms of how it develops and persists are poorly understood. Given that males have historically been utilized as the primary sex in preclinical studies, less is known about the female neuroinflammatory response to injury, formation of pain, or response to pain-relieving therapies. Macrophages contribute to the development of neuroinflammatory pain via the activation of their cyclooxygenase-2 (COX-2) enzyme, which leads to the production of prostaglandin E_2 (PGE_2). PGE_2 activates nociception and influences additional leukocyte infiltration. Attenuation of COX-2 activity decreases inflammatory pain, most commonly achieved by nonsteroidal anti-inflammatory drugs (NSAIDs), yet NSAIDs are considered ineffective for neuropathic pain due to off target toxicity. Using chronic constriction injury of the rat sciatic nerve, we show that males and females exhibit quantitatively the same degree of mechanical allodynia post injury. Furthermore, a low dose theranostic nanoemulsion containing the NSAID celecoxib is phagocytosed by circulating monocytes that then naturally accumulate at sites of injury as macrophages. Using this theranostic nanoemulsion, we show that treated males exhibit complete reversal of hypersensitivity, while the same dose of theranostic nanoemulsion in females provides an attenuated relief. The difference in behavioral response to the theranostic nanoemulsion is reflected in the reduction of infiltrating macrophages at the site of injury. The

observations contained in this study reinforce the notion that female neuroinflammation is different than males.

Reprinted from B. Deal, L. Reynolds, C. Patterson, J. M. Janjic, J. A. Pollock. (2022). Behavioral and inflammatory sex differences revealed by celecoxib nanotherapeutic treatment of peripheral neuroinflammation. *Scientific Reports*. 12, 8472. https://doi.org/10.1038/s41598-022-12248-8.

Contribution's statement:

In this analysis of 1X CXB-NE, Brooke Deal and Dr. John Pollock conceived and designed the experiments in a CCI rat neuropathic model. Dr. Jelena Janjic designed a macrophage-targeted COX-2 inhibition strategy for pain relief and formulated the nanoemulsions. Brooke conducted the animal experiments. Brooke, Charles Patterson (Figure 3.4) and Laura Reynolds (Figure 3.2 and 3.6) performed immunohistochemical assays. Brooke and Laura (Figure 3.2 and 3.6) imaged tissues and analyzed the results. Brooke was the primary author of the manuscript with assistance from Dr. John Pollock and edits from Dr. Jelena Janjic.

3.1 Introduction

Neuroinflammation is typically caused by injury, infection, or neurodegenerative disorders [85]. The hallmarks of neuroinflammation include rapid infiltration of immune cells at the site of injury that modulate the release of cytokines and chemokines [86]. As a result, specific inflammatory responses, such as cellular and molecular signaling, influence tissue repair, while other components of the inflammatory dialogue cause the sensitization of somatosensory neurons, driving them to hypersensitivity [87]. When these physiological processes are unregulated, the neuroinflammatory response can result in hypersensitivity and neuropathic pain. Furthermore, dysregulated neuroinflammation can interfere with the regenerative potential of the inflammatory response, impeding neuroregeneration and tissue functional recovery following injury [88].

At a cellular level, neuroinflammation is a complex cross-communication occurring between immune cells, neuronal cells, and glial cells that participates in teetering the cellular milieu between proinflammatory and anti-inflammatory [89-91]. Macrophages play a central role in this mediation, functioning at several levels in the inflammatory response as well as in the repair and regeneration of peripheral neurons. Once stimulated, one of the functions of macrophages is the activation of cyclooxygenase-2 (COX-2), an enzyme that in turn produces prostaglandin E_2 (PGE_2). The presence of PGE_2 has been linked to neuronal sensitization and pain through the increase of intracellular cAMP and Ca^+, allowing for heightened neurotransmitter release [92-95]. COX-2 and PGE_2 production has been a target for inhibition by many pharmaceuticals, including aspirin, ibuprofen, and celecoxib [96]. COX-2 inhibitors work by reducing the production of PGE_2, attenuating inflammation, and thereby providing pain relief. However, a problem with COX-2 inhibitors is that due to the systemic dosage needed to achieve neuropathic pain relief from nerve

injury and the associated reduction in inflammation at the site of injury, there are risks of off-target toxicity such as gastrointestinal bleeding, heart attack, stroke, and kidney damage [43]. As such, conventional non-steroidal anti-inflammatory drugs (NSAIDs) and COX-2 inhibitors were shown to be ineffective in the treatment of neuropathic pain [37].

One of the reasons for the need for high dosages is poor bioavailability of the drugs. In our previous work, we demonstrated that by directing the COX-2 inhibitor celecoxib (CXB) to macrophages by natural phagocytosis of the theranostic nanoemulsion formulation, both reduced systemic exposure and increased overall drug efficacy were achieved [51,54]. In these studies, a single intravenous dose of celecoxib theranostic nanoemulsion (CXB-NE) delivering 0.24 mg/kg celecoxib was found to provide 6 days of statistically significant relief from pain-like behavior caused by surgical chronic constriction injury (CCI) of the male rat sciatic nerve [51,54]. When compared to oral administration, this single dose represents approximately 2,000-fold less drug required to alleviate mechanical hypersensitivity for these 6 days [51-54]. This single dose is effective upon intravenous injection because circulating monocytes phagocytose the nanoemulsion and then naturally aggregate at the site of neuronal injury [51] or inflammatory insult [58]. Instead of an effective systemic dose, which presents the drug to all tissues, the theranostic nanoemulsion functions with macrophages acting as both a target and a vehicle. This allows for the drug to be brought to the site of inflammation, where macrophage-specific COX-2 inhibition attenuates the production of PGE_2. While recent work has evaluated CXB-NE's ability to reduce inflammatory signaling in male and female mice experiencing acute inflammation resulting from injection of Freund's Complete Adjuvant [58], CXB-NE has not yet been evaluated in female neuroinflammation and neuronal injury models.

In addition to macrophages exerting inflammatory effects at the site of injury, associated spinal microglia are reactive to peripheral inflammation in ways that can enhance pain signaling in the central nervous system [97]. Intrathecal injection of drugs can disrupt the functional proinflammatory role that activated microglia play in nociceptive signaling, preventing pain-like behavior in rodents [98]. However, blocking microglial cells alleviates pain in only males and not female rodents [26]. Interestingly, in mice that lack T cells, blocking microglia leads to pain relief in both sexes [27,73], and when T cells are restored, pain-like behavior returns only in female mice. This points to an influential role of T cells in the development of female neuroinflammatory pain. This is particularly interesting because during a typical neuroinflammatory response macrophages and T cells directly interact with one another through their major histocompatibility complex and T cell receptor, respectively. Macrophages infiltrate the site of injury within hours to days of injury. These infiltrating macrophages release cytokines and chemokines that attract T cells in the following days[10]. Once T cells communicate with antigen-presenting cells such as macrophages, they too contribute to the proinflammatory or anti-inflammatory milieu. Other studies have seen that without the infiltration of phagocytic cells such as macrophages, T cells are unable to infiltrate the nerve[12]. These observations reinforce the need to assess the influence of CXB-NE on macrophages and their relationship to the role of T cells in the neuroinflammatory response in both males and females.

In this study, we examined sex-specific relief from neuroinflammation and hypersensitivity following CCI injury achieved by COX-2 inhibition from a single intravenous injection of CXB-NE. This is of particular importance, because NSAIDs have been previously thought to be ineffective for neuroinflammatory pain relief at non-toxic dosages[37]. We found that male and female rats experiencing CCI of the sciatic nerve exhibited quantitatively equivalent

mechanical hypersensitivity as measured by the von Frey technique. When male and female CCI rats were given the same intravenous injection of CXB-NE, male rats exhibited a complete reversal of their mechanical allodynia persisting for five days, whereas female rats achieved only partial relief over the same time course. We also examined the presence of immunological cells within the fasciculated sciatic nerve such as CD68-positive macrophages, CD3e-positive T cells, CD4-positive cells, and CD8-positive cells to explore the sex differences between their involvement in inflammation, and the effect of treatment on their presence. Even though males and females exhibit quantitatively the same level of hypersensitivity to nerve injury as well as both having increased macrophages following CCI, the female response to the therapeutic nanoemulsion is quantitatively and qualitatively different, revealing previously unknown pharmacodynamic differences between male and female COX-2 inhibition in neuroinflammation.

3.2 Results

3.2.1 Treatment Effect on Mechanical Allodynia

Mechanical sensitivity was measured every other day prior to and after CCI surgery on the sciatic nerve using the up-down von Frey method [51,54,74,75] (Fig. 3.1a). Once CCI was performed, male and female rats exhibited quantitatively equivalent withdrawal thresholds across the experimental time course, ultimately exhibiting hypersensitivity averaging approximately 2-3 g, which dropped from a baseline of ~16 g (Fig. 3.1b, c). The injection of drug-free nanoemulsion (DF-NE) on day 8 did not exacerbate or alleviate mechanical hypersensitivity in either male or female rats (Fig. 3.1b, c). When CXB-NE was administered to male rats, significant mechanical hypersensitivity was relieved for 5 days post administration (Figure 3.1b) (*Treatment x Time* $F_{77,}$

$_{759}$ = 8.906, p < 0.0001; day 10 p = <0.0001, day 12 p = < 0.0001, day 14 p = < 0.0001). A similar bell curve response, representative of relief from hypersensitivity, could be seen in females beginning with the first measurement taken after injection on day 10 and lasting until day 16. However, the female response to CXB-NE was attenuated when compared to males, reaching statistically significant relief for 1 day at day 12 (Fig. 3.1c) (*Treatment x Time* $F_{77, 759}$ = 8.906, p < 0.0001; CXB-NE vs CCI p = 0.0031, CXB-NE vs DF-NE p = 0.0073). At days 10 (p = 0.0061) and 12 postsurgery (p < 0.0001), this relief was significantly different between the male and female CXB-NE groups (Fig. 3.1d).

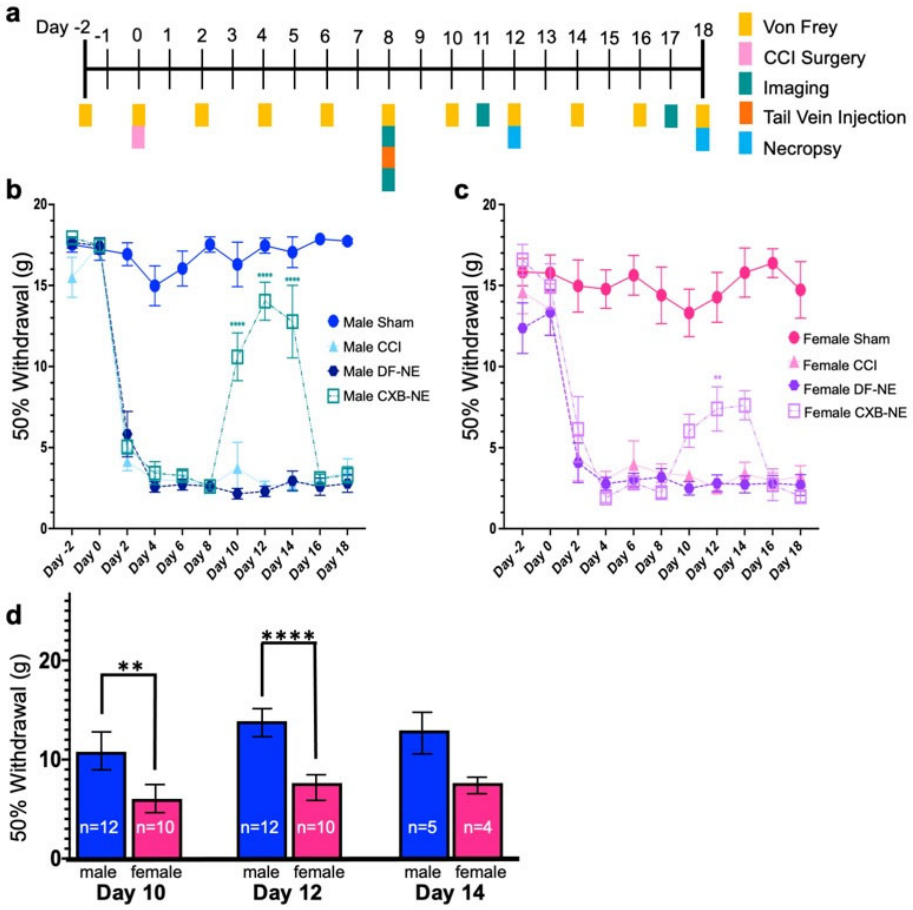

Figure 3.1. Mechanical hypersensitivity caused by CCI and the difference in pain relief from celecoxib-loaded nanoemulsion (CXB-NE). **a**. Timeline of animal behavior and drug

(Figure 3.1 continued) administration for both male and female groupings. **b**. Male hyperalgesia and allodynia was significantly relieved for at least 5 days following CXB-NE administration compared to both the CCI and DF-NE treatment groups. **c**. Female allodynia and hyperalgesia were significantly relieved 1 day after CXB-NE administration via tail vein injection compared to the CCI and DF-NE treatment groups. **d**. Summary of the sex differences in pain relief in drug-treated CCI animals at days 10, 12, and 14, with females (pink) experiencing significantly less relief than males (blue). Data is displayed as averages ± SEM. * ≤ 0.05, ** ≤ 0.01, *** ≤ 0.001, **** ≤ 0.0001. Number of animals included at 12 days post CCI (Sham ♂ = 4, ♀ = 4, CCI ♂ = 6, ♀ = 5, DF-NE ♂ = 5, ♀ = 4, CXBNE ♂ = 6, ♀ = 6). Number of animals included at 18 days post CCI (Sham ♂ = 4, ♀ = 5, CCI ♂ = 5, ♀ = 5, DF-NE ♂ = 6, ♀ = 5, CXBNE ♂ = 5, ♀ = 4). Male and female behavioral data was compared using a two-way ANOVA with a Tukey's post hoc analysis.

3.2.2 Assessment of Cellular Involvement of Neuroinflammation

Both males and females treated with CXB-NE experienced the peak of their relief from mechanical hypersensitivity four days following injection (Fig. 3.1b, c); therefore, a subset of animals were sacrificed on day 12 to examine the changes in the infiltration of immune cells at the site of injury on that day. A second set of animals of both sexes were sacrificed on day 18 to examine cellular infiltration once relief from hypersensitivity had dissipated. The status of the estrous cycle in the females did not affect the results as all the females appeared to be on the same cycle (Fig A1.1). Furthermore, given that female rats have a 4-day estrous cycle, and that the female progression to and degree of hypersensitivity perfectly matches that of the males (Fig 3.1b, c), it appears that the estrous cycle is not playing a significant role in influencing the rat's

behavior for these conditions. Because CXB-NE is phagocytosed and delivered by infiltrating macrophages, the presence of the infiltrating macrophages, which would have the most direct effect on the nerves was quantified in the sciatic nerve (Fig. 3.2 and Fig. A2.2)

During maximum relief at day 12, the sham surgical control had few if any CD68-positive (CD68+) macrophages detected within the sciatic nerve in either sex (Fig. 3.2b, f). Once CCI was performed, a significant number of infiltrating macrophages could be detected in the sciatic nerve in both males and females (Fig. 3.2c, g). CCI animals that received an injection of drug free nanoemulsion (DF-NE) exhibited a level of CD68+ macrophages (Fig. 3.2d, h) that was similar to that seen in CCI only animals (Fig. 3.2c, g). The animals that were given CXB-NE had a significant reduction in the number of infiltrating macrophages at the site of injury (female $F_{3,15} = 28.99$, $p < 0.0001$; male $F_{3,17} = 30.10$, $p < 0.0001$) when compared to their CCI (female $p = 0.0450$, male $p = 0.0019$) and DF-NE (female $p = 0.0175$, male $p = 0.0006$) counterparts (Fig. 3.2e, i). While day 12 CCI females treated with CXB-NE presented with a significant reduction in the number of infiltrating macrophages compared to their CCI and DF-NE same sex counterparts, they interestingly had significantly more macrophages than males treated with CXB-NE ($F_{5,5} = 1.732$, $p = 0.0088$). Assessment of the near infrared DiR signal from the nanoemulsion revealed no significant difference between the percentage of macrophages that phagocytosed the nanoemulsion, as observed between the sexes (Fig. 3.3).

Once male and female CXB-NE rats returned to mechanical hypersensitivity by day 18, the level of macrophage infiltration was equivalent to that of DF-NE treated animals as well as CCI animals that received no treatment (Fig. A2.2)

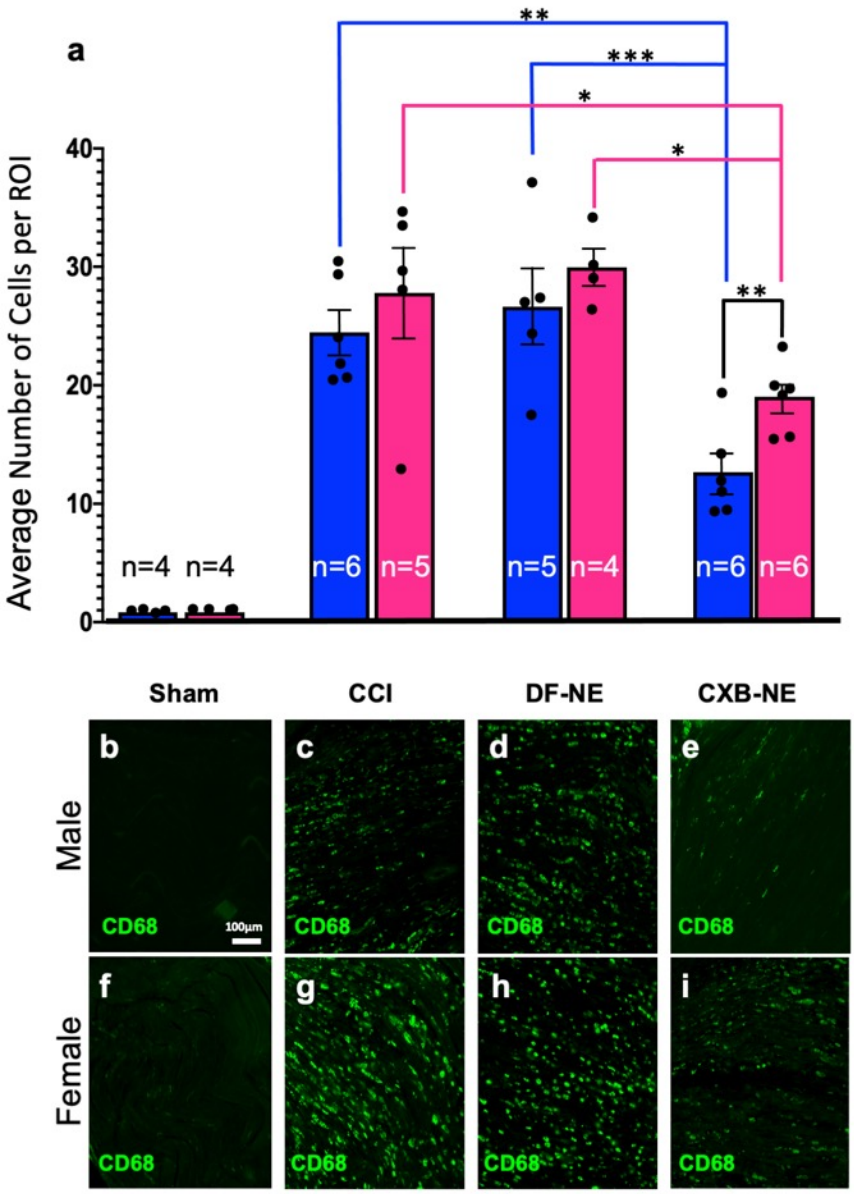

Figure 3.2. Day 12 macrophage infiltration after CCI decreases significantly in both male and female injured nerves treated with CXB-NE. However, CXB-NE treated females exhibited significantly more infiltrating CD68+ cells than similarly treated males. **a**. Average number of CD68+ macrophages per region of interest (ROI) across sex (male-blue, female-pink) and condition. Data is displayed as averages ± SEM. * ≤ 0.05, ** ≤ 0.01, *** ≤ 0.001, **** ≤ 0.0001. **b**. **- i**. Immunofluorescence staining for CD68+ macrophages in the sciatic nerve. Data

Figure 3.2 (continued) was analyzed using a two-way ANOVA and a Tukey's post-hoc analysis. Sex differences between treatment was done using For treatment, sex effects were examined using an unpaired two-tailed t-test.

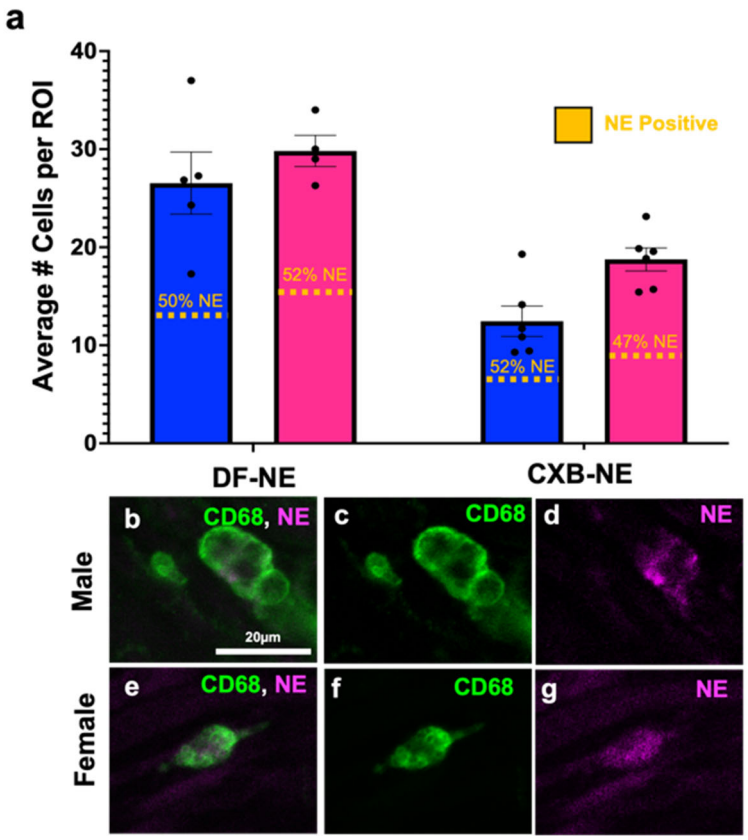

Figure 3.3. Nanoemulsion is equally phagocytosed by both male and female macrophages **a.** Nanoemulsion is taken up by 47-52% of macrophages regardless of sex or treatment. DF-NE n = 5 (male), 4 (female); and CXB-NE n = 6 (male), 6 (female). **b.**, **c.**, & **d.** CD68+ macrophage in male sciatic exhibit internalized nanoemulsion DiR signal **(d.),** as do infiltrating macrophages in the injured female sciatic nerve **e.**, **f.**, **& g.** with detectable DiR nanoemulsion **(g.).**

In order to examine the influence of the decreased number of inflammatory macrophages on other immune cells resulting from CXB-NE treatment, we examined the cell-specific

expression of CD3e, CD4 and CD8 by immunohistochemistry. When the sciatic nerve was examined 12 days post CCI, the majority of the CD3e+ T cells were localized to the epineurium (Fig. 3.4b, Fig. 3.4f), and little to no T cells were found within the nerve bundle itself in either sex or any condition (Fig. 3.5). While examining CD3e positive T cells, tissues were also co-stained for CD8 to visualize cytotoxic T cells that were positive for both CD3e and CD8 [12] (Fig. 3.4d, 3.4h), as well as CD4 to visualize helper T cells that were positive for both CD3e and CD4[99] (Fig. 3.4c, 3.4g). Even though the vast majority of T cells were localized in the epineurium of both males and females (Fig. 3.4b, 3.4f), cells singularly stained with CD8 could be seen infiltrating the fasciculated nervous tissue (Fig. 3.4d., 3.4h). We chose to quantify these CD8+ immune cells in the nerve track. Animals that underwent sham surgery had no CD8+ cell infiltration (Fig. 3.5b, 3.5f). All animals who underwent CCI surgery with or without injection of nanoemulsion had a significant increase in CD8+ cells (Fig. 3.5c-e and 3.5g-i) compared to the sham surgical control. Although there was no significant effect of CXB-NE treatment on CD8+ cells in either males or females, the female CCI, DF-NE, and CXB-NE groups all tended to have a higher relative abundance of CD8+ cells at the site of injury than their male counterparts.

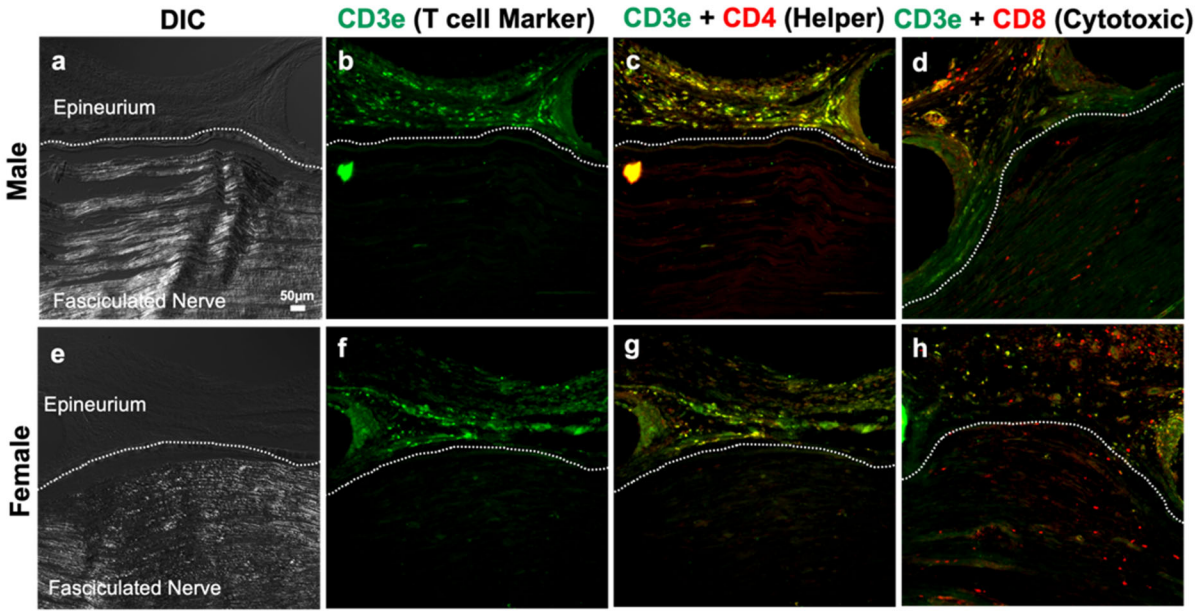

Figure 3.4. T cells localize to the epineurium of the sciatic nerve **a/e.** Demonstrate the ability to differentiate the fasciculated nerve from the epineurium using differential interference contrast (DIC). **b/f.** The CD3e pan-T cell marker shows localization of T cells in the epineurium. **c/g.** Shows that the CD4 subtype marker (red) co-localizes with CD3e (green) heavily in the epineurium with sparse occasional CD4 only staining occurring within the fasciculated nerve. **d/h.** Shows that CD8 (red) occasionally co-localizes with CD3e in the epineurium but also is more frequently present without CD3e within the fasciculated nerve. Panels d and h are located from a different slide than panels a-c and e-g due to compatibility of primary antibodies.

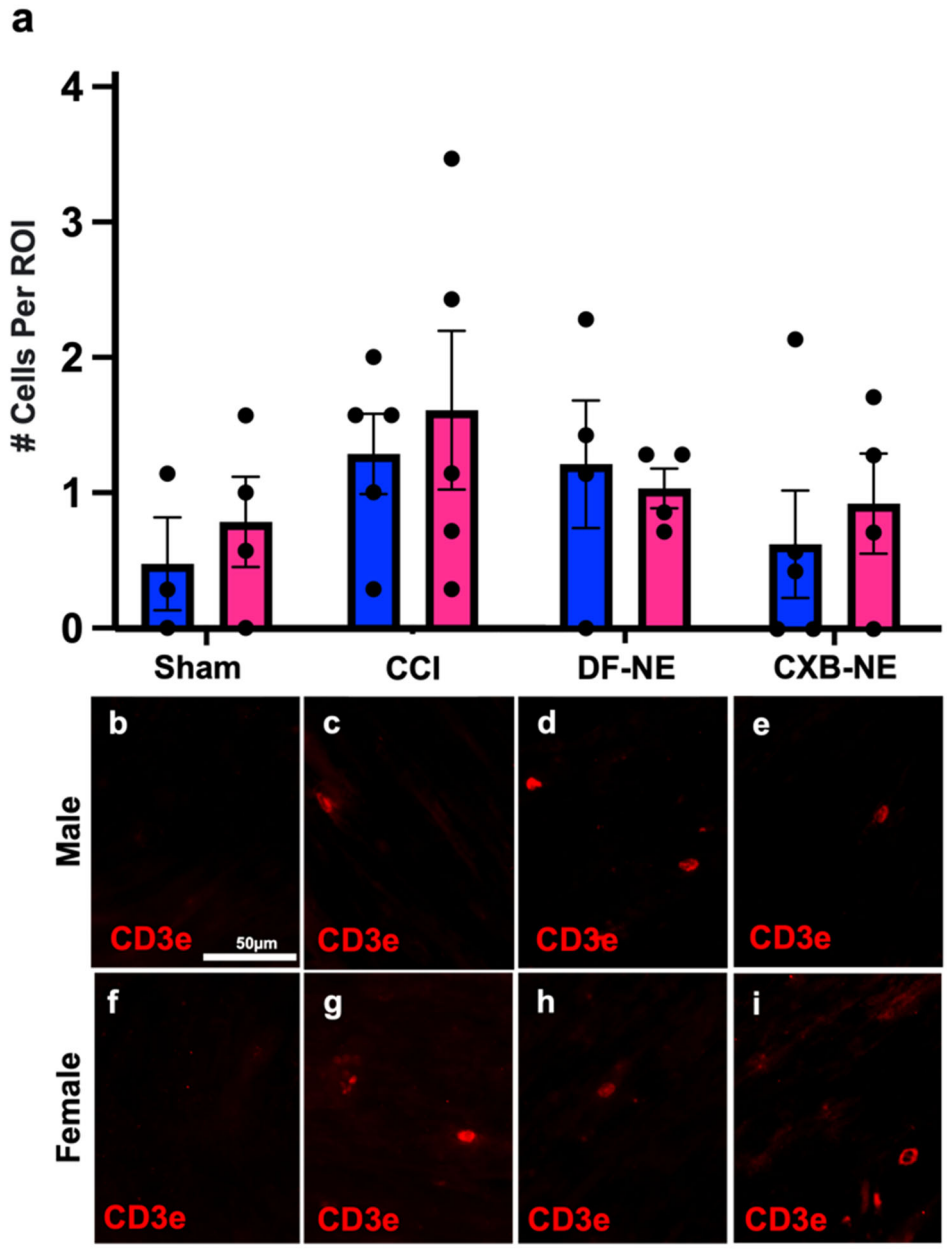

Figure 3.5. CD3e+ T cells are present at a low density in the fasciculated nerve; their number unchanged by CCI surgery, DF-NE or CXB-NE drug delivery. Data is displayed as averages ± SEM. Sham n = 3 (male), 4 (female); CCI n = 5 (male), 5 (female); DF-NE n = 4 (male), 4 (female); and CXB-NE n = 5 (male), 4 (female).

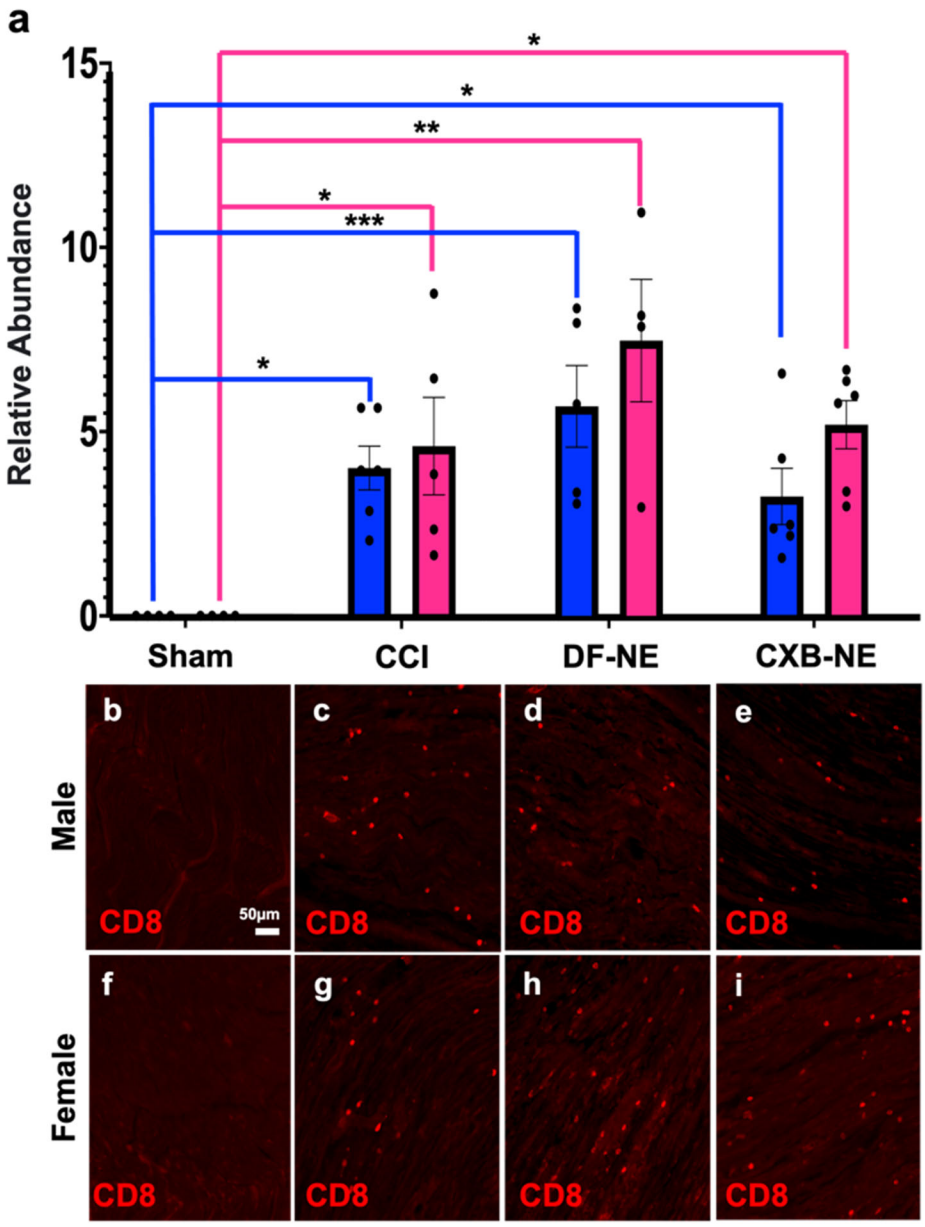

Figure 3.6. CD8+ cells are recruited to the site of injury after CCI and recruitment is not significantly affected by CXB-NE treatment. **a.** CD8+ cell recruitment into the injured nerve by sex (female-pink, male-blue). Data is displayed as averages ± SEM. * ≤ 0.05, ** ≤ 0.01, *** ≤ 0.001, **** ≤ 0.0001. **b.-i.** Immunofluorescence staining for CD8+ cells in the sciatic nerve. Sham n = 4 (male), 4 (female); CCI n = 6 (male), 5 (female); DF-NE n = 5 (male), 4 (female); and CXB-NE n = 6 (male), 6 (female). Data was analyzed using a two-way ANOVA and a

Figure 3.6 (continued) Tukey's post-hoc analysis. Sex differences between treatment was done using For treatment, sex effects were examined using an unpaired two-tailed t-test.

3.3 Discussion

Here, we demonstrate that under the same surgical conditions of nerve injury (CCI), male and female rats exhibit transitions to quantitatively equivalent hypersensitivity. Furthermore, we demonstrate for the first time that in females, a single low-dose injection of CXB-NE can reduce neuroinflammation and mechanical hypersensitivity. However, this reduction is not as effective as in male rats similarly treated [51,54,55,57]. We are therefore able to investigate how female neuroinflammation and associated hypersensitivity can be attenuated using celecoxib nanotherapy. This is noteworthy because previously, the use of COX-2 inhibitors were not thought to be effective in treating female neuroinflammation at non-toxic dosages[37]. The histological observations reveal that the density of infiltrating macrophages at the site of neuronal injury correlates with behavioral hypersensitivity. CCI females that were treated with CXB-NE exhibited a significant reduction in the number of infiltrating macrophages in the injured nerve as compared to female controls and behaviorally, they exhibited attenuated hypersensitivity. However, females did not achieve the same degree of relief from hypersensitivity as that observed in males similarly treated. Correspondingly, while the CXB-NE treated females had fewer infiltrating macrophages at the site of injury than the females experiencing hypersensitivity, they nonetheless exhibited a higher degree of inflammation than males. Assessment of the phagocytosis of the theranostic nanoemulsion revealed that there was equivalent engulfment of therapeutic by macrophages between sexes. Thus, these observations led us to investigate whether CXB-NE would alter the infiltration of other immune cells into the

site of injury, such as T cells, which have been shown to be sexually dimorphic at influencing inflammatory pain [27,73]. Taken together, the use of CXB-NE COX-2 inhibiting theranostic nanoemulsion reveals a pharmacodynamic sex difference in neuroinflammation and relief from hypersensitivity.

In order to examine sex differences in mechanical hypersensitivity relief, both male and female rats underwent CCI of the sciatic nerve. Mechanical withdrawal was measured before and after treatment with the theranostic nanoemulsion. Furthermore, to examine the involvement of inflammatory cells, the affected sciatic nerve tissues were collected at the peak of pain relief as well as at day 18 once hypersensitivity had returned. Here, we show that male and female rats that have experienced identical CCI of the right sciatic nerve exhibit an equivalent progression to mechanical hypersensitivity. In other words, males and females feel the same amount of pain with the same nerve injury. This study also found that male and female rats were both significantly relieved with a single injection of CXB-NE (Fig. 3.1b, c). However, when these injured male and female rats were treated with a theranostic nanoemulsion containing the NSAID celecoxib, we showed that while females achieved significant pain relief, they did not achieve the same level of pain relief as males (Fig. 3.1d). This sex difference in pain relief correlates with the density of infiltrating macrophages in the CXB-NE condition (Fig. 3.2). A few studies of NSAIDS in both sexes have also seen unequal relief from NSAID usage in females when compared to males. In one of these studies, healthy volunteers experienced induced inflammatory pain; the authors then assessed the ability of the nonselective COX inhibitor ibuprofen to provide relief. Here they found that male volunteers but not females received analgesia[100]. Chillingworth and colleagues[101] extended on these differences by examining COX involvement in hypersensitivity in mice. They showed that in the inflammatory

CFA model, COX-1 and COX-2 appear to play an additive role in female inflammation formation, while in males, the pain response is mainly driven by COX-2. Another study, exploring male and female response to CFA treatment in rats, found a similar phenomenon to that of Chillingworth et al[33] with the nonselective COX inhibitors working the best in females to reduce allodynia and the COX-2 inhibitor working the best in males to reduce inflammation[102]. Our study further adds to these findings by being the first to evaluate sex differences by inhibition of COX-2 in neuroinflammation with a celecoxib nanoemulsion (CXB-NE). Here we revealed sex differences resulting from the inhibition of COX-2 in both mechanical hypersensitivity and the extent of macrophage-driven inflammation. The results presented here, along with those of Chillingworth[101] and Craft[102], indicate that inhibition of COX-2 is most effective in providing relief for male neuroinflammation, while relief in females appear to include involvement of COX-2 activation as well as other factors that appear to contribute to their neuroinflammatory hypersensitivity.

While both males and females experience activation and recruitment of infiltrating macrophages during a neuroinflammatory response of an injured nerve, females have heightened responses to PGE_2 postinjury [103]. This fact along with the fact that there are more infiltrating macrophages could contribute to the behavioral difference in the females treated with CXB-NE where the relief from hypersensitivity is less than that of males receiving an equivalent dose. Why there are more macrophages infiltrating the injured nerve in females and what other underlying fundamental biological differences exist between males and females is unclear. Nonetheless, this is an important finding given that COX inhibitors are one of the most commonly prescribed pain treatments. Although NSAIDs have been shown to be effective in reducing inflammatory pain in both sexes [104], the research on the sex-specific efficacy of

NSAIDs for neuroinflammatory pain has been limited. One of the challenges is that with limited bioavailability of NSAIDs, safe systemic dosages are insufficient for providing effective therapy for human neuropathic pain [37]. Despite this fact, the composition of CXB-NE and the nanoemulsion's high surface-to-volume ratio increases the bioavailability of celecoxib [105]. Coupled with the fact that the theranostic nanoemulsion is internalized in the cytoplasm of macrophages, the cells that celecoxib can act on, the effective dosage is dramatically less than what is needed compared to oral systemic therapy [51,54]. In this way, the pharmacology of CXB-NE allows it to be effective in treating the hypersensitivity that is associated with neuroinflammatory pain. The increased efficacy at a low dosage avoids toxicity to off-target tissues and organs and is achieved by cell-specific delivery of the drug precisely in the injured tissue. To our knowledge, this is the first time that a safe systemic dosage of COX-2 inhibition has been reported to be effective at relieving female neuroinflammatory pain.

We also explored inflammation at the cellular level during CCI neuronal injury, demonstrating that macrophages infiltrate the injured nerve (Fig. 3.2). During maximum pain relief from CXB-NE, macrophages are still present at the site of injury; however, there is a significant decrease in their numbers when compared to both male and female DF-NE and CCI conditions. Here, we reveal that the response to CXB-NE differs between males and females at both the behavioral and cellular levels (Figs. 3.1 & 3.2). Furthermore, we show that when hypersensitivity returns, CXB-NE treated sciatic nerves exhibit to a similar macrophage infiltration as that of the DF-NE and CCI conditions (Fig. A2.2). This suggests that the presence of macrophages within the nerve directly correlates to the mechanical hypersensitivity being experienced. Furthermore, the difference in relief seen by males and females is not due to the percentage of infiltrating macrophages carrying CXB-NE or DF-NE as equivalent nanoemulsion

uptake was observed by both sexes (Fig. 3.3). Thus, it is not the ability to phagocytose the nanoemulsion and, in turn, deliver the theranostic nanoemulsion to the site of injury that is causing the difference in the relief from mechanical hyperalgesia or the level of inflammation, but how the attenuation of COX-2 causes differing neuroimmunological communication within the tissue for each of the sexes.

These data appear to contradict what others have reported about sex differences in phagocytic activity [23,106]. However, this prior observation involved an extremely different experimental model. A primary culture of splenic macrophages was derived from gonadectomized lizards, the wild gecko (*Hemidactylus flaviviridis*), which may function differently than macrophages in live rats. Mondal and Rai[106] treated these gecko-derived macrophages with dihydrotestosterone (DHT) or 17beta-estradiol (E2) at varying concentrations and found differences in phagocytic activity where the lizard cell culture macrophages treated with E2 had a higher rate of phagocytosis than those treated with DHT [106].

The transition to chronic pain is known to involve the interaction of the nervous system and the immune system[107]; knowing that other immune cells could be affected by the attenuation of COX-2 activity with CXB-NE[54,58] we focused specifically on T cells because they appear to have a unique contribution to female neuroinflammatory pain [23,67,108]. Furthermore, T cells can interact directly with macrophages during a neuroinflammatory response. Antigen-presenting cells such as macrophages can trigger a pro- or anti-inflammatory phenotype of T cells by affecting the cellular environment [109]. PGE_2 is able to alter regulatory T cells to inhibit activation, thereby attenuating neuroinflammation [110]. Helper T cells (CD3e and CD4 positive) have also been shown to help decrease neuroinflammation through the use of IL-10, while the role of cytotoxic T cells (CD3e and CD8 positive) is not well known[12]. While there was no

difference between sex or treatment for the presence of T cells in the facilitated nerve (Fig. 3.5); however, we did find that both cytotoxic and helper T cells were localized within the epineural sheath of the sciatic nerve near the site of injury rather than within the fasciculated nerve bundle (Fig. 3.4). Considering that these T cells appear to be confined to the epineural sheath, they nonetheless may influence neuropathy from afar via cytokine signaling rather than direct communication with the neurons themselves. IL-10 is a major cytokine used to communicate between macrophages and T cells influencing an anti-inflammatory response as well as aid in neuroregeneration[111]. Previous work has shown that IL-10 is essentially shut down shortly after CCI[112]. These finding regarding T cells are of particular interest because the majority of studies stating that T cells influence sexual dimorphism in the inflammatory response used indirect methods (flow cytometry, animal knockout models, adoptive splenocyte transfers, and qPCR [26,27,73,113,114]) and do not differentiate between the anatomical domains of the injured nerve.

We also observe a trend where a higher number of inflammatory cells appear to infiltrate the site of injury of the female sciatic nerve as compared to the similarly injured male sciatic nerve. The CCI, DF-NE, and CXB-NE conditions all exhibited higher infiltration of CD68+ and CD8+ cells in females (Fig. 3.2; Fig. 3.6). This observation is consistent with what has been reported by Klein and Flanagan [23], where females show stronger innate and adaptive immune responses than males. Given that human females exhibit more autoimmune diseases [115] and stronger reactions to immunization [116], it is of interest to consider that females may also have a sex specific peripheral neuroinflammatory response. Therefore, it is important that the evaluation of therapeutics is achieved in both sexes, as the immune responses to disease and treatment differ.

3.4 Conclusion

Here, we demonstrated that equivalent nerve injury results in quantitatively equivalent hypersensitivity in males and females. Our novel finding that the celecoxib nanoemulsion, CXB-NE, which we previously demonstrated as highly effective in males[51,54,57,76], is effective in females, but with reduced potency. Given that COX inhibitors are one of the most commonly prescribed analgesics[102], this sex differences in the response to therapy for neuroinflammation reiterates the need for therapeutics to be examined equally in males and females. Assuming that a given therapeutic will work equivalently in both sexes creates an opportunity for incomplete understanding of its effectiveness or its underlying fundamental biology[107]. Given the call to action to find a novel, non-opioid analgesic[107], the findings shown here are therefore, of great importance. Overall, these results show that there are similarities in the inception and perception of neuroinflammatory hypersensitivity between sexes, where both males and females report the same degree of pain-like behavior from equivalent nerve injury. Despite this, identical treatment with celecoxib theranostic nanoemulsion reveals a sex difference in the level of relief from hypersensitivity pain-like behavior achieved in chronic constriction injury. These results correlate with the sex difference in the degree of macrophage infiltration in the presence of CXB-NE, as well as the increased number of CD8+ cells at the site of injury in females. Lastly, our deeper evaluation of T cell involvement in neuroinflammation led to the discovery of T cells being confined to the epineural sheath and that the cytokines that they express may influence the injured nerves from that adjacent location. Our findings, along with others[58,101-103], further emphasize the need to clarify the mechanistic differences in the action of COX inhibition on the inflammatory milieu that result in these sex-specific differences in inflammation and in relief from hypersensitivity and pain-like behavior.

3.5 Material & Methods

3.5.1 Ethics Statement

Male (200 - 250 g) and female (150 - 200 g) Sprague-Dawley rats were purchased from Hilltop Lab Animals, Inc. (Springdale, PA). These experiments were carried out following the recommendations in the Guide for Care and Use of Laboratory Animals of the National Institutes of Health and the regulations of the Institutional Animal Care and Use Committee at Duquesne University under approved Protocol #1803-02 and in compliance with the ARRIVE guidelines (https://arriveguidelines.org). Rats were acclimated and maintained on a 12:12 hour light-dark cycle and housed on paper bedding with access to food and water *ad libitum*. Starting two days prior to surgery, animals were switched onto a special diet (Research Diets, Inc., New Brunswick NJ; Cat # AIN-93G) to avoid autofluorescence during near infrared imaging of the nanoemulsion in live animals. Animals were socially housed during acclimation. They were then individually housed once von Frey behavior began (two days prior to surgery) to establish baseline behavior; this was done to avoid rats from opening one another's wounds following surgery.

3.5.2 CCI Surgery

Male and female rats underwent chronic constriction injury (CCI) of the sciatic nerve as described by Bennett and Xie [75] and in accordance with our prior technique [51,54] to induce neuropathic pain and inflammation. Four sutures (McKesson 4-0 Chromic Gut Sutures, Cat # S635GX) were loosely tied around the sciatic nerve approximately 1 mm apart in CCI, DF-NE, and CXB-NE treated animals. Sham animals underwent identical surgery to expose the sciatic nerve, but no sutures were tied around the nerve.

3.5.3 Estrus Cycle Tracking

Vaginal swabs were collected for 4 consecutive days in order to establish their estrus cycle. Briefly, the vaginal canals of anesthetized rats were flushed with sterile saline and collected on a slide. The slide was allowed to dry. Then cells were fixed with 100% methanol and stained with 5% Giemsa stain for 20 minutes. Slides were then rinsed in diH_2O, dried, mounted with Permount (FisherScientific, Cat # SP15-100), and then imaged.

3.5.4 Behavioral Testing

To assess mechanical allodynia and the effectiveness of CXB-NE, von Frey Up-Down analysis was performed as previously described [51,54,74,81]. Testing was performed every other day including baseline behavior from 2 days before and on the day of surgery. Rodents were tested in separate same sex cohorts. Animals were acclimated for 30 minutes in individual plexiglass chambers with a mesh metal floor to allow access to paws. After acclimation, the left and right hind paws were tested using calibrated von Frey filaments (Stoelting Company, Cat # 58011). Rodents were probed with the filament in the middle of their hind paw for 3 seconds with the filament bent to a 30° angle. Positive responses were recorded through the visualization of a flick or quick lift. Animals were given a minimum of 30 seconds between probing of the same paw twice. Animals were randomly assigned to their groupings, and the behavioralist was blinded to animal treatment. Behavioral testing was scheduled as outlined in Figure 1a.

3.5.5 COX-2 Inhibiting Theranostic Nanoemulsion

The theranostic nanoemulsion used in this study was produced by microfluidization as reported earlier [51,58]. Briefly, celecoxib was dissolved in hydrocarbon oil, mixed with perfluoro-

15-crown-5 ether and nonionic surfactants, and emulsified using high shear processing, microfluidization on a M110 microfluidizer (Microfluidics, Westwood, MA, USA). CXB-NE and DF-NE were formulated with the near-infrared (NIR) fluorescent dye DiR and DiIC18(7) (1,1'-dioctadecyl-3,3,3',3' tetramethylindotricarbocyanine iodide) was added to hydrocarbon oil for fluorescent detection in tissues. Nanoemulsions were sterile filtered prior to use in animals and tested for colloidal properties, cell viability and stability as reported earlier [51,58].

3.5.6 Tail Vein Injection

Intravenous injections of DF-NE and CXB-NE were performed 8 days after surgery and following von Frey behavior analyses. Injections and near-infrared imaging inspection of injection quality were performed as described by Saleem et al. [76]. Investigators were blinded to the nanoemulsion treatment. Animals were anesthetized with respiratory isoflurane. Tails were warmed in water for 1 minute to dilate the lateral veins. Tails were then dried and sterilized with an alcohol pad. A 27G needle, bevel up, was placed distally into the lateral tail vein. Upon blood flashback, a syringe containing 300µL of DF-NE or CXB-NE (55.5 ng of celecoxib) was attached and slowly injected into the vein [51,54,76]; this dose was used for all animals. The quality of the tail vein injection was assessed using the near infrared LI-COR fluorescent imager (LI-COR BioSciences, Lincoln, NE). A quality injection should be cleared through the bloodstream, leaving little to no near infrared signal in the tail, except for the possibility of a tiny dot at the injection site. Animals with subcutaneous injections or a ruptured vein leading to an incomplete injection were removed from the study.

3.5.7 Tissue Processing

Rats were euthanized at the maximum relief from hypersensitivity at 12 days post CCI (Sham ♂ = 4, ♀ = 4, CCI ♂ = 6, ♀ = 5, DF-NE ♂ = 5, ♀ = 4, CXBNE ♂ = 6, ♀ = 6) or 18 days post CCI when the animals returned to pain-like behavior (Sham ♂ = 4, ♀ = 5, CCI ♂ = 5, ♀ = 5, DF-NE ♂ = 6, ♀ = 5, CXBNE ♂ = 5, ♀ = 4) by CO_2 asphyxiation. The sciatic nerves were immediately collected following euthanasia. All tissues were placed in 4% paraformaldehyde in 1X phosphate buffered saline (PBS) solution at 4°C for 24 hours. Tissues were then washed with 1X PBS, transferred into 30% sucrose in 1X PBS solution and kept at 4°C until embedded. Tissues were embedded in optimal cutting temperature compound (Tissue-Tek® OCT) and frozen in a bath of isopentane. Frozen tissue blocks acclimated to the cryostat (-25°C) were then sectioned on the cryostat at 20 μm thickness and collected on gelatin-coated slides (SouthernBioTech, Birmingham, AL; Cat # 100241-864). Slides were kept at -20°C until immunofluorescence staining was performed.

3.5.8 Immunofluorescence and Image Analysis

Tissues were stained with standard immunohistochemical protocols and recommendations of the antibody manufacturers as previously described [51,54]. Multistain procedures typically include nuclear staining (DAPI) and two other primary antibodies. Primary antibodies included an anti-CD68 [83] rabbit polyclonal antibody (ab125212) at a 1:400 dilution, an anti-CD3e mouse monoclonal antibody (MA1-90582) at a 1:500 dilution, an anti-CD4 mouse monoclonal antibody (ab33775) at a 1:500 dilution, and an anti-CD8 mouse monoclonal antibody (ab33786) at a 1:100 dilution. The secondary antibodies used were ThermoFisher's donkey anti-rabbit Alexa Fluor 488 (A21206) and goat anti-mouse Alexa Fluor 555 (A21127),

both at a 1:200 dilution. After the final washes, the slides were coverslipped with Prolong™ Diamond-DAPI (ThermoFisher).

Images were acquired and analyzed on a Nikon Eclipse Ni-U epifluorescence microscope with a 20X objective using Nikon NIS-Elements BR software (Version 5.02) for DAPI, 488 (FITC), 555 (TRITC), and DIC channels. Investigators were blinded to the treatment conditions while imaging and analyzing. Images were taken between the knots from the CCI surgery where inflammation was at its highest. Infiltrating immune cells were only counted if present within the fasciculated nerve bundle and not within the epineural sheath; this was determined by using the DIC overlay.

Quantification of macrophages and T cells used 7 regions of interest (140 μm x 140 μm) that were placed on the transmitted light image of the fasciculated axons of the sciatic nerve using the DIC view, and then individual CD68 positive or CD3e positive cells were counted. The average number of cells per region was compared across conditions.

When examining the percentage of CD68+ macrophages with the nanoemulsion, images were acquired on a Nikon Ti2 Eclipse inverted A1r confocal microscope. During this analysis, all macrophages in a field of view (212 μm X 212 μm) were counted, and then the number of those containing nanoemulsion were divided by the total number of macrophages in the field of view. Each animal was averaged within their treatment group to determine the percent of nanoemulsion-positive macrophages per sex and treatment.

Counting CD8-positive cells that infiltrated the fasciculated nerve required a different approach. Here, we counted the number of positive cells within the fasciculated nerve and divided this number by the total area counted. The cells per given area were then normalized. Data using CD68+ tissues for CCI and 1X CXB-NE males and females was used for a power

analysis to determine how many slides was necessary for IHC stains. An alpha value of 0.05 and a power of 80% were used. It was determined that an n of 2-3 was needed.

3.5.9 Statistical Analysis

All statistical analyses were performed using GraphPad 9.0.2 Prism Software. Quantification of the gram-force measures of pain-like withdrawal behavior utilizing the von Frey up-down method used a calculation of the 50% withdrawal thresholds [74] (50% withdrawal threshold = $(10^{[X_f + K\delta]})/10{,}000)$). The values for each time point, comparing sex and condition, were then analyzed by two-way ANOVA. Tukey's post hoc analysis for multiple comparisons of group means was performed following two-way ANOVA. The confidence interval was 95%, and the behavioral data displayed are presented as the mean ± SEM.

The immunofluorescent imaging data comparing macrophage, CD3e+ and CD8+ cell infiltration used two-way ANOVA to compare sex and treatment ANOVAs were used in conjunction with Tukey's post hoc analysis. For treatment, sex effects were examined using an unpaired two-tailed t-test. All immunofluorescent imaging data were calculated with a confidence interval of 95% and are displayed as the mean ± SEM with individual values plotted on the bar.

CHAPTER IV.

RNA-SEQ REVEALS SEX DIFFERENCES IN GENE EXPRESSION DURING PERIPHERAL NEUROINFLAMMATION AND IN RELIEF WITH COX-2 INHIBITING THERANOSTIC NANOEMULSION

Abstract

Given decades of neuroinflammatory research that focused on neuropathic pain only in males, there is an urgent need to better understand pain in females. This, paired with the fact that there currently is no long-term effective treatment for neuropathic pain furthers the need to evaluate how pain develops in both sexes and how it can be relieved. Here we show that CCI of the right sciatic nerve in male and female rats caused comparable levels of mechanical allodynia. Using a novel COX-2 inhibiting theranostic nanoemulsion, both sexes achieve equivalent sustained relief. Total RNA from affected DRG was sequenced to reveal sexually dimorphic differential gene expression responsive to neuroinflammation and also the COX-2 inhibition that caused relief. Of note, both males and females experience increased expression of *activating transcription factor 3* (*ATF3*) and *VGF nerve growth factor* (*VGF*); however, only the female DRG shows decreased expression of both following neuroinflammatory relief. Likewise, *corticotrophin releasing hormone* (*CRH*) expression increased in both sexes following neuroinflammation, but only decreased during relief in males. These are a few of the distinct sex differences in the differentially expressed genes identified in this study. Clearly, the underlying fundamental biology of pain and pain relief is different between the sexes.

Contribution's statement:

In this analysis of 10X CXB-NE, Brooke Deal and Dr. John Pollock conceived and designed the experiments in a CCI rat neuropathic model. Dr. Jelena Janjic designed the COX-2 inhibiting macrophage targeted theranostic nanoemulsion which Caitlin Crelli produced and validated *in vitro*. Brooke conducted the animal experiments with the assistance of Katy Philips. Qiagen performed the RNA extraction and RNA sequencing of the DRGs. Brooke performed all RNAseq data analysis. Brooke performed qPCR under the guidance of William King. Brooke and Katy (Figure 4.10) performed immunohistochemical assays. Katy and Dr. Pollock (Figure 4.10) imaged tissues and analyzed the results.

4.1 Introduction

Until recently, the vast majority of preclinical pain studies were performed exclusively in male rodent models with fundamental neurobiological studies exhibiting one of the biggest sex disparities[60]. Even though, in humans, females are more often affected by neuropathic pain[117, 118], the years of disproportionate research has led the chronic pain field to develop a male-biased literature[22]. For example, a recent review of pain literature found that for nearly a decade, the research published in a particular journal only reported results from male rodents or did not report sex as a variable 82% of the time[22]. In fact, this review summarized that for 127 different pain studies, an overwhelming 72.4% found their hypotheses to be true in males but not in females[22].

This biased body of research has skewed the understanding of pain biology and in turn led to issues in the translational aspect of therapeutics[119,120]. Current medications to treat pain include anticonvulsants, antidepressants, non-steroidal anti-inflammatory drugs (NSAIDs), and opioids[121, 122, 123, 45, 68]. However, for each, their adverse side effects often limit long-term use[5], and there is a growing body of research that is revealing sex differences in drug action[124, 125]. In order to help develop safer and more effective therapeutics, a closer evaluation of the development of neuropathic pain with a focus on sex differences is needed.

With the National Institute of Health's requirement for investigators to include sex as a biological variable (NOT-OD-15-102), more sex differences have been revealed in the development of neuropathic inflammatory pain [26, 27, 73, 103]. There have been a handful of studies evaluating the transcriptional differences between sexes experiencing neuroinflammatory pain [20,21,126-128]. During neuroinflammation, investigators have seen involvement from T cells, immune signaling pathways, changes in neuronal plasticity, as well as enrichment from other

genes involved in the neuronal immune crosstalk. However, the differential expression of genes that are responsive to pain relieving therapy between sexes has yet to be evaluated.

Previously, it has been thought that NSAIDs and COX-2 inhibitors were an ineffective treatment for neuropathic pain[37], nonetheless, our studies have repeatedly shown that a novel COX-2 inhibiting nanotheranostic nanoemulsion containing celecoxib (CXB-NE) is able to relieve mechanical allodynia caused by neuroinflammation at low, non-toxic dosages[51,54,55,57,58,68]. In our previous work using chronic constriction injury (CCI) of the rat sciatic nerve, we found that both males and females exhibited quantitatively equivalent hypersensitivity after injury as well as both sexes obtaining significant relief with a single dose of CXB-NE[68]. However, the amount of relief experienced is different between sexes with males experiencing about 5 days of relief, while females given the same dose achieve only partial relief for a shorter duration[68]. Considering that COX-2 inhibiting NSAIDs are one of the most commonly prescribed classes of pain-relieving drugs[129], and that over 80% of US adults reported using OTC pain medications each year[121], careful examination of the biological differences in pain relief between males and females is warranted.

This study elucidates transcriptional differences in the dorsal root ganglia (DRG), for male and female rats exhibiting hypersensitivity compared to animals experiencing relief. Distinct from our previous study[68], we find that by employing a modified 10X CXB-NE, we now can achieve complete pain relief in females, equivalent to males. The modified 10X CXB-NE has ten-times more celecoxib per nanodroplet than previous formulations[51,54,55,57,58,68].

The goal of this study is to assess transcriptional changes in both males and females during neuroinflammation and relief. Given that the males and females exhibit identical level of mechanical allodynia relief, we are now able to assess how the transcriptome changes in the

DRG following 10X CXB-NE treatment in both sexes; we are not revealing differences in the degree of behavioral pain relief. Even though both males and females are now experiencing similar allodynia and relief, sex differences that were evident while using 1X CXB-NE indicate that the underlying biology is different between sexes, which is verified through this study's results.

The sequencing of total RNA for each individual animal's L4/L5 DRG revealed significant differential expression in transcriptomes from naïve, hypersensitive, and animals experiencing relief. We find several hundred genes that exhibit differential expression in females in pain, distinct from that of males. Furthermore, we find that the gene expression that is responsive to celecoxib nanoemulsion therapy also differ between sexes. For example, the cAMP response element-binding (CREB) protein, *activating transcription factor 3* (*ATF3*) is differentially expressed being increased in the pain state. However, when pain-relieving therapy from the celecoxib nanoemulsion is present, *ATF3* RNA and protein are significantly reduced in females, but not so in males. These, and other observations demonstrate fundamental differences in the gene expression associated with pain and pain relief between the sexes.

4.2 Results

4.2.1 Celecoxib theranostic nanoemulsion alleviates mechanical hypersensitivity caused by neuroinflammation in both males and females

In order to assess the mechanical allodynia induced by CCI of the right sciatic nerve and demonstrate the relief received via 10X CXB-NE treatment, von Frey up-down analysis was used. The animal procedure timeline can be seen in Figure 1a. Briefly, baseline behavior was acquired 2 days prior to surgery and on day 0, preceding the CCI procedure. These two days

were averaged to give a baseline 50% withdrawal threshold of around 16-17 g for both sexes (Figure 4.1b and c). Following CCI, all groups that underwent the procedure showed decreased 50% withdrawal thresholds that levels off at about 5 g in both sexes. Similar time courses in the decrease in withdrawal were seen between both sexes. This indicates that both males and females are experiencing the same degree of provoked hypersensitivity resulting from the CCI surgery. Tail vein injections of either 10X CXB-NE or drug free nanoemulsion (DF-NE) were delivered on day 8 following von Frey behavior analysis. Receiving DF-NE did not decrease mechanical withdrawal threshold, nor did it produce any type of relief. On days 10 and 12, males (Figure 4.1b) and females (Figure 4.1c) both experienced significant relief when compared to their CCI (Day 10 ♂ $p = 0.0338$, Day 12 ♂$p< 0.0001$, Day 10♀$p < 0.0001$, Day 12♀< 0.0001) and DF-NE counterparts (Day 10 ♂ $p = 0.0404$, Day 12 ♂< 0.0001, Day 10♀$p < 0.0001$, Day 12♀< 0.0001). We also find that on day 12, the 10X CXB-NE treated males and females exhibit no statistically significant difference in behavior as compared to their naïve counterpart. Furthermore, by assessing the female estrus cycle, we find that it does not have an overt effect on the hypersensitivity behavior or the female response to 10X CXB-NE.

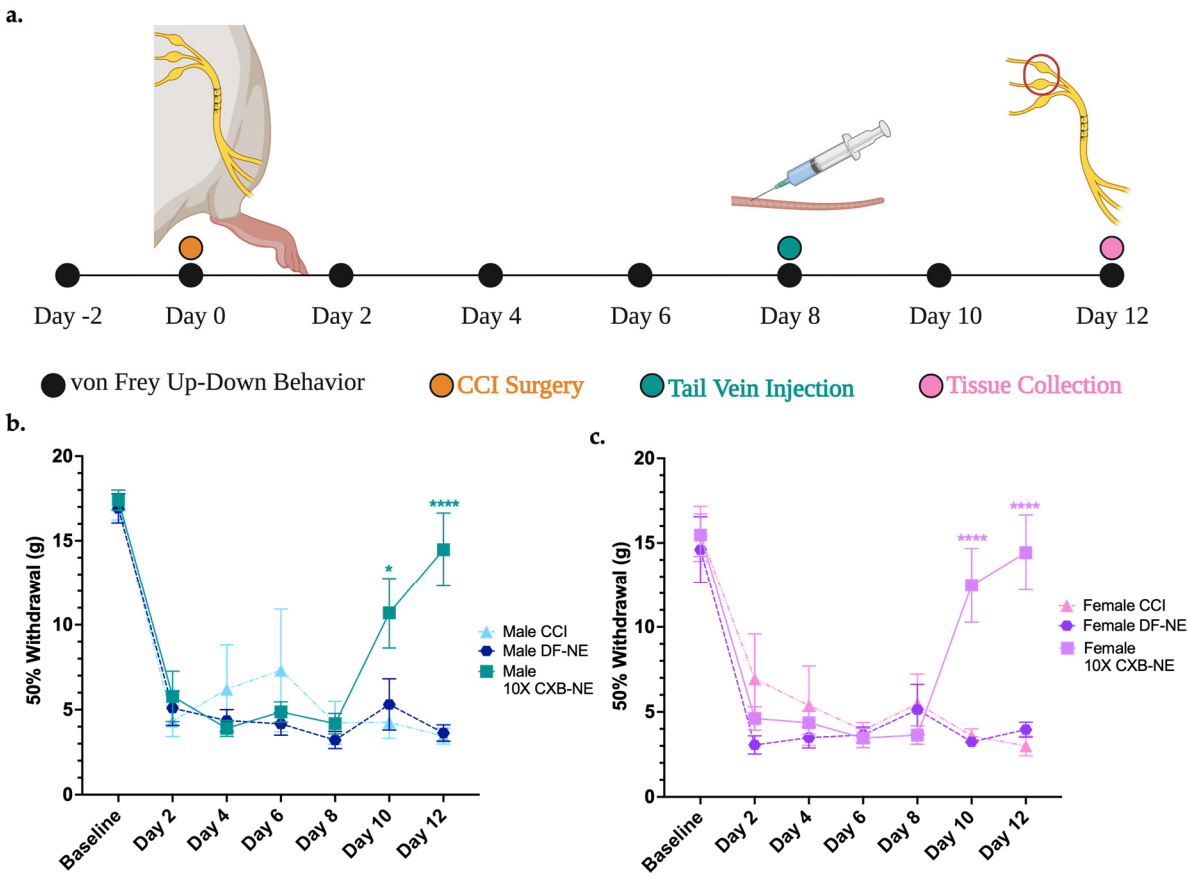

Figure 4.1. Mechanical allodynia relieved by single dose of Celecoxib theranostic nanoemulsion in both sexes. **(a)** Timeline of animal procedures, dosage treatment, and tissue collection for male and female cohorts. Estrus swabs collected on days 8-12. **(b)** Male mechanical allodynia observed post-surgery is significantly relieved following 10X CXB-NE on day 8 when compared to CCI and DF-NE groups. Number of animals included are CCI n = 4, DF-NE n = 7, and 10X CXB-NE n = 7. **(c)** Female von Frey behavioral data shows significant relief from mechanical allodynia following theranostic nanoemulsion treatment when compared to CCI and DF-NE groups. Number of animals included are CCI n = 6, DF-NE n = 7, and 10X CXB-NE n = 7. Data displayed as averaged ± SEM. *≤ 0.05, **≤ 0.01, ***≤ 0.001, ****≤ 0.0001. Male and female behavioral data was compared using a two-way ANOVA with a Tukey's post hoc analysis. Figure 1a. created with BioRender.com, and Figure 1b and c created using Prism 9.4.1.

4.2.2 Mechanical hypersensitivity induced by neuroinflammation and relief following 10X CXB-NE treatment causes a shift in gene expression in the DRG

The DRG corresponding to the right sciatic nerve were collected on day 12 (Figure 4.1a) and total RNA was extracted from both the RL4 and RL5 DRG for each animal. The RNA from the RL4 and the RL5 DRG were sequenced together as one sample per animal. Samples were sequenced using the NextSeq High Output flow cell instrument (Illumina Inc., San Diego, CA). An average of 74 million reads per sample were generated with lengths of 75bp; 85% of the raw reads on average were then mapped to the *Rattus norvegicus* (mRatBN7.2) genome using CLC Genomics Workbench 22.0.2 (Qiagen, Hilden, Germany).

A gene expression heatmap is used to look at the relatedness of the individual samples from each animal and the gene clusters shared across them. CLC Genomics Workbench was used to make hierarchically clustered heatmaps of both male (Figure 4.2a) and female (Figure 4.2b) rat transcriptomes. Using Euclidean distance and complete linkage of clusters, the top 90 genes with the highest coefficient of variation were used to cluster rat DRG transcriptomes by relatedness (genes listed in Tables A3.12 and A3.13). As seen in Figure 2a, male CCI and DF-NE cluster closest together sharing the most related transcriptomes while 10X CXB-NE animals are the least related to the other three groups having the most unique gene expression. Figure 2b shows a different pattern in the treated females where CCI is distinct from naïve, and 10X CXB-NE and DF-NE are most closely related.

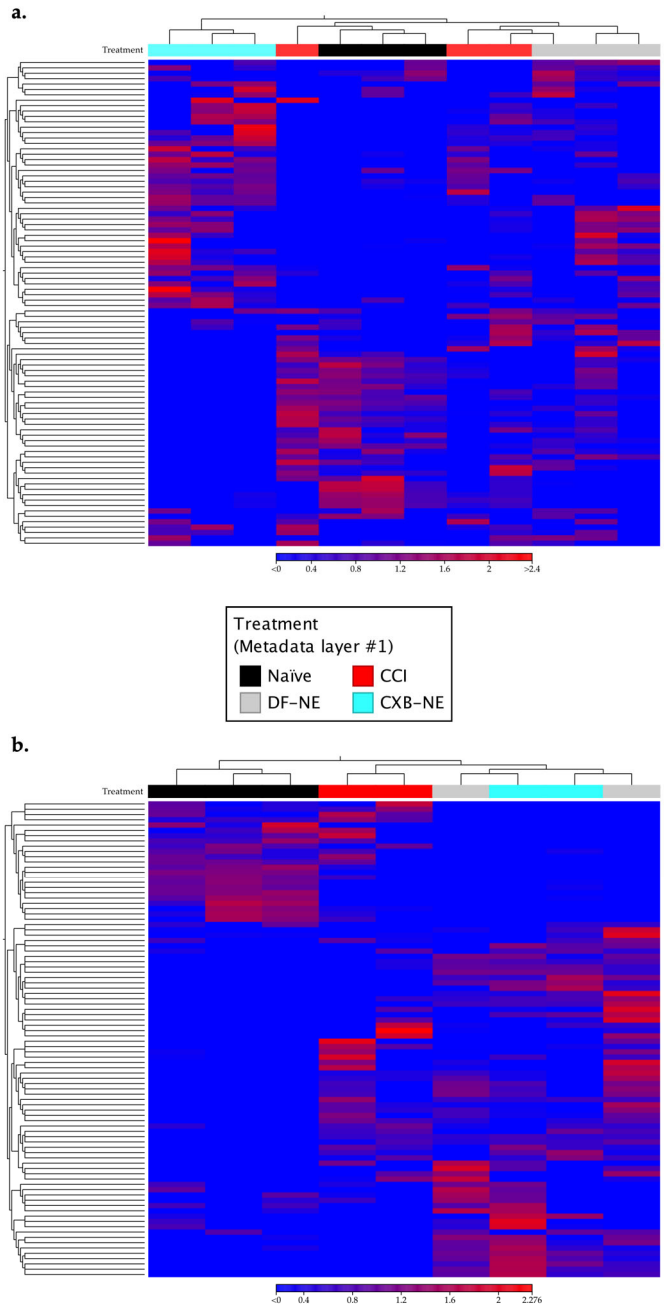

Figure 4.2. Heatmaps displaying the 90 genes with the highest coefficients of variation in male and female DRGs. **(a)** Euclidean linkage was used to display the normalized log counts per million (CPM) values to show the similarities and differences in male individual animals. Naïve n = 3, CCI n = 3, DF-NE n = 3, CXB-NE n = 3. Genes are listed in Table A3.12. **(b)** Female treated individual animals displayed along the x-axis separated by their Euclidean distance of

Figure 4.2 (continued) their gene's normalized log CPM values. Naïve n = 3, CCI n = 2, DF-NE n = 2, CXB-NE n = 2. Heatmaps made in CLC Genomics Workbench 22.0.2. Genes are listed in Table A3.13.

Differential gene expression analyses were then performed to examine those gene sets that are differentially expressed during male neuroinflammation (CCI vs Naïve), female neuroinflammation (CCI vs Naïve), male neuroinflammatory relief (10X CXB-NE vs DF-NE), and female neuroinflammatory relief (10X CXB-NE vs DF-NE) (Figure 4.3). With the genes filtered by fold change ≥ ± 1 and the adjusted p-value (false discovery rate (FDR)) of ≤ *0.05, there were 265 differentially expressed genes (DEGs) in male neuroinflammation, 977 DEGs in female neuroinflammation, 333 DEGs in male neuroinflammatory relief, and 16 DEGs in female neuroinflammatory relief.* These gene sets were then compared between sexes to look at gene expression changes unique to males, gene expression changes unique to females, and shared changes in gene expression across conditions.

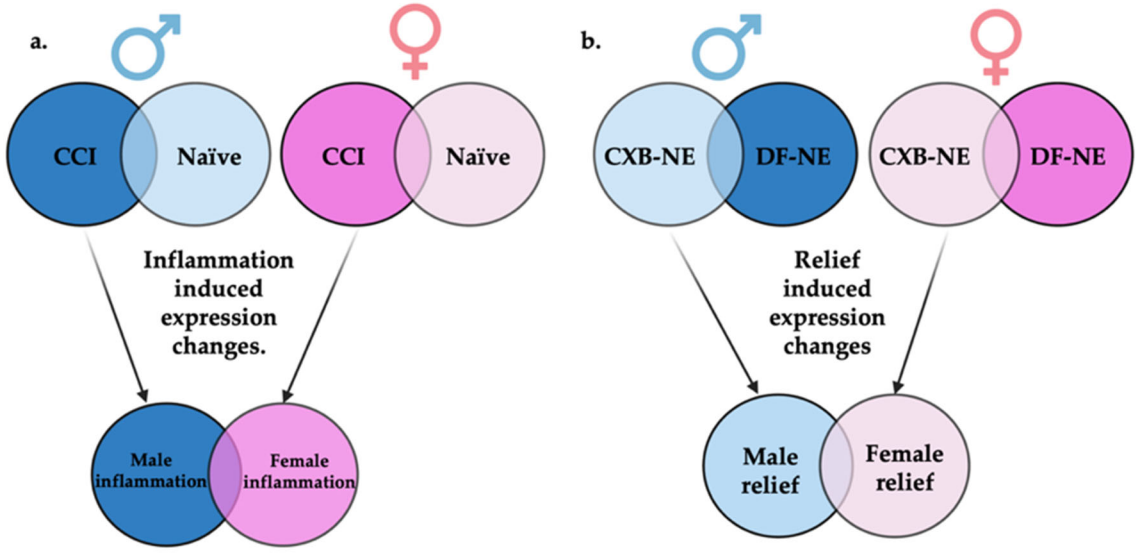

Figure 4.3. Display of comparisons made between RNA-seq generated gene sets. **(a)** Genes

Figure 4.3 (continued) differentially expressed between CCI and naïve of the same sex will be termed inflammatory induced gene expression changes. When these inflammatory gene sets are compared between sexes, genes uniquely differentially expressed in males or females can be identified. **(b)** Genes differentially expressed between 10X CXB-NE and DF-NE of the same sex will be termed relief induced gene expression changes. When these gene sets are compared between sexes, genes uniquely differentially expressed during relief in males or females associated can be identified. Figure made with BioRender.com.

4.2.3 Female neuroinflammation

CLC Genomics Workbench was used to perform a differential expression analysis between female CCI DRG transcriptomes and female naïve DRG transcriptomes. The genes differentially expressed between the two would be those attributed to neuroinflammation. Whole transcriptomes were compared and normalized using the internal normalization method of trimmed mean of M values (TMM).

Filtering using the FDR p-value $\leq$ *0.05 and fold change of* greater than $\pm$ 1, revealed that a total of 977 genes were differentially expressed following CCI in the female DRG. A total of 485 genes were significantly up-regulated, and 492 genes were significantly down-regulated. The top 25 significantly up-regulated (Table 4.1) and down-regulated (Table 4.2) genes are shown. These DEGs were then displayed using a volcano plot in Figure 4.4a with the top 10 DEGs highlighted. By focusing on the genes that exhibit differential expression with the greatest FDR significance, we identify some genes with very large fold-change, which represent genes that are either turned on or off, as well as genes with modest fold-change of less than 2.

Table 4.1. Top 25 significantly up-regulated genes in the female DRG following CCI of the sciatic nerve.

Gene Name	FDR p-value	Fold Change	ENSMBL ID
Npy	3.97E-42	12.38	ENSRNOG00000046449
Atf3	2.17E-23	7.83	ENSRNOG00000003745
Flrt3	2.46E-23	2.51	ENSRNOG00000004874
Igfbp3	4.67E-15	1.8	ENSRNOG00000061910
Gap43	8.54E-15	1.58	ENSRNOG00000001528
Cacna2d1	7.36E-13	1.91	ENSRNOG00000033531
Ktn1	1.04E-12	1.53	ENSRNOG00000012255
Stac2	2.03E-12	8.59	ENSRNOG00000004805
Gal	5.39E-12	2.92	ENSRNOG00000015156
Gadd45a	7.04E-12	2.25	ENSRNOG00000005615
Vip	9.71E-11	18.83	ENSRNOG00000018808
AC130970.1	1.41E-10	3.77	ENSRNOG00000042445
Csrp3	3.07E-10	43.49	ENSRNOG00000014327
Ccl2	1.04E-09	2.76	ENSRNOG00000007159
Sema6a	2.08E-09	2.06	ENSRNOG00000004033
gene:ENSRNOG00000067276	2.18E-09	1.81	ENSRNOG00000067276
Il7r	2.44E-09	1.98	ENSRNOG00000065741
Prkar2b	3.04E-09	1.46	ENSRNOG00000009079
Bdnf	8.06E-09	2.14	ENSRNOG00000047466
Vgf	1.52E-08	2.25	ENSRNOG00000001416
Stmn4	7.06E-08	1.83	ENSRNOG00000053334
Sox11	1.17E-07	2.53	ENSRNOG00000030034
Acsl4	1.23E-07	1.43	ENSRNOG00000019180
Hs2st1	1.53E-07	1.44	ENSRNOG00000012549
Il13ra1_2	1.69E-07	1.76	ENSRNOG00000013170

Table 4.2. Top 25 significantly down-regulated genes in the female DRG following CCI of the sciatic nerve.

Gene ID	FDR	Fold Change	ENSMBL Gene ID
Sema7a	2.41E-21	-1.82	ENSRNOG00000007687
Igfbp6	7.15E-15	-2.12	ENSRNOG00000010977
RT1-CE16	8.18E-15	-3.45	ENSRNOG00000065254
Tagln	4.07E-11	-2.27	ENSRNOG00000017628
Iscu	9.71E-11	-1.51	ENSRNOG00000000701
Hapln4	7.04E-10	-1.9	ENSRNOG00000049949
Gsn	2.18E-09	-1.46	ENSRNOG00000018991
Lgi3	2.08E-08	-1.44	ENSRNOG00000011323
Hcn2	1.02E-07	-1.46	ENSRNOG00000008831
gene:ENSRNOG00000070982	1.17E-07	-2.08	ENSRNOG00000070982
Capg	1.17E-07	-3.01	ENSRNOG00000013668
gene:ENSRNOG00000006471	1.51E-07	-1.69	ENSRNOG00000006471
gene:ENSRNOG00000062930	1.97E-07	-1.95	ENSRNOG00000062930
Fxyd6	2.21E-07	-1.44	ENSRNOG00000016412
Islr	3.48E-07	-1.76	ENSRNOG00000048924
Fxyd7	3.63E-07	-1.4	ENSRNOG00000021067
Abhd8	3.96E-07	-1.73	ENSRNOG00000000054
Tlcd3b	4.91E-07	-1.4	ENSRNOG00000019914
Sptb	4.94E-07	-1.39	ENSRNOG00000006911
Kcnh2	6.60E-07	-1.42	ENSRNOG00000009872
Kcnc3	7.18E-07	-1.41	ENSRNOG00000019959
Fbln2	7.35E-07	-1.37	ENSRNOG00000007338
Kcns1	7.67E-07	-1.67	ENSRNOG00000013681
Oaz1	1.08E-06	-1.4	ENSRNOG00000019459
Bphl	1.08E-06	-1.92	ENSRNOG00000017577

In order to better identify which classes of genes or pathways were overrepresented by these differentially expressed genes, a gene set enrichment analysis was performed using Metascape (Metascape.org). Metascape combines multiple enrichment analyses platforms such as Gene Ontology (GO) processes, Kyoto Encyclopedia of Genes and Genomics (KEGG) pathways, Reactome gene sets, Cytoscape and NCBI. All 977 differentially expressed genes in females were included in the pathway enrichment analysis with the upregulated genes being evaluated in one analysis and the downregulated genes being evaluated in a second analysis.

The two lists of significantly up-regulated and significantly down-regulated genes were analyzed separately. Figure 4b shows the top 20 enriched pathways that were significantly up-regulated including *cytokine signaling in immune system* (R-HSA-1280215) and *neuron projection development* (GO:0031155) among others. Figure 4c shows the top 20 enriched down-regulated pathways including the *synapse organization* (GO:0050808) and the *nervous system development* (R-HSA-9675108).

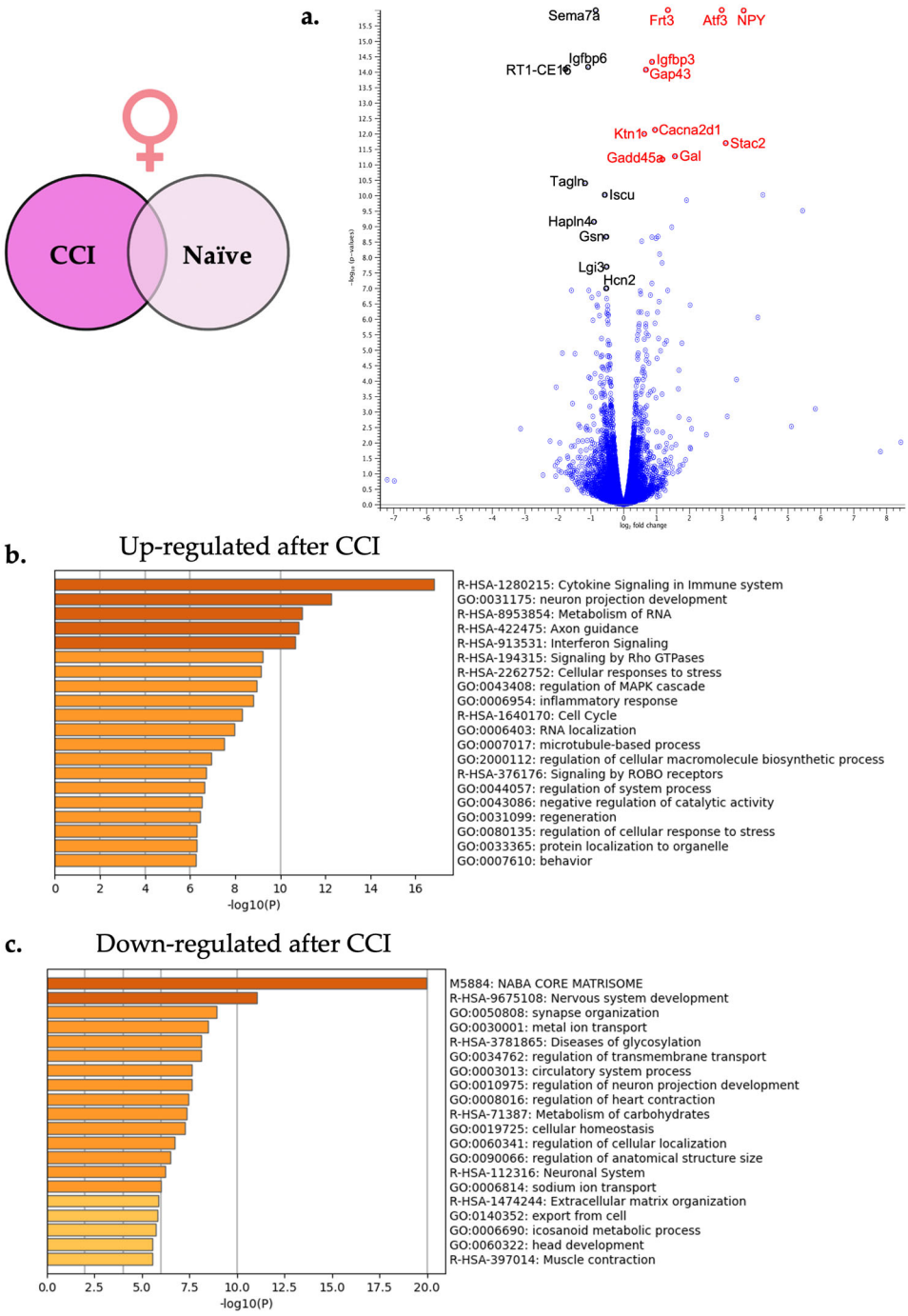

Figure 4.4. Neuroinflammation in females causes differential gene expression in the affected DRG. **(a)** For visual clarity the volcano plot features all of the differentially expressed genes due to neuroinflammation in the female DRG highlighting the top 10 significantly up-regulated (red) and top 10 significantly down-regulated genes (black). **(b)** Metascape enrichment analysis of the

Figure 4.4 (continued) top 20 up regulated biological pathways following neuroinflammatory induction. **(c)** Metascape enrichment analysis of the top 20 down-regulated biological pathways following neuroinflammatory induction.

4.2.4 Male neuroinflammation

Using a differentially expressed gene analysis as described above, expressed RNA sequences from male CCI DRG were compared to male naïve DRG to reveal differentially expressed genes altered by neuroinflammation. From this comparison, a total of 265 genes were differentially expressed following peripheral neuroinflammation with 126 genes significantly up-regulated and 139 genes significantly down-regulated. The top 25 up and down-regulated genes are featured in Tables 3 and 4 with the top 10 significantly up and down-regulated highlighted in the volcano plot in Figure 4.5a.

Table 4.3. Top 25 significantly up-regulated genes in the male DRG following CCI of the sciatic nerve.

Gene ID	FDR	Fold Change	ENSMBL Gene ID
Npy	2.67E-20	5.79	ENSRNOG00000046449
Thbs1	9.51E-14	1.88	ENSRNOG00000045829
Cfh	1.54E-09	1.49	ENSRNOG00000030715
NEWGENE_1308171	1.77E-07	1.58	ENSRNOG00000029792
RT1-Ba	5.72E-07	1.94	ENSRNOG00000000451
Atf3	1.26E-06	4.12	ENSRNOG00000003745
gene:ENSRNOG00000067832	1.55E-06	41.86	ENSRNOG00000067832
Lmo7	1.59E-06	1.62	ENSRNOG00000060775
Slc13a4	2.38E-06	1.63	ENSRNOG00000011184
H3f3c	2.63E-06	9.77	ENSRNOG00000032401
Phldb2	2.88E-06	1.43	ENSRNOG00000002171
Fyb1	3.53E-06	1.85	ENSRNOG00000013886
Aldh1a2	4.15E-06	2.52	ENSRNOG00000055049
Cp	4.44E-06	1.37	ENSRNOG00000011913
Sema3c	7.25E-06	1.33	ENSRNOG00000006526
Fbln1	9.61E-06	1.58	ENSRNOG00000014137
Emp1	1.65E-05	1.55	ENSRNOG00000008676
Slc6a20	3.23E-05	1.85	ENSRNOG00000068642
Thbd	3.55E-05	1.55	ENSRNOG00000004687
Cilp	4.37E-05	2.43	ENSRNOG00000029911
Crh	5.12E-05	33.5	ENSRNOG00000012703
Slc6a13	5.12E-05	1.99	ENSRNOG00000012876
Lcp1	5.12E-05	1.3	ENSRNOG00000010319
Cfb	5.12E-05	1.61	ENSRNOG00000051235
Fat4	6.83E-05	1.32	ENSRNOG00000028335

Table 4.4. Top 25 significantly down-regulated genes in the male DRG following CCI of the sciatic nerve.

Gene ID	FDR	Fold Change	ENSMBL Gene ID
Egr2	1.47E-20	-2.39	ENSRNOG00000000640
Zbtb16	1.27E-12	-3.05	ENSRNOG00000029980
Myh2	1.27E-12	-8.77	ENSRNOG00000065740
Sptbn5	1.39E-10	-1.45	ENSRNOG00000059260
Tnnc2	6.32E-08	-4.81	ENSRNOG00000015155
Dbp	7.66E-08	-1.49	ENSRNOG00000021027
Ttn	1.48E-07	-2.60	ENSRNOG00000069271
Tnnt3	1.77E-07	-3.66	ENSRNOG00000020332
Mertk	1.90E-07	-1.44	ENSRNOG00000017319
Tsc22d3	4.98E-07	-1.38	ENSRNOG00000056135
Eno3	6.24E-07	-2.42	ENSRNOG00000004078
Gpd1	6.88E-07	-1.73	ENSRNOG00000056457
Sgk1	1.55E-06	-1.58	ENSRNOG00000011815
AABR07005775.1	1.55E-06	-3.71	ENSRNOG00000047124
Neb	4.44E-06	-1.7	ENSRNOG00000006783
Hif3a	7.25E-06	-5.79	ENSRNOG00000017198
Acta1	7.25E-06	-3.23	ENSRNOG00000017786
Per1	8.28E-06	-1.94	ENSRNOG00000007387
Aatk	1.14E-05	-1.32	ENSRNOG00000004392
Fkbp5	1.19E-05	-1.56	ENSRNOG00000022523
Mb	1.30E-05	-5.5	ENSRNOG00000004583
Prx	1.34E-05	-1.3	ENSRNOG00000018369
Mylpf	2.18E-05	-3.55	ENSRNOG00000017645
Ntng2	3.12E-05	-1.34	ENSRNOG00000013694
Atp1a3	3.38E-05	-1.28	ENSRNOG00000020263

Enriched biological processes were elucidated using Metascape gene set enrichment analysis under express analysis parameters. Again, all 265 differentially expressed genes in males were included in the pathway enrichment analysis with the upregulated genes being evaluated in one analysis and the downregulated genes being evaluated in a second analysis. Overrepresented pathways in both the up and down-regulated differentially expressed gene sets are shown in Figure 4.5a and 4.5b. Some of the enriched up-regulated biological processes include *cytokine signaling in the immune system* (R-HSA-1280215) and *regulation of cell adhesion* (GO:0030155), while some down-regulated processes include *myelination* (GO:0042552) and *actin-filament based process* (GO:0030029).

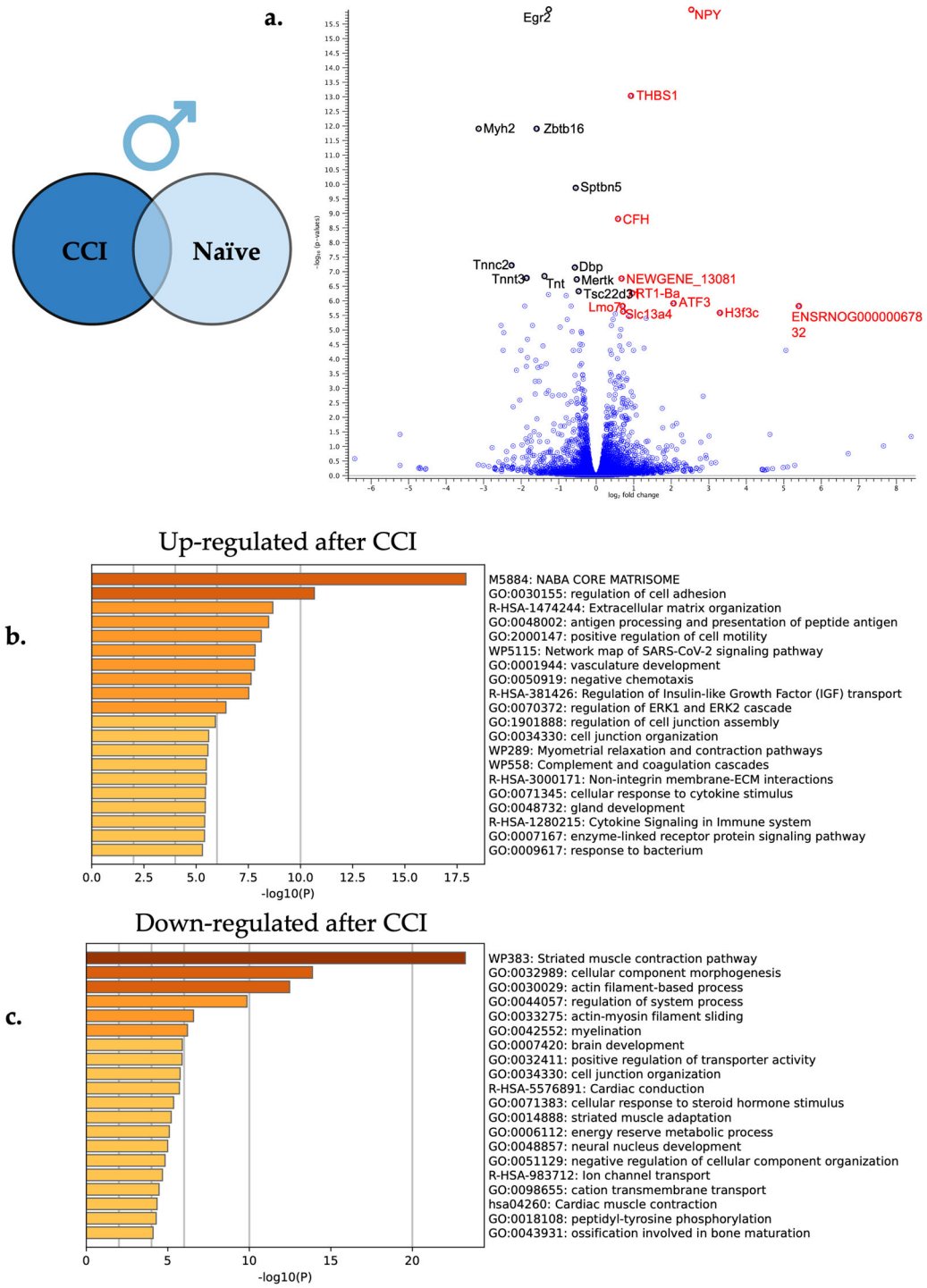

Figure 4.5. Neuroinflammation in males causes differential gene expression in the affected DRG**. (a)** For visual clarity the volcano plot features all of the differentially expressed genes due to neuroinflammation in the male DRG highlighting the top 10 significantly up-regulated (red)

Figure 4.5 (continued) and top 10 significantly down-regulated genes (black). **(b)** Metascape enrichment analysis of the top 20 up-regulated biological pathways following neuroinflammatory induction. **(c)** Metascape enrichment analysis of the top 20 down-regulated biological pathways following neuroinflammatory induction.

4.2.5 Female neuroinflammatory relief

Differential gene expression brought on by peripheral neuroinflammatory relief in females (Figure 4.1c) was examined using CLC Genomics Workbench and comparing the transcriptomes from female 10X CXB-NE DRG and female DF-NE DRG. Using the same filtering parameters of FDR p-value ≤ 0.05 and a fold change greater than ±1, this analysis showed a total of 16 DEGs. Of the 16 DEGs, 6 of them were significantly up-regulated (Table 4.5) and 10 of them were significantly down-regulated (Table 4.6). These 16 significant DEGs are featured on the volcano plot in Figure 6a.

Table 4.5. Most significantly up-regulated genes in the female DRG following neuroinflammatory reduction via COX-2 inhibition.

Gene ID	FDR	Fold Change	ENSMBL Gene ID
Myom3	1.10E-04	9.43	ENSRNOG00000032994
Grhl3	8.06E-04	13.29	ENSRNOG00000029427
Txnip	2.92E-03	1.35	ENSRNOG00000021201
Hba-a3	4.00E-02	2.51	ENSRNOG00000047321
Sptb	0.02	1.31	ENSRNOG00000006911
Gas2l3	0.03	1.3	ENSRNOG00000063755

Table 4.6. Most significantly down-regulated genes in the female DRG following neuroinflammatory reduction via COX-2 inhibition.

Gene ID	FDR	Fold Change	ENSMBL Gene ID
Ass1	3.44E-04	-2.4	ENSRNOG00000008837
Vgf	4.22E-04	-1.63	ENSRNOG00000001416
Atf3	8.06E-04	-2.09	ENSRNOG00000003745
Sox11	1.35E-03	-1.66	ENSRNOG00000030034
Lce1f_2	8.47E-03	-5.85	ENSRNOG00000066187
Sema6a	1.00E-02	-1.67	ENSRNOG00000004033
AABR07007068.1	2.00E-02	-1.3	ENSRNOG00000017438
Gadd45a	3.00E-02	-1.49	ENSRNOG00000005615
Jun	4.00E-02	-1.28	ENSRNOG00000026293
Rbp4	5.00E-02	-1.68	ENSRNOG00000015518

Metascape gene enrichment analysis using all 16 differentially expressed genes was performed as described earlier. The two separate lists of up-regulated DEGs and down-regulated DEGs did not show any enriched biological processes for up-regulated genes involved in female neuroinflammatory relief; however, 6 enriched biological processes were revealed from the down-regulated genes. These enriched biological processes include *PID ATF-2 pathway* (M166) and *cellular response to growth factor stimulus* (GO:0071363).

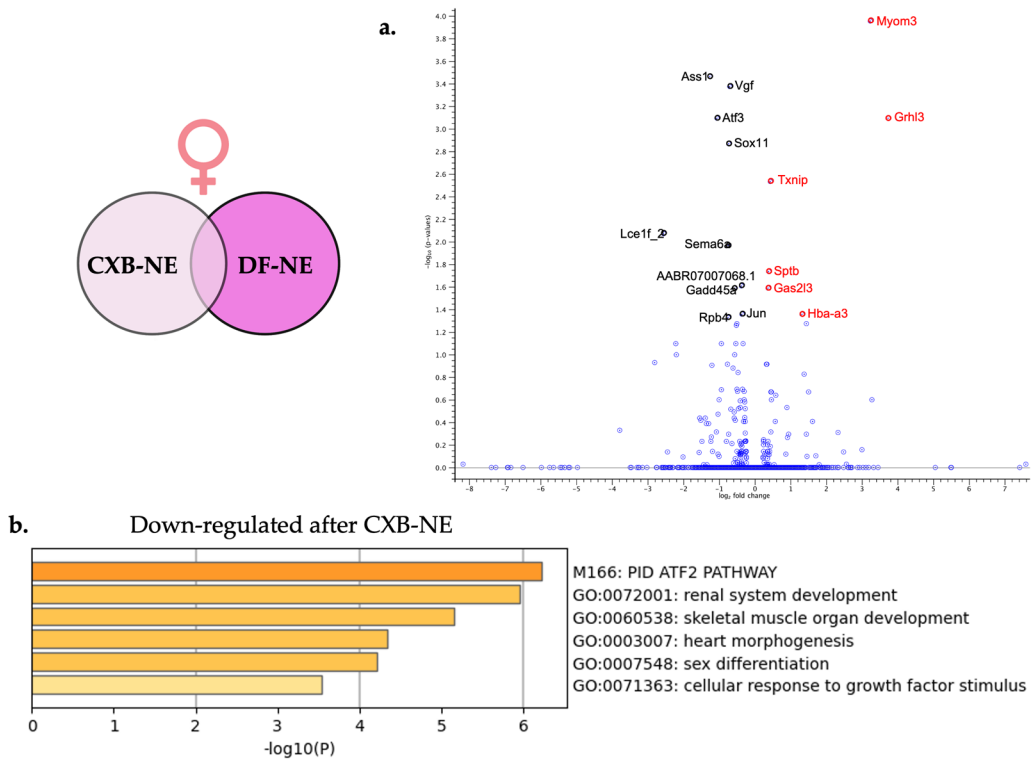

Figure 4.6. Neuroinflammatory relief via COX-2 inhibition in females causes differential gene expression in the affected DRG. **(a)** For visual clarity the volcano plot features all of the differentially expressed genes due to neuroinflammatory relief in the female DRG highlighting the top 6 significantly up-regulated (red) and top 10 significantly down-regulated genes (black). **(b)** Metascape enrichment analysis of the down-regulated biological pathways following neuroinflammatory reduction via COX-2 inhibition.

4.2.6 Male neuroinflammatory relief

Differential gene expression analysis comparing male 10X CXB-NE DRG transcriptomes to male DF-NE DRG transcriptomes was performed as described in previous sections. This comparison led to a gene list of 333 differentially expressed genes when males were experiencing neuroinflammatory relief (Figure 4.1b) compared to their drug free counterparts. Of these 333 differentially expressed genes, 302 were significantly up-regulated and 31 were

significantly down-regulated. The top 25 of these significantly up-regulated and down-regulated genes are featured in Tables 7 and 8 with the top 10 of each being highlighted in the volcano plot in Figure 4.7a.

Table 4.7. Top 25 most significantly up-regulated genes in the male DRG following neuroinflammatory reduction via COX-2 inhibition.

Gene ID	FDR	Fold Change	ENSMBL Gene ID
S100a9	9.37E-30	5.68	ENSRNOG00000011483
S100a8	4.11E-28	6.24	ENSRNOG00000011557
Mmp8	2.84E-20	7.53	ENSRNOG00000009907
Ngp	1.18E-18	5.2	ENSRNOG00000024330
Ighm	7.44E-17	3.2	ENSRNOG00000034190
Ccl21	3.78E-16	4.15	ENSRNOG00000034290
Slc4a1	2.75E-13	3.69	ENSRNOG00000020951
Fcnb	8.83E-13	5.16	ENSRNOG00000009342
Ccn3	1.45E-12	2.77	ENSRNOG00000008697
Mfap4	1.60E-12	2.41	ENSRNOG00000045683
NEWGENE_1308171	3.27E-11	1.45	ENSRNOG00000029792
Mpo	2.04E-10	5.12	ENSRNOG00000008310
Ptprc	2.46E-10	1.81	ENSRNOG00000000655
AABR07060872.1	4.76E-10	4.5	ENSRNOG00000049829
Serpinb1b	5.34E-10	11.78	ENSRNOG00000034229
Mki67	5.34E-10	2.22	ENSRNOG00000028137
Ccn2	1.13E-09	2.03	ENSRNOG00000015036
Sell	1.25E-09	3.82	ENSRNOG00000002776
Lyz2	1.25E-09	1.67	ENSRNOG00000005825
Prg2	3.12E-09	4.31	ENSRNOG00000008394
RatNP-3b	4.14E-09	7.22	ENSRNOG00000038135
Hemgn	1.29E-08	3.6	ENSRNOG00000009436
Slfn4_1	1.39E-08	2.24	ENSRNOG00000057092
Plac8	6.24E-08	3.18	ENSRNOG00000002217
Acta2	1.26E-07	1.77	ENSRNOG00000058039

Table 4.8. Top 25 most significantly down-regulated genes in the male DRG following neuroinflammatory reduction via COX-2 inhibition.

Gene ID	FDR	Fold Change	ENSMBL Gene ID
Dbp	8.42E-15	-1.72	ENSRNOG00000021027
Prim1	3.56E-05	-2.01	ENSRNOG00000031993
Hmgb1	6.42E-05	-2.03	ENSRNOG00000058908
Per1	9.79E-05	-1.53	ENSRNOG00000007387
Zbtb16	2.66E-04	-1.89	ENSRNOG00000029980
Gjc3	5.34E-04	-1.29	ENSRNOG00000001329
Sgk1	6.90E-04	-1.3	ENSRNOG00000011815
Clvs1	1.03E-03	-2.39	ENSRNOG00000006919
Chrna3	1.92E-03	-1.38	ENSRNOG00000013829
Acer2	1.95E-03	-1.52	ENSRNOG00000007637
Nptx1	2.13E-03	-1.23	ENSRNOG00000003741
Crh	3.52E-03	-21.61	ENSRNOG00000012703
Trim45	4.35E-03	-2.29	ENSRNOG00000015347
AABR07034445.1	7.52E-03	-2.27	ENSRNOG00000038610
Ntng1	7.98E-03	-1.25	ENSRNOG00000031136
Klf9	8.75E-03	-1.23	ENSRNOG00000014215
Sema7a	8.99E-03	-1.23	ENSRNOG00000007687
RGD1564899	0.01	-2.20	ENSRNOG00000049942
Nr1d1	0.02	-2.20	ENSRNOG00000009329
Gnai1	0.02	-1.21	ENSRNOG00000057096
Kcng1	0.03	-1.39	ENSRNOG00000054314
Chst2	0.03	-1.19	ENSRNOG00000047734
Slitrk2	0.03	-1.19	ENSRNOG00000011562
Svip	0.03	-1.19	ENSRNOG00000037137
Ncam2	0.03	-1.19	ENSRNOG00000002126

Enriched biological processes were evaluated with Metascape gene annotation and analysis resource under the express analysis settings. All 333 differentially expressed genes were included in the analysis split into two runs of upregulated and down regulated differentially expressed genes. The enriched biological processes from the up-regulated gene list are shown in Figure 7a with the two top enriched biological processes being *neutrophil degranulation* (R-HSA-6798695) and *leukocyte migration* (GO:0050900). The down-regulated differentially expressed genes influenced by neuroinflammatory relief enriched pathways such as *neuron*

projection development (GO:0031175) and *cellular response to steroid hormone stimulus* (GO:0071383).

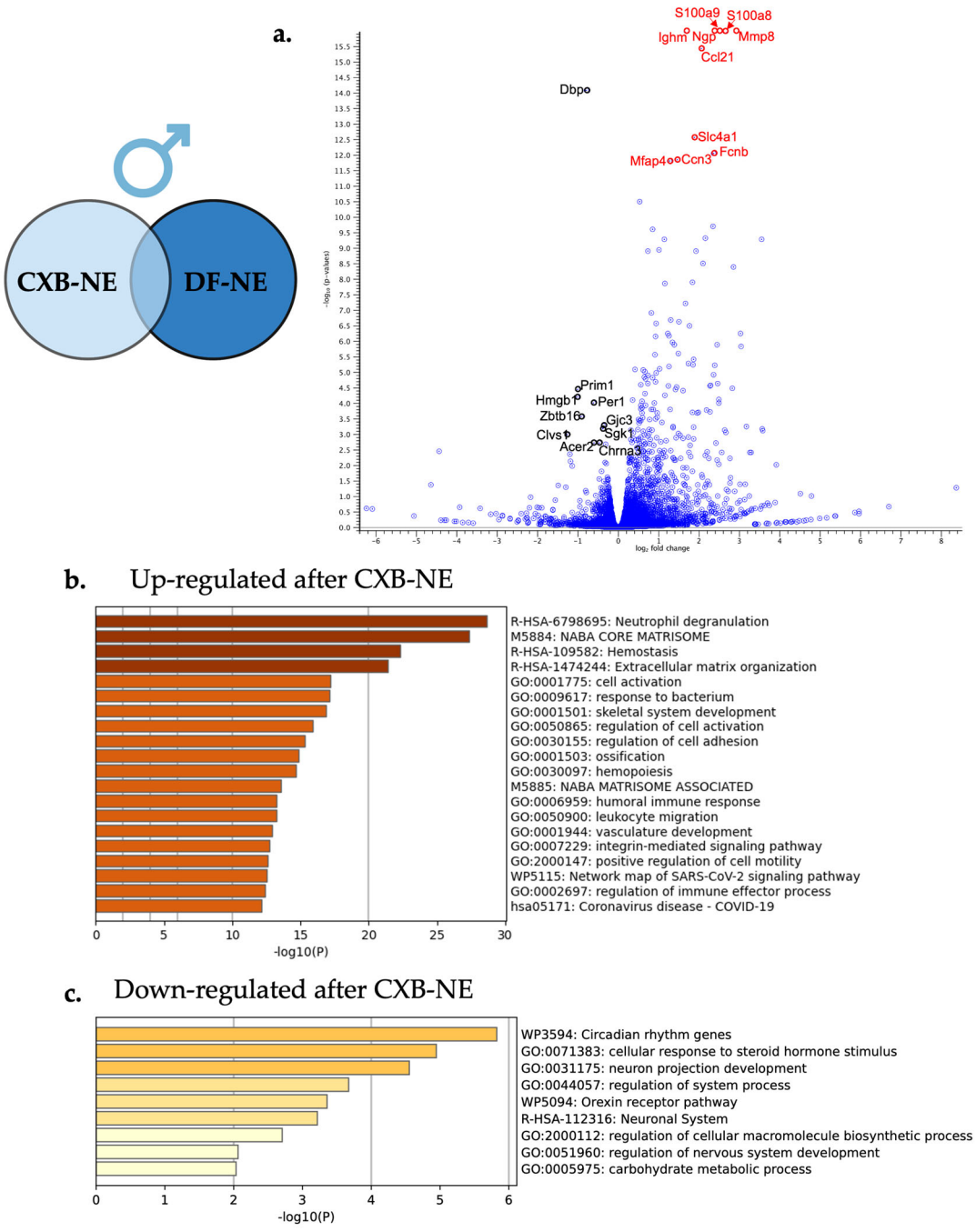

Figure 4.7. Neuroinflammatory relief via COX-2 inhibition in males causes differential gene expression in the affected DRG. **(a)** For visual clarity the volcano plot features all of the differentially expressed genes due to neuroinflammatory relief in the male DRG highlighting the

top 10 significantly up-regulated (red) and top 10 significantly down-regulated genes (black). **(b)** Metascape enrichment analysis of the top 20 up-regulated biological pathways following neuroinflammatory reduction via COX-**Figure 4.7 (continued)** 2 inhibition. **(c)** Metascape enrichment analysis of the top 9 down-regulated biological pathways following neuroinflammatory reduction via COX-2 inhibition.

4.2.7 Shared and unique gene expression changes across male and female neuroinflammation and relief.

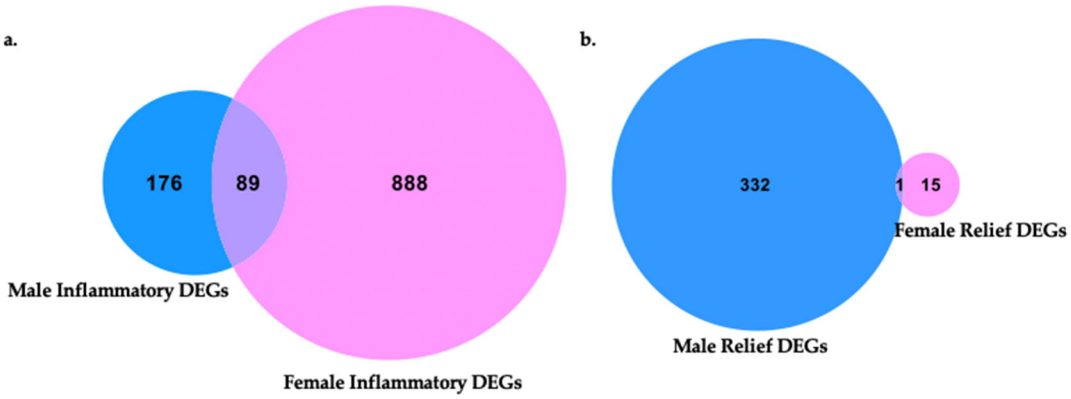

Figure 4.8. Venn diagrams of differentially expressed genes in each sex and shared genes in male and female neuroinflammation and relief. **(a)** Male and female differentially expressed neuroinflammatory genes compared between sexes for unique characteristics to males or females and those shared between sexes. Within each sex, neuroinflammatory gene sets originated from CCI vs naïve transcriptome comparisons. **(b)** Neuroinflammatory relief gene expression profiles of males and females were compared for shared features and those unique to a sex. Within each sex, neuroinflammatory relief gene sets originated from 10X CXB-NE vs DF-NE DRG transcriptome comparisons.

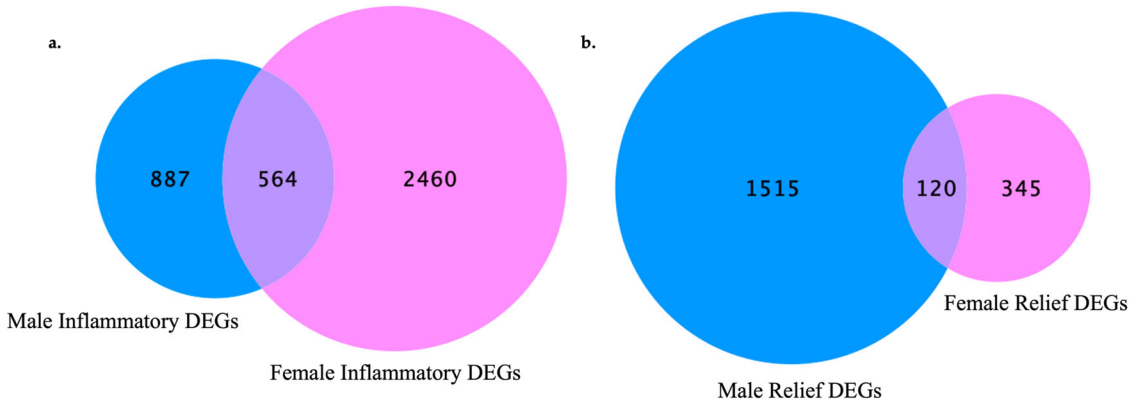

Figure 4.9 Venn Diagram of differentially expressed genes using p-value ≤ 0.05. (a) Male and female differentially expressed genes due to neuroinflammatory induction. **(b)** Male and female differentially expressed genes due to celecoxib theranostic nanoemulsion treatment.

Once the DEGs from male and female neuroinflammation and relief had been revealed, they were then compared and are presented in a Venn diagram generated by CLC Genomics Workbench (Figure 4.8). Again, only genes with an FDR p-value ≤ *0.05 and fold change of* greater than ±1 are included. Less stringent restrictions on gene filtering such as using a p-value rather than an FDR p-value ≤ 0.05 does provides a larger list of differentially expressed genes in both the inflammatory and relief gene sets for each sex (Figure 4.9 and Tables A.3.6 - A3.9). The raw p-value list shows a possible group of other genes to consider. However, a p-value assumes that 5% of all tests will be false positives, and when the number of tests increases like it does in a bioinformatic study like this one there is a need for more stringent guidelines. For this data analysis, FDR p-value was used to reduce false positive results. This is because, FDR p-value more conservatively assumes that 5% of all significant genes will be a false positive rather than 5% of the tests.

Following the induction of peripheral neuroinflammation by CCI of the right sciatic nerve there were 977 DEGs in the corresponding female dorsal root ganglia. Of these DEGs, 888 were unique to female neuroinflammation while 89 of them were shared with male neuroinflammation. DEGs distinctive to males from peripheral neuroinflammation included 176 genes (Figure 4.8a).

In contrast, during 10X CXB-NE driven neuroinflammatory relief from hypersensitivity, male dorsal root ganglia exhibited 333 DEGs while females have 16 DEGs (Figure 4.8b). In our analysis, males and females shared 1 common significant DEG following treatment, which was *hemoglobin alpha, adult chain 3* (*Hba-a3*).

These shared and sex associated genes were then examined for changes of expression between sexes following peripheral neuroinflammation and relief. A select group of them are listed in Table 9. Some of these include *corticotrophin releasing hormone* (*CRH*), which significantly increases in both sexes following CCI, but is down-regulated only in males following 10X CXB-NE treatment. There is also *activating transcription factor 3* (*ATF3*), which was upregulated in both sexes following peripheral neuroinflammation, but only significantly down-regulated in females following 10X CXB-NE treatment (Table 4.9). *ATF3* was also analyzed by quantitative PCR of the RNA extracted from the dorsal root ganglia to reveal equivalent trends of differential expression (Appendix Figure A3.1).

Table 4.9. List of differentially expressed genes that show unique patterns across sex and or treatment. Table information adapted from output data table from Metascape.com.

Gene Name	Official Name	GO	Protein Function	Pattern of Expression
Atf3	Activating transcription factor 3	GO:0061394 regulation of transcription from RNA polymerase II promoter in response to arsenic-containing substance; GO:1903984 positive regulation of TRAIL-activated apoptotic signaling pathway; GO:1903121 regulation of TRAIL-activated apoptotic signaling pathway	Transcription factors: Basic domains; Predicted intracellular proteins	Up regulation of ATF-3 in both males and females following CCI, down regulated with relief in females
Sema6a	Semaphorin 6A	GO:0106089 negative regulation of cell adhesion involved in sprouting angiogenesis; GO:0106088 regulation of cell adhesion involved in sprouting angiogenesis; GO:1900747 negative regulation of vascular endothelial growth factor signaling pathway	Predicted intracellular proteins	Up regulated in both sexes following CCI, down regulated with relief in females
Vgf	VGF nerve growth factor inducible	GO:0043084 penile erection; GO:0007620 copulation; GO:0002021 response to dietary excess	Predicted secreted proteins	Up regulated in both sexes following CCI, down regulated with relief in females
Flrt3	fibronectin leucine rich transmembrane protein 3	GO:0003345 proepicardium cell migration involved in pericardium morphogenesis; GO:0003344 pericardium morphogenesis; GO:0060973 cell migration involved in heart development	Disease related genes; Human disease related genes: Endocrine and metabolic diseases: Hypothalamus and pituitary gland disease	Up regulated in both sexes following CCI. No change with relief
Crh	corticotropin releasing hormone	GO:0042322 negative regulation of circadian sleep/wake cycle, REM sleep; GO:0010841 positive regulation of circadian sleep/wake cycle, wakefulness; GO:0042321 negative regulation of circadian sleep/wake cycle, sleep	Predicted secreted proteins	Up regulated in both sexes following CCI, down regulated with relief in males
Prim1	DNA primase subunit 1	GO:0006269 DNA replication, synthesis of RNA primer; GO:0006270 DNA replication initiation; GO:0006261 DNA-templated DNA replication	Predicted intracellular proteins	Up regulated in males following CCI, down regulated with relief in males
Prx	Periaxin	GO:0032287 peripheral nervous system myelin maintenance; GO:0043217 myelin maintenance; GO:0022011 myelination in peripheral nervous system	Disease related genes; Human disease related genes: Nervous system diseases: Other nervous and sensory system diseases; Human disease related genes: Nervous system diseases: Neurodegenerative diseases; Predicted intracellular proteins	Down regulated in both sexes following CCI, no significant change with drug
Myh2	Myosin heavy chain 2	GO:0030049 muscle filament sliding; GO:0033275 actin-myosin filament sliding; GO:0070252 actin-mediated cell contraction	Disease related genes; Human disease related genes: Musculoskeletal diseases: Muscular diseases; Predicted intracellular proteins	Up regulated in females following CCI, down regulated in males following CCI
Tnnt3	troponin T3, fast skeletal type	GO:1903612 positive regulation of calcium-dependent ATPase activity; GO:1903610 regulation of calcium-dependent ATPase activity; GO:0003009 skeletal muscle contraction	Disease related genes; Predicted intracellular proteins; Human disease related genes: Congenital malformations: Other congenital malformations	Up regulated in females following CCI, down regulated in males following CCI

Further examination of unique gene expression between male and female neuroinflammation and relief was investigated by immunofluorescent staining for the ATF3

protein. While examining the affected dorsal root ganglia recovered from animals on day 12, ATF3 protein was observed in all conditions. Naïve DRG of both males and females appeared to have low levels of this CREB protein dispersed in the cytoplasm (Figure 4.10a, d, and g). Once CCI was performed and neuroinflammation is evident at day 12, ATF3 presence increased and nuclear condensation is apparent 12 days after injury (Figure 4.10b and e). The apparent progression of ATF3 protein accumulation in the nucleus is evident in Figures 10g, h, and i. Following 10X CXB-NE treatment, which provided relief from mechanical allodynia, ATF3 expression decreased in both sexes (Figure 10c and f) with greater reduction evident in the female dorsal root ganglia neurons where no nuclear condensation was observed (Figure 10c). Examination of injured sciatic nerve at day 12 reveals some co-localization of ATF3 in CD68 positive macrophages (Figure 10j, k, and l).

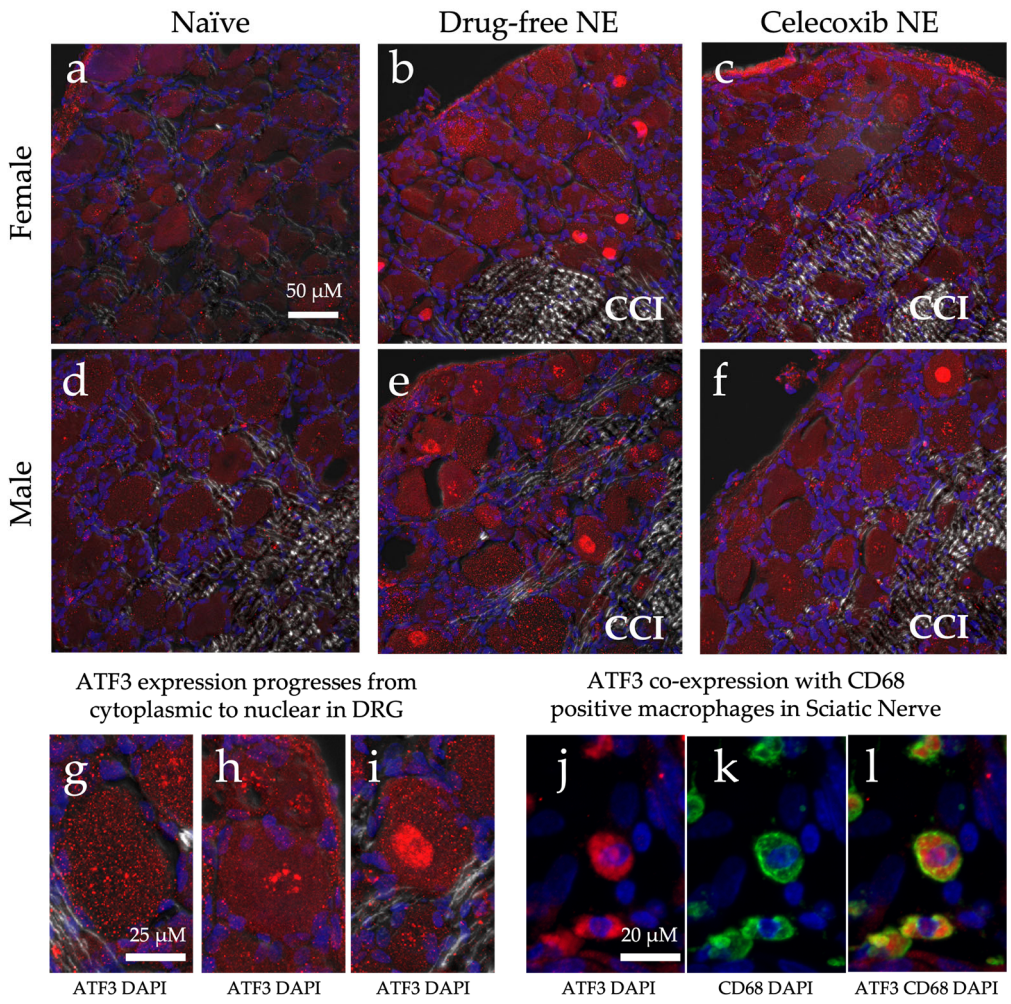

Figure 4.10. ATF3 protein expression changes in the ipsilateral DRG following hypersensitivity (DF-NE) and with relief (10X CXB-NE). Tissue recovered on day 12. **(a)** and **(d)** Naïve DRG tissue with dispersed ATF3 located throughout the cytosol. **(b)** and **(e)** ATF3 increased expression and condensing in the nucleus following neuroinflammatory hypersensitivity. **(c)** Disappearance of nuclear condensation of ATF3 following treatment in females. **(f)** Decreased nuclear condensation of ATF3 following 10X CXB-NE treatment in males. **(g)** Cytoplasmic ATF3 localization. **(h)** Beginning of condensation of ATF3 in the nucleus of the cell body. **(i)** Concentrated levels of nuclear ATF3. **(j)** Positive ATF-3 in macrophages of the sciatic nerve. **(k)** The same field of view as **j**, revealing positive staining of

Figure 4.10 (continued) macrophages with the anti-CD68 pan-marker. **(l)** Co-localization of ATF3 staining within CD68 positive macrophages within the sciatic nerve.

4.3 Discussion

This study set out to examine how allodynia induced by peripheral neuroinflammation causes changes in the transcriptome of the peripheral nerve cell bodies and associated cells of the dorsal root ganglia and how RNA expression is changed when this allodynia is relieved by a novel COX-2 inhibiting theranostic nanoemulsion. Here, we show that even though males and females develop quantitively similar hypersensitivity along the same time course (Figure 4.1), the gene expression within the affected dorsal root ganglia are distinct. While we also observe that there are some differences in RNA expression evident between individuals of the same sex and treatment group (Figure 4.2), we resolve statistically significant differences between sexes. For example, of more than 1,000 genes that exhibited differential expression in both males and females experiencing neuroinflammation, only 89 are shared between the two sexes (Figure 4.8a). Furthermore, with 10X CXB-NE providing equivalent mechanical hypersensitivity relief in both males and females, differences in changed gene expression are yet again evident between the sexes. Examining the differences in gene expression is beginning to reveal some of the fundamental similarities and sex differences in the cellular response to injury and differences in response to pain-relieving drug therapy. These are crucial findings given that there still no sufficient treatments for chronic neuroinflammatory pain, and the fact that there still remains a biased literature base towards male focused research leaving the molecular mechanisms of female neuroinflammation even more poorly understood[22].

4.3.1 Mechanical allodynia relief from NSAID theranostic nanoemulsion

In order to evaluate the transcriptomic changes associated with peripheral neuroinflammation and the relief from a theranostic nanoemulsion, CCI of the right sciatic nerve was performed for both sexes. Our previous work has seen that decreasing the neuroinflammatory response such as decreasing the overall number of infiltrating macrophages at the site of injury through treatment with CXB-NE has correlated to decreased mechanical hypersensitivity[51,54,68]. Quantifying mechanical allodynia by von Frey technique reveals that as compared to the naïve and base-line responsive of 16-17 g force for withdrawal for both male and females, both sexes develop equivalent hypersensitivity averaging around 5 grams of force as the 50% withdrawal threshold (Figure1b and c). This means that following identical surgeries, both sexes experienced equivalent levels of neuroinflammatory pain. Furthermore, once a single dose (2.4 mg/kg) of the COX-2 inhibiting theranostic nanoemulsion was administered on day 8 (Figure 4.1a), both males and females received multi-day relief from pain-like hypersensitivity (Figure 4.1b and c). In fact, at day 10 (♂ $p = 0.0919$, ♀$p = 0.3908$) and day 12 (♂ $p = 0.8712$, ♀$p = 0.8643$) there is no longer a significant difference in behavior between drug treated animals and their naïve counterparts. With the male and female rats experiencing similar levels of mechanical allodynia (CCI and DF-NE) and similar levels of relief (10X CXB-NE) on the day of tissue recovery, the analysis of RNA transcription during neuroinflammation and relief reveals associated changes in gene expression. While we have previously observed a sex difference in relief from CCI using celecoxib theranostic nanoemulsion[68], that study used a lower dose of celecoxib in the nanoemulsion droplets. Here, the higher drug loading in this new formulation completely closes the gap in relief with both sexes experiencing quantitatively identical alleviation. Previously

demonstrating that there is a sex difference in the degree of relief from the lower celecoxib dose unequivocally revealed that males and females are responding to pain and pain-relief differently.

While others have begun to examine the sex differences in neuroinflammatory induced pain[126, 21, 127, 128] or baseline sex differences in the naïve DRG[20], this is the first study examining the transcriptomic sex differences in neuroinflammatory relief by an effective COX-2 inhibitory treatment.

4.3.2 Male transcriptome changes in the DRG following CCI

Following peripheral nerve injury, the associated ganglia are impacted, and transcriptional changes occur due to interactions with glial cells, immune cells, and adjacent neuronal cells[113,130]. This crosstalk impacts neuronal hypersensitivity leading to the perception of pain[113]. We have previously seen immune cell infiltration in the DRG[54], and the findings in this study suggest that following neuroinflammation that immune cells have an impact on transcriptional regulation of the DRG (Figure 4.5b and c). Specifically, genes such as *neuropeptide y* (*NPY*), *thrombospondin-1* (*THBS-1*), *complement factor h* (*CFH*), and *activating transcription factor 3* (*ATF3*) are up regulated following neuroinflammation in the male DRG (Table 4.3). These genes ultimately result in the production of proteins that influence the inflammatory response[131-134].

Some genes such as *NYP* and *THBS-1* are known to induce phagocytosis of damaged cells by macrophages and neutrophils respectively[132, 133]. *NYP* is also well known to affect cell migration, cytokine secretion, and cell adhesion[133]. Other genes such as *CFH* have been shown to prevent the inflammatory response from overreacting and protect un-damaged cells by keeping the compliment system turned off[134]. *ATF3*, a member of the cAMP response element binding (CREB) protein family, has been shown to be both a repressor and an activator of the immune

response depending on the circumstances[131]. Other studies have also seen *ATF3* to be significantly upregulated following peripheral nerve injury indicating its importance in maintaining this inflammatory balance in the neuroimmune response[21]. Overall, stable changes in gene expression following peripheral neuronal injury can be seen to be a balance in maintaining an allostatic balance[135] while increasing the inflammatory response to facilitate tissue repair and regeneration.

Because of this damage, down regulation of *myelination* and *cytoskeleton dynamics* during Wallerian degeneration is known to occur following peripheral nerve injury[9]. During Wallerian degeneration, injured peripheral nerves signal to phagocytic immune cells and Schwann cells to phagocytose dying and damaged cells. During this process, the damaged axon retracts distally, and myelination significantly decreases[9]. These activities are seen to be enriched in the down regulated processes in this study (Figure 4.5c) as well with genes involved in myelination, such as *early growth response 2* (*EGR2*) and *zinc finger and BTB domain containing 16* (*ZBTB16*), both being significantly down regulated following CCI of the right sciatic nerve (Table 4.4). EGR2 is a DNA binding transcription factor known to regulate Schwann cell myelination by regulating other genes involved with myelination[136]. ZBTB16 is primarily known to be involved with neuronal differentiation; however, a recent study found it to be detrimental to neocortical myelination when knocked out of oligodendrocytes[137]. Cytoskeleton genes such as *spectrin beta, non-erythrocytic 5* (*SPTBN5*), who's role is in cytoskeleton dynamics and signaling, is also seen to be down regulated[138]. Interestingly, cytoskeleton elements seen in muscle and muscle contraction are also found to be down regulated in the DRG following injury (*Myosin heavy chain 2* (*myh2*)[139], *troponin* C2 (*Tnnc2*)[140], and *Troponin T3* (*Tnnt3*)[141]). This could indicate

multiple uses for these cytoskeleton components not only in muscle contraction but also in neuronal remodeling.

4.3.3 Female transcriptome changes in the DRG following CCI

Our understanding of the development of female neuropathic pain is just beginning to evolve, but from this past decade of research revealing both similarities and differences in the underlying biology is apparent as compared to neuropathic pain in males[21]. As with male neuroinflammation, female neuroinflammation also has up-regulation in the involvement of immune modulators such as *NPY*[133] and *ATF3*[131] (Table 4.1). This increase in *ATF3* in both sexes following nerve insult is in agreement with other transcriptional studies looking at sex differences following peripheral nerve injury[21,130]. However, we see a higher fold change of RNA expression in females (7.83) compared to that seen in males (4.12) (Tables 4.1 and 4.3). This heightened gene expression in females when compared to males is also seen with *NYP* where animals that have undergone CCI have 5.79-fold change in males when compared to naïve, but a 12.38-fold change in female neuroinflammation. In addition, other up-regulated enriched pathways in females following CCI include increased *cytokine signaling in the immune system* and *microtubule processing* (Figure 4.4b).

Some of these genes that are up-regulated and exhibit involvement in microtubule processing include *Fibronectin leucine rich transmembrane protein* (*FLRT3*) and *growth associated protein 43* (*GAP-43*) (Table 4.1). *FLRT3* has previously been seen to be upregulated in the DRG following peripheral nerve injury and modulates neuron growth[142]. While *GAP-43* is expressed in growing neurons, once retrograde axonal transport has been interrupted it is associated with neuron regeneration[143]. The increased gene enrichment in *microtubule processing* in females is

contradictory to what was observed in male neuroinflammation where a down regulation of *myelination* and decreased *cytoskeleton dynamics* were seen to be enriched, corresponding with Wallerian degeneration. This is not to say that Wallerian degeneration is not affecting the female DRG as well, but perhaps this process of clearing cellular debris is occurring differently in the female neuropathy than in the male. Further histological examination will be required to resolve this.

4.3.4 Macrophage associated COX-2 inhibitory effect causes transcriptional differences in the associated male DRG

While examining the transcriptomic changes uniquely associated with male mechanical allodynia relief, several enriched pathways come to light with one being an increased expression for *neutrophil degranulation* (Figure 4.7b). Neutrophils, under normal circumstances, have an antimicrobial role in clearing pathogens and cellular debris through phagocytosis, degranulation, and NETosis[144]. Once differentiated in the bone marrow they bear the CXCR2 motif and are held in the bone marrow by the CXCL12 ligand until signaled for by granulocyte colony stimulating factor (G-CSF)[145]. Macrophages at the injury are signaled to release G-CSF by the calcium binding proteins S100A8 and S100A9, which in turn initiate the neutrophil chemotaxis and then support the degranulation of enzymes such as myeloperoxidase (MPO). Our study shows upregulation of all of these components including *CXCR2*, *CXCL12*, *S100A8*, *S100A9*, and *MPO*. Neutrophil's presence is typically associated with acute inflammation, and their function is complete within 24 hours and then they are eliminated by macrophages once complete[144]. However, some recent studies have found that neutrophils can exhibit anti-inflammatory properties bearing the arginase 1 (Arg1) protein and have been termed N2 type neutrophils[146].

Another study built off of this found that immaturely delayed neutrophils expressing Arg1 also had enriched *Tgfb1* and excreted higher levels of nerve growth factor (NGF)[147]. Our study also sees a 2.42-fold increase of *Arg1* gene expression, 2.46-fold increase in *NGF*, and a 1.4-fold increase in *Tgfb* suggesting that these N2 anti-inflammatory neutrophils could also be present in the DRG. While it needs to be independently confirmed, it is interesting to consider that the relief in neuroinflammatory pain allows for a second set of neutrophils with the N2 phenotype to enter the DRG.

Down regulation of some enriched biological pathways were also present when mechanical allodynia was relieved including *regulation of system processes* (Figure 4.7c). One of the genes enriched in the *regulation of system processes* was *corticotrophin releasing hormone* (*CRH*). *CRH* was up regulated in male neuroinflammation (33.5-fold) and significantly down regulated only with male neuroinflammatory relief (-21.61-fold). Although *CRH* is primarily studied in the central nervous system, recent studies in the peripheral nervous system have shown it to be analgesic[148]; however these studies look at administration of corticotrophin releasing factor systemically[149, 150, 151, 152] rather than endogenous CRH function. Although our findings are counterintuitive to what these other studies have seen, Reinhold and colleagues using the CCI model saw that the most changed gene expression following DRG damage due to CCI was *CRH*[153]. Our findings are in agreement with this, showing the CRH's function endogenously may differ from its systemic effect. Although *CRH* is seen to also increase 34.48-fold following CCI in our study, it is only the males that have a significant decrease in *CRH* following mechanical allodynia relief; thereby, reveling an unknown pharmacodynamic sex difference.

4.3.5 Macrophage associated COX-2 inhibitory effect causes transcriptional differences in the associated female DRG

Females experiencing neuroinflammatory relief were affected very differently than males only showing 16 DEGs compared to 333 DEGs in males (Figure 4.8) (limit of FDR p-value ≤ *0.05 and fold change of* greater than ± 1); however, there were quite a few genes that were upregulated during mechanical allodynia and reduced when mechanical allodynia was relieved. Some of these genes include *ATF3*, *Transcription factor JUN* (*JUN*), and *VGF nerve inducible factor* (*VGF*).

VGF is a peptide that is increased with nerve growth factor and highly expressed in the peripheral and central nervous system following neurpathy[154]. And some studies administrating VGF peptide intrathecally have seen that it is associated with peripheral mechanical hypersensitivity[155]. Our study, as well as others have seen *VGF* to be transcriptomically increased in both the male and female DRG following peripheral neuroinflammatory induction[21]. However, here we see that only in the female DRG is VGF significantly reduced following treatment (-1.63-fold). Soliman and colleagues have written an extensive review about VGF and its increase in expression being undoubtedly related to inducing neuropathic hypersensitivity. They suggest that targeting VGF derived peptides may be a possible therapeutic for pain relief[154]; our studies support this claim that when VGF is reduced in females, mechanical hypersensitivity follows suit.

Another interesting enriched biological process is the *PID ATF2 Pathway* with *ATF3*, *JUN*, and *Sema6a* following within it. *ATF3* will be extensively discussed in the next section; however, *JUN* also has distinct roles in regulating neuroinflammatory pain. *JUN* is the gene encoding the c-Jun transcription factor highly associated with c-Jun N-terminal kinase (JNK).

The JNK pathway's typical role is in stress signaling within the cell. It has been observed to be upregulated following spinal nerve ligation in both the spinal cord and DRG and has a linked role in maintaining neuropathic hypersensitivity[156]. When an inhibitor to JNK was administered intrathecally via osmotic pump, a reversal of mechanical allodynia was observed[156]. Here in females, we also see that *JUN* is significantly down regulated when female neuropathic pain is relieved by 10X CXB-NE. This suggests that the JNK pathway can both relieve pain[156], but also is reduced when neuroinflammatory pain is reduced.

3.6 CREB protein involvement in the sex differences of neuroinflammation and mechanical hypersensitivity relief

One of the most interesting finds in this study was the involvement of the CREB protein ATF3 and the sex differences that were evident in the gene expression between components of the pathway during neuroinflammation and relief. *ATF3* is significantly upregulated in the DRG of both sexes following neuroinflammation, but only significantly down regulated in females following treatment.

ATF3 is a member of the CREB protein transcription factor family, which can be activated during an immune response by ER stress, cytokines, chemokines, hypoxia, DNA damage, and growth factors[157]. In turn, CREB proteins can lead to the activation of different toll-like receptors (TLRs)[131]. *ATF3* activation in a macrophage is known to down regulate the inflammatory response under normal conditions by regulating Th17 T cells, decreasing inflammatory cytokines (IL-6, IL-12b, and IL17) and promoting macrophage survival[131]. Interestingly, one study found that not only does the ATF3 protein regulate immune response, but it also is able to bind to the promotor of the *Ptgs2* gene, which transcriptionally regulates the COX-2 enzyme[158]. We find that some of the

CD68 positive macrophages in the injured sciatic nerve co-express ATF3 (Figure 4.10l). Because *Ptgs2* is involved in a regulatory feedback loop with its product prostaglandin E_2[159], it is intriguing to consider how attenuating the activity of the COX-2 enzyme in a macrophage with our novel COX-2 inhibiting theranostic nanoemulsion may play a role in influencing gene transcriptional changes, specifically with the CREB pathway components (summarized in Figure 4.11).

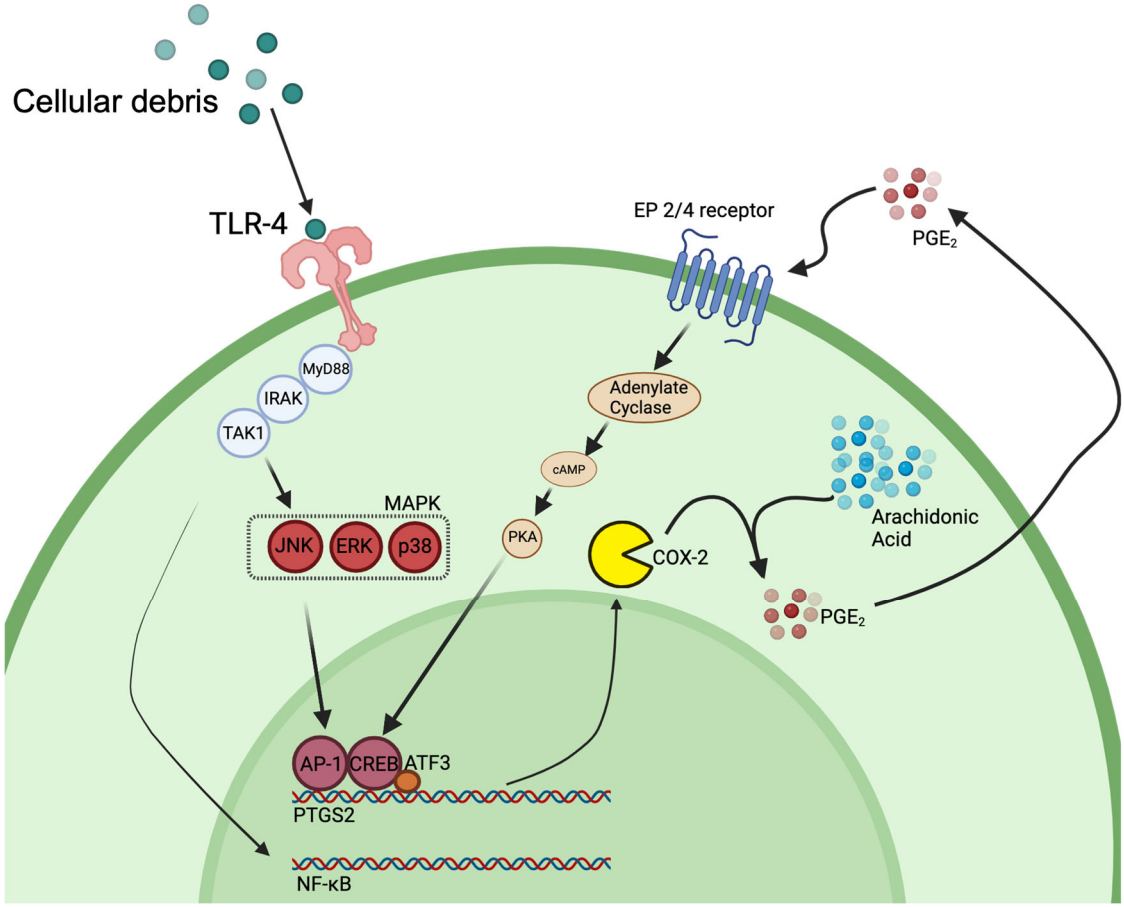

Figure 4.11. COX-2 feedback loop transcriptionally regulated by ATF3. TLR4 is activated by cellular debris from neuronal injury as well as certain cytokines, which then activates parts of the MAPK signaling cascade as well as NF-κB. Production of PGE_2 provides a positive feedback loop to support continued production of prostaglandin, which further support increased immune cell infiltration and activation. Model influenced by our research and multiple citations[131,158,160]. Figure made with BioRender.

ATF3 has been previously shown to also express unique functions in neuronal cells. Following nerve injury, ATF3 responds as an immediate early gene with transcription taking place to help regulate the neuronal response to inflammation[161]. For example, assessing skin incision injury on female rats revealed that ATF3 was upregulated in the DRG; DiI, placed at the site of injury facilitated the identification of the specific neuronal cell-bodies that innervate the injury[162]. The ATF3 upregulation persisted for weeks following the injury[162]. Our results show that ATF3 transcription and protein expression correlates with pain and pain relief suggesting increased expression of ATF3 could be involved in transcriptionally altering the nerve cells in ways that contribute to their hypersensitivity.

Mechanistically, our COX-2 inhibitor therapeutic may function indirectly to decrease ATF3 production in neurons (Figure 4.10) by decreasing overall PGE_2 in the cellular milieu, thus attenuating the PGE_2 feedback loop (Figure 4.11).

In the naïve DRG in both sexes, low levels of the ATF3 protein can be seen cytoplasmically located in neuronal cell bodies (Figure 4.10a and d). Following neuroinflammatory induction, RNA-seq detected significant increases in *ATF3* with a 7.83-fold increase in the female DRG and a 4.12-fold increase in the male DRG when compared to the respective naïve (Tables 4.2 and 4.3). Our observation is consistent with a similar study that also saw this sex difference following CCI induction where females had increased *ATF3* expression compared to males[21].

In injured tissue, ATF3 protein can be seen to progressively congregate in the nucleus of DRG neurons (Figure 4.10h) until it is densely located within (Figure 4.10i). We observed the highest number of neurons with ATF3 dense nuclear stains in those samples experiencing neuroinflammatory induced allodynia (Figure 4.10b and e), and reduced levels in those who

received 10X CXB-NE treatment (Figure 4.10c and f). Similarly, RNA-seq detected a significant decrease (2.09-fold) in *ATF3* expression in females treated with 10X CXB-NE while an increase in *ATF3 (*2-fold) was evident in treated males. This difference is again seen in other CREB pathway components downstream to ATF-3 such as *Jun* with both males and females having increased levels of expression following neuroinflammation (1.6-fold in females and 1.31-fold in males), but again, only females having significantly decreased expression of *Jun* following 10X CXB-NE treatment (-1.28-fold) while males again have a slight increase in expression of *Jun* (1.26-fold). *IL-6*, which is also downstream in the CREB response pathway, shows this similar pattern but at a more amplified manner in females (24.04-fold increase) when compared to males (3.77-fold). IL-6 is known to prevent *FoxP3* expression in T helper cells[163]; perhaps this change in IL-6 expression in females may in fact contribute to a pro-inflammatory role by not allowing T helper cells to differentiate into regulatory T cells. Following treatment, females again have decreased *IL-6* regulation (-4.56-fold) when comparing 10X CXB-NE to DF-NE, while males again have a slight increase in expression (2.03-fold).

4. Conclusion

Given that neuropathic pain currently has no effective long-term treatment, and that female neuropathic pain has been under studied, the need to evaluate the differences between male and female neuroinflammation and relief is warranted. This study elucidates some of these differences in the dorsal root ganglia transcriptome of male and females experiencing mechanical hypersensitivity and also while experiencing relief. Here we show that male and female rats who have undergone CCI of the right sciatic nerve experience similar levels of mechanical allodynia while a novel 10X COX-2 inhibiting theranostic nanoemulsion is able to provide sustained relief

equally to both males and females. This means that the transcriptomic differences seen between sexes are not due to different levels of pain or relief from pain, rather that they are due to sexual dimorphic expression of regulatory pathways. Some genes of interest playing unique roles in male neuroinflammation and relief include *CRH* as well as genes associated with neutrophil degranulation. While in females, some of the key genes include *ATF3*, *JUN*, and *VGF*. Overall, this study reveals that even though males and females may experience similar levels of neuropathic pain and can achieve equivalent relief from an NSAID, the basic underlying biology of how this occurs differs.

4.5 Materials and Methods

4.5.1 Animal Use and Ethics

The following experiments were carried out at Duquesne University, Pittsburgh, PA, USA, in compliance with the recommendations in the Guide for The Care and Use of Laboratory Animals and the regulations of the Institutional Animal Care and Use Committee (IACUC) under the approved protocol #2009-07 as well as the animal care and use review office (ACURO) for the Department of Defense (DM190725.e001, approved 12/21/2020).

Male and female Sprague Dawley rats were purchased through Hilltop Lab Animals, Inc. (Springdale, PA). Once received, animals were acclimated for 1 week and then handled for 1 week by the animal behavioralist prior to use. Prior to the experiment beginning, animals were socially housed; animals were individually housed once baseline von Frey behavior began (2 days prior to surgery). Individual housing was done to keep rats from opening one another's incisions. Animals were kept on a 12:12 h light-dark cycle with access to food and water *ad libitum*. Special diet (Research Diets, Inc., New Brunswick, Nj; Cat # AIN-93G) was used to avoid interference of

autofluorescence during near infrared imaging of the nanoemulsion. The number of animals used was based on a power analysis of our previous studies using 1X CXB-NE.

Groups used in this study included male and female naïve, CCI, DF-NE, and 10X CXB-NE. Naïve animals were selected instead of sham animals due to wanting data to be comparable to other published work[21] that examine CCI and sex differences in a way that reveals differential gene expression resulting from neuropathic injury and quantified hypersensitivity. Additionally, our previous work has shown that by 12 days after sham surgery at the sciatic nerve both cytokines[112] and the infiltration of macrophages[47] do not differ between sham and naive.

4.5.2 Up-down von Frey behavior

Cohorts of all male or all female rats were tested separately for hypersensitivity with the von Frey technique. In each case, behavioral analysis was assessed every other day before and following surgery as outlined in Figure 1a. Behavioralist was blinded to any treatment received. Rodents were first acclimated for 30 minutes in individual plexiglass containers with mesh floors. Once testing began, the left and right hind paws were probed with calibrated von Frey filaments (Stoelting Co., Catalog # 58011). Filaments (1.202 g, 1.479 g, 2.041 g, 3.630 g, 5.495 g, 8.511 g, 15.136 g) were applied to the hind paw at a 30-degree angle and for 3 seconds to look for positive (quick lift, flick, vocalization) or negative responses. If no response, the next largest filament would be used. If positive response, the next smallest filament would be used. This pattern continued until 4 responses were collected after the change in response such as used previously[74, 81, 68, 54, 51]. No less than 30 seconds separated probing of the same paw twice. The gram force of the 50% withdrawal threshold was then calculated using Chaplan's 50% withdrawal threshold formula[74].

4.5.3 Chronic Constriction Injury (CCI)

Neuroinflammation and mechanical hypersensitivity was induced via CCI as described by Bennet and Xie[75] and as previously done in our lab[51, 54, 68]. Surgery was performed under isoflurane anesthesia. The surgical area was first clipped of hair and sterilized with iodine and alcohol. An incision through the skin was made just beneath the right femur bone. The *biceps femoris* and *gluteus superficialis* were then bluntly separated to expose the right sciatic nerve. The sciatic nerve was freed from surrounding connective tissue and 4 sutures (McKesson 4-0 Chromic Gut Sutures, Catalog # S635GX) were loosely tied around the sciatic nerve approximately 1 mm apart. Muscles were closed with sutures and skin was stapled close with 9 mm autoclips (Braintree Scientific, Catalog # NC9281117).

4.5.4 COX-2 Inhibiting theranostic nanoemulsion

The therapeutic was produced by Janjic lab as reported earlier[51,58,68] with some modifications, the CXB-NE had drug concentration of 2.4mg/mL, 10X higher than in earlier studies.

4.5.5 Tail Vein Injection

10X CXB-NE or DF-NE was delivered via tail vein injection on day 8 following surgery as previously described[76]. The theranostic nanoemulsion is tagged with the near-infrared (NIR) DiR (1,1′-dioctadecyl-3,3,3′,3′-tetramethylindotricarbocyanine iodide) dye. Accuracy and quality of the tail vein injection can therefore be assessed using live animal NIRF imaging. Briefly, under anesthesia, the rat's lateral tail veins were dilated by placing the tail into a warmed water bath. A 27G needle was inserted into the lateral tail vein, and blood flashback was observed. Slowly, 300

μL of either 10X CXB-NE (55.5 micrograms of CXB) or DF-NE was injected into the tail vein[51, 54, 68]. The same dosage of celecoxib was used for all animals[68]. The injection quality was then assessed using the LI-COR Pearl Imager (LI-COR Biosciences, Lincoln, NE). A quality injection exhibits clearance from the site of injection leaving little to no NIRF signal in the tail. Any animals with 10X CXB-NE or DF-NE remaining in the tail from a ruptured vein or subcutaneous injection were removed from the study.

4.5.6 Estrus Cycle Tracking

Female's estrus cycle was tracked for four consecutive days (days 8 – 12 post-surgery) in order to track the estrus cycle and establish where in estrus cycle the individual was when receiving treatment. During this procedure, females were briefly anesthetized with isoflurane, vaginal canals were flushed with saline, and collection was allowed to dry on a slide. Once dry, slides were fixed with 100% methanol and stained with 5% Geisma stain for 20 minutes. Slides were then rinsed briefly with water and allowed to dry before mounting with Permount (FisherScientific, Cat # SP15-100). Using Cora and colleague's description of the estrus cycle[82], each female's cycle was established.

4.5.7 Dorsal Root Ganglion (DRG) Collection

Rats were euthanized on the 12th day following surgery at the peak of their mechanical hypersensitivity relief (Figure1b and c). Rats were euthanized by CO_2 asphyxiation, and the right L4 and L5 DRG were immediately dissected. DRG that were to be sequenced were placed into RNA*later*™ stabilizing solution (Invitrogen, Catalog # AM720) and solution was allowed to permeate tissue for 24 hours at room temperature. The RL4 and RL5 DRG of the same animal

were then combined into a new tube and stored at -20°C until shipment to Qiagen for RNA extraction, library preparation, and sequencing.

DRG that were to be used for immunohistochemistry were placed into 4% paraformaldehyde (PFA) in 1X PBS solution for 24 hours at 4°C. DRG were then placed in 30% sucrose solution in 1X PBS and kept at 4°C. Tissues were embedded in optimal cutting temperature (O.C.T.) compound and 20 μm frozen sections were collected on gelatin coded slides.

4.5.8 Sample preparation

RNA isolation was performed under contract by Qiagen as follows; RL4 and RL5 DRG were homogenized for RNA extraction using the RNeasy Plus Universal Mini Kit (Qiagen, Hilden, Germany). In order to include small RNAs, manufacturer instructions for the kit were followed using the Qiagen *Purification of Total RNA Containing miRNA appendix C*.

4.5.9 Library preparation and sequencing

Approximately 400 to 500 ng of extracted RNA was first heat fragmented, and then separated from any unwanted ribosomal RNA (rRNA) using the QIAseq FastSelect rRNA and globin deletion kit (Qiagen, Hilden, Germany). Samples were quality controlled by checking the RNA integrity number (RIN^e) gathered from the Agilent D1000 ScreenTape System (Agilent Technologies, Santa Clara, CA). Using the QIAseq Stranded Total RNA Library Kit (Qiagen, Hilden, Germany), library preparation was done. Briefly, sequencing adapters were added, and cDNA was amplified using PCR. All libraries were pooled in equimolar concentrations. Following the manufacturer's protocol, library pools were clustered on the surface of a flow cell before

sequencing on a NextSeq High Output flow cell (Illumina Inc., San Diego, CA) instrument (2x75, 2x8).

4.5.10 Bioinformatics analysis of RNA-seq data (Mapping and Differential Expression Analysis)

RNA-seq fastq data files were received by the authors from Qiagen and imported into CLC Genomics Workbench 22.0.2 (QIAGEN, Hilden, Germany). Data contained 3 naïve animals per sex, 3 CCI ♂ and 2 CCI ♀, 3 DF-NE ♂ and 2 DF-NE ♀, as well as 3 10X CXB-NE ♂ and 2 10X CXB-NE ♀. CLC was then used for quality assessment, alignment with the *Rattus norvegicus* genome (mRatBN7.2.106), heatmap comparisons, differential expression analyses, volcano plots, and Venn diagram comparisons of the differentially expressed genes.

Mapping was done under the CLC Genomics Workbench default settings in the forward direction. Genes included in most-mapping analyses had an adjusted p-value, false discovery rate (FDR), of ≤ 0.05 and a fold change greater than ±1. TMM normalization is internally used for DE, heatmaps, and principal component analyses (PCA).

To identify genes that were regulated by neuroinflammation (CCI vs Naïve) or relief (10X CXB-NE vs DF-NE) in each sex, DE analyses were performed. These gene sets that were differentially changed by neuroinflammation or relief were then compared between sexes as shown with Venn diagrams to see which genes are shared or distinct to a sex under these conditions.

4.5.11 Enrichment Analysis

Metascape (metascape.org) was used for enrichment analyses. Metascape is updated monthly and incorporates Gene Ontology (GO) processes, Kyoto Encyclopedia of Genes and Genomics (KEGG) pathways, Reactome gene sets, Cytoscape and NCBI as well as other publicly available

resources all incorporated into one platform[84]. This allows for reduced redundancy among ontology terms.

All differentially expressed genes were included and split into up or down regulated gene sets of differentially expressed genes due to neuroinflammation or relief by sex. These were then imported into Metascape using the express analysis version with the default settings. Enrichment heatmaps and protein interaction networks were then visualized for interpretation.

4.5.12 cDNA conversion and RT-qPCR validation

RNA received from Qiagen was converted to cDNA using the Verso cDNA conversion kit (ThermoFisher Scientific, Waltham, MA; AB-1453/A). RNA (500 ng) conversion was performed at 42°C for 1 hour and then inactivated for 2 minutes at 65°C. cDNA conv ersion was confirmed to be successful via PCR using GAPDH primers and visualization on an agarose gel.

Real time quantitative PCR (RT-qPCR) was done to verify gene expression changes in a subset of genes (*ATF3* and *Sema6a*). Maxima SYBR Green/ROX qPCR Master Mix (2X) (ThermoScientific, Catalog # K0221) was used on the Step One Plus qRT-PCR Instrument (Applied Biosystems, Waltham, MA). Primers are listed in Supplementary table 1. Briefly, 250 ng of template DNA was used in a 25µL reaction. Following the manufacturer's protocol, 40 cycles were run under the two-step reaction protocol. List of primers listed in Appendix A.3 Table A3.1.

4.5.13 Data Deposition

Fastq files are stored on the Mac in the Pollock Lab as well as on Pollock's personal external hardrive. Data analysis files are stored within CLC on Pollock's laptop.

4.5.14 Immunofluorescent Staining and Confocal Imaging

Fluorescent staining was performed using a rabbit anti-ATF3 primary antibody (Millipore Sigma, Burlington, MA; Cat # HPA001562) at a 1:500 dilution in combination with Alexa Fluor™ 555 donkey anti-rabbit poly-clonal antibody (ThermoFisher Scientific, Waltham, MA; Cat # A31572) secondary antibody. CD68 macrophage detection was done using a mouse monoclonal IgG1 anti-CD68 antibody (Bio-Rad, Hercules, CA; Cat # MCA341R) at 1:500 dilution in combination with Alexa Fluor™ 488 Goat anti-mouse poly-clonal antibody (ThermoFisher Scientific, Waltham, MA; Cat # A21121) following our standard protocols[68].

Briefly, slides were fixed in 4% paraformaldehyde for 15 minutes and then washed in 1X PBS. Next slides were permeabilized in 0.3% Triton X-100 for 15 minutes, washed, and then blocked in 5% normal donkey serum (NDS) for 1 hour at room temperature. Primary was then diluted in 5% NDS and allowed to incubate on the slides over night at 4°C. The next day, slides were washed, and secondary antibody diluted into 5% NDS was incubated on the tissue for 2 hours at room temperature. Slides were nuclear stained and mounted using ProLong™ Gold anti-fade reagent with DAPI (Invitrogen, Waltham, MA; Cat # P36935).

Images were acquired on a Nikon Ti2 Eclipse inverted A1r confocal microscope using a 40X 1.3 NA oil objective. Images were acquired using 3D Z-stacks through the entire DRG section. Images were then converted to a maximum intensity projection image in order to visualize signal throughout the whole section. All images were taken using the same exposure, gain, and LUTs settings.

CHAPTER V

DISCUSSION AND CONCULSIONS

Throughout the work presented in this dissertation, there is clear evidence that how males and females respond to peripheral neuropathic inflammation and how treatment changes the neuroinflammatory response to provide hypersensitivity relief are different. Seeing the initial sex differences in behavioral response with 1X CXB-NE gave insight to biological differences, which were then evident through the differentially expressed genes between drug treated males and females. COX-2 inhibiting theranostic nanoemulsion appears to shift the cellular environment at the site of injury which then leads to transcriptional changes at the DRG. Even though behaviorally, using 10X CXB-NE, males and females appear to behave the same, this study, along with others, reveal sex specific changes in the biology of neuroinflammation and now relief.

5.1 The use of chronic constriction injury and von Frey behavioral analysis to measure neuropathic pain-like behavior

In order to study neuropathic inflammatory hypersensitivity (which is an analog of pain sensation) and the relief from hypersensitivity, a model of neuroinflammation needed. One well-established peripheral neuroinflammatory model is the chronic constriction injury model. Chronic constriction injury of the rat sciatic nerve was established in 1988 by Bennet and Xie[75], and has been a standard technique ever since. The Pollock Lab has effectively used the CCI model of the rat sciatic nerve to study neuroinflammation and relief[47,48,51,54,55,57,68,112]. CCI is a form of complex regional pain syndrome II (CRPS II) where injury to a peripheral nerve causes long lasting neuropathic pain; more specifically, it is a model of compression induced CPRS

II[164, 165]. CCI is one of the only peripheral neuropathic pain models where the nerve remains intact[164], which allows for the animal's use of the limb, even though it is hypersensitive. The sciatic nerve is often used because the sciatic nerve is the largest nerve in the body, making it easily visible, as well as it is easily accessible with minimal damage to other tissues[166]. An additional advantage is that the sciatic nerve has afferent sensory nerves that innervate the paw pad making it possible to measure hypersensitivity to pressure, temperature, and chemical stimuli[166].

This study assessed mechanical allodynia induced by CCI and the relief achieved when CXB-NE was administered. This was made possible by using the von Frey behavioral assay where blunt filaments of calibrated forces are applied to the palm of the hind paw looking to see if it elicits a response of lifting, flicking, or licking[166,167]. The up-down version of analysis looks to predict at what gram force does the rat respond 50% of the time[74]. If this value is significantly decreased compared to what the animal's baseline withdrawal threshold is, the animal is deemed hypersensitive or that they are experiencing allodynia.

Our previous studies have been able to successfully induce mechanical allodynia in male Sprague Dawley rats to a 50% withdrawal threshold of about 5 grams by day 8 post-CCI[51,54,55,57]. This developmental timeline of neuropathic allodynia using CCI is comparable to what has been seen by other labs using rats of corresponding ages and timelines[53,113,168]. The studies included in this dissertation (Figure 3.1 and Figure 4.1) both align with our lab's own timeline as well as others showing male Sprague Dawley rats 50% withdrawal threshold to be anywhere between 3-5 grams of force by day 8 post-CCI induction.

5.1.1 Similar patterns of hypersensitivity in males and females

There is a debate between neuropathic pain researchers on whether age matched females experience higher levels of mechanical allodynia following induction of neuroinflammation of the peripheral nerve[97]. To begin, age matched male and female Sprague Dawley rats typically vary quite a bit in weight from one another with females of 7 weeks old being close to 180-190 g and males being close to 250-260 g (Hilltop Lab Animals Growth Chart). This weight discrepancy only continues to grow as both sexes age[169] being close to 200 g difference around 1 year of age (Hilltop Lab Animals Growth Chart). In rodent studies, some researchers have detected females to experience higher levels of neuropathic allodynia and hyperalgesia, while others have not seen this difference[73,170]. A difference in the ability to withstand larger forces may be due to differences in sizes. Others have accredited hypersensitivity differences to the rodent species (mouse, rat), strain, age, and neuroinflammatory model; however, there is no overall conclusion surrounding whether these sex differences are accepted norms[170,171]. Furthermore, in humans, there is a broad understanding that females report neuropathic pain more often[97]. This could be due to the societal and cultural acceptance of gender norms, or it could be due to underlying biological differences[87]. This remains to be further explored.
In the studies presented here, even though, at baseline, aged-matched males and females differ by 1-2 grams on average in 50% withdrawal threshold, no significant difference could be detected between the two. Males and females are also similar in the pattern of the development of neuropathic inflammatory pain; with both sexes showing almost immediate hypersensitivity by day 2 post-CCI as well as sustained mechanical allodynia of around 3-5 grams in 50% withdrawal threshold by day 8 (Figures 3.1 and 4.1). Again, no sex difference could be detected between the two. This means that in our protocol, given similar injuries, both male and female

Sprague Dawley rats (aged 6-7 weeks) develop quantitively identical levels of mechanical allodynia. This is a crucial finding because then both cellular and transcriptomic differences can then be accredited to inherit differences in the biology between sexes rather than due to the differences in the expression of mechanical hypersensitivity.

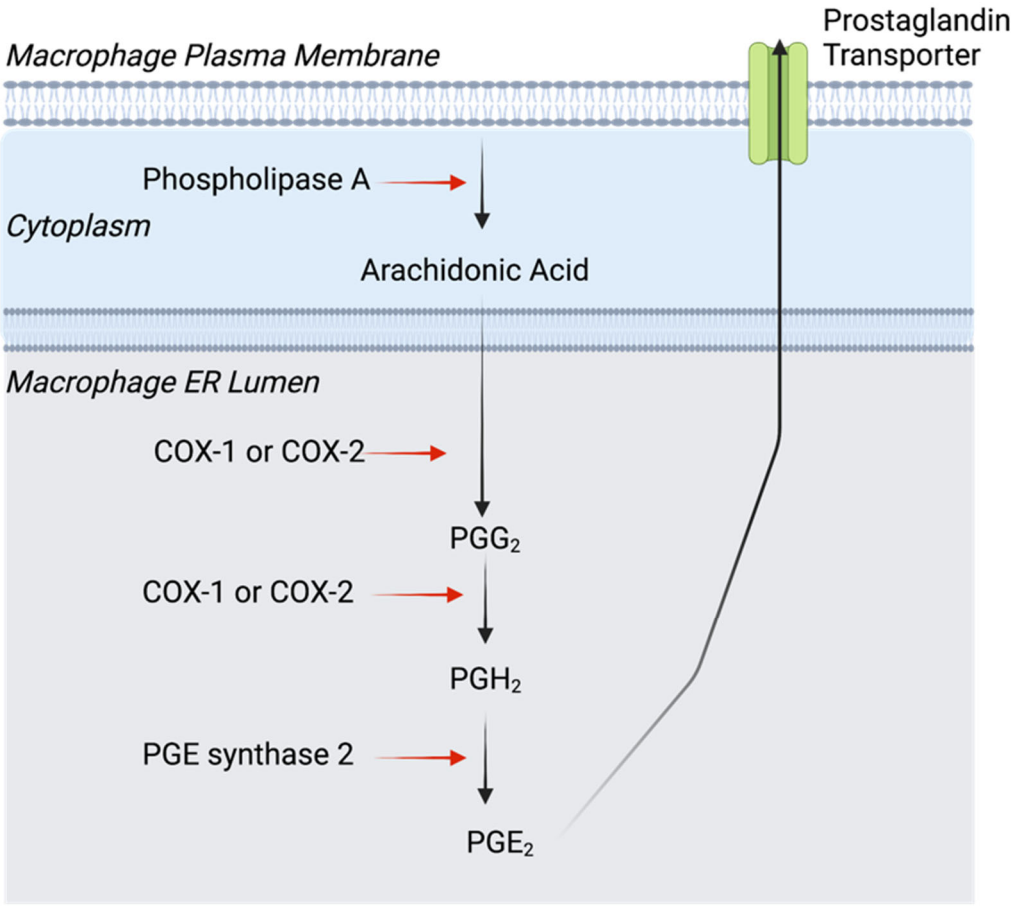

Figure 5.1. PGE_2 production by COX enzymes and PGE synthase 2.

5.1.2 Different responses to CXB-NE treatment

This celecoxib theranostic nanoemulsion has been previously seen to provide multi-day relief from mechanical allodynia in male CCI rats[51,54,55,57] with a single injection. It is able to reduce neuroinflammatory pain by decreasing levels of PGE_2[51,54] which would otherwise

sensitize the nerves. Because the nanoemulsion is present in about 50% of the infiltrated macrophages[54,114], Celecoxib is functioning as a selective COX-2 inhibitor, blocking the cyclooxygenase 2 enzyme from further production of PGE_2 in certain macrophages. The result is an attenuation of PGE_2 production, which decreases neuronal hypersensitivity (Figure 5.1). The study shown here (Figure 3.1b) reliably repeats what we have seen to be true, that a single dose of 1X CXB-NE theranostic nanoemulsion is able to provide around 5 days of significant relief from mechanical allodynia induced by neuropathic inflammation in males. However, what is revealed here is that the theranostic nanoemulsion works differently, and in this case less effectively on female neuropathic pain (Figure 3.1c) only providing 1 day of significant relief. Furthermore, the relief that females achieve is incomplete when compared to the males. This means that although males and females experience quantitively similar levels of mechanical hypersensitivity, when given the same dose, they do not experience similar levels of relief. However, once the theranostic nanoemulsion is loaded with 10 times the amount of celecoxib (10X CXB-NE), males and females exhibit nearly identical levels of mechanical allodynia relief (Figure 4.1b and c). Even though the increased drug loading leads to equivalent levels of relief, the previous demonstration that there is a sex difference from the 1X CXB-NE reveals that males and females may have different biological response to COX-2 inhibition. Therefore, even though the behavioral response to neuropathic inflammation evolves over the same time course and to the same degree in males and females, the underlying biology of that process appears to be sexually distinct.

This sex difference in 1X CXB-NE has also been seen in some recent work from the Janjic lab on inflammatory pain[58]. In the Janjic study, male and female mice who have induced inflammation of the paw pad by injection of complete Freund's adjuvant (CFA; heat killed

Mycobacterium tuberculosis) experience differences in the number of days of relief with males achieving 32 days of relief and females only achieving 11 days of relief[58]. Other researchers using the CFA inflammatory pain model in COX-1 and COX-2 knockout male and female mice also detected a difference in the involvement of these enzymes between sexes[101]. They saw that male inflammatory relief was most effective by COX-2 inhibition while females appeared to have an additive effect of COX-1 and COX-2 in the development of their inflammatory pain[101].

Non-steroidal anti-inflammatory drugs have been shown to be effective in treatment of inflammatory pain; however, it has previously been argued that NSAIDs are ineffective at treating neuropathic inflammation[37]. This is because in order to get to a systemic dosage to be effective, detrimental side effects occur such as gastrointestinal bleeding or cardiac issues[28,43]. The novelty presented here is that this is the first study to show that a COX-2 inhibiting NSAID can be used to treat female neuropathic pain. This portion of work addresses Specific Aim 1, which looked to "evaluate the efficiency of the COX-2 inhibiting celecoxib nanoemulsion to alleviate mechanical allodynia in both sexes". My hypothesis that females given CXB-NE treatment may experience relief differently than males is supported with these findings and the technicalities behind these differences will be discussed in the following sections.

Additional reasoning behind why 1X CXB-NE females responded differently than both the 10X CXB-NE females and their male counterparts could be that males and females appear to use COX-1 and COX-2 differently to induce inflammatory pain[101]. Here they found that COX-1 and COX-2 appear to play an additive role in female inflammation formation, while in males, the pain response is mainly driven by COX-2. Another study, looking at the effect of selective and nonselective COX inhibitors found that nonselective COX inhibitors work the best in females to reduce allodynia and the COX-2 specific inhibitor worked the best in males to reduce

inflammation[102]. Our study adds to these findings by showing that the COX-2 inhibiting theranostic nanoemulsion worked the most effectively in males at lower concentrations than females; however, celecoxib has slight COX-1 selectivity[172] and perhaps given at higher concentrations it then sufficiently blocked COX-1 leading to this behavioral phenomenon.

5.2 Neuroimmune response

Neuroinflammation due to injury involves the participation of multiple cell types including neuronal, immune, and glial cells[89]. A healthy response to injury induces heightened inflammation in order to recruit immune cells to clear cellular debris and give room for the growth of new axons[9] (Figure 1.1). Some of these phagocytic cells include macrophages, neutrophils, and activated Schwann cells, which typically function to myelinate axons, but when the axon is damaged, the Schwann cell changes its phenotype[9, 2,7]. Macrophages are a central component in this neuroinflammatory response with their ability to act as both pro-inflammatory (M1) and anti-inflammatory (M2) mediators[54,173]. Additionally, recent studies have seen neutrophils exhibiting both pro- or anti-inflammatory properties, being similarly referred to as N1 and N2 respectively. Impeding the entry of these cell types into the damaged tissue in the hours and days following injury has been shown to pro-longed neuroinflammatory pain[174]. Macrophages, because of their ability to produce pro-inflammatory mediators such as IL-1, IL-6, TNFα, and PGE_2[175], have been a target of neuroimmunologists with a focus on deciphering the macrophages role in the development of chronic pain. PGE_2 specifically has been a major focus because its presence has been linked to neuronal sensitization. Sensitization occurs through the binding of PGE_2 to its respective EP receptors, which when activated increases intracellular cAMP and Ca^{+}. These second messengers can cause heightened neurotransmitter release and

additional cytoplasmic signaling [92-95]. Similar to what we have previously reported, this current study shows that following CCI in the males, there is a significant increase in the number of infiltrating macrophages[47,51,54,55] compared to our sham animals (Figure 3.2c). In addition, for the first time, we reveal that neuroinflammation via CCI causes a dramatic increase in the number of infiltrating macrophages in females as well (Figure 3.2g).

This study shows that the number of macrophages in the sciatic nerve is correlated with neuronal hypersensitivity in both sexes. Sham animals, experiencing little to no hypersensitivity, have very few infiltrating CD68+ macrophages (Figure 3.2b and f) with the occasional residential macrophage present. However, following induction of neuroinflammation, the number of infiltrating macrophages rises as mechanical hypersensitivity increases (Figure 3.2c and g). This remains true at day 18 when the effect of 1X CXB-NE has subsided and mechanical hypersensitivity returns; the number of infiltrating macrophages remains high and is no different than the other treatment groups which did not experience relief and are still exhibiting hypersensitivity and pain-like behavior (Figure A.2). There was no statistical difference in the density of infiltrating macrophages between males and females experiencing hypersensitivity at any time point (day 12: CCI or DF-NE or Day 18: CCI, DF-NE or CXB-NE); however, females did trend to have slightly higher levels than males. This is not surprising considering that females are known to have a heightened immune response compared to males[176], which can sometimes lead to autoimmune disorders[23].

This finding is further supported by showing that when 1X CXB-NE is administered, the density of infiltrating macrophages decreases in parallel with the level of allodynia. Males who experience relief (Figure 3.1b) have significantly lower numbers of macrophages infiltrating the sciatic nerve as compared to their CCI and DF-NE at day 12 (Figure 3.2e). Females show a

similar pattern with their correlating density of macrophages mirroring their relief (Figures 3.1c and 3.2i). The most captivating finding from the 1X CXB-NE studies shows the correlation of sex differences in both behavior and infiltrating macrophages with 1X CXB-NE females experiencing statistically more allodynia than their male counterparts and having significantly more infiltrating macrophages in the sciatic nerve than their male counterparts (Figures 3.1 and 3.2).

Although these behavioral differences following treatment are parallel to the presence of macrophages, PGE_2 induces vasodilatation and recruits other immune cells such as additional macrophages, neutrophils, and mast cells[177]. Previous work with male rats from the Pollock lab showed that during neuroinflammation that macrophages had to undergo a phenotypic change in order to enter into the sciatic nerve. It was seen that macrophage cells "trapped" in the epineural sheath bared the CD11b marker while those macrophages that were infiltrated into the nerve bundle were CD68 expressing[55]. Macrophage phenotypic changes during neuroinflammation was further examined by looking at the presence of M1(pro-inflammatory) and M2 (anti-inflammatory) macrophages following CCI and 1X CXB-NE treatment[54]. Twelve days following injury in male rats, 75% of CD68+ macrophages infiltrating the sciatic nerve are M1 phenotype, with activated COX-2 generating increasing levels of PGE_2[54]. Additionally, mast cells were also present and were releasing mast cell protease 1 secretory granules. This is known to lead to cross talk between the two immune cell types increasing local inflammation. However, once males are treated with 1X CXB-NE, the phenotype of macrophages switches to M2 (60%) decreasing COX-2 expression, and reducing PGE_2 presence, as well as leading to a reduction in mast cell degranulation at the site of injury. It is seen that 18 days post CCI, that inflammation in the DRG significantly increases compared to day 12 indicating that inflammation distal to the neuronal

cell body is influencing the changes within the DRG milieu influencing neurogenic inflammation to these adjacent sites, millimeters away from the injury[54]. The ability to shift the environment at the DRG by shifting the environment at the site of injury is important to note given that this study looks at transcriptional changes at the DRG. Here we observed indicators for a shift in neutrophil phenotype seen in the DRG perhaps due to the switch in the macrophage phenotypes we know occur following CXB-NE treatment[54] Switching neutrophils towards an N2 or anti-inflammatory type phenotype secreting S100A8 and S100A9 and expressing Arginase 1 could additionally explain why males perhaps see more pain reduction than females at lower dosages given that others see these proteins providing pain relief[174].

Some explanation behind why 1X CXB-NE relieved mechanical allodynia and tissue level inflammation differently in females than in males may have to do with the TLR4 receptor, which activates PTGS-2 transcription for the COX-2 enzyme[158]. Studies have shown that blocking TLR4 in the spinal cord only leads to relief of neuropathic pain in males[26,27]. Other studies have shown that blocking p38[73], which is upstream from COX-2, also alleviates neuropathic pain only in males. Given that COX-2 is downstream from the TLR4 receptor and from p38 (Figure 4.11), blocking its function at this level appears to provide partial relief with 1X CXB-NE and almost total relief using 10X CXB-NE (Figures 3.1 and 4.1).

A different explanation for why these sex differences in relief arose could be due to the presence of other immune cells. Recent studies attributing sex differences in neuroinflammatory pain have focused on the adaptive immune system, specifically T cells in females. T cell presence and phenotype were a major focus of this work. Here I show that 12 days post-CCI, using the pan CD3e T cell marker, that T cells are located at the site of injury in both males and females, but appear mostly in the epineural sheath (Figure 3.4). Other studies have shown that T

cells take multiple weeks to infiltrate the nerve bundle[7] and that they achieve infiltration once other immune cells have created pathways for them to do so[12]. It is yet to be pinpointed what exactly it is about the T cell presence/absence that influences how females experience neuropathic allodynia[178]; however, one study linked it to the presence/absence of estrogen[27]. Nonetheless, estrus cycle was tracked along with our behavioral models (Figure A2.1), and no correlation between hypersensitivity or relief was found. What is known so far is that CD4+ T cells, also known as helper T (Tregs and Th2s), produce IL-10, which leads to a reduction of neuropathic hypersensitivity[12]. It has also been noted that rats experiencing neuroinflammatory pain have a higher number of CD4+/CD8+ cells in the DRG[179]. Another study depleted CD4+ T cells in male mice using antibodies and saw that hypersensitivity dissipated as well[180]; however, much of what we know of T cell involvement is from male inflammatory models[12]. Sex appears to be clearly linked in this response however, the molecular underpinnings need to be resolved. Here, I explored the CD4+/CD8+ presence and absence during neuroinflammation and relief (Figures 3.4, 3.5, and 3.6); however, in day-12 sciatic nerves, the T cells are predominately confined to the epineurium. Comparisons between sexes and treatments exhibited no difference. Figure 3.5 also shows how few of T cells were able to infiltrate the nerve. The presence of both CD4+ helper T cells and CD8+ cytotoxic T cells were there; yet, how they were influencing the cellular milieu remains to be uncovered. However, they may be influencing neuroinflammation and neuronal hypersensitivity via cytokine signaling from the adjacent position of the epineurium rather than directly from within the fasciculated axons themselves. Resolving this may also require analysis at different time points after CCI injury.

Taken together, this aspect of the work addresses specific aim 2, evaluating the presence of immune cells at the site of infiltration. The hypothesis that the presence of CD68+

macrophages in the cite of injury is an indicator of behavioral hypersensitivity is supported. However, the hypothesis that in females, T cell infiltration will decrease correlating with neuroinflammatory hypersensitivity and they will reflect more of a CD4+ phenotype is not supported. T cells do not appear to infiltrate the neuronal bundle and further evaluation exploring different time points and possibly using other methods such as flow cytometry should be considered.

5.3 Transcriptional differences

For decades, there was a sex disparity with most biological studies focused on males, especially in pain research. The result is that the foundational knowledge behind the development of chronic neuropathic pain is limited when it comes to females[22]. This, in addition to the fact that next generation sequencing was only commercially available starting around 2008, means that even less is known about female transcriptional regulation of neuropathic pain[19]. Evidence has shown that the transition from acute to chronic neuroinflammation is accompanied by gene expression changes in the neuronal cell bodies[79]. However, very few studies have begun to evaluate how these transcriptional changes then respond to neuroinflammatory treatment that provides relief. Here, I looked to address these concerns by using RNA-seq transcriptional analysis to evaluate the differential gene expression between male and female affected DRG during neuroinflammation and relief due to COX-2 inhibition.

Previous work in the Pollock Lab has looked at some transcriptional changes in the male DRG following chronic constriction injury and how these have responded to 1X CXB-NE treatment[55,57]. Here, I extend the work beyond this by assessing females as well as looking for transcriptional changes that occur in response to treatment with a 10X CXB-NE nanoemulsion.

This is important because this theranostic nanoemulsion treatment provides equivalent levels of relief in both males and females. In this way, differences in gene transcription between sexes should reveal biological differences rather than differences that result in the degree of pain relief. Using an FDR p-value ≤ 0.05 and a fold change greater than ±1, it was seen than males have 265 differentially expressed genes and that females have 977 differentially expressed genes following neuroinflammation via CCI. Of these differentially expressed genes, males and females share 89 genes. Some interesting genes include *activating transcription factor 3* (*ATF3*), *semaphorin 6a* (*SEMA6A*), *corticotropin releasing hormone* (*CRH*) and *VGF nerve factor inducible* (*VGF*) (Table 4.9). The interesting fact about these genes is that they are all responsive to 10X CXB-NE treatment, but in a sex dependent manner. *ATF3*, *SEMA6A*, *VGF* are all up regulated in both male and female neuroinflammation, but significantly decreased only in females following 10X CXB-NE treatment. Additionally, *CRH* is up regulated in males and females following neuroinflammation but only decreased in males following 10X CXB-NE treatment.

During neuroinflammation, males appear to follow the "typical" Wallerian degeneration pattern with increased induction of phagocytosis of macrophages and neutrophils (*NPY* and *THBS-1)* as well as decreased levels of myelination (*EGR2* and *ZBTB16*) and cytoskeleton processing (*SPTBN5*) (Figure 4.5 and Table A3.3)[7,9]. Other studies have seen that these basic properties such as Schwann cell de-differentiation[21], affecting myelination, changed following neuroinflammation. The Wallerian degeneration model is based off of decades of male based research and may not reflect what is happening in the female neuroinflammatory model as well.

In our model of female peripheral neuropathic pain we again see some immune regulators such as *NPY* and *ATF3* as well as an increase in cytokine signaling; however, when it comes to the cytoskeleton, there is an up regulation of microtubule processing with genes such as

FLRT3[142] and *GAP43*[143], which are known to be responsible for axon guidance after injury which is typical of Wallerian degeneration.

Once the theranostic nanoemulsion treatment has been administered, we observe a huge shift in differentially expressed genes when comparing 10X CXB-NE and DF-NE treatment groups; males exhibiting 333 differentially expressed genes while females, experiencing the same level of relief, only had 16 differentially expressed genes (using FDR p-value ≤ 0.05 and a fold change greater than ± 1) (Figure 4.8). Interestingly, even though the female response is small, it is influencing a significant decrease in *ATF3* expression and exhibiting a decreased biological enrichment for the *ATF2 Pathway* with *ATF3*, *JUN*, and *SEMA6A* within it (Figure 4.6). *ATF3* is a CREB transcription binding factor, which is activated similarly to COX-2 expression through toll like receptors[131]. ATF3 has been found to bind to the promotor of the *Ptgs2* gene regulating the production of the COX-2 enzyme[158] (Figure 4.11). With the reduction in the transcription of *ATF3*, which regulates COX-2, this could be why even though small numbers of genes significantly changed in females 10X CXB-NE animals causes such a dramatic change in behavior (Figure 4.1c). Other sex difference studies showed that when blocking Toll-like receptor 4[26,27] or p38[73], alleviation in female neuroinflammatory pain could not be achieved. Perhaps the true sex difference lies downstream at *ATF3* regulation and blocking this pathway earlier on doesn't give the ability to see where the divergence occurs.

Males undergoing neuroinflammatory relief also show an interesting pattern. One of the top biologically enriched pathways following 10X CXB-NE treatment is for neutrophil degranulation (Figure 4.7). Neutrophils are known to be acting within 24 hours in the neuroinflammatory response, functioning to help clear cellular debris, increase immune cell infiltration, and promote neuroregeneration[2,7]. However, it is intriguing that in tumors[145], it has

been recently shown that neutrophils are not only pro-inflammatory, but they can also be anti-inflammatory[146]. During this anti-inflammatory process, some studies have shown that the secretory proteins S100A8 and S100A9. These two proteins, S100A8 and S100A9, are neutrophil specific and have been shown to be a marker for neutrophil extracellular traps and activation[181], and treatment with these proteins has been shown to prevent the development of long lasting chronic pain[174]. These neutrophils influencing a healthy inflammatory response have been termed N2 and often bear the Arginase 1 protein[146]. In correlation with these, our studies see that *S100A8* and *S100A9* are only significantly increased following neuroinflammatory relief via 10X CXB-NE in males (Table A3.5). Additionally, arginase 1 increases 2.42-fold after treatment suggesting that one of the male exclusive factors contributing to relief could be the presence of N2 neutrophils.

Less stringent restrictions on gene filtering such as using a p-value rather than an FDR p-value ≤ 0.05 does provides a larger list of differentially expressed genes in both the inflammatory and relief gene sets for each sex (Figure 4.9 and Tables A.3.6 - A3.9); however, for this data analysis, FDR p-value was used to reduce false positive results.

5.4 10X CXB-NE Influence over COX-1, COX-2 and ATF3

While COX-2 expression measurements were not looked at between sexes within the sciatic nerve, the presence of the *PTGS2* gene (which codes for COX-2) was looked at within the DRG in both the CCI untreated and CCI treated states; however, it did not show any significant changes in expression in the DRG (Tables A3.2 - A3.9). This is an anticipated result given that the injury is at the sciatic nerve and not the DRG. The injury at the sciatic nerve recruits an influx of macrophages, and according to our previous work and the literature[182], these

macrophages are secreting PGE_2. One important point from Saleem et al (2019) shows that even though 1X CXB-NE leads to a reduction in the number of macrophages recruited to the sciatic nerve at day 12, it also blocks COX-2 production of PGE_2[54]. Nonetheless, the amount of COX-2 protein within each macrophage that is present does not appear to change based on the relative immunohistochemical fluorescence within a given cell[54]. Saleem also shows that what is going on at the sciatic nerve influences the environmental response in the DRG, but that at day 12, there are few macrophages being recruited into the DRG[54]. Given that the macrophages within the sciatic nerve are known to switch from pro-inflammatory to anti-inflammatory with CXB-NE treatment[54], it is not surprising that this response can indirectly influence a more anti-inflammatory response at the DRG, which may include N2 neutrophils being present there; an interpretation supported by the RNA sequencing data that will require further study.

The schematic (Figure 4.11) attempts to show how ATF3 can be transcriptionally regulated by the production of PGE_2 within the site of injury by being part of the feedback loop. ATF3 expression is known to increase with certain types of cellular stress[161]. Injury of the peripheral nerve of the DRG, but not the central projecting axons induces ATF3 expression [183]. In fact, the induction of ATF3 also seems rather selective for compounds or insults that may lead to nerve injury. Agents that cause inflammation, such as carrageenan or CFA, do not induce ATF3 expression [184], suggesting nerve injury, rather than the mere increased neuronal activation influences the shift in expression. So, possibly by increasing the concentration of CXB-NE additional changes in this feedback loop leads to signals that decreased cellular stress in 10X CXB-NE females as compared to 1X CXB-NE females.

Furthermore, given that others[101] have seen that females utilize an additive effect of COX1 and COX2 during neuropathic hypersensitivity. This could lead to an explanation for why

the 1X and 10X females are responding differently. Given that Celecoxib has some limited selectivity to COX-1[172], perhaps higher concentrations of Celecoxib begin to influence the activity of COX-1 to a sufficient level that we reveal similar levels of behavioral relief between sexes. Further assessment of COX-1 and COX-2 in females under these conditions is warranted.

Seeing that males and females develop equivalent behavioral hypersensitivity, along the same time-course and to the same degree, and when treated with 10X CXB-NE they exhibit quantitatively equivalent relief, the RNA sequencing data from the corresponding dorsal root ganglia reveal that the underlying biology of these behaviors are achieved through distinct mechanisms. Further study is needed to clarify the sex differences in the biology of pain and pain relief.

5.5 Future directions

The findings from this dissertation can be broken down into two major segments. Firstly, successful attenuation of both male and female neuropathic mechanical hypersensitivity was achieved. However, early studies using 1X CXB-NE in females reveal that this therapeutic treatment works differently and less effectively than in males. The 10X CXB-NE[77] seems to have minimized that difference; however, males seem to have hit a ceiling effect with no more relief being obtained. This could lead to personalized treatment with the 10X CXB-NE theranostic nanoemulsion.

Secondly, the transcriptomic studies reveal interesting fundamental sex differences in the underlying biology of both the development of neuroinflammatory pain between sexes and in relief via COX-2 inhibition with a theranostic nanoemulsion. Given that over 80% of adults

report using NSAIDs each year[121], and the fact that they are most commonly prescribed to women, these findings are very pertinent to daily use and future use of COX-2 inhibitors.

5.5.1 Longitudinal studies in neuroinflammatory relief

So far, the longest neuropathic pain study that we have evaluated is 18 days in both males and females using a single injection of 1X CXB-NE (Figure 3.1)[68]. Now that we have seen that females achieve equivalent relief over the same durations as compared to males using the 10X CXB-NE, a longitudinal study to see how long a single dose lasts is of utmost importance. Previous work went out to 18 days following CCI and saw that 1X CXB-NE in both males and females had a bell curve of around 6 days. The next study would to be to visualize the full extent of the drug behavioral response and then studies using a second dose of 10X CXB-NE should be performed using day 10 or 11 to continue to push the peak of relief outward a few days. This should be done in both male and female CCI animals in order to see if a prolonged relief can be achieved. Given that sustained relief is the overall goal of this theranostic nanoemulsion as well as the fact that COX-2 inhibitors can cause detrimental side effects with systemic long term use[43,44], demonstrating that multiple dosing of the theranostic nanoemulsion can provide extended relief from mechanical allodynia along with no evidence of toxicity is paramount.

5.5.2 Multiple assessments of neuroinflammatory pain relief

The Pollock Lab has routinely used the von Frey behavioral assessment to assay mechanical allodynia and relief in our neuroinflammatory model. Von Frey is an assessment of response to a provoked stimulus; however, an assessment of natural behavior to better understand how the pain is affecting function is also valuable. Studies evaluating pain and pain

relief at multiple levels in preclinical rodent models have been attributed to better clinical translation. Non-provoked assays such as CatWalk behavioral analyses or Grimace Scale could be done in order to assess natural behavior such as changes in locomotion, gait [185], or body language. Given the sciatic nerve does not only have nerves with mechanoreceptors but also chemoreceptors and thermoreceptors assays assessing hypersensitivity to temperature (Hargraves or acatone test) should be evaluated to test changes sensitivity to heat and cold during neuroinflammation and relief[167].

5.5.3. One suture CCI technique to lower variability

The traditional CCI technique involves the placement of 4 chromic gut sutures tied around the sciatic nerve tight enough to induce inflammation, but loose enough to not cut off function and flow of the vascular innervation of the nerve[75]. CCI is a technical surgery where reproducibility of knot tightness is important. Differences between one experimenter and the next or even between one knot in the next can add variation in a study[164]. In order to reduce variation, tighten results, and use less animals, fewer knots can be used. These studies have seen that a single knot causes similar levels of mechanical allodynia[186] to that which is seen with four knots from the Bennett and Xie model[75] and results last for up to 84 days[187].

5.5.4. Flow cytometry to phenotype immune cells at the site of injury and in the DRG

Immunohistochemistry provides for visualizing cellular location within a tissue, identification of cell type and even subcellular localization, which can provide information of protein function; e.g. nuclear, versus cell surface. Little manipulation is done to the tissue prior to use; therefore, visualized results should be representative to what is occurring *in vivo*.

However, when you visualize samples using IHC, you are limited to the small section of tissue on the slide unless you dedicate an entire tissue sample to serial sectioning analysis. When using flow, whole tissue samples can be analyzed for the presence/absence of certain immune cells and antigens. In fact, one study looking at the presence of an antigen in tumor cells found that flow cytometry had superior ability at detecting an antigen because it was present at lower quantities[188]. Flow cytometry can label up > 40 different markers at once allowing you to visualize a wide array of immune cell types at once while IHC is often limited to a four-stains maximum. This means that from a single sample, you are better able to phenotype multiple cell types using flow cytometry. However, the rat L4-L6 DRG contains about 41,000 neurons; yet, there are even fewer immune cells present at baseline. This means in order to run a flow study multiple animals would need to be pooled together for a successful run and the individuality of the data would be lost. Even so, this could give a good idea of targets to look for in the IHC tissue samples. T cells are a trending topic in the differentiation of female neuropathic pain with the major focus being in the central nervous system[26,27,97]. However, it is clear that they are present at the site of injury (Figure 3.4) and are taking place in the overall peripheral neuroinflammatory response. A better understanding of this interplay between Th1, Th2, Th17, T regs, and CD8 cells could give insight into how these cell types influence the pro- and anti-inflammatory response. It would also give us the ability to identify the singularly stained CD8+ cells infiltrating the sciatic nerve as pan IHC markers for dendritic cells are harder to come by. Lastly, phenotyping neutrophils to further research into N1 and N2 phenotype as well as seeing whether or not they phagocytize nanoemulsion is of extreme interest.

5.5.5 Assessment of early and long-term use of 10X CXB-NE

A recent study has provided some insight into the importance of the acute inflammatory response in the resolution of neuroinflammatory pain. Patients (n = 98) with acute lower back pain were tracked over a three-month period and peripheral blood samples were transcriptionally compared between those who developed long term pain and those who were now experiencing relief. Those in sustained pain had no differentially expressed genes from during their acute visit; however, those experiencing relief had 1700 differentially expressed genes compared to their acute visit. It was seen that some of the top hits had to do with neutrophil involvement including genes *S1008A* and *S1009A,* which are known to regulate inflammation levels. The scientists also found a correlation that using NSAIDs to decrease this early neuroinflammatory response, patients were twice as likely to develop long term neuropathic pain[174]. This was attributed to the reduction of neutrophils early on which typically function to clear cellular debris, give room for neuronal regeneration, and influence the local inflammatory response. To confirm the early use of NSAIDs can induce higher risk of chronic pain, and that it can be rescued by S1008A and S1009A proteins, the scientists moved to rodent studies. Mice who underwent CCI and CFA inflammatory induction were treated with the NSAID diclofenac for the 6 consecutive days following injury. (No sex is indicated for these rodent studies.) Once treatment wore off, the duration of mechanical allodynia was significantly greater in those treated with diclofenac in CFA models. Furthermore, in the CCI model, NSAID treatment was followed by prolonged duration of allodynia[174]. Scientists then saw that the prolonged hypersensitivity due to NSAID treatment could be reversed by injections of neutrophil specific proteins S100A8 and S100A9[174]. The authors claim that the initial acute response is key in resolution of long-term inflammation which may lead to chronic pain.

Given these findings, it is imperative to see how our NSAID therapeutic is affecting hypersensitivity long term. These studies use systemic wide dosages where our studies use significantly decreased dosages of NSAIDs encapsulated in nanoemulsions providing fewer off target effects. Future studies looking at allodynia and neuroregeneration at further time points are warranted in order to assure that early usage of CXB-NE does not pro-long neuroregeneration and resolution of the injury's healing.

APPENDIX 1.A

TAIL VEIN INJECTION PROTOCOL

Based on the publication:

M. Saleem*, A. Stevens*, **B. Deal**, L. Liu, J. M. Janjic, J. A. Pollock (2019) A new best practice for validating tail vein injections in rat with near infrared labeled agents. JoVE - J. Vis. Exp., e59295. *Co-authors contributed equally.

A.1.1 Abstract

Intravenous (IV) administration of agents into the tail vein of rats can be both difficult and inconsistent. Optimizing tail vein injections is a key part of many experimental procedures where reagents need to be introduced directly into the bloodstream. Unwittingly, the injection can be subcutaneous, possibly altering the scientific outcomes. Utilizing a nanoemulsion-based biological probe with an incorporated near-infrared fluorescent (NIRF) dye, this method offers the capability of imaging a successful tail vein injection in vivo. With the use of a NIRF imager, images are taken before and after the injection of the agent. An acceptable intravenous injection is then qualitatively or quantitatively determined based on the intensity of the NIRF signal at the site of injection.

A.1.2 Introduction

The route of administration of agents into small animals serves as a critical point of many experiments. It determines where the agent is to be delivered and, subsequently, what will happen to the agent thereafter. Although other routes can be used for agent administration[189], the intravenous route of delivery is a preferred route for certain agents. Intravenous injection allows agents to be directly injected into the bloodstream, bypassing first-pass tissue effects and the need for extraneous solute absorption[189]. This also allows for targeting cells in the bloodstream[49,51] and direct delivery to all tissues within the circulatory system. In rodents, several veins can be considered, including the jugular, the saphenous, and the tail vein.

In this method, a NIRF dye containing a biological probe—in this case, a nanoemulsion (Figure A1.1A)[48,49,190,191]—is injected into the lateral tail vein of rats. This particular NIRF-containing nanoemulsion has been used previously to image and track neuroinflammation in vivo and ex vivo[192,193] in a rat model[75] of neuropathic pain[47-49,51,112,190]. Imaging is conducted before and after the injection with a preclinical NIR fluorescence imager. This serves as a tool to validate the quality of the agent administration. Imaging prior to the tail vein injection serves as a basis for obtaining a baseline image.

Increasingly in animal studies, intravenously administered nanoemulsions are being utilized as biological probes and targeting agents[194-197]. It is a proven challenge to administer an agent via the tail vein[198,199]—be it a drug, a viral vector, or another probe—and to ensure that the entire contents of the injection have successfully entered the bloodstream and not the surrounding tissues[199]. Therefore, a method of visualizing and evaluating the quality of a successful injection is beneficial.

Typically, a heat lamp or warm water is used to warm the tail, which causes dilation of the

vein, permitting its visualization prior to injection. While this ensures easier entry into the vein, there is not a quantitative way to discern whether the compound has entered the bloodstream in its entirety[200-203]. This becomes more difficult still in strains of animals where the vein contrasts faintly with the skin, such as in black mice. Typically, the investigator can gauge a failed injection by experiencing resistance during the injection and, in some cases, visualizing a bulge on the tail, indicating a subcutaneous leakage of the agent[204,205].

In this study, NIRF imaging of the nanoemulsion injected into the lateral tail vein of live rats is performed on a small-animal NIRF imaging system. Rats are fed a special purified diet to reduce nonspecific gut fluorescence. Simultaneous image acquisition of white light and 800 nm fluorescence is captured using the NIRF imager and associated software. The relative fluorescence intensity is measured on the tail at the pre-injection and post-injection states. The fluorescence intensity for the region of interest at the site of injection is recorded and divided by the area of the ROI. Qualitative assessments can be made on which injections are acceptable. Optionally, further quantitative analysis can be performed by setting thresholds for acceptable injections and assigning region of interest measurements into groups, at which point statistical significance can be calculated.

By utilizing this validation strategy following tail vein injections, the standard of a research study improves due to increased consistency of agent administration. This method of assessing the quality of tail vein injection can be easily customized for different injectable agents to include infra-red fluorescent probes provided commercially by several companies.

A.1.3 Protocol

All protocols were performed in accordance with the guidelines in the Guide for the Care and

Use of Laboratory Animals of the National Institutes of Health and Institutional Animal Care and Use Committee (IACUC) at Duquesne University.

A.1.3.1 Preparation and anesthesia

NOTE: Aseptic techniques are used for the entirety of the procedure. Only new sterile materials and autoclaved sterile instruments are to be used. Personal protective equipment (sterile gloves, hair bonnet, surgical mask, scrubs) needs to be worn to avoid contamination.

1. Adult male Sprague-Dawley rats weighing 250–300 g were used in this protocol. Acclimate the rats to standard living conditions, keep them on a 12 h light/12 h dark cycle, and provide food and water ad libitum. House the animal socially, keep them on paper bedding, and provide a special diet to avoid autofluorescence during imaging.
2. With the use of a properly placed heating pad, anesthetize the animal under an initial 5% isoflurane in 20% oxygen, followed by a maintenance level of not less than 1.5% isoflurane and not more than 3%, unless the animal wakes up or retains feeling.
3. Confirm proper anesthesia via a lack of response to tail pinches. Monitor the blood flow as well via vital signs throughout the procedure.

A.1.3.2 Pre-injection

1. Image the animal in a preclinical NIR fluorescence imager by positioning the animal laterally to expose the injection site on the lateral tail to establish a baseline of fluorescence in the tail (Figure A1.1C, E). Perform a simultaneous image acquisition of both a white light (body view) and near infrared channels using the NIRF imager and associated software, with linked lookup tables (LUT).

2. Following imaging, move the animal back to the surgical table, and place it under anesthesia for the tail vein injection. NOTE: Continue monitoring the animal's vital signs and recheck proper anesthetization via tail pinch.

A.1.3.3 Tail vein injection with NIRF-containing agent

1. With the animal in the prone position, orient the tail with the dorsal side facing up. Dilate the tail vasculature in warm water for a minimum of 1 min. Orient the tail vein so the lateral side (either right or left) is turned 30° (clockwise or counterclockwise) to expose the right or left tail vein (Figure A1.1B).
    1. Once a lateral tail vein has been located (which appears dark-colored upon dilation), disinfect the entire tail with alcohol pads, repeating 2x.
    2. At an appropriate dosage based on the study design, begin injections in the distal coccygeal vertebrae region of the tail and moving more proximal if proper needle placement fails.
2. Insert a 25–27 G sterile needle, bevel up, into the lateral tail vein, with the tail at a 180° angle, inserting the needle parallel to the lifted tail. Observe blood flashback in the rim of the needle to ensure correct placement. If no flashback is apparent, slowly move the needle tip (without removing it from the tail) to find vein insertion. If placed subcutaneously, no blood flashback will occur.
3. Insert the syringe with the injectable materials into the rim of the needle. When proper placement is achieved, the injectable fluid will not incur resistance upon injection. The injection will advance smoothly and easily. Once injected, remove the needle and the syringe, apply pressure with sterile gauze for at least 1 min to ensure clotting, and mark

the spot of injection with a pen on the tail, ensuring it is visible on the white light image. NOTE: No hematoma or lesion will be visible at the site of injection.

4. If the needle tip moves during the syringe insertion, remove the needle and retry the needle entry procedure more proximal on the ipsilateral tail vein. Do not reuse the same needle if a different reentry point is tried.

   NOTE: Alternatively, the injection can be performed with an intravenous catheter with a blood-flow indicator. This has the benefit of visual confirmation of the catheter during venipuncture. Insert the catheter, bevel side up, at the angle previously described. Observe prompt flashback in the entire length of the blood-flow indicator to ensure correct placement. Slight back pressure can be used to pull blood into the syringe to confirm proper placement in the vessel before injecting. Again, no resistance will be felt.

A.1.3.4 Post-injection

1. Perform quality assessment following tail vein injection in a preclinical NIR fluorescence imager in the same orientation as the baseline pre- injection image. Ensure the animal is still properly anesthetized — and will be so for the duration of imaging — prior to placing it in the imager. NOTE: An imaging system containing a drawer housing with anesthesia connections and a mask for the animal should be used if available.
2. Orient the animal on its lateral side to expose the injection site (as marked) on the lateral tail. Check to see if a NIRF signal is present only at the site of injection. This indicates a successful tail vein injection (Figure A1.1D). NOTE: If the signal is dispersed throughout the entire tail, it is considered to be subcutaneous and, hence unsuccessful (Figure A1.1F). Figure A1.2 shows additional examples of failed injections.

A.1.4.5 Image quantification

NOTE: Image quantification can be performed with the imaging software that accompanies the NIR imager, if this function is available. Alternatively, other commercially available image analysis software may be used[206].

1. In the post-injection image, draw a region-of-interest around the area of fluorescence at the injection site[51,191].
2. Measure the area and relative fluorescence intensity and record as area/intensity. Compare post-injection and baseline pre-injection images either qualitatively or quantitively by using appropriate statistical analysis (dependent on study groups and conditions). NOTE: The researcher can decide on thresholds that discriminate good from bad injections or assign a percentage of quality to the injection.

A.1.4 Representative results

Rats were injected with NIRF-containing nanoemulsion into the lateral tail vein, and pre- and post-injection images were taken with the small- animal imager as described in the protocol. Post-injection images are qualitatively assessed for injection quality and placed into 'good injection' (n = 7) and 'bad injection' (n = 4) groups. Qualitative assessment was carried out by observing the post-injection area fluorescence intensity. In an optimal injection, the NIRF signal is confined to the site of injection. No signal will be seen if the injection is successful because the agent has been fully displaced into the bloodstream. A bad-quality injection displays a NIRF signal that is dispersed along the length of the tail.

Images were analyzed with the accompanying NIRF imager software. Regions-of-interest were drawn at the site of pre-injection images (Figure A1.1C, E) and around the area of

fluorescence in post-injection images (Figure A1.1D, F). Images where fluorescence was visible throughout the length of the tail were deemed unacceptable and removed from the analysis (Figure A1.2). Measurements of the area and fluorescence intensity were recorded. Values for area/fluorescence intensity were calculated and plotted (Figure A1.1G). A significant difference (unpaired *t*-test) in fluorescence intensity between pre- and post-injection images was observed in the 'bad injection' group (Figure A1.1G) ($p = 0.0024$).

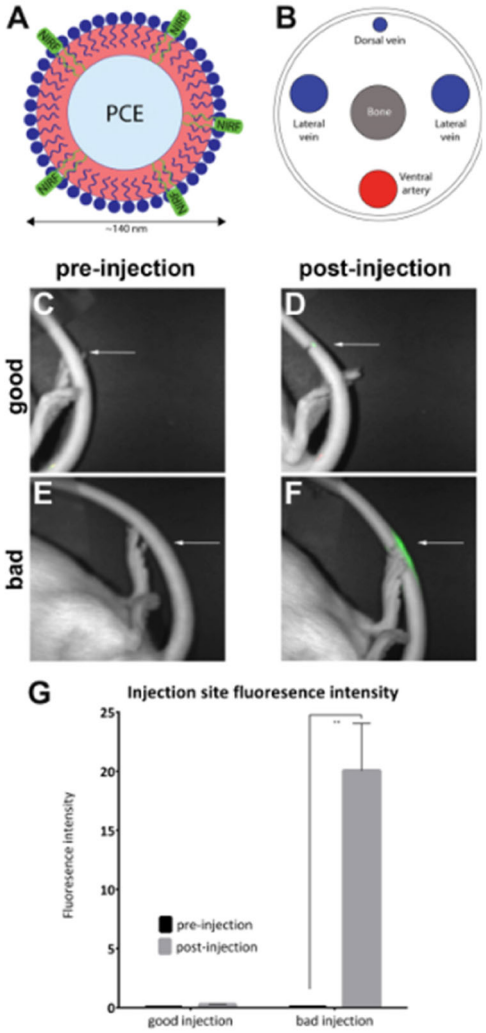

Figure A1.1: NIRF based nanoemulsion and images of tail vein. (**A**) A nanoemulsion-based biological probe containing NIRF dye was injected into (**B**) the lateral tail vein and imaged in a NIRF imager. (**C** and **D**) Pre- and postinjection images of a good injection. (**E** and **F**) Pre- and

Figure A1.1 (continued) post-injection images of a bad injection. White arrows indicate the point of injection. It is possible to qualitatively assess the success of a good injection compared to a bad injection by assessing the extent of the NIRF signal at the site of injection. Unacceptable injections display fluorescence throughout the length of the tail and were removed from the analysis (**Figure 2**). (**G**) The images can also be analyzed to reveal a quantitative measure of fluorescence intensity, with thresholds for injection quality assigned by the investigator. The error bars on the graph reflect the SEM. For the 'good injection' group, n = 7. For the 'bad injection' group, n = 4. There is a statistical difference in fluorescence intensity in the 'bad injection' group when comparing pre- and postinjection images (unpaired t-test; p = 0.0024).

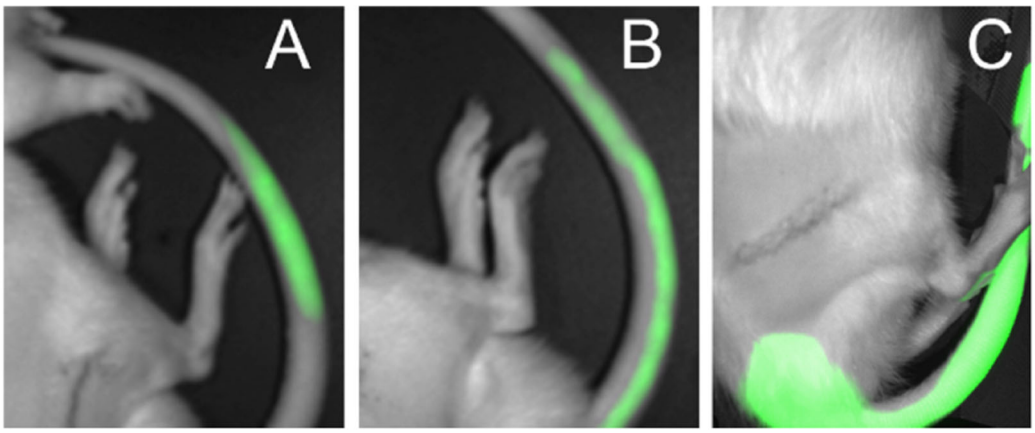

Figure A1.2. Examples of bad injections. (A) Fluorescent signal seen in part of the tail. (B) Fluorescent signal seen over the full length of the tail. (C) Fluorescent signal dispersed heavily in the entire tail and caudal area of the animal's body.

A.1.5 Discussion

Research laboratories incur significant costs as a result of the misadministration of testing agents. Tail vein injections are a difficult technique to master to attain consistent success rate, with

the most experienced of technologists often incurring misadministration errors. There is no reliable way to confirm a successful injection. This protocol offers a solution to this problem by giving researchers a qualitative and quantitative method to validate the success of a murine tail vein injection. Here, a NIRF-labelled nanoemulsion[192,193,207] incorporates the agent of choice (in this case, a drug) and is imaged at the site of injection in a NIRF small-animal imager. There is also the option to develop a non-nanoemulsion-based agent and use the same principle of NIRF imaging by incorporating commercially available infra-red dyes. Additionally, ready-to-use imaging agents with a variety of applications, such as tumor imaging, metabolic imaging, cell trafficking, and apoptosis are also commercially available. An injection is performed either by using a sterile needle or, alternatively, an intravenous catheter; this depends on the preference of the researcher. In addition, automated tail vein injectors[208] have been used to assist in this process and are compatible with this methodology. However, this technology has not yet become commercially available.

There are important steps in the tail vein injection method that ensure a higher rate of correct agent administration. First, the tail should be cleaned with ethanol to remove any dirt or debris, allowing researchers to better visualize the vein. Dilating the vein by submerging the tail in warm water is also a very important step in the method, as it allows a greater surface area for injection. Injecting at a more distal point on the tail vein allows for some error, in the event that multiple attempts are required. Injection should be attempted at a more proximal position in the tail as the tail vein increases in size as the caudal aspect of the animal's body is approached. In addition, the contralateral tail vein can be used if needle placement fails in more than three to five sites on the ipsilateral tail vein.

A successful administration of a test agent results in little to no NIRF signal at the point of

injection. If no resistance is felt during the administration of the injection and there is little to no fluorescence at the tail, then the injection can be recorded as successful. If resistance is felt during injection and there is a trail of NIRF signal along some length of the tail, then the injection is recorded as unsuccessful and is likely partly subcutaneous. Fluorescence images are taken pre- and post-injection, and the quality of the injection is assessed by observing qualitatively or analyzing quantitatively the fluorescence signal at the site of injection. The software accompanying the NIR fluorescence imager is often capable of performing this analysis.

The method can be adapted in several ways. It is applicable to tail vein injection in both mice and rats. Most small-animal NIR fluorescence imagers will be capable of accommodating murine rodents. Levels of anesthesia need to be adjusted depending on the weight of the animal, in accordance with the research laboratory's IACUC protocol. Another possible modification is the preparation of a non-nanoemulsion-based probe either by incorporating an infrared dye into the researcher's formulated agent or by purchasing a ready-to-use imaging agent, tailored to a specific biological application.

If a rat is relatively large, it can often be difficult to position it in the small-animal imager. It is thus recommended that a test image is taken with the animal in the drawer before injecting, and a field of view ascertained where the tail is visible. It is helpful to tape the tail to the drawer of the imager, to ensure it does not move during imaging.

Alternative methods seeking to assess the quality of tail vein injections in small animals are limited to the utilization of labeling reagents that do not interfere with concurrent experimental procedures and require euthanasia of the animals postinjection[194,195]. Some reagents may impact study outcomes and the therapeutic assessment of the animals involved, so care in experimental design is recommended.

This method can, in the future, be refined with advances in small-animal imaging technology, as well as improvements in infrared fluorescent probes. Biological probes with an incorporated infrared dye, designed for a variety of different applications, can be used at the agent administration stage of a study design to validate the quality of an injection, as outlined in this method[49,51,209-214].

APPENDIX A.2

SUPPLEMENTARY FIGURES FROM CHAPTER III

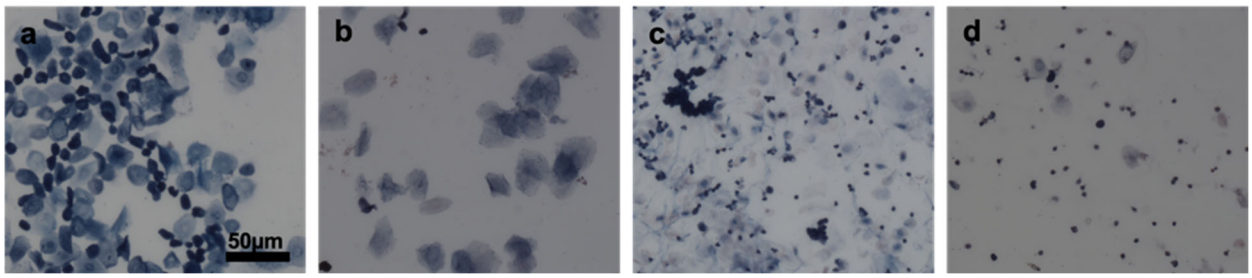

Figure A2.1. Vaginal smears were used to stage the ~ 4-day estrous cycle of all of the female rats; with the CXB-NE females all being cycled together in estrus such as seen in panel b. **a.** Proestrus is characterized by the vast majority of cells being nucleated epithelial cells with a small presence of neutrophils. **b.** Estrus is characterized by primarily anucleated keratinized epithelial cells. **c.** Metestrus is characterized by the combination of neutrophils and anucleated keratinized epithelial cells where neutrophils begin to outnumber epithelial cells and clump together. **d.** Diestrus is characterized by low numbers of cells with small numbers of both neutrophils and epithelial cells.

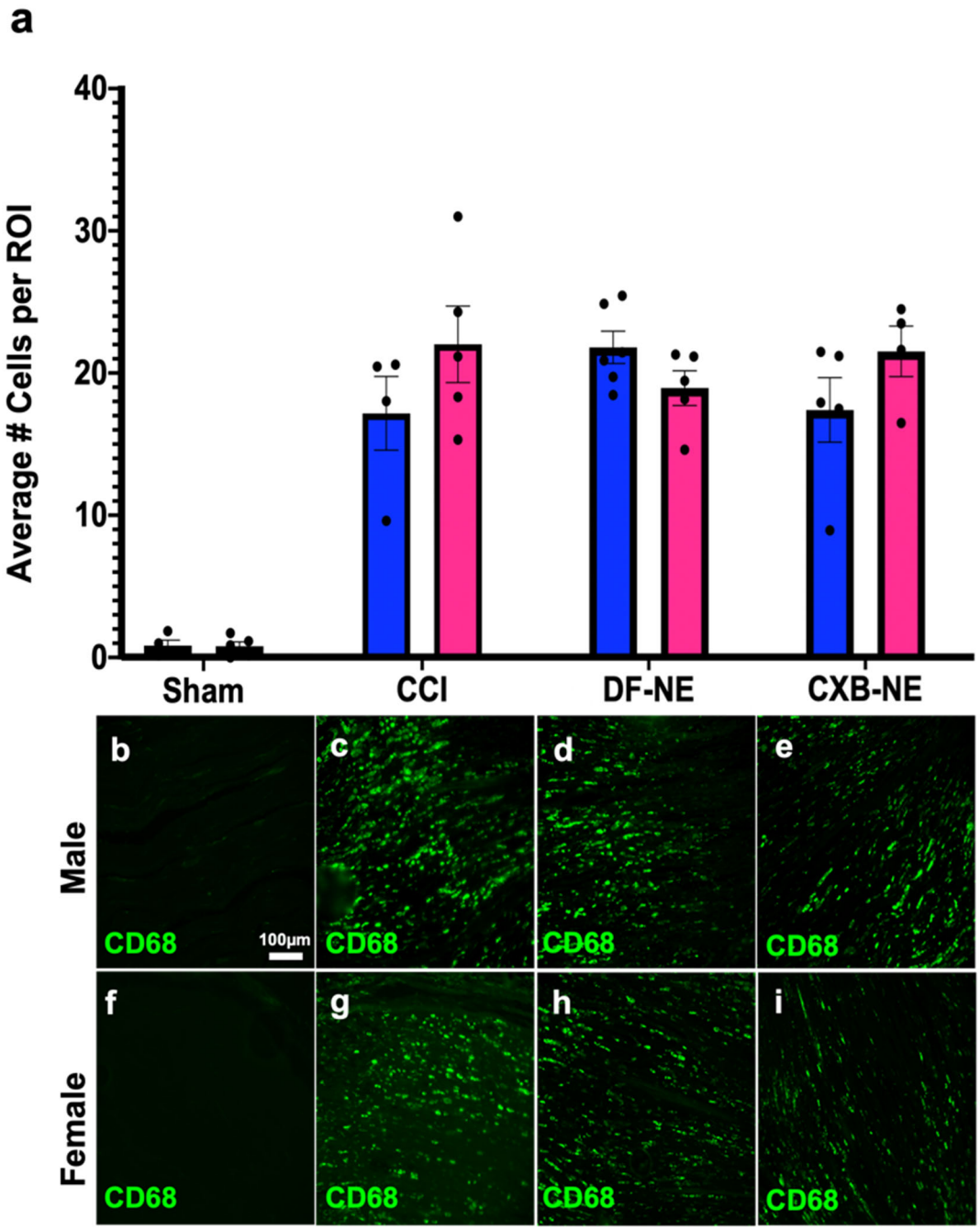

Figure A2.2. Day 18 macrophage infiltration in 1X CXB-NE heightens to a similar level of CCI and DF-NE as they return to hyperalgesia. **a.** Average number of CD68+ macrophages per region of interest across sex and condition. Male values are listed in blue and female values in pink. Data is displayed as averages ± SEM. Sham n = 4 (male), 4 (female); CCI n = 4 (male), 4 female; DF-NE n = 6 (male), 5 (female); and CXB-NE n = 5

Figure A2.2 (continued) (male), 4 (female). **b-i.** Immunofluorescence staining for CD68+ macrophages in the sciatic nerve. Male and female data was compared using a two-way ANOVA with a Tukey's post hoc analysis.

APPENDIX A.3

SUPPLEMENTARY FIGURES FROM CHAPTER IV

Table A3.1 Select table of primers used for qPCR including *ATF3*, *SEMA6A*, *VGF*, and the housekeeping gene *GAPDH*.

ATF3	Forward	5'-CCT GCA GAA GGA GTC AGA GAA-3'
	Reverse	5'-CGT TCT GAG CCC GGA CGA TA-3'
SEMA6A	Forward	5'-AGC AAG ACA TAG AGC GTG GC-3'
	Reverse	5'-TGG CAC GCC CAT TCA GT-3'
GAPDH	Forward	5'-GGC ACA GTC AAG GCT GAG AAT G-3'
	Reverse	5'-ATG GTG GTG AAG ACG CCA GTA -3'

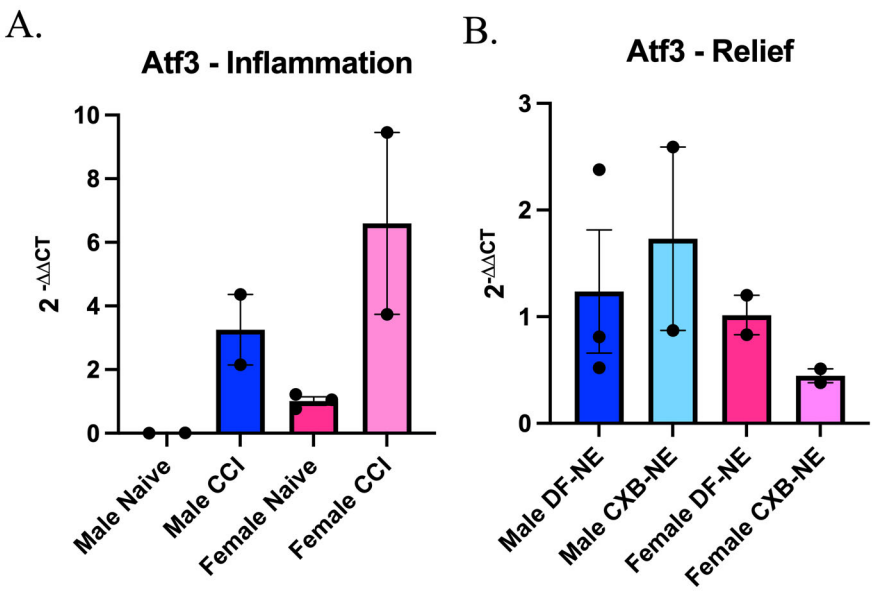

Figure A3.1 qPCR Results Looking at Expression Change in *ATF3*. A. Both male and female CCI DRGs show an increase in expression of *ATF3* following neuroinflammatory induction.

Figure A3.1 (continued) Male naïve n =2, female naïve n = 3, male CCI n = 2, female CCI n = 2. B. Female 10X CXB-NE appear to have a decrease in their *ATF3* expression when experiencing mechanical allodynia relief in contrast to their DF-NE counterparts. Male *ATF3* is unaffected. Male DF-NE n = 3, Female DF-NE n = 2, male 10X CXB-NE n = 2, Female 10X CXB-NE n = 2.

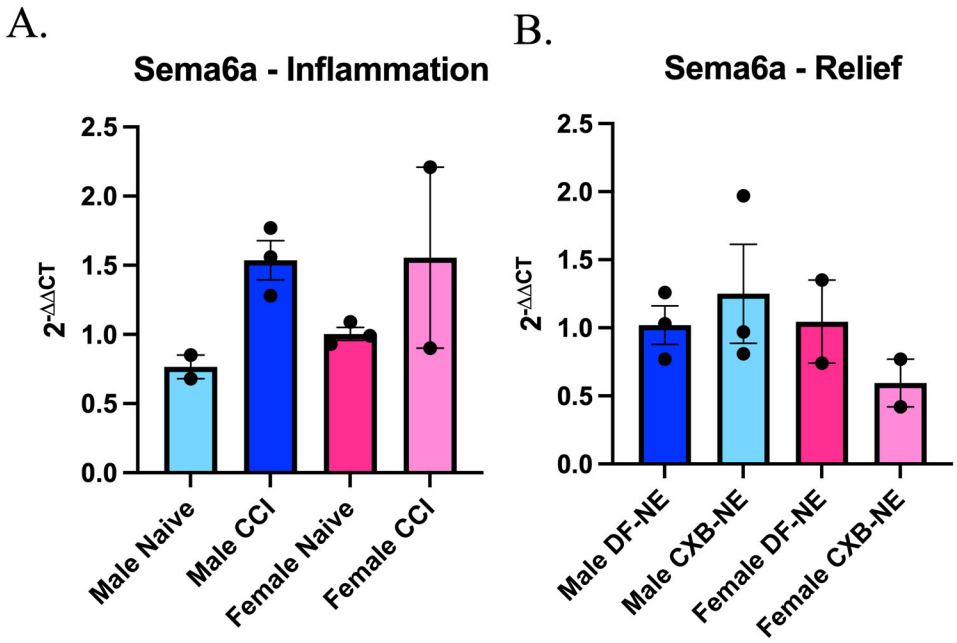

Figure A3.2 qPCR Results Looking at Expression Change in *SEMA6A*. A. Both male and female CCI DRGs show an increase in expression of *SEMA6A* following neuroinflammatory induction. Male naïve n =2, female naïve n = 3, male CCI n = 3, female CCI n = 2. B. Female 10X CXB-NE appear to have a decrease in their *SEMA6A* expression when experiencing mechanical allodynia relief in contrast to their DF-NE counterparts. Male *SEMA6A* is unaffected. Male DF-NE n = 3, Female DF-NE n = 2, male 10X CXB-NE n = 3, Female 10X CXB-NE n = 2.

Table A3.2. Master list of differentially expressed genes between Female CCI vs Naïve samples with a FDR p-value ≤ 0.05 and a fold change greater than ±1.

Name	Log_2 fold change	Fold change	P-value	FDR p-value	Bonferroni
AABR07001926.3	0.54	1.46	3.74E-05	2.18E-03	0.7
AABR07002774.1	0.57	1.49	2.79E-03	0.04	1
AABR07005844.1	-0.94	-1.91	2.16E-05	1.42E-03	0.4
AABR07007068.1	0.43	1.35	2.09E-04	8.02E-03	1
AABR07007675.1	-0.99	-1.99	2.30E-03	0.04	1
AABR07028902.1	0.25	1.19	1.20E-03	0.03	1
AABR07040412.1	0.5	1.41	1.77E-04	7.13E-03	1
AABR07040864.1	0.29	1.22	2.27E-03	0.04	1
AABR07040947.1	0.66	1.58	9.53E-06	7.45E-04	0.18
AABR07044388.2	-0.45	-1.37	1.16E-04	5.28E-03	1
Abca1	0.37	1.29	1.35E-03	0.03	1
Abca2	-0.32	-1.25	3.09E-05	1.88E-03	0.58
Abce1	0.3	1.23	1.37E-04	5.98E-03	1
Abcf3	-0.3	-1.23	5.93E-04	0.02	1
Abcg4	-0.41	-1.33	1.62E-03	0.03	1
Abhd16a	-0.47	-1.39	2.07E-07	3.06E-05	3.90E-03
Abhd17a	-0.49	-1.4	6.56E-07	8.29E-05	0.01
Abhd2	-0.23	-1.18	3.01E-03	0.05	1
Abhd8	-0.79	-1.73	1.22E-09	3.96E-07	2.29E-05
Ablim2	-0.47	-1.39	3.64E-04	0.01	1
AC105662.1	-0.89	-1.86	3.57E-04	0.01	1
AC130391.3	-0.98	-1.97	2.17E-04	8.12E-03	1
AC130970.1	1.92	3.77	1.68E-13	1.41E-10	3.15E-09
Acbd6	0.43	1.34	1.73E-03	0.03	1
Ache	-0.24	-1.18	3.18E-03	0.05	1
Acsl4	0.52	1.43	2.92E-10	1.23E-07	5.49E-06
Acta2	-0.66	-1.58	1.26E-05	9.30E-04	0.24
Actg2	-1.15	-2.22	1.69E-03	0.03	1
Actr6	0.3	1.23	1.86E-03	0.03	1
Adam11	-0.38	-1.31	5.22E-06	4.75E-04	0.1
Adam12	0.54	1.45	2.04E-04	7.89E-03	1
Adamts10	-0.42	-1.34	1.72E-03	0.03	1
Adamts2	-0.58	-1.49	5.34E-04	0.01	1

Adamtsl5	-0.99	-1.98	5.33E-04	0.01	1
Adcyap1	1.07	2.11	7.46E-10	2.66E-07	1.40E-05
Adgrg1	-0.25	-1.19	1.97E-03	0.04	1
Adra2c	-0.74	-1.67	1.74E-03	0.03	1
Aebp1	-0.39	-1.31	6.54E-06	5.81E-04	0.12
Agap3	-0.28	-1.21	6.50E-04	0.02	1
Ahdc1	-0.38	-1.3	2.41E-03	0.04	1
Ahr	0.39	1.31	4.38E-05	2.50E-03	0.82
Akap17b	0.41	1.33	1.38E-05	1.00E-03	0.26
Akap8l	-0.27	-1.21	3.38E-03	0.05	1
Akr1b1	-0.3	-1.23	2.22E-04	8.23E-03	1
Akr7a2	-0.46	-1.38	1.84E-03	0.03	1
Alad	-0.64	-1.56	1.08E-03	0.02	1
Alcam	0.28	1.21	2.68E-04	9.22E-03	1
Aldh1a3	-0.62	-1.54	6.51E-04	0.02	1
Aldoa_2	-0.88	-1.84	9.15E-04	0.02	1
Alkal2	2	3.99	2.88E-05	1.78E-03	0.54
Amigo1	-0.24	-1.18	3.36E-03	0.05	1
Amigo3	-0.47	-1.39	5.93E-09	1.44E-06	1.11E-04
Anapc4	0.29	1.22	7.31E-04	0.02	1
Ankfn1	-0.56	-1.48	2.67E-03	0.04	1
Ankrd1	2.52	5.73	1.24E-04	5.54E-03	1
Ankrd12	0.3	1.23	1.02E-04	4.72E-03	1
Ap1ar	0.25	1.19	3.07E-03	0.05	1
Ap2a1	-0.34	-1.26	2.76E-05	1.74E-03	0.52
Apbb1	-0.29	-1.23	1.97E-04	7.68E-03	1
Apc2	-0.31	-1.24	9.19E-05	4.34E-03	1
Aph1b	-1.32	-2.5	5.95E-05	3.14E-03	1
Apod	0.42	1.33	2.15E-04	8.09E-03	1
Appl1	0.27	1.2	1.55E-03	0.03	1
Arap1	-0.34	-1.27	2.24E-04	8.27E-03	1
Arf5	-0.41	-1.33	9.56E-04	0.02	1
Arhgap15	0.78	1.72	1.81E-03	0.03	1
Arhgap36	0.59	1.51	1.66E-04	6.84E-03	1
Arhgap44	-0.39	-1.31	7.65E-06	6.43E-04	0.14
Arhgap5	0.29	1.22	1.97E-04	7.68E-03	1
Arid4b	0.31	1.24	3.46E-04	0.01	1
Arl14ep	0.29	1.22	1.57E-03	0.03	1
Arpp19_2	0.51	1.42	6.70E-05	3.43E-03	1

Ascc3	0.3	1.23	2.78E-04	9.46E-03	1
Ash1l	0.25	1.19	1.05E-03	0.02	1
Atat1	-0.42	-1.34	3.79E-04	0.01	1
Atcay	-0.25	-1.19	2.46E-03	0.04	1
Atf3	2.97	7.83	3.04E-27	2.17E-23	5.71E-23
Atp13a2	-0.31	-1.24	1.72E-04	7.00E-03	1
Atp13a3	0.3	1.23	3.79E-04	0.01	1
Atp1a3	-0.41	-1.33	2.33E-04	8.46E-03	1
Atp2b1	0.23	1.17	2.88E-03	0.04	1
Atp2b2	-0.26	-1.2	7.04E-04	0.02	1
Atp2b4	0.28	1.21	8.70E-04	0.02	1
Atp5mc3	-0.39	-1.31	8.87E-07	1.06E-04	0.02
Atp5mg	-0.29	-1.22	7.41E-04	0.02	1
Atp6v0e2	-0.27	-1.2	1.01E-03	0.02	1
Atrx	0.38	1.31	7.18E-07	8.92E-05	0.01
Atxn10	0.3	1.23	1.21E-04	5.45E-03	1
B3gat3	-0.47	-1.39	2.55E-08	5.02E-06	4.78E-04
Bag3	-0.35	-1.28	7.60E-06	6.43E-04	0.14
Basp1	0.34	1.27	9.54E-06	7.45E-04	0.18
Bbln	-0.42	-1.34	7.34E-04	0.02	1
Bcan	-0.37	-1.29	2.66E-03	0.04	1
Bckdha	-0.57	-1.48	4.52E-05	2.52E-03	0.85
Bdnf	1.1	2.14	1.47E-11	8.06E-09	2.75E-07
Bgn	-0.52	-1.43	1.32E-05	9.71E-04	0.25
Bhlhe41	0.31	1.24	8.67E-04	0.02	1
Bicd1	0.31	1.24	8.63E-05	4.18E-03	1
Bphl	-0.94	-1.92	4.31E-09	1.08E-06	8.10E-05
Bpnt1	0.25	1.19	2.71E-03	0.04	1
Brsk2	-0.28	-1.22	8.69E-04	0.02	1
Brwd3	0.42	1.34	2.17E-03	0.04	1
Btbd2	-0.3	-1.23	6.35E-04	0.02	1
C1qb	0.45	1.37	2.83E-03	0.04	1
C2cd2	0.44	1.36	3.34E-04	0.01	1
Cabp1	-0.25	-1.19	2.52E-03	0.04	1
Cacna1g	-1.31	-2.47	1.55E-03	0.03	1
Cacna1h	-0.41	-1.33	8.12E-04	0.02	1
Cacna2d1	0.94	1.91	4.63E-16	7.36E-13	8.71E-12
Cacng2	-0.59	-1.5	8.80E-05	4.22E-03	1
Calb2	-0.65	-1.57	2.57E-07	3.67E-05	4.82E-03

Calca	0.53	1.44	2.71E-06	2.69E-04	0.05
Calm-ps2	-0.45	-1.36	5.90E-04	0.02	1
Calu	0.25	1.19	1.53E-03	0.03	1
Camk2d	0.42	1.34	3.41E-04	0.01	1
Capg	-1.59	-3.01	2.70E-10	1.17E-07	5.07E-06
Caprin1	0.23	1.17	2.93E-03	0.05	1
Car2	-0.58	-1.49	2.71E-06	2.69E-04	0.05
Caskin2	-0.37	-1.29	2.40E-03	0.04	1
Casp4	0.54	1.46	7.20E-04	0.02	1
Castor2	-0.32	-1.25	7.25E-04	0.02	1
Cav1	-0.31	-1.24	1.63E-04	6.78E-03	1
Cavin2	-0.53	-1.44	8.94E-05	4.26E-03	1
Cbln2	0.5	1.41	4.73E-05	2.61E-03	0.89
Cbr2	-0.67	-1.59	1.36E-03	0.03	1
Cbx6	-0.24	-1.18	2.74E-03	0.04	1
Cbx7	-0.42	-1.34	2.47E-03	0.04	1
Ccar1	0.32	1.25	1.46E-04	6.29E-03	1
Ccdc112	0.59	1.5	5.83E-05	3.08E-03	1
Ccdc172	0.8	1.75	1.15E-03	0.02	1
Ccl2	1.46	2.76	1.45E-12	1.04E-09	2.72E-08
Ccm2l	-0.78	-1.72	3.74E-04	0.01	1
Ccnc	0.38	1.3	1.87E-03	0.03	1
Ccpg1	0.29	1.22	2.44E-04	8.71E-03	1
Cct2	0.28	1.21	4.09E-04	0.01	1
Cd200	0.3	1.23	2.01E-04	7.82E-03	1
Cd24	0.24	1.18	3.24E-03	0.05	1
Cd248	-0.9	-1.87	1.74E-03	0.03	1
Cd44	0.25	1.19	1.07E-03	0.02	1
Cd47	0.24	1.18	1.81E-03	0.03	1
Cd55	0.34	1.26	2.83E-03	0.04	1
Cd59	0.35	1.28	1.71E-03	0.03	1
Cd74	0.49	1.41	1.98E-05	1.32E-03	0.37
Cdc27	0.29	1.22	3.05E-04	0.01	1
Cdh19	0.44	1.35	1.61E-04	6.75E-03	1
Cdk5r2	-0.41	-1.33	4.91E-04	0.01	1
Cdr2l	-0.38	-1.3	1.34E-06	1.49E-04	0.03
Cep170	0.27	1.2	5.00E-04	0.01	1
Cep250	-0.69	-1.61	5.73E-07	7.38E-05	0.01
Cers6	0.27	1.2	2.62E-03	0.04	1

Chchd10	-0.61	-1.53	3.04E-07	4.21E-05	5.70E-03
Chga	-0.4	-1.32	2.49E-06	2.56E-04	0.05
Chl1	0.58	1.49	3.28E-07	4.49E-05	6.16E-03
Chn1	0.3	1.23	4.69E-04	0.01	1
Chpf	-0.37	-1.29	2.37E-03	0.04	1
Chrm2	0.53	1.45	2.08E-09	6.05E-07	3.90E-05
Chst2	-0.24	-1.18	2.54E-03	0.04	1
Cilp	-1.1	-2.15	2.43E-04	8.70E-03	1
Ckb	-0.35	-1.27	2.00E-03	0.04	1
Ckmt1	-0.41	-1.33	1.82E-07	2.74E-05	3.42E-03
Cldn19	-0.46	-1.38	3.03E-04	0.01	1
Clec2l	-0.67	-1.6	2.02E-08	4.18E-06	3.80E-04
Clec3b	-0.82	-1.76	7.38E-04	0.02	1
Clec7a	0.84	1.79	8.77E-04	0.02	1
Clstn1	-0.26	-1.19	7.57E-04	0.02	1
Cmklr1	-0.69	-1.61	9.61E-04	0.02	1
Cmpk1	0.32	1.25	9.19E-05	4.34E-03	1
Cmtm5	-0.52	-1.43	3.50E-05	2.07E-03	0.66
Cmya5	0.74	1.67	8.48E-04	0.02	1
Cnnm1	-0.44	-1.36	6.34E-04	0.02	1
Coasy	-0.57	-1.48	2.32E-04	8.44E-03	1
Col28a1	0.29	1.22	4.64E-04	0.01	1
Col6a1	-0.36	-1.29	2.28E-03	0.04	1
Col6a2	-0.42	-1.34	9.37E-07	1.10E-04	0.02
Col8a1	-0.46	-1.37	1.16E-03	0.02	1
Coro6	-0.53	-1.44	1.30E-04	5.73E-03	1
Cox7a1	-1.36	-2.57	4.68E-05	2.59E-03	0.88
Cp	0.3	1.23	5.51E-04	0.01	1
Cpeb4	0.27	1.21	3.90E-04	0.01	1
Cped1	-0.41	-1.33	2.55E-03	0.04	1
Cpsf2	0.31	1.24	2.30E-04	8.40E-03	1
Cpxm2	-0.66	-1.58	5.72E-04	0.02	1
Crbn	0.24	1.18	2.13E-03	0.04	1
Crh	5.1	34.38	5.51E-05	2.95E-03	1
Crisp3	7.82	225.23	8.36E-04	0.02	1
Crtac1	0.52	1.43	1.22E-03	0.03	1
Crtc2	-0.51	-1.43	2.19E-04	8.16E-03	1
Cryab	-0.44	-1.36	9.61E-08	1.56E-05	1.81E-03
Csdc2	-0.35	-1.27	1.23E-04	5.51E-03	1

Csf1	0.7	1.62	1.41E-07	2.17E-05	2.65E-03
Csnk1g3	0.27	1.2	9.93E-04	0.02	1
Cspg4	-0.54	-1.45	1.64E-05	1.14E-03	0.31
Csrp1	-0.26	-1.2	1.67E-03	0.03	1
Csrp3	5.44	43.49	3.86E-13	3.07E-10	7.26E-09
Cst3	-0.38	-1.3	7.70E-04	0.02	1
Cstb	-0.3	-1.23	1.14E-03	0.02	1
Ctdsp1	-0.38	-1.3	2.50E-03	0.04	1
Cttnbp2nl	0.29	1.23	3.83E-04	0.01	1
Cxcl13	1.29	2.45	6.22E-04	0.02	1
Cyc1	-0.38	-1.31	1.81E-03	0.03	1
Cyp2s1	-1.03	-2.04	8.21E-06	6.71E-04	0.15
Cyrib	0.36	1.28	3.11E-03	0.05	1
Cysltr2	0.48	1.39	2.65E-03	0.04	1
Cystm1	-0.38	-1.3	2.48E-03	0.04	1
D030056L22Rik	0.61	1.53	2.12E-05	1.40E-03	0.4
D430041D05Rik	-0.39	-1.31	1.57E-03	0.03	1
Dagla	-0.3	-1.23	4.56E-04	0.01	1
Dars1	0.33	1.25	1.32E-04	5.81E-03	1
Dazap1	-0.33	-1.25	2.77E-04	9.46E-03	1
Dclk1	0.28	1.22	2.65E-04	9.14E-03	1
Ddr1	-0.27	-1.2	2.11E-03	0.04	1
Dgcr2	-0.32	-1.25	1.63E-04	6.77E-03	1
Dhfr	0.7	1.63	2.00E-03	0.04	1
Dhx15	0.27	1.21	6.42E-04	0.02	1
Dicer1	0.29	1.23	6.07E-04	0.02	1
Dip2a	-0.34	-1.27	2.10E-04	8.03E-03	1
Dipk1b	-0.27	-1.21	3.06E-03	0.05	1
Diras1	-0.55	-1.46	9.29E-06	7.37E-04	0.17
Dis3	0.45	1.36	7.53E-04	0.02	1
Dlg2	0.37	1.29	6.34E-06	5.67E-04	0.12
Dlgap3	-0.38	-1.3	2.53E-03	0.04	1
Dmtf1	0.25	1.19	2.28E-03	0.04	1
Dnah3	2.04	4.11	6.10E-04	0.02	1
Dnaja3	-0.28	-1.21	2.15E-03	0.04	1
Dnajc2	0.42	1.34	7.20E-04	0.02	1
Dnajc7	0.31	1.24	8.55E-05	4.17E-03	1
Dock11	0.24	1.18	2.02E-03	0.04	1
Dohh	-0.54	-1.45	2.30E-04	8.40E-03	1

Dok6	0.41	1.33	1.62E-03	0.03	1
Dolk	-0.54	-1.46	1.75E-04	7.10E-03	1
Dpp9	-0.28	-1.21	9.86E-04	0.02	1
Dpy19l4	0.29	1.22	1.45E-03	0.03	1
Draxin	3.15	8.88	2.22E-05	1.44E-03	0.42
Dtx1	-0.52	-1.43	1.16E-03	0.02	1
Dtx3	-0.49	-1.41	3.88E-04	0.01	1
Dusp7	0.56	1.48	1.34E-05	9.78E-04	0.25
Dynlt3	0.25	1.19	1.15E-03	0.02	1
Dyrk1b	-0.4	-1.32	3.27E-03	0.05	1
Ecel1	1.68	3.21	2.36E-05	1.51E-03	0.44
Ecm2	-0.63	-1.55	2.76E-03	0.04	1
Ecrg4	-1.55	-2.93	5.91E-06	5.35E-04	0.11
Edf1	-0.25	-1.19	2.84E-03	0.04	1
Efna5	-0.5	-1.41	3.31E-07	4.49E-05	6.23E-03
Ehd3	0.23	1.17	2.73E-03	0.04	1
Eif1a	0.31	1.24	1.38E-04	6.00E-03	1
Eif3a	0.26	1.2	8.90E-04	0.02	1
Eif4a1	0.32	1.25	4.42E-05	2.50E-03	0.83
Elavl4	0.24	1.18	1.91E-03	0.03	1
Ell2	0.29	1.22	5.61E-04	0.01	1
Eln	-0.63	-1.55	9.75E-04	0.02	1
Eloc	0.33	1.26	6.81E-05	3.46E-03	1
Emc10	-0.45	-1.36	3.13E-04	0.01	1
Emc2	0.37	1.29	4.86E-06	4.48E-04	0.09
Eme2	-0.6	-1.52	2.90E-03	0.04	1
Epha5	0.46	1.38	4.13E-04	0.01	1
Ephx1	-0.51	-1.43	1.55E-04	6.58E-03	1
Erbin	0.33	1.26	5.03E-05	2.72E-03	0.94
Erc2	0.39	1.31	1.54E-03	0.03	1
Esf1	0.39	1.31	2.38E-03	0.04	1
Esrra	-0.61	-1.53	2.95E-05	1.81E-03	0.55
F3	-0.61	-1.52	1.42E-03	0.03	1
F5	-1.04	-2.06	1.92E-03	0.03	1
Faim2	-0.59	-1.5	9.62E-07	1.12E-04	0.02
Fam163a	-0.84	-1.79	7.94E-04	0.02	1
Fam189b	-0.24	-1.18	2.02E-03	0.04	1
Fam234b	-0.28	-1.22	1.03E-03	0.02	1
Far1	0.24	1.18	2.11E-03	0.04	1

Faxc	0.23	1.17	2.77E-03	0.04	1
Fbll1	-0.56	-1.48	2.06E-03	0.04	1
Fbln2	-0.45	-1.37	2.73E-09	7.35E-07	5.12E-05
Fbxo2	-0.28	-1.21	4.08E-04	0.01	1
Fbxo44	-0.37	-1.3	2.43E-03	0.04	1
Fgd1	-0.53	-1.44	7.58E-04	0.02	1
Fgf13	0.27	1.21	3.23E-04	0.01	1
Flrt3	1.33	2.51	5.16E-27	2.46E-23	9.70E-23
Fmnl2	0.26	1.2	1.31E-03	0.03	1
Fndc1	-0.46	-1.38	1.74E-03	0.03	1
Fndc3a	0.25	1.19	2.01E-03	0.04	1
Foxc1	-0.85	-1.8	1.55E-03	0.03	1
Foxc2	-0.7	-1.63	1.22E-03	0.03	1
Foxd1	-0.88	-1.84	1.21E-03	0.03	1
Fra10ac1	0.45	1.37	1.29E-03	0.03	1
Frmpd1	-0.26	-1.2	1.05E-03	0.02	1
Fsd1l	0.28	1.22	2.55E-04	8.94E-03	1
Fth1	-0.4	-1.32	2.99E-04	9.97E-03	1
Ftl1_1	-0.44	-1.35	1.14E-04	5.24E-03	1
Ftl1_2	-0.4	-1.32	1.23E-03	0.03	1
Fxyd6	-0.52	-1.44	6.03E-10	2.21E-07	1.13E-05
Fxyd7	-0.49	-1.4	1.09E-09	3.63E-07	2.05E-05
Gaa	-0.34	-1.27	2.81E-05	1.76E-03	0.53
Gabra5	1.24	2.37	3.25E-08	6.19E-06	6.10E-04
Gadd45a	1.17	2.25	6.40E-15	7.04E-12	1.20E-10
Gadd45g	0.82	1.76	1.76E-03	0.03	1
Gal	1.55	2.92	4.53E-15	5.39E-12	8.50E-11
Galnt13	0.44	1.36	7.01E-08	1.25E-05	1.32E-03
Gap43	0.66	1.58	4.78E-18	8.54E-15	8.98E-14
Gas6	-0.42	-1.34	1.09E-07	1.74E-05	2.06E-03
Gas7	0.33	1.26	3.36E-03	0.05	1
Gatd3a	-0.3	-1.23	3.93E-04	0.01	1
Gbp2	0.81	1.76	2.18E-06	2.28E-04	0.04
Gbp5	0.73	1.65	4.79E-04	0.01	1
Gbp7	1.07	2.1	1.99E-08	4.17E-06	3.73E-04
Gdf1	-0.58	-1.49	3.40E-05	2.03E-03	0.64
Gdi2	0.26	1.2	7.45E-04	0.02	1
Gdpd1	0.33	1.26	5.81E-04	0.02	1
gene:ENSRNOG00000005840	-2.01	-4.03	2.69E-03	0.04	1

gene:ENSRNOG00000006471	-0.76	-1.69	3.69E-10	1.51E-07	6.93E-06
gene:ENSRNOG00000013579	-0.45	-1.36	2.19E-03	0.04	1
gene:ENSRNOG00000019778	-0.59	-1.51	1.39E-05	1.00E-03	0.26
gene:ENSRNOG00000027040	0.54	1.46	5.51E-05	2.95E-03	1
gene:ENSRNOG00000048258	0.42	1.34	3.99E-04	0.01	1
gene:ENSRNOG00000048337	1.78	3.44	3.07E-08	5.94E-06	5.78E-04
gene:ENSRNOG00000049075	0.24	1.18	2.67E-03	0.04	1
gene:ENSRNOG00000060288	0.38	1.3	2.08E-03	0.04	1
gene:ENSRNOG00000062272	-0.41	-1.33	3.14E-05	1.90E-03	0.59
gene:ENSRNOG00000062568	-1.71	-3.27	1.34E-03	0.03	1
gene:ENSRNOG00000062710	0.33	1.26	2.13E-04	8.08E-03	1
gene:ENSRNOG00000062927	-0.67	-1.59	1.09E-05	8.32E-04	0.21
gene:ENSRNOG00000062930	-0.96	-1.95	5.23E-10	1.97E-07	9.83E-06
gene:ENSRNOG00000063044	-0.76	-1.69	2.22E-03	0.04	1
gene:ENSRNOG00000063087	-0.95	-1.93	3.00E-04	9.98E-03	1
gene:ENSRNOG00000063675	-1.12	-2.17	5.42E-05	2.92E-03	1
gene:ENSRNOG00000063679	0.56	1.48	2.17E-03	0.04	1
gene:ENSRNOG00000064941	0.58	1.49	3.26E-03	0.05	1
gene:ENSRNOG00000065301	0.74	1.66	3.14E-03	0.05	1
gene:ENSRNOG00000065506	0.41	1.33	2.18E-03	0.04	1
gene:ENSRNOG00000065666	0.44	1.36	6.59E-04	0.02	1
gene:ENSRNOG00000065876	0.57	1.49	4.81E-04	0.01	1
gene:ENSRNOG00000066117	-0.46	-1.38	3.96E-04	0.01	1
gene:ENSRNOG00000066636	-0.87	-1.83	4.49E-07	5.88E-05	8.43E-03
gene:ENSRNOG00000067007	0.53	1.45	6.05E-04	0.02	1
gene:ENSRNOG00000067040	0.72	1.65	3.08E-04	0.01	1
gene:ENSRNOG00000067077	-2.04	-4.12	1.49E-06	1.63E-04	0.03
gene:ENSRNOG00000067276	0.86	1.81	3.41E-12	2.18E-09	6.40E-08
gene:ENSRNOG00000067344	0.6	1.52	7.59E-07	9.12E-05	0.01
gene:ENSRNOG00000068131	-3.13	-8.75	7.20E-05	3.61E-03	1
gene:ENSRNOG00000068148	1	2	9.12E-05	4.33E-03	1
gene:ENSRNOG00000069384	0.95	1.93	5.66E-09	1.40E-06	1.06E-04
gene:ENSRNOG00000069549	-1.05	-2.08	5.97E-07	7.62E-05	0.01
gene:ENSRNOG00000069773	0.91	1.88	1.46E-03	0.03	1
gene:ENSRNOG00000069969	2.02	4.07	5.33E-04	0.01	1
gene:ENSRNOG00000070106	0.38	1.3	2.35E-03	0.04	1
gene:ENSRNOG00000070285	-0.71	-1.64	1.01E-06	1.16E-04	0.02
gene:ENSRNOG00000070574	-0.28	-1.21	2.69E-03	0.04	1
gene:ENSRNOG00000070982	-1.06	-2.08	2.57E-10	1.17E-07	4.83E-06

gene:ENSRNOG00000071050	0.6	1.52	2.20E-04	8.18E-03	1
Gfap	0.62	1.54	7.70E-04	0.02	1
Ggt6	1.02	2.03	5.12E-04	0.01	1
Ggt7	-0.28	-1.21	9.51E-04	0.02	1
Glipr2	0.54	1.45	2.57E-04	8.97E-03	1
Glrx5	-0.47	-1.39	8.30E-04	0.02	1
Gls	0.25	1.19	1.24E-03	0.03	1
Gm45871	0.6	1.52	3.30E-03	0.05	1
Gmfb	0.28	1.21	2.59E-04	9.01E-03	1
Gmppb	0.7	1.62	4.63E-04	0.01	1
Gmpr	-0.38	-1.3	2.64E-03	0.04	1
Gna12	-0.27	-1.21	1.34E-03	0.03	1
Gnb2	-0.25	-1.19	2.60E-03	0.04	1
Golm2	0.26	1.2	9.03E-04	0.02	1
Gpc6	-0.44	-1.36	1.54E-03	0.03	1
Gpcpd1	0.3	1.23	2.04E-04	7.89E-03	1
Gpnmb	0.48	1.39	5.67E-04	0.02	1
Gpr137	-0.51	-1.42	2.83E-05	1.77E-03	0.53
Gpr180	-0.47	-1.39	6.41E-04	0.02	1
Gpx1	-0.31	-1.24	8.05E-04	0.02	1
Gpx4	-0.55	-1.47	3.14E-06	3.06E-04	0.06
Grin1	-0.38	-1.31	4.05E-06	3.79E-04	0.08
Grina	-0.33	-1.25	2.19E-05	1.43E-03	0.41
Grm4	-0.64	-1.56	1.23E-05	9.14E-04	0.23
Gsn	-0.54	-1.46	3.50E-12	2.18E-09	6.58E-08
Gvin1	0.69	1.61	3.26E-03	0.05	1
H1f10	-0.78	-1.72	8.82E-05	4.22E-03	1
H1f2	-0.41	-1.33	3.30E-04	0.01	1
Hamp	5.83	56.92	1.03E-05	7.96E-04	0.19
Hapln1	-0.6	-1.51	1.52E-05	1.08E-03	0.29
Hapln2	-1.25	-2.37	2.49E-04	8.79E-03	1
Hapln4	-0.92	-1.9	9.36E-13	7.04E-10	1.76E-08
Haus3	0.35	1.27	3.71E-04	0.01	1
Haus6	0.43	1.35	1.10E-03	0.02	1
Hcn2	-0.55	-1.46	2.14E-10	1.02E-07	4.02E-06
Hcn4	-0.52	-1.44	2.88E-04	9.73E-03	1
Hells	0.71	1.63	6.97E-04	0.02	1
Hhatl	-0.52	-1.43	3.82E-04	0.01	1
Hic1	-0.66	-1.58	1.91E-03	0.03	1

Hid1	-0.33	-1.26	1.16E-04	5.28E-03	1
Hif1a	0.37	1.29	4.89E-06	4.48E-04	0.09
Hist2h3c2_2	-0.89	-1.86	4.40E-05	2.50E-03	0.83
Hmga1	-0.43	-1.34	1.14E-03	0.02	1
Hnrnpa0	-0.58	-1.49	7.51E-06	6.39E-04	0.14
Hnrnpa1	0.25	1.19	1.27E-03	0.03	1
Hnrnpa2b1	0.34	1.26	1.53E-05	1.08E-03	0.29
Hnrnpa3	0.24	1.18	2.30E-03	0.04	1
Hopx	0.51	1.42	1.78E-05	1.21E-03	0.34
Hoxb8	-0.81	-1.75	2.94E-03	0.05	1
Hpse	-0.57	-1.49	2.03E-05	1.35E-03	0.38
Hrh3	-0.96	-1.95	3.15E-03	0.05	1
Hs2st1	0.52	1.44	3.85E-10	1.53E-07	7.23E-06
Hs3st2	-0.52	-1.43	2.21E-05	1.44E-03	0.41
Hspe1	0.44	1.36	2.70E-04	9.25E-03	1
Htr1d	-0.58	-1.5	6.22E-04	0.02	1
Htra3	-0.66	-1.58	2.89E-03	0.04	1
Idh1	0.25	1.19	1.37E-03	0.03	1
Ifit2	0.92	1.89	1.58E-03	0.03	1
Ifit3	1.88	3.69	2.03E-03	0.04	1
Ifngr2	0.4	1.32	2.82E-03	0.04	1
Ift20	0.39	1.31	4.79E-05	2.62E-03	0.9
Igf2	0.57	1.48	3.36E-03	0.05	1
Igfbp3	0.84	1.8	1.64E-18	4.67E-15	3.07E-14
Igfbp6	-1.08	-2.12	3.00E-18	7.15E-15	5.64E-14
Igsf21	-1.15	-2.22	6.72E-05	3.43E-03	1
Il11ra1	-0.51	-1.43	5.33E-04	0.01	1
Il13ra1_1	0.6	1.51	1.27E-04	5.60E-03	1
Il13ra1_2	0.81	1.76	4.36E-10	1.69E-07	8.20E-06
Il1r1	0.72	1.65	4.04E-05	2.33E-03	0.76
Il31ra	0.45	1.37	2.43E-03	0.04	1
Il7r	0.98	1.98	4.10E-12	2.44E-09	7.70E-08
Impdh1	-0.31	-1.24	1.17E-04	5.29E-03	1
Inhbb	-1.01	-2.01	6.74E-07	8.45E-05	0.01
Ints6	0.28	1.21	3.33E-03	0.05	1
Iqsec1	-0.28	-1.21	3.46E-04	0.01	1
Iqsec3	-0.38	-1.3	1.36E-04	5.93E-03	1
Iscu	-0.59	-1.51	1.09E-13	9.71E-11	2.04E-09
Islr	-0.81	-1.76	9.99E-10	3.48E-07	1.88E-05

Itga2b	-1.31	-2.48	7.72E-04	0.02	1
Itgb1	0.42	1.34	1.66E-04	6.85E-03	1
Itgb8	0.43	1.35	1.54E-08	3.33E-06	2.89E-04
Itm2c	-0.36	-1.28	4.45E-06	4.13E-04	0.08
Ivns1abp	0.32	1.25	2.90E-05	1.79E-03	0.55
Jak2	0.4	1.32	6.21E-06	5.58E-04	0.12
Josd2	-0.43	-1.35	1.67E-03	0.03	1
Jph3	-0.31	-1.24	2.08E-04	8.02E-03	1
Jun	0.68	1.6	6.08E-09	1.44E-06	1.14E-04
Kank4	-0.39	-1.31	7.10E-06	6.23E-04	0.13
Kcnc1	-0.63	-1.55	1.24E-06	1.40E-04	0.02
Kcnc3	-0.49	-1.41	2.61E-09	7.18E-07	4.91E-05
Kcnh2	-0.51	-1.42	2.31E-09	6.60E-07	4.34E-05
Kcnk1	-0.68	-1.6	1.02E-07	1.64E-05	1.92E-03
Kcns1	-0.74	-1.67	2.90E-09	7.67E-07	5.45E-05
Kctd14	-1.38	-2.6	1.54E-03	0.03	1
Kctd16	0.25	1.19	2.51E-03	0.04	1
Kdm7a	0.39	1.31	1.71E-03	0.03	1
Khk	-0.66	-1.58	1.48E-03	0.03	1
Kiaa0408L	0.29	1.22	2.42E-04	8.69E-03	1
Kif19	-0.51	-1.42	4.62E-05	2.57E-03	0.87
Kif21b	-0.41	-1.33	7.89E-04	0.02	1
Klf5	-0.41	-1.33	1.03E-03	0.02	1
Klf6	0.25	1.19	2.37E-03	0.04	1
Klhdc8b	-0.66	-1.58	1.66E-05	1.15E-03	0.31
Klrk1	1.08	2.11	2.37E-03	0.04	1
Kndc1	-0.42	-1.34	2.26E-05	1.46E-03	0.43
Kpna4	0.24	1.18	2.75E-03	0.04	1
Krt7	1.32	2.49	2.56E-08	5.02E-06	4.81E-04
Ktn1	0.62	1.53	7.24E-16	1.04E-12	1.36E-11
Lamb2	-0.4	-1.31	7.32E-07	9.00E-05	0.01
Lamp5	0.91	1.88	1.83E-06	1.97E-04	0.03
Large1	-0.34	-1.26	1.50E-05	1.07E-03	0.28
Larp4	0.39	1.31	1.33E-06	1.48E-04	0.02
Lcorl	0.38	1.3	2.96E-03	0.05	1
Lcp1	0.39	1.31	7.29E-04	0.02	1
Ldhb	-0.29	-1.22	1.57E-04	6.64E-03	1
Leng8	-0.25	-1.19	1.31E-03	0.03	1
Leng9	-0.52	-1.43	3.25E-04	0.01	1

Lgi3	-0.52	-1.44	4.08E-11	2.08E-08	7.66E-07
Lifr	0.42	1.34	2.31E-08	4.64E-06	4.33E-04
Lims1	0.25	1.19	2.07E-03	0.04	1
Lin7b	-0.68	-1.6	1.34E-03	0.03	1
Lingo1	-0.5	-1.41	3.75E-05	2.18E-03	0.7
Loxl1	-0.71	-1.64	4.81E-04	0.01	1
Lpar6	0.5	1.41	2.71E-03	0.04	1
Lpcat4	-0.43	-1.34	5.92E-04	0.02	1
Lrch4	-0.54	-1.46	3.27E-04	0.01	1
Lrp1	-0.33	-1.26	1.42E-05	1.02E-03	0.27
Lrp1b	0.31	1.24	5.58E-04	0.01	1
Lrrc24	-0.46	-1.37	1.51E-03	0.03	1
Lrrc32	-0.72	-1.65	9.59E-04	0.02	1
Lrrc58	0.25	1.19	1.31E-03	0.03	1
Lrrfip1	0.28	1.21	1.15E-03	0.02	1
Ltbp3	-0.29	-1.22	5.79E-04	0.02	1
Ltbp4	-0.58	-1.49	6.84E-06	6.04E-04	0.13
Luzp2	0.4	1.32	1.16E-03	0.02	1
Lxn	0.43	1.35	1.73E-04	7.03E-03	1
Maf	-0.38	-1.3	2.34E-03	0.04	1
Man1a1	0.43	1.34	1.07E-03	0.02	1
Maoa	0.56	1.47	2.02E-06	2.14E-04	0.04
Map1lc3a	-0.41	-1.33	6.20E-04	0.02	1
Map3k13	-0.46	-1.38	1.05E-03	0.02	1
Map7d2	0.24	1.18	1.47E-03	0.03	1
Mapre1	0.32	1.25	1.04E-04	4.77E-03	1
MAST1	-0.24	-1.18	1.67E-03	0.03	1
Matr3	0.26	1.2	7.44E-04	0.02	1
Mcpt1l1	-2.24	-4.72	2.56E-04	8.97E-03	1
Mdc1	-0.43	-1.35	1.69E-03	0.03	1
Med27	-0.42	-1.34	1.96E-03	0.04	1
Med9	-0.52	-1.44	6.86E-04	0.02	1
Mest	-0.35	-1.28	1.84E-05	1.24E-03	0.35
Mfap4	-0.67	-1.59	4.11E-04	0.01	1
Mfap5	-0.66	-1.58	2.96E-04	9.91E-03	1
Mfsd2a	-0.43	-1.35	2.46E-03	0.04	1
MGC108823	0.73	1.66	4.39E-04	0.01	1
Mgll	-0.26	-1.2	9.27E-04	0.02	1
Mgp	-0.42	-1.34	2.94E-07	4.12E-05	5.52E-03

Mgst3	-0.53	-1.45	1.49E-04	6.44E-03	1
Mif	-0.37	-1.29	7.45E-06	6.39E-04	0.14
Miga2	-0.39	-1.31	6.84E-05	3.46E-03	1
Mki67	0.56	1.48	3.74E-05	2.18E-03	0.7
Mknk2	-0.28	-1.22	3.07E-03	0.05	1
Mlf2	-0.3	-1.23	2.18E-04	8.12E-03	1
Mmgt1	0.32	1.25	6.97E-05	3.51E-03	1
Mmp16	0.56	1.47	7.73E-05	3.84E-03	1
Mpdu1	-0.4	-1.32	3.75E-05	2.18E-03	0.7
Mpz	-0.54	-1.46	3.77E-04	0.01	1
Mrc2	-0.51	-1.42	1.38E-04	5.98E-03	1
Mrpl45	-0.52	-1.44	9.96E-05	4.65E-03	1
Msrb1	-0.4	-1.32	3.15E-03	0.05	1
Mt-atp8	0.63	1.54	2.18E-08	4.45E-06	4.10E-04
Mt-nd3	0.43	1.35	2.17E-03	0.04	1
Mtarc1	-0.4	-1.32	3.37E-03	0.05	1
Mtch1	-0.31	-1.24	9.35E-05	4.39E-03	1
Mvb12a	-0.4	-1.32	2.86E-03	0.04	1
Mx2	1.18	2.27	1.00E-04	4.66E-03	1
Mxra8	-0.33	-1.25	3.82E-04	0.01	1
Myh11	-0.57	-1.48	9.73E-06	7.56E-04	0.18
Myh2	1.43	2.69	1.50E-04	6.46E-03	1
Myl9	-0.85	-1.81	3.61E-06	3.42E-04	0.07
Myo3a	0.48	1.39	2.28E-04	8.39E-03	1
Mypop	-0.6	-1.52	1.69E-04	6.91E-03	1
Mysm1	0.29	1.22	1.46E-03	0.03	1
Nabp1	0.7	1.62	3.83E-04	0.01	1
Nacc1	-0.27	-1.2	1.63E-03	0.03	1
Nagpa	-1.38	-2.6	2.44E-04	8.71E-03	1
Nalcn	0.26	1.2	1.02E-03	0.02	1
Nampt	0.37	1.29	6.17E-05	3.23E-03	1
Nap1l1	0.31	1.24	6.33E-05	3.28E-03	1
Nat8l	-0.4	-1.32	2.07E-07	3.06E-05	3.90E-03
Nbn	0.37	1.29	2.10E-03	0.04	1
Nckipsd	-0.42	-1.33	1.44E-03	0.03	1
Ncl	0.3	1.23	9.92E-05	4.65E-03	1
Ndst4	-0.27	-1.21	1.66E-03	0.03	1
Ndufb2_1	-0.3	-1.23	2.29E-03	0.04	1
Ndufb6	-0.39	-1.31	1.69E-03	0.03	1

Necab3	-0.29	-1.22	1.48E-03	0.03	1
Nectin3	0.37	1.29	2.59E-03	0.04	1
Nell1	0.27	1.21	1.18E-03	0.02	1
NEWGENE_1310680	-0.47	-1.38	3.77E-04	0.01	1
NEWGENE_619861	0.25	1.19	1.13E-03	0.02	1
Nfatc1	-0.47	-1.39	4.87E-04	0.01	1
Nfia	-0.25	-1.19	2.85E-03	0.04	1
Nfic	-0.23	-1.17	3.41E-03	0.05	1
Niban1	0.25	1.19	1.30E-03	0.03	1
Nlgn2	-0.36	-1.28	2.77E-03	0.04	1
Nlrx1	-0.97	-1.96	2.13E-06	2.24E-04	0.04
Nop58	0.3	1.23	8.94E-04	0.02	1
Notch3	-0.48	-1.39	4.49E-04	0.01	1
Npm1	0.37	1.3	2.26E-06	2.34E-04	0.04
Npy	3.63	12.38	2.78E-46	3.97E-42	5.22E-42
Npy1r	0.7	1.63	1.32E-08	2.91E-06	2.49E-04
Nrip1	0.46	1.38	7.53E-09	1.74E-06	1.42E-04
Nsg1	0.46	1.37	1.08E-08	2.42E-06	2.03E-04
Ntn1	-0.68	-1.6	8.73E-05	4.21E-03	1
Ntng1	-0.39	-1.31	1.33E-03	0.03	1
Ntng2	-0.65	-1.57	8.72E-08	1.48E-05	1.64E-03
Nts	2.03	4.09	1.03E-09	3.51E-07	1.94E-05
Nufip2	0.28	1.21	3.26E-04	0.01	1
Nxph4	-1.94	-3.84	1.91E-03	0.03	1
Oaf	-0.42	-1.34	1.09E-03	0.02	1
Oaz1	-0.49	-1.4	4.25E-09	1.08E-06	7.98E-05
Ociad2	0.74	1.66	1.56E-03	0.03	1
Ogfrl1	0.34	1.27	3.51E-05	2.07E-03	0.66
Olr1585	0.75	1.69	7.79E-05	3.84E-03	1
Olr318	8.44	347.93	2.85E-04	9.66E-03	1
Olr854	1.29	2.44	2.18E-03	0.04	1
Opn3	-1.53	-2.89	2.61E-03	0.04	1
Orc4	0.47	1.38	6.03E-04	0.02	1
Osbpl3	0.35	1.28	1.64E-05	1.14E-03	0.31
Osbpl8	0.31	1.24	1.26E-04	5.60E-03	1
Osmr	0.66	1.58	3.30E-05	1.97E-03	0.62
P2rx4	-0.6	-1.52	3.23E-03	0.05	1
P2rx6	-0.58	-1.5	3.24E-05	1.94E-03	0.61
Pafah1b1	0.33	1.26	3.10E-03	0.05	1

Paip1	0.44	1.35	2.34E-04	8.46E-03	1
Pak1ip1	1.1	2.15	4.48E-04	0.01	1
Pak6	1.44	2.72	1.61E-03	0.03	1
Panx2	-0.27	-1.21	1.08E-03	0.02	1
Pappa1	0.99	1.98	3.75E-06	3.52E-04	0.07
Paqr4	-0.3	-1.23	2.32E-04	8.44E-03	1
Paqr6	-0.57	-1.49	2.62E-05	1.67E-03	0.49
Parp14	0.56	1.47	1.67E-03	0.03	1
Parp3	0.43	1.35	1.01E-03	0.02	1
Patl1	0.43	1.35	7.43E-04	0.02	1
Pcf11	0.28	1.21	9.12E-04	0.02	1
PCOLCE2	0.62	1.53	1.10E-05	8.32E-04	0.21
Pcsk1n	-0.39	-1.31	6.08E-04	0.02	1
Pde6b	1.43	2.69	2.67E-03	0.04	1
Pde8b	0.51	1.42	3.63E-04	0.01	1
Pdgfa	-0.51	-1.42	2.23E-03	0.04	1
Pdpn	0.32	1.25	1.62E-04	6.77E-03	1
Pebp1	-0.33	-1.26	2.22E-05	1.44E-03	0.42
Perp	0.51	1.43	1.00E-03	0.02	1
Pex11b	-0.48	-1.39	2.03E-03	0.04	1
Pf4	-1.49	-2.81	4.29E-04	0.01	1
Pfas	-0.52	-1.43	1.02E-04	4.72E-03	1
Pfkm	-0.24	-1.18	2.67E-03	0.04	1
Pgrmc2	0.25	1.19	3.23E-03	0.05	1
Phactr2	0.48	1.4	6.16E-09	1.44E-06	1.16E-04
Phc2	-0.31	-1.24	6.36E-04	0.02	1
Phf1	-0.42	-1.34	2.57E-03	0.04	1
Phkb	0.27	1.21	1.08E-03	0.02	1
Phospho1	-0.5	-1.41	4.66E-04	0.01	1
Pim3	-0.6	-1.51	1.59E-05	1.11E-03	0.3
Pip4p1	-0.4	-1.32	2.09E-03	0.04	1
Piwil2	-0.88	-1.83	3.02E-03	0.05	1
Pkd1	-0.38	-1.3	1.26E-06	1.42E-04	0.02
Pkdcc	-0.64	-1.55	1.44E-03	0.03	1
Pkia	0.41	1.33	9.36E-07	1.10E-04	0.02
Pkib	0.71	1.64	7.80E-06	6.52E-04	0.15
Pla2g3	-0.42	-1.34	3.35E-03	0.05	1
Pla2g4e	-0.88	-1.84	2.03E-03	0.04	1
Pla2g7	-0.63	-1.55	2.59E-07	3.67E-05	4.87E-03

Plaa	0.26	1.19	1.64E-03	0.03	1
Plbd2	-0.31	-1.24	2.35E-04	8.47E-03	1
Pld3	-0.27	-1.2	1.51E-03	0.03	1
Plekha3	0.42	1.34	1.54E-03	0.03	1
Plekhg2	-0.4	-1.32	9.41E-04	0.02	1
Plekhh1	0.45	1.37	3.15E-04	0.01	1
Pllp	-0.41	-1.33	1.38E-03	0.03	1
Pls3	0.25	1.19	1.16E-03	0.02	1
Plxnb1	-0.39	-1.31	2.74E-03	0.04	1
Pmpca	-0.46	-1.38	3.47E-04	0.01	1
Pnkd	-0.37	-1.29	7.48E-06	6.39E-04	0.14
Pnpla1	-1.26	-2.39	2.76E-03	0.04	1
Pnpla8	0.24	1.18	2.26E-03	0.04	1
Pnpo	-0.54	-1.46	4.76E-05	2.61E-03	0.89
Pnpt1	0.38	1.3	2.11E-03	0.04	1
Pomp	0.32	1.25	6.45E-05	3.33E-03	1
Porcn	-0.56	-1.48	2.77E-03	0.04	1
Ppfia4	-0.44	-1.35	1.10E-05	8.32E-04	0.21
Ppig	0.32	1.25	1.52E-04	6.48E-03	1
Ppl	-0.9	-1.86	1.95E-03	0.04	1
Ppp1cb	0.26	1.2	6.83E-04	0.02	1
Ppp1r12a	0.32	1.24	7.62E-05	3.81E-03	1
Ppp1r14a	-1.69	-3.23	1.64E-03	0.03	1
Ppp1r36	0.43	1.35	2.43E-03	0.04	1
Ppp1r7	0.25	1.19	1.89E-03	0.03	1
Ppp2ca	0.31	1.24	6.00E-05	3.15E-03	1
Ppp2r2a	0.3	1.23	1.84E-04	7.34E-03	1
Ppt2	-0.46	-1.37	3.25E-03	0.05	1
Prdm2	0.26	1.19	1.32E-03	0.03	1
Prdx1	0.29	1.22	3.38E-04	0.01	1
Prdx2	-0.32	-1.25	4.92E-05	2.67E-03	0.92
Prdx5	-0.26	-1.19	2.32E-03	0.04	1
Prelp	-0.65	-1.57	3.55E-06	3.39E-04	0.07
Prep	-0.26	-1.2	2.26E-03	0.04	1
Prex2	0.28	1.22	5.61E-04	0.01	1
Prkaca	-0.28	-1.21	4.69E-04	0.01	1
Prkag2	0.24	1.18	3.38E-03	0.05	1
Prkar2b	0.55	1.46	5.31E-12	3.04E-09	9.98E-08
Prkcb	0.27	1.21	1.02E-03	0.02	1

Prpf19	-0.26	-1.19	1.32E-03	0.03	1
Prpf39	0.43	1.34	6.73E-04	0.02	1
Prpf40a	0.33	1.26	8.75E-05	4.21E-03	1
Prr13	0.31	1.24	1.93E-04	7.58E-03	1
Prr5	-0.59	-1.51	1.22E-04	5.49E-03	1
Prrg4	0.46	1.38	7.40E-04	0.02	1
Prrt1	-0.55	-1.46	2.71E-05	1.71E-03	0.51
Prx	-0.34	-1.27	2.38E-03	0.04	1
Psma3	0.25	1.19	2.02E-03	0.04	1
Psma6	0.27	1.2	9.57E-04	0.02	1
Psmc6	0.26	1.2	1.52E-03	0.03	1
Psme4	0.26	1.2	7.26E-04	0.02	1
Pstpip1	-1.08	-2.11	2.29E-03	0.04	1
Ptcd2	-0.45	-1.37	3.33E-03	0.05	1
Ptgfrn	0.31	1.24	1.93E-04	7.58E-03	1
Pth1r	-0.68	-1.6	6.12E-04	0.02	1
Ptp4a1	0.38	1.3	1.09E-05	8.32E-04	0.2
Ptpn12	0.4	1.32	3.38E-06	3.26E-04	0.06
Ptprt	0.63	1.54	3.94E-07	5.26E-05	7.40E-03
Ptprz1	0.23	1.17	2.96E-03	0.05	1
Pttg1ip	-0.27	-1.2	1.80E-03	0.03	1
Purb	0.27	1.21	4.72E-04	0.01	1
Pvr	0.81	1.75	1.10E-03	0.02	1
Pxn	-0.39	-1.31	1.48E-03	0.03	1
Rab3il1	-0.54	-1.45	5.65E-04	0.01	1
Rab7a	0.27	1.2	5.45E-04	0.01	1
Rabac1	-0.45	-1.36	2.41E-07	3.52E-05	4.53E-03
Rack1	-0.29	-1.23	5.72E-04	0.02	1
Ranbp2	0.28	1.21	2.89E-04	9.73E-03	1
Rap1b	0.28	1.21	4.00E-04	0.01	1
Rap1gap	-0.31	-1.24	2.67E-04	9.19E-03	1
Rarg	-0.42	-1.34	2.59E-03	0.04	1
Rassf10	0.67	1.59	5.81E-04	0.02	1
Rb1cc1	0.26	1.19	1.01E-03	0.02	1
Rbbp8	0.4	1.32	1.84E-03	0.03	1
Rbfox1	0.26	1.19	9.97E-04	0.02	1
Rbis_1	0.64	1.56	5.44E-07	7.07E-05	0.01
Rcn3	-0.46	-1.37	4.59E-04	0.01	1
Reg3b	4.09	17.03	3.37E-09	8.77E-07	6.34E-05

Rell2	-0.39	-1.31	1.76E-05	1.20E-03	0.33
Rem2	-0.68	-1.6	3.30E-04	0.01	1
Retsat	-0.47	-1.39	3.36E-04	0.01	1
Rfng	-0.42	-1.34	2.76E-03	0.04	1
RGD1304884	-0.27	-1.2	4.64E-04	0.01	1
RGD1307461	-0.45	-1.36	1.02E-03	0.02	1
RGD1308750	0.62	1.54	3.23E-05	1.94E-03	0.61
RGD1560394	-1.13	-2.18	7.78E-05	3.84E-03	1
RGD1563072	-0.26	-1.2	2.30E-03	0.04	1
RGD1565462_2	3.44	10.85	7.36E-07	9.00E-05	0.01
Rgs2	0.57	1.48	3.07E-05	1.87E-03	0.58
Rgs22	1.68	3.2	1.69E-06	1.83E-04	0.03
Rheb	0.35	1.28	3.20E-03	0.05	1
Rhou	0.45	1.37	1.14E-03	0.02	1
Rimkla	-0.32	-1.24	2.78E-04	9.46E-03	1
Riok3	0.36	1.29	1.78E-05	1.21E-03	0.33
Rnf157	-0.29	-1.22	1.57E-04	6.64E-03	1
Rnf167	-0.45	-1.37	3.01E-04	1.00E-02	1
Rnf208	-0.65	-1.56	8.00E-05	3.93E-03	1
Rnf43	1.24	2.36	8.51E-04	0.02	1
Rnpepl1	-0.47	-1.39	9.03E-04	0.02	1
Ro60	0.32	1.25	1.27E-04	5.60E-03	1
Rock2	0.32	1.25	4.44E-05	2.50E-03	0.83
Ror2	-0.85	-1.81	6.65E-04	0.02	1
Rpl10a	-0.32	-1.25	1.26E-04	5.60E-03	1
Rpl21_2	0.51	1.42	8.62E-05	4.18E-03	1
Rpl26	0.27	1.2	6.74E-04	0.02	1
Rpl30_1	0.38	1.3	9.31E-04	0.02	1
Rpl31l4	-1.86	-3.63	7.41E-08	1.29E-05	1.39E-03
Rpl35a_1	0.42	1.34	5.01E-04	0.01	1
Rpl4	0.22	1.17	3.35E-03	0.05	1
Rplp2	-0.46	-1.37	3.96E-04	0.01	1
Rps10l1	-0.69	-1.61	2.60E-06	2.63E-04	0.05
Rps15al4	1.68	3.21	3.33E-07	4.49E-05	6.26E-03
Rps18	-0.48	-1.39	2.94E-04	9.87E-03	1
Rps20_1	0.25	1.19	2.31E-03	0.04	1
Rps29_1	-0.3	-1.23	3.37E-04	0.01	1
Rps4x_1	-0.39	-1.31	7.84E-04	0.02	1
Rps4x_2	0.59	1.51	2.59E-04	9.01E-03	1

Rps6ka3	0.32	1.25	2.86E-05	1.78E-03	0.54
Rps9	-0.33	-1.26	4.34E-05	2.48E-03	0.82
Rspo2	0.58	1.5	1.41E-06	1.55E-04	0.03
RT1-Ba	0.67	1.59	5.55E-08	1.02E-05	1.04E-03
RT1-Bb	0.76	1.69	2.88E-06	2.82E-04	0.05
RT1-CE16	-1.79	-3.45	4.01E-18	8.18E-15	7.53E-14
RT1-Da	0.72	1.65	2.46E-09	6.90E-07	4.62E-05
RT1-Db1	0.5	1.41	1.94E-03	0.03	1
Rtkn	-0.29	-1.22	6.06E-04	0.02	1
Rtn4rl2	-0.83	-1.78	7.16E-08	1.26E-05	1.34E-03
S100a11	0.32	1.25	6.26E-05	3.25E-03	1
Samd9	0.76	1.7	1.78E-07	2.71E-05	3.35E-03
Sarnp	0.33	1.26	2.46E-04	8.73E-03	1
Sbk1	-0.33	-1.25	3.47E-04	0.01	1
Sbno2	0.75	1.69	1.57E-08	3.36E-06	2.96E-04
Sbspon	-0.69	-1.61	2.62E-04	9.08E-03	1
Scg2	0.35	1.27	2.08E-03	0.04	1
Scn1b	-0.41	-1.33	4.72E-04	0.01	1
Scn3a	0.51	1.42	2.48E-04	8.79E-03	1
Scn3b	0.38	1.3	1.58E-03	0.03	1
Scn7a	0.33	1.26	3.17E-03	0.05	1
Scn9a	0.34	1.27	2.40E-03	0.04	1
Scrt1	-0.58	-1.5	7.86E-06	6.54E-04	0.15
Sdhb	-0.25	-1.19	2.46E-03	0.04	1
Sec62	0.26	1.2	8.24E-04	0.02	1
Sec63	0.24	1.18	3.06E-03	0.05	1
Selenom	-0.41	-1.33	5.88E-04	0.02	1
Sema3b	-0.33	-1.25	5.82E-05	3.08E-03	1
Sema3c	0.43	1.34	2.51E-04	8.85E-03	1
Sema4g	-0.51	-1.42	3.97E-04	0.01	1
Sema5b	-0.98	-1.97	1.40E-03	0.03	1
Sema6a	1.05	2.06	3.06E-12	2.08E-09	5.75E-08
Sema7a	-0.87	-1.82	6.76E-25	2.41E-21	1.27E-20
Serp2	-0.62	-1.54	5.53E-04	0.01	1
Serpinb1a	0.51	1.43	9.09E-06	7.25E-04	0.17
Serpinb1b	1.13	2.18	5.81E-08	1.05E-05	1.09E-03
Serpinb9	0.4	1.32	8.16E-04	0.02	1
Serpini1	0.36	1.29	2.71E-03	0.04	1
Sestd1	0.38	1.3	9.47E-06	7.45E-04	0.18

Sez6l2	-0.35	-1.28	1.17E-05	8.72E-04	0.22
Sfrp5	-0.43	-1.34	3.50E-08	6.58E-06	6.58E-04
Sgcb	0.26	1.2	1.70E-03	0.03	1
Sh3bgrl	0.36	1.29	3.48E-06	3.34E-04	0.07
Sh3gl2	-0.38	-1.3	8.94E-06	7.18E-04	0.17
Sh3glb2	-0.35	-1.27	6.56E-05	3.37E-03	1
Shank1	-0.64	-1.55	2.56E-06	2.62E-04	0.05
Shisa3	-0.64	-1.56	7.80E-04	0.02	1
Skor2	-0.55	-1.47	2.74E-03	0.04	1
Slc13a4	-0.36	-1.28	1.82E-04	7.27E-03	1
Slc16a11	-0.64	-1.55	1.53E-04	6.50E-03	1
Slc17a6	0.35	1.27	2.34E-03	0.04	1
Slc17a7	-0.28	-1.21	3.98E-04	0.01	1
Slc22a17	-0.28	-1.21	4.64E-04	0.01	1
Slc25a12	-0.24	-1.18	2.48E-03	0.04	1
Slc25a22	-0.34	-1.27	1.87E-04	7.41E-03	1
Slc36a1	-0.37	-1.3	7.26E-06	6.29E-04	0.14
Slc38a1	-0.38	-1.3	2.33E-03	0.04	1
Slc39a6	0.31	1.24	2.14E-04	8.08E-03	1
Slc48a1	-0.39	-1.31	1.54E-03	0.03	1
Slc4a2	-0.27	-1.21	1.49E-03	0.03	1
Slc4a7	0.42	1.34	2.22E-03	0.04	1
Slc5a6	-0.47	-1.39	1.78E-04	7.15E-03	1
Slc66a2	-0.52	-1.43	1.72E-05	1.18E-03	0.32
Slc9a1	-0.39	-1.31	1.37E-03	0.03	1
Slc9a5	-0.91	-1.87	2.81E-03	0.04	1
Slco2a1	-0.86	-1.82	8.68E-04	0.02	1
Slco5a1	-0.38	-1.3	3.86E-05	2.23E-03	0.72
Slfn13	0.37	1.3	3.24E-03	0.05	1
Slit2	-0.28	-1.22	7.63E-04	0.02	1
Slit3	-0.31	-1.24	1.45E-03	0.03	1
Slk	0.43	1.35	9.00E-08	1.50E-05	1.69E-03
Smad1	0.38	1.3	2.49E-03	0.04	1
Smagp	1.59	3.01	3.87E-04	0.01	1
Smap1	0.29	1.23	2.13E-04	8.08E-03	1
Smarca5	0.26	1.2	8.49E-04	0.02	1
Smc6	0.37	1.3	8.55E-06	6.94E-04	0.16
Smdt1	-0.49	-1.4	9.55E-08	1.56E-05	1.79E-03
Smoc1	-1.48	-2.79	7.79E-08	1.34E-05	1.46E-03

Smpd1	-0.43	-1.35	4.61E-04	0.01	1
Sncb	-0.29	-1.22	7.21E-04	0.02	1
Snrpc	-1.59	-3	4.65E-04	0.01	1
Snrpel1	0.59	1.51	3.08E-03	0.05	1
Socs3	1.17	2.26	2.76E-06	2.72E-04	0.05
Sod2	0.28	1.21	2.61E-04	9.06E-03	1
Sox11	1.34	2.53	2.65E-10	1.17E-07	4.98E-06
Sparcl1	-0.34	-1.26	2.97E-03	0.05	1
Spata32	-1.94	-3.84	3.03E-04	0.01	1
Sphk2	-0.51	-1.43	8.49E-05	4.16E-03	1
Spire2	-0.27	-1.21	2.94E-03	0.05	1
Spp1	0.47	1.39	2.67E-05	1.70E-03	0.5
Spred1	0.29	1.22	3.47E-04	0.01	1
Sptb	-0.48	-1.39	1.59E-09	4.94E-07	2.98E-05
Sptbn5	-0.47	-1.39	4.48E-05	2.51E-03	0.84
Srebf1	-0.37	-1.29	3.09E-03	0.05	1
Srek1	0.31	1.24	3.06E-04	0.01	1
Srgap1	0.23	1.18	3.32E-03	0.05	1
Srsf2	-0.37	-1.29	5.66E-05	3.02E-03	1
Srsf5	0.24	1.18	2.82E-03	0.04	1
Ssb	0.43	1.34	1.25E-07	1.95E-05	2.36E-03
Ssc5d	0.68	1.61	1.92E-05	1.29E-03	0.36
Ssr3	0.31	1.24	1.67E-04	6.87E-03	1
Ssx2ip	0.41	1.33	5.82E-04	0.02	1
St7l	0.33	1.26	6.56E-04	0.02	1
Stab1	-0.51	-1.42	1.11E-04	5.10E-03	1
Stac2	3.1	8.59	1.56E-15	2.03E-12	2.94E-11
Stag1	0.27	1.21	2.26E-03	0.04	1
Stag2	0.28	1.22	5.17E-04	0.01	1
Stmn1	0.32	1.25	4.83E-05	2.63E-03	0.91
Stmn2	0.37	1.29	9.44E-04	0.02	1
Stmn4	0.87	1.83	1.43E-10	7.06E-08	2.69E-06
Stx3	1.03	2.04	1.20E-07	1.89E-05	2.26E-03
Stx7	0.23	1.17	3.06E-03	0.05	1
Susd4	-0.3	-1.23	1.91E-04	7.55E-03	1
Suz12	0.29	1.22	5.85E-04	0.02	1
Syncrip	0.28	1.22	4.04E-04	0.01	1
Syngr1	-0.38	-1.3	2.52E-03	0.04	1
Syt3	-0.59	-1.51	8.00E-06	6.61E-04	0.15

Syt4	0.5	1.41	1.54E-05	1.08E-03	0.29
Taf11	-0.45	-1.37	1.57E-03	0.03	1
Taf15	0.46	1.38	7.52E-07	9.11E-05	0.01
Tagln	-1.18	-2.27	3.99E-14	4.07E-11	7.49E-10
Taok1	0.28	1.21	3.19E-04	0.01	1
Tars2	-0.44	-1.36	1.86E-03	0.03	1
Tasor	0.26	1.2	1.70E-03	0.03	1
Tbcc	-0.52	-1.43	8.22E-04	0.02	1
Tbl1xr1	0.25	1.19	1.94E-03	0.03	1
Tcea1	0.46	1.38	1.91E-04	7.55E-03	1
Tdrd12	0.75	1.68	2.09E-03	0.04	1
Tdrd3	0.28	1.21	3.03E-03	0.05	1
Tedc1	-0.67	-1.59	2.37E-03	0.04	1
Tenm1	0.42	1.34	7.21E-04	0.02	1
Tesc	-0.43	-1.35	9.30E-04	0.02	1
Tex264	-0.4	-1.32	1.63E-03	0.03	1
Thoc1	0.47	1.39	3.28E-04	0.01	1
Thoc2	0.36	1.28	1.13E-05	8.46E-04	0.21
Tlcd3b	-0.49	-1.4	1.55E-09	4.91E-07	2.91E-05
Tm9sf3	0.29	1.23	2.11E-04	8.05E-03	1
Tmem130	-0.28	-1.22	4.99E-04	0.01	1
Tmem143	-0.44	-1.36	2.73E-03	0.04	1
Tmem158	-0.83	-1.78	3.24E-03	0.05	1
Tmem159	0.5	1.41	4.52E-04	0.01	1
Tmem176a	0.25	1.19	1.25E-03	0.03	1
Tmem179	-0.32	-1.25	6.01E-04	0.02	1
Tmem184b	-0.27	-1.2	1.35E-03	0.03	1
Tmem223	-0.44	-1.35	1.79E-03	0.03	1
Tmem229a	-0.5	-1.42	4.18E-04	0.01	1
Tmem25	-0.51	-1.42	1.64E-04	6.79E-03	1
Tmem256	-0.61	-1.53	2.39E-03	0.04	1
Tmem26	1.03	2.04	2.00E-09	6.05E-07	3.76E-05
Tmem38a	-0.41	-1.33	2.12E-03	0.04	1
Tmem59l	-0.31	-1.24	2.91E-04	9.79E-03	1
Tmem65	0.26	1.2	1.15E-03	0.02	1
Tmem8b	-0.44	-1.36	5.22E-04	0.01	1
Tmx1	0.29	1.22	7.67E-04	0.02	1
Tnfaip8l3	1.29	2.44	1.97E-03	0.04	1
Tnik	0.6	1.52	2.57E-07	3.67E-05	4.84E-03

Tnnc2	1.23	2.35	3.09E-03	0.05	1
Tnni2	2.08	4.23	6.94E-05	3.50E-03	1
Tnnt3	1.32	2.49	3.22E-04	0.01	1
Tnpo1	0.25	1.19	1.78E-03	0.03	1
Togaram1	0.31	1.24	2.25E-04	8.27E-03	1
Tomm70	0.26	1.2	5.85E-04	0.02	1
Tp53inp2	-0.26	-1.2	2.13E-03	0.04	1
Tpcn1	-0.41	-1.33	1.01E-06	1.16E-04	0.02
Tpm1	0.24	1.18	1.91E-03	0.03	1
Tpp2	0.28	1.21	4.71E-04	0.01	1
Tpr	0.25	1.19	1.17E-03	0.02	1
Tradd	-1.13	-2.19	6.92E-04	0.02	1
Trim67	-0.42	-1.34	2.75E-03	0.04	1
Trnp1	-0.46	-1.38	6.20E-05	3.24E-03	1
Trpa1	0.69	1.61	7.75E-09	1.76E-06	1.46E-04
Tsc22d3	-0.46	-1.38	3.62E-08	6.73E-06	6.81E-04
Tsfm	-0.53	-1.44	4.67E-04	0.01	1
Tspan13	0.27	1.21	8.84E-04	0.02	1
Tspan2	0.5	1.41	4.16E-05	2.39E-03	0.78
Tst	-0.61	-1.52	1.46E-03	0.03	1
Tubb2b	0.58	1.49	4.11E-07	5.44E-05	7.73E-03
Tubb6	0.64	1.56	3.58E-04	0.01	1
Tubg1	-0.41	-1.33	8.21E-06	6.71E-04	0.15
Twf1	0.38	1.3	1.63E-03	0.03	1
Txndc9	0.4	1.32	1.48E-03	0.03	1
Ube2k	0.25	1.19	1.52E-03	0.03	1
Ube2o	-0.23	-1.18	2.72E-03	0.04	1
Ube2ql1	-0.38	-1.3	3.20E-03	0.05	1
Ube2w	0.28	1.21	2.04E-03	0.04	1
Ube3b	-0.26	-1.2	1.09E-03	0.02	1
Ubl7	-0.47	-1.38	1.73E-04	7.03E-03	1
Uhrf1bp1l	0.47	1.38	2.04E-09	6.05E-07	3.84E-05
Uqcrq	-0.61	-1.53	1.91E-06	2.04E-04	0.04
Usp14	0.36	1.28	1.65E-03	0.03	1
Usp25	0.26	1.2	1.72E-03	0.03	1
Usp33	0.35	1.28	7.24E-06	6.29E-04	0.14
Usp53	0.32	1.25	1.52E-04	6.48E-03	1
Ust	-0.38	-1.3	2.40E-03	0.04	1
Vamp1	-0.49	-1.41	1.28E-05	9.40E-04	0.24

Vgf	1.17	2.25	2.87E-11	1.52E-08	5.39E-07
Vip	4.24	18.83	1.04E-13	9.71E-11	1.96E-09
Vps13a	0.3	1.23	1.17E-04	5.29E-03	1
Vps13c	0.25	1.19	8.12E-04	0.02	1
Vps35	0.23	1.17	3.01E-03	0.05	1
Vstm2b	-1.02	-2.03	7.66E-05	3.82E-03	1
Vstm2l	-0.47	-1.38	1.43E-03	0.03	1
Vwa5a	0.36	1.29	2.69E-06	2.69E-04	0.05
Vwa7	-0.36	-1.28	8.59E-06	6.94E-04	0.16
Washc4	0.24	1.18	2.50E-03	0.04	1
Wdr47	0.28	1.21	4.73E-04	0.01	1
Wipf2	-0.5	-1.42	4.11E-04	0.01	1
Wls	0.29	1.22	5.08E-04	0.01	1
Xpo1	0.28	1.22	3.54E-04	0.01	1
Yif1b	-0.5	-1.42	2.49E-04	8.79E-03	1
Yme1l1	0.29	1.23	2.18E-04	8.12E-03	1
Ypel3	-0.38	-1.3	1.24E-03	0.03	1
Ythdc2	0.45	1.37	2.36E-04	8.48E-03	1
Ythdf3	0.26	1.2	1.32E-03	0.03	1
Zbtb38	0.29	1.22	3.08E-04	0.01	1
Zc3h14	0.28	1.21	9.37E-04	0.02	1
Zdhhc22	-0.69	-1.61	1.94E-04	7.61E-03	1
Zdhhc8	-0.45	-1.37	2.81E-04	9.54E-03	1
Zeb2	0.28	1.21	3.06E-04	0.01	1
Zer1	-0.34	-1.26	4.48E-04	0.01	1
Zfand5	0.25	1.19	1.96E-03	0.04	1
Zfp300	1.47	2.77	5.37E-04	0.01	1
Zfp322a	0.38	1.3	3.34E-03	0.05	1
Zfp367	0.71	1.64	8.96E-08	1.50E-05	1.68E-03
Zfp385a	-0.45	-1.37	2.09E-04	8.02E-03	1
Zfp386	0.39	1.31	1.16E-03	0.02	1
Zfp423	-0.38	-1.3	2.71E-03	0.04	1
Zfp54	0.51	1.42	1.77E-04	7.13E-03	1
Zfp605	0.42	1.34	2.23E-03	0.04	1
Zfp622	0.29	1.22	1.79E-04	7.15E-03	1
Zfp638	0.28	1.22	3.16E-04	0.01	1
Zfp655	0.27	1.2	2.26E-03	0.04	1
Zfp68	0.28	1.21	7.47E-04	0.02	1
Zfp712	0.48	1.4	1.61E-04	6.75E-03	1

Zfp729a	0.45	1.37	4.48E-04	0.01	1
Zfp748_2	0.36	1.28	2.14E-04	8.08E-03	1
Zfp943	0.45	1.37	1.70E-03	0.03	1
Zfp949	0.42	1.34	2.27E-03	0.04	1
Zfp958_1	0.31	1.24	1.41E-03	0.03	1
Zfta	-0.45	-1.36	1.08E-03	0.02	1
Zhx1	0.26	1.19	1.27E-03	0.03	1
Zswim8	-0.28	-1.21	9.92E-04	0.02	1

Table A3.3. Master list of differentially expressed genes between Male CCI vs Naïve samples with a FDR p-value ≤ 0.05 and a fold change greater than ±1.

Name	Log_2 fold change	Fold change	P-value	FDR p-value	Bonferroni
AABR07005775.1	-1.89	-3.71	2.01E-09	1.55E-06	3.79E-05
AABR07057196.1	0.83	1.78	1.29E-04	1.00E-02	1
AABR07060610.1	2.85	7.23	1.22E-05	1.91E-03	0.23
AABR07071000.1	-1.14	-2.2	3.96E-04	0.03	1
Aatk	-0.4	-1.32	2.49E-08	1.14E-05	4.70E-04
Abcb9	-0.4	-1.32	7.10E-04	0.04	1
Abhd8	-0.4	-1.32	5.99E-06	1.08E-03	0.11
AC129365.1	2.04	4.12	2.48E-04	2.00E-02	1.00E+00
Acadsb	-0.37	-1.3	3.74E-04	0.03	1
Ace2	0.72	1.65	4.55E-06	8.62E-04	0.09
Ackr3	0.54	1.45	6.36E-05	7.16E-03	1
Acta1	-1.69	-3.23	1.41E-08	7.25E-06	2.67E-04
Actn2	-1.57	-2.97	1.16E-04	0.01	1
Actn3	-1.52	-2.87	2.91E-06	5.85E-04	0.05
Adamts20	-0.35	-1.27	2.43E-05	3.32E-03	4.60E-01
Ado	-0.29	-1.22	2.57E-04	2.00E-02	1
Aldh1a2	1.33	2.52	6.97E-09	4.15E-06	1.32E-04
Aldh1a3	0.7	1.62	8.74E-05	9.24E-03	1
Ampd1	-1.52	-2.87	6.09E-04	4.00E-02	1
Anxa8	0.99	1.99	3.95E-05	4.81E-03	0.75
Arhgap29	0.49	1.41	1.62E-05	2.37E-03	0.31
Arhgap39	-0.28	-1.22	9.37E-05	9.73E-03	1
Atf3	2.04	4.12	1.41E-09	1.26E-06	2.66E-05

Atp11a	-0.27	-1.21	4.14E-05	4.97E-03	0.78
Atp1a3	-0.36	-1.28	9.03E-08	3.38E-05	1.70E-03
Azin1	-0.27	-1.21	8.33E-05	9.00E-03	1
B3galt5	-0.56	-1.47	6.92E-06	1.22E-03	0.13
Bcan	-0.35	-1.27	2.54E-05	3.35E-03	0.48
Bcl2l1	-0.35	-1.27	1.88E-05	2.68E-03	0.36
Bgn	0.43	1.35	4.50E-05	5.31E-03	8.50E-01
Bnc2	0.38	1.3	2.79E-06	5.70E-04	0.05
C1s	0.45	1.36	3.66E-05	4.52E-03	0.69
C3	0.84	1.78	3.56E-05	4.44E-03	0.67
Ca3	-0.99	-1.99	1.09E-05	1.75E-03	0.21
Cacna1s	-1.62	-3.08	9.75E-06	1.63E-03	1.80E-01
Cadm4	-0.31	-1.24	1.74E-05	2.52E-03	0.33
Calb2	-0.6	-1.51	1.61E-07	5.12E-05	3.04E-03
Casq1	-1.32	-2.5	9.05E-06	1.53E-03	0.17
Cbln2	0.27	1.21	8.08E-04	5.00E-02	1
Ccdc3	0.85	1.8	1.91E-05	2.69E-03	0.36
Cd163	-0.83	-1.78	1.08E-05	1.75E-03	0.2
Cd74	0.73	1.66	1.30E-06	3.13E-04	0.02
Cdh15	-0.42	-1.34	1.28E-04	1.00E-02	1
Cdh5	0.41	1.33	2.05E-04	2.00E-02	1
Cfb	0.69	1.61	1.51E-07	5.12E-05	2.84E-03
Cfh	0.57	1.49	6.70E-13	1.54E-09	1.27E-08
Chchd4	-0.58	-1.5	3.55E-04	0.03	1
Chrm2	0.29	1.22	3.44E-04	0.03	1
Chrnb3	-0.26	-1.19	5.54E-04	4.00E-02	1.00E+00
Chst2	-0.25	-1.19	4.64E-04	0.03	1
Ciart	-1.11	-2.16	1.88E-04	2.00E-02	1
Cilp	1.28	2.43	1.25E-07	4.37E-05	2.36E-03
Ckb	-0.25	-1.19	1.97E-04	0.02	1
Ckm	-1.61	-3.04	3.99E-07	1.11E-04	7.53E-03
Cldn1	0.37	1.29	6.32E-04	4.00E-02	1
Cldn11	0.51	1.42	5.01E-04	0.04	1
Cldn19	-0.55	-1.47	1.58E-06	3.68E-04	0.03
Clec2g	0.3	1.23	3.32E-05	4.24E-03	6.30E-01
Clec2l	-0.39	-1.31	2.88E-04	0.02	1
Cmtm5	-0.32	-1.25	2.18E-04	0.02	1
Cmya5	-1.17	-2.24	1.16E-05	1.82E-03	0.22
Col12a1	0.38	1.3	1.85E-04	0.02	1

Col4a5	0.81	1.75	1.01E-04	1.00E-02	1
Col8a1	0.64	1.56	5.38E-04	4.00E-02	1
Cox6a2	-2.48	-5.56	1.76E-07	5.24E-05	3.32E-03
Cp	0.45	1.37	7.77E-09	4.44E-06	1.47E-04
Cpxm2	0.71	1.64	9.95E-05	0.01	1
Crh	5.07	33.5	1.64E-07	5.12E-05	3.09E-03
Csf1	0.5	1.41	6.90E-05	7.71E-03	1
Ctss	0.42	1.33	6.69E-04	4.00E-02	1
Cxcl13	1.77	3.4	4.10E-05	4.96E-03	0.77
Cxcl16	0.54	1.45	2.75E-04	0.02	1
Cyp2s1	0.93	1.91	2.61E-05	3.41E-03	0.49
Dab2	0.28	1.22	7.32E-04	5.00E-02	1
Dbp	-0.57	-1.49	4.28E-11	7.66E-08	8.08E-07
Ddr2	0.35	1.27	1.13E-05	1.80E-03	0.21
Dusp15	-0.34	-1.27	2.31E-06	4.90E-04	4.00E-02
Egr2	-1.26	-2.39	9.16E-25	1.47E-20	1.73E-20
Ehd1	-0.28	-1.21	3.52E-04	0.03	1
Eif2ak3	0.31	1.24	2.39E-04	0.02	1
Elk3	0.48	1.39	3.59E-04	3.00E-02	1
Emp1	0.63	1.55	4.00E-08	1.65E-05	7.55E-04
Eno3	-1.27	-2.42	6.21E-10	6.24E-07	1.17E-05
Errfi1	-0.43	-1.35	2.27E-04	2.00E-02	1
Fa2h	-0.39	-1.31	7.07E-04	4.00E-02	1.00E+00
Fam107a	-0.44	-1.36	5.33E-04	4.00E-02	1.00E+00
Fat4	0.41	1.32	2.33E-07	6.83E-05	4.40E-03
Fbln1	0.66	1.58	2.03E-08	9.61E-06	3.83E-04
Fbln2	-0.31	-1.24	6.99E-06	1.22E-03	0.13
Fgfr2	-0.44	-1.36	3.20E-04	2.00E-02	1.00E+00
Fkbp5	-0.64	-1.56	2.66E-08	1.19E-05	5.01E-04
Flrt2	0.29	1.23	2.26E-04	2.00E-02	1.00E+00
Flrt3	0.7	1.63	1.55E-05	2.31E-03	0.29
Foxd1	1.04	2.06	3.35E-05	4.25E-03	6.30E-01
Fyb1	0.89	1.85	5.71E-09	3.53E-06	1.08E-04
Fzd2	0.67	1.59	5.01E-06	9.38E-04	0.09
Gas2l3	-0.25	-1.19	3.76E-04	0.03	1
Gbp2	0.52	1.43	1.04E-05	1.70E-03	0.2
gene:ENSRNOG00000006471	-0.39	-1.31	3.29E-04	0.03	1
gene:ENSRNOG00000060288	0.33	1.26	4.37E-05	5.21E-03	0.83
gene:ENSRNOG00000063679	0.27	1.21	2.45E-04	0.02	1

gene:ENSRNOG00000067422	3.02	8.12	7.09E-04	0.04	1
gene:ENSRNOG00000067832	5.39	41.86	2.02E-09	1.55E-06	3.81E-05
Gjb2	0.94	1.91	8.06E-06	1.38E-03	0.15
Gjb6	0.88	1.84	7.37E-04	0.05	1
Gnb4	0.4	1.32	6.42E-04	0.04	1
Gpd1	-0.79	-1.73	7.27E-10	6.88E-07	1.37E-05
Gprc5b	-0.25	-1.19	3.20E-04	2.00E-02	1.00E+00
Gstm4	-0.48	-1.4	1.04E-04	1.00E-02	1.00E+00
Gvin1	0.72	1.65	5.76E-04	4.00E-02	1
H19	-1.26	-2.4	7.24E-06	1.25E-03	0.14
H3f3c	3.29	9.77	3.92E-09	2.63E-06	7.40E-05
Hamp	4.63	24.75	5.95E-04	0.04	1
Hapln1	-0.66	-1.58	2.10E-05	2.93E-03	0.4
Hapln4	-0.49	-1.4	2.36E-05	3.25E-03	0.45
Hba-a3	0.79	1.72	8.45E-05	9.07E-03	1.00E+00
Herpud1	-0.44	-1.36	1.69E-07	5.13E-05	3.19E-03
Hif3a	-2.53	-5.79	1.42E-08	7.25E-06	2.67E-04
Hmcn1	0.32	1.25	9.45E-05	9.75E-03	1
Hoxc6	0.38	1.3	1.22E-06	2.98E-04	0.02
Hpse	-0.43	-1.35	2.71E-04	2.00E-02	1.00E+00
Htra3	0.98	1.98	1.27E-05	1.96E-03	2.40E-01
Ifi47	0.81	1.76	1.36E-04	1.00E-02	1
Igf2	0.71	1.63	2.49E-05	3.34E-03	4.70E-01
Igfbp6	0.57	1.49	3.46E-07	9.78E-05	6.54E-03
Igfn1	-1.84	-3.57	2.77E-04	2.00E-02	1.00E+00
Inhbb	-0.73	-1.66	1.72E-04	0.02	1
Iscu	-0.35	-1.28	7.17E-04	5.00E-02	1
Islr	0.5	1.41	7.45E-04	5.00E-02	1.00E+00
Itgbl1	0.39	1.31	6.17E-04	4.00E-02	1
Itpr3	-0.24	-1.18	5.68E-04	4.00E-02	1.00E+00
Jun	0.39	1.31	2.02E-04	0.02	1
Kank4	-0.39	-1.31	5.48E-07	1.49E-04	1.00E-02
Kcnc1	-0.4	-1.32	6.18E-04	0.04	1
Kcnf1	-0.61	-1.52	1.35E-04	1.00E-02	1
Kcnip1	-0.29	-1.22	4.28E-04	0.03	1
Klf5	0.3	1.23	2.11E-04	0.02	1
Klhl31	-1.83	-3.55	3.22E-07	9.25E-05	6.08E-03
Lama4	0.26	1.2	1.99E-04	2.00E-02	1.00E+00
Lcp1	0.38	1.3	1.65E-07	5.12E-05	3.12E-03

Lepr	0.53	1.45	2.80E-06	5.70E-04	0.05
Lims2	-0.51	-1.43	1.53E-05	2.31E-03	0.29
Lmo7	0.7	1.62	2.17E-09	1.59E-06	4.10E-05
Ltbp1	0.42	1.33	1.65E-06	3.73E-04	3.00E-02
Maob	-0.34	-1.27	5.13E-05	5.93E-03	0.97
Map3k6	-1	-2	5.39E-04	4.00E-02	1
Mb	-2.46	-5.5	2.98E-08	1.30E-05	5.62E-04
Medag	0.62	1.53	6.51E-04	0.04	1
Meox2	0.74	1.67	2.00E-04	2.00E-02	1
Mertk	-0.53	-1.44	1.53E-10	1.90E-07	2.89E-06
Mest	-0.26	-1.2	3.66E-04	3.00E-02	1
Mfap4	0.67	1.59	3.04E-04	2.00E-02	1
Mfsd2a	-0.46	-1.37	5.38E-06	9.95E-04	0.1
MGC108823	0.82	1.77	2.16E-06	4.70E-04	0.04
Mgll	-0.28	-1.21	8.78E-05	9.24E-03	1
Mgp	0.42	1.34	7.80E-05	8.56E-03	1
Mpeg1	0.52	1.44	5.80E-06	1.06E-03	0.11
Mpz	-0.46	-1.38	3.54E-06	6.94E-04	7.00E-02
Mpzl2	1.08	2.11	7.55E-05	8.37E-03	1
Mrc2	0.49	1.4	8.86E-05	9.25E-03	1.00E+00
Mt3	-0.28	-1.21	8.77E-05	9.24E-03	1
Mtmr2	-0.28	-1.21	1.04E-04	1.00E-02	1
Mx1	0.74	1.67	2.05E-04	0.02	1
Mybpc1	-1.32	-2.5	5.58E-07	1.50E-04	0.01
Mybpc2	-2	-4.01	1.62E-07	5.12E-05	3.06E-03
Myh2	-3.13	-8.77	3.33E-16	1.27E-12	6.29E-12
Myh4	-1.61	-3.06	2.99E-06	5.94E-04	6.00E-02
Myl1	-1.54	-2.91	7.86E-07	1.98E-04	0.01
Mylpf	-1.83	-3.55	5.41E-08	2.18E-05	1.02E-03
Myoc	-0.39	-1.31	1.61E-04	0.01	1
Myom1	-0.95	-1.93	2.50E-04	2.00E-02	1.00E+00
Naa38	-0.29	-1.22	6.81E-04	4.00E-02	1
Ndst4	-0.3	-1.23	1.28E-04	0.01	1
Ndufs5_1	0.79	1.72	3.68E-05	4.52E-03	0.69
Neb	-0.76	-1.7	8.00E-09	4.44E-06	1.51E-04
Neil3	2.28	4.84	6.29E-04	4.00E-02	1
NEWGENE_1308171	0.66	1.58	1.32E-10	1.77E-07	2.50E-06
Nnat	0.47	1.38	5.86E-05	6.71E-03	1
Npy	2.53	5.79	3.32E-24	2.67E-20	6.26E-20

Nr1d1	-0.34	-1.26	1.60E-05	2.36E-03	0.3
Nr4a1	-0.4	-1.32	3.78E-04	3.00E-02	1.00E+00
Ntn1	0.7	1.62	2.28E-05	3.17E-03	0.43
Ntng2	-0.42	-1.34	7.94E-08	3.12E-05	1.50E-03
Obscn	-0.91	-1.88	6.04E-04	4.00E-02	1
Omd	0.8	1.74	1.23E-04	0.01	1
Osmr	0.48	1.4	5.88E-05	6.71E-03	1
Padi2	-0.42	-1.34	6.63E-07	1.75E-04	0.01
Pde5a	0.64	1.56	4.80E-05	5.60E-03	0.91
Per1	-0.96	-1.94	1.70E-08	8.28E-06	3.21E-04
Per2	-0.75	-1.68	2.81E-05	3.62E-03	0.53
Phldb2	0.51	1.43	4.47E-09	2.88E-06	8.43E-05
Piezo1	0.62	1.54	1.92E-06	4.23E-04	0.04
Plaat3	-0.3	-1.23	3.18E-04	2.00E-02	1
Pllp	-0.4	-1.32	5.40E-04	0.04	1
Plxnb1	-0.34	-1.27	1.42E-04	1.00E-02	1
Plxnb3	-0.37	-1.29	6.20E-06	1.11E-03	0.12
Pmepa1	-0.3	-1.23	5.12E-04	0.04	1
Ppp1r3a	-2.12	-4.34	9.79E-07	2.42E-04	2.00E-02
Prg4	0.74	1.67	4.00E-04	3.00E-02	1
Prim1	0.89	1.85	1.18E-04	1.00E-02	1
Prx	-0.38	-1.3	3.16E-08	1.34E-05	5.96E-04
Ptgds	0.8	1.74	2.76E-05	3.59E-03	0.52
Ptrh1	0.45	1.37	5.71E-04	4.00E-02	1
Pygm	-0.79	-1.73	1.05E-04	1.00E-02	1.00E+00
Rab1b_2	8.4	338.19	7.74E-04	0.05	1
Rassf4	-0.36	-1.28	1.45E-06	3.44E-04	0.03
Reln	-0.23	-1.17	7.53E-04	5.00E-02	1
RGD1310587	0.61	1.52	1.83E-06	4.08E-04	0.03
Rgs18	0.95	1.94	4.73E-04	3.00E-02	1
Rps4x_2	0.25	1.19	7.90E-04	0.05	1
RT1-Ba	0.96	1.94	5.33E-10	5.72E-07	1.01E-05
RT1-CE16	0.67	1.59	2.30E-06	4.90E-04	0.04
RT1-Da	0.81	1.75	2.55E-06	5.33E-04	0.05
RT1-Db1	0.74	1.67	1.55E-05	2.31E-03	0.29
RT1-N2	2.15	4.43	1.81E-04	0.02	1
Ryr1	-1.41	-2.66	1.00E-07	3.58E-05	1.89E-03
Scn1b	-0.3	-1.23	4.52E-05	5.31E-03	0.85
Sdc2	0.3	1.23	9.73E-05	9.97E-03	1.00E+00

Sema3b	-0.35	-1.27	1.63E-06	3.73E-04	0.03
Sema3c	0.41	1.33	1.44E-08	7.25E-06	2.72E-04
Sema3d	0.43	1.35	1.86E-04	0.02	1
Sema5a	-0.29	-1.22	2.49E-05	3.34E-03	0.47
Sema6a	0.5	1.42	3.65E-06	7.08E-04	0.07
Sema7a	-0.41	-1.33	1.12E-04	1.00E-02	1.00E+00
Sertm1	-0.51	-1.43	2.52E-05	3.35E-03	0.47
Sfrp5	-0.26	-1.19	2.32E-04	2.00E-02	1
Sgk1	-0.66	-1.58	1.87E-09	1.55E-06	3.53E-05
Slc13a4	0.7	1.63	3.40E-09	2.38E-06	6.41E-05
Slc25a22	-0.28	-1.22	7.23E-04	5.00E-02	1
Slc6a13	1	1.99	1.63E-07	5.12E-05	3.08E-03
Slc6a20	0.89	1.85	8.44E-08	3.23E-05	1.59E-03
Slc7a5	-0.3	-1.23	2.57E-04	2.00E-02	1
Slfn5	0.28	1.22	3.52E-04	0.03	1
Sncg	0.23	1.17	7.01E-04	4.00E-02	1.00E+00
Spry1	-0.6	-1.52	4.53E-04	3.00E-02	1
Sptb	-0.31	-1.24	1.45E-05	2.23E-03	0.27
Sptbn5	-0.54	-1.45	5.18E-14	1.39E-10	9.78E-10
Srl	-1.65	-3.14	4.41E-04	0.03	1
Stac2	1.78	3.43	2.99E-04	2.00E-02	1.00E+00
Svep1	0.64	1.56	4.24E-06	8.12E-04	0.08
Sypl2	-1.76	-3.38	7.35E-04	0.05	1
Syt4	0.28	1.22	6.13E-05	6.95E-03	1.00E+00
Tcap	-2.04	-4.1	1.86E-05	2.67E-03	3.50E-01
Tec	0.49	1.41	1.83E-04	0.02	1
Tef	-0.27	-1.21	5.38E-04	4.00E-02	1
Tent5b	-2.21	-4.64	3.49E-05	4.38E-03	0.66
Tesc	-0.44	-1.36	1.52E-04	1.00E-02	1.00E+00
Tgfbi	0.38	1.3	3.65E-04	3.00E-02	1
Thbd	0.63	1.55	9.70E-08	3.55E-05	1.83E-03
Thbs1	0.91	1.88	1.77E-17	9.51E-14	3.35E-13
Tnnc2	-2.27	-4.81	3.14E-11	6.32E-08	5.93E-07
Tnni2	-1.85	-3.6	7.22E-07	1.84E-04	1.00E-02
Tnnt3	-1.87	-3.66	1.26E-10	1.77E-07	2.38E-06
Tpm2	-0.49	-1.41	7.82E-05	8.56E-03	1
Tsc22d3	-0.46	-1.38	4.33E-10	4.98E-07	8.18E-06
Ttn	-1.38	-2.6	9.19E-11	1.48E-07	1.73E-06
Usp53	0.36	1.29	6.49E-04	4.00E-02	1.00E+00

Usp9y	-5.22	-37.21	5.88E-04	4.00E-02	1.00E+00
Vegfb	-0.43	-1.34	6.00E-04	4.00E-02	1
Vgf	0.39	1.31	3.99E-04	0.03	1
Vstm2b	-0.84	-1.79	2.52E-04	2.00E-02	1
Vwa1	-0.34	-1.26	1.03E-05	1.70E-03	0.19
Wee1	-0.48	-1.4	8.33E-05	9.00E-03	1
Xirp2	-1.46	-2.76	6.88E-07	1.79E-04	1.00E-02
Zbtb16	-1.61	-3.05	3.94E-16	1.27E-12	7.44E-12

Table A3.4. Master list of differentially expressed genes between female 10X CXB-NE vs DF-NE samples with a FDR p-value ≤ 0.05 and a fold change greater than ±1.

Name	**Log_2 fold change**	**Fold change**	**P-value**	**FDR p-value**	**Bonferroni**
AABR07007068.1	-0.38	-1.3	1.70E-05	2.00E-02	3.20E-01
Ass1	-1.26	-2.4	4.34E-08	3.44E-04	8.07E-04
Atf3	-1.06	-2.09	2.54E-07	8.06E-04	4.73E-03
Gadd45a	-0.57	-1.49	1.99E-05	3.00E-02	3.70E-01
Gas2l3	0.37	1.3	2.12E-05	0.03	0.39
Grhl3	3.73	13.29	2.20E-07	8.06E-04	4.10E-03
Hba-a3	1.33	2.51	3.91E-05	4.00E-02	7.30E-01
Jun	-0.36	-1.28	4.16E-05	4.00E-02	7.70E-01
Lce1f_2	-2.55	-5.85	4.27E-06	8.47E-03	0.08
Myom3	3.24	9.43	6.96E-09	1.10E-04	1.29E-04
Rbp4	-0.75	-1.68	4.72E-05	5.00E-02	0.88
Sema6a	-0.74	-1.67	6.13E-06	1.00E-02	1.10E-01
Sox11	-0.73	-1.66	5.12E-07	1.35E-03	9.53E-03
Sptb	0.38	1.31	1.15E-05	0.02	0.21
Txnip	0.44	1.35	1.29E-06	2.92E-03	0.02
Vgf	-0.71	-1.63	7.99E-08	4.22E-04	1.49E-03

Table A3.5. Master list of differentially expressed genes between male 10X CXB-NE vs DF-NE samples with an FDR p-value ≤ 0.05 and a fold change greater than ±1.

Name	Log_2 fold change	Fold change	P-value	FDR p-value	Bonferroni
1700092M07Rik	2.79	6.91	3.95E-04	0.03	1
AABR07005844.1	1.31	2.48	3.33E-10	2.07E-07	6.29E-06
AABR07034445.1	-1.18	-2.27	9.09E-05	7.52E-03	1
AABR07049329.1	0.83	1.78	8.27E-04	0.04	1
AABR07060872.1	2.17	4.5	4.25E-13	4.76E-10	8.03E-09
AC118772.1	3.29	9.8	3.78E-05	3.88E-03	0.71
Acap1	1.38	2.6	6.90E-05	6.13E-03	1
Ace2	0.54	1.46	4.58E-04	0.03	1
Acer2	-0.6	-1.52	1.63E-05	1.95E-03	0.31
Acta2	0.82	1.77	1.95E-10	1.26E-07	3.69E-06
Actn1	0.39	1.31	1.10E-05	1.42E-03	0.21
Adamts1	0.38	1.3	8.64E-04	0.04	1
Adamts12	0.57	1.49	7.14E-07	1.50E-04	0.01
Adh6_1	2.09	4.27	3.73E-04	0.02	1
Ahsp	1.37	2.58	3.43E-06	5.64E-04	0.06
Alas2	1.35	2.54	2.34E-09	1.12E-06	4.41E-05
Aldh1a3	0.58	1.49	8.11E-04	0.04	1
Alox15	1.36	2.57	6.18E-05	5.70E-03	1
Angpt1	0.64	1.56	3.32E-05	3.52E-03	0.63
Angptl1	1.31	2.48	2.49E-04	0.02	1
Ankrd1	2.16	4.46	5.06E-05	4.91E-03	0.96
Anpep	0.74	1.67	2.51E-04	0.02	1
Aox4	0.54	1.45	2.40E-05	2.68E-03	0.45
Arhgap45	0.63	1.55	5.14E-04	0.03	1
Arhgdib	0.58	1.5	2.01E-05	2.28E-03	0.38
Arntl	0.65	1.56	1.91E-05	2.20E-03	0.36
Aspn	1.4	2.63	2.88E-09	1.31E-06	5.44E-05
Bgn	0.57	1.48	8.83E-08	2.51E-05	1.67E-03
Bin2	1.05	2.08	1.20E-04	9.40E-03	1
Bmp4	1.31	2.47	3.07E-05	3.39E-03	0.58
Bmper	0.66	1.58	7.60E-06	1.06E-03	0.14
Boc	0.59	1.5	6.57E-07	1.40E-04	0.01
Btk	1.18	2.27	5.51E-05	5.29E-03	1

Btla	1.22	2.33	8.85E-04	0.05	1
C1qb	0.79	1.72	1.77E-05	2.06E-03	0.33
C1qtnf7	2.07	4.19	2.93E-04	0.02	1
C1r	0.39	1.31	3.15E-04	0.02	1
C1s	0.51	1.43	2.55E-06	4.28E-04	0.05
C3	0.62	1.53	8.96E-04	0.05	1
C4a	0.63	1.55	1.07E-04	8.60E-03	1
C4b	0.91	1.88	1.36E-04	0.01	1
Camp	2.4	5.27	1.55E-08	5.92E-06	2.93E-04
Ccbe1	1.61	3.06	1.68E-04	0.01	1
Ccdc3	0.89	1.85	2.07E-05	2.34E-03	0.39
Ccdc80	0.69	1.61	5.30E-07	1.16E-04	0.01
Ccl21	2.05	4.15	1.35E-19	3.78E-16	2.56E-15
Ccn1	0.76	1.69	8.18E-04	0.04	1
Ccn2	1.02	2.03	1.22E-12	1.13E-09	2.30E-08
Ccn3	1.47	2.77	8.62E-16	1.45E-12	1.63E-11
Ccr2	1.15	2.22	2.30E-07	5.59E-05	4.34E-03
Cd177	2.46	5.49	2.89E-09	1.31E-06	5.45E-05
Cd226	1.25	2.38	5.82E-04	0.03	1
Cd37	0.99	1.98	7.36E-04	0.04	1
Cd79b	2.46	5.49	7.82E-05	6.73E-03	1
Cdh11	0.31	1.24	1.18E-05	1.50E-03	0.22
Ceacam4	1.49	2.82	6.66E-06	9.56E-04	0.13
Cemip	0.52	1.43	4.46E-04	0.03	1
Cfp	0.96	1.95	6.04E-05	5.63E-03	1
Chi3l1	0.82	1.77	9.08E-04	0.05	1
Chrna3	-0.46	-1.38	1.59E-05	1.92E-03	0.3
Chst2	-0.25	-1.19	4.48E-04	0.03	1
Cilp	0.82	1.77	7.94E-07	1.61E-04	0.02
Clec4a3	0.83	1.78	7.91E-04	0.04	1
Clvs1	-1.26	-2.39	7.27E-06	1.03E-03	0.14
Cnn1	1.74	3.33	9.07E-06	1.24E-03	0.17
Cnn2	0.66	1.58	1.99E-07	4.92E-05	3.76E-03
Col12a1	0.35	1.28	3.44E-07	8.03E-05	6.51E-03
Col6a1	0.43	1.34	5.69E-05	5.40E-03	1
Col8a1	0.93	1.91	1.43E-09	7.06E-07	2.70E-05
Col9a1	0.88	1.83	8.26E-04	0.04	1
Cp	0.31	1.24	6.15E-05	5.70E-03	1
Cped1	0.47	1.38	1.25E-04	9.67E-03	1

Cpxm2	0.57	1.48	3.71E-04	0.02	1
Crh	-4.43	-21.61	3.33E-05	3.52E-03	0.63
Crisp3	3.18	9.06	3.51E-06	5.71E-04	0.07
Csf2rb	1.45	2.73	1.16E-07	3.09E-05	2.19E-03
Csf3r	1	2	1.72E-04	0.01	1
Csrp3	2.37	5.16	3.77E-08	1.24E-05	7.12E-04
Ctsg	3.27	9.62	3.79E-05	3.88E-03	0.72
Cxcl12	0.43	1.34	2.47E-04	0.02	1
Cxcr2	1.99	3.98	1.01E-06	1.96E-04	0.02
Cybb	0.56	1.47	9.34E-06	1.26E-03	0.18
Dab2	0.37	1.29	6.32E-06	9.15E-04	0.12
Dbp	-0.78	-1.72	3.51E-18	8.42E-15	6.64E-14
Ddah2	0.98	1.97	5.31E-04	0.03	1
Defa5	2.29	4.88	9.47E-08	2.65E-05	1.79E-03
Dio2	1.24	2.36	1.08E-09	5.72E-07	2.04E-05
Dpt	1	2	5.77E-05	5.44E-03	1
Ebf2	0.57	1.48	2.16E-06	3.69E-04	0.04
Eln	1.02	2.03	2.16E-08	7.87E-06	4.07E-04
Emp1	0.5	1.42	1.23E-05	1.55E-03	0.23
Epx	2.5	5.65	3.23E-07	7.64E-05	6.11E-03
Evi2b	0.9	1.87	6.69E-04	0.04	1
F13a1	0.87	1.82	7.83E-07	1.60E-04	0.01
F5	1.87	3.66	9.44E-09	3.87E-06	1.78E-04
Fabp4	1.79	3.46	5.61E-05	5.35E-03	1
Fam180a	0.94	1.92	1.20E-04	9.40E-03	1
Fat4	0.29	1.22	1.98E-04	0.01	1
Fbln1	0.49	1.41	5.78E-04	0.03	1
Fbn1	0.45	1.37	1.26E-05	1.57E-03	0.24
Fcgr2a_2	0.84	1.79	3.48E-05	3.63E-03	0.66
Fcnb	2.37	5.16	4.74E-16	8.83E-13	8.95E-12
Fermt3	1.05	2.07	1.46E-05	1.79E-03	0.28
Fes	1.01	2.02	4.65E-04	0.03	1
Fgr	1.43	2.7	9.66E-06	1.29E-03	0.18
Fhl1	0.37	1.29	8.48E-04	0.04	1
Filip1l	0.68	1.6	1.73E-05	2.05E-03	0.33
Flna	0.32	1.25	4.88E-06	7.31E-04	0.09
Flnc	0.6	1.51	1.10E-06	2.05E-04	0.02
Flt3	-0.3	-1.23	6.95E-04	0.04	1
Fn1	0.4	1.32	8.17E-05	6.89E-03	1

Foxc2	0.72	1.65	1.60E-04	0.01	1
Frmpd4	-0.26	-1.19	8.38E-04	0.04	1
Fut2	2.26	4.8	7.84E-04	0.04	1
Fxyd5	0.64	1.56	1.42E-05	1.76E-03	0.27
Fyb1	0.77	1.7	6.79E-06	9.66E-04	0.13
Fzd2	0.46	1.37	2.96E-04	0.02	1
Gal	1.42	2.68	1.45E-07	3.68E-05	2.74E-03
Gch1	1.15	2.21	3.35E-04	0.02	1
Gdf10	0.98	1.98	2.67E-04	0.02	1
gene:ENSRNOG00000002820	2.28	4.85	1.01E-07	2.74E-05	1.91E-03
gene:ENSRNOG00000004090	3.15	8.89	7.75E-04	0.04	1
gene:ENSRNOG00000031579	0.88	1.84	7.53E-05	6.58E-03	1
gene:ENSRNOG00000048967	1.2	2.3	4.77E-04	0.03	1
gene:ENSRNOG00000049075	0.25	1.19	6.21E-04	0.03	1
gene:ENSRNOG00000067832	3.57	11.84	4.40E-06	6.90E-04	0.08
gene:ENSRNOG00000068082	2.27	4.83	9.63E-07	1.90E-04	0.02
gene:ENSRNOG00000069384	0.91	1.89	6.60E-09	2.77E-06	1.25E-04
Gjb2	0.74	1.67	8.21E-06	1.13E-03	0.16
Gjc3	-0.36	-1.29	3.22E-06	5.34E-04	0.06
Gnai1	-0.27	-1.21	3.69E-04	0.02	1
Gng11	0.63	1.55	4.00E-04	0.03	1
Gp1ba	2.21	4.62	3.49E-05	3.63E-03	0.66
Gsn	0.62	1.53	3.59E-05	3.72E-03	0.68
Gvin1	0.83	1.78	4.70E-04	0.03	1
Gypa	1.86	3.64	1.50E-08	5.87E-06	2.84E-04
H1f4	0.45	1.37	1.76E-04	0.01	1
Hba-a2	1	1.99	8.13E-05	6.89E-03	1
Hba-a3	0.95	1.94	2.34E-04	0.02	1
Hbb-b1	0.99	1.99	1.34E-04	0.01	1
Hemgn	1.85	3.6	1.76E-11	1.29E-08	3.33E-07
Hist1h2ak	1.12	2.17	5.82E-04	0.03	1
Hist2h3c2_4	0.67	1.6	6.51E-05	5.94E-03	1
Hmgb1	-1.02	-2.03	2.68E-07	6.42E-05	5.06E-03
Hoxc6	0.34	1.27	1.53E-05	1.86E-03	0.29
Htra3	0.72	1.65	2.41E-04	0.02	1
Ifit1	2.18	4.52	7.34E-04	0.04	1
Ifitm3	0.31	1.24	3.14E-04	0.02	1
Ifitm6	1.54	2.92	6.69E-05	6.04E-03	1
Igfbp5	0.74	1.67	8.11E-08	2.36E-05	1.53E-03

Igfbp6	0.56	1.48	5.44E-07	1.17E-04	0.01
Igfbp7	0.29	1.22	5.49E-05	5.29E-03	1
Ighm	1.68	3.2	2.22E-20	7.44E-17	4.19E-16
Ikzf1	0.68	1.6	6.29E-05	5.77E-03	1
Ikzf3	1.76	3.38	3.89E-05	3.93E-03	0.73
Il13ra2	1.36	2.57	3.92E-06	6.27E-04	0.07
Il18rap	1.61	3.06	3.17E-04	0.02	1
Il2rg	0.82	1.76	8.85E-04	0.05	1
Il7r	0.44	1.36	5.23E-04	0.03	1
Irag1	0.45	1.37	8.62E-04	0.04	1
Itga11	0.77	1.71	5.49E-04	0.03	1
Itga2b	1.77	3.41	5.67E-10	3.17E-07	1.07E-05
Itgal	1.04	2.05	1.51E-04	0.01	1
Itgax	1.24	2.36	5.13E-04	0.03	1
Itgb2	1.24	2.37	9.96E-08	2.74E-05	1.88E-03
Jchain	1.61	3.05	1.05E-05	1.38E-03	0.2
Kcng1	-0.47	-1.39	4.32E-04	0.03	1
Klf9	-0.3	-1.23	1.10E-04	8.75E-03	1
Kxd1	0.25	1.19	4.96E-04	0.03	1
Lbp	0.98	1.98	5.17E-04	0.03	1
Lcn2	1.03	2.04	2.04E-04	0.01	1
Lcp2	0.68	1.6	2.27E-04	0.02	1
Lgals5	1.62	3.06	1.56E-07	3.91E-05	2.95E-03
Lilrb3a	3.59	12.03	5.18E-06	7.70E-04	0.1
Lmo7	0.45	1.37	8.99E-05	7.47E-03	1
Lox	0.92	1.9	6.85E-08	2.05E-05	1.29E-03
Loxl1	0.74	1.67	8.32E-05	6.95E-03	1
Lsp1	0.84	1.79	4.82E-06	7.29E-04	0.09
Lum	0.28	1.21	1.08E-04	8.69E-03	1
Ly49si2	1.62	3.08	7.07E-04	0.04	1
Ly6g6d	2.5	5.66	1.19E-04	9.35E-03	1
Lyl1	1.7	3.25	1.60E-04	0.01	1
Lyz2	0.74	1.67	1.46E-12	1.25E-09	2.76E-08
Map7d3	0.86	1.82	3.62E-04	0.02	1
Mcpt9	2.19	4.56	8.20E-07	1.64E-04	0.02
Medag	0.76	1.69	4.56E-04	0.03	1
Meox2	0.73	1.66	2.90E-04	0.02	1
Mfap4	1.27	2.41	1.05E-15	1.60E-12	1.98E-11
Mfap5	0.53	1.45	4.88E-05	4.79E-03	0.92

Mgp	0.5	1.41	1.94E-06	3.40E-04	0.04
Mki67	1.15	2.22	5.32E-13	5.34E-10	1.01E-08
Mmp2	0.42	1.34	1.32E-04	0.01	1
Mmp8	2.91	7.53	5.08E-24	2.84E-20	9.59E-20
Mmp9	2.46	5.51	8.17E-08	2.36E-05	1.54E-03
Mmrn1	1.74	3.35	1.30E-08	5.19E-06	2.45E-04
Mn1	1.13	2.19	4.17E-04	0.03	1
Mpig6b	1.78	3.44	2.01E-05	2.28E-03	0.38
Mpo	2.36	5.12	1.58E-13	2.04E-10	2.98E-09
Mrc2	0.45	1.36	2.38E-04	0.02	1
Mrpl51	-0.26	-1.2	6.01E-04	0.03	1
Ms4a1	3.91	15.06	1.29E-04	9.90E-03	1
Myh11	0.62	1.53	2.48E-08	8.67E-06	4.69E-04
Myh7	-1.48	-2.79	8.91E-04	0.05	1
Myl9	0.95	1.93	3.19E-08	1.07E-05	6.02E-04
Mylk	0.54	1.45	2.14E-06	3.69E-04	0.04
Myo1f	0.79	1.73	1.87E-06	3.30E-04	0.04
Myo1g	1.42	2.68	7.98E-05	6.83E-03	1
Napsa	1.84	3.57	2.17E-04	0.02	1
Ncam2	-0.25	-1.19	5.21E-04	0.03	1
Ncf1	0.77	1.7	4.64E-06	7.14E-04	0.09
Nckap1l	0.62	1.54	3.12E-05	3.42E-03	0.59
NEWGENE_1308171	0.53	1.45	2.34E-14	3.27E-11	4.41E-10
NEWGENE_2724	1.39	2.62	3.96E-04	0.03	1
Nfe2	1.84	3.59	1.04E-06	2.01E-04	0.02
Ngp	2.38	5.2	2.80E-22	1.18E-18	5.29E-18
Nnat	0.51	1.42	1.08E-05	1.41E-03	0.2
Np4	3.04	8.24	3.42E-09	1.51E-06	6.47E-05
Npas2	1.54	2.9	7.88E-06	1.09E-03	0.15
Nptx1	-0.3	-1.23	1.84E-05	2.13E-03	0.35
Npy	1.87	3.66	3.65E-06	5.90E-04	0.07
Nr1d1	-0.4	-1.32	2.19E-04	0.02	1
Nt5c3b	0.5	1.41	1.15E-04	9.09E-03	1
Ntng1	-0.32	-1.25	9.84E-05	7.98E-03	1
Pax5	2.78	6.85	6.91E-05	6.13E-03	1
Pcbd1_2	0.58	1.49	5.57E-04	0.03	1
Pde5a	0.68	1.6	5.35E-08	1.63E-05	1.01E-03
Pdgfrl	1.1	2.14	6.03E-05	5.63E-03	1
Per1	-0.61	-1.53	4.32E-07	9.79E-05	8.15E-03

Pf4	1.34	2.54	3.12E-04	0.02	1
Pglyrp1	3.02	8.12	7.64E-04	0.04	1
Phex	1.16	2.23	3.51E-04	0.02	1
Pi16	1.26	2.4	1.36E-09	6.94E-07	2.58E-05
Pik3ap1	0.97	1.96	1.54E-06	2.82E-04	0.03
Pkhd1l1	1.49	2.82	5.80E-09	2.49E-06	1.09E-04
Pla2g2a	1.43	2.7	5.66E-04	0.03	1
Plac8	1.67	3.18	9.30E-11	6.24E-08	1.76E-06
Plbd1	1.29	2.44	7.74E-07	1.60E-04	0.01
Plek	1.07	2.1	4.18E-05	4.15E-03	0.79
Prg2	2.11	4.31	3.91E-12	3.12E-09	7.38E-08
Prg3	2.82	7.07	1.24E-07	3.25E-05	2.34E-03
Prg4	0.79	1.72	1.88E-04	0.01	1
Prim1	-1.01	-2.01	1.38E-07	3.56E-05	2.60E-03
Prrx1	0.53	1.45	1.71E-04	0.01	1
Psd4	0.93	1.9	7.21E-04	0.04	1
Ptch1	0.4	1.32	1.24E-04	9.60E-03	1
Ptch2	0.86	1.81	3.82E-04	0.02	1
Ptpn6	0.77	1.7	3.26E-05	3.49E-03	0.62
Ptprc	0.86	1.81	2.05E-13	2.46E-10	3.87E-09
Ptprh	1.97	3.92	8.20E-04	0.04	1
Rab3il1	0.5	1.42	8.90E-04	0.05	1
Rab44	2.77	6.81	6.72E-04	0.04	1
Rac2	0.95	1.93	5.69E-04	0.03	1
Rack1	0.27	1.21	4.35E-04	0.03	1
Ranbp3l	0.73	1.66	4.17E-05	4.15E-03	0.79
Rassf2	0.49	1.4	1.37E-04	0.01	1
RatNP-3b	2.85	7.22	5.42E-12	4.14E-09	1.02E-07
Rbm38	1.26	2.39	1.80E-08	6.71E-06	3.40E-04
Retnlg	2.42	5.34	1.64E-05	1.95E-03	0.31
RGD1310587	0.43	1.35	5.30E-04	0.03	1
RGD1564899	-1.14	-2.2	1.38E-04	0.01	1
Rgs18	1.03	2.04	3.23E-05	3.47E-03	0.61
Rhag	1.87	3.65	1.09E-05	1.41E-03	0.21
Rhd	1.7	3.25	3.85E-04	0.02	1
Rhoj	0.34	1.27	7.48E-05	6.58E-03	1
Ror2	0.99	1.99	7.79E-05	6.73E-03	1
Rpl26	0.24	1.18	5.41E-04	0.03	1
Rpl31l4	1.39	2.61	8.23E-05	6.91E-03	1

Rpl39_3	0.32	1.25	7.61E-05	6.61E-03	1
Rplp1	0.27	1.21	6.65E-05	6.03E-03	1
Rps4x_1	0.26	1.19	4.81E-04	0.03	1
Rps8	0.26	1.19	4.66E-04	0.03	1
Rsad2	1.09	2.13	2.45E-06	4.16E-04	0.05
RT1-Ba	0.74	1.67	7.59E-04	0.04	1
S100a6	0.25	1.19	7.39E-04	0.04	1
S100a8	2.64	6.24	4.89E-32	4.11E-28	9.24E-28
S100a9	2.51	5.68	5.59E-34	9.37E-30	1.06E-29
Sdc2	0.3	1.23	9.29E-05	7.64E-03	1
Sell	1.93	3.82	1.49E-12	1.25E-09	2.81E-08
Selplg	0.95	1.93	9.65E-06	1.29E-03	0.18
Sema7a	-0.3	-1.23	1.13E-04	8.99E-03	1
Serpinb10	2.57	5.96	3.83E-05	3.90E-03	0.72
Serpinb1a	0.41	1.33	2.30E-08	8.22E-06	4.35E-04
Serpinb1b	3.56	11.78	5.41E-13	5.34E-10	1.02E-08
Serpinf1	0.67	1.59	2.83E-08	9.70E-06	5.35E-04
Serping1	0.46	1.38	2.47E-05	2.75E-03	0.47
Sfrp2	3.03	8.2	1.09E-09	5.72E-07	2.06E-05
Sfrp4	0.74	1.67	7.38E-05	6.52E-03	1
Sgk1	-0.38	-1.3	4.39E-06	6.90E-04	0.08
Shisa3	0.9	1.87	4.40E-07	9.84E-05	8.31E-03
Slc13a4	0.63	1.54	4.98E-05	4.86E-03	0.94
Slc16a11	0.51	1.42	3.17E-05	3.43E-03	0.6
Slc4a1	1.89	3.69	1.31E-16	2.75E-13	2.48E-12
Slfn4_1	1.16	2.24	1.99E-11	1.39E-08	3.76E-07
Slitrk2	-0.25	-1.19	4.80E-04	0.03	1
Smoc1	1.12	2.17	4.04E-05	4.06E-03	0.76
Spata32	1.42	2.68	5.73E-04	0.03	1
Spib	2.25	4.76	6.83E-05	6.13E-03	1
Spta1	1.51	2.86	4.05E-10	2.42E-07	7.64E-06
Srgn	0.94	1.92	4.69E-10	2.71E-07	8.85E-06
Stac2	1.66	3.15	7.99E-04	0.04	1
Stom	0.61	1.53	1.62E-06	2.93E-04	0.03
Stra6	0.99	1.99	1.60E-04	0.01	1
Svep1	0.63	1.54	5.52E-06	8.13E-04	0.1
Svip	-0.25	-1.19	4.89E-04	0.03	1
Syk	0.92	1.9	1.77E-06	3.17E-04	0.03
Synpo2	0.54	1.45	1.74E-05	2.05E-03	0.33

Tagap	1.15	2.22	3.16E-05	3.43E-03	0.6
Tagln	0.86	1.82	4.89E-08	1.52E-05	9.24E-04
Tal1	1.19	2.27	1.28E-05	1.59E-03	0.24
Tent5a	0.8	1.74	5.56E-04	0.03	1
Tf	0.39	1.31	3.70E-04	0.02	1
Tgm1	2.67	6.34	5.96E-06	8.70E-04	0.11
Tgm2	0.51	1.43	8.06E-05	6.86E-03	1
Thbd	0.59	1.5	3.79E-07	8.71E-05	7.16E-03
Thbs1	0.74	1.67	3.90E-08	1.26E-05	7.36E-04
Tmem71	1.65	3.14	8.46E-04	0.04	1
Tnik	0.35	1.28	8.61E-04	0.04	1
Tpm4	0.27	1.21	9.83E-05	7.98E-03	1
Treml1	2.22	4.64	5.83E-04	0.03	1
Treml2	2.64	6.25	4.81E-06	7.29E-04	0.09
Trim45	-1.19	-2.29	4.41E-05	4.35E-03	0.83
Tstd1	0.46	1.38	4.66E-04	0.03	1
Tubb1	1.96	3.9	1.10E-06	2.05E-04	0.02
Ucp2	0.29	1.23	9.36E-05	7.66E-03	1
Usp9y	-4.63	-24.75	7.97E-04	0.04	1
Vip	2.49	5.61	4.53E-07	1.00E-04	8.55E-03
Vwf	0.66	1.58	4.64E-08	1.47E-05	8.76E-04
Wdfy4	0.97	1.96	1.10E-06	2.05E-04	0.02
Xdh	0.57	1.49	9.26E-04	0.05	1
Ybx3	0.49	1.41	4.47E-06	6.95E-04	0.08
Zbtb16	-0.92	-1.89	1.44E-06	2.66E-04	0.03
Zfp2	-0.35	-1.27	5.66E-04	0.03	1
Zic1	0.8	1.74	1.16E-05	1.49E-03	0.22

Table A3.6. Master list of differentially expressed genes between Female CCI vs Naïve samples with a p-value ≤ 0.05 and a fold change greater than ±1.

Name	**Log_2 fold change**	**Fold change**	**P-value**	**FDR p-value**	**Bonferroni**
1110032F04Rik	-0.46	-1.38	0.04	0.22	1
AABR07001926.1	-1.28	-2.43	0.03	0.18	1
AABR07001926.3	0.54	1.46	3.74E-05	2.18E-03	0.7
AABR07002774.1	0.57	1.49	2.79E-03	0.04	1

AABR07003176.1	0.29	1.22	0.03	0.17	1
AABR07003537.1	0.33	1.26	0.04	0.21	1
AABR07005031.1	-0.77	-1.71	0.04	0.22	1
AABR07005844.1	-0.94	-1.91	2.16E-05	1.42E-03	0.4
AABR07006283.1	2.68	6.39	0.03	NaN	1
AABR07007068.1	0.43	1.35	2.09E-04	8.02E-03	1
AABR07007675.1	-0.99	-1.99	2.30E-03	0.04	1
AABR07015346.1	-0.35	-1.27	7.41E-03	0.08	1
AABR07017250.1	-3.06	-8.31	0.04	NaN	1
AABR07019403.1	0.33	1.26	0.01	0.11	1
AABR07021871.1	0.42	1.34	0.05	0.24	1
AABR07025140.1	0.85	1.8	0.05	0.24	1
AABR07026291.1	0.29	1.22	0.01	0.11	1
AABR07028349.1	-1.89	-3.7	0.04	NaN	1
AABR07028902.1	0.25	1.19	1.20E-03	0.03	1
AABR07029195.1	-1.5	-2.84	5.75E-03	0.07	1
AABR07029269.1	-0.55	-1.46	0.04	0.23	1
AABR07029605.1	0.3	1.23	0.01	0.12	1
AABR07030773.1	-3.63	-12.42	0.01	NaN	1
AABR07031480.1	0.39	1.31	0.04	0.22	1
AABR07038019.1	-0.59	-1.51	0.02	0.15	1
AABR07039303.2	-7.19	-145.93	0.02	0.16	1
AABR07040412.1	0.5	1.41	1.77E-04	7.13E-03	1
AABR07040864.1	0.29	1.22	2.27E-03	0.04	1
AABR07040947.1	0.66	1.58	9.53E-06	7.45E-04	0.18
AABR07044388.2	-0.45	-1.37	1.16E-04	5.28E-03	1
AABR07044631.2	0.36	1.29	6.46E-03	0.07	1
AABR07045621.1	1.02	2.02	0.02	0.13	1
AABR07048031.1	0.57	1.48	0.02	0.16	1
AABR07051450.1	-0.24	-1.18	5.08E-03	0.06	1
AABR07053185.1	0.38	1.31	0.02	0.12	1
AABR07054362.1	3.11	8.61	0.03	NaN	1
AABR07058914.1	-0.92	-1.9	8.99E-03	0.09	1
AABR07063281.1	-0.19	-1.14	0.04	0.2	1
AABR07070957.1	3.94	15.35	0.01	NaN	1
Abcb6	-0.26	-1.2	0.04	0.23	1
Abcb8	-0.31	-1.24	0.02	0.14	1
Abcc8	-0.42	-1.34	0.03	0.18	1
Abcc9	0.35	1.28	0.01	0.12	1

Abce1	0.3	1.23	1.37E-04	5.98E-03	1
Abcf3	-0.3	-1.23	5.93E-04	0.02	1
Abcg1	-0.22	-1.17	8.26E-03	0.09	1
Abcg3l3	0.37	1.29	6.36E-03	0.07	1
Abcg3l4	0.33	1.26	0.01	0.12	1
Abcg4	-0.41	-1.33	1.62E-03	0.03	1
Abhd12	-0.18	-1.14	0.02	0.15	1
Abhd14a	-0.7	-1.62	6.40E-03	0.07	1
Abhd17a	-0.49	-1.4	6.56E-07	8.29E-05	0.01
Abhd17b	0.27	1.21	0.04	0.2	1
Abhd2	-0.23	-1.18	3.01E-03	0.05	1
Abhd5	0.27	1.2	0.04	0.21	1
Ablim2	-0.47	-1.39	3.64E-04	0.01	1
Abracl	0.44	1.36	0.03	0.17	1
Abtb1	-0.42	-1.34	5.49E-03	0.07	1
Abtb2	-0.33	-1.26	9.83E-03	0.1	1
AC097784.1	0.34	1.27	8.78E-03	0.09	1
AC099450.1	-0.16	-1.12	0.05	0.23	1
AC105662.1	-0.89	-1.86	3.57E-04	0.01	1
AC109542.1	-0.39	-1.31	0.01	0.11	1
AC129049.1	-0.31	-1.24	0.03	0.18	1
AC130232.2	0.43	1.35	3.66E-03	0.05	1
AC130391.3	-0.98	-1.97	2.17E-04	8.12E-03	1
AC130970.1	1.92	3.77	1.68E-13	1.41E-10	3.15E-09
Acaa1a	-0.32	-1.25	0.03	0.18	1
Acads	-0.42	-1.34	4.20E-03	0.06	1
Acd	-0.42	-1.34	0.03	0.17	1
Ache	-0.24	-1.18	3.18E-03	0.05	1
Acin1	0.2	1.15	0.01	0.11	1
Ackr1	-0.44	-1.36	6.86E-03	0.08	1
Aco2	-0.16	-1.12	0.04	0.2	1
Acp3	0.2	1.15	0.01	0.1	1
Acsl3	0.17	1.13	0.04	0.2	1
Acsl4	0.52	1.43	2.92E-10	1.23E-07	5.49E-06
Acsl6	-0.19	-1.14	0.02	0.13	1
Acta2	-0.66	-1.58	1.26E-05	9.30E-04	0.24
Actr2	0.21	1.15	6.76E-03	0.08	1
Actr3	0.19	1.14	0.01	0.12	1
Actr6	0.3	1.23	1.86E-03	0.03	1

Acvr2a	0.31	1.24	0.02	0.13	1
Adam11	-0.38	-1.31	5.22E-06	4.75E-04	0.1
Adam12	0.54	1.45	2.04E-04	7.89E-03	1
Adam17	0.19	1.14	0.03	0.18	1
Adam19	0.2	1.15	0.01	0.1	1
Adamts14	-0.78	-1.71	0.01	0.11	1
Adamts17	0.28	1.21	0.04	0.2	1
Adamts2	-0.58	-1.49	5.34E-04	0.01	1
Adamts9	0.28	1.21	0.04	0.2	1
Adamtsl2	-0.97	-1.96	6.48E-03	0.07	1
Adamtsl5	-0.99	-1.98	5.33E-04	0.01	1
Adap1	-0.18	-1.13	0.03	0.19	1
Adcy6	-0.27	-1.2	0.04	0.2	1
Add2	0.18	1.13	0.03	0.16	1
Add3	0.23	1.17	3.64E-03	0.05	1
Adgrb2	-0.35	-1.28	0.04	0.21	1
Adgrg1	-0.25	-1.19	1.97E-03	0.04	1
Adgrl1	-0.23	-1.17	5.31E-03	0.07	1
Adgrl4	0.32	1.25	0.05	0.24	1
Adm	-0.83	-1.78	0.02	0.14	1
Adnp	0.16	1.12	0.04	0.21	1
Adpgk	-0.42	-1.34	6.43E-03	0.07	1
Adra2c	-0.74	-1.67	1.74E-03	0.03	1
Afap1l2	0.21	1.16	8.79E-03	0.09	1
Agap2	-0.5	-1.41	0.02	0.12	1
Agap3	-0.28	-1.21	6.50E-04	0.02	1
Agpat3	-0.21	-1.16	8.26E-03	0.09	1
Agps	0.17	1.12	0.05	0.23	1
Agrn	-0.24	-1.18	4.32E-03	0.06	1
Agtpbp1	0.26	1.19	0.02	0.16	1
Ahcy	-0.27	-1.21	5.73E-03	0.07	1
Ahdc1	-0.38	-1.3	2.41E-03	0.04	1
Ahr	0.39	1.31	4.38E-05	2.50E-03	0.82
Ajap1	0.88	1.85	0.01	0.11	1
Akap11	0.22	1.16	3.86E-03	0.05	1
Akap2	0.17	1.13	0.03	0.18	1
Akap6	0.28	1.21	0.01	0.11	1
Akap7	0.33	1.25	0.02	0.15	1
Akap8l	-0.27	-1.21	3.38E-03	0.05	1

Akirin1	0.19	1.14	0.02	0.16	1
Akr7a2	-0.46	-1.38	1.84E-03	0.03	1
Alad	-0.64	-1.56	1.08E-03	0.02	1
Alcam	0.28	1.21	2.68E-04	9.22E-03	1
Aldh1l2	0.82	1.76	0.01	0.11	1
Aldh4a1	-0.29	-1.22	0.02	0.15	1
Aldoa_1	-0.29	-1.22	0.01	0.1	1
Aldoa_2	-0.88	-1.84	9.15E-04	0.02	1
Alg10	0.3	1.23	0.03	0.19	1
Alg13_1	0.4	1.32	0.05	0.23	1
Alg3	-0.29	-1.22	0.04	0.23	1
Alkal2	2	3.99	2.88E-05	1.78E-03	0.54
Alkbh7	-0.47	-1.38	0.02	0.15	1
Alkbh8	0.27	1.21	0.05	0.24	1
Alms1	0.2	1.15	0.02	0.14	1
Alox12	-1	-2	0.04	0.22	1
Amh	3.61	12.19	9.44E-03	NaN	1
Amigo1	-0.24	-1.18	3.36E-03	0.05	1
Amph	-0.21	-1.16	7.86E-03	0.08	1
Anapc10	0.3	1.23	0.04	0.2	1
Anapc4	0.29	1.22	7.31E-04	0.02	1
Angptl7	-1.41	-2.66	7.72E-03	0.08	1
Ankh	-0.25	-1.19	0.04	0.2	1
Ankib1	0.17	1.12	0.04	0.23	1
Ankle2	0.17	1.13	0.03	0.19	1
Ankrd12	0.3	1.23	1.02E-04	4.72E-03	1
Ankrd13b	-0.26	-1.2	0.05	0.23	1
Ankrd28	0.19	1.14	0.02	0.14	1
Ankrd34a	-0.61	-1.52	0.03	0.19	1
Anks1a	-0.33	-1.26	7.54E-03	0.08	1
Anln	0.57	1.49	0.02	0.15	1
Anp32b	0.3	1.23	0.02	0.14	1
Anxa7	0.17	1.13	0.04	0.2	1
Ap1ar	0.25	1.19	3.07E-03	0.05	1
Ap1b1	-0.21	-1.15	0.01	0.11	1
Ap1g2	-0.2	-1.15	0.01	0.11	1
Ap1s1	0.23	1.17	6.77E-03	0.08	1
Ap2a1	-0.34	-1.26	2.76E-05	1.74E-03	0.52
Ap2b1	-0.16	-1.12	0.03	0.2	1

Ap4e1	0.27	1.21	0.04	0.23	1
Ap5m1	0.33	1.25	0.02	0.13	1
Apba2	-0.19	-1.14	0.02	0.16	1
Apc2	-0.31	-1.24	9.19E-05	4.34E-03	1
Aph1b	-1.32	-2.5	5.95E-05	3.14E-03	1
Apod	0.42	1.33	2.15E-04	8.09E-03	1
Apool	0.36	1.28	6.63E-03	0.08	1
Appl1	0.27	1.2	1.55E-03	0.03	1
Aqp1	-0.27	-1.21	0.02	0.16	1
Aqp4	-1.11	-2.15	0.03	0.17	1
Ar	-0.34	-1.26	0.02	0.13	1
Arap1	-0.34	-1.27	2.24E-04	8.27E-03	1
Arap3	-0.26	-1.2	0.04	0.23	1
Arcn1	0.16	1.11	0.05	0.24	1
Arf1	-0.18	-1.13	0.02	0.15	1
Arf5	-0.41	-1.33	9.56E-04	0.02	1
Arfgap1	-0.27	-1.21	0.05	0.24	1
Arg1	1.28	2.42	0.01	0.11	1
Arhgap12	0.24	1.18	4.30E-03	0.06	1
Arhgap15	0.78	1.72	1.81E-03	0.03	1
Arhgap27	-0.35	-1.28	0.01	0.1	1
Arhgap44	-0.39	-1.31	7.65E-06	6.43E-04	0.14
Arhgap5	0.29	1.22	1.97E-04	7.68E-03	1
Arhgap8	-0.73	-1.66	0.02	0.12	1
Arhgdig	-0.31	-1.24	0.02	0.12	1
Arhgef26	0.31	1.24	0.02	0.13	1
Arhgef37	-0.45	-1.37	4.24E-03	0.06	1
Arid4b	0.31	1.24	3.46E-04	0.01	1
Arl14ep	0.29	1.22	1.57E-03	0.03	1
Arl6	0.28	1.22	0.03	0.18	1
Armc7	-0.53	-1.44	0.04	0.23	1
Armcx1	0.22	1.17	7.99E-03	0.08	1
Armcx3	0.2	1.15	0.01	0.1	1
Arnt2	0.28	1.22	0.03	0.17	1
Arntl2	0.91	1.88	5.67E-03	0.07	1
Arpp19_1	0.16	1.12	0.04	0.23	1
Arpp19_2	0.51	1.42	6.70E-05	3.43E-03	1
Arrb2	-0.21	-1.16	0.03	0.17	1
Arrdc2	-0.52	-1.43	0.05	0.23	1

Arrdc4	0.31	1.24	0.01	0.1	1
Art3	0.22	1.16	7.00E-03	0.08	1
Asb18	-1.06	-2.09	0.03	0.19	1
Asb6	-0.36	-1.29	0.04	0.22	1
Ash1l	0.25	1.19	1.05E-03	0.02	1
Asic2	-0.32	-1.25	0.05	0.23	1
Asmtl	-0.34	-1.27	0.02	0.13	1
Asphd2	-0.47	-1.38	0.02	0.16	1
Atad1	0.21	1.16	8.68E-03	0.09	1
Atcay	-0.25	-1.19	2.46E-03	0.04	1
Atf2	0.22	1.16	7.93E-03	0.08	1
Atg13	-0.25	-1.19	0.04	0.2	1
Atg3	0.2	1.15	0.02	0.13	1
Atg4d	-0.43	-1.35	4.80E-03	0.06	1
Atg9a	-0.25	-1.19	0.04	0.21	1
Atl1	0.17	1.13	0.03	0.16	1
Atn1	-0.19	-1.14	0.02	0.13	1
Atox1	-0.3	-1.23	0.04	0.23	1
Atp11c	0.34	1.27	7.60E-03	0.08	1
Atp13a1	-0.3	-1.23	0.02	0.14	1
Atp13a2	-0.31	-1.24	1.72E-04	7.00E-03	1
Atp13a3	0.3	1.23	3.79E-04	0.01	1
Atp1b3	0.24	1.18	0.04	0.2	1
Atp2a3	-0.47	-1.38	0.02	0.15	1
Atp2b1	0.23	1.17	2.88E-03	0.04	1
Atp2b4	0.28	1.21	8.70E-04	0.02	1
Atp2c1	0.2	1.15	8.75E-03	0.09	1
Atp5f1d	-0.16	-1.12	0.04	0.21	1
Atp5mg	-0.29	-1.22	7.41E-04	0.02	1
Atp6v0e2	-0.27	-1.2	1.01E-03	0.02	1
Atp6v1h	0.17	1.13	0.03	0.18	1
Atp8b3	-1.1	-2.15	4.42E-03	0.06	1
Atpaf2	-0.41	-1.33	8.05E-03	0.08	1
Atr	0.2	1.15	0.02	0.13	1
Atrx	0.38	1.31	7.18E-07	8.92E-05	0.01
Atxn10	0.3	1.23	1.21E-04	5.45E-03	1
Atxn3	0.29	1.22	0.03	0.18	1
Aup1	-0.31	-1.24	0.01	0.11	1
B3gat3	-0.47	-1.39	2.55E-08	5.02E-06	4.78E-04

Baalc	0.4	1.32	4.51E-03	0.06	1
Babam2	0.19	1.14	0.04	0.21	1
Bag6	-0.23	-1.17	5.47E-03	0.07	1
Basp1	0.34	1.27	9.54E-06	7.45E-04	0.18
Baz1b	0.17	1.12	0.05	0.23	1
Baz2b	0.17	1.13	0.04	0.21	1
Bbx	0.35	1.28	5.06E-03	0.06	1
BC024063	0.45	1.36	4.68E-03	0.06	1
BC049762	-0.79	-1.73	0.03	0.17	1
Bckdha	-0.57	-1.48	4.52E-05	2.52E-03	0.85
Bckdhb	-0.37	-1.29	0.01	0.11	1
Bcl2	0.19	1.14	0.02	0.15	1
Bcl7c	-0.39	-1.31	0.01	0.12	1
Bclaf3	0.28	1.21	0.03	0.2	1
Bdnf	1.1	2.14	1.47E-11	8.06E-09	2.75E-07
Bean1	-0.24	-1.18	3.64E-03	0.05	1
Bex4	0.41	1.33	0.02	0.16	1
Bhlhe41	0.31	1.24	8.67E-04	0.02	1
Bicd1	0.31	1.24	8.63E-05	4.18E-03	1
Birc6	0.15	1.11	0.04	0.23	1
Bloc1s2	0.27	1.2	0.04	0.22	1
Bmp4	-0.96	-1.94	0.02	0.12	1
Bod1l1	0.19	1.14	0.02	0.13	1
Bola1	-0.68	-1.6	0.01	0.11	1
Borcs5	-0.51	-1.43	3.65E-03	0.05	1
Borcs6	-0.33	-1.25	0.02	0.16	1
Bpnt1	0.25	1.19	2.71E-03	0.04	1
Brat1	-0.46	-1.38	0.02	0.13	1
Brcc3	0.3	1.23	0.01	0.12	1
Bri3	-0.47	-1.38	4.19E-03	0.06	1
Brinp2	-0.32	-1.25	0.02	0.13	1
Brix1	0.31	1.24	0.03	0.19	1
Brsk1	-0.2	-1.15	0.01	0.11	1
Brsk2	-0.28	-1.22	8.69E-04	0.02	1
Brwd3	0.42	1.34	2.17E-03	0.04	1
Bsg	-0.3	-1.23	7.72E-03	0.08	1
Btbd11	-0.27	-1.21	0.04	0.21	1
Btbd6	-0.32	-1.25	9.80E-03	0.09	1
Btc	-1.93	-3.81	0.05	NaN	1

Bves	0.54	1.45	0.02	0.14	1
Bzw1	0.19	1.14	0.01	0.11	1
C1d	0.3	1.24	0.03	0.17	1
C1galt1c1	0.32	1.25	0.02	0.12	1
C1qb	0.45	1.37	2.83E-03	0.04	1
C1qtnf3	1.37	2.59	9.76E-03	0.09	1
C1qtnf4	-0.82	-1.77	0.03	0.2	1
C2cd2	0.44	1.36	3.34E-04	0.01	1
Ca12	-1.23	-2.34	0.03	0.2	1
Ca4	3.17	8.99	1.94E-03	NaN	1
Cacna1g	-1.31	-2.47	1.55E-03	0.03	1
Cacna1h	-0.41	-1.33	8.12E-04	0.02	1
Cacnb4	0.24	1.18	0.04	0.2	1
Cacng2	-0.59	-1.5	8.80E-05	4.22E-03	1
Cacng5	-0.43	-1.35	0.01	0.1	1
Cadm1	0.26	1.2	0.02	0.15	1
Calb1	0.5	1.41	0.04	0.2	1
Calca	0.53	1.44	2.71E-06	2.69E-04	0.05
Calr	0.3	1.23	7.42E-03	0.08	1
Calu	0.25	1.19	1.53E-03	0.03	1
Camkk1	-0.3	-1.23	0.02	0.15	1
Camp	-1.42	-2.68	0.01	0.1	1
Camsap3	-0.35	-1.28	9.66E-03	0.09	1
Camta2	-0.22	-1.17	7.82E-03	0.08	1
Canx	0.26	1.19	0.02	0.15	1
Capn15	-0.33	-1.26	0.02	0.12	1
Capn5	0.17	1.12	0.03	0.19	1
Caprin1	0.23	1.17	2.93E-03	0.05	1
Capza1	0.17	1.12	0.04	0.2	1
Capza2	0.32	1.25	5.00E-03	0.06	1
Card10	-0.61	-1.53	0.02	0.14	1
Carm1	-0.22	-1.17	7.07E-03	0.08	1
Carns1	-0.37	-1.29	8.56E-03	0.09	1
Cask	0.2	1.15	0.02	0.14	1
Caskin1	-0.23	-1.17	4.25E-03	0.06	1
Casp12	0.43	1.35	0.02	0.16	1
Casp3	0.36	1.28	0.01	0.1	1
Casp4	0.54	1.46	7.20E-04	0.02	1
Casp8ap2	0.27	1.21	0.03	0.18	1

Casq2	-1.04	-2.06	0.01	0.11	1
Cast	0.22	1.17	3.99E-03	0.06	1
Castor2	-0.32	-1.25	7.25E-04	0.02	1
Cbarp	-0.3	-1.23	0.01	0.12	1
Cbr2	-0.67	-1.59	1.36E-03	0.03	1
Cbx3	0.3	1.23	0.01	0.11	1
Cbx4	-0.3	-1.23	0.03	0.16	1
Cbx6	-0.24	-1.18	2.74E-03	0.04	1
Cbx7	-0.42	-1.34	2.47E-03	0.04	1
Ccar1	0.32	1.25	1.46E-04	6.29E-03	1
Ccdc112	0.59	1.5	5.83E-05	3.08E-03	1
Ccdc124	-0.34	-1.26	0.01	0.1	1
Ccdc152	0.88	1.83	0.03	0.17	1
Ccdc157	-0.66	-1.58	0.01	0.12	1
Ccdc172	0.8	1.75	1.15E-03	0.02	1
Ccdc18	0.46	1.38	0.05	0.24	1
Ccdc25	0.32	1.25	0.02	0.14	1
Ccdc50	0.22	1.16	9.79E-03	0.09	1
Ccdc59	0.58	1.5	3.83E-03	0.05	1
Ccdc66	0.26	1.2	0.05	0.24	1
Ccdc9	-0.25	-1.19	9.28E-03	0.09	1
Cckbr	1.21	2.31	0.02	0.14	1
Ccl12	2.79	6.92	7.01E-03	NaN	1
Ccl17	2.5	5.66	0.05	NaN	1
Ccm2l	-0.78	-1.72	3.74E-04	0.01	1
Ccnc	0.38	1.3	1.87E-03	0.03	1
Ccndbp1	0.26	1.2	0.04	0.23	1
Ccne2	0.67	1.59	0.02	0.16	1
Ccpg1	0.29	1.22	2.44E-04	8.71E-03	1
Cct2	0.28	1.21	4.09E-04	0.01	1
Cct6a	0.22	1.17	4.15E-03	0.06	1
Cd200	0.3	1.23	2.01E-04	7.82E-03	1
Cd248	-0.9	-1.87	1.74E-03	0.03	1
Cd2ap	0.21	1.16	6.02E-03	0.07	1
Cd47	0.24	1.18	1.81E-03	0.03	1
Cd84	0.45	1.37	0.03	0.18	1
Cd9	-0.23	-1.17	0.05	0.24	1
Cdc27	0.29	1.22	3.05E-04	0.01	1
Cdc42se2	0.19	1.14	0.04	0.21	1

Cdh13	-0.22	-1.16	0.01	0.1	1
Cdh19	0.44	1.35	1.61E-04	6.75E-03	1
Cdh2	0.2	1.15	0.01	0.1	1
Cdh8	0.5	1.42	0.03	0.19	1
Cdhr2	-0.73	-1.66	0.02	0.13	1
Cdk1	-1.08	-2.11	0.03	0.19	1
Cdk10	-0.29	-1.22	0.03	0.17	1
Cdk16	-0.23	-1.17	3.75E-03	0.05	1
Cdk2	-0.56	-1.48	0.04	0.23	1
Cdk2ap2	-0.43	-1.35	0.03	0.17	1
Cdk4	-0.27	-1.2	0.04	0.23	1
Cdk5	-0.22	-1.16	9.98E-03	0.1	1
Cdkn1a	0.5	1.42	0.04	0.23	1
Cebpb	-0.57	-1.48	0.03	0.18	1
Celf4	0.27	1.21	0.03	0.17	1
Cemip2	0.17	1.13	0.04	0.22	1
Cenpc	0.3	1.23	0.03	0.17	1
Cenpj	0.34	1.27	0.01	0.1	1
Cep120	0.25	1.19	6.31E-03	0.07	1
Cep170	0.27	1.2	5.00E-04	0.01	1
Cep192	0.2	1.15	0.03	0.19	1
Cep20	0.28	1.22	0.03	0.17	1
Cep250	-0.69	-1.61	5.73E-07	7.38E-05	0.01
Cep290	0.29	1.22	0.02	0.13	1
Cep57	0.42	1.34	0.01	0.11	1
Cep83	0.27	1.2	0.03	0.17	1
Cep95	-0.4	-1.32	0.01	0.12	1
Cep97	0.27	1.21	4.72E-03	0.06	1
Cercam	-0.48	-1.4	0.05	0.24	1
Cers2	-0.24	-1.18	6.28E-03	0.07	1
Cetn3	0.32	1.24	0.02	0.12	1
Cfap36	0.19	1.14	0.02	0.13	1
Cfap410	-0.35	-1.27	8.95E-03	0.09	1
Cfdp1	0.29	1.22	0.02	0.14	1
Cggbp1	0.31	1.24	9.55E-03	0.09	1
Cgnl1	-0.16	-1.12	0.05	0.24	1
Chd1	0.22	1.16	0.01	0.1	1
Chdh	-0.34	-1.26	0.01	0.1	1
Chek1	0.55	1.46	0.03	0.17	1

Chfr	0.26	1.2	4.99E-03	0.06	1
Chga	-0.4	-1.32	2.49E-06	2.56E-04	0.05
Chml	0.29	1.22	0.03	0.18	1
Chn1	0.3	1.23	4.69E-04	0.01	1
Chpf	-0.37	-1.29	2.37E-03	0.04	1
Chpf2	-0.31	-1.24	0.02	0.12	1
Chrm3	-0.5	-1.41	0.04	0.2	1
Chst15	-0.32	-1.25	7.51E-03	0.08	1
Ciao2a	0.46	1.37	0.02	0.16	1
Ckap5	0.2	1.15	9.15E-03	0.09	1
Ckmt1	-0.41	-1.33	1.82E-07	2.74E-05	3.42E-03
Clca2	0.66	1.58	0.03	0.2	1
Clcn2	-0.36	-1.29	9.49E-03	0.09	1
Cldn12	0.34	1.26	0.01	0.1	1
Cldn22	-1.51	-2.85	7.10E-03	0.08	1
Cldn4	2.68	6.4	0.02	NaN	1
Clec12a	0.68	1.6	0.02	0.15	1
Clec3b	-0.82	-1.76	7.38E-04	0.02	1
Clgn	0.2	1.15	0.01	0.11	1
Clic4	0.23	1.17	0.04	0.23	1
Clk1	0.28	1.22	0.02	0.13	1
Clmp	-0.24	-1.18	0.05	0.23	1
Clptm1	-0.16	-1.11	0.05	0.24	1
Clvs1	0.54	1.45	5.60E-03	0.07	1
Cmc2	0.29	1.23	0.04	0.21	1
Cmklr1	-0.69	-1.61	9.61E-04	0.02	1
Cmpk1	0.32	1.25	9.19E-05	4.34E-03	1
Cmtm2a	2.33	5.01	0.05	NaN	1
Cmtm7	-0.66	-1.58	0.02	0.15	1
Cnep1r1	0.27	1.21	4.10E-03	0.06	1
Cnih2	-0.56	-1.48	0.03	0.2	1
Cnn1	-1.11	-2.16	0.03	0.17	1
Cnnm3	-0.27	-1.21	0.05	0.24	1
Cnot2	0.17	1.12	0.05	0.24	1
Cnot6	0.26	1.2	0.04	0.21	1
Cnot6l	0.28	1.22	0.03	0.18	1
Cnpy2	-0.28	-1.22	0.04	0.2	1
Cnst	0.16	1.12	0.04	0.23	1
Cntfr	-0.32	-1.25	0.02	0.13	1

Cntn2	-0.18	-1.13	0.02	0.15	1
Coa3	-0.19	-1.14	0.05	0.24	1
Coasy	-0.57	-1.48	2.32E-04	8.44E-03	1
Col11a1	0.39	1.31	8.81E-03	0.09	1
Col16a1	0.3	1.23	0.01	0.1	1
Col28a1	0.29	1.22	4.64E-04	0.01	1
Col4a4	-0.38	-1.3	9.39E-03	0.09	1
Col6a1	-0.36	-1.29	2.28E-03	0.04	1
Col6a2	-0.42	-1.34	9.37E-07	1.10E-04	0.02
Col9a1	-0.89	-1.86	0.03	0.17	1
Colgalt2	-0.25	-1.19	4.35E-03	0.06	1
Copg2	0.17	1.12	0.04	0.2	1
Cops2	0.2	1.15	8.22E-03	0.09	1
Cops7a	-0.34	-1.27	5.07E-03	0.06	1
Coq9	-0.33	-1.26	0.01	0.12	1
Coro2b	-0.19	-1.14	0.02	0.13	1
Cox5b	-0.17	-1.13	0.04	0.2	1
Cox6a1	-0.19	-1.14	0.01	0.12	1
Cox6b1	0.27	1.21	0.02	0.14	1
Cox7a1	-1.36	-2.57	4.68E-05	2.59E-03	0.88
Cpeb4	0.27	1.21	3.90E-04	0.01	1
Cpne9	-0.64	-1.56	0.03	0.17	1
Cpped1	-0.35	-1.27	0.02	0.15	1
Cpsf2	0.31	1.24	2.30E-04	8.40E-03	1
Cpsf3	0.25	1.19	6.41E-03	0.07	1
Cpsf6	0.2	1.15	0.01	0.11	1
Cpt2	-0.3	-1.23	0.03	0.18	1
Cptp	-0.26	-1.2	0.04	0.21	1
Crbn	0.24	1.18	2.13E-03	0.04	1
Creb1	0.22	1.17	0.01	0.1	1
Creb3l1	-0.34	-1.26	0.01	0.11	1
Creld1	-0.25	-1.19	0.04	0.22	1
Crisp3	7.82	225.23	8.36E-04	0.02	1
Crmp1	0.18	1.13	0.04	0.21	1
Crtac1	0.52	1.43	1.22E-03	0.03	1
Crtc2	-0.51	-1.43	2.19E-04	8.16E-03	1
Cryzl1	0.27	1.2	0.04	0.2	1
Csdc2	-0.35	-1.27	1.23E-04	5.51E-03	1
Csde1	0.2	1.15	8.10E-03	0.09	1

Csnk1a1	0.22	1.16	4.16E-03	0.06	1
Csnk1g1	0.32	1.25	0.01	0.12	1
Csnk1g2	-0.16	-1.12	0.05	0.24	1
Csnk1g3	0.27	1.2	9.93E-04	0.02	1
Csrp1	-0.26	-1.2	1.67E-03	0.03	1
Cstb	-0.3	-1.23	1.14E-03	0.02	1
Cstf3	0.28	1.21	0.03	0.18	1
Ctcf	0.26	1.2	0.03	0.19	1
Ctdspl2	0.33	1.26	0.01	0.1	1
Ctf1	-1.06	-2.08	3.57E-03	0.05	1
Cthrc1	0.62	1.54	0.03	0.18	1
Ctif	-0.18	-1.13	0.03	0.18	1
Ctps2	0.27	1.21	0.03	0.17	1
Cttn	0.18	1.13	0.03	0.18	1
Cttnbp2nl	0.29	1.23	3.83E-04	0.01	1
Cul2	0.17	1.12	0.05	0.24	1
Cul3	0.18	1.14	0.02	0.13	1
Cul5	0.25	1.19	0.04	0.2	1
Cul9	-0.26	-1.2	0.03	0.19	1
Cxcl12	-0.35	-1.28	9.15E-03	0.09	1
Cyb5r1	-0.24	-1.18	3.46E-03	0.05	1
Cyb5r4	0.31	1.24	0.02	0.15	1
Cybrd1	-0.49	-1.4	0.02	0.14	1
Cygb	-0.53	-1.44	7.40E-03	0.08	1
Cyp2j4	0.3	1.23	0.02	0.14	1
Cyp46a1	-0.63	-1.55	0.04	0.22	1
Cyp4f1	-2.07	-4.19	0.01	NaN	1
Cyp4v3	0.4	1.32	0.02	0.15	1
Cyrib	0.36	1.28	3.11E-03	0.05	1
Cysrt1	-1.62	-3.07	4.32E-03	0.06	1
Cystm1	-0.38	-1.3	2.48E-03	0.04	1
D030056L22Rik	0.61	1.53	2.12E-05	1.40E-03	0.4
Dagla	-0.3	-1.23	4.56E-04	0.01	1
Dars1	0.33	1.25	1.32E-04	5.81E-03	1
Dazap1	-0.33	-1.25	2.77E-04	9.46E-03	1
Dbi	0.16	1.12	0.04	0.21	1
Dbndd2	-0.23	-1.18	0.01	0.1	1
Dbt	0.2	1.15	0.04	0.21	1
Dcdc2b	-0.82	-1.76	0.04	0.2	1

Dclk1	0.28	1.22	2.65E-04	9.14E-03	1
Dclk2	-0.19	-1.14	0.03	0.17	1
Dclre1a	0.34	1.26	0.03	0.19	1
Dclre1c	0.52	1.44	0.04	0.21	1
Dcn	-0.25	-1.19	0.03	0.18	1
Dcx	0.41	1.33	4.04E-03	0.06	1
Ddc	1.67	3.17	0.05	NaN	1
Ddn	-0.53	-1.44	0.03	0.2	1
Ddx1	0.2	1.15	0.01	0.1	1
Ddx42	0.23	1.18	4.50E-03	0.06	1
Ddx6	0.17	1.13	0.03	0.16	1
Degs1	-0.18	-1.13	0.03	0.17	1
Degs2	-1.64	-3.11	4.03E-03	0.06	1
Dennd10	0.28	1.21	0.03	0.19	1
Dennd2c	0.57	1.49	0.02	0.12	1
Dennd4a	0.21	1.16	6.61E-03	0.07	1
Denr	0.37	1.29	3.94E-03	0.05	1
Derl1	-0.28	-1.21	0.03	0.18	1
Derl3	-1.02	-2.03	0.02	0.16	1
Dgcr2	-0.32	-1.25	1.63E-04	6.77E-03	1
Dgkb	0.31	1.24	0.01	0.12	1
Dhfr	0.7	1.63	2.00E-03	0.04	1
Dhrs3	-0.32	-1.25	0.02	0.13	1
Dhrsx	-0.74	-1.67	0.04	0.21	1
Dhx15	0.27	1.21	6.42E-04	0.02	1
Dhx30	-0.21	-1.15	0.02	0.13	1
Dhx36	0.18	1.13	0.03	0.18	1
Dhx9	0.21	1.16	9.20E-03	0.09	1
Diablo	-0.23	-1.17	5.48E-03	0.07	1
Diaph3	0.45	1.37	0.04	0.21	1
Dicer1	0.29	1.23	6.07E-04	0.02	1
Dip2a	-0.34	-1.27	2.10E-04	8.03E-03	1
Dipk1b	-0.27	-1.21	3.06E-03	0.05	1
Dis3	0.45	1.36	7.53E-04	0.02	1
Disp3	-0.45	-1.37	0.02	0.12	1
Dld	0.23	1.17	3.72E-03	0.05	1
Dleu7	-0.63	-1.55	7.04E-03	0.08	1
Dlg2	0.37	1.29	6.34E-06	5.67E-04	0.12
Dmac2	-0.32	-1.25	0.02	0.15	1

Dmd	0.17	1.12	0.03	0.17	1
Dmtf1	0.25	1.19	2.28E-03	0.04	1
Dmtn	-0.18	-1.13	0.03	0.17	1
Dmxl1	0.17	1.12	0.03	0.18	1
Dnah3	2.04	4.11	6.10E-04	0.02	1
Dnah6	-1.07	-2.1	3.62E-03	0.05	1
Dnaja1	0.31	1.24	6.71E-03	0.08	1
Dnaja3	-0.28	-1.21	2.15E-03	0.04	1
Dnajb4	0.21	1.15	0.02	0.12	1
Dnajc10	0.16	1.11	0.04	0.23	1
Dnajc13	0.22	1.17	4.85E-03	0.06	1
Dnajc2	0.42	1.34	7.20E-04	0.02	1
Dnajc7	0.31	1.24	8.55E-05	4.17E-03	1
Dnajc8	0.2	1.15	0.02	0.14	1
Dnal1	0.19	1.14	0.03	0.18	1
Dnlz	-0.32	-1.25	0.04	0.2	1
Dnm1l	0.19	1.14	0.02	0.12	1
Doc2a	-0.43	-1.35	0.03	0.18	1
Dock4	0.18	1.13	0.03	0.19	1
Dock7	0.19	1.14	0.02	0.12	1
Dock9	-0.18	-1.13	0.02	0.15	1
Dohh	-0.54	-1.45	2.30E-04	8.40E-03	1
Dok6	0.41	1.33	1.62E-03	0.03	1
Dok7	-0.58	-1.5	0.03	0.17	1
Dolk	-0.54	-1.46	1.75E-04	7.10E-03	1
Dop1b	-0.17	-1.12	0.04	0.21	1
Dph2	-0.66	-1.58	0.04	0.2	1
Dpp9	-0.28	-1.21	9.86E-04	0.02	1
Dpt	-0.59	-1.5	0.03	0.17	1
Dpy19l4	0.29	1.22	1.45E-03	0.03	1
Dsel	0.33	1.26	7.07E-03	0.08	1
Dtnbp1	0.36	1.28	0.05	0.24	1
Dtx1	-0.52	-1.43	1.16E-03	0.02	1
Dtx3	-0.49	-1.41	3.88E-04	0.01	1
Duox1	-2.37	-5.17	0.03	NaN	1
Dusp26	0.24	1.18	4.73E-03	0.06	1
Dusp7	0.56	1.48	1.34E-05	9.78E-04	0.25
Dvl1	-0.38	-1.3	3.80E-03	0.05	1
Dvl2	-0.45	-1.37	0.02	0.14	1

Dync1i2	0.27	1.21	0.02	0.12	1
Dync2h1	0.17	1.13	0.04	0.2	1
Dynlt3	0.25	1.19	1.15E-03	0.02	1
Dynlt5	-1.26	-2.39	0.01	0.11	1
Dyrk1b	-0.4	-1.32	3.27E-03	0.05	1
Dyrk2	0.21	1.16	0.02	0.12	1
Dzip1	-0.17	-1.12	0.05	0.24	1
Dzip3	0.31	1.24	8.51E-03	0.09	1
Eapp	0.17	1.13	0.04	0.22	1
Ebf1	0.19	1.14	0.02	0.14	1
Ecel1	1.68	3.21	2.36E-05	1.51E-03	0.44
Ech1	-0.2	-1.15	0.02	0.14	1
Echdc1	0.34	1.27	9.96E-03	0.1	1
Ecpas	0.19	1.14	0.01	0.11	1
Ecrg4	-1.55	-2.93	5.91E-06	5.35E-04	0.11
Ect2	0.79	1.73	0.01	0.1	1
Eefsec	-0.42	-1.34	0.01	0.1	1
Eepd1	0.19	1.14	0.02	0.15	1
Efcab15	-1.8	-3.48	0.04	NaN	1
Efcc1	-0.56	-1.47	0.04	0.22	1
Efhd1	-0.51	-1.43	0.01	0.12	1
Efna5	-0.5	-1.41	3.31E-07	4.49E-05	6.23E-03
Efs	-0.5	-1.41	6.60E-03	0.07	1
Egfr	-0.29	-1.22	0.03	0.19	1
Egln2	-0.32	-1.25	0.01	0.1	1
Ehbp1	0.2	1.15	0.01	0.1	1
Ehbp1l1	-0.3	-1.23	0.02	0.16	1
Ehd2	-0.31	-1.24	0.02	0.13	1
Ehd3	0.23	1.17	2.73E-03	0.04	1
Ehmt2	-0.28	-1.22	0.02	0.15	1
Eif1a	0.31	1.24	1.38E-04	6.00E-03	1
Eif1b	-0.19	-1.14	0.03	0.16	1
Eif2s2	0.2	1.15	0.01	0.11	1
Eif2s3x	0.22	1.17	4.00E-03	0.06	1
Eif3a	0.26	1.2	8.90E-04	0.02	1
Eif3el1	0.25	1.19	0.04	0.21	1
Eif3j	0.19	1.14	0.02	0.16	1
Eif3m	0.26	1.2	0.03	0.19	1
Eif4a1	0.32	1.25	4.42E-05	2.50E-03	0.83

Eif4a2	0.27	1.21	0.02	0.12	1
Eif4ebp3	0.17	1.12	0.04	0.21	1
Elapor1	-0.5	-1.42	0.04	0.21	1
Elapor2	0.16	1.11	0.05	0.24	1
Elavl2	0.26	1.19	0.02	0.16	1
Elavl4	0.24	1.18	1.91E-03	0.03	1
Elfn1	-0.32	-1.25	0.01	0.12	1
Ell	-0.43	-1.34	5.21E-03	0.06	1
Ell2	0.29	1.22	5.61E-04	0.01	1
Elmod1	0.27	1.2	0.04	0.23	1
Eloc	0.33	1.26	6.81E-05	3.46E-03	1
Elovl5	0.22	1.16	3.95E-03	0.05	1
Emc2	0.37	1.29	4.86E-06	4.48E-04	0.09
Emc3	0.18	1.13	0.03	0.18	1
Eme2	-0.6	-1.52	2.90E-03	0.04	1
Eml1	0.16	1.11	0.04	0.23	1
Eml5	0.38	1.3	7.07E-03	0.08	1
Enkd1	-0.99	-1.98	0.03	0.17	1
Enpep	-0.47	-1.39	3.90E-03	0.05	1
Entpd4	-0.19	-1.14	0.01	0.12	1
Eola2	0.35	1.27	0.01	0.11	1
Epb41l4a	0.28	1.21	0.05	0.23	1
Epha5	0.46	1.38	4.13E-04	0.01	1
Ephx1	-0.51	-1.43	1.55E-04	6.58E-03	1
Epm2a	0.32	1.25	0.02	0.16	1
Epm2aip1	0.16	1.11	0.04	0.22	1
Epn1	-0.26	-1.2	0.03	0.18	1
Epn3	-0.28	-1.21	0.02	0.15	1
Erc2	0.39	1.31	1.54E-03	0.03	1
Ercc6l2	0.28	1.22	0.02	0.15	1
Erich3	0.3	1.23	0.01	0.11	1
Erlec1	0.17	1.12	0.05	0.24	1
Esf1	0.39	1.31	2.38E-03	0.04	1
Esrrb	-0.9	-1.87	0.04	0.21	1
Etf1	0.18	1.13	0.04	0.21	1
Etfrf1	0.58	1.5	0.01	0.12	1
Ethe1	-0.47	-1.39	0.03	0.18	1
Etl4	-0.31	-1.24	7.00E-03	0.08	1
Exoc3l4	-2.13	-4.37	0.03	NaN	1

Exoc5	0.33	1.25	5.40E-03	0.07	1
Extl3	-0.16	-1.12	0.05	0.23	1
Eya2	-0.41	-1.33	0.02	0.13	1
F3	-0.61	-1.52	1.42E-03	0.03	1
Faap20	0.4	1.32	0.03	0.19	1
Faim2	-0.59	-1.5	9.62E-07	1.12E-04	0.02
Fam117a	-0.63	-1.55	4.91E-03	0.06	1
Fam126b	0.23	1.17	7.64E-03	0.08	1
Fam131a	-0.32	-1.25	0.04	0.22	1
Fam13a	-0.28	-1.21	0.05	0.24	1
Fam163a	-0.84	-1.79	7.94E-04	0.02	1
Fam177a1	0.3	1.23	0.01	0.11	1
Fam178b	-1.22	-2.34	0.02	0.15	1
Fam184b	0.3	1.23	0.05	0.24	1
Fam189a1	-0.53	-1.44	0.04	0.22	1
Fam189b	-0.24	-1.18	2.02E-03	0.04	1
Fam20a	-0.78	-1.71	4.29E-03	0.06	1
Fam217b	-0.36	-1.28	0.01	0.1	1
Fam222a	-0.59	-1.51	0.03	0.18	1
Fam234b	-0.28	-1.22	1.03E-03	0.02	1
Fam43a	-0.36	-1.28	0.03	0.2	1
Fam76b	0.37	1.29	5.65E-03	0.07	1
Fam89b	-0.23	-1.17	0.01	0.11	1
Fam91a1	0.2	1.15	0.01	0.12	1
Fan1	0.31	1.24	0.03	0.19	1
Far1	0.24	1.18	2.11E-03	0.04	1
Fastk	-0.36	-1.28	7.95E-03	0.08	1
Faxc	0.23	1.17	2.77E-03	0.04	1
Fbll1	-0.56	-1.48	2.06E-03	0.04	1
Fbn1	-0.18	-1.13	0.02	0.16	1
Fbrs	-0.37	-1.29	4.10E-03	0.06	1
Fbxl16	-0.33	-1.25	0.01	0.1	1
Fbxl7	-0.38	-1.3	0.04	0.2	1
Fbxl8	-1.14	-2.21	0.01	0.1	1
Fbxo2	-0.28	-1.21	4.08E-04	0.01	1
Fbxo34	0.2	1.15	0.04	0.2	1
Fbxo44	-0.37	-1.3	2.43E-03	0.04	1
Fbxw5	-0.33	-1.25	0.02	0.13	1
Fcer1g	0.28	1.22	3.91E-03	0.05	1

Fcgr3a	1.7	3.25	7.29E-03	0.08	1
Fcho2	0.25	1.19	0.04	0.23	1
Fcsk	-0.61	-1.53	0.01	0.1	1
Fem1c	0.2	1.15	0.02	0.16	1
Fgd1	-0.53	-1.44	7.58E-04	0.02	1
Fgf13	0.27	1.21	3.23E-04	0.01	1
Fgfr1	-0.22	-1.16	5.98E-03	0.07	1
Fgfr4	-1.06	-2.08	0.01	0.1	1
Fhip2b	-0.28	-1.21	0.04	0.21	1
Fhl3	-0.61	-1.53	0.03	0.18	1
Fibcd1	-2.29	-4.9	0.03	NaN	1
Fig4	0.25	1.19	0.04	0.22	1
Fis1	-0.23	-1.18	5.51E-03	0.07	1
Fkbp1a	0.19	1.14	0.01	0.11	1
Fkbpl	-0.54	-1.46	0.02	0.13	1
Flii	-0.17	-1.13	0.03	0.19	1
Fmn1	0.19	1.14	0.02	0.14	1
Fmnl2	0.26	1.2	1.31E-03	0.03	1
Fmo3	-0.68	-1.6	0.04	0.21	1
Fmo9	2.13	4.38	0.02	NaN	1
Fndc1	-0.46	-1.38	1.74E-03	0.03	1
Fndc3a	0.25	1.19	2.01E-03	0.04	1
Foxc1	-0.85	-1.8	1.55E-03	0.03	1
Foxc2	-0.7	-1.63	1.22E-03	0.03	1
Foxm1	4.18	18.14	2.27E-03	NaN	1
Fra10ac1	0.45	1.37	1.29E-03	0.03	1
Frg1	0.38	1.3	6.67E-03	0.08	1
Frmpd1	-0.26	-1.2	1.05E-03	0.02	1
Frmpd4	-0.22	-1.16	8.85E-03	0.09	1
Fry	-0.22	-1.17	3.95E-03	0.05	1
Fsd1	-0.2	-1.15	0.04	0.23	1
Fsd1l	0.28	1.22	2.55E-04	8.94E-03	1
Fth1	-0.4	-1.32	2.99E-04	9.97E-03	1
Ftl1_1	-0.44	-1.35	1.14E-04	5.24E-03	1
Ftl1_2	-0.4	-1.32	1.23E-03	0.03	1
Fubp1	0.17	1.12	0.04	0.22	1
Fundc1	0.25	1.19	0.05	0.24	1
Fundc2	-0.29	-1.23	0.02	0.15	1
Fus	-0.21	-1.16	0.01	0.1	1

Fxr1	0.29	1.22	0.01	0.11	1
Fxyd6	-0.52	-1.44	6.03E-10	2.21E-07	1.13E-05
Fxyd7	-0.49	-1.4	1.09E-09	3.63E-07	2.05E-05
Fyttd1	0.21	1.15	0.01	0.1	1
G6pc3	-0.34	-1.27	8.45E-03	0.09	1
Gabarap	0.21	1.16	6.32E-03	0.07	1
Gabra2	0.17	1.13	0.03	0.18	1
Gabrb3	0.19	1.14	0.02	0.16	1
Gabrg1	0.34	1.27	3.79E-03	0.05	1
Gabrr1	0.83	1.78	0.05	0.23	1
Gadd45g	0.82	1.76	1.76E-03	0.03	1
Gal	1.55	2.92	4.53E-15	5.39E-12	8.50E-11
Gas2l1	-0.25	-1.19	3.54E-03	0.05	1
Gas7	0.33	1.26	3.36E-03	0.05	1
Gbp4	0.58	1.49	0.04	0.23	1
Gcc2	0.17	1.12	0.04	0.22	1
Gcnt2	0.23	1.18	0.05	0.24	1
Gdap1	0.19	1.14	0.02	0.14	1
Gdf1	-0.58	-1.49	3.40E-05	2.03E-03	0.64
Gdi2	0.26	1.2	7.45E-04	0.02	1
Gdpd1	0.33	1.26	5.81E-04	0.02	1
Gemin5	-0.36	-1.28	8.70E-03	0.09	1
Gemin7	-0.5	-1.42	9.09E-03	0.09	1
gene:ENSRNOG00000005736	0.18	1.13	0.03	0.2	1
gene:ENSRNOG00000005840	-2.01	-4.03	2.69E-03	0.04	1
gene:ENSRNOG00000007879	0.51	1.42	0.05	0.24	1
gene:ENSRNOG00000013579	-0.45	-1.36	2.19E-03	0.04	1
gene:ENSRNOG00000016452	0.17	1.12	0.04	0.22	1
gene:ENSRNOG00000017586	0.58	1.49	5.60E-03	0.07	1
gene:ENSRNOG00000017864	0.18	1.13	0.02	0.16	1
gene:ENSRNOG00000018936	0.31	1.24	0.02	0.14	1
gene:ENSRNOG00000019655	-0.32	-1.24	0.01	0.11	1
gene:ENSRNOG00000019657	-1.7	-3.25	9.11E-03	0.09	1
gene:ENSRNOG00000019778	-0.59	-1.51	1.39E-05	1.00E-03	0.26
gene:ENSRNOG00000025261	0.6	1.51	0.02	0.14	1
gene:ENSRNOG00000027040	0.54	1.46	5.51E-05	2.95E-03	1
gene:ENSRNOG00000028430	4.95	31	0.05	NaN	1
gene:ENSRNOG00000031167	-0.61	-1.52	0.02	0.15	1
gene:ENSRNOG00000031859	-0.56	-1.48	0.03	0.18	1

gene:ENSRNOG00000032531	-1.07	-2.1	0.02	0.13	1
gene:ENSRNOG00000033776	-0.33	-1.26	0.02	0.12	1
gene:ENSRNOG00000037341	-1.7	-3.25	0.04	NaN	1
gene:ENSRNOG00000037661	0.38	1.3	6.81E-03	0.08	1
gene:ENSRNOG00000038074	5.72	52.53	0.02	NaN	1
gene:ENSRNOG00000047931	0.29	1.23	8.71E-03	0.09	1
gene:ENSRNOG00000048258	0.42	1.34	3.99E-04	0.01	1
gene:ENSRNOG00000048337	1.78	3.44	3.07E-08	5.94E-06	5.78E-04
gene:ENSRNOG00000048606	0.26	1.19	0.04	0.21	1
gene:ENSRNOG00000048967	1.15	2.22	5.22E-03	0.06	1
gene:ENSRNOG00000049075	0.24	1.18	2.67E-03	0.04	1
gene:ENSRNOG00000051237	-1.1	-2.15	8.97E-03	0.09	1
gene:ENSRNOG00000055496	3.08	8.46	9.62E-03	NaN	1
gene:ENSRNOG00000057159	0.52	1.43	0.01	0.1	1
gene:ENSRNOG00000058856	2.68	6.4	0.02	NaN	1
gene:ENSRNOG00000060262	0.2	1.15	0.02	0.15	1
gene:ENSRNOG00000061597	1.68	3.21	0.03	NaN	1
gene:ENSRNOG00000062272	-0.41	-1.33	3.14E-05	1.90E-03	0.59
gene:ENSRNOG00000062325	0.31	1.24	0.01	0.12	1
gene:ENSRNOG00000062568	-1.71	-3.27	1.34E-03	0.03	1
gene:ENSRNOG00000062629	0.32	1.25	0.03	0.18	1
gene:ENSRNOG00000062644	-1.65	-3.15	4.67E-03	0.06	1
gene:ENSRNOG00000062652	-0.21	-1.15	0.01	0.12	1
gene:ENSRNOG00000062661	0.54	1.46	4.38E-03	0.06	1
gene:ENSRNOG00000062710	0.33	1.26	2.13E-04	8.08E-03	1
gene:ENSRNOG00000062896	-0.6	-1.52	0.02	0.16	1
gene:ENSRNOG00000062927	-0.67	-1.59	1.09E-05	8.32E-04	0.21
gene:ENSRNOG00000062930	-0.96	-1.95	5.23E-10	1.97E-07	9.83E-06
gene:ENSRNOG00000063044	-0.76	-1.69	2.22E-03	0.04	1
gene:ENSRNOG00000063081	1.13	2.19	0.03	0.17	1
gene:ENSRNOG00000063087	-0.95	-1.93	3.00E-04	9.98E-03	1
gene:ENSRNOG00000063189	-0.76	-1.69	0.01	0.12	1
gene:ENSRNOG00000063205	0.35	1.27	4.28E-03	0.06	1
gene:ENSRNOG00000063289	-3.14	-8.81	0.01	NaN	1
gene:ENSRNOG00000063301	-0.79	-1.73	3.65E-03	0.05	1
gene:ENSRNOG00000063490	1.59	3.01	0.05	NaN	1
gene:ENSRNOG00000063649	0.42	1.34	0.03	0.19	1
gene:ENSRNOG00000063675	-1.12	-2.17	5.42E-05	2.92E-03	1
gene:ENSRNOG00000063700	0.52	1.43	0.03	0.18	1

gene:ENSRNOG00000063885	2.33	5.01	0.04	NaN	1
gene:ENSRNOG00000064149	0.54	1.45	7.43E-03	0.08	1
gene:ENSRNOG00000064392	0.32	1.25	0.02	0.16	1
gene:ENSRNOG00000064485	0.47	1.39	9.76E-03	0.09	1
gene:ENSRNOG00000064882	-2.06	-4.17	0.02	0.12	1
gene:ENSRNOG00000064941	0.58	1.49	3.26E-03	0.05	1
gene:ENSRNOG00000064986	0.42	1.34	0.03	0.2	1
gene:ENSRNOG00000065042	-2.19	-4.55	0.03	NaN	1
gene:ENSRNOG00000065095	0.26	1.19	0.04	0.21	1
gene:ENSRNOG00000065100	3.78	13.75	0.02	NaN	1
gene:ENSRNOG00000065205	0.29	1.22	0.02	0.15	1
gene:ENSRNOG00000065208	0.98	1.97	0.02	0.14	1
gene:ENSRNOG00000065506	0.41	1.33	2.18E-03	0.04	1
gene:ENSRNOG00000065630	0.28	1.22	0.04	0.2	1
gene:ENSRNOG00000065666	0.44	1.36	6.59E-04	0.02	1
gene:ENSRNOG00000065876	0.57	1.49	4.81E-04	0.01	1
gene:ENSRNOG00000065971	2.13	4.39	2.81E-03	NaN	1
gene:ENSRNOG00000066094	0.29	1.22	0.04	0.23	1
gene:ENSRNOG00000066117	-0.46	-1.38	3.96E-04	0.01	1
gene:ENSRNOG00000066386	-2.2	-4.6	0.03	NaN	1
gene:ENSRNOG00000066415	-1.26	-2.39	0.01	0.1	1
gene:ENSRNOG00000066471	0.49	1.41	5.82E-03	0.07	1
gene:ENSRNOG00000066473	-0.55	-1.47	0.04	0.22	1
gene:ENSRNOG00000066633	-0.63	-1.55	0.05	0.23	1
gene:ENSRNOG00000066838	0.37	1.29	0.01	0.11	1
gene:ENSRNOG00000066877	0.3	1.23	0.02	0.13	1
gene:ENSRNOG00000067007	0.53	1.45	6.05E-04	0.02	1
gene:ENSRNOG00000067040	0.72	1.65	3.08E-04	0.01	1
gene:ENSRNOG00000067077	-2.04	-4.12	1.49E-06	1.63E-04	0.03
gene:ENSRNOG00000067229	-0.94	-1.92	0.03	0.17	1
gene:ENSRNOG00000067240	0.34	1.27	4.92E-03	0.06	1
gene:ENSRNOG00000067344	0.6	1.52	7.59E-07	9.12E-05	0.01
gene:ENSRNOG00000067370	-0.69	-1.61	7.73E-03	0.08	1
gene:ENSRNOG00000067741	-0.54	-1.46	0.01	0.12	1
gene:ENSRNOG00000067762	-1.42	-2.68	0.02	0.14	1
gene:ENSRNOG00000067926	0.35	1.27	0.03	0.18	1
gene:ENSRNOG00000067970	0.26	1.2	0.05	0.24	1
gene:ENSRNOG00000068131	-3.13	-8.75	7.20E-05	3.61E-03	1
gene:ENSRNOG00000068148	1	2	9.12E-05	4.33E-03	1

gene:ENSRNOG00000068241	0.49	1.41	0.05	0.23	1
gene:ENSRNOG00000068362	1.71	3.27	4.26E-03	0.06	1
gene:ENSRNOG00000068427	-0.69	-1.61	0.03	0.19	1
gene:ENSRNOG00000068528	0.32	1.25	0.02	0.14	1
gene:ENSRNOG00000068777	2.33	5.01	0.04	NaN	1
gene:ENSRNOG00000068784	1.79	3.46	0.05	NaN	1
gene:ENSRNOG00000068893	0.64	1.56	0.02	0.15	1
gene:ENSRNOG00000068936	2.89	7.42	0.04	NaN	1
gene:ENSRNOG00000069113	1.51	2.84	0.01	0.1	1
gene:ENSRNOG00000069276	0.29	1.22	0.02	0.16	1
gene:ENSRNOG00000069384	0.95	1.93	5.66E-09	1.40E-06	1.06E-04
gene:ENSRNOG00000069449	0.67	1.59	0.03	0.17	1
gene:ENSRNOG00000069549	-1.05	-2.08	5.97E-07	7.62E-05	0.01
gene:ENSRNOG00000069647	0.25	1.19	0.04	0.22	1
gene:ENSRNOG00000069648	-0.19	-1.14	0.03	0.17	1
gene:ENSRNOG00000069969	2.02	4.07	5.33E-04	0.01	1
gene:ENSRNOG00000070106	0.38	1.3	2.35E-03	0.04	1
gene:ENSRNOG00000070334	1.52	2.86	0.04	NaN	1
gene:ENSRNOG00000070474	0.54	1.45	8.81E-03	0.09	1
gene:ENSRNOG00000070509	2.89	7.42	0.04	NaN	1
gene:ENSRNOG00000070513	0.35	1.27	0.03	0.18	1
gene:ENSRNOG00000070574	-0.28	-1.21	2.69E-03	0.04	1
gene:ENSRNOG00000070909	-1.19	-2.29	0.04	0.2	1
gene:ENSRNOG00000070917	0.89	1.86	0.02	0.14	1
gene:ENSRNOG00000071050	0.6	1.52	2.20E-04	8.18E-03	1
gene:ENSRNOG00000071060	4.17	17.97	9.12E-04	NaN	1
gene:ENSRNOG00000071146	1.95	3.85	0.02	NaN	1
Gfap	0.62	1.54	7.70E-04	0.02	1
Gfpt1	0.21	1.16	8.69E-03	0.09	1
Ggcx	-0.32	-1.25	0.02	0.12	1
Ggt6	1.02	2.03	5.12E-04	0.01	1
Ggt7	-0.28	-1.21	9.51E-04	0.02	1
Ggta1	0.21	1.15	0.02	0.16	1
Ghr	0.26	1.2	0.03	0.2	1
Gid4	-0.31	-1.24	0.02	0.16	1
Gigyf1	-0.3	-1.23	0.03	0.18	1
Giot1	0.39	1.31	0.02	0.15	1
Gk	0.26	1.2	0.05	0.23	1
Gkap1	0.4	1.32	6.59E-03	0.07	1

Glb1l2	-0.54	-1.45	0.01	0.11	1
Glipr2	0.54	1.45	2.57E-04	8.97E-03	1
Glrx3	0.21	1.16	8.26E-03	0.09	1
Glrx5	-0.47	-1.39	8.30E-04	0.02	1
Gls	0.25	1.19	1.24E-03	0.03	1
Gls2	-0.3	-1.23	0.03	0.18	1
Gm45871	0.6	1.52	3.30E-03	0.05	1
Gmfb	0.28	1.21	2.59E-04	9.01E-03	1
Gmppb	0.7	1.62	4.63E-04	0.01	1
Gmps	0.3	1.23	0.01	0.11	1
Gna12	-0.27	-1.21	1.34E-03	0.03	1
Gnb1l	-0.71	-1.63	0.03	0.17	1
Gnb2	-0.25	-1.19	2.60E-03	0.04	1
Gnb3	1.32	2.5	0.03	NaN	1
Gng8	-0.56	-1.48	0.03	0.17	1
Gnpda2	0.26	1.2	0.03	0.19	1
Golga2	-0.17	-1.12	0.04	0.21	1
Golm2	0.26	1.2	9.03E-04	0.02	1
Gorasp1	-0.31	-1.24	0.03	0.19	1
Gpaa1	-0.38	-1.3	6.10E-03	0.07	1
Gpbp1	0.2	1.15	0.01	0.12	1
Gpcpd1	0.3	1.23	2.04E-04	7.89E-03	1
Gpm6b	0.3	1.23	9.06E-03	0.09	1
Gpnmb	0.48	1.39	5.67E-04	0.02	1
Gpr137	-0.51	-1.42	2.83E-05	1.77E-03	0.53
Gpr157	-0.55	-1.47	0.03	0.18	1
Gpr180	-0.47	-1.39	6.41E-04	0.02	1
Gpr37l1	-0.3	-1.23	0.01	0.11	1
Gprasp1	0.16	1.12	0.04	0.21	1
Gprc5c	-0.32	-1.25	0.02	0.12	1
Gprin3	0.29	1.22	0.04	0.23	1
Gps1	-0.24	-1.18	0.05	0.24	1
Gpx1	-0.31	-1.24	8.05E-04	0.02	1
Gpx4	-0.55	-1.47	3.14E-06	3.06E-04	0.06
Gramd2a	1.07	2.1	0.03	0.18	1
Gramd4	-0.28	-1.21	5.80E-03	0.07	1
Gria4	0.38	1.3	4.43E-03	0.06	1
Grik2	0.39	1.31	6.19E-03	0.07	1
Grik5	-0.32	-1.25	0.02	0.14	1

Grin1	-0.38	-1.31	4.05E-06	3.79E-04	0.08
Grina	-0.33	-1.25	2.19E-05	1.43E-03	0.41
Grm4	-0.64	-1.56	1.23E-05	9.14E-04	0.23
Grsf1	0.21	1.15	9.94E-03	0.1	1
Grxcr2	0.66	1.58	0.02	0.13	1
Gsn	-0.54	-1.46	3.50E-12	2.18E-09	6.58E-08
Gstk1	-0.3	-1.23	0.04	0.2	1
Gstm3	-0.39	-1.31	0.01	0.1	1
Gstm6l	-0.26	-1.2	0.05	0.24	1
Gstp1	-0.25	-1.19	0.05	0.24	1
Gtf2a1	0.22	1.17	5.39E-03	0.07	1
Gtf2a2	0.51	1.42	0.01	0.1	1
Gtf2h5	0.25	1.19	9.18E-03	0.09	1
Gucy1a1	-0.48	-1.4	0.03	0.17	1
Guk1	-0.26	-1.2	0.03	0.19	1
Gzmbl2	1.61	3.05	0.04	NaN	1
H1f1	-0.54	-1.45	0.03	0.2	1
H1f10	-0.78	-1.72	8.82E-05	4.22E-03	1
H1f2	-0.41	-1.33	3.30E-04	0.01	1
H1f4	-0.28	-1.21	0.04	0.2	1
Hapln2	-1.25	-2.37	2.49E-04	8.79E-03	1
Hapln3	-0.53	-1.44	0.04	0.2	1
Has3	-1.07	-2.1	0.04	0.23	1
Haus3	0.35	1.27	3.71E-04	0.01	1
Haus6	0.43	1.35	1.10E-03	0.02	1
Hbb-bs	-1.35	-2.54	0.02	0.14	1
Hcfc1r1	-0.22	-1.17	8.20E-03	0.09	1
Hcls1	0.64	1.56	0.03	0.19	1
Hdac11	-0.3	-1.23	0.03	0.18	1
Hdac2	0.2	1.14	0.02	0.15	1
Hdac5	-0.28	-1.22	0.03	0.19	1
Hdgfl3	0.31	1.24	0.01	0.11	1
Hdx	0.48	1.39	0.02	0.12	1
Helb	0.28	1.21	0.04	0.21	1
Hells	0.71	1.63	6.97E-04	0.02	1
Hepacam	-0.29	-1.22	0.02	0.14	1
Herc1	0.18	1.14	0.01	0.12	1
Herc6	0.94	1.92	4.56E-03	0.06	1
Hhatl	-0.52	-1.43	3.82E-04	0.01	1

Hic1	-0.66	-1.58	1.91E-03	0.03	1
Hid1	-0.33	-1.26	1.16E-04	5.28E-03	1
Hif1a	0.37	1.29	4.89E-06	4.48E-04	0.09
Higd2a	-0.38	-1.3	4.49E-03	0.06	1
Hist1h2ak	0.87	1.82	0.04	0.2	1
Hist2h3c2_2	-0.89	-1.86	4.40E-05	2.50E-03	0.83
Hist2h3c2_3	-0.51	-1.42	6.73E-03	0.08	1
Hivep3	0.23	1.17	0.01	0.1	1
Hltf	0.24	1.18	0.01	0.11	1
Hmga1	-0.43	-1.34	1.14E-03	0.02	1
Hmgn2	0.27	1.2	0.03	0.19	1
Hmgn3	0.38	1.3	5.58E-03	0.07	1
Hmx1	-1.06	-2.09	0.02	0.12	1
Hnrnpa0	-0.58	-1.49	7.51E-06	6.39E-04	0.14
Hnrnpa1	0.25	1.19	1.27E-03	0.03	1
Hnrnpa2b1	0.34	1.26	1.53E-05	1.08E-03	0.29
Hnrnpa3	0.24	1.18	2.30E-03	0.04	1
Hnrnph3	0.25	1.19	0.05	0.23	1
Hnrnpul1	-0.17	-1.13	0.04	0.2	1
Hopx	0.51	1.42	1.78E-05	1.21E-03	0.34
Hoxb3	-0.57	-1.49	0.02	0.15	1
Hoxb5	-0.57	-1.49	0.02	0.15	1
Hpf1	0.32	1.24	0.03	0.16	1
Hps3	0.2	1.15	0.04	0.21	1
Hrh3	-0.96	-1.95	3.15E-03	0.05	1
Hs2st1	0.52	1.44	3.85E-10	1.53E-07	7.23E-06
Hsd17b12	0.19	1.14	0.02	0.16	1
Hsf1	-0.24	-1.18	0.02	0.12	1
Hsf2	0.26	1.19	0.04	0.2	1
Hsp90aa1	0.25	1.19	0.03	0.17	1
Hsp90b1	0.26	1.2	0.02	0.14	1
Hspa4	0.21	1.16	4.76E-03	0.06	1
Hspa5	0.25	1.19	0.03	0.17	1
Hspd1	0.15	1.11	0.05	0.24	1
Hspe1	0.44	1.36	2.70E-04	9.25E-03	1
Htatsf1	0.19	1.14	0.03	0.19	1
Htr1d	-0.58	-1.5	6.22E-04	0.02	1
Htr3a	-0.27	-1.21	0.02	0.16	1
Htr3b	-0.31	-1.24	0.01	0.11	1

Ibsp	0.96	1.95	6.49E-03	0.07	1
Idi1	0.19	1.14	0.01	0.12	1
Ids	0.2	1.15	9.21E-03	0.09	1
Ifi27	-0.35	-1.27	3.60E-03	0.05	1
Ifi27l2b	-0.32	-1.25	0.01	0.1	1
Ifitm10	-0.33	-1.25	0.02	0.16	1
Ifnar2	0.32	1.25	0.01	0.1	1
Ifngr2	0.4	1.32	2.82E-03	0.04	1
Ifrd1	0.28	1.21	0.04	0.21	1
Ift20	0.39	1.31	4.79E-05	2.62E-03	0.9
Ift27	-0.48	-1.39	0.01	0.1	1
Ift74	0.35	1.27	0.01	0.12	1
Igf1r	-0.2	-1.15	0.02	0.15	1
Igfbp3	0.84	1.8	1.64E-18	4.67E-15	3.07E-14
Igfbp4	-0.29	-1.22	0.02	0.14	1
Igsf21	-1.15	-2.22	6.72E-05	3.43E-03	1
Ikzf2	0.46	1.37	0.01	0.1	1
Il11ra1	-0.51	-1.43	5.33E-04	0.01	1
Il13ra1_1	0.6	1.51	1.27E-04	5.60E-03	1
Il15ra	0.99	1.99	0.02	0.16	1
Il1r1	0.72	1.65	4.04E-05	2.33E-03	0.76
Il22ra2	-1.57	-2.97	0.01	0.11	1
Il31ra	0.45	1.37	2.43E-03	0.04	1
Impa1	0.29	1.22	0.02	0.13	1
Impact	0.17	1.13	0.04	0.21	1
Inf2	-0.32	-1.25	6.88E-03	0.08	1
Inha	-0.56	-1.48	0.02	0.15	1
Ints13	0.33	1.26	0.01	0.11	1
Ints4	-0.19	-1.14	0.04	0.22	1
Ints5	-0.4	-1.32	8.04E-03	0.08	1
Ints6	0.28	1.21	3.33E-03	0.05	1
Ipo13	-0.27	-1.21	4.46E-03	0.06	1
Ipo5	0.2	1.15	0.01	0.1	1
Ipo7	0.21	1.16	9.02E-03	0.09	1
Iqsec1	-0.28	-1.21	3.46E-04	0.01	1
Iqsec2	-0.24	-1.18	7.09E-03	0.08	1
Iqsec3	-0.38	-1.3	1.36E-04	5.93E-03	1
Ireb2	0.2	1.15	0.01	0.12	1
Irf1	0.5	1.42	6.66E-03	0.08	1

Irf2bp1	-0.36	-1.28	0.01	0.11	1
Irgq	-0.17	-1.13	0.03	0.2	1
Irs2	-0.17	-1.12	0.04	0.21	1
Isg15	1.65	3.14	8.01E-03	0.08	1
Islr2	-0.94	-1.91	0.01	0.11	1
Isyna1	-0.5	-1.41	3.99E-03	0.06	1
Itga2b	-1.31	-2.48	7.72E-04	0.02	1
Itga4	0.35	1.28	0.02	0.13	1
Itga9	-0.46	-1.38	0.01	0.12	1
Itgb5	-0.29	-1.22	0.02	0.14	1
Itgb6	-0.49	-1.4	0.05	0.24	1
Itgb8	0.43	1.35	1.54E-08	3.33E-06	2.89E-04
Itm2c	-0.36	-1.28	4.45E-06	4.13E-04	0.08
Itpkc	0.51	1.43	0.01	0.12	1
Ivns1abp	0.32	1.25	2.90E-05	1.79E-03	0.55
Jakmip2	0.21	1.16	0.01	0.1	1
Josd2	-0.43	-1.35	1.67E-03	0.03	1
Jph3	-0.31	-1.24	2.08E-04	8.02E-03	1
Kat2b	0.2	1.15	0.02	0.13	1
Kazn	-0.28	-1.21	0.02	0.16	1
Kbtbd12	1.91	3.76	0.04	NaN	1
Kcna3	0.52	1.44	5.91E-03	0.07	1
Kcnd1	-0.16	-1.12	0.04	0.21	1
Kcne4	0.39	1.31	0.05	0.24	1
Kcng1	0.37	1.3	4.84E-03	0.06	1
Kcnh7	-0.2	-1.15	0.01	0.11	1
Kcnip3	-0.27	-1.21	0.02	0.15	1
Kcnj4	-0.79	-1.72	0.03	0.2	1
Kcnk12	-0.66	-1.58	4.78E-03	0.06	1
Kcnk5	-0.54	-1.45	0.03	0.17	1
Kcnq5	-0.29	-1.22	0.02	0.12	1
Kcns3	-0.26	-1.2	0.04	0.2	1
Kctd14	-1.38	-2.6	1.54E-03	0.03	1
Kctd16	0.25	1.19	2.51E-03	0.04	1
Kctd17	-0.26	-1.2	0.04	0.2	1
Kctd2	-0.39	-1.31	6.05E-03	0.07	1
Kdelr1	-0.26	-1.2	0.04	0.23	1
Kdm3a	0.28	1.21	0.02	0.16	1
Kdm7a	0.39	1.31	1.71E-03	0.03	1

Khdrbs2	0.91	1.87	6.30E-03	0.07	1
Khk	-0.66	-1.58	1.48E-03	0.03	1
Kiaa0408L	0.29	1.22	2.42E-04	8.69E-03	1
Kif11	0.57	1.49	0.02	0.15	1
Kif20b	0.48	1.39	0.04	0.23	1
Kif22	3.46	11	0.01	NaN	1
Kif2a	0.18	1.14	0.02	0.14	1
Kif3b	0.17	1.13	0.03	0.2	1
Kifc2	-0.31	-1.24	0.02	0.15	1
Kitlg	0.24	1.18	0.04	0.21	1
Kiz	0.3	1.23	0.03	0.18	1
Klf2	-0.51	-1.43	0.03	0.2	1
Klf6	0.25	1.19	2.37E-03	0.04	1
Klf7	0.22	1.16	4.94E-03	0.06	1
Klhdc2	0.22	1.17	8.94E-03	0.09	1
Klhdc8a	-0.76	-1.69	6.57E-03	0.07	1
Klhdc8b	-0.66	-1.58	1.66E-05	1.15E-03	0.31
Klhl14	-0.42	-1.34	0.04	0.22	1
Klhl17	-0.32	-1.25	0.03	0.17	1
Klhl2	0.22	1.17	0.02	0.14	1
Klhl25	-0.52	-1.43	0.05	0.23	1
Klhl28	0.31	1.24	0.02	0.12	1
Klrg2	-0.85	-1.81	0.02	0.14	1
Kndc1	-0.42	-1.34	2.26E-05	1.46E-03	0.43
Knl1	0.29	1.22	0.04	0.21	1
Kpna1	0.18	1.13	0.02	0.16	1
Kpna4	0.24	1.18	2.75E-03	0.04	1
Kpna5	0.33	1.26	5.51E-03	0.07	1
Kpnb1	0.16	1.12	0.03	0.19	1
Krba1	-0.43	-1.34	0.03	0.18	1
Krit1	0.29	1.22	0.02	0.13	1
Krt15	-1.02	-2.03	4.05E-03	0.06	1
Ksr2	-0.18	-1.13	0.04	0.22	1
L3mbtl1	-0.87	-1.83	0.05	0.23	1
Lamb2	-0.4	-1.31	7.32E-07	9.00E-05	0.01
Lamp2	0.16	1.12	0.04	0.2	1
Lamp5	0.91	1.88	1.83E-06	1.97E-04	0.03
Lancl2	0.24	1.18	0.05	0.24	1
Lap3	0.26	1.2	0.03	0.19	1

Larp4	0.39	1.31	1.33E-06	1.48E-04	0.02
Lck	0.95	1.93	0.05	0.23	1
Lcorl	0.38	1.3	2.96E-03	0.05	1
Ldlr	0.17	1.12	0.03	0.18	1
Ldlrap1	-0.77	-1.7	5.17E-03	0.06	1
Leng8	-0.25	-1.19	1.31E-03	0.03	1
Leng9	-0.52	-1.43	3.25E-04	0.01	1
Leo1	0.21	1.16	0.02	0.15	1
Letmd1	-0.25	-1.19	0.04	0.23	1
Lgals3	0.22	1.16	9.62E-03	0.09	1
Lgi3	-0.52	-1.44	4.08E-11	2.08E-08	7.66E-07
Lhfpl4	-0.18	-1.13	0.03	0.17	1
Lifr	0.42	1.34	2.31E-08	4.64E-06	4.33E-04
Lig4	0.3	1.23	0.01	0.1	1
Lilrb2	-2.3	-4.93	0.02	NaN	1
Lin7c	0.23	1.18	0.05	0.24	1
Lingo1	-0.5	-1.41	3.75E-05	2.18E-03	0.7
Lipa	-0.18	-1.13	0.03	0.18	1
Lipe	-0.41	-1.32	5.44E-03	0.07	1
Llgl1	-0.31	-1.24	0.02	0.16	1
Lmbrd2	0.17	1.12	0.04	0.22	1
Loxl1	-0.71	-1.64	4.81E-04	0.01	1
Lpar6	0.5	1.41	2.71E-03	0.04	1
Lrch4	-0.54	-1.46	3.27E-04	0.01	1
Lrfn1	-0.3	-1.23	0.03	0.2	1
Lrfn3	-0.72	-1.64	0.01	0.11	1
Lrif1	0.28	1.22	0.04	0.2	1
Lrp1	-0.33	-1.26	1.42E-05	1.02E-03	0.27
Lrp11	-0.17	-1.13	0.03	0.18	1
Lrp1b	0.31	1.24	5.58E-04	0.01	1
Lrp3	-0.28	-1.21	0.03	0.17	1
Lrp5	-0.28	-1.21	0.04	0.22	1
Lrrc2	0.39	1.31	0.04	0.22	1
Lrrc24	-0.46	-1.37	1.51E-03	0.03	1
Lrrc32	-0.72	-1.65	9.59E-04	0.02	1
Lrrc58	0.25	1.19	1.31E-03	0.03	1
Lrrc61	-0.38	-1.3	0.02	0.13	1
Lrrc71	-0.91	-1.88	3.94E-03	0.05	1
Lrrc74b	0.53	1.44	0.04	0.21	1

Lrrfip1	0.28	1.21	1.15E-03	0.02	1
Lrrfip2	0.31	1.24	0.01	0.1	1
Lsm5_1	0.55	1.46	7.87E-03	0.08	1
Ltbp3	-0.29	-1.22	5.79E-04	0.02	1
Ltbp4	-0.58	-1.49	6.84E-06	6.04E-04	0.13
Luc7l	0.2	1.15	0.03	0.17	1
Luc7l2	0.2	1.15	0.01	0.1	1
Luc7l3	0.18	1.13	0.03	0.19	1
Lxn	0.43	1.35	1.73E-04	7.03E-03	1
Lypd1	-0.76	-1.69	4.12E-03	0.06	1
Lypd3	-1.61	-3.04	0.04	NaN	1
Lztfl1	0.34	1.27	0.03	0.19	1
Lzts2	-0.28	-1.22	0.05	0.24	1
Mab21l3	0.96	1.95	0.01	0.1	1
Madd	-0.16	-1.12	0.04	0.22	1
Maf	-0.38	-1.3	2.34E-03	0.04	1
Maf1	-0.28	-1.21	4.25E-03	0.06	1
Mafa	-0.95	-1.93	0.03	0.17	1
Maged1	0.21	1.16	5.21E-03	0.06	1
Maged2	-0.18	-1.13	0.05	0.24	1
Magt1	0.19	1.14	0.02	0.16	1
Man1a1	0.43	1.34	1.07E-03	0.02	1
Man1a2	0.18	1.14	0.02	0.15	1
Manea	0.27	1.2	0.03	0.17	1
Maoa	0.56	1.47	2.02E-06	2.14E-04	0.04
Map1s	-0.3	-1.23	0.02	0.16	1
Map2k2	-0.34	-1.26	0.01	0.1	1
Map3k10	-0.3	-1.23	0.02	0.14	1
Map3k11	-0.26	-1.2	0.04	0.22	1
Map3k13	-0.46	-1.38	1.05E-03	0.02	1
Map4k4	0.19	1.14	0.02	0.12	1
Map4k5	0.22	1.17	8.60E-03	0.09	1
Map7	0.21	1.15	0.01	0.11	1
Map7d2	0.24	1.18	1.47E-03	0.03	1
Map9	0.29	1.22	0.02	0.13	1
Mapk12	-0.37	-1.29	5.87E-03	0.07	1
Mapk8ip1	-0.27	-1.21	0.02	0.13	1
Mapk9	0.19	1.14	0.02	0.12	1
Mapkbp1	-0.3	-1.23	0.03	0.2	1

Mapre1	0.32	1.25	1.04E-04	4.77E-03	1
Marchf2	-0.31	-1.24	0.02	0.12	1
Marveld1	-0.3	-1.24	0.04	0.23	1
MAST1	-0.24	-1.18	1.67E-03	0.03	1
Mast4	-0.26	-1.2	0.04	0.22	1
Matk	-0.44	-1.36	0.03	0.19	1
Matn4	-3.25	-9.49	0.02	NaN	1
Matr3	0.26	1.2	7.44E-04	0.02	1
Mau2	-0.35	-1.28	0.01	0.11	1
Mbd5	0.2	1.15	0.02	0.13	1
Mc4r	-1.37	-2.59	0.03	0.19	1
Mcl1	0.33	1.26	5.51E-03	0.07	1
Mcoln1	-0.3	-1.23	0.02	0.16	1
Mcpt1l1	-2.24	-4.72	2.56E-04	8.97E-03	1
Mdc1	-0.43	-1.35	1.69E-03	0.03	1
Mdm2	0.27	1.21	0.05	0.23	1
Med13	0.17	1.13	0.03	0.19	1
Med24	-0.24	-1.18	9.17E-03	0.09	1
Med25	-0.37	-1.3	4.73E-03	0.06	1
Med27	-0.42	-1.34	1.96E-03	0.04	1
Med29	-0.39	-1.31	3.95E-03	0.05	1
Med7	0.32	1.24	0.02	0.16	1
Med9	-0.52	-1.44	6.86E-04	0.02	1
Mef2a	0.19	1.14	0.03	0.18	1
Megf8	-0.19	-1.14	0.02	0.14	1
Memo1	0.24	1.18	4.14E-03	0.06	1
Mettl1	0.53	1.45	0.03	0.19	1
Mettl2	0.38	1.3	0.04	0.21	1
Mettl7a	-0.29	-1.23	0.04	0.22	1
Mettl7b	-1.82	-3.53	0.03	NaN	1
Mfap1a	0.19	1.14	0.04	0.21	1
Mfap3l	0.24	1.18	0.04	0.22	1
Mfsd12	-0.28	-1.21	0.05	0.23	1
Mfsd3	-0.53	-1.45	0.04	0.21	1
Mga	0.19	1.14	0.01	0.12	1
Mgat4a	0.36	1.28	4.99E-03	0.06	1
Mgmt	-0.74	-1.67	0.01	0.12	1
Mgst3	-0.53	-1.45	1.49E-04	6.44E-03	1
Mia2	0.24	1.18	8.42E-03	0.09	1

Mia3	0.17	1.13	0.03	0.17	1
Micu2	0.19	1.14	0.04	0.21	1
Mien1	-0.3	-1.23	0.02	0.14	1
Mif	-0.37	-1.29	7.45E-06	6.39E-04	0.14
Miga2	-0.39	-1.31	6.84E-05	3.46E-03	1
Mindy3	0.15	1.11	0.05	0.24	1
Mki67	0.56	1.48	3.74E-05	2.18E-03	0.7
Mknk2	-0.28	-1.22	3.07E-03	0.05	1
Mlf1	0.74	1.67	5.51E-03	0.07	1
Mlf2	-0.3	-1.23	2.18E-04	8.12E-03	1
Mlip	-0.17	-1.13	0.04	0.21	1
Mllt6	-0.31	-1.24	0.02	0.13	1
Mmgt1	0.32	1.25	6.97E-05	3.51E-03	1
Mmp16	0.56	1.47	7.73E-05	3.84E-03	1
Mmp3	2.65	6.28	9.38E-03	NaN	1
Mmrn1	-0.87	-1.83	0.01	0.1	1
Mn1	-0.77	-1.71	0.03	0.18	1
Mobp	-1.65	-3.13	0.01	0.11	1
Morf4l1	0.25	1.19	0.03	0.18	1
Morn4	-0.3	-1.23	0.03	0.18	1
Mpl	-1.14	-2.21	0.04	0.21	1
Mpp5	0.36	1.28	3.49E-03	0.05	1
Mrm2	-0.73	-1.66	0.01	0.11	1
Mroh7	0.6	1.51	0.05	0.24	1
Mrpl12	-0.38	-1.3	6.39E-03	0.07	1
Mrpl30	0.32	1.25	0.01	0.11	1
Mrpl38	-0.36	-1.28	0.01	0.11	1
Mrpl43	-0.33	-1.26	0.01	0.12	1
Mrpl45	-0.52	-1.44	9.96E-05	4.65E-03	1
Mrpl47	0.34	1.26	9.58E-03	0.09	1
Mrps17	0.92	1.89	0.02	0.16	1
Ms4a3	-3.11	-8.63	0.03	NaN	1
Ms4a6bl_2	0.61	1.53	0.02	0.13	1
Msmo1	0.18	1.13	0.03	0.17	1
Msrb1	-0.4	-1.32	3.15E-03	0.05	1
Mst1r	-0.32	-1.25	0.04	0.21	1
Mt-atp8	0.63	1.54	2.18E-08	4.45E-06	4.10E-04
Mt-co2	0.24	1.18	0.03	0.18	1
Mt-nd3	0.43	1.35	2.17E-03	0.04	1

Mtarc1	-0.4	-1.32	3.37E-03	0.05	1
Mtdh	0.19	1.14	0.03	0.17	1
Mthfd2	0.32	1.25	0.05	0.24	1
Mtif2	0.36	1.28	0.04	0.2	1
Mtm1	-0.24	-1.18	0.02	0.13	1
Mtmr11	-0.53	-1.44	0.02	0.15	1
Mtmr3	-0.32	-1.24	9.09E-03	0.09	1
Mtpn	0.19	1.14	0.02	0.12	1
Mtx2	-0.32	-1.25	0.03	0.18	1
Mvb12a	-0.4	-1.32	2.86E-03	0.04	1
Mx2	1.18	2.27	1.00E-04	4.66E-03	1
Mxra8	-0.33	-1.25	3.82E-04	0.01	1
Myadml2	-1.06	-2.08	0.01	0.1	1
Mybl1	0.51	1.42	4.11E-03	0.06	1
Myc	0.56	1.48	5.74E-03	0.07	1
Myh11	-0.57	-1.48	9.73E-06	7.56E-04	0.18
Myl6	-0.16	-1.12	0.04	0.22	1
Myl9	-0.85	-1.81	3.61E-06	3.42E-04	0.07
Myo10	0.21	1.16	8.80E-03	0.09	1
Myo1g	-0.83	-1.78	0.04	0.23	1
Myo3a	0.48	1.39	2.28E-04	8.39E-03	1
Myo9a	0.29	1.22	9.60E-03	0.09	1
Myof	0.37	1.29	3.44E-03	0.05	1
Myom2	0.39	1.31	0.04	0.2	1
Myoz2	1.21	2.31	0.03	0.18	1
Mypop	-0.6	-1.52	1.69E-04	6.91E-03	1
Mysm1	0.29	1.22	1.46E-03	0.03	1
Naa15	0.3	1.23	9.22E-03	0.09	1
Naa50	0.24	1.18	0.04	0.21	1
Nabp1	0.7	1.62	3.83E-04	0.01	1
Nacc1	-0.27	-1.2	1.63E-03	0.03	1
Nacc2	-0.24	-1.18	3.47E-03	0.05	1
Nadk2	0.4	1.32	4.40E-03	0.06	1
Naglt1	2.08	4.24	0.03	NaN	1
Nalcn	0.26	1.2	1.02E-03	0.02	1
Nampt	0.37	1.29	6.17E-05	3.23E-03	1
Nap1l1	0.31	1.24	6.33E-05	3.28E-03	1
Nbeal1	0.21	1.16	6.59E-03	0.07	1
Nbl1	-0.18	-1.14	0.03	0.17	1

Nbn	0.37	1.29	2.10E-03	0.04	1
Ncam1	0.18	1.13	0.02	0.15	1
Ncam2	0.3	1.23	9.10E-03	0.09	1
Ncbp2as2	-0.35	-1.27	0.05	0.23	1
Ncdn	-0.19	-1.14	0.01	0.11	1
Nckipsd	-0.42	-1.33	1.44E-03	0.03	1
Ncl	0.3	1.23	9.92E-05	4.65E-03	1
Ncln	-0.32	-1.25	7.94E-03	0.08	1
Ncoa1	0.16	1.12	0.04	0.22	1
Ncoa4_2	0.45	1.36	0.01	0.1	1
Ncoa7	0.25	1.19	0.03	0.18	1
Ndc80	0.67	1.59	0.03	0.17	1
Ndrg4	-0.22	-1.17	0.05	0.24	1
Ndufa11	-0.28	-1.22	0.02	0.15	1
Ndufa3	-0.21	-1.16	0.01	0.1	1
Ndufa4	0.18	1.13	0.03	0.17	1
Ndufa6	-0.25	-1.19	5.79E-03	0.07	1
Ndufa8	-0.23	-1.17	5.35E-03	0.07	1
Ndufaf4	0.36	1.28	8.51E-03	0.09	1
Ndufb10	-0.19	-1.14	0.02	0.12	1
Ndufb2_1	-0.3	-1.23	2.29E-03	0.04	1
Ndufb6	-0.39	-1.31	1.69E-03	0.03	1
Ndufb8	-0.24	-1.18	0.04	0.23	1
Ndufs2	-0.22	-1.16	6.95E-03	0.08	1
Necab3	-0.29	-1.22	1.48E-03	0.03	1
Necap1	-0.18	-1.13	0.03	0.17	1
Nectin3	0.37	1.29	2.59E-03	0.04	1
Nedd8	0.21	1.15	0.01	0.1	1
Nefh	-0.22	-1.16	0.05	0.24	1
Nefl	-0.23	-1.17	0.04	0.22	1
Nek1	0.21	1.16	0.01	0.1	1
Nell1	0.27	1.21	1.18E-03	0.02	1
Neo1	0.18	1.13	0.04	0.21	1
NEWGENE_1310680	-0.47	-1.38	3.77E-04	0.01	1
NEWGENE_1559832	0.22	1.17	8.33E-03	0.09	1
NEWGENE_1565644	-0.37	-1.29	0.05	0.24	1
NEWGENE_619861	0.25	1.19	1.13E-03	0.02	1
NEWGENE_6497122	-0.84	-1.79	7.44E-03	0.08	1
Nexmif	0.42	1.34	0.03	0.18	1

Nfatc2	-0.62	-1.54	0.03	0.18	1
Nfatc2ip	-0.41	-1.33	0.03	0.17	1
Nfatc4	-0.57	-1.49	0.02	0.16	1
Nfia	-0.25	-1.19	2.85E-03	0.04	1
Nfic	-0.23	-1.17	3.41E-03	0.05	1
Nfkbie	-0.33	-1.26	8.99E-03	0.09	1
Nfyb	0.27	1.21	0.04	0.22	1
Nicn1	-0.35	-1.27	0.01	0.1	1
Nipa1	0.16	1.12	0.04	0.2	1
Nipbl	0.17	1.12	0.03	0.19	1
Nkd2	-0.64	-1.56	0.01	0.12	1
Nlgn2	-0.36	-1.28	2.77E-03	0.04	1
Nln	0.38	1.3	4.30E-03	0.06	1
Nlrx1	-0.97	-1.96	2.13E-06	2.24E-04	0.04
Nmb	-0.48	-1.39	6.29E-03	0.07	1
Nmd3	0.29	1.22	0.03	0.2	1
Nmnat2	0.23	1.17	6.00E-03	0.07	1
Noc3l	0.33	1.26	0.01	0.11	1
Nol6	-0.3	-1.23	0.02	0.13	1
Nop10	0.17	1.12	0.03	0.19	1
Nop14	0.28	1.21	0.03	0.18	1
Nop53	-0.3	-1.23	0.02	0.13	1
Nop58	0.3	1.23	8.94E-04	0.02	1
Nos1	0.69	1.61	0.01	0.1	1
Notch3	-0.48	-1.39	4.49E-04	0.01	1
Npat	0.33	1.26	8.46E-03	0.09	1
Nppa	0.59	1.51	0.01	0.12	1
Nprl2	-0.31	-1.24	0.03	0.18	1
Nptxr	0.17	1.12	0.04	0.2	1
Npy1r	0.7	1.63	1.32E-08	2.91E-06	2.49E-04
Nr1h2	-0.36	-1.29	3.95E-03	0.05	1
Nr2f6	-0.51	-1.43	0.01	0.1	1
Nras	0.27	1.2	0.03	0.17	1
Nrbp2	-0.24	-1.18	0.04	0.22	1
Nrcam	0.23	1.18	0.04	0.22	1
Nrdc	0.19	1.14	0.02	0.15	1
Nrg2	-0.35	-1.27	0.04	0.23	1
Nrip1	0.46	1.38	7.53E-09	1.74E-06	1.42E-04
Nrip2	-0.55	-1.46	5.00E-03	0.06	1

Nrip3	0.19	1.14	0.02	0.13	1
Nrm	0.25	1.19	0.05	0.24	1
Nrp2	-0.2	-1.15	0.01	0.12	1
Nrxn2	-0.21	-1.16	7.30E-03	0.08	1
Nsa2	0.27	1.21	0.02	0.15	1
Nsd2	0.17	1.12	0.05	0.24	1
Nsdhl	0.2	1.15	0.02	0.13	1
Nsun6	0.5	1.41	0.04	0.22	1
Nt5dc3	0.29	1.23	0.01	0.11	1
Ntf3	-2.9	-7.47	0.05	NaN	1
Ntm	-0.33	-1.26	0.03	0.17	1
Ntn3	-1.26	-2.39	0.02	0.14	1
Ntng1	-0.39	-1.31	1.33E-03	0.03	1
Ntrk3	-0.21	-1.16	8.07E-03	0.08	1
Nucks1	0.16	1.12	0.05	0.24	1
Nudc	-0.19	-1.14	0.02	0.16	1
Nudt14	-0.67	-1.59	0.01	0.1	1
Nudt21	0.32	1.25	8.62E-03	0.09	1
Nudt3	-0.2	-1.15	0.01	0.11	1
Nufip2	0.28	1.21	3.26E-04	0.01	1
Nup188	-0.3	-1.23	0.03	0.18	1
Nup214	-0.22	-1.16	0.01	0.11	1
Nup62	-0.32	-1.25	0.02	0.14	1
Nus1	0.2	1.15	0.02	0.15	1
Nxf1	0.21	1.15	0.01	0.1	1
Nxph4	-1.94	-3.84	1.91E-03	0.03	1
Oasl2	0.63	1.54	0.04	0.22	1
Oat	0.17	1.13	0.03	0.19	1
Ociad2	0.74	1.66	1.56E-03	0.03	1
Ofd1	0.38	1.3	0.01	0.12	1
Oga	0.18	1.13	0.02	0.15	1
Olfr1417	3.29	9.8	0.02	NaN	1
Olr1585	0.75	1.69	7.79E-05	3.84E-03	1
Olr318	8.44	347.93	2.85E-04	9.66E-03	1
Olr854	1.29	2.44	2.18E-03	0.04	1
Onecut1	-0.29	-1.22	0.04	0.23	1
Orai2	-0.31	-1.24	0.02	0.13	1
Orai3	-0.3	-1.23	0.03	0.18	1
Orc4	0.47	1.38	6.03E-04	0.02	1

Orc5	0.33	1.26	0.01	0.1	1
Osbp2	-0.29	-1.23	0.03	0.19	1
Osbpl10	-0.37	-1.3	4.14E-03	0.06	1
Osbpl5	-0.31	-1.24	0.01	0.11	1
Osbpl8	0.31	1.24	1.26E-04	5.60E-03	1
Osgin2	0.36	1.28	0.04	0.21	1
Ostf1	0.17	1.12	0.03	0.18	1
Otub1	-0.16	-1.12	0.05	0.24	1
Oxa1l	-0.25	-1.19	0.05	0.23	1
Oxld1	-0.67	-1.59	0.04	0.2	1
P2rx4	-0.6	-1.52	3.23E-03	0.05	1
P2rx6	-0.58	-1.5	3.24E-05	1.94E-03	0.61
P3h3	-0.19	-1.14	0.03	0.18	1
P4ha1	0.19	1.14	0.02	0.16	1
P4htm	-0.37	-1.29	4.03E-03	0.06	1
Pacrgl	0.63	1.55	0.02	0.12	1
Pacsin2	-0.2	-1.15	0.02	0.13	1
Padi3	1.64	3.11	0.01	NaN	1
Pafah1b1	0.33	1.26	3.10E-03	0.05	1
Pafah1b3	-0.56	-1.48	7.06E-03	0.08	1
Paip1	0.44	1.35	2.34E-04	8.46E-03	1
Pak1ip1	1.1	2.15	4.48E-04	0.01	1
Pak6	1.44	2.72	1.61E-03	0.03	1
Pald1	-0.31	-1.24	0.02	0.13	1
Pam	0.16	1.12	0.04	0.22	1
Pam16	-0.45	-1.37	0.01	0.12	1
Panx2	-0.27	-1.21	1.08E-03	0.02	1
Pappa2	0.57	1.49	0.01	0.12	1
Paqr3	-0.42	-1.33	5.74E-03	0.07	1
Paqr4	-0.3	-1.23	2.32E-04	8.44E-03	1
Paqr7	-0.28	-1.21	4.35E-03	0.06	1
Parp3	0.43	1.35	1.01E-03	0.02	1
Parp9	0.52	1.43	4.27E-03	0.06	1
Parpbp	0.83	1.78	0.05	0.24	1
Patl1	0.43	1.35	7.43E-04	0.02	1
Patz1	-0.29	-1.22	0.05	0.23	1
Paxx	-0.5	-1.42	0.02	0.12	1
Pbdc1	0.25	1.19	5.27E-03	0.06	1
Pbk	1.08	2.12	0.05	0.24	1

Pbrm1	0.21	1.16	6.51E-03	0.07	1
Pbx4	-0.9	-1.87	0.03	0.19	1
Pcdh18	0.37	1.3	4.47E-03	0.06	1
Pcdh7_2	-0.51	-1.43	0.05	0.23	1
Pcdh9	0.19	1.14	0.02	0.13	1
Pced1a	-0.32	-1.25	0.02	0.15	1
Pcf11	0.28	1.21	9.12E-04	0.02	1
Pcm1	0.17	1.12	0.03	0.19	1
Pcnp	0.22	1.16	5.37E-03	0.07	1
Pcnx2	-0.19	-1.14	0.02	0.12	1
Pcnx3	-0.33	-1.26	8.26E-03	0.09	1
Pcolce	-0.33	-1.26	0.03	0.17	1
PCOLCE2	0.62	1.53	1.10E-05	8.32E-04	0.21
Pcp4	0.21	1.15	6.05E-03	0.07	1
Pcsk1	0.28	1.21	0.02	0.13	1
Pcsk1n	-0.39	-1.31	6.08E-04	0.02	1
Pcsk6	-0.38	-1.3	8.61E-03	0.09	1
Pctp	-0.47	-1.39	4.12E-03	0.06	1
Pcyt1b	-0.21	-1.16	0.03	0.18	1
Pdcd5	0.35	1.28	5.23E-03	0.06	1
Pdcl3	0.22	1.17	0.02	0.14	1
Pde1a	0.38	1.31	0.01	0.1	1
Pde6b	1.43	2.69	2.67E-03	0.04	1
Pde8b	0.51	1.42	3.63E-04	0.01	1
Pdgfa	-0.51	-1.42	2.23E-03	0.04	1
Pdha1	0.3	1.23	7.75E-03	0.08	1
Pdpn	0.32	1.25	1.62E-04	6.77E-03	1
Pds5a	0.21	1.16	0.01	0.11	1
Pea15	0.17	1.12	0.02	0.16	1
Pear1	-0.29	-1.22	0.03	0.19	1
Pebp1	-0.33	-1.26	2.22E-05	1.44E-03	0.42
Perp	0.51	1.43	1.00E-03	0.02	1
Pex11b	-0.48	-1.39	2.03E-03	0.04	1
Pex14	-0.29	-1.22	0.03	0.2	1
Pex2	0.27	1.21	0.04	0.2	1
Pfas	-0.52	-1.43	1.02E-04	4.72E-03	1
Pfdn6	-0.31	-1.24	0.02	0.14	1
Pgap1	0.28	1.22	0.03	0.2	1
Pgap2	-0.36	-1.29	0.05	0.24	1

Pgap4	-0.33	-1.26	0.01	0.1	1
Pgbd5	-0.35	-1.27	7.37E-03	0.08	1
Pgm2	0.29	1.22	0.05	0.24	1
Pgm2l1	0.16	1.12	0.04	0.21	1
Pgrmc2	0.25	1.19	3.23E-03	0.05	1
Phactr2	0.48	1.4	6.16E-09	1.44E-06	1.16E-04
Phc2	-0.31	-1.24	6.36E-04	0.02	1
Phf1	-0.42	-1.34	2.57E-03	0.04	1
Phf14	0.22	1.16	6.73E-03	0.08	1
Phf20l1	0.2	1.15	0.02	0.15	1
Phf3	0.17	1.13	0.03	0.19	1
Phf6	0.32	1.24	0.01	0.1	1
Phldb3	0.84	1.79	0.02	0.15	1
Phyh	-0.25	-1.19	0.04	0.21	1
Phyhipl	-0.17	-1.13	0.03	0.17	1
Pi16	-0.61	-1.53	0.03	0.18	1
Pi4k2a	-0.17	-1.12	0.05	0.24	1
Pias4	-0.33	-1.25	0.02	0.15	1
Picalm	0.22	1.16	4.30E-03	0.06	1
Pick1	-0.45	-1.36	0.02	0.14	1
Pign	0.39	1.31	0.02	0.15	1
Pik3ca	0.21	1.16	7.47E-03	0.08	1
Pik3cg	0.46	1.38	0.03	0.2	1
Pik3ip1	-0.25	-1.19	0.05	0.24	1
Pin1	-0.22	-1.16	0.01	0.1	1
Pip4p1	-0.4	-1.32	2.09E-03	0.04	1
Pipox	-1.89	-3.72	8.76E-03	0.09	1
Pitpnm1	-0.42	-1.34	6.12E-03	0.07	1
Piwil2	-0.88	-1.83	3.02E-03	0.05	1
Pja1	-0.2	-1.15	0.01	0.11	1
Pkd1	-0.38	-1.3	1.26E-06	1.42E-04	0.02
Pkd1l1	0.66	1.58	0.03	0.2	1
Pkdcc	-0.64	-1.55	1.44E-03	0.03	1
Pkhd1	0.6	1.52	0.02	0.13	1
Pkia	0.41	1.33	9.36E-07	1.10E-04	0.02
Pkn3	0.22	1.16	8.37E-03	0.09	1
Pla2g3	-0.42	-1.34	3.35E-03	0.05	1
Pla2g4e	-0.88	-1.84	2.03E-03	0.04	1
Plaa	0.26	1.19	1.64E-03	0.03	1

Plac8	-0.79	-1.74	0.02	0.13	1
Plat	0.31	1.24	7.91E-03	0.08	1
Plaur	0.43	1.35	0.04	0.2	1
Plbd2	-0.31	-1.24	2.35E-04	8.47E-03	1
Pld1	0.24	1.18	7.43E-03	0.08	1
Pld3	-0.27	-1.2	1.51E-03	0.03	1
Plekha3	0.42	1.34	1.54E-03	0.03	1
Plekha6	-0.19	-1.14	0.01	0.11	1
Plekhb1	-0.21	-1.16	6.00E-03	0.07	1
Plekhg2	-0.4	-1.32	9.41E-04	0.02	1
Plpp3	-0.23	-1.17	3.53E-03	0.05	1
Plpp5	0.19	1.14	0.02	0.15	1
Plppr2	-0.26	-1.19	0.05	0.24	1
Pls3	0.25	1.19	1.16E-03	0.02	1
Plscr5	-1.75	-3.37	9.53E-03	0.09	1
Plvap	-0.59	-1.51	0.03	0.19	1
Plxna2	0.31	1.24	5.46E-03	0.07	1
Plxnc1	0.26	1.2	0.03	0.17	1
Pmm1	-0.18	-1.13	0.04	0.2	1
Pmm2	-0.3	-1.23	0.02	0.16	1
Pmpca	-0.46	-1.38	3.47E-04	0.01	1
Pmvk	-0.2	-1.15	0.04	0.2	1
Pnisr	0.16	1.12	0.05	0.24	1
Pnma1	-0.65	-1.57	8.19E-03	0.09	1
Pnn	0.25	1.19	3.72E-03	0.05	1
Pnpla1	-1.26	-2.39	2.76E-03	0.04	1
Pnpla6	-0.25	-1.19	0.04	0.2	1
Pnpla8	0.24	1.18	2.26E-03	0.04	1
Pnpo	-0.54	-1.46	4.76E-05	2.61E-03	0.89
Pnpt1	0.38	1.3	2.11E-03	0.04	1
Pnrc2_1	0.21	1.15	0.02	0.13	1
Poc1a	-1.37	-2.59	0.04	0.2	1
Pogk	0.18	1.13	0.04	0.2	1
Polr3g	0.2	1.15	0.01	0.11	1
Pom121	-0.31	-1.24	0.01	0.12	1
Pomgnt2	-0.33	-1.26	0.01	0.11	1
Pomp	0.32	1.25	6.45E-05	3.33E-03	1
Porcn	-0.56	-1.48	2.77E-03	0.04	1
Pot1	0.32	1.25	0.05	0.24	1

Ppfia3	-0.23	-1.18	9.17E-03	0.09	1
Ppfia4	-0.44	-1.35	1.10E-05	8.32E-04	0.21
Ppif	-0.44	-1.36	0.03	0.19	1
Ppig	0.32	1.25	1.52E-04	6.48E-03	1
Ppl	-0.9	-1.86	1.95E-03	0.04	1
Ppm1j	-0.33	-1.25	0.01	0.1	1
Ppp1cb	0.26	1.2	6.83E-04	0.02	1
Ppp1r12a	0.32	1.24	7.62E-05	3.81E-03	1
Ppp1r14a	-1.69	-3.23	1.64E-03	0.03	1
Ppp1r1c	0.29	1.22	0.01	0.1	1
Ppp1r36	0.43	1.35	2.43E-03	0.04	1
Ppp1r3b	-0.56	-1.48	7.39E-03	0.08	1
Ppp1r42	2.16	4.47	0.04	NaN	1
Ppp1r7	0.25	1.19	1.89E-03	0.03	1
Ppp1r9a	0.19	1.14	0.03	0.17	1
Ppp1r9b	-0.18	-1.13	0.03	0.18	1
Ppp2ca	0.31	1.24	6.00E-05	3.15E-03	1
Ppp2r2a	0.3	1.23	1.84E-04	7.34E-03	1
Ppp2r2b	0.18	1.13	0.02	0.16	1
Ppp4r2	0.2	1.15	0.02	0.13	1
Ppp4r3a	0.32	1.25	0.01	0.11	1
Ppp5c	-0.19	-1.14	0.02	0.16	1
Ppt2	-0.46	-1.37	3.25E-03	0.05	1
Ppwd1	0.28	1.22	0.05	0.24	1
Praf2	-0.17	-1.12	0.05	0.24	1
Prc1	0.74	1.67	0.01	0.12	1
Prdm2	0.26	1.19	1.32E-03	0.03	1
Prdx1	0.29	1.22	3.38E-04	0.01	1
Prdx5	-0.26	-1.19	2.32E-03	0.04	1
Prdx6	0.35	1.28	4.58E-03	0.06	1
Prelp	-0.65	-1.57	3.55E-06	3.39E-04	0.07
Prep	-0.26	-1.2	2.26E-03	0.04	1
Prickle1	-0.3	-1.23	0.03	0.18	1
Prkaa2	0.36	1.28	4.20E-03	0.06	1
Prkaca	-0.28	-1.21	4.69E-04	0.01	1
Prkag2	0.24	1.18	3.38E-03	0.05	1
Prkar2b	0.55	1.46	5.31E-12	3.04E-09	9.98E-08
Prkcb	0.27	1.21	1.02E-03	0.02	1
Prkdc	0.26	1.19	0.03	0.18	1

Prlr	0.69	1.61	7.78E-03	0.08	1
Prpf19	-0.26	-1.19	1.32E-03	0.03	1
Prpf39	0.43	1.34	6.73E-04	0.02	1
Prpf40a	0.33	1.26	8.75E-05	4.21E-03	1
Prpf4b	0.23	1.17	5.15E-03	0.06	1
Prpsap1	-0.28	-1.21	0.04	0.22	1
Prr12	-0.32	-1.25	0.01	0.1	1
Prr13	0.31	1.24	1.93E-04	7.58E-03	1
Prrg1	0.25	1.19	0.05	0.24	1
Prrg4	0.46	1.38	7.40E-04	0.02	1
Prrt1	-0.55	-1.46	2.71E-05	1.71E-03	0.51
Prrt2	-0.19	-1.14	0.02	0.15	1
Prtfdc1	0.38	1.3	4.35E-03	0.06	1
Psd	-0.72	-1.65	6.03E-03	0.07	1
Psma3	0.25	1.19	2.02E-03	0.04	1
Psma6	0.27	1.2	9.57E-04	0.02	1
Psmb5	-0.22	-1.17	7.61E-03	0.08	1
Psmc6	0.26	1.2	1.52E-03	0.03	1
Psmd1	0.19	1.14	0.01	0.11	1
Psmd14	0.2	1.15	0.02	0.14	1
Psme4	0.26	1.2	7.26E-04	0.02	1
Psmf1	-0.22	-1.17	8.81E-03	0.09	1
Pstpip1	-1.08	-2.11	2.29E-03	0.04	1
Ptbp2	0.22	1.17	4.94E-03	0.06	1
Ptcd2	-0.45	-1.37	3.33E-03	0.05	1
Ptch2	-0.71	-1.63	9.65E-03	0.09	1
Pten	0.18	1.13	0.02	0.15	1
Pter	0.74	1.67	0.01	0.12	1
Ptgdrl	-2.64	-6.23	0.02	NaN	1
Ptges2	-0.39	-1.31	7.63E-03	0.08	1
Ptges3	0.16	1.12	0.04	0.22	1
Ptgfrn	0.31	1.24	1.93E-04	7.58E-03	1
Ptgir	-0.4	-1.32	0.04	0.22	1
Ptgr2	0.26	1.2	0.05	0.24	1
Pth1r	-0.68	-1.6	6.12E-04	0.02	1
Ptk7	-0.34	-1.26	9.61E-03	0.09	1
Ptma_1	0.3	1.23	8.84E-03	0.09	1
Ptp4a1	0.38	1.3	1.09E-05	8.32E-04	0.2
Ptp4a2	0.18	1.13	0.02	0.16	1

Ptpmt1	-0.41	-1.33	0.01	0.1	1
Ptpn12	0.4	1.32	3.38E-06	3.26E-04	0.06
Ptpn5	0.51	1.42	0.01	0.11	1
Ptprg	0.19	1.14	0.02	0.16	1
Ptprj	0.2	1.15	0.02	0.12	1
Ptpro	0.31	1.24	0.02	0.15	1
Ptprs	-0.2	-1.15	8.21E-03	0.09	1
Ptprt	0.63	1.54	3.94E-07	5.26E-05	7.40E-03
Ptprz1	0.23	1.17	2.96E-03	0.05	1
Ptrhd1	0.4	1.32	0.04	0.21	1
Pts	0.65	1.57	6.01E-03	0.07	1
Pttg1ip	-0.27	-1.2	1.80E-03	0.03	1
Pum2	0.2	1.15	9.89E-03	0.1	1
Purb	0.27	1.21	4.72E-04	0.01	1
Pus3	0.36	1.29	0.01	0.12	1
Pvr	0.81	1.75	1.10E-03	0.02	1
Pxn	-0.39	-1.31	1.48E-03	0.03	1
Pygb	-0.18	-1.14	0.02	0.12	1
Qdpr	0.2	1.15	0.01	0.12	1
Qpctl	-0.44	-1.36	9.21E-03	0.09	1
Qser1	0.23	1.18	6.32E-03	0.07	1
R3hdm4	-0.31	-1.24	0.02	0.13	1
Rab10	0.18	1.14	0.02	0.13	1
Rab11a	0.2	1.15	9.64E-03	0.09	1
Rab11fip2	0.25	1.19	4.28E-03	0.06	1
Rab1b_1	-0.18	-1.13	0.03	0.18	1
Rab39a	0.19	1.14	0.03	0.2	1
Rab3a	-0.16	-1.12	0.04	0.21	1
Rab3il1	-0.54	-1.45	5.65E-04	0.01	1
Rab5a	0.2	1.15	0.01	0.1	1
Rab7a	0.27	1.2	5.45E-04	0.01	1
Rab9b	0.3	1.23	0.01	0.1	1
Rabac1	-0.45	-1.36	2.41E-07	3.52E-05	4.53E-03
Rabgap1l	0.17	1.13	0.04	0.22	1
Rabggtb	0.28	1.21	0.02	0.16	1
Rac3	-0.22	-1.16	0.02	0.14	1
Rack1	-0.29	-1.23	5.72E-04	0.02	1
Rad23b	0.17	1.12	0.03	0.19	1
Rad50	0.17	1.12	0.05	0.24	1

Rala	0.3	1.23	0.01	0.12	1
Ralgapa2	-0.22	-1.16	5.53E-03	0.07	1
Ralgps2	0.28	1.22	0.02	0.15	1
Ralyl	0.33	1.26	7.60E-03	0.08	1
Ranbp1	0.16	1.12	0.04	0.22	1
Ranbp2	0.28	1.21	2.89E-04	9.73E-03	1
Ranbp6	0.22	1.16	8.27E-03	0.09	1
Rap1b	0.28	1.21	4.00E-04	0.01	1
Rap1gap	-0.31	-1.24	2.67E-04	9.19E-03	1
Rap1gap2	-0.21	-1.15	0.01	0.1	1
Raph1	0.17	1.13	0.03	0.18	1
Rarg	-0.42	-1.34	2.59E-03	0.04	1
Rasa1	0.17	1.12	0.04	0.2	1
Rasa2	0.28	1.21	3.62E-03	0.05	1
Rasef	0.55	1.46	0.02	0.14	1
Rasgrp1	0.37	1.29	0.03	0.18	1
Rasip1	-0.45	-1.37	0.03	0.19	1
Rasl10b	-0.29	-1.22	0.03	0.18	1
Rassf10	0.67	1.59	5.81E-04	0.02	1
RatNP-3b	-1.57	-2.97	0.01	0.12	1
Rb1	0.18	1.13	0.04	0.21	1
Rb1cc1	0.26	1.19	1.01E-03	0.02	1
Rbbp4	0.19	1.14	0.02	0.14	1
Rbbp8	0.4	1.32	1.84E-03	0.03	1
Rbck1	-0.36	-1.29	8.06E-03	0.08	1
Rbfox1	0.26	1.19	9.97E-04	0.02	1
Rbis_1	0.64	1.56	5.44E-07	7.07E-05	0.01
Rbm18	0.19	1.14	0.04	0.21	1
Rbm25l1	5.1	34.39	0.04	NaN	1
Rbm26	0.22	1.17	6.85E-03	0.08	1
Rbm42	-0.31	-1.24	0.02	0.13	1
Rbms1	0.18	1.13	0.02	0.16	1
Rbpms2	-1.13	-2.18	0.02	0.15	1
Rc3h2	0.2	1.15	9.65E-03	0.09	1
Rcn3	-0.46	-1.37	4.59E-04	0.01	1
Rcsd1	-0.38	-1.3	0.03	0.2	1
Recql	0.25	1.19	0.05	0.24	1
Reep1	0.15	1.11	0.04	0.22	1
Rel	0.49	1.4	0.04	0.23	1

Rell2	-0.39	-1.31	1.76E-05	1.20E-03	0.33
Rem2	-0.68	-1.6	3.30E-04	0.01	1
Resp18	-0.35	-1.28	4.16E-03	0.06	1
Retsat	-0.47	-1.39	3.36E-04	0.01	1
Rex1bd	-0.5	-1.42	0.01	0.11	1
Rfng	-0.42	-1.34	2.76E-03	0.04	1
RGD1304884	-0.27	-1.2	4.64E-04	0.01	1
RGD1305110	0.21	1.15	0.01	0.1	1
RGD1305350	-0.33	-1.26	0.01	0.11	1
RGD1307461	-0.45	-1.36	1.02E-03	0.02	1
RGD1308750	0.62	1.54	3.23E-05	1.94E-03	0.61
RGD1309748	0.16	1.12	0.04	0.22	1
RGD1311744	0.32	1.25	0.02	0.12	1
RGD1559747	-0.61	-1.53	4.39E-03	0.06	1
RGD1559896	-0.23	-1.17	0.01	0.1	1
RGD1560212	-0.34	-1.27	4.86E-03	0.06	1
RGD1560394	-1.13	-2.18	7.78E-05	3.84E-03	1
RGD1561413	0.41	1.33	0.01	0.11	1
RGD1562339	0.22	1.17	6.10E-03	0.07	1
RGD1563072	-0.26	-1.2	2.30E-03	0.04	1
RGD1563159	1.26	2.4	7.93E-03	0.08	1
RGD1564899	-0.73	-1.66	0.03	0.18	1
RGD1565059	0.47	1.39	0.04	0.21	1
Rgs2	0.57	1.48	3.07E-05	1.87E-03	0.58
Rgs20	0.64	1.56	0.04	0.22	1
Rgs22	1.68	3.2	1.69E-06	1.83E-04	0.03
Rgs4	0.31	1.24	5.32E-03	0.07	1
Rgs7	0.18	1.14	0.03	0.19	1
Rhbdd2	-0.36	-1.28	0.01	0.1	1
Rhbdd3	-0.75	-1.68	3.56E-03	0.05	1
Rhbdf2	-0.59	-1.51	5.03E-03	0.06	1
Rhbdl1	-0.6	-1.52	0.03	0.17	1
Rheb	0.35	1.28	3.20E-03	0.05	1
Rhobtb2	-0.27	-1.2	0.04	0.22	1
Rhoc	0.28	1.21	0.03	0.17	1
Rhou	0.45	1.37	1.14E-03	0.02	1
Rimkla	-0.32	-1.24	2.78E-04	9.46E-03	1
Ring1	-0.29	-1.22	0.03	0.2	1
Riok3	0.36	1.29	1.78E-05	1.21E-03	0.33

Ripor3	-1.08	-2.11	0.01	0.1	1
Rita1	-0.28	-1.22	0.04	0.23	1
Rnase4	-0.3	-1.23	0.05	0.24	1
Rnaseh2a_1	-0.4	-1.32	7.48E-03	0.08	1
Rnasel	0.31	1.24	0.03	0.2	1
Rnd3	0.22	1.16	0.02	0.13	1
Rnf115	0.27	1.2	0.02	0.16	1
Rnf111l	0.19	1.14	0.02	0.14	1
Rnf123	-0.29	-1.23	0.02	0.12	1
Rnf144a	-0.35	-1.27	0.02	0.12	1
Rnf157	-0.29	-1.22	1.57E-04	6.64E-03	1
Rnf167	-0.45	-1.37	3.01E-04	1.00E-02	1
Rnf168	0.35	1.27	8.73E-03	0.09	1
Rnf208	-0.65	-1.56	8.00E-05	3.93E-03	1
Rnf213	0.44	1.36	3.82E-03	0.05	1
Rnf220	-0.31	-1.24	0.02	0.12	1
Rnf40	-0.2	-1.15	0.05	0.23	1
Rnf43	1.24	2.36	8.51E-04	0.02	1
Rnf44	-0.29	-1.22	0.03	0.18	1
Rnft2	-0.26	-1.2	0.04	0.21	1
Rnpc3	0.27	1.21	0.04	0.23	1
Rnpepl1	-0.47	-1.39	9.03E-04	0.02	1
Ro60	0.32	1.25	1.27E-04	5.60E-03	1
Rock2	0.32	1.25	4.44E-05	2.50E-03	0.83
Ror2	-0.85	-1.81	6.65E-04	0.02	1
Rpap1	-0.42	-1.34	0.02	0.14	1
Rpe	0.27	1.21	4.28E-03	0.06	1
Rpgrip1l	0.22	1.16	0.02	0.15	1
Rpl10a	-0.32	-1.25	1.26E-04	5.60E-03	1
Rpl14	-0.23	-1.17	6.74E-03	0.08	1
Rpl23a	0.19	1.14	0.02	0.12	1
Rpl26	0.27	1.2	6.74E-04	0.02	1
Rpl28	-0.17	-1.12	0.03	0.19	1
Rpl30_1	0.38	1.3	9.31E-04	0.02	1
Rpl31	0.22	1.17	7.21E-03	0.08	1
Rpl31l4	-1.86	-3.63	7.41E-08	1.29E-05	1.39E-03
Rpl36a_1	0.54	1.45	4.08E-03	0.06	1
Rpl4	0.22	1.17	3.35E-03	0.05	1
Rplp0	-0.2	-1.15	8.86E-03	0.09	1

Rplp2	-0.46	-1.37	3.96E-04	0.01	1
Rps10l1	-0.69	-1.61	2.60E-06	2.63E-04	0.05
Rps15al4	1.68	3.21	3.33E-07	4.49E-05	6.26E-03
Rps18l1	-0.24	-1.18	4.99E-03	0.06	1
Rps19	-0.19	-1.14	0.03	0.17	1
Rps19bp1	-0.37	-1.29	0.03	0.18	1
Rps20_1	0.25	1.19	2.31E-03	0.04	1
Rps25	0.22	1.16	9.13E-03	0.09	1
Rps29_1	-0.3	-1.23	3.37E-04	0.01	1
Rps3a	0.18	1.13	0.02	0.15	1
Rps4x_1	-0.39	-1.31	7.84E-04	0.02	1
Rps6ka3	0.32	1.25	2.86E-05	1.78E-03	0.54
Rps9	-0.33	-1.26	4.34E-05	2.48E-03	0.82
Rpusd1	-0.6	-1.52	0.02	0.12	1
Rras	-0.56	-1.48	4.82E-03	0.06	1
Rrm2	0.49	1.41	0.05	0.24	1
Rsrc1	0.18	1.13	0.05	0.23	1
Rsrc2	0.28	1.22	0.02	0.15	1
RT1-Bb	0.76	1.69	2.88E-06	2.82E-04	0.05
RT1-CE15	1.3	2.47	8.64E-03	0.09	1
Rtkn	-0.29	-1.22	6.06E-04	0.02	1
Rtn2	-0.26	-1.2	0.03	0.19	1
Rtn4	0.22	1.17	0.05	0.24	1
Rtn4r	-0.57	-1.48	0.01	0.1	1
Rusf1	-0.29	-1.22	0.03	0.2	1
Rxrb	-0.32	-1.25	0.02	0.13	1
Rybp	0.19	1.14	0.04	0.2	1
S100a1	-0.58	-1.49	0.02	0.14	1
S100a10	0.16	1.11	0.04	0.22	1
S100a4	-0.28	-1.21	0.03	0.18	1
S100a6	-0.19	-1.14	0.02	0.14	1
S100a9	-0.97	-1.96	0.04	0.21	1
S100b	-0.26	-1.2	0.02	0.14	1
S100pbp	0.2	1.15	0.02	0.16	1
Samd11	0.39	1.31	0.02	0.14	1
Sars2	-0.55	-1.46	8.56E-03	0.09	1
Sat1	0.19	1.14	0.04	0.2	1
Scap	-0.2	-1.15	0.02	0.14	1
Scaper	0.24	1.18	4.94E-03	0.06	1

Scg2	0.35	1.27	2.08E-03	0.04	1
Schip1	0.18	1.13	0.03	0.19	1
Scn3a	0.51	1.42	2.48E-04	8.79E-03	1
Scn3b	0.38	1.3	1.58E-03	0.03	1
Scn5a	-0.87	-1.82	0.04	0.21	1
Scn8a	-0.19	-1.14	0.01	0.1	1
Scn9a	0.34	1.27	2.40E-03	0.04	1
Sco2	-0.58	-1.49	0.03	0.19	1
Scrib	-0.31	-1.24	0.01	0.1	1
Scube3	-0.6	-1.52	0.02	0.15	1
Scx	-0.57	-1.48	0.03	0.17	1
Sdhb	-0.25	-1.19	2.46E-03	0.04	1
Sec13	0.22	1.17	9.84E-03	0.1	1
Sec23ip	0.18	1.14	0.04	0.22	1
Sec24b	-0.19	-1.14	0.03	0.17	1
Sec62	0.26	1.2	8.24E-04	0.02	1
Sec63	0.24	1.18	3.06E-03	0.05	1
Selenof	0.16	1.12	0.04	0.22	1
Selenom	-0.41	-1.33	5.88E-04	0.02	1
Selenop	-0.2	-1.15	7.63E-03	0.08	1
Selenot	0.26	1.2	0.02	0.15	1
Sema5b	-0.98	-1.97	1.40E-03	0.03	1
Sema6c	-0.52	-1.44	0.01	0.1	1
Senp18	3.11	8.61	0.03	NaN	1
Senp6	0.18	1.14	0.02	0.14	1
Septin2	0.17	1.12	0.04	0.2	1
Septin4	-0.22	-1.16	0.01	0.1	1
Septin7	0.27	1.21	0.02	0.12	1
Septin8	0.18	1.13	0.02	0.16	1
Serbp1	0.2	1.15	9.24E-03	0.09	1
Serf2	0.17	1.12	0.04	0.22	1
Serinc1	0.23	1.18	0.04	0.21	1
Serp1	0.25	1.19	0.04	0.21	1
Serp2	-0.62	-1.54	5.53E-04	0.01	1
Serpinb1b	1.13	2.18	5.81E-08	1.05E-05	1.09E-03
Serpine3	2.89	7.42	0.04	NaN	1
Sestd1	0.38	1.3	9.47E-06	7.45E-04	0.18
Setd2	0.21	1.15	9.28E-03	0.09	1
Sf3b5	-0.29	-1.23	0.03	0.18	1

Sfr1	0.32	1.25	7.77E-03	0.08	1
Sfrp2	-1.35	-2.54	4.69E-03	0.06	1
Sfxn1	0.19	1.14	0.02	0.16	1
Sgcb	0.26	1.2	1.70E-03	0.03	1
Sgip1	0.23	1.17	4.52E-03	0.06	1
Sgpp2	-0.3	-1.23	0.02	0.14	1
Sh3bgrl	0.36	1.29	3.48E-06	3.34E-04	0.07
Sh3d19	0.18	1.13	0.03	0.17	1
Sh3gl2	-0.38	-1.3	8.94E-06	7.18E-04	0.17
Sh3glb1	0.29	1.23	0.01	0.11	1
Sh3glb2	-0.35	-1.27	6.56E-05	3.37E-03	1
Shank1	-0.64	-1.55	2.56E-06	2.62E-04	0.05
Shank3	-0.32	-1.25	0.03	0.19	1
Shoc2	0.18	1.13	0.03	0.18	1
Shtn1	0.33	1.25	8.21E-03	0.09	1
Sirt1	0.36	1.28	7.63E-03	0.08	1
Skap2	0.33	1.26	0.02	0.15	1
Skint10	1.87	3.66	0.02	NaN	1
Skor2	-0.55	-1.47	2.74E-03	0.04	1
Slain2	0.19	1.14	0.03	0.18	1
Slc12a7	-0.18	-1.13	0.04	0.23	1
Slc13a3	-0.47	-1.38	0.04	0.2	1
Slc15a4	0.32	1.25	0.02	0.13	1
Slc16a3	-1.6	-3.03	0.01	0.1	1
Slc17a6	0.35	1.27	2.34E-03	0.04	1
Slc1a4	-0.2	-1.15	0.02	0.15	1
Slc25a1	-0.33	-1.26	7.19E-03	0.08	1
Slc25a12	-0.24	-1.18	2.48E-03	0.04	1
Slc25a19	-0.31	-1.24	0.03	0.2	1
Slc25a25	-0.27	-1.21	0.03	0.17	1
Slc25a30	0.27	1.21	0.03	0.2	1
Slc25a4	0.2	1.15	9.74E-03	0.09	1
Slc25a42	-0.47	-1.38	0.02	0.16	1
Slc25a5	-0.19	-1.14	0.02	0.14	1
Slc25a6	-2.46	-5.51	0.03	NaN	1
Slc27a1	-0.34	-1.26	5.37E-03	0.07	1
Slc27a3	-0.53	-1.45	7.85E-03	0.08	1
Slc2a3	0.3	1.23	0.01	0.1	1
Slc2a8	-0.44	-1.36	5.81E-03	0.07	1

Slc37a4	-0.3	-1.23	0.03	0.19	1
Slc39a10	0.17	1.12	0.04	0.23	1
Slc3a1	-0.94	-1.92	6.95E-03	0.08	1
Slc41a2	0.19	1.14	0.03	0.17	1
Slc45a4	-0.23	-1.18	0.01	0.1	1
Slc4a2	-0.27	-1.21	1.49E-03	0.03	1
Slc4a4	-0.19	-1.14	0.02	0.13	1
Slc4a7	0.42	1.34	2.22E-03	0.04	1
Slc5a3	0.16	1.11	0.05	0.24	1
Slc7a2	-0.29	-1.22	0.03	0.17	1
Slc8b1	-0.4	-1.32	9.85E-03	0.1	1
Slc9a1	-0.39	-1.31	1.37E-03	0.03	1
Slc9a3r1	-0.21	-1.15	0.01	0.12	1
Slc9a5	-0.91	-1.87	2.81E-03	0.04	1
Slc9a6	0.23	1.17	4.72E-03	0.06	1
Slco2a1	-0.86	-1.82	8.68E-04	0.02	1
Slco5a1	-0.38	-1.3	3.86E-05	2.23E-03	0.72
Slf2	0.27	1.2	0.03	0.17	1
Slirp	0.39	1.31	9.77E-03	0.09	1
Slit3	-0.31	-1.24	1.45E-03	0.03	1
Slitrk2	0.23	1.18	3.66E-03	0.05	1
Slitrk3	-0.21	-1.16	0.01	0.1	1
Slk	0.43	1.35	9.00E-08	1.50E-05	1.69E-03
Slmap	0.16	1.12	0.05	0.24	1
Sltm	0.18	1.13	0.04	0.21	1
Smad2	0.21	1.16	0.01	0.11	1
Smagp	1.59	3.01	3.87E-04	0.01	1
Smap1	0.29	1.23	2.13E-04	8.08E-03	1
Smarca1	0.38	1.3	3.93E-03	0.05	1
Smarca5	0.26	1.2	8.49E-04	0.02	1
Smc4	0.35	1.27	3.59E-03	0.05	1
Smc5	0.31	1.24	0.01	0.1	1
Smc6	0.37	1.3	8.55E-06	6.94E-04	0.16
Smdt1	-0.49	-1.4	9.55E-08	1.56E-05	1.79E-03
Smim27	-0.57	-1.49	0.03	0.19	1
Smim29	-0.41	-1.33	4.46E-03	0.06	1
Smo	-0.38	-1.3	0.01	0.1	1
Smoc1	-1.48	-2.79	7.79E-08	1.34E-05	1.46E-03
Smpd3	0.26	1.2	3.67E-03	0.05	1

Snph	-0.3	-1.23	0.02	0.12	1
Snrnp70	-0.16	-1.12	0.05	0.24	1
Snrpb	-0.28	-1.22	0.03	0.19	1
Snrpb2	0.32	1.25	0.01	0.12	1
Snrpc	-1.59	-3	4.65E-04	0.01	1
Snrpel1	0.59	1.51	3.08E-03	0.05	1
Snrpg_1	5.31	39.62	0.04	NaN	1
Snx16	0.26	1.2	0.04	0.2	1
Snx18	0.17	1.13	0.04	0.23	1
Snx2	0.32	1.25	5.95E-03	0.07	1
Snx21	-0.26	-1.2	0.05	0.24	1
Snx33	-0.39	-1.31	7.52E-03	0.08	1
Snx6	0.22	1.16	6.16E-03	0.07	1
Socs3	1.17	2.26	2.76E-06	2.72E-04	0.05
Socs4	0.21	1.16	0.02	0.14	1
Sod2	0.28	1.21	2.61E-04	9.06E-03	1
Sorbs2	0.4	1.32	9.80E-03	0.09	1
Sorl1	-0.2	-1.15	8.30E-03	0.09	1
Sowaha	-1.43	-2.7	0.04	0.21	1
Sox10	-0.29	-1.22	0.01	0.12	1
Sox13	-0.4	-1.32	4.29E-03	0.06	1
Sox18	-1.1	-2.14	0.01	0.1	1
Sox3	-1.13	-2.19	0.04	0.23	1
Spart	0.19	1.14	0.03	0.17	1
Spata17	-1.57	-2.96	0.02	0.14	1
Spata24	-1.07	-2.09	0.03	0.18	1
Spata32	-1.94	-3.84	3.03E-04	0.01	1
Spata5	0.3	1.23	0.03	0.19	1
Spata5l1	-0.76	-1.7	0.04	0.23	1
Spcs1	-0.19	-1.14	0.05	0.23	1
Spcs3	0.33	1.26	5.90E-03	0.07	1
Speg	-0.33	-1.26	0.02	0.12	1
Spem1	-0.77	-1.7	0.04	0.23	1
Sphk1	-0.44	-1.36	0.03	0.18	1
Sphk2	-0.51	-1.43	8.49E-05	4.16E-03	1
Sphkap	0.2	1.15	0.02	0.13	1
Spint1	-0.94	-1.91	9.71E-03	0.09	1
Spns1	-0.34	-1.26	0.01	0.11	1
Spns2	-0.47	-1.38	0.02	0.14	1

Spopl	0.3	1.23	0.03	0.19	1
Spp1	0.47	1.39	2.67E-05	1.70E-03	0.5
Spred1	0.29	1.22	3.47E-04	0.01	1
Spryd3	-0.16	-1.12	0.05	0.24	1
Sptbn4	-0.25	-1.19	0.04	0.23	1
Srebf1	-0.37	-1.29	3.09E-03	0.05	1
Srgap1	0.23	1.18	3.32E-03	0.05	1
Srgn	-0.41	-1.33	0.05	0.23	1
Sri	0.18	1.13	0.03	0.17	1
Srp14	0.34	1.27	3.67E-03	0.05	1
Srsf10	0.26	1.2	0.03	0.19	1
Srsf11	0.18	1.14	0.04	0.22	1
Srsf12	-0.65	-1.57	0.02	0.15	1
Srsf6	0.21	1.15	0.01	0.1	1
Ss18l2	-0.39	-1.31	0.04	0.23	1
Ssb	0.43	1.34	1.25E-07	1.95E-05	2.36E-03
Ssbp4	-0.35	-1.27	0.01	0.11	1
Ssr1	0.19	1.14	0.02	0.13	1
Ssr3	0.31	1.24	1.67E-04	6.87E-03	1
Ssrp1	0.16	1.12	0.05	0.24	1
Ssx2ip	0.41	1.33	5.82E-04	0.02	1
St7l	0.33	1.26	6.56E-04	0.02	1
Stab1	-0.51	-1.42	1.11E-04	5.10E-03	1
Stag1	0.27	1.21	2.26E-03	0.04	1
Stag2	0.28	1.22	5.17E-04	0.01	1
Stap1	1.27	2.41	0.02	0.16	1
Stat5a	-0.37	-1.3	0.04	0.22	1
Stc1	0.7	1.63	0.04	0.2	1
Steap4	0.32	1.25	0.02	0.13	1
Stk32a	0.83	1.77	6.47E-03	0.07	1
Stmn1	0.32	1.25	4.83E-05	2.63E-03	0.91
Stmn2	0.37	1.29	9.44E-04	0.02	1
Stoml2	-0.29	-1.22	0.04	0.2	1
Stpg2	1.2	2.3	0.01	0.1	1
Stra6	-0.8	-1.74	7.25E-03	0.08	1
Strada	-0.34	-1.27	0.02	0.12	1
Strbp	0.18	1.13	0.02	0.16	1
Strn3	0.18	1.14	0.03	0.18	1
Sts	-0.39	-1.31	0.02	0.14	1

Stx11	0.37	1.29	0.02	0.16	1
Stx17	0.36	1.28	7.25E-03	0.08	1
Stx3	1.03	2.04	1.20E-07	1.89E-05	2.26E-03
Stx7	0.23	1.17	3.06E-03	0.05	1
Sub1_2	0.31	1.24	6.80E-03	0.08	1
Sucla2	0.24	1.18	0.04	0.21	1
Suco	0.21	1.16	0.01	0.1	1
Sult1a1	-0.47	-1.38	0.01	0.12	1
Sult2b1	-0.88	-1.84	0.02	0.16	1
Sumo1	0.27	1.2	0.03	0.17	1
Sun2	-0.18	-1.13	0.03	0.18	1
Supt6h	0.19	1.14	0.01	0.11	1
Suz12	0.29	1.22	5.85E-04	0.02	1
Sv2a	-0.39	-1.31	0.01	0.1	1
Svip	0.21	1.15	0.01	0.1	1
Svop	-0.3	-1.23	0.03	0.18	1
Swt1	0.28	1.21	0.04	0.2	1
Sycp2	0.86	1.81	0.02	0.15	1
Sympk	-0.2	-1.15	0.02	0.13	1
Syn3	-0.34	-1.27	6.33E-03	0.07	1
Syncrip	0.28	1.22	4.04E-04	0.01	1
Synpr	0.33	1.26	3.53E-03	0.05	1
Syp	-0.2	-1.15	8.31E-03	0.09	1
Syt12	-0.5	-1.41	0.04	0.2	1
Sytl2	0.21	1.16	7.01E-03	0.08	1
Syvn1	-0.33	-1.26	8.61E-03	0.09	1
Tacstd2	3.11	8.61	0.03	NaN	1
Taf11	-0.45	-1.37	1.57E-03	0.03	1
Taf12	0.36	1.28	7.42E-03	0.08	1
Taf6	-0.23	-1.17	0.03	0.17	1
Tafa2	-0.23	-1.17	0.02	0.13	1
Tafa4	0.59	1.5	9.51E-03	0.09	1
Taok1	0.28	1.21	3.19E-04	0.01	1
Tardbp	0.16	1.12	0.04	0.22	1
Tars2	-0.44	-1.36	1.86E-03	0.03	1
Tasor	0.26	1.2	1.70E-03	0.03	1
Tax1bp1	0.19	1.14	0.01	0.12	1
Tbc1d13	-0.18	-1.13	0.05	0.23	1
Tbcc	-0.52	-1.43	8.22E-04	0.02	1

Tbl1xr1	0.25	1.19	1.94E-03	0.03	1
Tbpl1_1	0.31	1.24	0.02	0.16	1
Tbx3	-0.37	-1.29	0.01	0.1	1
Tc2n	0.55	1.46	3.64E-03	0.05	1
Tcea2	-0.29	-1.23	0.02	0.14	1
Tceal8	0.19	1.14	0.03	0.17	1
Tceal9	0.3	1.23	0.01	0.12	1
Tcf21	2.89	7.42	0.04	NaN	1
Tcf7l1	-0.34	-1.27	0.01	0.11	1
Tdrd12	0.75	1.68	2.09E-03	0.04	1
Tdrd3	0.28	1.21	3.03E-03	0.05	1
Tdrd5	1.13	2.19	0.03	0.18	1
Tecr	-0.23	-1.17	0.04	0.23	1
Tectb	2.51	5.71	0.03	NaN	1
Tedc1	-0.67	-1.59	2.37E-03	0.04	1
Tenm1	0.42	1.34	7.21E-04	0.02	1
Tenm2	-0.33	-1.25	6.38E-03	0.07	1
Tes	0.3	1.23	0.01	0.12	1
Tex264	-0.4	-1.32	1.63E-03	0.03	1
Tf	-0.31	-1.24	0.01	0.11	1
Tfeb	-0.56	-1.48	0.01	0.12	1
Tfrc	0.22	1.16	5.70E-03	0.07	1
Tgm1	1.72	3.29	0.04	NaN	1
Tgm2	-0.38	-1.31	7.16E-03	0.08	1
Tgs1	0.29	1.22	0.04	0.2	1
Thbs4	-0.34	-1.27	0.01	0.1	1
Them6	-0.32	-1.24	8.98E-03	0.09	1
Thoc1	0.47	1.39	3.28E-04	0.01	1
Thoc2	0.36	1.28	1.13E-05	8.46E-04	0.21
Thoc2l	0.21	1.16	0.01	0.12	1
Thoc7	0.33	1.26	0.01	0.1	1
Thtpa	-0.19	-1.14	0.05	0.24	1
Ticam2	0.89	1.85	0.04	0.22	1
Tifa	0.47	1.39	4.58E-03	0.06	1
Timm50	-0.41	-1.33	4.16E-03	0.06	1
Tipin	0.38	1.3	0.04	0.21	1
Tlcd2	-2.46	-5.51	0.03	NaN	1
Tlcd3b	-0.49	-1.4	1.55E-09	4.91E-07	2.91E-05
Tle5	-0.15	-1.11	0.04	0.23	1

Tlr4	0.33	1.26	0.03	0.2	1
Tlx2	-0.31	-1.24	0.02	0.15	1
Tlx3	-0.27	-1.21	0.05	0.24	1
Tm2d2	-0.29	-1.22	0.02	0.14	1
Tm9sf3	0.29	1.23	2.11E-04	8.05E-03	1
Tma7	0.22	1.16	9.06E-03	0.09	1
Tmem106b	0.28	1.21	0.02	0.16	1
Tmem129	-0.33	-1.25	0.03	0.18	1
Tmem132e	-0.21	-1.16	0.01	0.11	1
Tmem143	-0.44	-1.36	2.73E-03	0.04	1
Tmem150c	-0.19	-1.14	0.03	0.18	1
Tmem158	-0.83	-1.78	3.24E-03	0.05	1
Tmem159	0.5	1.41	4.52E-04	0.01	1
Tmem163	-0.39	-1.31	8.32E-03	0.09	1
Tmem175	-0.39	-1.31	0.01	0.1	1
Tmem176a	0.25	1.19	1.25E-03	0.03	1
Tmem178a	-0.71	-1.64	0.05	0.24	1
Tmem179	-0.32	-1.25	6.01E-04	0.02	1
Tmem184b	-0.27	-1.2	1.35E-03	0.03	1
Tmem196	-0.54	-1.45	0.04	0.22	1
Tmem205	-0.54	-1.46	6.92E-03	0.08	1
Tmem229a	-0.5	-1.42	4.18E-04	0.01	1
Tmem25	-0.51	-1.42	1.64E-04	6.79E-03	1
Tmem256	-0.61	-1.53	2.39E-03	0.04	1
Tmem26	1.03	2.04	2.00E-09	6.05E-07	3.76E-05
Tmem33	0.2	1.15	0.01	0.1	1
Tmem41b	0.16	1.12	0.05	0.24	1
Tmem42	-0.51	-1.42	0.01	0.12	1
Tmem59l	-0.31	-1.24	2.91E-04	9.79E-03	1
Tmem63b	-0.19	-1.14	0.02	0.12	1
Tmem64	-0.81	-1.76	0.01	0.12	1
Tmem65	0.26	1.2	1.15E-03	0.02	1
Tmem88	-1.18	-2.27	5.14E-03	0.06	1
Tmem8b	-0.44	-1.36	5.22E-04	0.01	1
Tmf1	0.22	1.17	5.03E-03	0.06	1
Tmlhe	0.34	1.27	0.04	0.21	1
Tmod2	0.21	1.16	6.76E-03	0.08	1
Tmprss11f	1.06	2.09	0.02	0.13	1
Tmtc2	0.25	1.19	4.27E-03	0.06	1

Tmtc3	0.27	1.21	0.03	0.16	1
Tmub1	-0.44	-1.36	0.03	0.19	1
Tmx1	0.29	1.22	7.67E-04	0.02	1
Tmx3	0.26	1.2	0.03	0.17	1
Tmx4	0.21	1.16	7.05E-03	0.08	1
Tnfaip1	0.17	1.12	0.05	0.24	1
Tnfaip8l3	1.29	2.44	1.97E-03	0.04	1
Tnfrsf21	0.23	1.17	0.05	0.23	1
Tnfrsf9	1.03	2.05	0.03	0.18	1
Tnfsf12	-0.54	-1.45	9.32E-03	0.09	1
Tnik	0.6	1.52	2.57E-07	3.67E-05	4.84E-03
Tnk2	-0.23	-1.17	6.42E-03	0.07	1
Tnks2	0.16	1.12	0.04	0.22	1
Tnnt1	1.8	3.49	3.56E-03	0.05	1
Tnpo1	0.25	1.19	1.78E-03	0.03	1
Tns1	-0.23	-1.17	0.04	0.22	1
Togaram1	0.31	1.24	2.25E-04	8.27E-03	1
Tom1l1	0.35	1.27	0.03	0.18	1
Tomm20	0.24	1.18	3.60E-03	0.05	1
Tomm40	-0.33	-1.26	0.01	0.1	1
Tomm5	-0.2	-1.15	0.03	0.18	1
Tomm70	0.26	1.2	5.85E-04	0.02	1
Top1	0.24	1.18	3.59E-03	0.05	1
Top2a	0.54	1.45	7.10E-03	0.08	1
Top2b	0.21	1.15	0.01	0.1	1
Tor1aip2_2	0.26	1.2	7.10E-03	0.08	1
Tox2	-0.37	-1.29	7.05E-03	0.08	1
Tp53i13	-0.88	-1.84	0.02	0.13	1
Tp53inp2	-0.26	-1.2	2.13E-03	0.04	1
Tpbgl	-0.5	-1.41	0.02	0.14	1
Tpcn1	-0.41	-1.33	1.01E-06	1.16E-04	0.02
Tpgs1	-0.33	-1.25	0.04	0.22	1
Tph2	0.44	1.36	0.01	0.1	1
Tpm1	0.24	1.18	1.91E-03	0.03	1
Tpp2	0.28	1.21	4.71E-04	0.01	1
Tpr	0.25	1.19	1.17E-03	0.02	1
Tpra1	-0.35	-1.27	0.02	0.13	1
Tradd	-1.13	-2.19	6.92E-04	0.02	1
Trafd1	0.19	1.14	0.04	0.22	1

Tram1	0.17	1.12	0.05	0.23	1
Trappc14	-0.29	-1.22	0.02	0.13	1
Trappc2	0.24	1.18	3.72E-03	0.05	1
Trhr	1.16	2.24	0.04	0.23	1
Trim13	0.28	1.22	0.04	0.21	1
Trim24	0.25	1.19	6.09E-03	0.07	1
Trim54	1.76	3.39	0.01	NaN	1
Trim56	0.33	1.26	6.14E-03	0.07	1
Trim59	0.61	1.53	0.02	0.15	1
Trim67	-0.42	-1.34	2.75E-03	0.04	1
Trim8	-0.21	-1.16	0.02	0.12	1
Trip10	-0.35	-1.27	5.84E-03	0.07	1
Trip11	0.2	1.15	0.01	0.1	1
Trmt13	0.59	1.51	5.66E-03	0.07	1
Trpa1	0.69	1.61	7.75E-09	1.76E-06	1.46E-04
Trpm1	2.33	5.01	0.05	NaN	1
Trpm3	0.22	1.17	4.04E-03	0.06	1
Trpm7	0.22	1.16	6.59E-03	0.07	1
Tsc2	-0.18	-1.13	0.05	0.23	1
Tsc22d4	-0.29	-1.22	0.03	0.18	1
Tsfm	-0.53	-1.44	4.67E-04	0.01	1
Tshz2	0.2	1.15	0.01	0.1	1
Tspan12	0.25	1.19	0.03	0.19	1
Tspan13	0.27	1.21	8.84E-04	0.02	1
Tspan2	0.5	1.41	4.16E-05	2.39E-03	0.78
Tspyl4	-0.2	-1.15	8.71E-03	0.09	1
Tst	-0.61	-1.52	1.46E-03	0.03	1
Ttbk2	0.17	1.13	0.03	0.17	1
Ttc28	-0.33	-1.25	0.01	0.11	1
Ttc3	0.23	1.17	0.04	0.23	1
Ttc37	0.22	1.17	5.58E-03	0.07	1
Ttc9b	-0.34	-1.26	0.03	0.18	1
Tti1	-0.31	-1.24	0.02	0.15	1
Tuba4a	-0.18	-1.13	0.02	0.14	1
Tuba8	-0.74	-1.67	0.04	0.22	1
Tubb6	0.64	1.56	3.58E-04	0.01	1
Tubg1	-0.41	-1.33	8.21E-06	6.71E-04	0.15
Tubg2	-0.43	-1.34	5.30E-03	0.07	1
Twf1	0.38	1.3	1.63E-03	0.03	1

Txndc5	-0.27	-1.21	0.03	0.17	1
Txndc9	0.4	1.32	1.48E-03	0.03	1
Txnip	-0.32	-1.25	7.03E-03	0.08	1
Txnrd1	0.2	1.15	0.01	0.1	1
Tysnd1	-0.47	-1.38	0.04	0.21	1
U2surp	0.22	1.17	6.63E-03	0.08	1
Uba3	0.19	1.14	0.02	0.16	1
Uba6	0.23	1.17	4.30E-03	0.06	1
Ubac2	-0.34	-1.27	0.01	0.12	1
Ubald1	-0.28	-1.21	0.04	0.21	1
Ubash3a	-3.27	-9.62	3.83E-03	NaN	1
Ube2d1	0.21	1.15	0.03	0.19	1
Ube2d2	0.16	1.12	0.04	0.22	1
Ube2d3	0.19	1.14	0.01	0.12	1
Ube2g1	0.31	1.24	0.01	0.1	1
Ube2h	0.18	1.14	0.02	0.15	1
Ube2k	0.25	1.19	1.52E-03	0.03	1
Ube2o	-0.23	-1.18	2.72E-03	0.04	1
Ube2q2	0.24	1.18	0.04	0.23	1
Ube2ql1	-0.38	-1.3	3.20E-03	0.05	1
Ube2s	-0.33	-1.26	0.01	0.11	1
Ube3a	0.17	1.13	0.03	0.18	1
Ube3b	-0.26	-1.2	1.09E-03	0.02	1
Ube4a	0.19	1.14	0.01	0.12	1
Ubl4a	-0.39	-1.31	0.03	0.17	1
Ubl7	-0.47	-1.38	1.73E-04	7.03E-03	1
Ubqln4	-0.31	-1.24	0.01	0.12	1
Ubxn8	0.35	1.28	0.01	0.12	1
Uchl5	0.29	1.23	0.02	0.16	1
Ucn	4.94	30.61	0.04	NaN	1
Ugdh	0.3	1.23	0.03	0.18	1
Ugp2	0.29	1.22	0.02	0.13	1
Ulk1	-0.25	-1.19	0.04	0.23	1
Unc13c	0.3	1.23	0.01	0.11	1
Unc13d	-0.79	-1.73	0.01	0.11	1
Unc50	-0.33	-1.26	0.02	0.13	1
Upf3b	0.33	1.25	0.01	0.12	1
Uprt	0.27	1.2	0.03	0.18	1
Uqcr10	-0.21	-1.16	0.03	0.17	1

Uqcrb_2	-0.2	-1.15	0.02	0.12	1
Uqcrc2	0.16	1.12	0.05	0.23	1
Uri1	0.26	1.19	6.64E-03	0.08	1
Usp1	0.28	1.21	0.05	0.24	1
Usp14	0.36	1.28	1.65E-03	0.03	1
Usp15	0.17	1.13	0.03	0.18	1
Usp16	0.35	1.28	6.39E-03	0.07	1
Usp19	-0.24	-1.18	4.60E-03	0.06	1
Usp20	-0.18	-1.13	0.03	0.18	1
Usp21	-0.41	-1.33	7.66E-03	0.08	1
Usp25	0.26	1.2	1.72E-03	0.03	1
Usp32	0.19	1.14	0.01	0.11	1
Usp33	0.35	1.28	7.24E-06	6.29E-04	0.14
Usp34	0.19	1.14	0.01	0.12	1
Usp45	0.18	1.13	0.04	0.22	1
Usp9x	0.24	1.18	0.03	0.2	1
Ust	-0.38	-1.3	2.40E-03	0.04	1
Vasn	-0.58	-1.49	3.47E-03	0.05	1
Vom2r18	2.96	7.79	9.47E-03	NaN	1
Vom2r44	0.6	1.52	0.03	0.18	1
Vps13a	0.3	1.23	1.17E-04	5.29E-03	1
Vps13c	0.25	1.19	8.12E-04	0.02	1
Vps25	-0.23	-1.17	6.27E-03	0.07	1
Vps35	0.23	1.17	3.01E-03	0.05	1
Vps4b	0.16	1.12	0.05	0.24	1
Vstm2a	-0.32	-1.25	0.04	0.21	1
Vstm2l	-0.47	-1.38	1.43E-03	0.03	1
Vwa7	-0.36	-1.28	8.59E-06	6.94E-04	0.16
Vwa8	-0.17	-1.12	0.05	0.23	1
Wac	0.23	1.17	3.88E-03	0.05	1
Wapl	0.19	1.14	0.02	0.16	1
Washc4	0.24	1.18	2.50E-03	0.04	1
Wbp1l	-0.23	-1.17	0.01	0.11	1
Wbp2	-0.27	-1.21	0.02	0.13	1
Wbp4	0.24	1.18	4.89E-03	0.06	1
Wdr1	0.18	1.13	0.02	0.15	1
Wdr12	0.33	1.26	0.03	0.17	1
Wdr35	0.28	1.21	0.03	0.19	1
Wdr44	0.18	1.13	0.04	0.21	1

Wdr46	-0.3	-1.23	0.04	0.21	1
Wdr90	-0.52	-1.43	0.04	0.21	1
Wdtc1	-0.24	-1.18	0.05	0.24	1
Wipf2	-0.5	-1.42	4.11E-04	0.01	1
Wiz	-0.27	-1.2	0.03	0.19	1
Wrn	0.22	1.16	0.02	0.15	1
Xdh	0.49	1.4	0.02	0.12	1
Xiap	0.26	1.19	4.29E-03	0.06	1
Xkr4	0.3	1.23	0.03	0.2	1
Xpo1	0.28	1.22	3.54E-04	0.01	1
Yars2	-0.68	-1.61	0.01	0.11	1
Yif1b	-0.5	-1.42	2.49E-04	8.79E-03	1
Yme1l1	0.29	1.23	2.18E-04	8.12E-03	1
Ypel3	-0.38	-1.3	1.24E-03	0.03	1
Ythdc2	0.45	1.37	2.36E-04	8.48E-03	1
Ythdf3	0.26	1.2	1.32E-03	0.03	1
Zbed4	0.41	1.32	3.53E-03	0.05	1
Zbp1	1.24	2.37	0.03	0.19	1
Zbtb33	0.28	1.21	0.03	0.2	1
Zbtb38	0.29	1.22	3.08E-04	0.01	1
Zbtb4	-0.18	-1.13	0.03	0.18	1
Zbtb6	0.28	1.22	0.03	0.19	1
Zbtb7a	-0.29	-1.22	0.02	0.15	1
Zc3h10	0.19	1.14	0.02	0.13	1
Zc3h11a	0.17	1.12	0.03	0.17	1
Zc3h14	0.28	1.21	9.37E-04	0.02	1
Zc3h15	0.25	1.19	0.03	0.19	1
Zc3h7a	0.26	1.19	0.04	0.22	1
Zc4h2	0.3	1.23	0.03	0.17	1
Zcchc18	0.2	1.15	9.23E-03	0.09	1
Zcchc7	0.27	1.2	4.39E-03	0.06	1
Zdbf2	0.72	1.64	7.08E-03	0.08	1
Zdhhc20	0.35	1.28	4.59E-03	0.06	1
Zdhhc8	-0.45	-1.37	2.81E-04	9.54E-03	1
Zeb1	0.23	1.17	4.21E-03	0.06	1
Zer1	-0.34	-1.26	4.48E-04	0.01	1
Zfand3	-0.2	-1.15	0.02	0.15	1
Zfand5	0.25	1.19	1.96E-03	0.04	1
Zfand6	0.27	1.21	0.03	0.18	1

Zfc3h1	0.23	1.18	3.72E-03	0.05	1
Zfhx4	0.25	1.19	0.05	0.23	1
Zfp133	0.35	1.28	0.01	0.11	1
Zfp148	0.17	1.13	0.04	0.23	1
Zfp160	0.32	1.25	0.01	0.12	1
Zfp229	0.34	1.27	9.87E-03	0.1	1
Zfp26	0.25	1.19	5.01E-03	0.06	1
Zfp280c	0.39	1.31	3.53E-03	0.05	1
Zfp280d	0.29	1.22	0.02	0.14	1
Zfp292	0.2	1.15	0.02	0.13	1
Zfp317	0.26	1.2	0.05	0.24	1
Zfp322a	0.38	1.3	3.34E-03	0.05	1
Zfp329	0.3	1.23	0.02	0.14	1
Zfp330	0.31	1.24	0.03	0.17	1
Zfp347	0.24	1.18	3.52E-03	0.05	1
Zfp367	0.71	1.64	8.96E-08	1.50E-05	1.68E-03
Zfp384	-0.25	-1.19	8.56E-03	0.09	1
Zfp385a	-0.45	-1.37	2.09E-04	8.02E-03	1
Zfp386	0.39	1.31	1.16E-03	0.02	1
Zfp39	0.35	1.28	0.05	0.24	1
Zfp423	-0.38	-1.3	2.71E-03	0.04	1
Zfp451	0.23	1.17	6.03E-03	0.07	1
Zfp51_1	0.46	1.38	6.52E-03	0.07	1
Zfp512b	-0.36	-1.29	7.25E-03	0.08	1
Zfp52	0.49	1.41	4.49E-03	0.06	1
Zfp53	0.4	1.32	0.03	0.18	1
Zfp54	0.51	1.42	1.77E-04	7.13E-03	1
Zfp541	-1.67	-3.18	0.03	NaN	1
Zfp563	0.39	1.31	0.03	0.2	1
Zfp583	0.36	1.28	0.02	0.16	1
Zfp605	0.42	1.34	2.23E-03	0.04	1
Zfp606	0.34	1.26	0.01	0.12	1
Zfp612	0.18	1.14	0.03	0.18	1
Zfp62	0.3	1.23	0.02	0.12	1
Zfp622	0.29	1.22	1.79E-04	7.15E-03	1
Zfp655	0.27	1.2	2.26E-03	0.04	1
Zfp667	0.4	1.32	0.05	0.23	1
Zfp668	-0.49	-1.41	0.04	0.23	1
Zfp703	-0.26	-1.2	0.05	0.24	1

Zfp709l1	0.31	1.24	0.01	0.1	1
Zfp712	0.48	1.4	1.61E-04	6.75E-03	1
Zfp729a	0.45	1.37	4.48E-04	0.01	1
Zfp748_1	0.27	1.2	0.05	0.23	1
Zfp748_2	0.36	1.28	2.14E-04	8.08E-03	1
Zfp758	0.47	1.38	3.65E-03	0.05	1
Zfp770	0.28	1.21	0.03	0.19	1
Zfp771	-0.34	-1.27	0.01	0.1	1
Zfp780b	0.32	1.25	0.02	0.16	1
Zfp810	0.24	1.18	0.04	0.22	1
Zfp846	0.25	1.19	0.04	0.21	1
Zfp87	0.41	1.33	7.27E-03	0.08	1
Zfp871	0.16	1.11	0.04	0.23	1
Zfp875	0.31	1.24	0.02	0.14	1
Zfp91	0.21	1.16	7.54E-03	0.08	1
Zfp938	0.37	1.3	0.01	0.1	1
Zfp943	0.45	1.37	1.70E-03	0.03	1
Zfp949	0.42	1.34	2.27E-03	0.04	1
Zfp950	0.35	1.27	9.90E-03	0.1	1
Zfp955a	0.4	1.32	0.01	0.1	1
Zfp958_1	0.31	1.24	1.41E-03	0.03	1
Zfp958l1	0.34	1.27	0.04	0.2	1
Zfpm1	-0.33	-1.26	0.02	0.16	1
Zfr2	-0.31	-1.24	0.03	0.18	1
Zfta	-0.45	-1.36	1.08E-03	0.02	1
Zfx	0.26	1.2	0.03	0.2	1
Zhx1	0.26	1.19	1.27E-03	0.03	1
Zmiz2	-0.32	-1.25	6.63E-03	0.08	1
Zmym5	0.34	1.27	6.66E-03	0.08	1
Zmynd11	0.18	1.13	0.03	0.18	1
Znfx1	0.17	1.12	0.04	0.23	1
Znhit2	-0.39	-1.31	0.05	0.24	1
Znrd2	-0.33	-1.26	0.01	0.11	1
Zscan26	0.18	1.13	0.04	0.22	1
Zswim1	-0.47	-1.39	0.01	0.1	1
Zswim8	-0.28	-1.21	9.92E-04	0.02	1
Zw10	0.35	1.27	8.80E-03	0.09	1
Zyx	-0.35	-1.27	6.56E-03	0.07	1

Table A3.7. Master list of differentially expressed genes between Male CCI vs Naïve samples with a p-value ≤ 0.05 and a fold change greater than ±1

Name	Log_2 fold change	Fold change	P-value	FDR p-value	Bonferroni
1500009L16Rik	-0.32	-1.25	0.05	0.54	1
A3galt2	0.15	1.11	0.04	0.5	1
AABR07007905.2	-2.48	-5.57	0.03	0.44	1
AABR07015812.1	-0.17	-1.13	0.04	0.49	1
AABR07017902.1	1.62	3.08	0.01	0.27	1
AABR07028769.1	-0.22	-1.16	2.54E-03	0.11	1
AABR07030861.1	-0.37	-1.29	2.78E-03	0.12	1
AABR07041778.1	0.46	1.37	0.02	0.36	1
AABR07045032.1	-0.7	-1.62	0.03	0.44	1
AABR07051787.1	0.42	1.34	9.40E-03	0.25	1
AABR07057196.1	0.83	1.78	1.29E-04	0.01	1
AABR07059632.3	0.32	1.25	0.03	0.43	1
AABR07060610.1	2.85	7.23	1.22E-05	1.91E-03	0.23
AABR07062138.2	0.96	1.95	0.02	0.39	1
AABR07062154.1	-1.11	-2.16	0.02	0.36	1
AABR07071000.1	-1.14	-2.2	3.96E-04	0.03	1
AABR07071198.1	1.44	2.71	0.02	0.42	1
Abcb9	-0.4	-1.32	7.10E-04	0.04	1
Abcg3	2.2	4.6	0.02	0.36	1
Abi3bp	0.24	1.18	0.02	0.4	1
AC121415.1	0.82	1.77	0.05	0.54	1
AC129365.1	2.04	4.12	2.48E-04	0.02	1
Acbd4	-0.38	-1.31	0.04	0.52	1
Ace2	0.72	1.65	4.55E-06	8.62E-04	0.09
Acer2	-0.47	-1.39	5.76E-03	0.18	1
Ackr3	0.54	1.45	6.36E-05	7.16E-03	1
Acrbp	-0.33	-1.26	0.01	0.31	1
Actn2	-1.57	-2.97	1.16E-04	0.01	1
Adamts1	0.38	1.3	1.09E-03	0.06	1
Adamts20	-0.35	-1.27	2.43E-05	3.32E-03	0.46
Adamts5	0.24	1.18	1.84E-03	0.09	1
Adamtsl1	-0.36	-1.28	2.89E-03	0.12	1
Adamtsl3	0.36	1.28	2.32E-03	0.1	1
Adgrb1	-0.24	-1.18	4.73E-03	0.16	1

Adgre1	0.4	1.32	0.03	0.48	1
Adgrf1	2.33	5.03	1.28E-03	0.07	1
Adhfe1	-0.81	-1.76	0.04	0.53	1
Ado	-0.29	-1.22	2.57E-04	0.02	1
Adprh	-0.27	-1.2	0.03	0.44	1
Adra1a	-0.55	-1.47	0.02	0.35	1
Adrm1	-0.2	-1.15	0.02	0.33	1
Adssl1	-1.26	-2.4	4.41E-03	0.16	1
Afdn	0.19	1.14	0.01	0.26	1
Akap5	0.82	1.77	3.55E-03	0.14	1
Aldh1a2	1.33	2.52	6.97E-09	4.15E-06	1.32E-04
Alpk3	-1.5	-2.83	1.28E-03	0.07	1
Ampd1	-1.52	-2.87	6.09E-04	0.04	1
Ankrd23	-1.2	-2.3	3.42E-03	0.13	1
Ankrd33b	0.66	1.58	0.03	0.45	1
Ankrd60	1.14	2.21	0.02	0.35	1
Ankrd63	3.19	9.13	0.02	0.37	1
Ano1	-0.34	-1.27	0.03	0.46	1
Ano5	-0.9	-1.86	0.05	0.54	1
Ano7	-3.01	-8.04	0.03	0.45	1
Ano8	-0.16	-1.12	0.05	0.55	1
Anxa3	0.42	1.33	0.02	0.35	1
Anxa8	0.99	1.99	3.95E-05	4.81E-03	0.75
Aox4	0.31	1.24	0.02	0.35	1
Aplnr	0.59	1.51	4.90E-03	0.17	1
Apobec1	0.94	1.91	0.03	0.46	1
Apobec2	-1.04	-2.05	0.04	0.52	1
Apoe	-0.15	-1.11	0.03	0.44	1
Apol3	0.87	1.83	0.01	0.26	1
Arc	-0.73	-1.66	0.04	0.52	1
Arhgap10	0.2	1.15	0.02	0.37	1
Arhgap19	-0.2	-1.15	0.01	0.3	1
Arhgap20	0.3	1.23	0.03	0.44	1
Arhgap25	0.43	1.34	0.02	0.41	1
Arhgap29	0.49	1.41	1.62E-05	2.37E-03	0.31
Arhgap39	-0.28	-1.22	9.37E-05	9.73E-03	1
Arhgef10	-0.16	-1.11	0.03	0.48	1
Arhgef18	0.33	1.25	0.04	0.49	1
Arid5b	0.17	1.12	0.05	0.54	1

Armh4	0.17	1.13	0.03	0.48	1
Arntl	0.38	1.3	0.02	0.32	1
Arpp21	-0.19	-1.14	0.03	0.45	1
Arsi	1.23	2.35	2.59E-03	0.11	1
Arvcf	-0.21	-1.15	0.01	0.31	1
Asap3	0.39	1.31	3.31E-03	0.13	1
Aspn	0.95	1.93	2.13E-03	0.1	1
Atp10d	0.38	1.3	3.81E-03	0.14	1
Atp9b	0.15	1.11	0.04	0.5	1
Atpaf1	-0.19	-1.14	0.02	0.41	1
Avpr1b	-1.48	-2.79	0.02	0.33	1
Azin1	-0.27	-1.21	8.33E-05	9.00E-03	1
B2m	0.16	1.11	0.02	0.38	1
B3galt5	-0.56	-1.47	6.92E-06	1.22E-03	0.13
B9d1	-0.41	-1.32	0.04	0.52	1
Bcar3	-0.21	-1.16	0.03	0.46	1
Bcdin3d	-0.47	-1.38	0.05	0.54	1
Bcl2a1	1.05	2.07	6.97E-03	0.21	1
Bcl2l1	-0.35	-1.27	1.88E-05	2.68E-03	0.36
Bcl2l15	1.96	3.89	0.03	0.45	1
Bglap	-1.22	-2.33	0.04	0.49	1
Bloc1s3	-0.53	-1.44	0.03	0.47	1
Bmp3	0.91	1.88	0.02	0.39	1
Bmp5	0.44	1.35	0.01	0.26	1
Bnc2	0.38	1.3	2.79E-06	5.70E-04	0.05
Boc	0.37	1.29	1.80E-03	0.09	1
Bscl2	0.25	1.19	0.03	0.42	1
Btbd16	-1.1	-2.14	0.01	0.29	1
Btbd17	-1.95	-3.87	9.70E-03	0.25	1
Btn2a2	1.24	2.36	0.03	0.49	1
C1qa	0.44	1.36	0.02	0.33	1
C1qtnf7	1.07	2.09	0.05	0.55	1
C1r	0.25	1.19	0.02	0.36	1
C4b	0.46	1.37	0.03	0.44	1
Ca3	-0.99	-1.99	1.09E-05	1.75E-03	0.21
Cables1	-0.36	-1.29	6.09E-03	0.19	1
Cables2	-0.16	-1.11	0.04	0.49	1
Cacna1f	-1.31	-2.49	0.05	0.54	1
Cacna1s	-1.62	-3.08	9.75E-06	1.63E-03	0.18

Cacng4	-0.23	-1.17	9.29E-03	0.25	1
Cadm4	-0.31	-1.24	1.74E-05	2.52E-03	0.33
Camk1d	-0.18	-1.13	0.03	0.43	1
Capn10	-0.35	-1.27	0.01	0.31	1
Card6	0.33	1.26	7.15E-03	0.21	1
Casq1	-1.32	-2.5	9.05E-06	1.53E-03	0.17
Cass4	1.25	2.37	0.01	0.31	1
Cbfa2t3	0.47	1.39	0.02	0.38	1
Ccdc28b	-0.91	-1.88	0.04	0.5	1
Ccdc3	0.85	1.8	1.91E-05	2.69E-03	0.36
Ccdc39	0.42	1.33	0.02	0.34	1
Ccl4	2.12	4.34	0.01	0.3	1
Ccn4	-0.28	-1.21	0.03	0.44	1
Ccr2	0.83	1.78	1.91E-03	0.09	1
Ccr5	0.41	1.33	0.04	0.51	1
Ccr7	1.67	3.18	0.04	0.53	1
Cd101	0.97	1.96	0.01	0.29	1
Cd163	-0.83	-1.78	1.08E-05	1.75E-03	0.2
Cd226	1.31	2.47	3.73E-03	0.14	1
Cd34	0.34	1.27	5.36E-03	0.18	1
Cd6	1.21	2.32	0.04	0.51	1
Cd79b	-1.18	-2.27	0.02	0.36	1
Cd93	0.32	1.25	0.01	0.28	1
Cdh1	-0.15	-1.11	0.03	0.43	1
Cdh11	0.2	1.15	5.46E-03	0.18	1
Cdh15	-0.42	-1.34	1.28E-04	0.01	1
Cdh3	0.33	1.26	7.71E-03	0.22	1
Cdk9	-0.31	-1.24	9.11E-03	0.25	1
Cep85	-0.27	-1.21	0.03	0.44	1
Cfap100	-0.55	-1.47	7.95E-03	0.22	1
Cfap157	-1.46	-2.74	0.03	0.45	1
Cfap52	-1.34	-2.53	0.04	0.49	1
Cfd	0.97	1.95	0.02	0.38	1
Cflar	0.25	1.19	0.04	0.49	1
Chadl	-0.37	-1.29	0.03	0.44	1
Chchd2_2	-0.16	-1.11	0.03	0.48	1
Chchd4	-0.58	-1.5	3.55E-04	0.03	1
Chgb	-0.19	-1.14	7.41E-03	0.22	1
Chka	-0.19	-1.14	0.02	0.38	1

Chmp4bl1	-0.64	-1.56	0.05	0.55	1
Chn2	-0.18	-1.13	0.03	0.43	1
Chodl	-0.42	-1.34	0.01	0.31	1
Chrna5	-0.37	-1.29	0.03	0.48	1
Chrnb3	-0.26	-1.19	5.54E-04	0.04	1
Ciao1	-0.18	-1.13	0.03	0.43	1
Ciart	-1.11	-2.16	1.88E-04	0.02	1
Ckmt2	-0.71	-1.64	1.21E-03	0.07	1
Clasrp	-0.18	-1.13	0.04	0.52	1
Clcn1	-0.72	-1.65	0.04	0.49	1
Cldn11	0.51	1.42	5.01E-04	0.04	1
Clec1b	1.51	2.84	9.67E-03	0.25	1
Clec2g	0.3	1.23	3.32E-05	4.24E-03	0.63
Clec4a3	0.57	1.48	0.04	0.49	1
Cmtm6	-0.19	-1.14	0.02	0.36	1
Cnn2	0.33	1.26	8.71E-03	0.24	1
Cnot4	0.15	1.11	0.04	0.53	1
Cnp	-0.14	-1.1	0.05	0.55	1
Coch	1.24	2.36	4.87E-03	0.17	1
Col11a2	-0.37	-1.3	0.03	0.49	1
Col12a1	0.38	1.3	1.85E-04	0.02	1
Col23a1	-0.24	-1.19	0.05	0.54	1
Col24a1	-0.27	-1.21	1.28E-03	0.07	1
Col4a5	0.81	1.75	1.01E-04	0.01	1
Col9a3	-0.26	-1.19	0.04	0.53	1
Coq6	-0.31	-1.24	0.02	0.4	1
Coro1a	-0.34	-1.26	6.06E-03	0.19	1
Cox6a2	-2.48	-5.56	1.76E-07	5.24E-05	3.32E-03
Cpa2	1.11	2.16	0.04	0.51	1
Cpne7	-1.03	-2.04	4.69E-03	0.16	1
Cracd	-0.14	-1.1	0.04	0.53	1
Creb5	0.31	1.24	0.02	0.4	1
Crisp2	3.08	8.45	0.02	0.38	1
Crtapl1	0.31	1.24	0.03	0.46	1
Crybg2	1.54	2.91	0.04	0.49	1
Cryz	-0.45	-1.37	0.02	0.35	1
Csad	-0.29	-1.22	0.02	0.41	1
Csf1r	0.28	1.21	0.02	0.33	1
Csnk2b	-0.19	-1.14	0.02	0.36	1

Ctns	-0.19	-1.14	0.02	0.36	1
Ctsk	0.33	1.26	0.04	0.53	1
Ctso	0.32	1.25	0.03	0.43	1
Ctss	0.42	1.33	6.69E-04	0.04	1
Cx3cr1	0.57	1.49	0.01	0.28	1
Cxadr	0.33	1.26	7.66E-03	0.22	1
Cxcl16	0.54	1.45	2.75E-04	0.02	1
Cxcr4	0.32	1.25	0.04	0.52	1
Cybb	0.28	1.21	0.03	0.44	1
Cyp11b2	-3.14	-8.81	0.03	0.43	1
Cyp2a3	-1.8	-3.48	4.13E-03	0.15	1
Cyp7b1	0.53	1.44	0.03	0.49	1
Cysltr1	0.94	1.92	0.02	0.42	1
Cyth4	0.54	1.45	5.68E-03	0.18	1
Dab2	0.28	1.22	7.32E-04	0.05	1
Dact2	0.51	1.42	0.01	0.31	1
Dag1	-0.21	-1.16	1.79E-03	0.09	1
Dapk2	0.36	1.29	0.04	0.52	1
Dbp	-0.57	-1.49	4.28E-11	7.66E-08	8.08E-07
Dchs1	0.45	1.37	5.94E-03	0.19	1
Ddit4	-0.48	-1.39	4.60E-03	0.16	1
Ddr2	0.35	1.27	1.13E-05	1.80E-03	0.21
Ddx11	-0.51	-1.42	0.03	0.45	1
Ddx28	-0.29	-1.22	0.05	0.54	1
Ddx39b	-0.17	-1.13	0.03	0.44	1
Ddx41	-0.27	-1.2	0.04	0.5	1
Dek	0.26	1.2	2.71E-03	0.11	1
Dennd4c	0.25	1.19	1.65E-03	0.08	1
Dennd6b	-0.43	-1.34	0.01	0.31	1
Dhh	-0.19	-1.14	0.02	0.37	1
Dio2	0.56	1.48	9.43E-03	0.25	1
Dmp1	-1.87	-3.66	9.15E-04	0.05	1
Dnah11	-0.33	-1.26	0.02	0.41	1
Dnajc18	0.17	1.12	0.03	0.47	1
Dock5	0.2	1.15	3.85E-03	0.14	1
Dock6	0.28	1.22	0.01	0.3	1
Dock8	0.34	1.27	5.78E-03	0.18	1
Dpcd	-0.21	-1.16	0.01	0.31	1
Dpp4	0.52	1.43	6.85E-03	0.21	1

Dpys	1.71	3.28	0.05	0.54	1
Drg1	0.17	1.13	0.05	0.54	1
Duox2	-0.7	-1.63	0.03	0.46	1
Dusp5	-0.5	-1.42	0.02	0.33	1
Dux4	-0.56	-1.47	0.02	0.42	1
Ebf2	0.42	1.34	2.00E-03	0.09	1
Ecscr	-0.5	-1.42	0.04	0.5	1
Ect2l	1.59	3.01	0.04	0.53	1
Efna3	-0.78	-1.71	0.02	0.35	1
Efnb1	0.18	1.13	0.04	0.53	1
Efr3b	-0.22	-1.16	3.27E-03	0.13	1
Eif4enif1	0.18	1.14	0.03	0.48	1
Elf2	0.17	1.12	0.05	0.55	1
Elk3	0.48	1.39	3.59E-04	0.03	1
Emp1	0.63	1.55	4.00E-08	1.65E-05	7.55E-04
Eng	0.31	1.24	0.01	0.29	1
Eno3	-1.27	-2.42	6.21E-10	6.24E-07	1.17E-05
Enpp3	0.39	1.31	2.64E-03	0.11	1
Enpp4	-0.22	-1.17	3.61E-03	0.14	1
Entpd1	0.31	1.24	7.40E-03	0.22	1
Epha3	0.68	1.6	0.02	0.38	1
Ephb4	0.36	1.28	0.05	0.54	1
Erbb4	-0.43	-1.35	4.41E-03	0.16	1
Errfi1	-0.43	-1.35	2.27E-04	0.02	1
Etnk2	-0.96	-1.94	0.02	0.4	1
Ets2	0.3	1.23	0.02	0.39	1
Evi2a	0.51	1.42	0.04	0.53	1
Exoc8	-0.16	-1.11	0.04	0.52	1
Eya1	0.58	1.49	1.54E-03	0.08	1
F13a1	0.55	1.46	0.04	0.49	1
F2rl2	0.36	1.29	0.03	0.45	1
Fam107a	-0.44	-1.36	5.33E-04	0.04	1
Fam111a	1.15	2.22	7.18E-03	0.21	1
Fam174b	0.77	1.71	0.02	0.36	1
Fam180a	0.69	1.62	3.44E-03	0.13	1
Fam181b_1	-0.36	-1.28	0.01	0.31	1
Fam205a	2.28	4.87	0.04	0.5	1
Fam207a	-0.26	-1.2	0.05	0.54	1
Fam20c	-0.17	-1.12	0.05	0.55	1

Fam214a	0.19	1.14	0.03	0.45	1
Fam83f	-0.31	-1.24	0.04	0.53	1
Farp2	-0.22	-1.16	2.20E-03	0.1	1
Farsa	-0.27	-1.21	0.03	0.44	1
Fat4	0.41	1.32	2.33E-07	6.83E-05	4.40E-03
Fbln5	-0.17	-1.12	0.02	0.4	1
Fbn2	0.3	1.23	0.02	0.37	1
Fbxl4	-0.29	-1.23	0.02	0.39	1
Fbxw4	-0.29	-1.22	0.03	0.43	1
Fcgr1a	0.54	1.45	0.04	0.5	1
Fer	0.21	1.15	0.01	0.31	1
Fgf20	-1.34	-2.53	0.04	0.5	1
Fgfr2	-0.44	-1.36	3.20E-04	0.02	1
Fgl2	-0.28	-1.21	6.30E-03	0.2	1
Fkbp5	-0.64	-1.56	2.66E-08	1.19E-05	5.01E-04
Fn1	0.25	1.19	0.02	0.33	1
Fndc7	0.76	1.7	0.03	0.43	1
Folh1	-0.23	-1.17	0.05	0.54	1
Fos	0.6	1.51	0.02	0.34	1
Foxf1	-1.45	-2.73	0.01	0.3	1
Foxj2	-0.19	-1.14	0.03	0.43	1
Foxo3	-0.18	-1.13	0.02	0.36	1
Frem1	0.64	1.56	5.42E-03	0.18	1
Frmd6	0.16	1.12	0.04	0.5	1
Fscn1	-0.24	-1.18	0.05	0.55	1
Fsd2	-2.21	-4.61	2.20E-03	0.1	1
Fstl3	-0.44	-1.36	9.61E-03	0.25	1
Fut8	-0.21	-1.16	0.05	0.55	1
Fzd4	-0.32	-1.25	0.03	0.44	1
Fzd6	0.66	1.58	5.76E-03	0.18	1
Fzd7	0.52	1.44	3.54E-03	0.14	1
Gabbr1	-0.14	-1.1	0.04	0.5	1
Gabpb2	0.27	1.21	0.05	0.54	1
Galnt3	0.67	1.59	6.21E-03	0.19	1
Gas2l3	-0.25	-1.19	3.76E-04	0.03	1
Gatm	-0.23	-1.18	0.04	0.49	1
Gemin6	0.46	1.38	0.03	0.43	1
gene:ENSRNOG00000000866	0.19	1.14	0.03	0.46	1
gene:ENSRNOG00000007238	-2.7	-6.49	0.05	0.55	1

gene:ENSRNOG00000030021	0.54	1.46	0.04	0.52	1
gene:ENSRNOG00000042660	-2.36	-5.12	0.04	0.5	1
gene:ENSRNOG00000047276	0.47	1.38	8.90E-03	0.24	1
gene:ENSRNOG00000055911	-2.48	-5.58	0.04	0.49	1
gene:ENSRNOG00000062480	1.04	2.06	4.22E-03	0.15	1
gene:ENSRNOG00000062779	1.12	2.18	0.02	0.33	1
gene:ENSRNOG00000062881	0.94	1.92	0.03	0.47	1
gene:ENSRNOG00000063011	0.94	1.92	0.02	0.42	1
gene:ENSRNOG00000063038	2.34	5.06	0.02	0.38	1
gene:ENSRNOG00000063471	1.57	2.98	0.03	0.48	1
gene:ENSRNOG00000063741	-1.11	-2.15	0.02	0.38	1
gene:ENSRNOG00000063781	-1.85	-3.6	7.78E-03	0.22	1
gene:ENSRNOG00000063986	2.09	4.26	0.01	0.3	1
gene:ENSRNOG00000064080	0.19	1.14	0.02	0.36	1
gene:ENSRNOG00000065098	0.15	1.11	0.05	0.54	1
gene:ENSRNOG00000065389	-0.83	-1.78	0.01	0.31	1
gene:ENSRNOG00000065543	0.94	1.92	0.04	0.49	1
gene:ENSRNOG00000065823	2.68	6.4	0.05	0.55	1
gene:ENSRNOG00000066655	-0.8	-1.74	0.02	0.36	1
gene:ENSRNOG00000067090	-2.21	-4.62	0.01	0.28	1
gene:ENSRNOG00000067422	3.02	8.12	7.09E-04	0.04	1
gene:ENSRNOG00000067560	0.24	1.18	2.24E-03	0.1	1
gene:ENSRNOG00000067650	2.4	5.29	0.04	0.5	1
gene:ENSRNOG00000068025	-1.23	-2.34	4.20E-03	0.15	1
gene:ENSRNOG00000068953	0.25	1.19	0.04	0.51	1
gene:ENSRNOG00000069032	1.11	2.16	0.03	0.45	1
gene:ENSRNOG00000069157	2.78	6.87	0.01	0.27	1
gene:ENSRNOG00000069624	-1.81	-3.51	0.02	0.39	1
gene:ENSRNOG00000070264	2.82	7.08	0.04	0.53	1
Gimap1	1.44	2.72	0.03	0.48	1
Gja1	0.26	1.2	9.82E-04	0.06	1
Gja6	1.33	2.51	0.05	0.55	1
Gjb2	0.94	1.91	8.06E-06	1.38E-03	0.15
Gjb6	0.88	1.84	7.37E-04	0.05	1
Gldn	-0.29	-1.22	9.59E-03	0.25	1
Glul	-0.15	-1.11	0.03	0.43	1
Gm11992	-2.59	-6.03	0.02	0.36	1
Gm2a	0.23	1.17	0.04	0.52	1
Gna15	0.89	1.86	0.03	0.48	1

Gnai1	-0.18	-1.13	0.01	0.32	1
Gnb4	0.4	1.32	6.42E-04	0.04	1
Gnl1	-0.25	-1.19	4.44E-03	0.16	1
Gpc1	0.15	1.11	0.04	0.53	1
Gpsm2	0.31	1.24	6.86E-03	0.21	1
Grk3	0.4	1.32	1.79E-03	0.09	1
Grk5	0.23	1.17	7.10E-03	0.21	1
Grxcr1	1.15	2.22	0.04	0.51	1
Gsg1l	-1.24	-2.36	0.02	0.42	1
Gstm2	0.37	1.29	0.02	0.37	1
Gstm4	-0.48	-1.4	1.04E-04	0.01	1
Gsto1	0.18	1.13	0.03	0.47	1
Gtf2a1l	-0.6	-1.52	0.04	0.52	1
Gys1	-0.19	-1.14	0.03	0.43	1
H19	-1.26	-2.4	7.24E-06	1.25E-03	0.14
H2az1	-0.17	-1.13	0.04	0.53	1
H2bc18	0.22	1.17	5.35E-03	0.18	1
H3c1	-0.73	-1.65	0.05	0.55	1
H3f3c	3.29	9.77	3.92E-09	2.63E-06	7.40E-05
Hba-a2	0.38	1.3	0.02	0.38	1
Hba-a3	0.79	1.72	8.45E-05	9.07E-03	1
Hbb-b1	0.35	1.28	0.04	0.5	1
Hbegf	-0.4	-1.32	1.95E-03	0.09	1
Hbp1	0.18	1.13	0.03	0.44	1
Hdhd3	-0.48	-1.4	0.04	0.49	1
Hebp2	-0.36	-1.29	0.02	0.35	1
Herpud1	-0.44	-1.36	1.69E-07	5.13E-05	3.19E-03
Hexa	-0.19	-1.14	0.01	0.32	1
Hhip	1.18	2.27	2.31E-03	0.1	1
Hif3a	-2.53	-5.79	1.42E-08	7.25E-06	2.67E-04
Hip1	-0.16	-1.12	0.03	0.46	1
Hjv	-1.4	-2.64	0.02	0.34	1
Hmcn1	0.32	1.25	9.45E-05	9.75E-03	1
Hmg1l1	1.3	2.47	0.03	0.48	1
Hoxa9	0.27	1.2	0.03	0.47	1
Hoxc6	0.38	1.3	1.22E-06	2.98E-04	0.02
Hoxc8	0.44	1.36	0.03	0.48	1
Hs6st1	0.22	1.16	0.04	0.53	1
Hspa2	-0.24	-1.18	0.03	0.46	1

Hspb6	-0.39	-1.31	0.01	0.27	1
Hvcn1	-0.66	-1.58	4.96E-03	0.17	1
Id3	-0.24	-1.18	0.03	0.46	1
Ifi47	0.81	1.76	1.36E-04	0.01	1
Ifitm1	0.38	1.3	0.02	0.33	1
Ifitm2	0.24	1.18	0.05	0.55	1
Ift140	0.19	1.14	0.02	0.42	1
Ift80	0.18	1.13	0.05	0.55	1
Igdcc3	0.66	1.58	7.01E-03	0.21	1
Igdcc4	-0.2	-1.15	0.02	0.37	1
Igfn1	-1.84	-3.57	2.77E-04	0.02	1
Igsf11	-0.24	-1.18	0.02	0.42	1
Il12rb2	1.89	3.71	3.36E-03	0.13	1
Il16	-0.29	-1.23	0.01	0.26	1
Il1rl1	0.65	1.57	0.02	0.35	1
Il20ra	-2.86	-7.26	0.04	0.49	1
Ino80e	-0.3	-1.23	0.04	0.53	1
Ints12	0.41	1.33	8.39E-03	0.23	1
Iqgap2	-0.36	-1.29	5.04E-03	0.17	1
Irf5	0.74	1.67	7.20E-03	0.21	1
Irf7	0.52	1.43	0.03	0.49	1
Irf8	0.62	1.54	0.02	0.39	1
Isca2	-0.21	-1.15	0.02	0.36	1
Itga1	0.36	1.29	2.12E-03	0.1	1
Itga8	0.67	1.59	1.12E-03	0.06	1
Itgal	0.84	1.79	1.88E-03	0.09	1
Itgb3	0.36	1.28	0.03	0.44	1
Itgbl1	0.39	1.31	6.17E-04	0.04	1
Itih2	1.34	2.53	0.02	0.32	1
Itpkb	-0.18	-1.13	0.02	0.38	1
Itpr2	0.23	1.18	3.15E-03	0.13	1
Jag2	-0.15	-1.11	0.05	0.55	1
Jcad	0.23	1.17	4.18E-03	0.15	1
Jph1	-1.15	-2.22	8.21E-03	0.23	1
Jph2	-0.94	-1.92	9.04E-03	0.24	1
Katnal1	-0.17	-1.12	0.05	0.54	1
Katnal2	1.3	2.46	0.02	0.37	1
Kbtbd11	-0.23	-1.17	8.69E-03	0.24	1
Kcna1	-0.17	-1.12	0.01	0.29	1

Kcna5	-0.28	-1.21	0.03	0.49	1
Kcna7	-2.38	-5.2	0.01	0.3	1
Kcnf1	-0.61	-1.52	1.35E-04	0.01	1
Kcnip1	-0.29	-1.22	4.28E-04	0.03	1
Kcnj13	0.56	1.48	0.05	0.54	1
Kcnk2	0.57	1.48	2.40E-03	0.11	1
Kcnq3	-0.17	-1.13	0.03	0.47	1
Kcp	-1.29	-2.45	1.28E-03	0.07	1
Kctd11	-0.5	-1.41	0.01	0.32	1
Kdr	0.19	1.14	0.03	0.48	1
Kif19b	0.69	1.62	0.02	0.38	1
Kif5c	0.14	1.1	0.04	0.51	1
Klf12	0.27	1.2	0.04	0.51	1
Klf13	-0.21	-1.16	9.70E-03	0.25	1
Klf15	-0.62	-1.54	1.18E-03	0.07	1
Klf3	0.2	1.15	0.02	0.33	1
Klf9	-0.29	-1.22	6.52E-03	0.2	1
Klhl26	-0.36	-1.29	7.45E-03	0.22	1
Klhl41	-0.89	-1.86	0.02	0.34	1
Klra2	0.85	1.81	1.23E-03	0.07	1
Kmt2e	0.14	1.1	0.04	0.53	1
Ky	-0.9	-1.86	0.04	0.49	1
Kynu	2.4	5.26	0.03	0.44	1
Lama4	0.26	1.2	1.99E-04	0.02	1
Lamc3	-0.33	-1.25	0.02	0.36	1
Lamtor4	-0.27	-1.21	2.43E-03	0.11	1
Lancl3	-0.33	-1.25	0.05	0.54	1
Laptm5	0.41	1.33	0.04	0.51	1
Ldb3	-0.31	-1.24	9.12E-03	0.25	1
Lgals1	-0.15	-1.11	0.03	0.44	1
Lgalsl	-0.25	-1.19	1.19E-03	0.07	1
Lgi4	-0.26	-1.2	0.01	0.3	1
Lilrb3	1.38	2.6	1.24E-03	0.07	1
Lilrb3a	1.81	3.52	4.01E-03	0.15	1
Lilrb3l	1.71	3.28	0.05	0.54	1
Limch1	-0.17	-1.12	0.02	0.37	1
Lmo7	0.7	1.62	2.17E-09	1.59E-06	4.10E-05
Lmod3	-1.6	-3.02	0.02	0.36	1
Loxhd1	1.49	2.82	0.02	0.33	1

Lpin3	-0.8	-1.74	1.91E-03	0.09	1
Lpp	0.24	1.18	1.87E-03	0.09	1
Lpxn	0.6	1.52	0.02	0.37	1
Lrig2	0.16	1.12	0.03	0.48	1
Lrp6	0.17	1.13	0.02	0.39	1
Lrrc14b	-1.64	-3.11	0.05	0.54	1
Lrrc4b	-0.28	-1.21	8.34E-04	0.05	1
Lrrc70	0.75	1.68	0.04	0.52	1
Lrrtm2	0.35	1.28	5.52E-03	0.18	1
Lsm10	0.4	1.32	0.03	0.46	1
Lsmem2	-0.24	-1.18	0.02	0.42	1
Lss	-0.26	-1.2	0.01	0.3	1
Ltbp1	0.42	1.33	1.65E-06	3.73E-04	0.03
Ly49si1	2.21	4.64	0.02	0.37	1
Lyc2	0.59	1.5	0.04	0.53	1
Lysmd2	-0.16	-1.12	0.05	0.54	1
Mag	-0.52	-1.44	1.01E-03	0.06	1
Mal	-0.23	-1.17	0.03	0.43	1
Man2a1	0.19	1.14	0.03	0.44	1
Map3k6	-1	-2	5.39E-04	0.04	1
Mapkapk5	-0.26	-1.2	0.04	0.53	1
Marchf1	0.84	1.79	8.07E-03	0.23	1
Marcksl1	-0.22	-1.17	0.04	0.52	1
Mars1	-0.16	-1.12	0.04	0.52	1
Mat2a	-0.17	-1.12	0.02	0.37	1
Mbp	-0.24	-1.18	0.02	0.34	1
Mdfic	0.23	1.18	0.05	0.55	1
Medag	0.62	1.53	6.51E-04	0.04	1
Meox2	0.74	1.67	2.00E-04	0.02	1
Mertk	-0.53	-1.44	1.53E-10	1.90E-07	2.89E-06
Met	0.47	1.39	4.87E-03	0.17	1
Mgat2	0.27	1.21	0.04	0.52	1
MGC105567	0.49	1.41	7.88E-03	0.22	1
MGC109340_2	-5.22	-37.4	0.03	0.46	1
MGC94207	-0.35	-1.27	5.30E-03	0.18	1
Mical1	-0.21	-1.16	6.99E-03	0.21	1
Mical2	-0.17	-1.13	0.03	0.49	1
Mllt1	-0.3	-1.23	0.02	0.36	1
Mmp19	0.55	1.47	9.85E-03	0.25	1

Mnda	0.77	1.7	0.02	0.35	1
Mns1	-0.74	-1.67	3.72E-03	0.14	1
Mon2	0.15	1.11	0.04	0.53	1
Mpdz	-0.15	-1.11	0.04	0.52	1
Mrap	-0.45	-1.36	4.65E-03	0.16	1
Mrgprb4	0.4	1.32	7.67E-03	0.22	1
Ms4a14	1.35	2.54	0.04	0.49	1
Msc	-0.6	-1.51	9.55E-03	0.25	1
Msr1	0.67	1.59	0.01	0.26	1
Msrb2	-0.4	-1.32	2.08E-03	0.1	1
Msrb3	0.28	1.21	0.03	0.44	1
Mtmr12	-0.24	-1.18	0.04	0.53	1
Mtrf1l	-0.38	-1.3	0.04	0.49	1
Mvp	0.25	1.19	0.04	0.49	1
Mybpc1	-1.32	-2.5	5.58E-07	1.50E-04	0.01
Myf6	-2.36	-5.12	0.04	0.51	1
Myh7	-1.1	-2.15	7.83E-03	0.22	1
Mylk2	-1.73	-3.32	2.61E-03	0.11	1
Mylk3	-1.21	-2.32	0.05	0.55	1
Myoc	-0.39	-1.31	1.61E-04	0.01	1
Myom1	-0.95	-1.93	2.50E-04	0.02	1
Myoz1	-0.98	-1.98	0.01	0.27	1
N4bp2	0.35	1.27	8.17E-03	0.23	1
Naa11	1.75	3.36	0.03	0.46	1
Naaladl2	0.47	1.38	0.01	0.27	1
Nap1l5	-0.17	-1.13	0.01	0.28	1
Ncmap	-0.25	-1.19	0.04	0.53	1
Ncoa3	-0.16	-1.12	0.04	0.52	1
Ndnf	0.79	1.73	0.02	0.33	1
Ndrg1	-0.16	-1.11	0.02	0.39	1
Ndufa13	-0.23	-1.18	5.08E-03	0.17	1
Ndufs5_1	0.79	1.72	3.68E-05	4.52E-03	0.69
Ndufs5_2	-0.41	-1.32	5.52E-03	0.18	1
Neil3	2.28	4.84	6.29E-04	0.04	1
NEWGENE_1308171	0.66	1.58	1.32E-10	1.77E-07	2.50E-06
Nfkbia	-0.4	-1.32	6.65E-03	0.2	1
Nhsl1	0.34	1.27	0.04	0.52	1
Nkain2	-0.17	-1.13	0.03	0.45	1
Nlgn1	0.26	1.2	0.03	0.44	1

Nlrc4	0.87	1.83	0.02	0.35	1
Nlrp1a	0.57	1.48	6.83E-03	0.21	1
Nlrp3	0.66	1.58	0.01	0.31	1
Nnat	0.47	1.38	5.86E-05	6.71E-03	1
Npas2	0.65	1.57	0.05	0.55	1
Npffr1	-2.22	-4.67	0.04	0.53	1
Nphp4	-0.37	-1.29	0.05	0.54	1
Npnt	0.3	1.23	0.03	0.47	1
Nr1d1	-0.34	-1.26	1.60E-05	2.36E-03	0.3
Nr1h4	1.82	3.53	0.02	0.35	1
Nr3c1	0.15	1.11	0.04	0.53	1
Nr3c2	0.18	1.13	0.03	0.47	1
Nr4a1	-0.4	-1.32	3.78E-04	0.03	1
Nrap	-1.38	-2.61	9.88E-03	0.25	1
Nrg1	-0.16	-1.12	0.02	0.4	1
Nrk	1.8	3.49	5.31E-03	0.18	1
Ntn4	-0.39	-1.31	0.05	0.54	1
Nudt9	-0.23	-1.17	0.01	0.26	1
Nyx	-2.48	-5.58	0.03	0.46	1
Obp3	1.36	2.56	0.01	0.3	1
Obscn	-0.91	-1.88	6.04E-04	0.04	1
Olr1193	-2.22	-4.67	0.04	0.53	1
Olr1388	2.16	4.48	0.05	0.54	1
Omd	0.8	1.74	1.23E-04	0.01	1
Ophn1	0.16	1.12	0.05	0.54	1
Oscp1	-0.27	-1.21	0.02	0.42	1
Osr1	0.55	1.47	0.04	0.53	1
Otud7b	-0.2	-1.15	0.01	0.31	1
P2ry4	0.19	1.14	0.03	0.43	1
P4ha2	-0.27	-1.2	0.04	0.53	1
Pacs2	-0.16	-1.12	0.02	0.42	1
Padi4	-1.82	-3.52	0.04	0.49	1
Paip2b	-0.16	-1.12	0.04	0.5	1
Palmd	0.25	1.19	1.51E-03	0.08	1
Pamr1	0.62	1.54	0.03	0.43	1
Paqr8	-0.16	-1.12	0.03	0.44	1
Parp11	0.48	1.39	0.02	0.41	1
Parvb	0.22	1.17	1.79E-03	0.09	1
Pawr	0.79	1.73	4.78E-03	0.17	1

Pax9	0.54	1.46	0.02	0.42	1
Pcdh20	-1.69	-3.23	6.71E-03	0.2	1
Pde3a	0.34	1.26	0.03	0.48	1
Pde4c_1	-0.79	-1.73	3.36E-03	0.13	1
Pde6a	2.93	7.64	6.67E-03	0.2	1
Pdgfd	-0.26	-1.2	0.02	0.41	1
Pdgfrl	0.84	1.79	8.63E-03	0.24	1
Pdlim1	0.21	1.16	0.02	0.33	1
Pdlim3	-0.85	-1.81	0.03	0.48	1
Pecam1	0.31	1.24	0.01	0.32	1
Peli2	-0.36	-1.29	1.11E-03	0.06	1
Per1	-0.96	-1.94	1.70E-08	8.28E-06	3.21E-04
Per2	-0.75	-1.68	2.81E-05	3.62E-03	0.53
Perm1	-1.04	-2.06	0.01	0.3	1
Pgam2	-1.82	-3.53	1.41E-03	0.07	1
Pgf	0.38	1.3	0.04	0.53	1
Pgm5	0.66	1.58	0.04	0.49	1
Phb2	-0.19	-1.14	0.02	0.38	1
Phf21a	0.24	1.18	0.04	0.53	1
Phldb2	0.51	1.43	4.47E-09	2.88E-06	8.43E-05
Piezo1	0.62	1.54	1.92E-06	4.23E-04	0.04
Pim1	0.5	1.41	0.05	0.55	1
Pink1	-0.15	-1.11	0.05	0.55	1
Pip5k1b	0.27	1.2	0.04	0.53	1
Pkdrej	1.67	3.18	0.03	0.48	1
Pkn1	-0.29	-1.23	0.02	0.36	1
Pla2g4f	1.35	2.54	0.03	0.44	1
Plaat3	-0.3	-1.23	3.18E-04	0.02	1
Plce1	-0.21	-1.16	0.04	0.52	1
Plek	1.06	2.08	2.43E-03	0.11	1
Plekhg5	-0.34	-1.27	9.23E-03	0.25	1
Plekhh2	0.44	1.36	0.02	0.39	1
Plxnb3	-0.37	-1.29	6.20E-06	1.11E-03	0.12
Pmepa1	-0.3	-1.23	5.12E-04	0.04	1
Pmp2	-0.39	-1.31	0.01	0.28	1
Pnpla2	-0.27	-1.2	0.03	0.44	1
Pon3	1.11	2.16	0.03	0.45	1
Postn	0.44	1.36	0.03	0.48	1
Pou2f2	0.99	1.98	3.75E-03	0.14	1

Ppp1r3a	-2.12	-4.34	9.79E-07	2.42E-04	0.02
Ppp2r5a	0.32	1.25	0.01	0.29	1
Prelid2	0.39	1.31	0.05	0.55	1
Prf1	1.89	3.7	0.04	0.53	1
Prg4	0.74	1.67	4.00E-04	0.03	1
Prim1	0.89	1.85	1.18E-04	0.01	1
Prmt2	-0.18	-1.13	0.04	0.53	1
Prokr2	0.62	1.53	0.02	0.42	1
Prr5l	0.79	1.73	0.05	0.54	1
Psip1	0.21	1.16	0.05	0.55	1
Psrc1	-1.55	-2.93	0.04	0.53	1
Ptafr	0.39	1.31	0.05	0.54	1
Ptch1	0.24	1.18	0.02	0.38	1
Ptgfr	0.28	1.22	0.03	0.44	1
Pthlh	0.8	1.74	0.01	0.28	1
Ptpn13	-0.16	-1.12	0.03	0.47	1
Ptpn7	1.13	2.18	0.04	0.52	1
Ptprc	0.48	1.4	6.29E-03	0.2	1
Ptprh	0.88	1.85	0.05	0.55	1
Ptpru	-0.34	-1.27	0.02	0.38	1
Ptrh1	0.45	1.37	5.71E-04	0.04	1
Pwwp3a	-0.26	-1.19	0.03	0.48	1
Pycard	1.09	2.13	0.03	0.45	1
Pycr1	-0.7	-1.63	0.04	0.51	1
Pygm	-0.79	-1.73	1.05E-04	0.01	1
Rab11fip1	0.54	1.45	0.03	0.44	1
Rab1b_2	8.4	338.19	7.74E-04	0.05	1
Rac2	0.63	1.55	0.05	0.55	1
Rae1	-0.26	-1.2	0.04	0.53	1
Ralgds	-0.22	-1.17	0.04	0.49	1
Rapgef6	0.22	1.16	3.50E-03	0.13	1
Rasl11b	-0.65	-1.57	9.75E-04	0.06	1
Rassf4	-0.36	-1.28	1.45E-06	3.44E-04	0.03
Rassf9	0.59	1.5	2.18E-03	0.1	1
Rbm15b	-0.22	-1.17	0.04	0.49	1
Rbp4	0.41	1.33	0.05	0.54	1
Reln	-0.23	-1.17	7.53E-04	0.05	1
Retreg2	-0.17	-1.12	0.05	0.55	1
Rexo1	-0.21	-1.16	0.02	0.34	1

Rgcc	-0.31	-1.24	0.01	0.31	1
RGD1308706	-0.33	-1.25	9.80E-03	0.25	1
RGD1310507	0.9	1.87	0.01	0.29	1
RGD1310587	0.61	1.52	1.83E-06	4.08E-04	0.03
RGD1311595	0.17	1.13	0.03	0.44	1
RGD1560813	-2.39	-5.24	4.16E-03	0.15	1
RGD1561662	1.33	2.52	0.03	0.48	1
RGD1562726	1.64	3.12	0.03	0.44	1
RGD1563888	0.33	1.25	0.04	0.51	1
RGD1565323	-1.52	-2.87	0.01	0.3	1
RGD1565784	-0.26	-1.2	0.05	0.54	1
Rgs18	0.95	1.94	4.73E-04	0.03	1
Rhbdf1	-0.21	-1.16	0.02	0.35	1
Rhod	1.98	3.95	0.05	0.55	1
Rhoj	0.26	1.19	2.63E-03	0.11	1
Rhpn1	-0.33	-1.26	4.69E-03	0.16	1
Rin3	-0.31	-1.24	0.02	0.37	1
Rlf	0.21	1.16	7.83E-03	0.22	1
Rnf113a2	0.48	1.4	0.03	0.46	1
Rnf32	0.54	1.45	0.02	0.37	1
Rpl11	0.14	1.1	0.05	0.55	1
Rpl23	0.17	1.12	0.02	0.36	1
Rpl38_2	0.75	1.68	7.98E-03	0.22	1
Rpl3l	-1.81	-3.51	0.01	0.29	1
Rps20_3	6.73	106.08	5.58E-03	0.18	1
Rps8	0.17	1.13	0.02	0.36	1
Rrh	-4.7	-26	0.05	0.55	1
Rsad2	1.02	2.02	2.25E-03	0.1	1
Rspo3	0.98	1.98	0.02	0.37	1
RT1-CE2	1.5	2.83	0.03	0.43	1
RT1-DMb	0.45	1.37	0.04	0.53	1
RT1-M1-4	1.31	2.49	0.05	0.55	1
RT1-N2	2.15	4.43	1.81E-04	0.02	1
Runx3	-0.35	-1.27	9.54E-03	0.25	1
Rxfp2	-2.7	-6.49	0.05	0.54	1
Ryr1	-1.41	-2.66	1.00E-07	3.58E-05	1.89E-03
Sars1	-0.15	-1.11	0.04	0.52	1
Satb1	-0.17	-1.12	0.04	0.51	1
Scara3	0.34	1.27	0.04	0.51	1

Scube1	-0.18	-1.13	0.03	0.48	1
Sdc2	0.3	1.23	9.73E-05	9.97E-03	1
Sdf2l1	-0.26	-1.19	0.05	0.55	1
Sdk2	-0.23	-1.17	0.04	0.52	1
Sec11a	-0.2	-1.15	0.02	0.41	1
Sec14l1	-0.19	-1.14	8.80E-03	0.24	1
Sec14l2	-0.2	-1.15	0.02	0.37	1
Sec14l5	-0.62	-1.54	0.01	0.3	1
Secisbp2l	-0.22	-1.17	0.03	0.44	1
Sema3d	0.43	1.35	1.86E-04	0.02	1
Sema3g	-0.22	-1.17	8.74E-03	0.24	1
Sema4c	-0.28	-1.21	0.02	0.35	1
Sema5a	-0.29	-1.22	2.49E-05	3.34E-03	0.47
Sephs2	-0.32	-1.25	0.02	0.33	1
Septin3	-0.17	-1.13	0.02	0.36	1
Serpinb6b	1.41	2.66	8.40E-03	0.23	1
Serpine1	-0.77	-1.71	2.44E-03	0.11	1
Serpinf1	0.38	1.3	1.63E-03	0.08	1
Serping1	0.33	1.26	2.72E-03	0.11	1
Sfswap	-0.2	-1.15	0.02	0.33	1
Sgk1	-0.66	-1.58	1.87E-09	1.55E-06	3.53E-05
Shc3	-0.28	-1.22	0.05	0.55	1
Shisa4	-0.23	-1.18	4.37E-03	0.16	1
Shox2	-0.22	-1.16	5.33E-03	0.18	1
Sipa1l2	-0.28	-1.21	8.77E-03	0.24	1
Sirt5	-0.16	-1.12	0.04	0.53	1
Slc10a6	-0.7	-1.63	0.04	0.51	1
Slc11a1	1.07	2.1	0.01	0.29	1
Slc12a4	-0.17	-1.13	0.04	0.52	1
Slc14a2	-1.97	-3.93	0.05	0.54	1
Slc15a2	-0.24	-1.18	0.01	0.28	1
Slc15a3	0.84	1.79	0.03	0.44	1
Slc18a1	-1.79	-3.46	3.68E-03	0.14	1
Slc22a8	0.95	1.93	0.04	0.52	1
Slc25a48	-1.32	-2.5	4.75E-03	0.16	1
Slc2a1	-0.19	-1.14	0.02	0.33	1
Slc2a10	1.02	2.03	0.01	0.28	1
Slc35d2	0.38	1.3	0.03	0.46	1
Slc35e2b	-0.32	-1.25	0.02	0.38	1

Slc36a2	-0.46	-1.38	1.67E-03	0.08	1
Slc39a14	-0.25	-1.19	0.04	0.52	1
Slc43a2	-0.19	-1.14	0.02	0.35	1
Slc47a1	0.67	1.59	1.18E-03	0.07	1
Slc6a11	-0.46	-1.37	0.05	0.54	1
Slc6a12	1.24	2.37	0.01	0.27	1
Slc6a13	1	1.99	1.63E-07	5.12E-05	3.08E-03
Slc6a20	0.89	1.85	8.44E-08	3.23E-05	1.59E-03
Slc6a4	1.85	3.6	0.04	0.5	1
Slc6a8	-0.2	-1.15	9.35E-03	0.25	1
Slc7a11	0.57	1.48	0.03	0.44	1
Slc7a5	-0.3	-1.23	2.57E-04	0.02	1
Slc7a8	-0.32	-1.25	6.59E-03	0.2	1
Slc8a2	-0.24	-1.18	0.05	0.55	1
Slc9a3	-0.52	-1.43	4.26E-03	0.15	1
Slco1a4	0.19	1.14	0.02	0.37	1
Slfn4_1	0.46	1.37	0.03	0.49	1
Slfn5	0.28	1.22	3.52E-04	0.03	1
Slx1b	-0.34	-1.26	0.01	0.27	1
Smad9	-0.16	-1.11	0.04	0.49	1
Smim18	-0.38	-1.3	0.03	0.46	1
Smtnl2	-1.4	-2.64	9.62E-03	0.25	1
Smyd1	-1.65	-3.14	7.18E-03	0.21	1
Snai2	0.9	1.87	0.01	0.27	1
Sncg	0.23	1.17	7.01E-04	0.04	1
Sned1	0.23	1.17	0.04	0.53	1
Snta1	-0.38	-1.3	5.66E-03	0.18	1
Sort1	-0.2	-1.15	4.71E-03	0.16	1
Sox17	-0.57	-1.48	0.01	0.3	1
Sox5	0.37	1.3	0.03	0.44	1
Sp140	0.32	1.25	0.05	0.54	1
Sp2	0.27	1.21	0.03	0.46	1
Spata2	-0.26	-1.19	7.98E-03	0.22	1
Spata21	-1.29	-2.45	0.04	0.53	1
Spats2l	0.22	1.16	0.03	0.43	1
Sppl2b	-0.26	-1.2	0.04	0.49	1
Spry1	-0.6	-1.52	4.53E-04	0.03	1
Src	-0.22	-1.16	8.08E-03	0.23	1
Srebf2	-0.15	-1.11	0.03	0.47	1

Srl	-1.65	-3.14	4.41E-04	0.03	1
Srrd	-0.41	-1.33	0.04	0.52	1
Srrm4	-0.39	-1.31	0.02	0.35	1
St3gal5	-0.28	-1.22	9.81E-04	0.06	1
St6galnac2_1	0.77	1.7	0.04	0.52	1
Stard3	-0.29	-1.22	3.04E-03	0.12	1
Stard3nl	-0.19	-1.14	0.03	0.44	1
Stat2	0.16	1.12	0.04	0.5	1
Steap1	1.27	2.41	0.04	0.51	1
Stom	0.41	1.33	5.54E-03	0.18	1
Ston1	-0.16	-1.12	0.04	0.51	1
Strn4	-0.2	-1.15	0.02	0.37	1
Stxbp6	0.33	1.26	0.01	0.3	1
Sult5a1	-0.88	-1.84	2.98E-03	0.12	1
Suv39h2	0.37	1.29	0.02	0.34	1
Syce3	-0.72	-1.65	0.04	0.54	1
Sypl2	-1.76	-3.38	7.35E-04	0.05	1
Syt2	-0.15	-1.11	0.03	0.46	1
Sytl3	0.28	1.22	0.03	0.44	1
Tacc1	-0.14	-1.11	0.03	0.48	1
Taf13	0.24	1.18	4.02E-03	0.15	1
Taf7	0.27	1.2	1.98E-03	0.09	1
Tafa5	-0.29	-1.22	0.02	0.36	1
Tapbp	0.21	1.16	0.01	0.28	1
Tasl	1.21	2.32	0.02	0.41	1
Tbata	0.99	1.98	0.02	0.35	1
Tbpl1_2	0.27	1.2	0.03	0.46	1
Tbx18	0.39	1.31	0.04	0.49	1
Tcap	-2.04	-4.1	1.86E-05	2.67E-03	0.35
Tcf7	0.61	1.53	0.01	0.29	1
Tcfl5	-1.14	-2.2	0.02	0.35	1
Tcp11l2	0.27	1.2	0.04	0.5	1
Tdrd15	0.59	1.5	0.05	0.55	1
Tdrp	-0.24	-1.18	0.04	0.5	1
Tec	0.49	1.41	1.83E-04	0.02	1
Tef	-0.27	-1.21	5.38E-04	0.04	1
Tent5b	-2.21	-4.64	3.49E-05	4.38E-03	0.66
Tesk2	-0.56	-1.48	0.01	0.26	1
Tfpi	0.39	1.31	1.05E-03	0.06	1

Tgfb1	0.63	1.55	4.43E-03	0.16	1
Tgfbr1	0.22	1.17	0.04	0.53	1
Tgfbr2	0.2	1.15	4.63E-03	0.16	1
Thap11	-0.37	-1.29	0.02	0.36	1
Thbd	0.63	1.55	9.70E-08	3.55E-05	1.83E-03
Thbs1	0.91	1.88	1.77E-17	9.51E-14	3.35E-13
Themis	1.89	3.7	0.05	0.55	1
Ticrr	0.98	1.97	0.05	0.54	1
Tinag	-2.48	-5.57	0.03	0.44	1
Tinagl1	-0.44	-1.35	0.01	0.32	1
Tle3	-0.2	-1.15	0.01	0.27	1
Tlr11	2.09	4.25	0.03	0.43	1
Tlr2	0.62	1.54	0.03	0.47	1
Tlr8	0.51	1.42	0.02	0.41	1
Tm4sf1	0.28	1.22	0.03	0.46	1
Tmem117	-0.2	-1.15	7.93E-03	0.22	1
Tmem182	-1.27	-2.41	0.03	0.45	1
Tmem200c	-0.34	-1.26	0.04	0.53	1
Tmem266	-0.97	-1.96	8.88E-03	0.24	1
Tnfrsf1b	0.59	1.51	8.73E-03	0.24	1
Tnni1	-1.81	-3.52	0.02	0.38	1
Tnnt2	0.89	1.85	4.83E-03	0.17	1
Tnpo3	0.17	1.13	0.02	0.37	1
Topors	0.19	1.14	0.03	0.48	1
Tph1	0.61	1.53	3.06E-03	0.12	1
Trdn	-0.86	-1.81	4.70E-03	0.16	1
Trem1	2.39	5.25	0.03	0.48	1
Trhde	-0.7	-1.62	1.35E-03	0.07	1
Trim36	0.25	1.19	0.02	0.36	1
Trim9	-0.25	-1.19	0.04	0.49	1
Trmt9b	-0.37	-1.29	0.03	0.45	1
Trpc5	0.39	1.31	0.02	0.39	1
Trps1	0.31	1.24	9.26E-03	0.25	1
Trpt1	-0.51	-1.42	0.03	0.49	1
Trpv1	-0.14	-1.1	0.05	0.55	1
Tspan1	-1.07	-2.1	0.03	0.45	1
Tspan15	-0.26	-1.2	3.43E-03	0.13	1
Ttc39d	-2.76	-6.79	2.66E-03	0.11	1
Ttll4	0.29	1.22	0.03	0.46	1

Ttr	-2.19	-4.57	0.03	0.44	1
Twsg1	0.26	1.2	0.02	0.42	1
Txndc12	-0.29	-1.22	2.61E-03	0.11	1
Tyrobp	0.51	1.42	0.03	0.47	1
Uaca	0.23	1.17	3.37E-03	0.13	1
Uckl1	0.25	1.19	0.03	0.48	1
Ugt1a3	0.28	1.21	0.03	0.48	1
Ugt8	-0.23	-1.17	8.50E-04	0.05	1
Unc5b	-0.32	-1.24	0.04	0.53	1
Uox	-1.97	-3.93	0.05	0.54	1
Usp35	-0.19	-1.14	0.02	0.42	1
Usp54	-0.27	-1.2	0.01	0.29	1
Usp9y	-5.22	-37.21	5.88E-04	0.04	1
Vegfb	-0.43	-1.34	6.00E-04	0.04	1
Vsir	0.26	1.2	0.04	0.53	1
Vtn	0.42	1.34	3.57E-03	0.14	1
Vwa1	-0.34	-1.26	1.03E-05	1.70E-03	0.19
Wdr4	-0.67	-1.59	6.22E-03	0.19	1
Wee1	-0.48	-1.4	8.33E-05	9.00E-03	1
Whrn	-0.25	-1.19	2.19E-03	0.1	1
Wscd1	-0.83	-1.77	0.04	0.49	1
Yrdc	-0.53	-1.45	0.01	0.31	1
Zbtb11	0.17	1.13	0.03	0.43	1
Zbtb16	-1.61	-3.05	3.94E-16	1.27E-12	7.44E-12
Zbtb9	-0.3	-1.23	0.03	0.44	1
Zfp36l1	0.19	1.14	0.01	0.27	1
Zfp407	0.18	1.14	0.01	0.27	1
Zfp428	-0.33	-1.25	0.04	0.51	1
Zfp513	-0.37	-1.29	0.02	0.36	1
Zfp804b	-0.39	-1.31	0.03	0.48	1
Zfp84_2	0.51	1.42	2.11E-03	0.1	1
Zfp963	-0.73	-1.65	2.27E-03	0.1	1
Zic1	0.65	1.57	1.49E-03	0.08	1
Zzz3	0.22	1.16	7.48E-03	0.22	1

Table A3.8. Master list of differentially expressed genes between female 10X CXB-NE vs DF-NE samples with a p-value ≤ 0.05 and a fold change greater than ±1.

Name	Log_2 fold change	Fold change	P-value	FDR p-value	Bonferroni
1700102P08Rik	0.88	1.83	5.80E-03	0.76	1
A4galt	-0.44	-1.36	0.03	1	1
AABR07005775.1	-2.01	-4.03	6.67E-03	0.8	1
AABR07014550.1	-1.98	-3.95	0.04	1	1
AABR07026317.1	-2.53	-5.77	0.01	1	1
AABR07028349.1	3.28	9.73	7.23E-04	0.25	1
AABR07049516.1	3.44	10.89	0.02	1	1
AABR07052523.1	2.6	6.08	0.03	1	1
AABR07060610.1	-7.39	-167.33	0.01	1	1
AABR07062466.1	-2.37	-5.17	0.02	1	1
AABR07063279.1	-0.51	-1.43	0.01	1	1
Abat	-0.46	-1.37	1.02E-03	0.3	1
Abca1	-0.33	-1.25	1.08E-04	0.08	1
Abca12	-1.26	-2.4	0.03	1	1
Abca3	-0.19	-1.14	0.02	1	1
Abcg3	-6.49	-90.13	0.03	1	1
AC099453.1	1.19	2.29	0.04	1	1
AC128848.1	0.6	1.51	0.02	1	1
AC128901.1	-2.1	-4.29	0.01	1	1
AC131360.2	-1.22	-2.33	2.63E-03	0.53	1
Acadsb	0.54	1.45	9.18E-03	0.95	1
Acsf2	-0.37	-1.3	0.04	1	1
Acsl4	-0.3	-1.23	7.45E-04	0.25	1
Acta1	-1.48	-2.8	3.14E-03	0.59	1
Adam22	0.17	1.13	0.04	1	1
Adcyap1	-0.58	-1.49	1.14E-03	0.32	1
Add2	-0.2	-1.15	0.02	1	1
Agbl2	2.49	5.6	5.21E-03	0.73	1
Akr1b1	0.33	1.26	2.18E-04	0.12	1
Albfm1	1.13	2.19	0.04	1	1
Aldh7a1	-0.29	-1.22	0.04	1	1
Amph	0.22	1.16	0.01	1	1
Anapc15	0.38	1.3	0.05	1	1

Ankfn1	0.49	1.41	0.02	1	1
Apobec1	0.96	1.94	0.04	1	1
Arap2	0.28	1.22	0.03	1	1
Arhgap36	-0.33	-1.26	0.02	1	1
Arhgef9	0.19	1.14	0.04	1	1
Armh4	0.29	1.22	0.03	1	1
Ascl2	1.72	3.29	0.03	1	1
Ascl3	2.72	6.58	0.02	1	1
Ass1	-1.26	-2.4	4.34E-08	3.44E-04	8.07E-04
Atp2b4	-0.54	-1.46	1.51E-03	0.38	1
Atp5mk_1	-0.22	-1.16	0.03	1	1
Atxn2l	-0.19	-1.14	0.03	1	1
Basp1	-0.28	-1.21	1.01E-03	0.3	1
Blvra	0.41	1.33	4.64E-03	0.72	1
Bmx	1.42	2.67	0.04	1	1
C1qa	-0.59	-1.5	8.15E-03	0.91	1
C1qbp	-0.2	-1.15	0.04	1	1
Ca3	-1.55	-2.93	0.04	1	1
Cabp2	-2.02	-4.04	0.02	1	1
Cacng5	-0.55	-1.47	0.03	1	1
Calb2	0.36	1.28	0.01	1	1
Camk2d	-0.24	-1.18	6.73E-03	0.8	1
Camkmt	0.44	1.36	0.04	1	1
Capn5	-0.24	-1.18	4.95E-03	0.72	1
Car2	0.28	1.21	0.04	1	1
Cartpt	0.82	1.77	0.03	1	1
Cck	-3.24	-9.44	0.03	1	1
Cd82	-0.2	-1.15	0.03	1	1
Cds2	-0.27	-1.2	2.31E-03	0.49	1
Cep250	0.41	1.33	0.03	1	1
Cers1	1.98	3.94	0.02	1	1
Cers6	-0.19	-1.14	0.04	1	1
Cgn	1.5	2.83	5.76E-04	0.21	1
Chchd2_1	2.48	5.58	0.04	1	1
Chrm2	-0.2	-1.15	0.04	1	1
Chst11	-0.33	-1.26	0.03	1	1
Ckm	-1.66	-3.15	0.04	1	1
Ckmt1	0.24	1.18	4.91E-03	0.72	1
Cldn19	0.36	1.28	0.01	1	1

Clic4	-0.26	-1.2	0.04	1	1
Cnmd	0.33	1.26	0.01	1	1
Col16a1	-0.34	-1.26	9.27E-03	0.95	1
Cr2	-1.85	-3.6	0.03	1	1
Crabp2	-0.4	-1.32	0.05	1	1
Cracdl	1.7	3.25	6.28E-03	0.78	1
Creld2	-0.64	-1.55	3.60E-03	0.61	1
Crmp1	-0.21	-1.15	0.03	1	1
Crybg1	-0.91	-1.88	0.04	1	1
Csf1	-0.58	-1.5	1.41E-03	0.37	1
Csk	-0.21	-1.15	0.02	1	1
Csmd3	0.33	1.26	0.02	1	1
Ctnnal1	0.27	1.21	0.04	1	1
Cxcl10	-0.98	-1.97	0.03	1	1
Cxcl9	-1.08	-2.12	2.20E-03	0.48	1
Cxxc4	0.3	1.23	0.05	1	1
Cyp27b1	-1.86	-3.62	0.04	1	1
D430041D05Rik	0.27	1.21	0.05	1	1
Ddah1	0.28	1.21	0.04	1	1
Ddx3y	0.74	1.67	0.03	1	1
Dhfr	-0.57	-1.48	1.64E-04	0.1	1
Dnah3	-1.54	-2.9	1.40E-03	0.37	1
Dnajb9	-0.28	-1.21	0.03	1	1
Dock10	0.19	1.14	0.03	1	1
Dtx3l	-0.38	-1.3	5.44E-03	0.74	1
Ebna1bp2	0.34	1.27	0.02	1	1
Eea1	0.19	1.14	0.03	1	1
Eif2ak2	-0.18	-1.14	0.05	1	1
Eml1	-0.17	-1.12	0.05	1	1
Epb41	0.19	1.14	0.03	1	1
Erich3	0.25	1.19	0.01	1	1
Etl4	0.37	1.29	3.26E-03	0.59	1
Exd1	-1	-2	0.05	1	1
Extl2	0.21	1.16	0.02	1	1
Fads3	-0.33	-1.25	0.02	1	1
Fam111a	1.38	2.59	3.19E-04	0.15	1
Fam222b	-0.21	-1.15	0.03	1	1
Fam83d	-1.67	-3.17	0.04	1	1
Fcgr3a	-1.12	-2.17	0.04	1	1

Filip1	0.27	1.21	5.87E-03	0.76	1
Fndc7	-1.15	-2.21	0.02	1	1
Frmd3	0.28	1.21	0.04	1	1
Frmd8	-0.31	-1.24	1.57E-03	0.39	1
Fscn1	-0.46	-1.38	0.02	1	1
Fsd2	3.19	9.11	0.03	1	1
Gabarap	-0.17	-1.12	0.05	1	1
Gabra5	-0.49	-1.4	7.93E-03	0.9	1
Gadd45g	-0.94	-1.92	4.79E-04	0.21	1
gene:ENSRNOG00000025211	3.19	9.11	0.03	1	1
gene:ENSRNOG00000031060	2.48	5.58	0.04	1	1
gene:ENSRNOG00000037661	-0.41	-1.33	5.63E-03	0.76	1
gene:ENSRNOG00000049579	-2.4	-5.27	0.04	1	1
gene:ENSRNOG00000054017	0.2	1.15	0.04	1	1
gene:ENSRNOG00000061597	-2.17	-4.5	0.04	1	1
gene:ENSRNOG00000062467	-3.46	-10.98	0.02	1	1
gene:ENSRNOG00000062492	-1.5	-2.83	0.05	1	1
gene:ENSRNOG00000063112	-1.71	-3.27	0.05	1	1
gene:ENSRNOG00000063986	-2.43	-5.38	0.01	1	1
gene:ENSRNOG00000064332	2.6	6.08	0.03	1	1
gene:ENSRNOG00000064423	1.08	2.11	0.04	1	1
gene:ENSRNOG00000065633	2.57	5.94	8.85E-03	0.94	1
gene:ENSRNOG00000067240	0.27	1.21	0.04	1	1
gene:ENSRNOG00000068362	-1.68	-3.21	0.04	1	1
gene:ENSRNOG00000070474	-0.56	-1.48	0.01	1	1
gene:ENSRNOG00000071148	7.6	193.81	8.80E-03	0.94	1
Gfra3	-0.49	-1.41	4.85E-03	0.72	1
Ghsr	-2.5	-5.67	0.04	1	1
Glipr2	-0.29	-1.22	0.04	1	1
Gm17266	1.63	3.1	0.01	1	1
Gmppb	-0.35	-1.27	0.02	1	1
Gpc1	-0.28	-1.22	0.03	1	1
Grhl3	3.73	13.29	2.20E-07	8.06E-04	4.10E-03
Grk2	-0.19	-1.14	0.04	1	1
Gstm2	-0.34	-1.26	0.01	1	1
H2bc18	0.32	1.25	0.01	1	1
Hapln1	0.58	1.49	1.63E-03	0.39	1
Hbb-bs	1.58	2.99	0.01	1	1
Hif1a	-0.18	-1.13	0.04	1	1

Hmcn2	1.45	2.72	6.02E-05	0.05	1
Hoxa9	-0.33	-1.26	0.03	1	1
Hoxb6	0.78	1.72	0.01	1	1
Hoxd10	-1.34	-2.53	9.35E-03	0.95	1
Hpse	0.59	1.5	6.37E-04	0.23	1
Hrh3	1.18	2.27	0.01	1	1
Hs2st1	-0.27	-1.21	0.03	1	1
Hspa5	-0.41	-1.32	0.02	1	1
Hspb1	-0.28	-1.22	8.28E-04	0.26	1
Htr2b	-3.25	-9.54	0.03	1	1
Hyou1	-0.36	-1.28	4.81E-03	0.72	1
Ifih1	-0.39	-1.31	6.74E-03	0.8	1
Ifnlr1	-1	-2	7.60E-04	0.25	1
Igf2	-0.67	-1.59	0.01	1	1
Igfbp3	-0.34	-1.27	0.01	1	1
Igsf23	-1.85	-3.6	0.02	1	1
Il21r	-1.23	-2.34	3.37E-03	0.59	1
Il6	-2.22	-4.65	1.16E-04	0.08	1
Isg15	-1.14	-2.2	0.04	1	1
Itga3	-0.29	-1.22	0.03	1	1
Kcnc1	0.37	1.29	0.01	1	1
Kcnc4	-0.23	-1.18	0.01	1	1
Khdrbs2	-0.83	-1.77	0.03	1	1
Klrk1	-1.01	-2.02	0.03	1	1
Larp4	-0.23	-1.17	8.31E-03	0.92	1
Lce1f_2	-2.55	-5.85	4.27E-06	8.47E-03	0.08
Lck	-1.31	-2.48	0.03	1	1
Lcp1	-0.25	-1.19	2.95E-03	0.58	1
Ldhb	0.18	1.13	0.04	1	1
Ldlr	-0.17	-1.12	0.05	1	1
Lgals3bp	-0.32	-1.25	0.02	1	1
Lhfpl4	0.19	1.14	0.03	1	1
Lif	2.26	4.79	0.02	1	1
Lingo4	0.7	1.62	0.03	1	1
Lmo4	-0.29	-1.22	0.03	1	1
Lypd1	0.68	1.6	0.02	1	1
Mad1l1	0.32	1.25	0.03	1	1
Magi3	-0.23	-1.18	6.98E-03	0.83	1
Man1a1	-0.32	-1.25	0.02	1	1

Manf	-0.44	-1.36	5.80E-03	0.76	1
Maoa	-0.37	-1.29	4.04E-03	0.65	1
Mboat7	-0.4	-1.32	5.16E-03	0.73	1
Mbp	0.28	1.22	0.02	1	1
Me1	-0.18	-1.14	0.04	1	1
Mex3c	-0.23	-1.17	0.02	1	1
Mgst3	0.37	1.29	6.14E-03	0.77	1
Mmd	-0.39	-1.31	3.81E-03	0.63	1
Mrps17	1.62	3.07	1.62E-03	0.39	1
Mt-co2	0.26	1.2	0.04	1	1
Mt-nd6	0.36	1.29	3.06E-03	0.58	1
Mthfd2	-0.55	-1.47	7.19E-03	0.84	1
Mybpc1	1.44	2.72	2.40E-03	0.51	1
Myh4	-2.2	-4.6	1.59E-04	0.1	1
Myl1	-3.78	-13.73	2.06E-03	0.47	1
Myo10	-0.25	-1.19	4.97E-03	0.72	1
Myom3	3.24	9.43	6.96E-09	1.10E-04	1.29E-04
Nadsyn1	0.58	1.49	0.01	1	1
Ncr3lg1	3.04	8.22	0.04	1	1
Ndrg3	-0.37	-1.29	4.59E-03	0.72	1
Nefl	0.24	1.18	0.05	1	1
Nefm	0.25	1.19	0.04	1	1
Neurl1	-0.3	-1.23	0.04	1	1
Npas4	3.19	9.11	0.04	1	1
Nrap	-2.13	-4.38	0.01	1	1
Nrip1	-0.3	-1.23	5.35E-04	0.21	1
Nsun4_1	0.35	1.27	0.03	1	1
Nts	-0.83	-1.78	0.02	1	1
Oasl2	-0.74	-1.67	2.47E-03	0.51	1
Olr1877	-2.62	-6.13	0.03	1	1
Olr318	7.41	170.43	0.01	1	1
Os9	-0.19	-1.14	0.03	1	1
Otulinl	-0.44	-1.36	0.05	1	1
P2ry10b	1.56	2.94	0.03	1	1
Paip1	-0.21	-1.16	0.02	1	1
Pappa1	-0.39	-1.31	6.11E-03	0.77	1
Pappa2	-0.68	-1.6	1.06E-03	0.3	1
Parp14	-0.35	-1.27	0.01	1	1
Pctp	0.43	1.35	0.04	1	1

Pdcl3	-0.48	-1.4	5.25E-04	0.21	1
Pde10a	-0.45	-1.37	0.03	1	1
Pdia4	-0.29	-1.23	0.02	1	1
Pdpn	-0.19	-1.14	0.04	1	1
Phf11	-6.93	-121.68	0.02	1	1
Pkib	-0.51	-1.42	7.81E-03	0.89	1
Pla2g7	0.36	1.28	7.24E-03	0.84	1
Plcl1	0.4	1.32	0.03	1	1
Pld5	-0.44	-1.36	0.02	1	1
Plekhb1	0.23	1.17	7.06E-03	0.83	1
Plekhh1	-0.36	-1.28	9.01E-03	0.94	1
Pllp	0.45	1.36	2.20E-03	0.48	1
Pmp2	0.41	1.33	8.84E-03	0.94	1
Pmp22	0.25	1.19	0.04	1	1
Pnpla1	1.29	2.44	0.02	1	1
Polr3b	0.21	1.16	0.03	1	1
Pomt1	-0.51	-1.42	0.03	1	1
Ppm1k	0.3	1.23	0.04	1	1
Prelid3a	0.69	1.61	0.05	1	1
Prkcq	0.43	1.35	4.02E-03	0.65	1
Prr13	-0.25	-1.19	0.05	1	1
Ptp4a1	-0.3	-1.23	0.02	1	1
Ptpn5	-0.52	-1.44	0.01	1	1
Ptprn	-0.25	-1.19	3.21E-03	0.59	1
Ptpro	-0.51	-1.42	4.62E-04	0.2	1
Qdpr	-0.26	-1.2	0.04	1	1
Rab15	-0.38	-1.3	3.55E-03	0.61	1
Rab33b	-0.3	-1.23	0.03	1	1
Rab3ip	0.33	1.25	0.05	1	1
Rai14	0.28	1.21	0.05	1	1
Ralgps2	-0.29	-1.23	0.03	1	1
Rbm15b	-0.32	-1.25	0.01	1	1
Rbp4	-0.75	-1.68	4.72E-05	0.05	0.88
Rfc1	0.18	1.13	0.05	1	1
RGD1309350	3.32	10	0.03	1	1
RGD1561662	-2.04	-4.12	0.02	1	1
RGD1564409	0.48	1.39	0.05	1	1
Rhoc	-0.29	-1.22	3.33E-03	0.59	1
Rhof	-0.47	-1.39	0.01	1	1

Ripk3	-1.02	-2.03	0.04	1	1
Rnf213	-0.27	-1.21	1.66E-03	0.39	1
Rorb	-1.32	-2.49	0.05	1	1
Rpl21_2	-0.34	-1.26	0.01	1	1
Rspo2	-0.52	-1.44	6.57E-05	0.05	1
RT1-CE1	-1.21	-2.31	0.03	1	1
RT1-N2	2.33	5.04	2.25E-03	0.49	1
RT1-S3	-0.47	-1.38	0.03	1	1
Rtel1	0.46	1.37	7.50E-04	0.25	1
Ryr1	-1	-2	0.02	1	1
S100a11	-0.28	-1.22	1.32E-03	0.36	1
S1pr4	-3.3	-9.82	0.03	1	1
Sbf2	0.19	1.14	0.03	1	1
Sbspon	0.5	1.41	0.04	1	1
Sdf2l1	-0.61	-1.52	0.02	1	1
Sema4f	-0.37	-1.29	7.70E-03	0.89	1
Sema6d	0.19	1.14	0.03	1	1
Serpina1	-0.45	-1.37	0.04	1	1
Serpini1	-0.24	-1.18	0.01	1	1
Set	-0.46	-1.37	0.01	1	1
Shank2	-0.26	-1.2	0.04	1	1
Shisal2b	1.84	3.57	0.01	1	1
Slc13a3	-0.45	-1.37	0.04	1	1
Slc27a4	-0.3	-1.23	0.03	1	1
Slc36a2	0.46	1.38	0.02	1	1
Slc7a5	-0.28	-1.21	0.04	1	1
Smagp	-0.99	-1.99	0.03	1	1
Smap1	-0.19	-1.14	0.03	1	1
Snrpg_1	-2.45	-5.48	5.14E-03	0.73	1
Sod3	0.22	1.16	0.02	1	1
Sorbs2	0.41	1.33	6.09E-03	0.77	1
Sparcl1	0.2	1.14	0.02	1	1
Spata17	1.36	2.56	0.05	1	1
Sptb	0.38	1.31	1.15E-05	0.02	0.21
Sptbn5	0.29	1.22	0.02	1	1
Srgap1	-0.21	-1.16	0.02	1	1
Strip1	-0.34	-1.26	0.01	1	1
Sypl2	-3.02	-8.1	0.04	1	1
Syt4	-0.3	-1.23	5.08E-04	0.21	1

Tbc1d8	-0.41	-1.33	0.01	1	1
Tceal9	-0.29	-1.22	0.03	1	1
Tecta	-1.36	-2.56	1.76E-03	0.41	1
Tesc	0.3	1.23	0.04	1	1
Tex15	0.6	1.51	0.03	1	1
Tex38	3.32	10	0.03	1	1
Thap3	0.76	1.7	0.02	1	1
Thegl	-3.49	-11.25	0.04	1	1
Tmem139	3.01	8.04	4.35E-03	0.7	1
Tmem255a	0.25	1.19	2.85E-03	0.56	1
Tnc	-0.25	-1.19	5.24E-03	0.73	1
Tnfaip1	-0.27	-1.2	3.33E-03	0.59	1
Tnmd	1.88	3.68	0.03	1	1
Tnnc2	-3.23	-9.41	0.05	1	1
Tp53i11	-0.45	-1.37	0.03	1	1
Trim56	-0.19	-1.14	0.05	1	1
Trpv2	-0.22	-1.17	0.03	1	1
Trub2	0.41	1.33	0.03	1	1
Tspan13	-0.18	-1.13	0.04	1	1
Ttc27	-0.31	-1.24	0.03	1	1
Ttn	-0.53	-1.44	0.02	1	1
Txnip	0.44	1.35	1.29E-06	2.92E-03	0.02
Txnrd1	-0.18	-1.13	0.04	1	1
Ube2a	-0.22	-1.17	0.02	1	1
Ubl5	-0.22	-1.17	0.02	1	1
Vat1	-0.2	-1.15	0.02	1	1
Vgf	-0.71	-1.63	7.99E-08	4.22E-04	1.49E-03
Vwa5a	-0.21	-1.16	0.01	1	1
Xirp2	-0.99	-1.99	6.49E-03	0.8	1
Yes1	-0.21	-1.16	0.03	1	1
Zbtb38	-0.18	-1.13	0.04	1	1
Zdhhc22	0.51	1.42	0.04	1	1
Zfp407	0.24	1.18	6.67E-03	0.8	1
Zfp622	-0.2	-1.14	0.02	1	1
Zfp804a	0.27	1.2	0.05	1	1
Zfp938	0.39	1.31	0.03	1	1
Zgrf1	0.62	1.53	0.02	1	1

Table A3.9. Master list of differentially expressed genes between male 10X CXB-NE vs DF-NE samples with a p-value ≤ 0.05 and a fold change greater than ±1

Name	Log_2 fold change	Fold change	P-value	FDR p-value	Bonferroni
1110038F14Rik	0.45	1.36	0.05	0.5	1
1700092M07Rik	2.79	6.91	3.95E-04	0.03	1
4833439L19Rik	-0.16	-1.12	0.04	0.44	1
4930563E22Rik	0.2	1.15	0.03	0.37	1
6330403K07Rik	0.26	1.19	0.04	0.48	1
AABR07005844.1	1.31	2.48	3.33E-10	2.07E-07	6.29E-06
AABR07006275.1	3.56	11.76	8.87E-03	0.21	1
AABR07015812.1	-0.2	-1.15	0.02	0.32	1
AABR07018556.1	1.7	3.26	0.05	0.5	1
AABR07021955.1	0.26	1.2	0.01	0.23	1
AABR07025140.1	0.55	1.47	0.03	0.42	1
AABR07029195.1	1.28	2.44	0.02	0.32	1
AABR07029272.1	0.35	1.28	0.01	0.28	1
AABR07029596.1	0.75	1.69	0.02	0.35	1
AABR07030773.1	2.42	5.35	0.02	0.36	1
AABR07034445.1	-1.18	-2.27	9.09E-05	7.52E-03	1
AABR07041109.1	-0.8	-1.75	1.46E-03	0.07	1
AABR07049329.1	0.83	1.78	8.27E-04	0.04	1
AABR07051450.1	-0.16	-1.11	0.05	0.5	1
AABR07054614.1	0.74	1.67	0.04	0.48	1
AABR07058412.1	-2.87	-7.29	0.03	0.42	1
AABR07060872.1	2.17	4.5	4.25E-13	4.76E-10	8.03E-09
AABR07062138.2	0.99	1.98	0.01	0.26	1
AABR07066700.1	-0.43	-1.34	0.02	0.28	1
AABR07069837.1	2.76	6.79	0.02	0.3	1
AABR07070957.1	3.2	9.18	0.02	0.34	1
Aard	1.08	2.12	0.02	0.35	1
AB124611	1.04	2.06	0.05	0.5	1
Abca13	0.98	1.97	1.50E-03	0.07	1
Abca2	-0.15	-1.11	0.04	0.44	1
Abca5	-0.16	-1.12	0.04	0.44	1
Abcc9	0.3	1.23	0.03	0.37	1
Abcd2	-0.27	-1.2	0.02	0.29	1

Abcg2	-0.37	-1.3	2.78E-03	0.1	1
Abhd14b	0.3	1.23	0.03	0.38	1
Abi3	1.22	2.33	1.53E-03	0.07	1
Abi3bp	0.29	1.22	7.22E-03	0.19	1
Ablim2	-0.29	-1.22	0.02	0.32	1
AC118772.1	3.29	9.8	3.78E-05	3.88E-03	0.71
AC128859.3	1.37	2.59	0.02	0.31	1
Acacb	-0.3	-1.23	0.04	0.46	1
Acap1	1.38	2.6	6.90E-05	6.13E-03	1
Ace2	0.54	1.46	4.58E-04	0.03	1
Acer2	-0.6	-1.52	1.63E-05	1.95E-03	0.31
Acta2	0.82	1.77	1.95E-10	1.26E-07	3.69E-06
Actg2	1.34	2.54	1.05E-03	0.05	1
Actn1	0.39	1.31	1.10E-05	1.42E-03	0.21
Acvrl1	0.37	1.29	0.04	0.47	1
Adam11	-0.21	-1.15	7.54E-03	0.19	1
Adam15	0.27	1.2	0.03	0.38	1
Adam23	-0.16	-1.12	0.02	0.31	1
Adam33	0.73	1.66	0.03	0.38	1
Adamts1	0.38	1.3	8.64E-04	0.04	1
Adamts12	0.57	1.49	7.14E-07	1.50E-04	0.01
Adamts2	0.38	1.3	9.11E-03	0.21	1
Adamts20	-0.25	-1.19	0.02	0.36	1
Adamts9	0.35	1.28	8.30E-03	0.2	1
Adamtsl1	-0.33	-1.26	5.88E-03	0.17	1
Adcy1	-0.15	-1.11	0.04	0.45	1
Adcy7	0.29	1.23	0.02	0.32	1
Adcy8	-0.35	-1.28	0.02	0.31	1
Adgrd1	0.41	1.32	0.01	0.25	1
Adgre1	0.41	1.33	0.03	0.38	1
Adgre4	1.63	3.09	6.72E-03	0.18	1
Adgrf3	2.08	4.23	0.03	0.37	1
Adgrl1	-0.17	-1.13	0.02	0.33	1
Adipoq	3.13	8.75	0.03	0.37	1
Ado	-0.18	-1.13	0.03	0.41	1
Aebp1	0.28	1.22	8.20E-03	0.2	1
Agt	-0.89	-1.85	0.02	0.32	1
Ahctf1	-0.16	-1.12	0.03	0.43	1
Ahsp	1.37	2.58	3.43E-06	5.64E-04	0.06

AI593442	-0.15	-1.11	0.03	0.4	1
Aif1	0.71	1.64	2.20E-03	0.09	1
Aif1l	-0.24	-1.18	0.03	0.43	1
Akna	0.39	1.31	4.48E-03	0.14	1
Aldh1a2	0.51	1.43	0.02	0.32	1
Aldh1a3	0.58	1.49	8.11E-04	0.04	1
Alk	-0.27	-1.2	2.61E-03	0.1	1
Alox12	1.03	2.04	2.06E-03	0.08	1
Alox15	1.36	2.57	6.18E-05	5.70E-03	1
Alox5ap	0.84	1.79	1.83E-03	0.08	1
Amotl2	0.37	1.29	2.98E-03	0.11	1
Angpt1	0.64	1.56	3.32E-05	3.52E-03	0.63
Angptl1	1.31	2.48	2.49E-04	0.02	1
Angptl7	0.76	1.69	0.05	0.49	1
Ankle1	3.4	10.55	0.01	0.25	1
Ankrd37	1.26	2.39	0.04	0.49	1
Ano2	-2.26	-4.8	0.05	0.5	1
Ano3	-0.15	-1.11	0.03	0.38	1
Anpep	0.74	1.67	2.51E-04	0.02	1
Antxr1	0.24	1.18	5.85E-03	0.16	1
Anxa1	0.36	1.28	1.26E-03	0.06	1
Anxa3	0.39	1.31	6.85E-03	0.18	1
Anxa8	0.49	1.4	0.03	0.43	1
Aox1	0.33	1.26	3.85E-03	0.13	1
Aox4	0.54	1.45	2.40E-05	2.68E-03	0.45
Ap1s2	-0.14	-1.1	0.05	0.5	1
Ap3d1	-0.15	-1.11	0.03	0.43	1
Apobr	0.74	1.67	0.02	0.36	1
Apol2	2.73	6.64	1.49E-03	0.07	1
Apol9a	0.55	1.47	0.04	0.46	1
Appbp2	-0.18	-1.13	0.02	0.3	1
Aprt	0.26	1.19	0.03	0.41	1
Aqp4	-0.86	-1.81	0.04	0.48	1
Arap1	0.23	1.17	7.63E-03	0.19	1
Arhgap15	0.49	1.41	0.02	0.33	1
Arhgap25	0.37	1.29	0.04	0.46	1
Arhgap29	0.31	1.24	5.91E-03	0.17	1
Arhgap39	-0.23	-1.17	1.71E-03	0.07	1
Arhgap45	0.63	1.55	5.14E-04	0.03	1

Arhgap9	0.67	1.59	0.04	0.44	1
Arhgdib	0.58	1.5	2.01E-05	2.28E-03	0.38
Arntl	0.65	1.56	1.91E-05	2.20E-03	0.36
Arsi	0.76	1.7	0.03	0.42	1
Art4	2.46	5.5	2.58E-03	0.1	1
Asns	-0.16	-1.12	0.03	0.4	1
Aspn	1.4	2.63	2.88E-09	1.31E-06	5.44E-05
Astn2	-0.18	-1.13	0.05	0.49	1
Atp11a	-0.14	-1.1	0.03	0.43	1
Atp1a1	-0.18	-1.13	7.92E-03	0.2	1
Atp2a2	-0.14	-1.1	0.04	0.44	1
Atp2b2	-0.17	-1.13	0.01	0.26	1
Atp2b3	-0.19	-1.14	0.01	0.23	1
Atp5mc2	0.17	1.13	0.04	0.45	1
Atp5me	0.76	1.69	8.18E-03	0.2	1
Atp5mg	0.22	1.16	4.13E-03	0.13	1
Atp8a2	-0.14	-1.1	0.03	0.42	1
Atp8b4	1.08	2.12	4.12E-03	0.13	1
Atpaf1	-0.2	-1.15	0.02	0.3	1
Avpr1b	-1.97	-3.91	0.01	0.23	1
B3galt5	-0.3	-1.24	0.02	0.3	1
B4galt6	-0.15	-1.11	0.04	0.48	1
Bag3	-0.18	-1.13	0.01	0.27	1
Bank1	1.27	2.41	0.01	0.27	1
Bcl2	-0.22	-1.16	4.67E-03	0.14	1
Bcl2l15	-2.4	-5.29	0.03	0.37	1
Bcl6b	0.7	1.62	0.04	0.46	1
Bglap	1.7	3.25	0.01	0.24	1
Bgn	0.57	1.48	8.83E-08	2.51E-05	1.67E-03
Bicd1	-0.15	-1.11	0.04	0.46	1
Bin2	1.05	2.08	1.20E-04	9.40E-03	1
Birc3	0.73	1.65	0.03	0.43	1
Blk	1.49	2.81	0.04	0.44	1
Bmp1	0.21	1.15	0.02	0.3	1
Bmp4	1.31	2.47	3.07E-05	3.39E-03	0.58
Bmper	0.66	1.58	7.60E-06	1.06E-03	0.14
Bnc2	0.25	1.19	0.02	0.36	1
Boc	0.59	1.5	6.57E-07	1.40E-04	0.01
Bpifc	-2.4	-5.29	0.03	0.37	1

Brms1l	-0.18	-1.13	0.04	0.44	1
Btbd17	2.42	5.35	0.02	0.37	1
Btbd3	-0.17	-1.12	0.03	0.39	1
Btg2	0.41	1.33	0.02	0.3	1
Btk	1.18	2.27	5.51E-05	5.29E-03	1
Btla	1.22	2.33	8.85E-04	0.05	1
C1qc	0.5	1.41	5.58E-03	0.16	1
C1qtnf2	0.35	1.28	0.05	0.51	1
C1qtnf7	2.07	4.19	2.93E-04	0.02	1
C1r	0.39	1.31	3.15E-04	0.02	1
C1rl	0.85	1.8	0.04	0.45	1
C1s	0.51	1.43	2.55E-06	4.28E-04	0.05
C3	0.62	1.53	8.96E-04	0.05	1
C4a	0.63	1.55	1.07E-04	8.60E-03	1
C4b	0.91	1.88	1.36E-04	0.01	1
C5ar2	0.51	1.43	0.03	0.42	1
C8g	0.5	1.42	0.02	0.36	1
Cabyr	2.16	4.47	0.03	0.37	1
Cacna1g	1.09	2.12	1.05E-03	0.05	1
Cacna1h	-0.2	-1.15	0.01	0.27	1
Cacna2d3	-0.16	-1.12	0.03	0.43	1
Cacybp	-0.17	-1.12	0.02	0.32	1
Cadm3	-0.19	-1.14	4.54E-03	0.14	1
Cadps2	-0.23	-1.17	7.50E-03	0.19	1
Cage1	-0.59	-1.5	0.04	0.49	1
Camp	2.4	5.27	1.55E-08	5.92E-06	2.93E-04
Car1	2.16	4.46	2.23E-03	0.09	1
Card10	0.56	1.48	2.34E-03	0.09	1
Carhsp1	0.19	1.14	0.02	0.36	1
Casp3	0.28	1.21	0.03	0.42	1
Castor2	-0.2	-1.15	0.02	0.35	1
Cavin2	0.31	1.24	9.97E-03	0.23	1
Ccbe1	1.61	3.06	1.68E-04	0.01	1
Ccdc12	0.4	1.32	0.02	0.34	1
Ccdc126	-0.23	-1.17	9.44E-03	0.22	1
Ccdc172	0.61	1.52	0.02	0.29	1
Ccdc3	0.89	1.85	2.07E-05	2.34E-03	0.39
Ccdc6	-0.2	-1.15	5.90E-03	0.17	1
Ccdc80	0.69	1.61	5.30E-07	1.16E-04	1.00E-02

Ccl21	2.05	4.15	1.35E-19	3.78E-16	2.56E-15
Ccl24	1.26	2.39	0.03	0.4	1
Ccl4	-1.79	-3.45	0.04	0.45	1
Ccn2	1.02	2.03	1.22E-12	1.13E-09	2.30E-08
Ccn3	1.47	2.77	8.62E-16	1.45E-12	1.63E-11
Ccn5	1.52	2.86	1.52E-03	0.07	1
Ccna2	0.68	1.6	0.02	0.36	1
Ccnb2	1.11	2.15	1.57E-03	0.07	1
Ccnf	0.55	1.46	0.05	0.49	1
Ccr2	1.15	2.22	2.30E-07	5.59E-05	4.34E-03
Ccr7	3.22	9.33	0.02	0.3	1
Ccser2	-0.18	-1.14	5.83E-03	0.16	1
Cd109	0.54	1.46	0.04	0.49	1
Cd14	0.72	1.65	0.03	0.37	1
Cd177	2.46	5.49	2.89E-09	1.31E-06	5.45E-05
Cd19	1.15	2.21	0.05	0.51	1
Cd22	0.91	1.88	0.02	0.3	1
Cd226	1.25	2.38	5.82E-04	0.03	1
Cd33	1.11	2.16	0.02	0.29	1
Cd37	0.99	1.98	7.36E-04	0.04	1
Cd3e	2	4	0.02	0.33	1
Cd40	2.68	6.42	3.47E-03	0.12	1
Cd53	0.6	1.52	1.85E-03	0.08	1
Cd6	1.17	2.25	0.05	0.5	1
Cd7	0.93	1.9	0.03	0.37	1
Cd79a	0.79	1.73	3.70E-03	0.13	1
Cd79b	2.46	5.49	7.82E-05	6.73E-03	1
Cd8a	1.93	3.82	0.02	0.36	1
Cd93	0.26	1.2	0.04	0.46	1
Cdc25b	0.29	1.22	8.41E-03	0.2	1
Cdc34	0.25	1.19	5.17E-03	0.15	1
Cdc45_2	-0.36	-1.29	4.62E-03	0.14	1
Cdca2	1.25	2.38	1.84E-03	0.08	1
Cdh1	-0.23	-1.17	1.11E-03	0.05	1
Cdh11	0.31	1.24	1.18E-05	1.50E-03	0.22
Cdh15	0.43	1.35	0.02	0.3	1
Cdh4	-0.34	-1.26	0.01	0.23	1
Cdh5	0.22	1.16	0.05	0.49	1
Cdhr2	0.64	1.56	8.38E-03	0.2	1

Cdk20	-0.47	-1.38	0.03	0.37	1
Cdk5r2	-0.15	-1.11	0.05	0.49	1
Cdr2l	-0.18	-1.13	0.01	0.24	1
Ceacam1	0.26	1.2	0.04	0.49	1
Ceacam4	1.49	2.82	6.66E-06	9.56E-04	0.13
Cebpe	1.7	3.25	0.04	0.46	1
Cenpa	1.12	2.18	0.03	0.43	1
Cenpf	0.57	1.48	0.01	0.23	1
Cenpi	0.68	1.6	0.03	0.38	1
Cenpu	0.79	1.73	0.03	0.39	1
Cep83	-0.22	-1.17	0.04	0.49	1
Ces2b	1.64	3.13	0.03	0.37	1
Cesl1_1	1.43	2.69	0.03	0.37	1
Cfb	0.5	1.41	9.69E-03	0.22	1
Cfh	0.24	1.18	0.03	0.37	1
Cfp	0.96	1.95	6.04E-05	5.63E-03	1
Cftr	-1.1	-2.15	0.05	0.49	1
Chi3l1	0.82	1.77	9.08E-04	0.05	1
Chordc1	-0.24	-1.18	1.26E-03	0.06	1
Chrdl2	0.93	1.9	0.01	0.26	1
Chrm3	-0.5	-1.42	4.59E-03	0.14	1
Chrm5	2.26	4.77	3.39E-03	0.12	1
Chrna3	-0.46	-1.38	1.59E-05	1.92E-03	0.3
Chrnb4	-0.45	-1.37	0.01	0.28	1
Chst15	-0.19	-1.14	0.01	0.28	1
Chst2	-0.25	-1.19	4.48E-04	0.03	1
Ciart	-0.95	-1.93	4.23E-03	0.14	1
Ciita	0.69	1.61	0.03	0.43	1
Cilp	0.82	1.77	7.94E-07	1.61E-04	0.02
Clcn4	-0.14	-1.11	0.05	0.49	1
Clec11a	0.62	1.54	6.92E-03	0.18	1
Clec12a	0.62	1.54	0.02	0.33	1
Clec14a	0.7	1.63	1.18E-03	0.06	1
Clec1b	1.39	2.62	0.01	0.26	1
Clec2d2	1.34	2.53	0.03	0.42	1
Clec2g	0.19	1.14	0.01	0.23	1
Clec4a3	0.83	1.78	7.91E-04	0.04	1
Clec4d	2.31	4.96	0.02	0.3	1
Clec7a	0.67	1.59	1.53E-03	0.07	1

Clic2	0.49	1.41	0.03	0.38	1
Clint1	-0.15	-1.11	0.05	0.49	1
Clk1	-0.23	-1.18	0.03	0.39	1
Cln6	-0.28	-1.21	0.04	0.45	1
Clspn	1.15	2.22	0.03	0.37	1
Clstn1	-0.15	-1.11	0.03	0.41	1
Cltb	-0.2	-1.15	6.42E-03	0.17	1
Cltc	-0.15	-1.11	0.03	0.39	1
Cluh	-0.18	-1.13	0.01	0.27	1
Clvs1	-1.26	-2.39	7.27E-06	1.03E-03	0.14
Cmahp	1.22	2.33	0.01	0.23	1
Cmtm3	0.4	1.32	0.04	0.47	1
Cnksr3	0.37	1.29	0.03	0.39	1
Cnn1	1.74	3.33	9.07E-06	1.24E-03	0.17
Cnn2	0.66	1.58	1.99E-07	4.92E-05	3.76E-03
Cnnm2	-0.27	-1.21	0.03	0.41	1
Cnot4	-0.18	-1.13	0.02	0.33	1
Cnr1	-0.28	-1.21	0.02	0.32	1
Cntn4	-0.33	-1.26	5.38E-03	0.16	1
Cntnap4	-0.33	-1.26	0.02	0.32	1
Cntrl	0.23	1.17	0.01	0.24	1
Col12a1	0.35	1.28	3.44E-07	8.03E-05	6.51E-03
Col1a1	0.23	1.17	0.02	0.33	1
Col1a2	0.29	1.22	4.05E-03	0.13	1
Col3a1	0.4	1.32	2.68E-03	0.1	1
Col4a5	0.6	1.51	2.03E-03	0.08	1
Col5a1	0.19	1.14	0.01	0.23	1
Col5a2	0.2	1.15	6.91E-03	0.18	1
Col6a1	0.43	1.34	5.69E-05	5.40E-03	1
Col6a2	0.29	1.22	6.09E-03	0.17	1
Col6a3	0.28	1.21	8.67E-03	0.21	1
Col8a1	0.93	1.91	1.43E-09	7.06E-07	2.70E-05
Col9a1	0.88	1.83	8.26E-04	0.04	1
Colec11	0.16	1.12	0.02	0.32	1
Coq8b	0.48	1.39	2.09E-03	0.08	1
Coro1a	0.36	1.28	4.22E-03	0.14	1
Cp	0.31	1.24	6.15E-05	5.70E-03	1
Cpeb3	-0.15	-1.11	0.04	0.46	1
Cped1	0.47	1.38	1.25E-04	9.67E-03	1

Cpne4	-0.17	-1.12	0.02	0.35	1
Cpxm2	0.57	1.48	3.71E-04	0.02	1
Cracd	-0.14	-1.1	0.04	0.49	1
Cracr2a	1.24	2.35	0.01	0.26	1
Crh	-4.43	-21.61	3.33E-05	3.52E-03	0.63
Crim1	0.27	1.21	7.88E-03	0.2	1
Crisp3	3.18	9.06	3.51E-06	5.71E-04	0.07
Cryab	-0.22	-1.16	3.05E-03	0.11	1
Crybg2	3.13	8.78	3.73E-03	0.13	1
Csf1r	0.33	1.26	0.02	0.33	1
Csf2ra	0.48	1.4	0.03	0.37	1
Csf2rb	1.45	2.73	1.16E-07	3.09E-05	2.19E-03
Csf3r	1	2	1.72E-04	0.01	1
Csnk2b	-0.17	-1.12	0.05	0.5	1
Csrp3	2.37	5.16	3.77E-08	1.24E-05	7.12E-04
Cst12	0.69	1.61	0.05	0.49	1
Ctsc	0.27	1.21	0.03	0.37	1
Ctse	0.82	1.76	0.02	0.36	1
Ctsg	3.27	9.62	3.79E-05	3.88E-03	0.72
Ctsk	0.41	1.33	4.70E-03	0.15	1
Ctxn3	0.41	1.33	0.01	0.25	1
Cul3	-0.2	-1.15	4.30E-03	0.14	1
Cx3cl1	0.5	1.41	0.03	0.43	1
Cx3cr1	0.68	1.6	3.47E-03	0.12	1
Cxcl12	0.43	1.34	2.47E-04	0.02	1
Cxcl13	1.14	2.21	4.52E-03	0.14	1
Cxcr2	1.99	3.98	1.01E-06	1.96E-04	0.02
Cxcr4	0.33	1.26	0.03	0.43	1
Cyb5a_2	0.16	1.11	0.05	0.5	1
Cyb5rl	0.91	1.88	0.01	0.28	1
Cybb	0.56	1.47	9.34E-06	1.26E-03	0.18
Cyp1b1	0.28	1.22	0.01	0.24	1
Cyp26b1	0.59	1.51	2.64E-03	0.1	1
Cyp2s1	0.65	1.57	0.01	0.27	1
Cyp3a9	-0.63	-1.54	0.01	0.27	1
Cyp4f18	1.74	3.35	6.08E-03	0.17	1
Cysrt1	-1.33	-2.52	0.04	0.47	1
Cyth4	0.42	1.34	0.04	0.49	1
Cytip	0.87	1.83	0.02	0.33	1

Daam2	-0.2	-1.15	0.01	0.23	1
Dab2	0.37	1.29	6.32E-06	9.15E-04	0.12
Dact1	0.5	1.41	0.02	0.3	1
Dag1	-0.14	-1.1	0.04	0.44	1
Dapp1	0.72	1.65	0.02	0.37	1
Dbh	-3.93	-15.2	0.01	0.23	1
Dbp	-0.78	-1.72	3.51E-18	8.42E-15	6.64E-14
Dchs1	0.44	1.36	4.36E-03	0.14	1
Dchs2	0.86	1.81	0.01	0.28	1
Dcn	0.24	1.18	0.02	0.31	1
Dctn1	-0.14	-1.1	0.04	0.48	1
Ddit4	-0.23	-1.17	5.23E-03	0.16	1
Ddr2	0.26	1.2	0.02	0.29	1
Ddx39b	0.24	1.18	2.11E-03	0.09	1
Ddx58	0.41	1.33	4.09E-03	0.13	1
Defa5	2.29	4.88	9.47E-08	2.65E-05	1.79E-03
Dennd3	0.36	1.28	0.03	0.41	1
Depdc1	1.26	2.4	0.03	0.43	1
Dgki	-0.18	-1.13	0.01	0.28	1
Dhrs2	-0.82	-1.76	0.03	0.43	1
Dhrs9	1.04	2.05	0.02	0.32	1
Dio2	1.24	2.36	1.08E-09	5.72E-07	2.04E-05
Dlgap5	0.58	1.5	0.01	0.23	1
Dmxl2	-0.13	-1.1	0.05	0.51	1
Dnah11	0.27	1.21	0.02	0.36	1
Dnajb4	-0.17	-1.12	0.03	0.41	1
Dnase1l3	1.41	2.66	0.01	0.25	1
Dner	-0.17	-1.12	0.02	0.31	1
Dock3	-0.15	-1.11	0.04	0.48	1
Dock6	0.24	1.18	4.00E-03	0.13	1
Dock8	0.37	1.29	0.01	0.27	1
Dok2	0.73	1.66	0.04	0.45	1
Dop1b	-0.19	-1.14	0.01	0.23	1
Dpp10	-0.2	-1.15	4.00E-03	0.13	1
Dpt	1	2	5.77E-05	5.44E-03	1
Dpysl2	-0.17	-1.12	0.01	0.23	1
Drc7	1.93	3.82	0.02	0.36	1
Dtx1	0.34	1.27	0.03	0.38	1
Dusp7	0.38	1.3	0.01	0.23	1

Dusp8	-0.27	-1.21	0.04	0.48	1
E2f2	0.84	1.79	7.73E-03	0.2	1
E2f3	-0.29	-1.22	0.04	0.44	1
E2f8	1.46	2.75	0.02	0.3	1
Ebf2	0.57	1.48	2.16E-06	3.69E-04	0.04
Ecel1	1.35	2.56	9.44E-03	0.22	1
Ecm2	0.38	1.3	0.02	0.36	1
Ecrg4	-0.42	-1.34	0.03	0.4	1
Ect2	0.66	1.58	0.02	0.33	1
Edil3	-0.2	-1.15	4.95E-03	0.15	1
Efemp1	0.18	1.13	0.02	0.34	1
Egf	0.59	1.5	0.01	0.24	1
Egfr	0.36	1.28	3.89E-03	0.13	1
Egr3	-0.45	-1.36	0.02	0.29	1
Ehbp1l1	0.31	1.24	0.01	0.24	1
Ehd1	-0.24	-1.18	0.03	0.39	1
Ehd2	0.26	1.2	3.75E-03	0.13	1
Eif1	-0.16	-1.12	0.02	0.36	1
Eif3j	-0.16	-1.12	0.03	0.39	1
Eif5a2	-0.16	-1.12	0.02	0.32	1
Elane	2.75	6.73	0.01	0.24	1
Elf1	0.39	1.31	2.06E-03	0.08	1
Elk3	0.34	1.27	0.01	0.23	1
Eln	1.02	2.03	2.16E-08	7.87E-06	4.07E-04
Emilin2	0.41	1.33	0.04	0.49	1
Eml5	0.27	1.2	0.04	0.47	1
Emp1	0.5	1.42	1.23E-05	1.55E-03	0.23
Eng	0.26	1.2	0.03	0.42	1
Entpd4	-0.15	-1.11	0.04	0.46	1
Ep300_1	0.78	1.72	0.04	0.44	1
Epb41l1	-0.14	-1.1	0.04	0.48	1
Epb42	1.07	2.09	2.06E-03	0.08	1
Epha3	0.65	1.57	0.02	0.31	1
Epha6	-0.26	-1.2	1.98E-03	0.08	1
Ephb1	-0.33	-1.25	6.53E-03	0.18	1
Ephb2	0.44	1.36	0.03	0.39	1
Ephb4	0.41	1.33	5.37E-03	0.16	1
Ephx1	-0.25	-1.19	0.04	0.46	1
Epor	3.15	8.85	0.02	0.36	1

Epsti1	0.73	1.66	0.01	0.23	1
Epx	2.5	5.65	3.23E-07	7.64E-05	6.11E-03
Eral1	-0.35	-1.27	0.01	0.24	1
Ermap	1.99	3.98	4.60E-03	0.14	1
Ermp1	-0.16	-1.11	0.04	0.45	1
Esyt1	0.2	1.15	4.10E-03	0.13	1
Esyt2	-0.19	-1.14	7.57E-03	0.19	1
Etfa	-0.16	-1.12	0.03	0.41	1
Ets1	0.32	1.25	7.60E-03	0.19	1
Etv1	-0.15	-1.11	0.03	0.37	1
Evi2b	0.9	1.87	6.69E-04	0.04	1
Exo5	0.45	1.37	7.87E-03	0.2	1
Exoc3l2	1.1	2.15	0.02	0.29	1
Exosc8	0.38	1.31	0.03	0.37	1
Eya1	0.53	1.44	2.46E-03	0.1	1
F13a1	0.87	1.82	7.83E-07	1.60E-04	0.01
F5	1.87	3.66	9.44E-09	3.87E-06	1.78E-04
Faap20	-0.43	-1.34	0.01	0.25	1
Fam114a1l1	3.02	8.12	0.03	0.39	1
Fam171a1	-0.16	-1.12	0.02	0.36	1
Fam180a	0.94	1.92	1.20E-04	9.40E-03	1
Fam193a	-0.15	-1.11	0.05	0.5	1
Fam205c	-1.89	-3.7	0.01	0.24	1
Fam234b	-0.24	-1.18	0.03	0.4	1
Fam81a	-0.45	-1.37	0.01	0.24	1
Fastkd3	0.31	1.24	0.04	0.44	1
Fat3	-0.2	-1.15	4.66E-03	0.14	1
Fat4	0.29	1.22	1.98E-04	0.01	1
Fbl	0.31	1.24	0.03	0.37	1
Fbln1	0.49	1.41	5.78E-04	0.03	1
Fbln7	0.77	1.7	2.35E-03	0.09	1
Fbn1	0.45	1.37	1.26E-05	1.57E-03	0.24
Fbn2	0.31	1.24	0.01	0.26	1
Fbxo21	-0.17	-1.13	0.02	0.35	1
Fcgr2a_2	0.84	1.79	3.48E-05	3.63E-03	0.66
Fcnb	2.37	5.16	4.74E-16	8.83E-13	8.95E-12
Fcrl2	1.46	2.75	3.56E-03	0.12	1
Fcrla	1.33	2.51	0.01	0.28	1
Fech	0.28	1.21	1.08E-03	0.05	1

Fem1b	-0.25	-1.19	1.52E-03	0.07	1
Fermt3	1.05	2.07	1.46E-05	1.79E-03	0.28
Fes	1.01	2.02	4.65E-04	0.03	1
Fgd3	0.93	1.9	2.29E-03	0.09	1
Fgf11	1.09	2.13	0.03	0.4	1
Fgf2	0.89	1.86	7.09E-03	0.19	1
Fgr	1.43	2.7	9.66E-06	1.29E-03	0.18
Fhip1a	1.58	2.99	5.95E-03	0.17	1
Fhl1	0.37	1.29	8.48E-04	0.04	1
Fig4	-0.2	-1.15	0.01	0.27	1
Filip1l	0.68	1.6	1.73E-05	2.05E-03	0.33
Fkbp5	-0.38	-1.3	1.67E-03	0.07	1
Flna	0.32	1.25	4.88E-06	7.31E-04	0.09
Flrt1	-0.29	-1.22	0.02	0.32	1
Flrt2	0.31	1.24	4.36E-03	0.14	1
Flt3	-0.3	-1.23	6.95E-04	0.04	1
Flt4	0.81	1.75	1.96E-03	0.08	1
Fmn1	-0.17	-1.12	0.02	0.32	1
Fmnl3	0.28	1.22	0.04	0.47	1
Fmo3	0.58	1.49	0.03	0.42	1
Fmod	0.5	1.42	4.52E-03	0.14	1
Fn1	0.4	1.32	8.17E-05	6.89E-03	1
Fnbp4	0.21	1.16	0.01	0.24	1
Fndc1	0.37	1.3	7.14E-03	0.19	1
Fosb	1.09	2.12	0.04	0.46	1
Foxc1	0.71	1.63	1.07E-03	0.05	1
Foxc2	0.72	1.65	1.60E-04	0.01	1
Foxo1	-0.19	-1.14	0.03	0.37	1
Foxo4	-0.27	-1.21	0.03	0.43	1
Foxp1	0.28	1.22	0.02	0.34	1
Fpgt	-0.24	-1.18	0.04	0.49	1
Fpr1	1.81	3.51	0.01	0.25	1
Frem1	0.44	1.36	0.04	0.46	1
Frmd6	0.25	1.19	1.13E-03	0.05	1
Frmpd4	-0.26	-1.19	8.38E-04	0.04	1
Fry	-0.17	-1.12	0.02	0.3	1
Fryl	-0.16	-1.12	0.02	0.32	1
Fundc2	-0.27	-1.2	0.04	0.47	1
Furin	0.25	1.19	4.97E-03	0.15	1

Fut2	2.26	4.8	7.84E-04	0.04	1
Fxyd1	0.34	1.27	1.31E-03	0.06	1
Fxyd5	0.64	1.56	1.42E-05	1.76E-03	0.27
Fyb1	0.77	1.7	6.79E-06	9.66E-04	0.13
Fzd2	0.46	1.37	2.96E-04	0.02	1
Fzd6	0.61	1.53	6.04E-03	0.17	1
Fzd7	0.4	1.32	3.75E-03	0.13	1
Gabarapl1	-0.17	-1.13	0.01	0.23	1
Gabpb1l	-5.05	-33.16	0.03	0.43	1
Gabra2	-0.19	-1.14	8.30E-03	0.2	1
Gabrg1	-0.18	-1.13	0.02	0.3	1
Gabrg2	-0.18	-1.13	0.01	0.26	1
Galnt18	-0.3	-1.23	0.01	0.24	1
Galnt7	0.28	1.22	0.04	0.49	1
Galr2	0.43	1.35	0.03	0.41	1
Gata1	1.86	3.63	0.04	0.44	1
Gch1	1.15	2.21	3.35E-04	0.02	1
Gcsam	1.7	3.25	2.57E-03	0.1	1
Gdf10	0.98	1.98	2.67E-04	0.02	1
Gdf15	-1.8	-3.49	0.03	0.43	1
gene:ENSRNOG00000001474	1.78	3.44	0.04	0.44	1
gene:ENSRNOG00000002820	2.28	4.85	1.01E-07	2.74E-05	1.91E-03
gene:ENSRNOG00000004090	3.15	8.89	7.75E-04	0.04	1
gene:ENSRNOG00000007238	2.45	5.45	8.95E-03	0.21	1
gene:ENSRNOG00000011042	2.42	5.35	0.02	0.36	1
gene:ENSRNOG00000018113	2.64	6.22	6.45E-03	0.17	1
gene:ENSRNOG00000029512	0.33	1.25	0.02	0.3	1
gene:ENSRNOG00000030021	0.47	1.38	0.02	0.3	1
gene:ENSRNOG00000031579	0.88	1.84	7.53E-05	6.58E-03	1
gene:ENSRNOG00000031859	0.44	1.35	0.04	0.48	1
gene:ENSRNOG00000042308	0.49	1.41	0.05	0.49	1
gene:ENSRNOG00000048109	-0.49	-1.41	0.05	0.51	1
gene:ENSRNOG00000049075	0.25	1.19	6.21E-04	0.03	1
gene:ENSRNOG00000058590	2.91	7.52	0.03	0.41	1
gene:ENSRNOG00000062480	0.82	1.77	0.02	0.34	1
gene:ENSRNOG00000062652	0.17	1.12	0.03	0.39	1
gene:ENSRNOG00000062798	0.91	1.88	0.04	0.48	1
gene:ENSRNOG00000062907	2.69	6.44	0.02	0.33	1
gene:ENSRNOG00000063038	3.31	9.94	0.01	0.26	1

gene:ENSRNOG00000063301	-0.78	-1.72	1.71E-03	0.07	1
gene:ENSRNOG00000063679	0.19	1.14	0.01	0.27	1
gene:ENSRNOG00000063700	0.51	1.42	0.01	0.27	1
gene:ENSRNOG00000063781	-2.01	-4.02	0.01	0.23	1
gene:ENSRNOG00000064399	0.19	1.14	7.98E-03	0.2	1
gene:ENSRNOG00000064524	3.89	14.83	5.55E-03	0.16	1
gene:ENSRNOG00000064569	-0.94	-1.92	0.04	0.44	1
gene:ENSRNOG00000064589	2.12	4.36	2.63E-03	0.1	1
gene:ENSRNOG00000065182	1.77	3.41	0.03	0.39	1
gene:ENSRNOG00000065602	-0.46	-1.37	0.02	0.37	1
gene:ENSRNOG00000065745	-0.62	-1.54	0.02	0.31	1
gene:ENSRNOG00000065746	-0.45	-1.36	0.05	0.51	1
gene:ENSRNOG00000065952	2.91	7.54	0.04	0.44	1
gene:ENSRNOG00000066080	1.42	2.67	0.03	0.41	1
gene:ENSRNOG00000066348	-0.33	-1.25	0.04	0.48	1
gene:ENSRNOG00000066471	0.28	1.22	0.04	0.47	1
gene:ENSRNOG00000066473	0.51	1.42	0.02	0.3	1
gene:ENSRNOG00000067018	1.17	2.26	0.04	0.48	1
gene:ENSRNOG00000067072	0.86	1.82	0.04	0.45	1
gene:ENSRNOG00000067229	-0.82	-1.76	0.04	0.46	1
gene:ENSRNOG00000067259	2.79	6.91	0.04	0.46	1
gene:ENSRNOG00000067276	-0.19	-1.14	0.02	0.33	1
gene:ENSRNOG00000067278	-0.56	-1.48	0.01	0.28	1
gene:ENSRNOG00000067347	1.34	2.54	0.04	0.49	1
gene:ENSRNOG00000067516	3.13	8.73	0.02	0.33	1
gene:ENSRNOG00000067711	-2.26	-4.78	0.05	0.5	1
gene:ENSRNOG00000067740	5.86	58.28	0.02	0.33	1
gene:ENSRNOG00000067762	1.37	2.59	0.05	0.49	1
gene:ENSRNOG00000067786	0.45	1.37	0.04	0.46	1
gene:ENSRNOG00000067832	3.57	11.84	4.40E-06	6.90E-04	0.08
gene:ENSRNOG00000068082	2.27	4.83	9.63E-07	1.90E-04	0.02
gene:ENSRNOG00000068306	-0.55	-1.46	6.88E-03	0.18	1
gene:ENSRNOG00000068602	0.59	1.51	0.02	0.29	1
gene:ENSRNOG00000068784	3.63	12.38	8.04E-03	0.2	1
gene:ENSRNOG00000068796	1.75	3.37	1.24E-03	0.06	1
gene:ENSRNOG00000069024	0.61	1.52	0.02	0.3	1
gene:ENSRNOG00000069032	1.24	2.37	7.73E-03	0.2	1
gene:ENSRNOG00000069140	1.7	3.26	0.05	0.51	1
gene:ENSRNOG00000069647	-0.22	-1.17	8.39E-03	0.2	1

gene:ENSRNOG00000069878	1.25	2.38	2.45E-03	0.1	1
gene:ENSRNOG00000069899	-6.08	-67.77	0.01	0.26	1
gene:ENSRNOG00000069961	-2.19	-4.57	0.01	0.24	1
gene:ENSRNOG00000070319	2.88	7.34	0.04	0.48	1
gene:ENSRNOG00000070434	1.3	2.46	3.29E-03	0.12	1
gene:ENSRNOG00000070444	1.62	3.08	0.01	0.23	1
gene:ENSRNOG00000070540	2.89	7.39	1.54E-03	0.07	1
gene:ENSRNOG00000070737	2.09	4.25	0.03	0.43	1
gene:ENSRNOG00000070861	1.92	3.77	2.20E-03	0.09	1
Gfi1	3.02	8.12	0.03	0.38	1
Gfi1b	3.31	9.94	0.02	0.29	1
Gfra2	-0.15	-1.11	0.05	0.49	1
Gimap8	0.4	1.32	0.03	0.39	1
Gjb2	0.74	1.67	8.21E-06	1.13E-03	0.16
Gjc3	-0.36	-1.29	3.22E-06	5.34E-04	0.06
Glb1l2	-0.59	-1.5	0.01	0.26	1
Gldn	-0.21	-1.16	0.01	0.24	1
Gli1	0.37	1.29	0.02	0.36	1
Glipr1	0.92	1.9	4.30E-03	0.14	1
Glis2	0.33	1.26	0.02	0.36	1
Glrb	-0.16	-1.12	0.03	0.38	1
Gm14137	0.94	1.92	8.46E-03	0.2	1
Gmip	0.28	1.22	0.04	0.48	1
Gnai1	-0.27	-1.21	3.69E-04	0.02	1
Gnb2	0.16	1.12	0.04	0.44	1
Gne	0.33	1.26	9.42E-03	0.22	1
Gng11	0.63	1.55	4.00E-04	0.03	1
Gnpnat1	-0.38	-1.3	0.03	0.37	1
Gp1ba	2.21	4.62	3.49E-05	3.63E-03	0.66
Gp9	1.76	3.38	0.04	0.44	1
Gpam	-0.18	-1.13	0.01	0.23	1
Gpd2	-0.18	-1.14	0.03	0.41	1
Gpr137b	-0.19	-1.14	0.03	0.42	1
Gpr141	2.31	4.96	0.02	0.3	1
Gpr161	0.25	1.19	0.04	0.48	1
Gpr22	-0.25	-1.19	0.05	0.49	1
Gprc5a	2.3	4.94	5.75E-03	0.16	1
Gpx1	0.25	1.19	0.03	0.41	1
Gria3	-0.28	-1.21	0.02	0.35	1

Grik2	-0.49	-1.41	0.02	0.33	1
Gsn	0.62	1.53	3.59E-05	3.72E-03	0.68
Gstm1	0.18	1.13	0.02	0.3	1
Gtf3c2	0.18	1.13	0.04	0.45	1
Gucy1a1	0.41	1.33	0.02	0.28	1
Gvin1	0.83	1.78	4.70E-04	0.03	1
Gxylt2	0.65	1.57	0.03	0.43	1
Gypa	1.86	3.64	1.50E-08	5.87E-06	2.84E-04
Gypc	0.59	1.51	5.87E-03	0.16	1
H1f1	0.6	1.51	7.70E-03	0.2	1
H1f4	0.45	1.37	1.76E-04	0.01	1
H2ac10	1.06	2.08	8.29E-03	0.2	1
H3c1	0.84	1.8	0.04	0.44	1
H4f3	0.43	1.34	3.17E-03	0.11	1
Hamp	1.99	3.98	1.50E-03	0.07	1
Has1	2.14	4.4	0.04	0.44	1
Hcls1	0.58	1.49	0.02	0.36	1
Heg1	0.22	1.17	2.83E-03	0.11	1
Hemgn	1.85	3.6	1.76E-11	1.29E-08	3.33E-07
Herc3	-0.15	-1.11	0.03	0.43	1
Heyl	-0.34	-1.27	5.72E-03	0.16	1
Hgf	0.38	1.3	0.05	0.5	1
Hhat	-0.81	-1.75	0.04	0.44	1
Hhip	0.81	1.75	0.01	0.25	1
Hif1an	-0.18	-1.13	0.03	0.42	1
Hist1h2ak	1.12	2.17	5.82E-04	0.03	1
Hist1h2bg	0.96	1.95	0.03	0.37	1
Hist1h2bq_2	0.86	1.81	0.01	0.23	1
Hist1h3b	0.89	1.85	1.87E-03	0.08	1
Hist2h3c2_2	0.5	1.41	0.04	0.48	1
Hist2h3c2_4	0.67	1.6	6.51E-05	5.94E-03	1
Hist2h3c2_6	0.43	1.35	0.03	0.39	1
Hk2	0.6	1.52	8.53E-03	0.21	1
Hk3	2.3	4.94	7.12E-03	0.19	1
Hmcn1	0.32	1.25	3.90E-03	0.13	1
Hmgb1	-1.02	-2.03	2.68E-07	6.42E-05	5.06E-03
Hmgb2l1_1	0.71	1.63	1.03E-03	0.05	1
Hmgn2	0.21	1.16	9.88E-03	0.22	1
Hoxb5	0.55	1.47	0.01	0.26	1

Hoxc5	0.45	1.36	0.04	0.44	1
Hoxc6	0.34	1.27	1.53E-05	1.86E-03	0.29
Hp	0.73	1.66	0.02	0.3	1
Hsd17b1	-2.17	-4.49	2.93E-03	0.11	1
Hsd17b8	0.54	1.45	4.13E-03	0.13	1
Hsh2d	1.36	2.57	0.04	0.48	1
Hspbap1	0.47	1.38	0.04	0.45	1
Hsph1	-0.2	-1.14	3.91E-03	0.13	1
Htra3	0.72	1.65	2.41E-04	0.02	1
Ibsp	0.66	1.58	0.04	0.44	1
Id3	-0.27	-1.21	0.02	0.37	1
Ier5	0.76	1.69	0.01	0.27	1
Ifi30	0.47	1.39	0.02	0.29	1
Ifi47	0.57	1.48	8.29E-03	0.2	1
Ifit1	2.18	4.52	7.34E-04	0.04	1
Ifit1bl	0.5	1.42	9.09E-03	0.21	1
Ifit3	0.74	1.67	0.02	0.36	1
Ifitm2	0.37	1.29	1.72E-03	0.07	1
Ifitm6	1.54	2.92	6.69E-05	6.04E-03	1
Igfbp5	0.74	1.67	8.11E-08	2.36E-05	1.53E-03
Igfbp6	0.56	1.48	5.44E-07	1.17E-04	0.01
Igfbp7	0.29	1.22	5.49E-05	5.29E-03	1
Igfn1	1.55	2.92	0.04	0.48	1
Ighm	1.68	3.2	2.22E-20	7.44E-17	4.19E-16
Igsf10	0.53	1.45	6.92E-03	0.18	1
Igsf6	0.9	1.87	5.37E-03	0.16	1
Ikzf1	0.68	1.6	6.29E-05	5.77E-03	1
Ikzf3	1.76	3.38	3.89E-05	3.93E-03	0.73
Il10ra	0.76	1.7	2.90E-03	0.11	1
Il13ra2	1.36	2.57	3.92E-06	6.27E-04	0.07
Il17ra	0.32	1.25	9.26E-03	0.22	1
Il17rd	0.32	1.25	0.01	0.24	1
Il18	1.02	2.03	0.02	0.29	1
Il18rap	1.61	3.06	3.17E-04	0.02	1
Il1a	2.3	4.92	0.02	0.34	1
Il1b	1.6	3.02	1.79E-03	0.08	1
Il1r1	0.34	1.26	0.04	0.46	1
Il1r2	2.38	5.2	0.01	0.23	1
Il1rl1	0.63	1.54	0.02	0.31	1

Il1rn	1.4	2.63	5.06E-03	0.15	1
Il24	2.81	7.03	0.01	0.26	1
Il2rg	0.82	1.76	8.85E-04	0.05	1
Il4r	0.58	1.49	0.02	0.3	1
Il7r	0.44	1.36	5.23E-04	0.03	1
Ildr2	0.64	1.56	0.01	0.28	1
Inka2	-0.29	-1.22	7.97E-03	0.2	1
Insc	-0.35	-1.27	6.22E-03	0.17	1
Insyn1	-0.25	-1.19	0.05	0.49	1
Insyn2a	0.3	1.23	0.04	0.49	1
Iqgap1	0.15	1.11	0.04	0.46	1
Irag1	0.45	1.37	8.62E-04	0.04	1
Irak3	0.32	1.25	0.01	0.26	1
Irf1	0.41	1.33	0.03	0.37	1
Irf2bp2	-0.17	-1.12	0.03	0.4	1
Irf4	0.96	1.95	3.03E-03	0.11	1
Irf5	0.74	1.67	2.15E-03	0.09	1
Irf7	0.38	1.31	0.04	0.47	1
Iscu	0.21	1.16	0.04	0.47	1
Islr	0.37	1.3	6.49E-03	0.18	1
Ism1	0.71	1.63	0.02	0.36	1
Itga1	0.32	1.25	6.38E-03	0.17	1
Itga11	0.77	1.71	5.49E-04	0.03	1
Itga2b	1.77	3.41	5.67E-10	3.17E-07	1.07E-05
Itga4	0.34	1.27	0.04	0.48	1
Itga8	0.46	1.37	9.01E-03	0.21	1
Itga9	0.49	1.4	9.12E-03	0.21	1
Itgal	1.04	2.05	1.51E-04	0.01	1
Itgam	0.96	1.94	1.22E-03	0.06	1
Itgav	-0.14	-1.1	0.04	0.44	1
Itgax	1.24	2.36	5.13E-04	0.03	1
Itgb2	1.24	2.37	9.96E-08	2.74E-05	1.88E-03
Itgb7	1.4	2.63	3.81E-03	0.13	1
Itgbl1	0.31	1.24	6.06E-03	0.17	1
Itpr1	0.23	1.18	0.05	0.51	1
Ivns1abp	-0.18	-1.13	0.01	0.23	1
Jade3	-0.61	-1.53	6.82E-03	0.18	1
Jchain	1.61	3.05	1.05E-05	1.38E-03	0.2
Kank2	0.19	1.14	0.02	0.33	1

Katnal1	-0.28	-1.21	1.25E-03	0.06	1
Kbtbd11	-0.25	-1.19	0.03	0.41	1
Kcna1	-0.17	-1.13	0.01	0.23	1
Kcna2	-0.19	-1.14	4.27E-03	0.14	1
Kcna4	-0.2	-1.15	4.15E-03	0.13	1
Kcnc3	-0.18	-1.13	0.02	0.3	1
Kcng1	-0.47	-1.39	4.32E-04	0.03	1
Kcnj10	-0.19	-1.14	5.70E-03	0.16	1
Kcnj15	0.54	1.45	0.04	0.44	1
Kcnk1	-0.2	-1.15	0.02	0.34	1
Kcnv2	2.58	5.97	0.05	0.51	1
Kcp	-0.71	-1.64	0.05	0.51	1
Kctd12	-0.14	-1.1	0.05	0.5	1
Kctd3	-0.2	-1.15	0.01	0.27	1
Kel	1.45	2.73	8.08E-03	0.2	1
Kif14	0.89	1.85	0.02	0.36	1
Kif15	0.7	1.63	2.30E-03	0.09	1
Kif20a	0.83	1.78	2.77E-03	0.1	1
Kif20b	0.5	1.41	0.02	0.3	1
Kif21a	-0.19	-1.14	4.80E-03	0.15	1
Kif23	0.59	1.51	0.03	0.43	1
Kif5b	-0.13	-1.1	0.05	0.49	1
Kifc1	0.88	1.85	0.01	0.26	1
Klf13	-0.23	-1.17	6.02E-03	0.17	1
Klf15	-0.37	-1.3	0.03	0.37	1
Klf5	0.25	1.19	0.02	0.37	1
Klf9	-0.3	-1.23	1.10E-04	8.75E-03	1
Kmo	1.65	3.15	0.04	0.48	1
Kndc1	-0.33	-1.25	6.29E-03	0.17	1
Knl1	0.31	1.24	0.01	0.25	1
Kpna6	-0.18	-1.13	0.03	0.41	1
Krt7	0.43	1.35	0.04	0.47	1
Kxd1	0.25	1.19	4.96E-04	0.03	1
Lama4	0.15	1.11	0.03	0.37	1
Laptm5	0.42	1.34	0.03	0.38	1
Large1	-0.2	-1.15	4.27E-03	0.14	1
Lbp	0.98	1.98	5.17E-04	0.03	1
Lcn2	1.03	2.04	2.04E-04	0.01	1
Lcp2	0.68	1.6	2.27E-04	0.02	1

Leng8	0.17	1.12	0.02	0.31	1
Lepr	0.32	1.25	0.05	0.51	1
Lgals3	0.24	1.18	1.89E-03	0.08	1
Lhcgr	1.86	3.63	0.03	0.4	1
Lhx6	3.56	11.76	8.64E-03	0.21	1
Lhx9	-1.13	-2.19	0.02	0.33	1
Lilrb2	0.85	1.8	0.04	0.45	1
Lilrb3a	3.59	12.03	5.18E-06	7.70E-04	0.1
Lilrb3l	5.97	62.61	0.02	0.31	1
Lilrb4	1.11	2.16	0.04	0.46	1
Lilrc2	2.22	4.65	0.04	0.45	1
Lima1	0.33	1.26	7.70E-03	0.2	1
Limd2	0.46	1.37	0.02	0.3	1
Litaf	0.22	1.17	0.01	0.26	1
Lman2l	-0.2	-1.15	0.02	0.35	1
Lmbrd2	-0.17	-1.13	0.02	0.32	1
Lmnb1	0.81	1.76	1.16E-03	0.06	1
Lmo7	0.45	1.37	8.99E-05	7.47E-03	1
Lox	0.92	1.9	6.85E-08	2.05E-05	1.29E-03
Loxhd1	-1.61	-3.05	0.01	0.28	1
Loxl1	0.74	1.67	8.32E-05	6.95E-03	1
Loxl2	0.3	1.23	0.02	0.34	1
Lrg1	0.54	1.45	0.05	0.51	1
Lrp1	0.2	1.15	3.07E-03	0.11	1
Lrrc4	-0.29	-1.22	0.02	0.37	1
Lrrc75b	0.28	1.21	0.05	0.49	1
Lsp1	0.84	1.79	4.82E-06	7.29E-04	0.09
Ltb	1.01	2.01	0.04	0.47	1
Lum	0.28	1.21	1.08E-04	8.69E-03	1
Lvrn	-0.33	-1.26	0.04	0.45	1
Ly6c	1.29	2.45	0.01	0.23	1
Ly6g6d	2.5	5.66	1.19E-04	9.35E-03	1
Lyc2	0.7	1.62	0.01	0.23	1
Lyl1	1.7	3.25	1.60E-04	0.01	1
Lyn	0.46	1.38	3.05E-03	0.11	1
Lyz2	0.74	1.67	1.46E-12	1.25E-09	2.76E-08
Mafg	-0.17	-1.12	0.03	0.4	1
Magee1	-0.15	-1.11	0.04	0.44	1
Majin	-3.03	-8.16	0.02	0.37	1

Maml1	0.31	1.24	0.02	0.35	1
Man2a1	0.2	1.15	0.03	0.37	1
Man2b1	0.21	1.15	0.01	0.26	1
Mansc1	0.52	1.43	0.04	0.44	1
Maob	-0.23	-1.17	0.05	0.5	1
Map3k1	0.28	1.21	1.13E-03	0.05	1
Map3k13	-0.33	-1.25	0.01	0.24	1
Map4k1	0.85	1.8	1.08E-03	0.05	1
Map7	-0.17	-1.13	0.02	0.34	1
Map7d3	0.86	1.82	3.62E-04	0.02	1
Mapk8ip2	-0.15	-1.11	0.04	0.45	1
Mboat1	-0.33	-1.26	8.23E-03	0.2	1
Mcc	0.29	1.22	0.03	0.41	1
Mcemp1	1.43	2.7	0.02	0.36	1
Mcm5	0.51	1.42	0.04	0.47	1
Mcm6	0.58	1.49	0.02	0.29	1
Mcph1	0.3	1.23	0.04	0.47	1
Mcpt9	2.19	4.56	8.20E-07	1.64E-04	0.02
Mecom	-0.43	-1.35	0.02	0.29	1
Med17	-0.3	-1.23	0.02	0.36	1
Medag	0.76	1.69	4.56E-04	0.03	1
Megf10	-0.2	-1.15	9.44E-03	0.22	1
Megf9	-0.21	-1.15	4.09E-03	0.13	1
Meis2	-0.3	-1.23	0.02	0.31	1
Meox1	0.73	1.65	0.03	0.43	1
Meox2	0.73	1.66	2.90E-04	0.02	1
Mest	-0.19	-1.14	0.01	0.25	1
Mfap4	1.27	2.41	1.05E-15	1.60E-12	1.98E-11
Mfap5	0.53	1.45	4.88E-05	4.79E-03	0.92
Mgp	0.5	1.41	1.94E-06	3.40E-04	0.04
Miga1	-0.18	-1.13	0.03	0.37	1
Minar1	-0.23	-1.17	0.04	0.47	1
Mki67	1.15	2.22	5.32E-13	5.34E-10	1.01E-08
Mkks	-0.4	-1.32	1.58E-03	0.07	1
Mks1	0.5	1.42	0.02	0.3	1
Mlec_1	0.25	1.19	0.02	0.33	1
Mmd2	-0.2	-1.15	0.01	0.23	1
Mmp13	1.2	2.3	2.94E-03	0.11	1
Mmp15	-0.17	-1.12	0.02	0.34	1

Mmp16	0.41	1.33	0.02	0.3	1
Mmp2	0.42	1.34	1.32E-04	1.00E-02	1
Mmp8	2.91	7.53	5.08E-24	2.84E-20	9.59E-20
Mmp9	2.46	5.51	8.17E-08	2.36E-05	1.54E-03
Mmrn1	1.74	3.35	1.30E-08	5.19E-06	2.45E-04
Mn1	1.13	2.19	4.17E-04	0.03	1
Mpeg1	0.52	1.43	1.12E-03	0.05	1
Mpig6b	1.78	3.44	2.01E-05	2.28E-03	0.38
Mpl	1.17	2.25	2.93E-03	0.11	1
Mpo	2.36	5.12	1.58E-13	2.04E-10	2.98E-09
Mrc2	0.45	1.36	2.38E-04	0.02	1
Mrpl51	-0.26	-1.2	6.01E-04	0.03	1
Mrps35	0.25	1.19	0.04	0.47	1
Mrps6	-0.25	-1.19	0.04	0.48	1
Ms4a1	3.91	15.06	1.29E-04	9.90E-03	1
Ms4a3	2.37	5.18	0.02	0.32	1
Mt3	-0.18	-1.13	0.01	0.25	1
Mtm1	-0.2	-1.15	0.03	0.43	1
Muc20	1.96	3.89	6.97E-03	0.18	1
Mx1	0.45	1.36	0.02	0.29	1
Mxra7	-0.25	-1.19	0.04	0.49	1
Myb	1.33	2.51	3.88E-03	0.13	1
Mybl2	1.71	3.26	3.00E-03	0.11	1
Myct1	0.99	1.99	4.88E-03	0.15	1
Myd88	0.4	1.32	0.04	0.46	1
Myh11	0.62	1.53	2.48E-08	8.67E-06	4.69E-04
Myh7	-1.48	-2.79	8.91E-04	0.05	1
Myl9	0.95	1.93	3.19E-08	1.07E-05	6.02E-04
Mylk	0.54	1.45	2.14E-06	3.69E-04	0.04
Myo1c	0.2	1.15	0.01	0.26	1
Myo1f	0.79	1.73	1.87E-06	3.30E-04	0.04
Myo1g	1.42	2.68	7.98E-05	6.83E-03	1
Myo5c	0.68	1.6	0.01	0.24	1
Myo7a	0.88	1.84	0.02	0.3	1
Myocd	0.86	1.82	0.04	0.44	1
N4bp2	0.3	1.23	0.02	0.32	1
N4bp2l1	0.64	1.56	0.03	0.37	1
Naglu	0.42	1.34	0.02	0.3	1
Napsa	1.84	3.57	2.17E-04	0.02	1

Nat8f3	-0.42	-1.34	1.06E-03	0.05	1
Nbeal1	-0.17	-1.12	0.02	0.31	1
Ncam2	-0.25	-1.19	5.21E-04	0.03	1
Ncan	-0.28	-1.21	0.02	0.31	1
Ncf1	0.77	1.7	4.64E-06	7.14E-04	0.09
Ncf2	0.85	1.8	0.04	0.45	1
Ncf4	1	2	4.87E-03	0.15	1
Nckap1l	0.62	1.54	3.12E-05	3.42E-03	0.59
Ncoa7	-0.15	-1.11	0.02	0.36	1
Ndc80	0.68	1.61	0.01	0.25	1
Ndrg1	-0.14	-1.1	0.04	0.47	1
Ndrg2	0.15	1.11	0.03	0.39	1
Ndufa3	0.2	1.15	9.30E-03	0.22	1
Ndufa4	0.18	1.13	0.02	0.3	1
Ndufa6	0.2	1.14	0.02	0.34	1
Ndufs8	0.19	1.14	0.03	0.38	1
Nedd9	0.25	1.19	0.04	0.48	1
Nek3	-0.42	-1.34	0.05	0.49	1
Nes	-0.16	-1.12	0.03	0.38	1
NEWGENE_1308171	0.53	1.45	2.34E-14	3.27E-11	4.41E-10
NEWGENE_2724	1.39	2.62	3.96E-04	0.03	1
NEWGENE_620180	0.43	1.34	5.31E-03	0.16	1
Nfam1	0.61	1.52	0.03	0.4	1
Nfatc1	0.29	1.22	0.02	0.31	1
Nfatc4	0.51	1.42	0.02	0.34	1
Nfe2	1.84	3.59	1.04E-06	2.01E-04	0.02
Nfe2l3	-1	-1.99	0.03	0.38	1
Nfkbia	0.24	1.19	0.04	0.47	1
Ngf	1.3	2.46	0.02	0.34	1
Ngly1	-0.16	-1.12	0.05	0.51	1
Ngp	2.38	5.2	2.80E-22	1.18E-18	5.29E-18
Nkg7	2.58	5.97	0.03	0.38	1
Nkiras1	-0.21	-1.16	6.55E-03	0.18	1
Nkx6-1	1.91	3.75	0.04	0.48	1
Nlrp12	3.7	12.97	5.70E-03	0.16	1
Nlrp1a	0.48	1.4	0.01	0.24	1
Nme3	0.75	1.68	0.05	0.5	1
Nmnat3	0.81	1.75	0.04	0.47	1
Nmt2	-0.15	-1.11	0.05	0.5	1

Nnat	0.51	1.42	1.08E-05	1.41E-03	0.2
Nop53	0.17	1.12	0.05	0.51	1
Notch1	-0.19	-1.14	9.16E-03	0.21	1
Nox3	-3.16	-8.93	0.03	0.37	1
Nox4	2.14	4.41	1.05E-03	0.05	1
Np4	3.04	8.24	3.42E-09	1.51E-06	6.47E-05
Npas2	1.54	2.9	7.88E-06	1.09E-03	0.15
Nphp3	0.43	1.34	0.05	0.5	1
Nphp4	-0.48	-1.4	0.01	0.24	1
Npr1	0.66	1.58	0.03	0.41	1
Nptx1	-0.3	-1.23	1.84E-05	2.13E-03	0.35
Nptx2	-0.24	-1.18	0.03	0.41	1
Npy5r	0.7	1.62	0.02	0.32	1
Nqo2	-0.49	-1.4	7.84E-03	0.2	1
Nr1d1	-0.4	-1.32	2.19E-04	0.02	1
Nr1d2	-0.23	-1.17	2.58E-03	0.1	1
Nr1h2	0.23	1.18	6.66E-03	0.18	1
Nrcam	-0.19	-1.14	5.87E-03	0.16	1
Nrg1	-0.15	-1.11	0.03	0.42	1
Nrp1	0.21	1.16	6.27E-03	0.17	1
Nrxn1	-0.15	-1.11	0.03	0.41	1
Nsf	-0.14	-1.1	0.03	0.43	1
Nsg2	-0.18	-1.13	0.01	0.23	1
Nt5c3b	0.5	1.41	1.15E-04	9.09E-03	1
Ntn1	0.57	1.49	1.54E-03	0.07	1
Ntng1	-0.32	-1.25	9.84E-05	7.98E-03	1
Ntrk1	-0.19	-1.14	9.08E-03	0.21	1
Ntrk2	-0.18	-1.13	9.15E-03	0.21	1
Nup210l	0.8	1.74	0.03	0.39	1
Nup93	-0.15	-1.11	0.05	0.49	1
Nwd1	-0.42	-1.34	8.97E-03	0.21	1
Nxpe3	-0.24	-1.18	6.35E-03	0.17	1
Nxt2	-0.57	-1.49	0.01	0.24	1
Oaf	-0.22	-1.16	0.01	0.27	1
Obp3	1.95	3.86	3.49E-03	0.12	1
Odf2	0.21	1.16	0.02	0.31	1
Olfm4	1.44	2.71	0.01	0.24	1
Olfml3	0.27	1.21	0.03	0.37	1
Olr1585	0.47	1.39	0.01	0.26	1

Omd	0.37	1.29	0.05	0.49	1
Oprk1	-0.53	-1.45	7.72E-03	0.2	1
Oprm1	-0.27	-1.21	0.02	0.36	1
Osbpl3	-0.15	-1.11	0.05	0.49	1
Osr1	0.58	1.5	0.02	0.36	1
Oxr1	-0.16	-1.12	0.02	0.3	1
P2rx4	0.38	1.3	0.02	0.33	1
P2ry10	1.45	2.73	5.28E-03	0.16	1
P3h3	0.22	1.17	4.10E-03	0.13	1
Pabpc1	0.16	1.12	0.02	0.34	1
Pacc1	0.37	1.29	0.05	0.5	1
Pacsin1	-0.19	-1.14	0.02	0.32	1
Pank1	-0.39	-1.31	2.07E-03	0.08	1
Pank3	-0.15	-1.11	0.03	0.43	1
Paqr8	-0.18	-1.13	0.02	0.28	1
Parl	0.28	1.22	0.03	0.39	1
Parp10	0.35	1.27	0.05	0.5	1
Parp3	0.27	1.21	0.02	0.37	1
Pawr	0.68	1.6	0.02	0.29	1
Pax5	2.78	6.85	6.91E-05	6.13E-03	1
Pcbd1_2	0.58	1.49	5.57E-04	0.03	1
Pcdh18	0.25	1.19	0.03	0.43	1
Pcdh7_1	-0.15	-1.11	0.04	0.45	1
Pcdh7_2	-0.51	-1.42	0.05	0.49	1
Pcdhb12	0.62	1.54	0.04	0.46	1
Pcdhb5	-0.74	-1.67	5.26E-03	0.16	1
Pclo	-0.14	-1.1	0.04	0.47	1
Pcolce	0.27	1.2	0.04	0.45	1
PCOLCE2	0.37	1.29	0.03	0.37	1
Pde2a	0.18	1.13	0.03	0.41	1
Pde3a	0.37	1.29	0.03	0.39	1
Pde4d	-0.17	-1.12	0.04	0.48	1
Pde5a	0.68	1.6	5.35E-08	1.63E-05	1.01E-03
Pde7b	-0.32	-1.25	5.87E-03	0.16	1
Pdgfd	-0.23	-1.18	0.05	0.5	1
Pdgfra	0.23	1.17	0.03	0.42	1
Pdgfrl	1.1	2.14	6.03E-05	5.63E-03	1
Pdlim1	0.31	1.24	7.89E-03	0.2	1
Pdpk1	-0.22	-1.16	5.25E-03	0.16	1

Pdzd8	-0.17	-1.13	0.01	0.26	1
Pecam1	0.4	1.32	1.88E-03	0.08	1
Per1	-0.61	-1.53	4.32E-07	9.79E-05	8.15E-03
Per2	-0.5	-1.41	5.53E-03	0.16	1
Pex5l	-0.16	-1.12	0.04	0.46	1
Pgam5	0.27	1.21	0.04	0.48	1
Pgd	-0.14	-1.1	0.04	0.46	1
Pglyrp1	3.02	8.12	7.64E-04	0.04	1
Pgm2	0.28	1.21	0.04	0.46	1
Pgm5	0.59	1.51	0.03	0.43	1
Phex	1.16	2.23	3.51E-04	0.02	1
Phldb2	0.18	1.13	0.04	0.45	1
Pi15	0.85	1.81	1.10E-03	0.05	1
Pi16	1.26	2.4	1.36E-09	6.94E-07	2.58E-05
Pi4k2a	-0.17	-1.13	0.03	0.4	1
Piezo1	0.35	1.27	8.12E-03	0.2	1
Pign	-0.26	-1.2	0.04	0.49	1
Pigq	0.23	1.17	0.05	0.5	1
Pik3ap1	0.97	1.96	1.54E-06	2.82E-04	0.03
Pik3c2a	-0.17	-1.12	0.02	0.36	1
Pik3cg	0.42	1.34	0.03	0.4	1
Pik3r1	-0.18	-1.13	9.61E-03	0.22	1
Pink1	-0.16	-1.12	0.03	0.41	1
Pir	-0.25	-1.19	0.04	0.46	1
Pkdcc	0.49	1.4	0.01	0.25	1
Pkhd1l1	1.49	2.82	5.80E-09	2.49E-06	1.09E-04
Pla1a	0.71	1.63	0.03	0.42	1
Pla2g2a	1.43	2.7	5.66E-04	0.03	1
Pla2g4a	0.7	1.62	1.62E-03	0.07	1
Plac8	1.67	3.18	9.30E-11	6.24E-08	1.76E-06
Plac9	1.84	3.58	5.38E-03	0.16	1
Plat	0.22	1.17	1.86E-03	0.08	1
Plbd1	1.29	2.44	7.74E-07	1.60E-04	0.01
Plcd3	0.42	1.33	0.03	0.37	1
Plcg2	0.75	1.68	6.70E-03	0.18	1
Plek	1.07	2.1	4.18E-05	4.15E-03	0.79
Plin1	5.38	41.58	0.03	0.43	1
Plin2	0.16	1.12	0.04	0.48	1
Plk1	1.04	2.06	0.01	0.23	1

Plscr2_1	0.74	1.67	0.05	0.49	1
Plvap	0.63	1.54	5.80E-03	0.16	1
Plxnb2	0.16	1.12	0.04	0.46	1
Pml	0.27	1.2	0.05	0.49	1
Pnma2	-0.16	-1.12	0.03	0.37	1
Pold3	0.44	1.35	9.19E-03	0.21	1
Pomgnt2	-0.26	-1.2	0.03	0.42	1
Pou2af1	2.03	4.08	2.67E-03	0.1	1
Pou3f1	-0.47	-1.38	0.01	0.26	1
Ppa1	-0.15	-1.11	0.04	0.48	1
Ppbp	5.39	41.84	0.03	0.43	1
Ppdpf	0.29	1.22	1.00E-02	0.23	1
Ppic	0.25	1.19	0.05	0.5	1
Ppp1r15b	-0.17	-1.13	0.02	0.36	1
Ppp1r21	0.19	1.14	0.03	0.42	1
Ppp2r2a	-0.16	-1.12	0.03	0.4	1
Ppp3cb	-0.16	-1.12	0.02	0.35	1
Ppp3cc	0.27	1.21	0.02	0.34	1
Ppp4r2	-0.2	-1.15	0.01	0.23	1
Prc1	0.59	1.51	4.93E-03	0.15	1
Prdm16	0.28	1.21	0.02	0.3	1
Prdm5	0.46	1.37	0.01	0.23	1
Prdm6	0.87	1.83	1.80E-03	0.08	1
Prdx4	0.39	1.31	3.09E-03	0.11	1
Prelp	0.39	1.31	1.71E-03	0.07	1
Prex2	-0.21	-1.16	0.04	0.47	1
Prg2	2.11	4.31	3.91E-12	3.12E-09	7.38E-08
Prg3	2.82	7.07	1.24E-07	3.25E-05	2.34E-03
Prg4	0.79	1.72	1.88E-04	0.01	1
Prim1	-1.01	-2.01	1.38E-07	3.56E-05	2.60E-03
Prkca	-0.14	-1.11	0.04	0.46	1
Prkce	-0.15	-1.11	0.04	0.49	1
Prox1	1.31	2.49	1.67E-03	0.07	1
Prr5	-0.34	-1.27	0.02	0.32	1
Prrg3	-0.19	-1.14	0.02	0.33	1
Prrx1	0.53	1.45	1.71E-04	0.01	1
Prrx2	0.91	1.88	0.05	0.51	1
Prss29	5.16	35.87	0.05	0.49	1
Prune2	-0.14	-1.1	0.04	0.44	1

Psd4	0.93	1.9	7.21E-04	0.04	1
Psmb8	0.65	1.57	0.04	0.47	1
Psme1	0.32	1.25	8.51E-03	0.21	1
Psph	0.44	1.36	0.03	0.37	1
Pstpip1	0.65	1.56	0.01	0.23	1
Ptch1	0.4	1.32	1.24E-04	9.60E-03	1
Ptch2	0.86	1.81	3.82E-04	0.02	1
Ptgdrl	-2.27	-4.82	0.02	0.35	1
Ptgs1	0.5	1.42	0.02	0.29	1
Ptpn22	1.38	2.59	3.45E-03	0.12	1
Ptpn6	0.77	1.7	3.26E-05	3.49E-03	0.62
Ptprc	0.86	1.81	2.05E-13	2.46E-10	3.87E-09
Ptprcap	1.75	3.36	0.01	0.26	1
Ptprh	1.97	3.92	8.20E-04	0.04	1
Ptprj	0.15	1.11	0.04	0.48	1
Ptprz1	-0.18	-1.14	8.32E-03	0.2	1
Pura	-0.17	-1.13	0.01	0.23	1
Pygm	0.5	1.42	6.41E-03	0.17	1
Qk	-0.15	-1.11	0.03	0.41	1
R3hdm1	-0.23	-1.17	0.04	0.46	1
Rab11fip1	0.56	1.47	2.09E-03	0.08	1
Rab3gap1	-0.16	-1.11	0.04	0.48	1
Rab3il1	0.5	1.42	8.90E-04	0.05	1
Rab44	2.77	6.81	6.72E-04	0.04	1
Rac2	0.95	1.93	5.69E-04	0.03	1
Rack1	0.27	1.21	4.35E-04	0.03	1
Rag1	1.7	3.25	4.30E-03	0.14	1
Rag2	2.26	4.81	0.01	0.24	1
Ralgapa2	-0.2	-1.15	5.07E-03	0.15	1
Ralgds	-0.25	-1.19	0.02	0.34	1
Rapgef4	-0.16	-1.12	0.02	0.36	1
Rasa1	-0.15	-1.11	0.04	0.47	1
Rasgrp3	0.49	1.41	2.57E-03	0.1	1
Rasgrp4	1.36	2.57	0.01	0.25	1
Rassf2	0.49	1.4	1.37E-04	0.01	1
RatNP-3b	2.85	7.22	5.42E-12	4.14E-09	1.02E-07
Rbfox3	-0.21	-1.16	3.42E-03	0.12	1
Rbm38	1.26	2.39	1.80E-08	6.71E-06	3.40E-04
Rbpjl	1.78	3.44	0.04	0.48	1

Rcc1	0.61	1.53	0.01	0.24	1
Rcsd1	0.36	1.28	0.01	0.24	1
Rdh16	0.84	1.78	3.18E-03	0.11	1
Reep2	-0.15	-1.11	0.04	0.47	1
Reep5	-0.13	-1.1	0.04	0.49	1
Reg3b	1.6	3.02	8.57E-03	0.21	1
Rem2	-0.46	-1.38	0.03	0.39	1
Ret	-0.15	-1.11	0.03	0.43	1
Retn	2.51	5.69	0.02	0.33	1
Retnlg	2.42	5.34	1.64E-05	1.95E-03	0.31
Rftn1	0.55	1.47	0.03	0.39	1
RGD1306271	-0.23	-1.18	7.47E-03	0.19	1
RGD1306941	-0.26	-1.2	1.46E-03	0.07	1
RGD1310587	0.43	1.35	5.30E-04	0.03	1
RGD1560464	-6.24	-75.51	0.01	0.25	1
RGD1561958	-2.87	-7.29	0.04	0.44	1
RGD1565355	0.29	1.22	0.05	0.5	1
RGD1565989	-3.42	-10.69	0.01	0.25	1
Rgl1	-0.17	-1.12	0.03	0.37	1
Rgs14	1.08	2.11	3.16E-03	0.11	1
Rgs18	1.03	2.04	3.23E-05	3.47E-03	0.61
Rhag	1.87	3.65	1.09E-05	1.41E-03	0.21
Rhd	1.7	3.25	3.85E-04	0.02	1
Rhoh	0.82	1.76	0.03	0.4	1
Rhoj	0.34	1.27	7.48E-05	6.58E-03	1
Rims1	-0.16	-1.12	0.03	0.42	1
Rin1	1.09	2.12	9.67E-03	0.22	1
Ripk1	0.34	1.26	0.02	0.32	1
Ripor2	0.29	1.23	0.03	0.42	1
Rlbp1	-0.8	-1.75	0.01	0.27	1
Rmdn1	0.45	1.37	1.40E-03	0.07	1
Rnase2	2.16	4.47	0.02	0.36	1
Rnase3_1	2.07	4.19	0.01	0.27	1
Rnase3_2	3.53	11.54	0.01	0.26	1
Rnf149	-0.26	-1.19	0.03	0.4	1
Rnf212	-1.61	-3.06	0.01	0.27	1
Rnf214	-0.21	-1.15	7.58E-03	0.19	1
Rnh1	0.3	1.23	0.01	0.23	1
Ror2	0.99	1.99	7.79E-05	6.73E-03	1

Rph3a	-0.15	-1.11	0.03	0.43	1
Rph3al	0.82	1.76	0.05	0.5	1
Rpl11	0.15	1.11	0.04	0.44	1
Rpl13	0.2	1.15	7.71E-03	0.2	1
Rpl15	0.18	1.13	0.02	0.29	1
Rpl18	0.19	1.14	0.03	0.39	1
Rpl19	0.21	1.15	3.62E-03	0.13	1
Rpl26	0.24	1.18	5.41E-04	0.03	1
Rpl29	0.16	1.12	0.05	0.5	1
Rpl31	0.2	1.15	8.56E-03	0.21	1
Rpl31l4	1.39	2.61	8.23E-05	6.91E-03	1
Rpl32	0.19	1.14	0.01	0.24	1
Rpl35	0.17	1.12	0.02	0.29	1
Rpl35a_1	0.25	1.19	0.02	0.32	1
Rpl36a_2	0.27	1.21	0.02	0.36	1
Rpl38_4	0.16	1.12	0.03	0.43	1
Rpl39_3	0.32	1.25	7.61E-05	6.61E-03	1
Rpl5	0.21	1.16	3.14E-03	0.11	1
Rpl6	0.14	1.1	0.05	0.5	1
Rpl7a	0.2	1.15	4.46E-03	0.14	1
Rplp1	0.27	1.21	6.65E-05	6.03E-03	1
Rps10l1	0.47	1.38	0.01	0.23	1
Rps12	0.25	1.19	5.26E-03	0.16	1
Rps14	0.16	1.12	0.03	0.43	1
Rps15	0.18	1.14	9.65E-03	0.22	1
Rps16	0.16	1.12	0.02	0.36	1
Rps17_1	0.24	1.18	1.43E-03	0.07	1
Rps18l1	0.33	1.26	2.24E-03	0.09	1
Rps2	0.14	1.1	0.05	0.5	1
Rps20_1	0.24	1.18	1.26E-03	0.06	1
Rps24	0.15	1.11	0.03	0.43	1
Rps28	0.2	1.15	0.03	0.38	1
Rps29_1	0.2	1.15	9.84E-03	0.22	1
Rps3a	0.21	1.16	2.53E-03	0.1	1
Rps4x_1	0.26	1.19	4.81E-04	0.03	1
Rps5	0.21	1.15	5.80E-03	0.16	1
Rps8	0.26	1.19	4.66E-04	0.03	1
Rpsa	0.15	1.11	0.03	0.43	1
Rragd	-0.44	-1.36	0.01	0.24	1

Rrm2b	-0.19	-1.14	0.02	0.31	1
Rsad2	1.09	2.13	2.45E-06	4.16E-04	0.05
RT1-Ba	0.74	1.67	7.59E-04	0.04	1
RT1-Bb	1.06	2.08	0.02	0.31	1
RT1-CE2	-1.55	-2.93	4.11E-03	0.13	1
RT1-Da	0.61	1.53	2.03E-03	0.08	1
RT1-Db1	0.62	1.54	0.03	0.39	1
RT1-DMb	0.61	1.52	0.03	0.37	1
Rtn4	-0.15	-1.11	0.02	0.35	1
Rtn4ip1	-0.37	-1.29	9.87E-03	0.22	1
Runx2	0.52	1.43	0.01	0.24	1
Ryr2	-0.19	-1.14	7.00E-03	0.18	1
S100a6	0.25	1.19	7.39E-04	0.04	1
S100a8	2.64	6.24	4.89E-32	4.11E-28	9.24E-28
Sacs	-0.14	-1.1	0.04	0.45	1
Samd8	-0.18	-1.13	0.04	0.44	1
Samd9	0.24	1.18	1.74E-03	0.07	1
Satb2	1.15	2.21	0.02	0.3	1
Scand1	0.27	1.2	7.77E-03	0.2	1
Scara3	0.41	1.33	3.70E-03	0.13	1
Scarf2	0.41	1.33	0.03	0.41	1
Scd	-0.18	-1.13	8.54E-03	0.21	1
Scd3	-0.42	-1.34	0.02	0.32	1
Scgb1a1	-1.98	-3.94	0.03	0.42	1
Scml4	-0.42	-1.33	1.99E-03	0.08	1
Scn1a	-0.21	-1.15	2.68E-03	0.1	1
Scn4b	-0.14	-1.1	0.04	0.47	1
Scn8a	-0.19	-1.14	7.19E-03	0.19	1
Scpep1	0.25	1.19	3.32E-03	0.12	1
Scrn3	-0.18	-1.14	0.03	0.41	1
Sdc1	0.52	1.43	0.03	0.41	1
Sdc2	0.3	1.23	9.29E-05	7.64E-03	1
Sdc4	-0.16	-1.12	0.04	0.48	1
Sec11c	-0.19	-1.14	0.03	0.43	1
Sec14l1	-0.18	-1.13	0.01	0.27	1
Selenbp1	0.5	1.41	0.03	0.37	1
Selenof	0.22	1.17	1.95E-03	0.08	1
Sell	1.93	3.82	1.49E-12	1.25E-09	2.81E-08
Selplg	0.95	1.93	9.65E-06	1.29E-03	0.18

Sema3c	0.22	1.16	2.86E-03	0.11	1
Sema3g	-0.25	-1.19	0.03	0.42	1
Sema5a	-0.21	-1.15	2.91E-03	0.11	1
Senp8	-0.26	-1.2	0.04	0.48	1
Serpinb10	2.57	5.96	3.83E-05	3.90E-03	0.72
Serpinb11	3.13	8.73	0.02	0.34	1
Serpinb1a	0.41	1.33	2.30E-08	8.22E-06	4.35E-04
Serpinb6a	-0.28	-1.22	5.10E-03	0.15	1
Serpinf1	0.67	1.59	2.83E-08	9.70E-06	5.35E-04
Serping1	0.46	1.38	2.47E-05	2.75E-03	0.47
Sf3a1	-0.16	-1.12	0.04	0.46	1
Sfrp2	3.03	8.2	1.09E-09	5.72E-07	2.06E-05
Sfrp4	0.74	1.67	7.38E-05	6.52E-03	1
Sgk1	-0.38	-1.3	4.39E-06	6.90E-04	0.08
Sgpp2	-0.3	-1.23	0.01	0.27	1
Sgta	0.17	1.12	0.04	0.47	1
Sh2d1b2	0.79	1.73	0.02	0.31	1
Sh2d3c	0.29	1.22	0.04	0.49	1
Sh2d4a	0.53	1.45	0.04	0.47	1
Sh3d19	-0.17	-1.13	0.02	0.3	1
Shisa3	0.9	1.87	4.40E-07	9.84E-05	8.31E-03
Shisa9	-0.47	-1.39	0.05	0.5	1
Shroom4	0.3	1.23	0.04	0.46	1
Siglec10	2.68	6.42	1.30E-03	0.06	1
Six1	-0.16	-1.11	0.05	0.49	1
Six4	-0.18	-1.14	0.02	0.31	1
Sla	1.03	2.04	5.72E-03	0.16	1
Slamf6	2.96	7.77	5.74E-03	0.16	1
Slc13a4	0.63	1.54	4.98E-05	4.86E-03	0.94
Slc14a1	0.57	1.48	0.02	0.35	1
Slc15a2	-0.33	-1.26	8.36E-03	0.2	1
Slc16a11	0.51	1.42	3.17E-05	3.43E-03	0.6
Slc17a7	-0.19	-1.14	8.41E-03	0.2	1
Slc17a8	-1.3	-2.46	1.02E-03	0.05	1
Slc19a1	0.6	1.52	4.20E-03	0.14	1
Slc1a4	-0.16	-1.11	0.05	0.5	1
Slc22a17	-0.15	-1.11	0.04	0.46	1
Slc25a25	-0.25	-1.19	0.03	0.37	1
Slc25a37	0.62	1.53	4.61E-03	0.14	1

Slc25a45	-0.35	-1.28	0.03	0.41	1
Slc26a11	-0.65	-1.57	8.55E-03	0.21	1
Slc26a2	0.33	1.26	0.05	0.5	1
Slc28a2	0.72	1.65	6.17E-03	0.17	1
Slc33a1	-0.33	-1.25	9.34E-03	0.22	1
Slc35f1	-0.15	-1.11	0.04	0.49	1
Slc38a3	-0.95	-1.93	8.90E-03	0.21	1
Slc38a5	1.53	2.88	0.02	0.33	1
Slc39a10	-0.23	-1.17	2.47E-03	0.1	1
Slc43a1	0.92	1.89	0.02	0.33	1
Slc43a3	-0.25	-1.19	0.03	0.4	1
Slc47a1	0.51	1.42	0.01	0.26	1
Slc4a1	1.89	3.69	1.31E-16	2.75E-13	2.48E-12
Slc4a10	0.72	1.65	0.02	0.32	1
Slc5a3	-0.26	-1.2	0.01	0.25	1
Slc6a13	0.47	1.39	3.93E-03	0.13	1
Slc6a17	-0.19	-1.14	6.96E-03	0.18	1
Slc6a4	1.61	3.06	0.02	0.33	1
Slc6a6	0.28	1.21	0.02	0.36	1
Slc9a3r1	-0.22	-1.17	3.70E-03	0.13	1
Slfn13	0.35	1.28	5.80E-03	0.16	1
Slfn2	0.56	1.47	5.00E-03	0.15	1
Slitrk2	-0.25	-1.19	4.80E-04	0.03	1
Slitrk3	-0.15	-1.11	0.04	0.47	1
Smad9	-0.16	-1.12	0.03	0.41	1
Smap2	-0.16	-1.12	0.04	0.44	1
Smim14	0.15	1.11	0.05	0.49	1
Smoc1	1.12	2.17	4.04E-05	4.06E-03	0.76
Snai2	0.83	1.77	0.01	0.25	1
Snx10	0.38	1.3	9.04E-03	0.21	1
Socs3	0.75	1.68	5.38E-03	0.16	1
Sorl1	-0.22	-1.16	0.03	0.42	1
Sos1	-0.16	-1.12	0.02	0.33	1
Sox10	-0.18	-1.13	0.02	0.3	1
Sp100	0.37	1.29	2.27E-03	0.09	1
Sp110	0.38	1.3	7.61E-03	0.19	1
Sp140	0.31	1.24	0.03	0.39	1
Sp5	2.59	6.04	0.01	0.27	1
Spag17	3.25	9.54	2.49E-03	0.1	1

Spata32	1.42	2.68	5.73E-04	0.03	1
Sphk1	-0.45	-1.36	0.02	0.32	1
Spib	2.25	4.76	6.83E-05	6.13E-03	1
Spint2	0.32	1.25	0.05	0.5	1
Spn	0.86	1.82	1.79E-03	0.08	1
Sppl3	-0.17	-1.13	0.03	0.4	1
Spta1	1.51	2.86	4.05E-10	2.42E-07	7.64E-06
Srgn	0.94	1.92	4.69E-10	2.71E-07	8.85E-06
Srpx2	0.88	1.85	0.02	0.3	1
Ssc5d	0.29	1.22	0.04	0.44	1
St14	1.25	2.38	3.60E-03	0.12	1
St6gal2	-0.55	-1.46	0.03	0.43	1
St6galnac2_1	0.74	1.67	0.03	0.41	1
St8sia3	-0.18	-1.13	0.02	0.33	1
Stab2	1.47	2.76	0.03	0.37	1
Stard13	0.16	1.12	0.04	0.44	1
Steap3	-0.17	-1.12	0.04	0.46	1
Stk32a	0.67	1.59	0.02	0.32	1
Stom	0.61	1.53	1.62E-06	2.93E-04	0.03
Ston1	-0.16	-1.11	0.05	0.49	1
Stra6	0.99	1.99	1.60E-04	0.01	1
Strip2	0.35	1.28	0.04	0.46	1
Stx11	0.4	1.32	0.01	0.25	1
Stxbp1	-0.18	-1.13	8.73E-03	0.21	1
Stxbp2	0.62	1.53	0.03	0.41	1
Stxbp5	-0.15	-1.11	0.05	0.51	1
Stxbp6	0.34	1.26	0.02	0.34	1
Sulf2	0.32	1.25	3.77E-03	0.13	1
Sv2c	-0.16	-1.12	0.02	0.3	1
Svep1	0.63	1.54	5.52E-06	8.13E-04	0.1
Svil	0.16	1.12	0.03	0.41	1
Svip	-0.25	-1.19	4.89E-04	0.03	1
Syk	0.92	1.9	1.77E-06	3.17E-04	0.03
Syn2	-0.15	-1.11	0.05	0.49	1
Syngr2	0.34	1.27	0.02	0.3	1
Synm	-0.26	-1.2	9.69E-03	0.22	1
Synpo2	0.54	1.45	1.74E-05	2.05E-03	0.33
Syt2	-0.2	-1.15	4.63E-03	0.14	1
Sytl2	0.15	1.11	0.03	0.41	1

Tacc3	0.69	1.61	0.01	0.26	1
Tagap	1.15	2.22	3.16E-05	3.43E-03	0.6
Tagln	0.86	1.82	4.89E-08	1.52E-05	9.24E-04
Tagln2	0.21	1.16	3.25E-03	0.12	1
Tal1	1.19	2.27	1.28E-05	1.59E-03	0.24
Tars3	-0.18	-1.13	0.03	0.42	1
Tasl	1.12	2.18	0.05	0.49	1
Tax1bp3	0.25	1.19	0.04	0.44	1
Tbx15	0.69	1.61	1.74E-03	0.07	1
Tbx2	-0.28	-1.21	1.63E-03	0.07	1
Tbx3	-0.31	-1.24	0.02	0.31	1
Tec	0.34	1.27	8.24E-03	0.2	1
Tef	-0.32	-1.24	3.90E-03	0.13	1
Tek	0.26	1.2	0.03	0.43	1
Tent5a	0.8	1.74	5.56E-04	0.03	1
Tf	0.39	1.31	3.70E-04	0.02	1
Tfpt	0.29	1.23	0.05	0.51	1
Tgfb1	0.49	1.4	0.01	0.25	1
Tgfbi	0.32	1.25	2.17E-03	0.09	1
Tgfbr1	0.18	1.13	0.03	0.39	1
Tgm2	0.51	1.43	8.06E-05	6.86E-03	1
Thbd	0.59	1.5	3.79E-07	8.71E-05	7.16E-03
Thbs1	0.74	1.67	3.90E-08	1.26E-05	7.36E-04
Thrsp	2.91	7.52	0.04	0.45	1
Ticrr	1.4	2.64	8.98E-03	0.21	1
Tifa	0.33	1.26	0.03	0.43	1
Timm44	0.26	1.19	0.04	0.46	1
Timmdc1	0.25	1.19	0.05	0.51	1
Timp4	-0.56	-1.47	2.47E-03	0.1	1
Tinagl1	0.35	1.28	0.04	0.49	1
Tlcd4	-0.31	-1.24	7.51E-03	0.19	1
Tln1	0.14	1.11	0.04	0.46	1
Tlr3	0.35	1.28	0.03	0.37	1
Tlr8	0.43	1.35	0.03	0.39	1
Tm6sf1	-0.16	-1.12	0.04	0.46	1
Tmc7	-0.31	-1.24	8.63E-03	0.21	1
Tmc8	1.16	2.24	0.03	0.41	1
Tmem132c	-0.38	-1.3	1.14E-03	0.05	1
Tmem150c	-0.19	-1.14	0.01	0.27	1

Tmem176b	0.27	1.21	6.96E-03	0.18	1
Tmem179	-0.17	-1.13	0.04	0.48	1
Tmem204	0.57	1.48	6.80E-03	0.18	1
Tmem229a	-0.45	-1.36	3.43E-03	0.12	1
Tmem33	-0.16	-1.12	0.02	0.36	1
Tmem35a	-0.18	-1.13	0.02	0.34	1
Tmem41b	-0.16	-1.12	0.03	0.43	1
Tmem60	-0.27	-1.2	0.04	0.45	1
Tmem71	1.65	3.14	8.46E-04	0.04	1
Tmx3	-0.18	-1.13	0.02	0.29	1
Tnfaip8l2	0.69	1.61	0.02	0.28	1
Tnfrsf1b	0.59	1.5	3.06E-03	0.11	1
Tnn	2.15	4.45	0.03	0.38	1
Tnpo3	-0.18	-1.13	0.02	0.32	1
Tomm34	-0.18	-1.13	0.03	0.37	1
Top2a	0.44	1.36	8.15E-03	0.2	1
Tp53i13	0.68	1.6	0.04	0.46	1
Tpm2	0.42	1.34	0.02	0.29	1
Tpm4	0.27	1.21	9.83E-05	7.98E-03	1
Tpsb2	2.11	4.31	0.03	0.43	1
Tpst1	0.25	1.19	0.04	0.49	1
Tpx2	0.49	1.41	5.87E-03	0.16	1
Tradd	0.78	1.72	0.02	0.32	1
Traf3ip3	1.06	2.09	7.15E-03	0.19	1
Treml2	2.64	6.25	4.81E-06	7.29E-04	0.09
Trib1	-0.31	-1.24	0.04	0.47	1
Tril	-0.17	-1.12	0.02	0.37	1
Trim32	-0.19	-1.14	0.03	0.39	1
Trim37	-0.2	-1.15	4.40E-03	0.14	1
Trim45	-1.19	-2.29	4.41E-05	4.35E-03	0.83
Trim6	1.78	3.44	0.04	0.48	1
Trim9	-0.25	-1.19	0.04	0.46	1
Trir	-0.24	-1.18	6.35E-03	0.17	1
Trpm4	-0.29	-1.22	0.05	0.5	1
Tspan11	0.4	1.32	6.13E-03	0.17	1
Tstd1	0.46	1.38	4.66E-04	0.03	1
Ttc7a	0.36	1.29	0.04	0.45	1
Ttc9	-0.15	-1.11	0.03	0.42	1
Ttll7	-0.19	-1.14	4.77E-03	0.15	1

Ttyh1	-0.18	-1.13	0.01	0.25	1
Tubb1	1.96	3.9	1.10E-06	2.05E-04	0.02
Tubb2a	0.14	1.1	0.04	0.49	1
Tubb6	0.5	1.41	0.02	0.32	1
Twist1	0.74	1.67	9.75E-03	0.22	1
Txnrd3	-0.29	-1.22	0.03	0.39	1
Tyrobp	0.77	1.7	3.46E-03	0.12	1
Ube2c	1.16	2.24	4.89E-03	0.15	1
Ube2q2	-0.18	-1.13	0.01	0.26	1
Ube4b	-0.14	-1.1	0.04	0.48	1
Ubqln1	-0.14	-1.1	0.04	0.49	1
Ubr3	-0.19	-1.14	5.71E-03	0.16	1
Ubxn2a_1	-0.18	-1.13	0.02	0.3	1
Ugcg	-0.23	-1.17	3.35E-03	0.12	1
Uhrf1	0.65	1.57	0.03	0.4	1
Unc13a	-0.18	-1.13	0.02	0.32	1
Unc5b	0.31	1.24	0.03	0.43	1
Uqcr10	0.24	1.18	0.04	0.45	1
Usp20	-0.18	-1.13	0.02	0.33	1
Usp3	0.31	1.24	0.03	0.4	1
Usp32	-0.14	-1.1	0.04	0.49	1
Usp9y	-4.63	-24.75	7.97E-04	0.04	1
Ust	-0.18	-1.13	0.03	0.41	1
Vav1	0.59	1.5	0.02	0.3	1
Vim	0.14	1.1	0.03	0.43	1
Vip	2.49	5.61	4.53E-07	1.00E-04	8.55E-03
Vipr2	0.5	1.41	0.03	0.42	1
Vpreb3	3.02	8.12	4.47E-03	0.14	1
Vps35	-0.17	-1.12	0.02	0.3	1
Vsig10l	-0.48	-1.4	8.59E-03	0.21	1
Vsir	0.31	1.24	0.02	0.29	1
Vstm1	2.35	5.08	6.78E-03	0.18	1
Vstm2b	-0.48	-1.39	0.02	0.32	1
Vwf	0.66	1.58	4.64E-08	1.47E-05	8.76E-04
Wasl	-0.18	-1.14	0.01	0.25	1
Wdfy4	0.97	1.96	1.10E-06	2.05E-04	0.02
Wdr46	0.31	1.24	0.04	0.44	1
Wdr70	-0.31	-1.24	0.01	0.26	1
Wee1	-0.38	-1.3	2.89E-03	0.11	1

Wipf3	-0.23	-1.17	2.13E-03	0.09	1
Wnt2b	0.54	1.46	0.04	0.48	1
Xdh	0.57	1.49	9.26E-04	0.05	1
Ybx3	0.49	1.41	4.47E-06	6.95E-04	0.08
Ypel3	0.17	1.13	0.02	0.34	1
Ywhag	-0.19	-1.14	4.75E-03	0.15	1
Zbp1	1.3	2.46	0.02	0.29	1
Zbtb16	-0.92	-1.89	1.44E-06	2.66E-04	0.03
Zc2hc1a	-0.15	-1.11	0.04	0.47	1
Zc3h10	0.17	1.12	0.02	0.31	1
Zc3h12d	1.01	2.01	0.02	0.33	1
Zc3h15	-0.17	-1.12	0.02	0.36	1
Zcchc24	-0.22	-1.16	5.15E-03	0.15	1
Zdhhc16	0.37	1.29	0.03	0.39	1
Zfp14	0.3	1.23	0.02	0.32	1
Zfp2	-0.35	-1.27	5.66E-04	0.03	1
Zfp202	0.37	1.29	0.02	0.37	1
Zfp217	0.42	1.33	0.03	0.38	1
Zfp260	-0.17	-1.12	0.04	0.44	1
Zfp36	0.41	1.33	4.40E-03	0.14	1
Zfp385b	-0.24	-1.18	0.04	0.44	1
Zfp516	-0.22	-1.16	4.90E-03	0.15	1
Zfp646	0.29	1.22	0.02	0.3	1
Zfp663	4.79	27.62	2.50E-03	0.1	1
Zfp84_2	0.42	1.34	1.73E-03	0.07	1
Zfp862	0.58	1.49	2.57E-03	0.1	1
Zfp871	-0.17	-1.13	0.01	0.27	1
Zic1	0.8	1.74	1.16E-05	1.49E-03	0.22
Zmat3	-0.15	-1.11	0.04	0.46	1
Znf660	1.02	2.03	0.03	0.43	1
Zyx	0.24	1.18	0.04	0.47	1

Table A3.10. Master list of differentially expressed genes between female 10X CXB-NE vs male 10X CXB-NE samples with an FDR p-value ≤ 0.05 and a fold change greater than ±1.

Name	Log_2 fold change	Fold change	P-value	FDR p-value	Bonferroni
AABR07005775.1	-2.94	-7.7	6.58E-05	0.01	1
AABR07034445.1	1.34	2.53	1.27E-04	0.02	1
AABR07073181.1	-0.31	-1.24	4.90E-05	8.83E-03	0.93
Abat	-0.45	-1.36	4.92E-04	0.04	1
Acsf2	-0.6	-1.52	2.56E-05	5.65E-03	0.48
Acta1	-1.82	-3.53	2.30E-04	0.03	1
Acta2	-0.86	-1.82	9.34E-05	0.01	1
Adh6_1	-2.8	-6.97	1.21E-04	0.02	1
Ano3	0.31	1.24	6.36E-05	0.01	1
Aox4	-0.75	-1.68	2.99E-06	1.31E-03	0.06
Apcdd1	-0.6	-1.52	1.15E-05	3.32E-03	0.22
Ass1	-1.38	-2.6	2.58E-15	1.90E-11	4.87E-11
Atp1a2	-0.45	-1.37	6.43E-05	0.01	1
Bahcc1	-0.49	-1.4	5.51E-04	0.05	1
Banp	0.51	1.42	1.26E-04	0.02	1
Bcas1	-0.56	-1.48	3.62E-06	1.49E-03	0.07
Bicd1	0.3	1.23	1.29E-04	0.02	1
C1ql3	-0.61	-1.53	1.72E-05	4.31E-03	0.33
Ca3	-1.95	-3.87	2.56E-05	5.65E-03	0.48
Cacybp	0.27	1.21	4.37E-04	0.04	1
Cav1	-0.42	-1.34	3.61E-04	0.04	1
Cav2	-0.49	-1.4	1.57E-04	0.02	1
Cdh18	0.39	1.31	1.33E-05	3.60E-03	0.25
Cdh5	-0.46	-1.38	1.91E-04	0.02	1
Ceacam4	-1.44	-2.71	8.75E-05	0.01	1
Chmp4bl1	-1.19	-2.28	5.04E-04	0.05	1
Ckm	-2.48	-5.57	1.34E-04	0.02	1
Clvs1	1.36	2.57	6.16E-05	0.01	1
Cntf	-0.44	-1.36	3.18E-04	0.03	1
Col15a1	-0.41	-1.33	3.86E-04	0.04	1
Col1a1	-0.55	-1.46	8.97E-05	0.01	1
Col1a2	-0.43	-1.35	1.15E-04	0.02	1
Col2a1	-1.29	-2.44	2.96E-07	2.19E-04	5.60E-03

Col4a1	-0.36	-1.28	5.62E-06	1.96E-03	0.11
Col4a2	-0.32	-1.24	7.43E-05	0.01	1
Col6a1	-0.56	-1.47	1.86E-04	0.02	1
Col6a2	-0.54	-1.45	1.12E-04	0.02	1
Col9a1	-1.41	-2.65	7.54E-05	0.01	1
Csmd3	0.6	1.51	5.52E-06	1.96E-03	0.1
Cxcl12	-0.55	-1.46	2.18E-05	5.03E-03	0.41
Cyyr1	-0.45	-1.37	4.70E-04	0.04	1
Dbp	-1.15	-2.23	5.95E-15	2.93E-11	1.13E-10
Dcdc2	-1.03	-2.04	4.77E-04	0.04	1
Ddx3	-13.44	-11,081.59	2.73E-06	1.30E-03	0.05
Ddx3x	0.33	1.25	1.57E-05	4.15E-03	0.3
Ddx3y	1.15	2.23	3.30E-04	0.03	1
Dmd	0.44	1.36	5.08E-09	6.26E-06	9.61E-05
Dnah11	-0.56	-1.48	3.08E-05	6.17E-03	0.58
Drp2	-0.34	-1.27	5.70E-06	1.96E-03	0.11
Ebf2	-0.49	-1.41	5.06E-04	0.05	1
Edil3	0.3	1.23	1.59E-04	0.02	1
Eif2s3x	0.89	1.86	4.35E-30	6.44E-26	8.23E-26
Eif2s3y	-13.37	-10,621.72	3.00E-06	1.31E-03	0.06
Eif3el1	0.33	1.26	1.59E-04	0.02	1
Eif5a2	0.28	1.22	2.49E-04	0.03	1
Emb	0.33	1.26	1.09E-04	0.02	1
Eng	-0.67	-1.59	3.02E-05	6.17E-03	0.57
Epas1	-0.34	-1.27	1.34E-05	3.60E-03	0.25
Epb41l2	-0.28	-1.21	3.40E-04	0.04	1
Esyt2	0.29	1.22	2.10E-04	0.02	1
Fam111a	1.38	2.59	2.71E-04	0.03	1
Fgf7	-0.59	-1.51	7.61E-05	0.01	1
Fgl2	-0.47	-1.38	4.63E-05	8.55E-03	0.88
Flt1	-0.55	-1.46	3.09E-05	6.17E-03	0.58
Fn1	-0.45	-1.36	2.36E-04	0.03	1
Frem2	-0.9	-1.86	1.16E-04	0.02	1
Fxyd6	-0.44	-1.36	2.30E-04	0.03	1
gene:ENSRNOG00000028747	-0.88	-1.84	4.87E-06	1.84E-03	0.09
gene:ENSRNOG00000032224	0.44	1.36	2.88E-04	0.03	1
gene:ENSRNOG00000048109	0.72	1.65	9.25E-09	1.05E-05	1.75E-04
gene:ENSRNOG00000062930	-0.57	-1.48	3.76E-07	2.52E-04	7.10E-03
gene:ENSRNOG00000065189	4.83	28.42	3.24E-04	0.03	1

gene:ENSRNOG00000065273	-0.5	-1.41	1.59E-04	0.02	1
gene:ENSRNOG00000067240	0.49	1.41	3.95E-05	7.58E-03	0.75
gene:ENSRNOG00000068362	-4.23	-18.78	1.33E-12	4.90E-09	2.51E-08
Grhl3	2.56	5.89	1.75E-04	0.02	1
Gria4	-0.54	-1.46	7.44E-05	0.01	1
H2bc18	0.62	1.54	1.94E-07	1.69E-04	3.67E-03
Hlf	-0.81	-1.75	4.53E-04	0.04	1
Islr	-0.55	-1.47	3.89E-04	0.04	1
Itga6	-0.31	-1.24	6.70E-05	0.01	1
Kcnh7	0.27	1.21	5.68E-04	0.05	1
Kdm5c	0.53	1.44	4.31E-10	1.06E-06	8.15E-06
Kdm5d	-12.35	-5,231.88	1.62E-05	4.20E-03	0.31
Kdm6a	0.73	1.66	3.30E-09	4.44E-06	6.25E-05
Kif13b	-0.34	-1.26	2.95E-05	6.14E-03	0.56
Lama5	-0.54	-1.45	7.01E-05	0.01	1
Lamb1	-0.29	-1.22	1.62E-04	0.02	1
Lhfpl6	-0.33	-1.26	3.24E-04	0.03	1
Limch1	-0.48	-1.39	4.24E-05	7.94E-03	0.8
Lpl	-0.78	-1.72	2.34E-07	1.92E-04	4.42E-03
Lrp4	-0.38	-1.3	4.81E-05	8.79E-03	0.91
Lrpprc	0.31	1.24	9.56E-05	0.01	1
Mag	-0.68	-1.61	2.75E-06	1.30E-03	0.05
Mal	-0.58	-1.5	3.71E-07	2.52E-04	7.02E-03
Mapk8	0.3	1.23	1.95E-04	0.02	1
Mbp	-0.49	-1.41	1.05E-05	3.23E-03	0.2
Mgll	-0.43	-1.34	9.51E-08	8.79E-05	1.80E-03
Mlec_1	-0.32	-1.24	3.60E-04	0.04	1
Mpz	-0.63	-1.55	2.00E-08	2.12E-05	3.79E-04
Mt-nd1	0.54	1.45	1.54E-06	8.66E-04	0.03
Mt-nd2	0.48	1.39	1.85E-05	4.48E-03	0.35
Mt-nd4	0.52	1.44	2.81E-06	1.30E-03	0.05
Mt-nd4l	0.61	1.53	5.29E-08	5.21E-05	1.00E-03
Mxra8	-0.42	-1.34	7.34E-06	2.46E-03	0.14
Myh4	-3.56	-11.76	2.79E-09	4.44E-06	5.28E-05
Myl1	-4.62	-24.58	9.82E-05	0.01	1
Mylk	-0.53	-1.45	3.61E-04	0.04	1
Myom2	-1.22	-2.33	3.00E-09	4.44E-06	5.67E-05
Myom3	2.95	7.73	2.20E-12	6.51E-09	4.16E-08
Nbl1	-0.35	-1.27	2.89E-05	6.11E-03	0.55

Nes	-0.42	-1.34	2.62E-07	2.04E-04	4.95E-03
Notch4	-0.86	-1.81	2.85E-04	0.03	1
Nr1d1	-0.68	-1.6	9.06E-05	0.01	1
Nr1d2	-0.39	-1.31	1.14E-05	3.32E-03	0.21
Nup93	0.37	1.29	8.82E-06	2.83E-03	0.17
Olr318	5.4	42.16	3.47E-04	0.04	1
Osbpl5	-0.54	-1.45	2.12E-05	4.98E-03	0.4
Pbdc1	0.56	1.47	1.61E-09	2.97E-06	3.04E-05
Pde7b	0.61	1.52	4.22E-05	7.94E-03	0.8
Plce1	0.35	1.27	2.02E-05	4.82E-03	0.38
Plekha7	-0.62	-1.54	3.75E-06	1.50E-03	0.07
Pmp2	-1.2	-2.3	8.61E-10	1.82E-06	1.63E-05
Pmp22	-0.43	-1.35	1.12E-04	0.02	1
Podxl	-0.53	-1.44	2.76E-05	5.99E-03	0.52
Ppa1	0.29	1.23	3.02E-04	0.03	1
Prrg3	-0.39	-1.31	2.84E-05	6.09E-03	0.54
Prx	-0.5	-1.41	1.03E-05	3.23E-03	0.19
Ptgds	-0.94	-1.92	2.12E-04	0.02	1
Ptprb	-0.53	-1.44	1.33E-05	3.60E-03	0.25
Rars1	0.31	1.24	4.59E-04	0.04	1
RatNP-3b	-1.71	-3.28	4.14E-04	0.04	1
Rbp4	-0.52	-1.43	5.10E-04	0.05	1
Rev3l	0.39	1.31	2.40E-06	1.22E-03	0.05
RGD1310587	-0.68	-1.6	9.31E-07	5.74E-04	0.02
Ro60	0.29	1.22	4.91E-04	0.04	1
Rpl10l	1.34	2.54	1.94E-04	0.02	1
Rufy3	0.33	1.25	1.80E-05	4.43E-03	0.34
Sacs	0.26	1.2	4.18E-04	0.04	1
Scube1	-0.52	-1.43	2.01E-04	0.02	1
Sema3b	-0.31	-1.24	1.35E-04	0.02	1
Serping1	-0.53	-1.44	1.71E-05	4.31E-03	0.32
Shisa3	-0.84	-1.79	1.71E-04	0.02	1
Slc13a3	-0.69	-1.61	3.61E-06	1.49E-03	0.07
Slc16a11	-0.63	-1.55	6.38E-07	4.10E-04	0.01
Slc41a1	-0.51	-1.42	7.58E-05	0.01	1
Slc47a1	-1.32	-2.5	6.54E-05	0.01	1
Slc6a6	-0.52	-1.43	1.53E-04	0.02	1
Slc6a8	-0.33	-1.26	2.11E-04	0.02	1
Slc7a5	-0.43	-1.35	5.00E-06	1.85E-03	0.09

Slfn4_1	-0.75	-1.68	8.63E-06	2.83E-03	0.16
Smurf1	-0.31	-1.24	5.21E-04	0.05	1
Sptb	-0.36	-1.29	4.14E-06	1.61E-03	0.08
Tbccd1	0.35	1.28	1.71E-04	0.02	1
Tf	-0.38	-1.3	1.30E-05	3.60E-03	0.25
Thbs2	-0.62	-1.53	1.08E-06	6.36E-04	0.02
Timp3	-0.28	-1.21	4.35E-04	0.04	1
Tnnt3	-1.85	-3.61	2.28E-06	1.21E-03	0.04
Tpm4	-0.29	-1.22	1.88E-04	0.02	1
Trim45	1.23	2.34	3.70E-04	0.04	1
Trnp1	-0.28	-1.22	4.59E-04	0.04	1
Tuba1c	-0.54	-1.45	1.13E-05	3.32E-03	0.21
Tyrp1	0.36	1.29	1.58E-06	8.66E-04	0.03
Ucp2	-0.34	-1.27	3.54E-05	6.89E-03	0.67
Uty	-11.9	-3,828.55	3.26E-05	6.43E-03	0.62
Wwtr1	-0.32	-1.24	1.28E-04	0.02	1
Zfp518a	0.32	1.25	4.14E-04	0.04	1
Zfp709l1	0.29	1.23	5.67E-04	0.05	1
Zgrf1	0.99	1.99	2.45E-05	5.58E-03	0.46

Table A3.11. Master list of differentially expressed genes between female 10X DF-NE vs male 10X DF-NE samples with an FDR p-value ≤ 0.05 and a fold change greater than ±1.

Name	**Log_2 fold change**	**Fold change**	**P-value**	**FDR p-value**	**Bonferroni**
4833439L19Rik	-0.38	-1.3	6.55E-06	4.96E-04	0.12
AABR07003537.1	0.53	1.44	2.78E-04	0.01	1
AABR07005844.1	0.94	1.92	1.31E-03	0.04	1
AABR07007068.1	0.55	1.46	1.36E-11	3.31E-09	2.52E-07
AABR07017241.1	0.83	1.78	5.16E-04	0.02	1
AABR07021465.1	-1.39	-2.61	9.04E-04	0.03	1
AABR07028769.1	-0.36	-1.28	8.86E-06	6.30E-04	0.16
AABR07040947.1	-0.44	-1.36	8.10E-04	0.03	1
AABR07060872.1	1.79	3.45	1.55E-03	0.04	1
AABR07073181.1	-0.41	-1.33	2.62E-04	0.01	1
Abca1	0.24	1.18	1.73E-03	0.04	1
Abca2	-0.28	-1.22	2.93E-04	0.01	1

Abcb1b_1	-0.8	-1.74	1.19E-09	1.99E-07	2.22E-05
Abcd2	-0.34	-1.26	1.54E-04	6.99E-03	1
Acer2	-0.67	-1.59	1.86E-04	8.13E-03	1
Acox3	0.4	1.32	1.52E-03	0.04	1
Acsl4	0.36	1.28	8.79E-06	6.29E-04	0.16
Acsl6	-0.39	-1.31	1.01E-03	0.03	1
Adamts20	-0.42	-1.34	8.61E-04	0.03	1
Adamtsl1	-0.9	-1.86	2.12E-16	8.87E-14	3.95E-12
Adcy1	-0.36	-1.29	1.11E-05	7.61E-04	0.21
Adcyap1	0.78	1.72	3.45E-11	7.39E-09	6.42E-07
Adgre4	2.27	4.82	2.04E-03	0.05	1
Adgrf5	-0.49	-1.41	3.30E-07	3.67E-05	6.14E-03
Adgrl1	-0.28	-1.21	5.78E-04	0.02	1
Afg3l2	-0.28	-1.22	1.30E-03	0.04	1
Agfg2	-0.55	-1.47	1.87E-04	8.15E-03	1
Aif1	0.83	1.78	9.13E-04	0.03	1
Aif1l	-0.9	-1.86	5.28E-12	1.40E-09	9.82E-08
Ajuba	-0.78	-1.72	2.90E-04	0.01	1
Akr1b1	-0.7	-1.63	1.16E-17	5.95E-15	2.16E-13
Ankfn1	-0.7	-1.63	2.31E-05	1.46E-03	0.43
Ankrd1	2.96	7.76	2.59E-10	4.67E-08	4.81E-06
Ap1s1	0.34	1.27	5.99E-05	3.23E-03	1
Apcdd1	-0.53	-1.45	7.22E-05	3.82E-03	1
Appl2	0.4	1.32	1.72E-03	0.04	1
Arg1	1.85	3.61	7.46E-06	5.51E-04	0.14
Arhgap19	-0.56	-1.47	9.12E-10	1.56E-07	1.70E-05
Arhgap24	-0.45	-1.36	1.46E-03	0.04	1
Arhgap31	-0.37	-1.3	2.77E-05	1.70E-03	0.52
Arhgef10	-0.28	-1.21	7.09E-04	0.02	1
Arntl	1.25	2.38	2.09E-11	4.87E-09	3.88E-07
Arrdc4	0.4	1.32	1.06E-03	0.03	1
Atf3	1.81	3.51	1.04E-10	2.03E-08	1.93E-06
Atg12	0.31	1.24	3.02E-04	0.01	1
Atp2b2	-0.26	-1.2	8.01E-04	0.03	1
Atp2b4	0.5	1.42	1.72E-05	1.12E-03	0.32
Atp6v1fnb	0.28	1.21	8.53E-04	0.03	1
B3galnt1	0.44	1.35	1.72E-03	0.04	1
Bcas1	-1.03	-2.04	3.43E-31	7.78E-28	6.38E-27
Bhlhe40	-0.6	-1.51	4.64E-05	2.59E-03	0.86

C1qa	0.8	1.74	4.62E-05	2.58E-03	0.86
C1qb	0.83	1.78	5.71E-06	4.39E-04	0.11
C1qc	0.67	1.59	4.40E-06	3.60E-04	0.08
C1ql3	-0.82	-1.76	7.81E-09	1.19E-06	1.45E-04
C2cd2	0.28	1.22	1.88E-03	0.05	1
C3	0.92	1.89	1.44E-05	9.71E-04	0.27
C4a	0.57	1.48	4.90E-04	0.02	1
Cacna2d1	0.87	1.83	6.31E-29	1.25E-25	1.18E-24
Cadm3	-0.32	-1.24	3.19E-05	1.90E-03	0.59
Cadm4	-0.63	-1.55	1.30E-14	4.60E-12	2.43E-10
Calb1	0.96	1.95	1.44E-04	6.60E-03	1
Camk2d	0.34	1.26	2.96E-05	1.79E-03	0.55
Capn5	0.26	1.2	8.07E-04	0.03	1
Caskin2	-0.45	-1.36	8.09E-07	8.34E-05	0.02
Casp3	0.46	1.38	9.35E-04	0.03	1
Cav1	-0.39	-1.31	9.53E-04	0.03	1
Cbln2	0.67	1.59	2.70E-14	8.93E-12	5.03E-10
Ccbe1	1.61	3.06	4.45E-04	0.02	1
Ccdc172	1.01	2.01	3.51E-05	2.04E-03	0.65
Ccdc6	-0.25	-1.19	1.76E-03	0.05	1
Cckbr	2.31	4.95	5.49E-07	5.90E-05	0.01
Ccl2	1.03	2.04	2.10E-08	2.90E-06	3.91E-04
Ccl21	1.73	3.32	4.92E-08	6.39E-06	9.16E-04
Ccn4	-0.65	-1.57	7.08E-06	5.26E-04	0.13
Ccr2	1.14	2.2	1.35E-04	6.26E-03	1
Cct4	0.26	1.2	1.10E-03	0.03	1
Cd34	-0.52	-1.44	2.63E-04	0.01	1
Cd44	0.27	1.21	4.17E-04	0.02	1
Cd74	1.25	2.38	6.87E-56	3.64E-52	1.28E-51
Cdc42se2	0.39	1.31	1.01E-05	7.03E-04	0.19
Cdc45_2	-0.95	-1.93	1.54E-10	2.92E-08	2.87E-06
Cdh1	-0.3	-1.23	1.24E-04	5.85E-03	1
Cdk5r2	-0.29	-1.22	5.43E-04	0.02	1
Cdr2l	-0.37	-1.3	2.99E-06	2.54E-04	0.06
Cebpd	0.8	1.74	1.35E-04	6.26E-03	1
Celsr2	-0.34	-1.26	2.49E-05	1.55E-03	0.46
Cenpb	-0.27	-1.2	1.92E-03	0.05	1
Cfap410	-0.56	-1.48	2.37E-05	1.49E-03	0.44
Cgn	-1.39	-2.63	3.03E-04	0.01	1

Chchd6	0.61	1.53	1.60E-03	0.04	1
Chga	-0.35	-1.27	6.03E-05	3.23E-03	1
Chl1	0.39	1.31	3.87E-07	4.24E-05	7.21E-03
Chrm2	0.29	1.22	1.17E-03	0.03	1
Chrna3	-0.41	-1.33	1.37E-06	1.29E-04	0.03
Chrnb3	-0.29	-1.22	5.28E-04	0.02	1
Chst2	-0.66	-1.59	1.60E-16	7.07E-14	2.98E-12
Ciart	-1.63	-3.11	1.87E-04	8.15E-03	1
Ciita	1.18	2.27	3.99E-04	0.01	1
Clcn4	-0.25	-1.19	2.00E-03	0.05	1
Cldn19	-0.86	-1.81	8.51E-11	1.69E-08	1.59E-06
Cldn4	3.41	10.66	9.00E-05	4.58E-03	1
Clec7a	0.93	1.9	2.66E-05	1.64E-03	0.5
Clstn1	-0.33	-1.25	1.87E-05	1.20E-03	0.35
Cmtm6	-0.47	-1.39	1.23E-04	5.85E-03	1
Cnmd	-0.8	-1.74	2.29E-11	5.27E-09	4.26E-07
Cnn2	0.55	1.46	1.02E-04	5.00E-03	1
Cnp	-0.26	-1.2	1.01E-03	0.03	1
Cntf	-0.54	-1.46	1.50E-05	9.94E-04	0.28
Col15a1	-0.44	-1.35	1.56E-04	7.07E-03	1
Col23a1	-0.63	-1.55	8.62E-06	6.22E-04	0.16
Col24a1	-0.45	-1.37	7.48E-04	0.02	1
Col2a1	-1.69	-3.23	1.25E-17	6.21E-15	2.33E-13
Col4a1	-0.33	-1.25	3.44E-05	2.01E-03	0.64
Col4a2	-0.39	-1.31	8.55E-07	8.71E-05	0.02
Colec11	0.26	1.2	7.24E-04	0.02	1
Crabp2	0.53	1.45	2.26E-04	9.64E-03	1
Cracdl	-1.96	-3.9	2.00E-04	8.61E-03	1
Creld2	1.06	2.08	6.71E-08	8.40E-06	1.25E-03
Crisp3	4.04	16.46	7.83E-15	2.96E-12	1.46E-10
Crispld2	-0.61	-1.53	4.16E-05	2.36E-03	0.78
Cryab	-0.41	-1.33	5.51E-04	0.02	1
Crybg1	1.04	2.06	8.61E-06	6.22E-04	0.16
Csf1	0.61	1.52	3.41E-06	2.88E-04	0.06
Csf1r	0.41	1.33	1.06E-03	0.03	1
Csrp3	3.07	8.4	1.28E-18	7.83E-16	2.39E-14
Ctnnal1	-0.71	-1.63	7.82E-17	3.65E-14	1.46E-12
Ctss	0.8	1.74	1.56E-09	2.52E-07	2.90E-05
Cx3cr1	1.41	2.66	1.46E-08	2.07E-06	2.72E-04

Cxcl10	1.67	3.19	1.34E-04	6.26E-03	1
Cxcl13	1.72	3.29	2.34E-06	2.12E-04	0.04
Cyb5r2	-0.71	-1.63	2.56E-06	2.24E-04	0.05
Cyb5r3	0.31	1.24	7.74E-05	4.04E-03	1
Cyyr1	-0.48	-1.39	2.57E-04	0.01	1
D430041D05Rik	-0.7	-1.62	6.94E-14	2.19E-11	1.29E-09
Dbp	-2.24	-4.73	9.37E-52	3.72E-48	1.74E-47
Dclk3	-0.88	-1.85	1.58E-04	7.09E-03	1
Ddah1	-0.48	-1.4	8.99E-05	4.58E-03	1
Ddit4	-0.51	-1.42	5.14E-05	2.81E-03	0.96
Ddr1	-0.29	-1.22	1.19E-03	0.03	1
Ddx3	-11.32	-2,556.26	4.21E-19	3.04E-16	7.84E-15
Ddx58	0.47	1.38	9.32E-04	0.03	1
Desi1	-0.36	-1.29	7.70E-05	4.04E-03	1
Dhfr	1.11	2.16	2.87E-14	9.29E-12	5.34E-10
Dio2	1.37	2.59	1.66E-05	1.09E-03	0.31
Dlc1	-0.25	-1.19	1.82E-03	0.05	1
Dmd	0.3	1.23	8.06E-05	4.20E-03	1
Dop1b	-0.27	-1.2	1.13E-03	0.03	1
Drp2	-0.53	-1.44	2.86E-06	2.45E-04	0.05
Dusp15	-0.79	-1.73	1.82E-21	1.52E-18	3.40E-17
Dusp26	0.62	1.53	2.62E-13	7.86E-11	4.88E-09
Ecel1	2.21	4.62	9.68E-09	1.45E-06	1.80E-04
Efcc1	-0.95	-1.94	3.64E-05	2.10E-03	0.68
Egr2	-0.72	-1.64	9.96E-07	9.88E-05	0.02
Eif1	-0.25	-1.19	1.87E-03	0.05	1
Eif2s3x	0.75	1.68	1.42E-21	1.25E-18	2.65E-17
Eif2s3y	-11.24	-2,417.61	7.46E-19	4.74E-16	1.39E-14
Eif3j	-0.29	-1.22	4.50E-04	0.02	1
Eif3k	0.3	1.23	5.66E-04	0.02	1
Emb	0.28	1.21	1.44E-03	0.04	1
Emid1	-1.03	-2.04	1.20E-04	5.73E-03	1
Emp2	-0.48	-1.39	2.79E-04	0.01	1
Eng	-0.47	-1.38	1.11E-03	0.03	1
Eno1	0.24	1.18	1.83E-03	0.05	1
Epas1	-0.43	-1.35	3.67E-08	4.86E-06	6.83E-04
Epb41l2	-0.35	-1.27	7.70E-06	5.66E-04	0.14
Epx	2.43	5.38	5.08E-04	0.02	1
Erbb4	-0.72	-1.65	6.54E-04	0.02	1

Esrra	-0.64	-1.56	1.57E-04	7.08E-03	1
Esyt1	0.28	1.21	3.22E-04	0.01	1
Etl4	-0.5	-1.41	2.54E-10	4.64E-08	4.73E-06
Etv1	-0.24	-1.18	1.96E-03	0.05	1
Fa2h	-0.87	-1.83	8.31E-11	1.67E-08	1.55E-06
Fam107a	-0.72	-1.64	1.44E-06	1.35E-04	0.03
Fam234b	-0.28	-1.21	1.56E-03	0.04	1
Fam83f	-0.7	-1.62	1.00E-03	0.03	1
Fcgr2a_2	1.36	2.57	6.18E-09	9.62E-07	1.15E-04
Fcrl2	2.05	4.14	1.11E-04	5.38E-03	1
Fermt3	1.13	2.19	3.57E-04	0.01	1
Fgf7	-0.98	-1.97	1.36E-10	2.60E-08	2.53E-06
Fgf9	-0.5	-1.42	5.85E-05	3.18E-03	1
Fgl2	-0.79	-1.73	6.30E-12	1.62E-09	1.17E-07
Filip1	-0.65	-1.57	4.98E-13	1.44E-10	9.27E-09
Flnc	0.61	1.53	5.00E-05	2.75E-03	0.93
Flrt3	1.41	2.65	2.58E-27	3.72E-24	4.80E-23
Flt1	-0.48	-1.4	2.22E-04	9.50E-03	1
Foxo4	-0.55	-1.47	1.07E-04	5.22E-03	1
Frem2	-0.81	-1.76	3.76E-04	0.01	1
Frmd3	-0.28	-1.21	1.86E-03	0.05	1
Frmpd1	-0.28	-1.22	4.18E-04	0.02	1
Fry	-0.26	-1.2	6.53E-04	0.02	1
Fryl	-0.27	-1.21	4.59E-04	0.02	1
Fut8	-0.39	-1.31	5.48E-06	4.27E-04	0.1
Fxyd1	0.57	1.49	1.19E-06	1.14E-04	0.02
Fxyd6	-0.57	-1.48	2.48E-06	2.23E-04	0.05
Gabra5	1.05	2.07	1.22E-09	2.01E-07	2.27E-05
Gadd45a	1.02	2.03	1.92E-11	4.55E-09	3.58E-07
Gadd45g	0.99	1.98	9.08E-05	4.61E-03	1
Gal	2.39	5.24	4.15E-56	3.30E-52	7.73E-52
Gap43	0.75	1.69	5.60E-23	5.82E-20	1.04E-18
Gas2l3	-0.6	-1.52	7.04E-14	2.19E-11	1.31E-09
Gatm	-0.63	-1.55	2.50E-11	5.67E-09	4.65E-07
Gbp2	0.45	1.36	6.19E-04	0.02	1
Gch1	1.5	2.83	1.35E-06	1.29E-04	0.03
gene:ENSRNOG00000032224	0.52	1.43	3.16E-05	1.89E-03	0.59
gene:ENSRNOG00000037191	1.83	3.56	3.91E-04	0.01	1
gene:ENSRNOG00000048967	1.58	3	4.87E-06	3.89E-04	0.09

gene:ENSRNOG00000049075	0.48	1.4	2.96E-05	1.79E-03	0.55
gene:ENSRNOG00000051885	0.96	1.94	8.77E-06	6.29E-04	0.16
gene:ENSRNOG00000063044	1.02	2.03	9.96E-10	1.68E-07	1.86E-05
gene:ENSRNOG00000063189	1.14	2.21	1.07E-06	1.04E-04	0.02
gene:ENSRNOG00000063301	-1.14	-2.21	3.16E-04	0.01	1
gene:ENSRNOG00000063418	0.26	1.2	1.43E-03	0.04	1
gene:ENSRNOG00000063679	0.42	1.34	3.53E-04	0.01	1
gene:ENSRNOG00000064025	0.51	1.42	9.37E-05	4.73E-03	1
gene:ENSRNOG00000064399	0.27	1.21	7.93E-04	0.03	1
gene:ENSRNOG00000065189	2.51	5.71	4.88E-04	0.02	1
gene:ENSRNOG00000065195	-0.39	-1.31	4.30E-04	0.02	1
gene:ENSRNOG00000065301	-0.9	-1.86	8.55E-04	0.03	1
gene:ENSRNOG00000066876	0.35	1.27	7.26E-05	3.82E-03	1
gene:ENSRNOG00000067347	2.17	4.49	1.00E-04	4.94E-03	1
gene:ENSRNOG00000067560	0.38	1.3	1.71E-03	0.04	1
gene:ENSRNOG00000068362	-1.86	-3.64	1.20E-03	0.03	1
gene:ENSRNOG00000068784	4.29	19.53	1.94E-03	0.05	1
gene:ENSRNOG00000069384	1.42	2.68	6.84E-18	3.74E-15	1.27E-13
gene:ENSRNOG00000069549	-1.29	-2.45	1.50E-07	1.76E-05	2.79E-03
gene:ENSRNOG00000070513	0.63	1.55	5.07E-07	5.48E-05	9.44E-03
gene:ENSRNOG00000070706	0.63	1.54	2.33E-04	9.75E-03	1
Gfra3	0.43	1.35	1.82E-03	0.05	1
Gfus	0.47	1.38	1.38E-03	0.04	1
Git1	-0.27	-1.2	1.11E-03	0.03	1
Gjb1	-0.7	-1.63	1.30E-03	0.04	1
Gjc3	-0.5	-1.41	1.11E-08	1.64E-06	2.07E-04
Gldc	-1.15	-2.22	5.04E-04	0.02	1
Gldn	-0.81	-1.76	1.76E-10	3.30E-08	3.28E-06
Glipr2	0.35	1.28	9.02E-04	0.03	1
Glrx	0.27	1.21	1.19E-03	0.03	1
Gnai1	-0.28	-1.22	7.71E-04	0.02	1
Got2	0.25	1.19	1.13E-03	0.03	1
Gpc1	0.27	1.21	7.99E-04	0.03	1
Gpd1	-0.6	-1.51	3.30E-05	1.96E-03	0.62
Gpr171	1.16	2.24	2.68E-04	0.01	1
Gprc5b	-0.53	-1.44	3.49E-11	7.39E-09	6.49E-07
Gvin1	0.96	1.95	3.34E-05	1.97E-03	0.62
H1f4	0.55	1.47	2.57E-05	1.59E-03	0.48
H4f3	0.52	1.43	9.65E-05	4.81E-03	1

Hamp	3	7.98	1.32E-08	1.91E-06	2.46E-04
Hapln1	-0.68	-1.6	6.45E-05	3.44E-03	1
Hapln4	-0.62	-1.53	4.27E-06	3.54E-04	0.08
Hist1h4m	0.51	1.42	2.79E-04	0.01	1
Hist2h3c2_3	0.65	1.57	2.45E-05	1.53E-03	0.46
Hist2h3c2_4	0.86	1.81	9.93E-06	6.95E-04	0.18
Hist2h3c2_6	0.82	1.77	5.82E-04	0.02	1
Hmgb1	-0.87	-1.83	9.87E-05	4.90E-03	1
Hnrnpdl	-0.28	-1.21	1.39E-03	0.04	1
Hopx	0.42	1.33	4.40E-04	0.02	1
Hpse	-0.71	-1.63	2.74E-07	3.11E-05	5.10E-03
Hrh3	-1.4	-2.64	5.78E-04	0.02	1
Hs3st2	-0.56	-1.47	6.71E-06	5.05E-04	0.13
Hspa2	-0.46	-1.37	9.62E-04	0.03	1
Hspa5	0.63	1.55	6.47E-06	4.92E-04	0.12
Hspb1	0.4	1.32	3.25E-07	3.66E-05	6.05E-03
Ifi47	0.93	1.91	3.69E-05	2.12E-03	0.69
Ifitm3	0.52	1.43	3.73E-05	2.14E-03	0.69
Igf2bp2	-0.97	-1.96	8.50E-04	0.03	1
Il10ra	1.09	2.14	9.66E-05	4.81E-03	1
Il13ra1_1	0.51	1.43	2.90E-04	0.01	1
Il13ra1_2	0.42	1.34	1.11E-03	0.03	1
Il1a	3.07	8.42	1.45E-03	0.04	1
Il1r1	0.54	1.46	1.20E-04	5.73E-03	1
Il1rl1	0.88	1.84	1.29E-03	0.04	1
Il24	3.64	12.5	9.61E-04	0.03	1
Il6	2.18	4.52	5.98E-05	3.23E-03	1
Ildr2	1.03	2.05	8.03E-04	0.03	1
Impdh1	-0.32	-1.24	8.90E-05	4.56E-03	1
Impdh2	0.53	1.44	5.85E-04	0.02	1
Iqsec1	-0.34	-1.26	1.60E-05	1.06E-03	0.3
Irs1	-0.33	-1.26	3.24E-04	0.01	1
Isg15	1.56	2.95	1.60E-03	0.04	1
Itga6	-0.31	-1.24	5.89E-05	3.19E-03	1
Itgam	1.1	2.14	6.50E-04	0.02	1
Itgb2	1.33	2.52	5.19E-06	4.10E-04	0.1
Itpr3	-0.34	-1.26	1.74E-05	1.12E-03	0.32
Jam2	-0.27	-1.21	1.63E-03	0.04	1
Jmy	-0.28	-1.21	1.65E-03	0.04	1

Jun	0.63	1.54	6.83E-08	8.48E-06	1.27E-03
Kank4	-0.39	-1.31	1.16E-05	7.95E-04	0.22
Kazn	-0.3	-1.23	8.74E-04	0.03	1
Kcnb1	-0.31	-1.24	1.57E-04	7.08E-03	1
Kcnc1	-0.45	-1.37	1.96E-05	1.26E-03	0.37
Kcnc3	-0.29	-1.22	5.01E-04	0.02	1
Kcnh2	-0.27	-1.2	1.87E-03	0.05	1
Kcnip3	-0.39	-1.31	1.06E-03	0.03	1
Kcnk1	-0.43	-1.35	9.82E-04	0.03	1
Kcns1	-0.41	-1.33	1.27E-03	0.04	1
Kdm5c	0.48	1.39	2.78E-08	3.71E-06	5.18E-04
Kdm5d	-12.31	-5,089.05	2.95E-06	2.52E-04	0.05
Kdm6a	0.85	1.81	7.13E-20	5.66E-17	1.33E-15
Khdrbs2	1.15	2.22	2.87E-04	0.01	1
Kif13b	-0.53	-1.44	7.59E-11	1.55E-08	1.41E-06
Klf13	-0.34	-1.26	2.29E-04	9.72E-03	1
Klf15	-0.76	-1.69	7.58E-04	0.02	1
Klf6	0.28	1.21	6.34E-04	0.02	1
Klf9	-0.42	-1.34	8.16E-07	8.36E-05	0.02
Kmt5a	-0.27	-1.21	9.16E-04	0.03	1
Krt7	1.13	2.18	9.52E-07	9.51E-05	0.02
Ktn1	0.31	1.24	6.37E-05	3.41E-03	1
Lamb1	-0.24	-1.18	1.75E-03	0.04	1
Large1	-0.28	-1.21	3.80E-04	0.01	1
Lce1f_2	3.24	9.43	8.56E-09	1.29E-06	1.59E-04
Lcp1	0.49	1.41	5.08E-10	8.97E-08	9.46E-06
Lgals3	0.47	1.38	1.91E-08	2.69E-06	3.56E-04
Lhfpl4	-0.31	-1.24	8.30E-05	4.31E-03	1
Lilrb3	1.94	3.83	1.20E-03	0.03	1
Lilrb3a	3.93	15.2	7.33E-07	7.76E-05	0.01
Limch1	-0.56	-1.48	6.00E-12	1.56E-09	1.12E-07
Limk1	-0.31	-1.24	1.18E-04	5.68E-03	1
Lims1	0.3	1.23	1.90E-04	8.25E-03	1
Lims2	-0.6	-1.52	1.06E-05	7.35E-04	0.2
Lmo4	0.4	1.32	2.55E-06	2.24E-04	0.05
Lnp1	2.61	6.11	6.49E-04	0.02	1
Lpl	-0.89	-1.86	9.49E-05	4.77E-03	1
Lrrc4	-0.44	-1.36	2.04E-03	0.05	1
Lrrc49	-0.28	-1.21	4.70E-04	0.02	1

Lrrk2	-0.31	-1.24	1.47E-04	6.75E-03	1
Lsmem2	-0.49	-1.41	4.92E-05	2.71E-03	0.92
Lurap1	-0.57	-1.48	8.38E-06	6.11E-04	0.16
Lvrn	-0.78	-1.71	8.35E-04	0.03	1
Lxn	0.26	1.2	5.83E-04	0.02	1
Ly49si2	1.82	3.53	3.32E-04	0.01	1
Lypd1	-0.66	-1.58	1.20E-03	0.03	1
Lyz2	0.81	1.76	1.02E-06	1.00E-04	0.02
Maf	-0.33	-1.25	7.15E-04	0.02	1
Mafg	-0.27	-1.2	1.94E-03	0.05	1
Mag	-0.88	-1.85	3.33E-07	3.67E-05	6.19E-03
Maged1	0.25	1.19	1.39E-03	0.04	1
Magi2	-0.29	-1.22	1.10E-03	0.03	1
Mal	-0.78	-1.72	3.51E-23	3.98E-20	6.53E-19
Manf	0.93	1.9	3.01E-13	8.86E-11	5.61E-09
Maoa	0.4	1.32	7.70E-07	8.10E-05	0.01
Maob	-0.7	-1.63	4.95E-08	6.39E-06	9.21E-04
Mapk8ip1	-0.29	-1.23	1.32E-04	6.21E-03	1
Mboat1	-0.89	-1.85	6.16E-10	1.08E-07	1.15E-05
Mbp	-0.86	-1.81	2.22E-14	7.50E-12	4.13E-10
Mecom	-0.75	-1.68	4.67E-04	0.02	1
Megf9	-0.34	-1.26	2.39E-05	1.49E-03	0.44
Mest	-0.4	-1.32	2.56E-06	2.24E-04	0.05
Mgat3	-0.29	-1.22	5.47E-04	0.02	1
Mgll	-0.64	-1.56	1.25E-15	5.08E-13	2.32E-11
Mki67	1.1	2.14	1.44E-06	1.35E-04	0.03
Mlip	-0.75	-1.69	5.83E-19	3.86E-16	1.09E-14
Mmgt2	-0.49	-1.41	2.89E-04	0.01	1
Mmp15	-0.28	-1.21	6.28E-04	0.02	1
Mmp16	0.6	1.52	1.38E-05	9.29E-04	0.26
Mmp8	2.07	4.19	3.47E-04	0.01	1
Mob3b	-0.47	-1.38	4.53E-04	0.02	1
Mogat2	1.07	2.1	1.22E-04	5.83E-03	1
Mpeg1	0.66	1.58	2.43E-07	2.80E-05	4.53E-03
Mpz	-1.18	-2.26	8.44E-26	1.03E-22	1.57E-21
Mrc1	0.58	1.49	4.70E-06	3.79E-04	0.09
Mrpl51	-0.27	-1.21	1.11E-03	0.03	1
Ms4a6a	1.18	2.27	7.05E-04	0.02	1
Mt-cyb	0.39	1.31	4.72E-04	0.02	1

Mt-nd1	0.41	1.33	2.32E-04	9.75E-03	1
Mt-nd2	0.37	1.3	1.73E-03	0.04	1
Mt-nd3	0.54	1.45	1.72E-06	1.58E-04	0.03
Mt3	-0.28	-1.22	3.46E-04	0.01	1
Mvb12b	-0.32	-1.25	1.11E-04	5.37E-03	1
Mx1	0.86	1.82	3.38E-05	1.98E-03	0.63
Mx2	1.25	2.39	3.30E-11	7.19E-09	6.15E-07
Myadm	0.43	1.35	1.43E-07	1.70E-05	2.66E-03
Myh14	-0.29	-1.22	3.83E-04	0.01	1
Myo1b	-0.31	-1.24	4.22E-04	0.02	1
Myo1f	0.74	1.67	1.59E-03	0.04	1
Myoc	-0.66	-1.58	1.30E-08	1.90E-06	2.43E-04
Myom2	-0.98	-1.97	3.48E-04	0.01	1
Nat8f3	-0.8	-1.74	1.22E-05	8.27E-04	0.23
Nat8l	-0.32	-1.25	4.90E-05	2.71E-03	0.91
Nav2	0.51	1.42	2.35E-10	4.34E-08	4.37E-06
Nckap1l	0.82	1.76	1.41E-07	1.69E-05	2.63E-03
Ncmap	-0.68	-1.61	9.40E-07	9.45E-05	0.02
Ndrg1	-0.43	-1.35	1.35E-04	6.26E-03	1
Ndrg2	0.26	1.2	8.17E-04	0.03	1
Ndrg3	0.28	1.21	9.96E-04	0.03	1
Ndufa10l1_1	-0.48	-1.4	1.59E-03	0.04	1
Ndufb10	0.27	1.2	8.83E-04	0.03	1
Nefl	-0.37	-1.3	8.23E-04	0.03	1
Nefm	-0.44	-1.35	9.67E-05	4.81E-03	1
Nes	-0.64	-1.56	5.44E-15	2.11E-12	1.01E-10
Nfasc	-0.33	-1.25	1.74E-05	1.12E-03	0.32
Nfia	-0.34	-1.27	4.50E-05	2.53E-03	0.84
Nfil3	1.01	2.02	9.90E-04	0.03	1
Ngly1	-0.33	-1.26	3.39E-04	0.01	1
Nop56	0.3	1.23	6.69E-04	0.02	1
Notch4	-0.91	-1.88	1.61E-04	7.19E-03	1
Npas2	2.22	4.65	6.41E-08	8.08E-06	1.19E-03
Nptx1	-0.42	-1.34	8.96E-08	1.10E-05	1.67E-03
Npy	2.68	6.41	2.32E-19	1.76E-16	4.32E-15
Npy1r	0.39	1.31	1.46E-03	0.04	1
Nqo2	-0.71	-1.64	8.08E-07	8.34E-05	0.02
Nr1d1	-1.49	-2.81	2.56E-18	1.51E-15	4.77E-14
Nr1d2	-0.71	-1.64	4.72E-09	7.42E-07	8.79E-05

Nrarp	-0.58	-1.49	1.49E-05	9.94E-04	0.28
Nrip1	0.35	1.28	1.03E-05	7.15E-04	0.19
Nsg1	0.62	1.54	4.88E-15	1.94E-12	9.08E-11
Nt5c3b	0.63	1.55	1.80E-04	7.88E-03	1
Ntng1	-0.29	-1.22	1.26E-03	0.04	1
Ntng2	-0.6	-1.52	9.27E-07	9.37E-05	0.02
Nts	0.87	1.83	1.83E-03	0.05	1
Oasl2	0.81	1.75	1.40E-04	6.46E-03	1
Odc1	-0.29	-1.22	1.61E-03	0.04	1
Olr1585	0.79	1.73	1.49E-03	0.04	1
Osbpl5	-0.57	-1.49	6.74E-06	5.05E-04	0.13
Ostf1	0.24	1.18	1.58E-03	0.04	1
Otud7b	-0.39	-1.31	1.73E-05	1.12E-03	0.32
P2ry2	-0.52	-1.43	3.48E-04	0.01	1
Pacs2	-0.33	-1.25	4.30E-05	2.43E-03	0.8
Padi2	-0.67	-1.59	1.87E-07	2.18E-05	3.48E-03
Pam	-0.29	-1.22	2.30E-04	9.73E-03	1
Pank1	-0.49	-1.41	4.95E-04	0.02	1
Panx2	-0.28	-1.21	1.09E-03	0.03	1
Pappa2	0.8	1.74	2.91E-05	1.77E-03	0.54
Paqr8	-0.3	-1.23	3.36E-04	0.01	1
Parp3	0.5	1.41	1.61E-04	7.19E-03	1
Pbdc1	0.66	1.58	2.38E-12	6.51E-10	4.43E-08
Pcnx2	-0.26	-1.19	1.40E-03	0.04	1
PCOLCE2	0.75	1.68	4.60E-08	6.04E-06	8.57E-04
Pde2a	0.29	1.22	1.61E-03	0.04	1
Pde6b	1.63	3.09	8.63E-05	4.44E-03	1
Pdgfrb	-0.36	-1.29	5.38E-05	2.94E-03	1
Pdia4	0.49	1.4	3.08E-05	1.85E-03	0.57
Pdlim1	0.55	1.46	1.46E-05	9.79E-04	0.27
Pdzd8	-0.27	-1.21	4.54E-04	0.02	1
Peli2	-0.47	-1.39	6.14E-07	6.55E-05	0.01
Peli3	0.76	1.69	1.19E-03	0.03	1
Per1	-1.26	-2.4	4.53E-19	3.13E-16	8.43E-15
Per2	-0.73	-1.66	3.81E-05	2.18E-03	0.71
Per3	-0.9	-1.87	5.06E-12	1.36E-09	9.43E-08
Phyhipl	-0.26	-1.2	8.71E-04	0.03	1
Pik3ap1	0.83	1.77	7.09E-04	0.02	1
Pink1	-0.3	-1.23	4.33E-04	0.02	1

Pla2g7	-0.44	-1.35	3.51E-04	0.01	1
Plaat3	-0.47	-1.39	2.04E-04	8.72E-03	1
Plat	0.27	1.21	5.09E-04	0.02	1
Plce1	0.27	1.2	1.21E-03	0.03	1
Plekha7	-0.72	-1.65	1.03E-07	1.25E-05	1.92E-03
Plekhb1	-0.37	-1.3	1.18E-06	1.14E-04	0.02
Plekhb2	0.26	1.19	7.20E-04	0.02	1
Plekhg2	-0.38	-1.3	2.21E-05	1.40E-03	0.41
Plekhh1	0.39	1.31	1.64E-03	0.04	1
Plk2	0.36	1.28	8.60E-05	4.43E-03	1
Pllp	-0.87	-1.83	5.68E-11	1.17E-08	1.06E-06
Pmp2	-1.73	-3.32	1.31E-49	4.17E-46	2.44E-45
Pmp22	-0.86	-1.82	1.34E-14	4.63E-12	2.50E-10
Podxl	-0.52	-1.43	5.40E-08	6.92E-06	1.01E-03
Pomp	0.25	1.19	1.58E-03	0.04	1
Pou3f1	-0.76	-1.7	9.22E-04	0.03	1
Ppp1r16b	-0.81	-1.75	7.87E-10	1.36E-07	1.47E-05
Pptc7	-0.27	-1.21	1.90E-03	0.05	1
Prdx6	0.32	1.25	3.90E-04	0.01	1
Prex2	-0.3	-1.23	2.32E-04	9.75E-03	1
Prg2	2.1	4.28	3.49E-05	2.03E-03	0.65
Prg3	2.83	7.11	1.65E-04	7.32E-03	1
Prkca	-0.36	-1.28	5.72E-06	4.39E-04	0.11
Prkcq	-0.64	-1.56	3.50E-06	2.94E-04	0.07
Prp2l1	0.34	1.27	1.01E-04	4.97E-03	1
Prrg3	-0.66	-1.58	1.34E-07	1.61E-05	2.49E-03
Prx	-0.98	-1.97	7.23E-18	3.83E-15	1.35E-13
Ptpn13	-0.26	-1.2	1.84E-03	0.05	1
Ptpn14	-0.56	-1.48	9.30E-05	4.71E-03	1
Ptpn5	1.1	2.14	2.32E-08	3.15E-06	4.32E-04
Ptprb	-0.57	-1.48	2.61E-06	2.27E-04	0.05
Ptprc	0.6	1.51	9.73E-04	0.03	1
Ptprh	2.78	6.89	2.44E-13	7.46E-11	4.55E-09
Ptpro	0.66	1.58	1.02E-06	1.00E-04	0.02
Ptprt	0.6	1.52	1.22E-11	3.02E-09	2.26E-07
Qdpr	0.38	1.3	5.02E-06	3.99E-04	0.09
Ralgapa2	-0.25	-1.19	1.73E-03	0.04	1
Ralgds	-0.29	-1.23	7.28E-04	0.02	1
Ralgps2	0.41	1.32	8.17E-04	0.03	1

Ranbp3l	0.82	1.77	5.16E-04	0.02	1
Rap1gap2	-0.3	-1.23	3.09E-04	0.01	1
Rapgef4	-0.26	-1.19	1.35E-03	0.04	1
Rapgef5	-0.43	-1.34	5.41E-04	0.02	1
Rasal2	-0.3	-1.23	1.26E-04	5.94E-03	1
Rasgef1a	-0.44	-1.36	1.19E-03	0.03	1
Rassf3	-0.46	-1.37	1.38E-03	0.04	1
Rbfox3	-0.27	-1.21	8.55E-04	0.03	1
Rbm15b	0.51	1.43	1.82E-03	0.05	1
Rcn1	-0.28	-1.21	4.92E-04	0.02	1
Reg3b	2.38	5.19	2.65E-06	2.28E-04	0.05
RGD1304694	-0.27	-1.21	1.45E-03	0.04	1
RGD1559896	-0.38	-1.3	2.90E-05	1.77E-03	0.54
RGD1563354	-0.79	-1.73	4.68E-06	3.79E-04	0.09
RGD1564409	-0.6	-1.51	1.10E-03	0.03	1
RGD1564899	-2.07	-4.21	7.95E-07	8.30E-05	0.01
RGD1565462_2	1.94	3.84	1.83E-06	1.66E-04	0.03
Rgs2	0.74	1.67	2.67E-08	3.59E-06	4.97E-04
Rhobtb3	-0.71	-1.63	1.17E-16	5.31E-14	2.18E-12
Rhoc	0.44	1.36	3.98E-04	0.01	1
Rimklb	-0.33	-1.26	5.82E-04	0.02	1
rnf141	-0.4	-1.32	2.56E-06	2.24E-04	0.05
Rnf157	-0.33	-1.25	2.25E-05	1.42E-03	0.42
Rnh1	0.45	1.37	4.45E-04	0.02	1
Ro60	0.26	1.19	2.00E-03	0.05	1
Rpl19	0.24	1.18	1.90E-03	0.05	1
Rpl26	0.32	1.25	3.93E-05	2.24E-03	0.73
Rpl27	0.28	1.22	5.01E-04	0.02	1
Rpl35	0.3	1.23	1.14E-04	5.53E-03	1
Rplp1	0.27	1.2	4.35E-04	0.02	1
Rps13	0.32	1.25	4.18E-04	0.02	1
Rps15	0.26	1.2	1.04E-03	0.03	1
Rps2	0.25	1.19	1.68E-03	0.04	1
Rps20_1	0.29	1.22	3.70E-04	0.01	1
Rps23	0.28	1.21	5.93E-04	0.02	1
Rps28	0.41	1.33	1.34E-03	0.04	1
Rps8	0.34	1.26	2.98E-05	1.80E-03	0.56
Rpsa	0.27	1.2	5.69E-04	0.02	1
Rrbp1	-0.25	-1.19	1.97E-03	0.05	1

Rsad2	1.17	2.24	8.92E-06	6.30E-04	0.17
RT1-Ba	1.36	2.57	9.23E-28	1.63E-24	1.72E-23
RT1-Bb	1.26	2.4	1.44E-03	0.04	1
RT1-Da	1.42	2.67	1.13E-31	3.00E-28	2.11E-27
RT1-Db1	1.14	2.2	3.78E-09	6.00E-07	7.03E-05
RT1-DMb	0.97	1.96	2.00E-04	8.61E-03	1
Rtn4rl2	-0.52	-1.44	8.18E-04	0.03	1
S100a11	0.45	1.37	2.21E-08	3.03E-06	4.12E-04
S100b	-0.36	-1.28	1.30E-03	0.04	1
Samd9	0.72	1.65	2.83E-18	1.60E-15	5.26E-14
Sash3	1.26	2.4	2.03E-03	0.05	1
Satb1	-0.3	-1.23	9.61E-04	0.03	1
Sbno2	0.6	1.52	6.22E-06	4.75E-04	0.12
Sbspon	-0.75	-1.68	1.95E-04	8.46E-03	1
Scn3a	0.46	1.38	8.12E-04	0.03	1
Scn3b	0.39	1.31	1.22E-03	0.03	1
Scn8a	-0.29	-1.22	1.62E-04	7.20E-03	1
Scrt1	-0.47	-1.38	4.20E-04	0.02	1
Scube1	-0.48	-1.4	1.37E-04	6.33E-03	1
Sdc1	0.87	1.82	1.44E-03	0.04	1
Secisbp2l	-0.63	-1.55	1.94E-08	2.71E-06	3.62E-04
Selplg	0.91	1.88	2.52E-04	0.01	1
Sema3b	-0.4	-1.32	1.16E-06	1.13E-04	0.02
Sema3c	0.45	1.37	1.45E-08	2.07E-06	2.70E-04
Sema4c	-0.41	-1.32	2.04E-03	0.05	1
Sema4g	-0.71	-1.64	1.79E-06	1.64E-04	0.03
Sema5a	-0.53	-1.44	9.64E-12	2.43E-09	1.80E-07
Sema6a	0.97	1.96	1.78E-16	7.66E-14	3.32E-12
Sema7a	-0.65	-1.57	6.30E-08	8.01E-06	1.17E-03
Serpina1	1.03	2.05	1.98E-07	2.30E-05	3.69E-03
Serpinb1a	0.88	1.84	1.60E-27	2.55E-24	2.99E-23
Serpinb1b	4.28	19.42	#######	5.22E-298	6.11E-298
Serpinb2	4.29	19.53	1.95E-03	0.05	1
Serpinb9	0.39	1.31	4.22E-06	3.51E-04	0.08
Serpini1	0.38	1.3	1.61E-05	1.06E-03	0.3
Sgk1	-0.39	-1.31	1.54E-03	0.04	1
Sipa1l1	-0.42	-1.33	5.12E-04	0.02	1
Slc14a1	1.08	2.11	3.35E-05	1.97E-03	0.62
Slc22a17	-0.3	-1.23	2.03E-04	8.71E-03	1

Slc2a1	-0.29	-1.22	9.84E-04	0.03	1
Slc30a1	-0.62	-1.53	1.30E-03	0.04	1
Slc36a2	-0.9	-1.86	2.63E-09	4.22E-07	4.90E-05
Slc39a6	0.26	1.2	1.38E-03	0.04	1
Slc39a8	-0.52	-1.43	3.32E-04	0.01	1
Slc6a17	-0.25	-1.19	1.70E-03	0.04	1
Slc6a6	-0.45	-1.37	1.31E-03	0.04	1
Slc6a8	-0.45	-1.37	4.16E-07	4.52E-05	7.74E-03
Slc7a1	-0.46	-1.38	1.00E-04	4.94E-03	1
Slc9a3r2	-0.34	-1.27	3.29E-04	0.01	1
Slco1a4	-0.41	-1.33	8.92E-06	6.30E-04	0.17
Slco1c1	-0.9	-1.87	1.80E-03	0.05	1
Slfn13	0.62	1.54	1.56E-06	1.44E-04	0.03
Slfn4_1	0.83	1.78	4.60E-06	3.75E-04	0.09
Slit2	-0.4	-1.32	3.95E-06	3.30E-04	0.07
Slit3	-0.44	-1.36	6.93E-04	0.02	1
Smad1	0.35	1.28	1.24E-04	5.85E-03	1
Smagp	1.5	2.83	1.19E-03	0.03	1
Snn	-0.59	-1.5	1.57E-11	3.77E-09	2.92E-07
Socs3	0.79	1.73	1.83E-03	0.05	1
Sod2	0.27	1.2	4.99E-04	0.02	1
Sorbs2	-0.57	-1.49	5.28E-06	4.13E-04	0.1
Sort1	-0.3	-1.24	1.69E-04	7.49E-03	1
Sox11	1.44	2.71	5.07E-17	2.44E-14	9.45E-13
Spire2	-0.3	-1.23	1.59E-03	0.04	1
Sprr1a	3.12	8.67	1.56E-04	7.07E-03	1
Spta1	1.5	2.84	5.58E-04	0.02	1
Sptb	-0.79	-1.73	5.87E-23	5.82E-20	1.09E-18
Sptbn5	-0.68	-1.6	7.58E-09	1.17E-06	1.41E-04
Srpra	-0.28	-1.22	4.99E-04	0.02	1
Ssc5d	0.52	1.43	7.25E-05	3.82E-03	1
Stac2	2.52	5.74	9.31E-13	2.64E-10	1.73E-08
Stard9	-0.36	-1.29	1.17E-05	8.00E-04	0.22
Stat4	0.3	1.23	4.87E-04	0.02	1
Stmn4	1.02	2.03	9.49E-15	3.43E-12	1.77E-10
Ston1	-0.58	-1.5	4.03E-11	8.41E-09	7.50E-07
Stx11	0.45	1.37	1.87E-03	0.05	1
Svip	-0.64	-1.56	8.98E-15	3.32E-12	1.67E-10
Synm	-0.42	-1.34	1.71E-04	7.56E-03	1

Syt2	-0.26	-1.2	9.82E-04	0.03	1
Syt4	0.52	1.44	2.81E-11	6.20E-09	5.23E-07
Syt5	0.5	1.42	5.45E-04	0.02	1
Sytl2	0.28	1.22	2.51E-04	0.01	1
Tagln2	0.26	1.2	7.68E-04	0.02	1
Tagln3	0.39	1.31	2.53E-06	2.24E-04	0.05
Tcte1_1	-0.32	-1.25	3.21E-04	0.01	1
Tef	-0.58	-1.49	1.06E-10	2.06E-08	1.98E-06
Tesc	-0.49	-1.4	2.46E-04	0.01	1
Tgfbr1	0.38	1.3	1.98E-03	0.05	1
Tgm1	3.45	10.93	2.66E-11	5.95E-09	4.96E-07
Timp3	-0.26	-1.2	9.18E-04	0.03	1
Timp4	-1.29	-2.44	4.39E-06	3.60E-04	0.08
Tjp2	-0.49	-1.4	1.10E-04	5.36E-03	1
Tll1	-0.69	-1.61	3.32E-07	3.67E-05	6.19E-03
Tm6sf1	-0.39	-1.31	5.64E-06	4.37E-04	0.1
Tmem150c	-0.32	-1.25	1.76E-04	7.76E-03	1
Tmem176b	0.5	1.41	9.19E-06	6.46E-04	0.17
Tmem229a	-0.49	-1.41	7.93E-04	0.03	1
Tmem26	0.68	1.6	8.13E-06	5.95E-04	0.15
Tnc	0.32	1.25	8.45E-05	4.37E-03	1
Tnik	0.57	1.49	1.72E-12	4.80E-10	3.21E-08
Tob2	-0.59	-1.51	4.85E-06	3.89E-04	0.09
Tph2	0.91	1.88	4.30E-10	7.68E-08	8.01E-06
Tril	-0.3	-1.23	2.98E-04	0.01	1
Trim37	-0.25	-1.19	1.15E-03	0.03	1
Tuba1c	-0.52	-1.44	2.00E-05	1.28E-03	0.37
Tubb2b	0.46	1.38	1.41E-09	2.31E-07	2.63E-05
Tubb6	0.8	1.74	4.62E-05	2.58E-03	0.86
Txnip	-0.34	-1.27	4.73E-05	2.63E-03	0.88
Tyrobp	0.94	1.93	2.29E-04	9.72E-03	1
Ube2l6	0.53	1.45	5.21E-04	0.02	1
Ugdh	0.53	1.45	7.00E-05	3.72E-03	1
Ugt8	-0.76	-1.69	2.63E-22	2.45E-19	4.89E-18
Uty	-11.84	-3,654.80	7.03E-06	5.24E-04	0.13
Vip	3.82	14.09	7.65E-27	1.01E-23	1.43E-22
Vopp1	-0.28	-1.21	9.52E-04	0.03	1
Vsnl1	-0.26	-1.2	1.08E-03	0.03	1
Vtcn1	3.25	9.49	1.10E-08	1.64E-06	2.06E-04

Vwa5a	0.37	1.29	1.53E-06	1.42E-04	0.03
Vwc2l	-0.36	-1.28	3.73E-04	0.01	1
Wdfy4	0.92	1.89	3.99E-04	0.01	1
Wipf3	-0.31	-1.24	1.35E-04	6.26E-03	1
Wwc2	-0.47	-1.39	1.54E-04	6.99E-03	1
Xbp1	0.65	1.57	1.03E-07	1.25E-05	1.91E-03
Zbtb16	-1.19	-2.29	2.64E-07	3.02E-05	4.91E-03
Zbtb18	-0.27	-1.21	1.51E-03	0.04	1
Zbtb38	0.25	1.19	1.82E-03	0.05	1
Zbtb47	-0.42	-1.34	5.22E-06	4.11E-04	0.1
Zcchc24	-0.31	-1.24	3.08E-04	0.01	1
Zdhhc21	0.27	1.2	8.29E-04	0.03	1
Zfp367	0.48	1.39	3.33E-04	0.01	1
Zfp84_2	0.51	1.43	4.26E-04	0.02	1
Zik1	0.48	1.4	1.69E-03	0.04	1

Table A3.12. List of 90 genes from male heat map gene tree (Figure 4.2a). Genes are listed in order of the gene heatmap tree from top to bottom.

Scd2
Mbp
Mpz
Pmp22
Fth1
Tuba1b
Actb
gene:ENSRNOG00000051885
Tubb3
Cd74
Prph
Ctsb
Actg1
Stmn2
Npy
Anxa2
Sparc
Ubb
gene:ENSRNOG00000047931

Gapdh
Serpinb1b
Col3a1
Col1a1
Col1a2
Igfbp5
Hba-a2
Hbb-b1
gene:ENSRNOG00000062930
Mt-nd1
Mt-nd4
Mt-nd5
Mt-nd2
Mt-cyb
Mt-nd3
Cst3
Mt-co1
Mt-atp6
Mt-co3
NEWGENE_1308171
Ptgds
Ahnak
Eef1a1
Mt-co2
Mt-atp8
Apod
Dcn
Hspa8
Ywhaz
gene:ENSRNOG00000065195
Sptan1
Sptbn1
Prune2
Hsp90aa1
Fstl1
Rtn3
Snap25
Nefh
Nefm

Nefl
Ywhah
Atp1b1
Dync1h1
Kif1a
Map1a
Atp1a1
Epb41l3
Map1b
Rtn4
Kif5a
Kcna1
Ywhag
Pgd
Calm1_2
Cltc
Hsp90ab1
Dst
Ank2
Gnas_2
Ttn
Neb
Acta1
Myh4
AABR07005775.1
Apoe
Uchl1
Zwint
Sncg
Thy1
Scn7a
Rgs4

Table A3.13. List of 90 genes from female heat map gene tree (Figure 4.2b). Genes are listed in order of the gene heatmap tree from top to bottom.

Ttn
Myh4

Dpysl2
Kif5a
gene:ENSRNOG00000062930
Scd2
Map1b
Dync1h1
Atp1a1
Nefm
Map1a
Ywhag
Atp1a3
Atp11a
Kcna1
Nefh
Nefl
Ndrg4
Vamp1
Fth1
Mbp
Mpz
Pmp22
Cst3
Apoe
Uchl1
Rtn3
Sptan1
Fstl1
Mt-nd3
Nedd4
Hsp90aa1
Eef1a1
Hspa8
Mt-co1
Mt-co2
Tmem176b
gene:ENSRNOG00000047931
Anxa2
Sncg
Gapdh

Thy1
Rgs4
Serpinb1b
Mx2
Dst
Epb41l3
Ank2
Sptbn1
Tuba1b
Tubb3
Prph
Stmn2
Npy
Gap43
Cacna2d1
Spp1
Cd59
Ywhaz
Akap6
Pafah1b1
Calm1_2
Cltc
Usp9x
Scn9a
Prune2
Mt-atp8
Scn7a
Apod
Hspa5
Actg1
Hsp90ab1
Ahnak
Dcn
Col1a1
Col1a2
Igfbp5
Col3a1
Mt-nd6
Hba-a2

Hbb-b1
Actb
Mt-cyb
Mt-atp6
Mt-nd2
Mt-co3
Mt-nd4l
Mt-nd5
Mt-nd4
Mt-nd1

REFERENCES:

1 Ren, K. & Dubner, R. Interactions between the immune and nervous systems in pain. *Nature Medicine* **16**, 1267-1276 (2010). https://doi.org:10.1038/nm.2234

2 Totsch, S. K. & Sorge, R. E. Immune system involvement in specific pain conditions. *Molecular Pain* **13**, 1744806917724559 (2017). https://doi.org:10.1177/1744806917724559

3 Bouhassira, D. Neuropathic pain: Definition, assessment and epidemiology. *Rev Neurol (Paris)* **175**, 16-25 (2019). https://doi.org:10.1016/j.neurol.2018.09.016

4 Chapman, C. R. & Vierck, C. J. The Transition of Acute Postoperative Pain to Chronic Pain: An Integrative Overview of Research on Mechanisms. *J Pain* **18**, 359.e351-359.e338 (2017). https://doi.org:10.1016/j.jpain.2016.11.004

5 Cavalli, E., Mammana, S., Nicoletti, F., Bramanti, P. & Mazzon, E. The neuropathic pain: An overview of the current treatment and future therapeutic approaches. *International Journal of Immunopathology and Pharmacology* **33**, 1-10 (2019). https://doi.org:10.1177/2058738419838383

6 Finnerup, N. B., Kuner, R. & Jensen, T. S. Neuropathic Pain: From Mechanisms to Treatment. *Physiological Reviews* **101**, 259-301 (2021). https://doi.org:10.1152/physrev.00045.2019

7 Gaudet, A. D., Popovich, P. G. & Ramer, M. S. Wallerian degeneration: gaining perspective on inflammatory events after peripheral nerve injury. *Journal of Neuroinflammation* **8**, 110 (2011). https://doi.org:10.1186/1742-2094-8-110

8 Baron, R. Mechanisms of Disease: neuropathic pain—a clinical perspective. *Nature Clinical Practice Neurology* **2**, 95-106 (2006). https://doi.org:10.1038/ncpneuro0113

9 Liu, J. *et al.* Role of microtubule dynamics in Wallerian degeneration and nerve regeneration after peripheral nerve injury. *Neural Regen Res* **17**, 673-681 (2022). https://doi.org:10.4103/1673-5374.320997

10 Kim, C. F. & Moalem-Taylor, G. Detailed characterization of neuro-immune responses following neuropathic injury in mice. *Brain Res* **1405**, 95-108 (2011). https://doi.org:10.1016/j.brainres.2011.06.022

11 Moalem, G., Xu, K. & Yu, L. T lymphocytes play a role in neuropathic pain following peripheral nerve injury in rats. *Neuroscience* **129**, 767-777 (2004). https://doi.org:10.1016/j.neuroscience.2004.08.035

12 Laumet, G. *et al.* T Cells as an Emerging Target for Chronic Pain Therapy. *Front Mol Neurosci* **12**, 216 (2019). https://doi.org:10.3389/fnmol.2019.00216

13 Cherry, J. D., Olschowka, J. A. & O'Banion, M. K. Neuroinflammation and M2 microglia: the good, the bad, and the inflamed. *Journal of Neuroinflammation* **11**, 98 (2014). https://doi.org:10.1186/1742-2094-11-98

14 Hore, Z. & Denk, F. Neuroimmune interactions in chronic pain - An interdisciplinary perspective. *Brain Behav Immun* **79**, 56-62 (2019). https://doi.org:10.1016/j.bbi.2019.04.033

15 Wang, J., Ou, S. W. & Wang, Y. J. Distribution and function of voltage-gated sodium channels in the nervous system. *Channels (Austin)* **11**, 534-554 (2017). https://doi.org:10.1080/19336950.2017.1380758

16 Metzker, M. L. Sequencing technologies — the next generation. *Nature Reviews Genetics* **11**, 31-46 (2010). https://doi.org:10.1038/nrg2626

17 Sanger, F., Nicklen, S. & Coulson, A. R. DNA sequencing with chain-terminating inhibitors. *Proc Natl Acad Sci U S A* **74**, 5463-5467 (1977). https://doi.org:10.1073/pnas.74.12.5463

18 Tse-Wen, C. Binding of cells to matrixes of distinct antibodies coated on solid surface. *Journal of Immunological Methods* **65**, 217-223 (1983). https://doi.org:https://doi.org/10.1016/0022-1759(83)90318-6

19 Koch, C. M. *et al.* A Beginner's Guide to Analysis of RNA Sequencing Data. *Am J Respir Cell Mol Biol* **59**, 145-157 (2018). https://doi.org:10.1165/rcmb.2017-0430TR

20 Mecklenburg, J. *et al.* Transcriptomic sex differences in sensory neuronal populations of mice. *Scientific Reports* **10**, 1 - 18 (2020). https://doi.org:10.1038/s41598-020-72285-z

21 Stephens, K. E. *et al.* Sex differences in gene regulation in the dorsal root ganglion after nerve injury. *BMC Genomics* **20**, 1 - 18 (2019). https://doi.org:10.1186/s12864-019-5512-9

22 Mogil, J. S. Qualitative sex differences in pain processing: emerging evidence of a biased literature. *Nature Reviews Neuroscience* **21**, 353 - 365 (2020). https://doi.org:10.1038/s41583-020-0310-6

23 Klein, S. L. & Flanagan, K. L. Sex differences in immune responses. *Nat Rev Immunol* **16**, 626-638 (2016). https://doi.org:10.1038/nri.2016.90

24 Ray, P. R. *et al.* Transcriptome Analysis of the Human Tibial Nerve Identifies Sexually Dimorphic Expression of Genes Involved in Pain, Inflammation, and Neuro-Immunity. *Front Mol Neurosci* **12**, 37 (2019). https://doi.org:10.3389/fnmol.2019.00037

25 North, R. Y. *et al.* Electrophysiological and transcriptomic correlates of neuropathic pain in human dorsal root ganglion neurons. *Brain* **142**, 1215-1226 (2019). https://doi.org:10.1093/brain/awz063

26 Sorge, R. E. *et al.* Spinal cord Toll-like receptor 4 mediates inflammatory and neuropathic hypersensitivity in male but not female mice. *J Neurosci* **31**, 15450-15454 (2011). https://doi.org:10.1523/JNEUROSCI.3859-11.2011

27 Sorge, R. E. *et al.* Different immune cells mediate mechanical pain hypersensitivity in male and female mice. *Nat Neurosci* **18**, 1081-1083 (2015). https://doi.org:10.1038/nn.4053

28 Rayar, A. M. *et al.* Update on COX-2 Selective Inhibitors: Chemical Classification, Side Effects and their Use in Cancers and Neuronal Diseases. *Curr Top Med Chem* **17**, 2935-2956 (2017). https://doi.org:10.2174/1568026617666170821124947

29 Gilron, I., Baron, R. & Jensen, T. Neuropathic pain: principles of diagnosis and treatment. *Mayo Clin Proc* **90**, 532-545 (2015). https://doi.org:10.1016/j.mayocp.2015.01.018

30 Finnerup, N. B. *et al.* Pharmacotherapy for neuropathic pain in adults: a systematic review and meta-analysis. *Lancet Neurol* **14**, 162-173 (2015). https://doi.org:10.1016/s1474-4422(14)70251-0

31 Attal, N., Lanteri-Minet, M., Laurent, B., Fermanian, J. & Bouhassira, D. The specific disease burden of neuropathic pain: results of a French nationwide survey. *Pain* **152**, 2836-2843 (2011). https://doi.org:10.1016/j.pain.2011.09.014

32 Torrance, N. *et al.* Neuropathic pain in the community: more under-treated than refractory? *Pain* **154**, 690-699 (2013). https://doi.org:10.1016/j.pain.2012.12.022

33 Ghayur, M. N. Potential Adverse Consequences of Combination Therapy with Gabapentin and Pregabalin. *Case Rep Med* **2021**, 5559981 (2021). https://doi.org:10.1155/2021/5559981

34 Sansone, R. A. & Sansone, L. A. Pain, pain, go away: antidepressants and pain management. *Psychiatry (Edgmont)* **5**, 16-19 (2008).

35 Golzari, S. E., Soleimanpour, H., Mahmoodpoor, A., Safari, S. & Ala, A. Lidocaine and pain management in the emergency department: a review article. *Anesth Pain Med* **4**, e15444 (2014). https://doi.org:10.5812/aapm.15444

36 Peppin, J. F. & Pappagallo, M. Capsaicinoids in the treatment of neuropathic pain: a review. *Ther Adv Neurol Disord* **7**, 22-32 (2014). https://doi.org:10.1177/1756285613501576

37 Moore, R. A., Chi, C. C., Wiffen, P. J., Derry, S. & Rice, A. S. Oral nonsteroidal anti-inflammatory drugs for neuropathic pain. *Cochrane Database Syst Rev*, CD010902 (2015). https://doi.org:10.1002/14651858.CD010902.pub2

38 Hemler, M. & Lands, W. E. Purification of the cyclooxygenase that forms prostaglandins. Demonstration of two forms of iron in the holoenzyme. *J Biol Chem* **251**, 5575-5579 (1976).

39 Kujubu, D. A., Fletcher, B. S., Varnum, B. C., Lim, R. W. & Herschman, H. R. TIS10, a phorbol ester tumor promoter-inducible mRNA from Swiss 3T3 cells, encodes a novel prostaglandin synthase/cyclooxygenase homologue. *Journal of Biological Chemistry* **266**, 12866-12872 (1991). https://doi.org:https://doi.org/10.1016/S0021-9258(18)98774-0

40 Xie, W. L., Chipman, J. G., Robertson, D. L., Erikson, R. L. & Simmons, D. L. Expression of a mitogen-responsive gene encoding prostaglandin synthase is regulated by mRNA splicing. *Proc Natl Acad Sci U S A* **88**, 2692-2696 (1991). https://doi.org:10.1073/pnas.88.7.2692

41 Sibbald, B. Rofecoxib (Vioxx) voluntarily withdrawn from market. *Cmaj* **171**, 1027-1028 (2004). https://doi.org:10.1503/cmaj.1041606

42 Burton, B. COX 2 inhibitor rejected in North America but retained in Europe. *Bmj* **335**, 791 (2007). https://doi.org:10.1136/bmj.39370.401597.13

43 Gong, L. *et al.* Celecoxib pathways: pharmacokinetics and pharmacodynamics. *Pharmacogenet Genomics* **22**, 310-318 (2012). https://doi.org:10.1097/FPC.0b013e32834f94cb

44 Nissen, S. E. *et al.* Cardiovascular Safety of Celecoxib, Naproxen, or Ibuprofen for Arthritis. *New England Journal of Medicine* **375**, 2519-2529 (2016). https://doi.org:10.1056/NEJMoa1611593

45 Farkouh, A. *et al.* Sex-Related Differences in Drugs with Anti-Inflammatory Properties. *Journal of Clinical Medicine* **10** (2021). https://doi.org: 10.3390/jcm10071441

46 Balducci, A. *et al.* A novel probe for the non-invasive detection of tumor-associated inflammation. *OncoImmunology* **2**, e23034 (2013). https://doi.org:10.4161/onci.23034

47 Vasudeva, K. *et al.* Imaging Neuroinflammation In Vivo in a Neuropathic Pain Rat Model with Near-Infrared Fluorescence and 19F Magnetic Resonance. *PLOS ONE* **9**, e90589 (2014). https://doi.org:10.1371/journal.pone.0090589

48 Patel, S. K., Zhang, Y., Pollock, J. A. & Janjic, J. M. Cyclooxgenase-2 Inhibiting Perfluoropoly (Ethylene Glycol) Ether Theranostic Nanoemulsions—In Vitro Study. *PLOS ONE* **8**, e55802 (2013). https://doi.org:10.1371/journal.pone.0055802

49 Patel, S. K., Beaino, W., Anderson, C. J. & Janjic, J. M. Theranostic nanoemulsions for macrophage COX-2 inhibition in a murine inflammation model. *Clin Immunol* **160**, 59-70 (2015). https://doi.org:10.1016/j.clim.2015.04.019

50 Ghasemlou, N., Chiu, I. M., Julien, J.-P. & Woolf, C. J. CD11b+/Ly6G- myeloid cells mediate mechanical inflammatory pain hypersensitivity. *Proceedings of the National*

Academy of Sciences **112**, E6808-E6817 (2015). https://doi.org:doi:10.1073/pnas.1501372112

51 Janjic, J. M. *et al.* Low-dose NSAIDs reduce pain via macrophage targeted nanoemulsion delivery to neuroinflammation of the sciatic nerve in rat. *J Neuroimmunol* **318**, 72-79 (2018). https://doi.org:10.1016/j.jneuroim.2018.02.010

52 Wang, Y. *et al.* Cyclooxygenase inhibitors suppress the expression of P2X(3) receptors in the DRG and attenuate hyperalgesia following chronic constriction injury in rats. *Neurosci Lett* **478**, 77-81 (2010). https://doi.org:10.1016/j.neulet.2010.04.069

53 Schafers, M., Marziniak, M., Sorkin, L. S., Yaksh, T. L. & Sommer, C. Cyclooxygenase inhibition in nerve-injury- and TNF-induced hyperalgesia in the rat. *Exp Neurol* **185**, 160-168 (2004). https://doi.org:10.1016/j.expneurol.2003.09.015

54 Saleem, M., Deal, B., Nehl, E., Janjic, J. M. & Pollock, J. A. Nanomedicine-driven neuropathic pain relief in a rat model is associated with macrophage polarity and mast cell activation. *Acta Neuropathol Commun* **7**, 108 (2019). https://doi.org:10.1186/s40478-019-0762-y

55 Stevens, A. M., Liu, L., Bertovich, D., Janjic, J. M. & Pollock, J. A. Differential Expression of Neuroinflammatory mRNAs in the Rat Sciatic Nerve Following Chronic Constriction Injury and Pain-Relieving Nanoemulsion NSAID Delivery to Infiltrating Macrophages. *Int J Mol Sci* **20** (2019). https://doi.org:10.3390/ijms20215269

56 Swett, J. E., Torigoe, Y., Elie, V. R., Bourassa, C. M. & Miller, P. G. Sensory neurons of the rat sciatic nerve. *Experimental Neurology* **114**, 82-103 (1991). https://doi.org:https://doi.org/10.1016/0014-4886(91)90087-S

57 Stevens, A. M., Saleem, M., Deal, B., Janjic, J. & Pollock, J. A. Targeted cyclooxygenase-2 inhibiting nanomedicine results in pain-relief and differential expression of the RNA transcriptome in the dorsal root ganglia of injured male rats. *Mol Pain* **16**, 1744806920943309 (2020). https://doi.org:10.1177/1744806920943309

58 Liu, L. *et al.* Sex Differences Revealed in a Mouse CFA Inflammation Model with Macrophage Targeted Nanotheranostics. *Theranostics* **10**, 1694-1707 (2020). https://doi.org:10.7150/thno.41309

59 Xu, Q. & Yaksh, T. L. A brief comparison of the pathophysiology of inflammatory versus neuropathic pain. *Curr Opin Anaesthesiol* **24**, 400-407 (2011). https://doi.org:10.1097/ACO.0b013e32834871df

60 Beery, A. K. & Zucker, I. Sex bias in neuroscience and biomedical research. *Neuroscience & Biobehavioral Reviews* **35**, 565-572 (2011). https://doi.org:doi:10.1016/j.neubiorev.2010.07.002

61 Office, U. G. A. Drug Safety: Most Drugs Withdrawn in Recent Years Had Greater Health Risks for Women *Government Publishing Office, Washington, DC* (2001).

62 Klein, S. L. *et al.* Sex inclusion in basic research drives discovery. *Proceedings of the National Academy of Sciences* **112**, 5257-5258 (2015). https://doi.org:doi:10.1073/pnas.1502843112

63 Mogil, J. S. & Chanda, M. L. The case for the inclusion of female subjects in basic science studies of pain. *Pain* **117**, 1-5 (2005). https://doi.org:10.1016/j.pain.2005.06.020

64 Meziane, H., Ouagazzal, A.-M., Aubert, L., Wietrzych, M. & Krezel, W. Estrous cycle effects on behavior of C57BL/6J and BALB/cByJ female mice: implications for phenotyping strategies. *Genes, Brain and Behavior* **6**, 192-200 (2007). https://doi.org:https://doi.org/10.1111/j.1601-183X.2006.00249.x

65 Becker, J. B., Prendergast, B. J. & Liang, J. W. Female rats are not more variable than male rats: a meta-analysis of neuroscience studies. *Biol Sex Differ* **7**, 34 (2016). https://doi.org:10.1186/s13293-016-0087-5

66 Prendergast, B. J., Onishi, K. G. & Zucker, I. Female mice liberated for inclusion in neuroscience and biomedical research. *Neurosci Biobehav Rev* **40**, 1-5 (2014). https://doi.org:10.1016/j.neubiorev.2014.01.001

67 Dance, A. The Pain Gap. *Nature* **567**, 448-450 (2019). https://doi.org:10.1038/d41586-019-00895-3

68 Deal, B., Reynolds, L. M., Patterson, C., Janjic, J. M. & Pollock, J. A. Behavioral and inflammatory sex differences revealed by celecoxib nanotherapeutic treatment of peripheral neuroinflammation. *Scientific Reports* **12**, 1-12 (2022). https://doi.org:10.1038/s41598-022-12248-8

69 Molteni, M., Gemma, S. & Rossetti, C. The Role of Toll-Like Receptor 4 in Infectious and Noninfectious Inflammation. *Mediators of Inflammation* **2016**, 6978936 (2016). https://doi.org:10.1155/2016/6978936

70 Fukata, M. *et al.* Cox-2 Is Regulated by Toll-Like Receptor-4 (TLR4) Signaling: Role in Proliferation and Apoptosis in the Intestine. *Gastroenterology* **131**, 862-877 (2006). https://doi.org:https://doi.org/10.1053/j.gastro.2006.06.017

71 Wang, W. & Wang, J. Toll-Like Receptor 4 (TLR4)/Cyclooxygenase-2 (COX-2) Regulates Prostate Cancer Cell Proliferation, Migration, and Invasion by NF-κB Activation. *Med Sci Monit* **24**, 5588-5597 (2018). https://doi.org:10.12659/msm.906857

72 Pietruszewska, W. *et al.* Expression of Transcript Variants of PTGS1 and PTGS2 Genes among Patients with Chronic Rhinosinusitis with Nasal Polyps. *Diagnostics* **11**, 135 (2021).

73 Taves, S. *et al.* Spinal inhibition of p38 MAP kinase reduces inflammatory and neuropathic pain in male but not female mice: Sex-dependent microglial signaling in the spinal cord. *Brain Behav Immun* **55**, 70-81 (2016). https://doi.org:10.1016/j.bbi.2015.10.006

74 Chaplan, S. R., Bach, F. W., Pogrel, J. W., Chung, J. M. & Yaksh, T. L. Quantitative assessment of tactile allodynia in the rat paw. *J Neurosci Methods* **53**, 55-63 (1994). https://doi.org:10.1016/0165-0270(94)90144-9

75 Bennett, G. J. & Xie, Y. K. A peripheral mononeuropathy in rat that produces disorders of pain sensation like those seen in man. *Pain* **33**, 87-107 (1988). https://doi.org:10.1016/0304-3959(88)90209-6

76 Saleem, M. *et al.* A New Best Practice for Validating Tail Vein Injections in Rat with Near-infrared-Labeled Agents. *J Vis Exp* (2019). https://doi.org:10.3791/59295

77 Herneisey, M. *et al.* Development of Theranostic Perfluorocarbon Nanoemulsions as a Model Non-Opioid Pain Nanomedicine Using a Quality by Design (QbD) Approach. *AAPS PharmSciTech* **20**, 65 (2019). https://doi.org:10.1208/s12249-018-1287-6

78 Berta, T., Qadri, Y., Tan, P. H. & Ji, R. R. Targeting dorsal root ganglia and primary sensory neurons for the treatment of chronic pain. *Expert Opin Ther Targets* **21**, 695-703 (2017). https://doi.org:10.1080/14728222.2017.1328057

79 LaCroix-Fralish, M. L., Austin, J. S., Zheng, F. Y., Levitin, D. J. & Mogil, J. S. Patterns of pain: meta-analysis of microarray studies of pain. *Pain* **152**, 1888-1898 (2011). https://doi.org:10.1016/j.pain.2011.04.014

80 Berta, T. *et al.* Gene Expression Profiling of Cutaneous Injured and Non-Injured Nociceptors in SNI Animal Model of Neuropathic Pain. *Sci Rep* **7**, 9367 (2017). https://doi.org:10.1038/s41598-017-08865-3

81 Dixon, W. J. Efficient analysis of experimental observations. *Annu Rev Pharmacol Toxicol* **20**, 441-462 (1980). https://doi.org:10.1146/annurev.pa.20.040180.002301

82 Cora, M. C., Kooistra, L. & Travlos, G. Vaginal Cytology of the Laboratory Rat and Mouse: Review and Criteria for the Staging of the Estrous Cycle Using Stained Vaginal Smears. *Toxicologic Pathology* **43**, 776-793 (2015). https://doi.org:10.1177/0192623315570339

83 Damoiseaux, J. G. *et al.* Rat macrophage lysosomal membrane antigen recognized by monoclonal antibody ED1. *Immunology* **83**, 140-147 (1994).

84 Zhou, Y. *et al.* Metascape provides a biologist-oriented resource for the analysis of systems-level datasets. *Nature Communications* **10**, 1-10 (2019). https://doi.org:10.1038/s41467-019-09234-6

85 Haanpää, M. & Treede, R. Diagnosis and Classification of Neuropathic Pain. *PAIN Clinical Updates* **18**, 1-6 (2010).

86 Zhang, J. M. & An, J. Cytokines, inflammation, and pain. *Int Anesthesiol Clin* **45**, 27-37 (2007). https://doi.org:10.1097/AIA.0b013e318034194e

87 Rosen, S., Ham, B. & Mogil, J. S. Sex differences in neuroimmunity and pain. *J Neurosci Res* **95**, 500-508 (2017). https://doi.org:10.1002/jnr.23831

88 Kempuraj, D. *et al.* Brain and Peripheral Atypical Inflammatory Mediators Potentiate Neuroinflammation and Neurodegeneration. *Front Cell Neurosci* **11**, 216 (2017). https://doi.org:10.3389/fncel.2017.00216

89 Ren, K. & Dubner, R. Neuron-glia crosstalk gets serious: role in pain hypersensitivity. *Curr Opin Anaesthesiol* **21**, 570-579 (2008). https://doi.org:10.1097/ACO.0b013e32830edbdf

90 Austin, P. J. *et al.* Evidence for a distinct neuro-immune signature in rats that develop behavioural disability after nerve injury. *J Neuroinflammation* **12**, 96 (2015). https://doi.org:10.1186/s12974-015-0318-4

91 DiSabato, D. J., Quan, N. & Godbout, J. P. Neuroinflammation: the devil is in the details. *J Neurochem* **139 Suppl 2**, 136-153 (2016). https://doi.org:10.1111/jnc.13607

92 Vanegas, H. & Schaible, H. G. Prostaglandins and cyclooxygenases in the spinal cord. *Prog Neurobiol* **64**, 327-363 (2001). https://doi.org:10.1016/s0301-0082(00)00063-0

93 Ricciotti, E. & FitzGerald, G. A. Prostaglandins and inflammation. *Arterioscler Thromb Vasc Biol* **31**, 986-1000 (2011). https://doi.org:10.1161/ATVBAHA.110.207449

94 Funk, C. D. Prostaglandins and leukotrienes: advances in eicosanoid biology. *Science* **294**, 1871-1875 (2001). https://doi.org:10.1126/science.294.5548.1871

95 Lopshire, J. C. & Nicol, G. D. Activation and recovery of the PGE2-mediated sensitization of the capsaicin response in rat sensory neurons. *J Neurophysiol* **78**, 3154-3164 (1997). https://doi.org:10.1152/jn.1997.78.6.3154

96 Hawkey, C. J. COX-1 and COX-2 inhibitors. *Best Pract Res Clin Gastroenterol* **15**, 801-820 (2001). https://doi.org:10.1053/bega.2001.0236

97 Sorge, R. E. & Strath, L. J. Sex differences in pain responses. *Current Opinion in Physiology* **6**, 75-81 (2018). https://doi.org:10.1016/j.cophys.2018.05.006

98 Watkins, L. R. & Maier, S. F. Glia: a novel drug discovery target for clinical pain. *Nat Rev Drug Discov* **2**, 973-985 (2003). https://doi.org:10.1038/nrd1251

99 Adoga, M. P. *et al.* CD4- and CD3-T Lymphocyte Reference Values of Immunocompetent Urban and Rural Subjects in an African Nation. **76**, 33 (2012). https://doi.org:10.1111/j.1365-3083.2012.02700.x

100 Walker, J. S. & Carmody, J. J. Experimental Pain in Healthy Human Subjects: Gender Differencds in Nociception in Response to Ibuprofen. *The International Anesthesia Research Society* **86**, 1257 - 1262 (1998). https://doi.org:10.1097/00000539-199806000-00023

101 Chillingworth, N. L., Morham, S. G. & Donaldson, L. F. Sex differences in inflammation and inflammatory pain in cyclooxygenase-deficient mice. *Am J Physiol Regul Integr Comp Physiol* **291**, R327-334 (2006). https://doi.org:10.1152/ajpregu.00901.2005

102 Craft, R. M., Hewitt, K. A. & Britch, S. C. Antinociception produced by nonsteroidal anti-inflammatory drugs in female vs male rats. *Behavioral Pharmacology* **32**, 153 - 169 (2021). https://doi.org:10.1097/FBP.0000000000000584

103 Tavares-Ferreira, D. *et al.* Sex Differences in Nociceptor Translatomes Contribute to Divergent Prostaglandin Signaling in Male and Female Mice. *Biol Psychiatry* (2022). https://doi.org:10.1016/j.biopsych.2020.09.022

104 Marjoribanks, J., Ayeleke, R. O., Farquhar, C. & Proctor, M. Nonsteroidal anti-inflammatory drugs for dysmenorrhoea. *Cochrane Database Syst Rev*, CD001751 (2015). https://doi.org:10.1002/14651858.CD001751.pub3

105 Patel, R. B., Patel, M. R., Thakore, S. D. & Patel, B. G. in *Nano- and Microscale Drug Delivery Systems: Design and Fabrication* (ed A. M. Grumezescu) Ch. Chapter 17 - Nanoemulsion as Valuable Nanostructure Platform for Pharmaceutical Drug Delivery, 321-339 (Elsevier, 2017).

106 Mondal, S. & Rai, U. In vitro effect of sex steroids on cytotoxic activity of splenic macrophages in wall lizard (Hemidactylus flaviviridis). *Gen Comp Endocrinol* **125**, 264-271 (2002). https://doi.org:10.1006/gcen.2001.7744

107 Price, T. J. *et al.* Transition to chronic pain: opportunities for novel theraputics. *Nature Reviews Neuroscience* **19**, 383 - 384 (2018). https://doi.org:10.1038/s41583-018-0012-5

108 Klein, S. L. & Schwarz, J. M. Sex-Specific Regulation of Peripheral and Central Immune Responses. *Oxford Research Encyclopedia of Neuroscience*, 1-32 (2018). https://doi.org:10.1093/acrefore/9780190264086.013.223

109 Gonzalez, H. & Pacheco, R. T-cell-mediated regulation of neuroinflammation involved in neurodegenerative diseases. *J Neuroinflammation* **11**, 201 (2014). https://doi.org:10.1186/s12974-014-0201-8

110 Goodwin, J. S., Bankhurst, A. D. & Messner, R. P. Suppression of human T-cell mitogenesis by prostaglandin. Existence of a prostaglandin-producing suppressor cell. *J Exp Med* **146**, 1719-1734 (1977). https://doi.org:10.1084/jem.146.6.1719

111 Fregnan, F., Muratori, L., Simões, A. R., Giacobini-Robecchi, M. G. & Raimondo, S. Role of inflammatory cytokines in peripheral injury. *Neural Regeneration Research* **7**, 2259-2266 (2012). https://doi.org:10.3969/j.issn.1673-5374.2012.29.003

112 Vasudeva, K. *et al.* In vivo and systems biology studies implicate IL-18 as a central mediator in chronic pain. *Journal of Immunology* **283**, 43-49 (2015). https://doi.org:10.1016/j.jneuroim.2015.04.012

113 Mapplebeck, J. C. S. *et al.* Microglial P2X4R-evoked pain hypersensitivity is sexually dimorphic in rats. *Pain* **159**, 1752-1763 (2018). https://doi.org:10.1097/j.pain.0000000000001265

114 Aloisi, A. M. *et al.* Cross-sex hormone administration changes pain in transsexual women and men. *Pain* **132 Suppl 1**, S60-S67 (2007). https://doi.org:10.1016/j.pain.2007.02.006

115 Fairweather, D. & Rose, N. R. Women and autoimmune diseases. *Emerg Infect Dis* **10**, 2005-2011 (2004). https://doi.org:10.3201/eid1011.040367

116 Giefing-Kroll, C., Berger, P., Lepperdinger, G. & Grubeck-Loebenstein, B. How sex and age affect immune responses, susceptibility to infections, and response to vaccination. *Aging Cell* **14**, 309-321 (2015). https://doi.org:10.1111/acel.12326

117 Bouhassira, D., Lante´ri-Minet, M., Attal, N., Laurent, B. & Touboul, C. Prevalence of chronic pain with neuropathic characteristics in the general population. *Pain* **136**, 380-387 (2008). https://doi.org:10.1016/j.pain.2007.08.013

118 Bartley, E. J. & Fillingim, R. B. Sex differences in pain: a brief review of clinical and experimental findings. *British Journal of Anaesthesia* **111**, 52-58 (2013). https://doi.org:10.1093/bja/aet127

119 Demyanets, S. & Wojta, J. Sex differences in effects and use of anti-inflammatory drugs. *Handb Exp Pharmacol*, 443-472 (2012). https://doi.org:10.1007/978-3-642-30726-3_20

120 Leresche, L. Defining gender disparities in pain management. *Clin Orthop Relat Res* **469**, 1871-1877 (2011). https://doi.org:10.1007/s11999-010-1759-9

121 Kim, J., Kinney, K., Nyquist, M., Capellari, E. & Vordenberg, S. E. Factors that influence how adults select oral over-the-counter analgesics: A systematic review. *J Am Pharm Assoc (2003)* **62**, 1113-1123.e1118 (2022). https://doi.org:10.1016/j.japh.2022.03.007

122 Dowell, D., Ragan, K. R., Jones, C. M., Baldwin, G. T. & Chou, R. CDC Clinical Practice Guideline for Prescribing Opioids for Pain — United States, 2022. *MMWR Recomm Rep 2022* **71**, 1-95 (2022). https://doi.org:10.15585/mmwr.rr7103a1

123 Nasser, S. A. & Afify, E. A. Sex differences in pain and opioid mediated antinociception: Modulatory role of gonadal hormones. *Life Sciences* **237**, 116926 (2019). https://doi.org:https://doi.org/10.1016/j.lfs.2019.116926

124 Butlen-Ducuing, F. *et al.* Implications of sex-related differences in central nervous system disorders for drug research and development. *Nat Rev Drug Discov* **20**, 881-882 (2021). https://doi.org:10.1038/d41573-021-00115-6

125 Samba Reddy, D. Sex differences in the anticonvulsant activity of neurosteroids. *Journal of Neuroscience Research* **95**, 661-670 (2017). https://doi.org:https://doi.org/10.1002/jnr.23853

126 Ray, P. R. *et al.* RNA profiling of human dorsal root ganglia reveals sex-differences in mechanisms promoting neuropathic pain. *Brain* **Advance online publication** (2022). https://doi.org:10.1093/brain/awac266

127 Ahlström, F. H. G. *et al.* Spared Nerve Injury Causes Sexually Dimorphic Mechanical Allodynia and Differential Gene Expression in Spinal Cords and Dorsal Root Ganglia in Rats. *Molecular Neurobiology* **58**, 5396 - 5419 (2021). https://doi.org:10.1007/s12035-021-02447-1

128 Johnston, K. J. A. *et al.* Sex-stratified genome-wide association study of multisite chronic pain in UK Biobank. *PLOS Genetics* **17**, 1 - 27 (2021). https://doi.org:10.1371/journal.pgen.1009428

129 Wongrakpanich, S., Wongrakpanich, A., Melhado, K. & Rangaswami, J. A Comprehensive Review of Non-Steroidal Anti-Inflammatory Drug Use in The Elderly. *Aging Dis* **9**, 143-150 (2018). https://doi.org:10.14336/ad.2017.0306

130 Chernov, A. V. & Shubayev, V. I. Sexual Dimorphism of Early Transcriptional Reprogramming in Dorsal Root Ganglia After Peripheral Nerve Injury. *Frontiers in Molecular Neuroscience* **14** (2021). https://doi.org:10.3389/fnmol.2021.779024

131 Ku, H. & Cheng, C. Master Regulator Activating Transcription Factor 3 (ATF3) in Metabolic Homeostasis and Cancer. *Frontiers in Endocrinology* **11**, 1-16 (2020). https://doi.org:10.3389/fendo.2020.00556

132 Lopez-Dee, Z., Pidcock, K. & Gutierrez, L. S. Thrombospondin-1: Multiple Paths to Inflammation. *Mediators of Inflammation* **2011**, 1-10 (2011). https://doi.org:10.1155/2011/296069

133 Zhang, Y. *et al.* Regulation of neuropeptide Y in body microenvironments and its potential application in therapies: a review. *Cell and Bioscience* **11**, 1-14 (2021). https://doi.org:10.1186/s13578-021-00657-7

134 Boon, C. J. *et al.* Basal laminar drusen caused by compound heterozygous variants in the CFH gene. *American Journal of Human Genetics* **82**, 516-523 (2008). https://doi.org:10.1016/j.ajhg.2007.11.007

135 McEwen, B. S. Stress: Homeostasis, Rheostasis, Reactive Scope, Allostasis and Allostatic Load. *Reference Module in Neuroscience and Biobehavioral Psychology* (2017). https://doi.org:10.1016/B978-0-12-809324-5.02867-4.

136 Martinez-Moreno, M. *et al.* Regulation of Peripheral Myelination through Transcriptional Buffering of Egr2 by an Antisense Long Non-coding RNA. *Cell Reports* **20**, 1950-1963 (2017). https://doi.org:10.1016/j.celrep.2017.07.068

137 Usui, N. *et al.* Zbtb16 regulates social cognitive behaviors and neocortical development. *Translational Psychiatry* **11**, 1-15 (2021). https://doi.org:10.1038/s41398-021-01358-y

138 Khan, A. *et al.* SPTBN5, Encoding the βV-Spectrin Protein, Leads to a Syndrome of Intellectual Disability, Developmental Delay, and Seizures. *Frontiers in Molecular Neuroscience* **15** (2022). https://doi.org:10.3389/fnmol.2022.877258

139 Madigan, N. N. *et al.* Filamentous tangles with nemaline rods in MYH2 myopathy: a novel phenotype. *Acta Neuropathologica Communications* **9**, 79 (2021). https://doi.org:10.1186/s40478-021-01168-9

140 van de Locht, M. *et al.* Pathogenic variants in TNNC2 cause congenital myopathy due to an impaired force response to calcium. *The Journal of clinical investigation* **131** (2021). https://doi.org:doi.org/10.1172/JCI145700

141 Gigli, M. *et al.* A Review of the Giant Protein Titin in Clinical Molecular Diagnostics of Cardiomyopathies. *Frontiers in Cardiovascular Medicine* **3** (2016). https://doi.org:10.3389/fcvm.2016.00021

142 Yamada, M. *et al.* Increased Expression of Fibronectin Leucine-Rich Transmembrane Protein 3 in the Dorsal Root Ganglion Induces Neuropathic Pain in Rats. *Neurobiology of Disease* **39**, 7615-7627 (2019). https://doi.org:10.1523/JNEUROSCI.0295-19.2019

143 Kato, N., Nemoto, K., Arino, H. & Fujikawa, K. Influence of peripheral inflammation on growth-associated

phosphoprotein (GAP-43) expression in dorsal root ganglia and on

nerve recovery after crush injury. *Neuroscience Research* **45**, 297-303 (2003). https://doi.org:10.1016/s0168-0102(02)00234-1

144 Kanashiro, A. *et al.* The role of neutrophils in neuro-immune modulation. *Pharmacol Res* **151**, 104580 (2020). https://doi.org:10.1016/j.phrs.2019.104580

145 Rosales, C. Neutrophil: A Cell with Many Roles in Inflammation or Several Cell Types? *Frontiers in Physiology* **9** (2018). https://doi.org:10.3389/fphys.2018.00113

146 McGettrick, H. M. Bridging the gap—Immune cells that can repair nerves. *Cellular & Molecular Immunology* **18**, 784-786 (2021). https://doi.org:10.1038/s41423-021-00642-7

147 Sas, A. R. *et al.* A new neutrophil subset promotes CNS neuron survival and axon regeneration. *Nat Immunol* **21**, 1496-1505 (2020). https://doi.org:10.1038/s41590-020-00813-0

148 Zheng, H., Lim, J. Y., Seong, J. Y. & Hwang, S. W. The Role of Corticotropin-Releasing Hormone at Peripheral Nociceptors: Implications for Pain Modulation. *Biomedicines* **8** (2020). https://doi.org:10.3390/biomedicines8120623

149 Hargreaves, K. M., Mueller, G. P., Dubner, R., Goldstein, D. & Dionne, R. A. Corticotropin-releasing factor (CRF) produces analgesia in humans and rats. *Brain*

Research **422**, 154-157 (1987). https://doi.org:https://doi.org/10.1016/0006-8993(87)90550-6

150 Hargreaves, K. M., Dubner, R. & Costello, A. H. Corticotropin releasing factor (CRF) has a peripheral site of action for antinociception. *European Journal of Pharmacology* **170**, 275-279 (1989). https://doi.org:https://doi.org/10.1016/0014-2999(89)90550-5

151 Hargreaves, K. M., Flores, C. M., Dionne, R. A. & Mueller, G. P. The role of pituitary beta-endorphin in mediating corticotropin-releasing factor-induced antinociception. *American Journal of Physiology-Endocrinology and Metabolism* **258**, E235-E242 (1990). https://doi.org:10.1152/ajpendo.1990.258.2.E235

152 Yarushkina, N. I. & Filaretova, L. P. The peripheral corticotropin-releasing factor (CRF)-induced analgesic effect on somatic pain sensitivity in conscious rats: involving CRF, opioid and glucocorticoid receptors. *Inflammopharmacology* **26**, 305-318 (2018). https://doi.org:10.1007/s10787-018-0445-5

153 Reinhold, A. K. *et al.* Differential Transcriptional Profiling of Damaged and Intact Adjacent Dorsal Root Ganglia Neurons in Neuropathic Pain. *PLOS ONE* **10**, e0123342 (2015). https://doi.org:10.1371/journal.pone.0123342

154 Soliman, N., Okuse, K. & Rice, A. S. C. VGF: a biomarker and potential target for the treatment of neuropathic pain? *Pain Rep* **4**, e786 (2019). https://doi.org:10.1097/pr9.0000000000000786

155 Moss, A. *et al.* Origins, actions and dynamic expression patterns of the neuropeptide VGF in rat peripheral and central sensory neurones following peripheral nerve injury. *Mol Pain* **4**, 62 (2008). https://doi.org:10.1186/1744-8069-4-62

156 Zhuang, Z. Y. *et al.* A peptide c-Jun N-terminal kinase (JNK) inhibitor blocks mechanical allodynia after spinal nerve ligation: respective roles of JNK activation in primary sensory neurons and spinal astrocytes for neuropathic pain development and maintenance. *J Neurosci* **26**, 3551-3560 (2006). https://doi.org:10.1523/jneurosci.5290-05.2006

157 Hai, T., Wolford, C. C. & Chang, Y. S. ATF3, a hub of the cellular adaptive-response network, in the pathogenesis of diseases: is modulation of inflammation a unifying component? *Gene Expr* **15**, 1-11 (2010). https://doi.org:10.3727/105221610x12819686555015

158 Hellmann, J. *et al.* Atf3 negatively regulates Ptgs2/Cox2 expression during acute inflammation. *Prostaglandins Other Lipid Mediat* **116-117**, 49-56 (2015). https://doi.org:10.1016/j.prostaglandins.2015.01.001

159 Bradbury, D. A. *et al.* Cyclooxygenase-2 Induction by Bradykinin in Human Pulmonary Artery Smooth Muscle Cells Is Mediated by the Cyclic AMP Response Element through a Novel Autocrine Loop Involving Endogenous Prostaglandin E₂, E-

prostanoid 2 (EP2), and EP4 Receptors *. *Journal of Biological Chemistry* **278**, 49954-49964 (2003). https://doi.org:10.1074/jbc.M307964200

160 Yu, T. *et al.* The Regulatory Role of Activating Transcription Factor 2 in Inflammation. *Mediators of Inflammation* **2014**, 950472 (2014). https://doi.org:10.1155/2014/950472

161 Tsujino, H. *et al.* Activating Transcription Factor 3 (ATF3) Induction by Axotomy in Sensory and Motoneurons: A Novel Neuronal Marker of Nerve Injury. *Molecular and Cellular Neuroscience* **15**, 170-182 (2000). https://doi.org:https://doi.org/10.1006/mcne.1999.0814

162 Rau, K. K. *et al.* Cutaneous tissue damage induces long-lasting nociceptive sensitization and regulation of cellular stress- and nerve injury-associated genes in sensory neurons. *Experimental Neurology* **283**, 413-427 (2016). https://doi.org:https://doi.org/10.1016/j.expneurol.2016.06.002

163 Becher, B., Spath, S. & Goverman, J. Cytokine networks in neuroinflammation. *Nature Reviews Immunology* **17**, 49-59 (2017). https://doi.org:10.1038/nri.2016.123

164 Chen, S.-H., Huang, T.-C., Wang, J.-Y., Wu, C.-C. & Hsueh, Y.-Y. Controllable forces for reproducible chronic constriction injury mimicking compressive neuropathy in rat sciatic nerve. *Journal of Neuroscience Methods* **335**, 108615 (2020). https://doi.org:https://doi.org/10.1016/j.jneumeth.2020.108615

165 Chen, S.-H. *et al.* Investigation of Neuropathology after Nerve Release in Chronic Constriction Injury of Rat Sciatic Nerve. *International Journal of Molecular Sciences* **22**, 4746 (2021).

166 Barrot, M. Tests and models of nociception and pain in rodents. *Neuroscience* **211**, 39-50 (2012). https://doi.org:10.1016/j.neuroscience.2011.12.041

167 Deuis, J. R., Dvorakova, L. S. & Vetter, I. Methods Used to Evaluate Pain Behaviors in Rodents. *Frontiers in Molecular Neuroscience* **10** (2017). https://doi.org:10.3389/fnmol.2017.00284

168 Lin, J. P. *et al.* Dexmedetomidine Attenuates Neuropathic Pain by Inhibiting P2X7R Expression and ERK Phosphorylation in Rats. *Exp Neurobiol* **27**, 267-276 (2018). https://doi.org:10.5607/en.2018.27.4.267

169 Ghasemi, A., Jeddi, S. & Kashfi, K. The laboratory rat: Age and body weight matter. *Excli j* **20**, 1431-1445 (2021). https://doi.org:10.17179/excli2021-4072

170 Racine, M. *et al.* A systematic literature review of 10 years of research on sex/gender and experimental pain perception – Part 1: Are there really differences between women and men? *PAIN* **153**, 602-618 (2012). https://doi.org:10.1016/j.pain.2011.11.025

171 Hurley, R. W. & Adams, M. C. Sex, gender, and pain: an overview of a complex field. *Anesth Analg* **107**, 309-317 (2008). https://doi.org:10.1213/01.ane.0b013e31816ba437

172 Rimon, G. *et al.* Coxibs interfere with the action of aspirin by binding tightly to one monomer of cyclooxygenase-1. *Proceedings of the National Academy of Sciences* **107**, 28-33 (2010). https://doi.org:doi:10.1073/pnas.0909765106

173 Italiani, P. & Boraschi, D. From Monocytes to M1/M2 Macrophages: Phenotypical vs. Functional Differentiation. *Frontiers in Immunology* **5** (2014). https://doi.org:10.3389/fimmu.2014.00514

174 Parisien, M. *et al.* Acute inflammatory response via neutrophil activation protects against the development of chronic pain. *Science Translational Medicine* **14**, eabj9954 (2022). https://doi.org:doi:10.1126/scitranslmed.abj9954

175 Arango Duque, G. & Descoteaux, A. Macrophage cytokines: involvement in immunity and infectious diseases. *Front Immunol* **5**, 491 (2014). https://doi.org:10.3389/fimmu.2014.00491

176 Gregus, A. M., Levine, I. S., Eddinger, K. A., Yaksh, T. L. & Buczynski, M. W. Sex differences in neuroimmune and glial mechanisms of pain. *PAIN* **162**, 2186-2200 (2021). https://doi.org:10.1097/j.pain.0000000000002215

177 Kalinski, P. Regulation of immune responses by prostaglandin E2. *J Immunol* **188**, 21-28 (2012). https://doi.org:10.4049/jimmunol.1101029

178 Linher-Melville, K., Shah, A. & Singh, G. Sex differences in neuro(auto)immunity and chronic sciatic nerve pain. *Biology of Sex Differences* **11**, 62 (2020). https://doi.org:10.1186/s13293-020-00339-y

179 McLachlan, E. M. & Hu, P. Inflammation in dorsal root ganglia after peripheral nerve injury: effects of the sympathetic innervation. *Auton Neurosci* **182**, 108-117 (2014). https://doi.org:10.1016/j.autneu.2013.12.009

180 Kobayashi, Y. *et al.* Macrophage-T cell interactions mediate neuropathic pain through the glucocorticoid-induced tumor necrosis factor ligand system. *J Biol Chem* **290**, 12603-12613 (2015). https://doi.org:10.1016/j.autneu.2013.12.009

181 Sprenkeler, E. G. G. *et al.* S100A8/A9 Is a Marker for the Release of Neutrophil Extracellular Traps and Induces Neutrophil Activation. *Cells* **11** (2022). https://doi.org:10.3390/cells11020236

182 Camara-Lemarroy, C. R., Gonzalez-Moreno, E. I., Guzman-de la Garza, F. J. & Fernandez-Garza, N. E. Arachidonic acid derivatives and their role in peripheral nerve degeneration and regeneration. *ScientificWorldJournal* **2012**, 168953 (2012). https://doi.org:10.1100/2012/168953

183 Bloechlinger, S., Karchewski, L. A. & Woolf, C. J. Dynamic changes in glypican-1 expression in dorsal root ganglion neurons after peripheral and central axonal injury. *Eur J Neurosci* **19**, 1119-1132 (2004). https://doi.org:10.1111/j.1460-9568.2004.03262.x

184 Bráz, J. M. & Basbaum, A. I. Differential ATF3 expression in dorsal root ganglion neurons reveals the profile of primary afferents engaged by diverse noxious chemical stimuli. *Pain* **150**, 290-301 (2010). https://doi.org:10.1016/j.pain.2010.05.005

185 Vrinten, D. H. & Hamers, F. F. 'CatWalk' automated quantitative gait analysis as a novel method to assess mechanical allodynia in the rat; a comparison with von Frey testing. *Pain* **102**, 203-209 (2003). https://doi.org:10.1016/s0304-3959(02)00382-2

186 Dias, Q. M., Rossaneis, A. C., Fais, R. S. & Prado, W. A. An improved experimental model for peripheral neuropathy in rats. . *Brazilian Journal of Medical and Biological Research* **46**, 253-256 (2013). https://doi.org:10.1590/1414-431X20122462

187 Gopalsamy, B. *et al.* Experimental Characterization of the Chronic Constriction Injury-Induced Neuropathic Pain Model in Mice. *Neurochemical Research* **44**, 2123-2138 (2019). https://doi.org:10.1007/s11064-019-02850-0

188 Diederichsen, A. C. P. *et al.* A comparison of flow cytometry and immunohistochemistry in human colorectal cancers. *APMIS* **106**, 562-570 (1998). https://doi.org:https://doi.org/10.1111/j.1699-0463.1998.tb01385.x

189 Turner, P. V., Brabb, T., Pekow, C. & Vasbinder, M. A. Administration of substances to laboratory animals: routes of administration and factors to consider. *J Am Assoc Lab Anim Sci* **50**, 600-613 (2011).

190 Patel, S. K. & Janjic, J. M. Macrophage targeted theranostics as personalized nanomedicine strategies for inflammatory diseases. *Theranostics* **5**, 150-172 (2015). https://doi.org:10.7150/thno.9476

191 Liu, L., Bagia, C. & Janjic, J. M. The First Scale-Up Production of Theranostic Nanoemulsions. *Biores Open Access* **4**, 218-228 (2015). https://doi.org:10.1089/biores.2014.0030

192 Patel, S. K., Patrick, M. J., Pollock, J. A. & Janjic, J. M. Two-color fluorescent (near-infrared and visible) triphasic perfluorocarbon nanoemuslions. *J Biomed Opt* **18**, 101312 (2013). https://doi.org:10.1117/1.Jbo.18.10.101312

193 O'Hanlon, C. E., Amede, K. G., O'Hear, M. R. & Janjic, J. M. NIR-labeled perfluoropolyether nanoemulsions for drug delivery and imaging. *J Fluor Chem* **137**, 27-33 (2012). https://doi.org:10.1016/j.jfluchem.2012.02.004

194 Cheng, Y., Liu, M., Hu, H.-j., Liu, D.-z. & Zhou, S.-y. Development, Optimization, and Characterization of PEGylated Nanoemulsion of Prostaglandin E1 for Long Circulation. *AAPS PharmSciTech* **17**, 409-417 (2016).

195 Fofaria, N. M., Qhattal, H. S., Liu, X. & Srivastava, S. K. Nanoemulsion formulations for anti-cancer agent piplartine--Characterization, toxicological, pharmacokinetics and efficacy studies. *Int J Pharm* **498**, 12-22 (2016). https://doi.org:10.1016/j.ijpharm.2015.11.045

196 Ganta, S. *et al.* EGFR Targeted Theranostic Nanoemulsion for Image-Guided Ovarian Cancer Therapy. *Pharm Res* **32**, 2753-2763 (2015). https://doi.org:10.1007/s11095-015-1660-z

197 Shah, L., Kulkarni, P., Ferris, C. & Amiji, M. M. Analgesic efficacy and safety of DALDA peptide analog delivery to the brain using oil-in-water nanoemulsion formulation. *Pharm Res* **31**, 2724-2734 (2014). https://doi.org:10.1007/s11095-014-1370-y

198 Maruyama, H. *et al.* High-level expression of naked DNA delivered to rat liver via tail vein injection. *J Gene Med* **4**, 333-341 (2002). https://doi.org:10.1002/jgm.281

199 Hibbitt, O. C. *et al.* Delivery and long-term expression of a 135 kb LDLR genomic DNA locus in vivo by hydrodynamic tail vein injection. *The Journal of Gene Medicine* **9**, 488-497 (2007). https://doi.org:https://doi.org/10.1002/jgm.1041

200 Sebestyén, M. G. *et al.* Mechanism of plasmid delivery by hydrodynamic tail vein injection. I. Hepatocyte uptake of various molecules. *J Gene Med* **8**, 852-873 (2006). https://doi.org:10.1002/jgm.921

201 Budker, V. G. *et al.* Mechanism of plasmid delivery by hydrodynamic tail vein injection. II. Morphological studies. *J Gene Med* **8**, 874-888 (2006). https://doi.org:10.1002/jgm.920

202 Lecocq, M. *et al.* Uptake by mouse liver and intracellular fate of plasmid DNA after a rapid tail vein injection of a small or a large volume. *J Gene Med* **5**, 142-156 (2003). https://doi.org:10.1002/jgm.328

203 Park, S., Park, H. M. & Sun, S. H. Single-dose Intravenous Injection Toxicity of Water-soluble Danggui Pharmacopuncture (WDP) in Sprague-Dawley Rats. *J Pharmacopuncture* **21**, 104-111 (2018). https://doi.org:10.3831/kpi.2018.21.013

204 Zhang, X. *et al.* Activatable fluorescence detection of epidermal growth factor receptor positive mediastinal lymph nodes in murine lung cancer model. *PLOS ONE* **13**, e0198224 (2018). https://doi.org:10.1371/journal.pone.0198224

205 Liu, G. *et al.* Tracking of transplanted human umbilical cord-derived mesenchymal stem cells labeled with fluorescent probe in a mouse model of acute lung injury. *Int J Mol Med* **41**, 2527-2534 (2018). https://doi.org:10.3892/ijmm.2018.3491

206 Schindelin, J. *et al.* Fiji: an open-source platform for biological-image analysis. *Nature Methods* **9**, 676-682 (2012). https://doi.org:10.1038/nmeth.2019

207 Janjic, J. M., Srinivas, M., Kadayakkara, D. K. K. & Ahrens, E. T. Self-delivering nanoemulsions for dual fluorine-19 MRI and fluorescence detection. *J Am Chem Soc* **130**, 2832-2841 (2008). https://doi.org:10.1021/ja077388j

208 Chang, Y. C. *et al.* An Automated Mouse Tail Vascular Access System by Vision and Pressure Feedback. *IEEE ASME Trans Mechatron* **20**, 1616-1623 (2015). https://doi.org:10.1109/tmech.2014.2360886

209 Chen, Q. *et al.* Theranostic imaging of liver cancer using targeted optical/MRI dual-modal probes. *Oncotarget* **8**, 32741-32751 (2017). https://doi.org:10.18632/oncotarget.15642

210 Tansi, F. L. *et al.* Activatable bispecific liposomes bearing fibroblast activation protein directed single chain fragment/Trastuzumab deliver encapsulated cargo into the nuclei of tumor cells and the tumor microenvironment simultaneously. *Acta Biomater* **54**, 281-293 (2017). https://doi.org:10.1016/j.actbio.2017.03.033

211 Li, S., Johnson, J., Peck, A. & Xie, Q. Near infrared fluorescent imaging of brain tumor with IR780 dye incorporated phospholipid nanoparticles. *Journal of Translational Medicine* **15**, 18 (2017). https://doi.org:10.1186/s12967-016-1115-2

212 Wang, R., Han, X., You, J., Yu, F. & Chen, L. Ratiometric Near-Infrared Fluorescent Probe for Synergistic Detection of Monoamine Oxidase B and Its Contribution to Oxidative Stress in Cell and Mice Aging Models. *Analytical Chemistry* **90**, 4054-4061 (2018). https://doi.org:10.1021/acs.analchem.7b05297

213 Gao, M., Yu, F., Lv, C., Choo, J. & Chen, L. Fluorescent chemical probes for accurate tumor diagnosis and targeting therapy. *Chemical Society Reviews* **46**, 2237-2271 (2017). https://doi.org:10.1039/C6CS00908E

214 Han, X., Song, X., Yu, F. & Chen, L. A Ratiometric Near-Infrared Fluorescent Probe for Quantification and Evaluation of Selenocysteine-Protective Effects in Acute Inflammation. *Advanced Functional Materials* **27**, 1700769 (2017). https://doi.org:https://doi.org/10.1002/adfm.201700769